PB90-131111

Transactions: Effects of Air Pollution on Western Forests

(U.S.) Corvallis Environmental Research Lab., OR

1989

U.S. Department of Commerce
National Technical Information Service
NTIS

ERL-COR-1056D

TECHNICAL REPORT DATA

(Please read Instructions on the reverse before completir

1. REPORT NO.
EPA/600/D-89/195

2.

3.
PB90-131111

4. TITLE AND SUBTITLE
Transactions of the Air and Waste Management Association: Effects of Air Pollution on Western Forests

5. REPORT DATE

6. PERFORMING ORGANIZATION CODE

7. AUTHOR(S)
Richard K. Olson and Allen S. LeFohn (eds).

8. PERFORMING ORGANIZATION REPORT NO.

9. PERFORMING ORGANIZATION NAME AND ADDRESS
NSI, US EPA, ERL-Corvallis, and ASL & Assoc., Helena, MT

10. PROGRAM ELEMENT NO.

11. CONTRACT/GRANT NO.

12. SPONSORING AGENCY NAME AND ADDRESS
US Environmental Protection Agency
Environmental Research Laboratory
200 SW 35th Street
Corvallis, OR 97333

13. TYPE OF REPORT AND PERIOD COVERED
Symposium Paper

14. SPONSORING AGENCY CODE
EPA/600/2

15. SUPPLEMENTARY NOTES
Volume in the AWMA Transactions series.

16. ABSTRACT

This volume contains 35 papers from a Symposium held June 29-30, 1989 in Anaheim, CA. Topics addressed include air quality and deposition, forest condition and growth trends, physiological mechanism of effects, and effects of air pollution on forest soils. Among the conclusions reached at the Symposium were: (1) large areas of forests in California have been damaged by ozone; (2) highly acidic clouds impact forests in Washington, California and Colorado; (3) most western forest soils are not currently at risk from acid deposition; (4) forests in southern Arizona are experiencing unexplained growth declines.

17. KEY WORDS AND DOCUMENT ANALYSIS

a. DESCRIPTORS	b. IDENTIFIERS/OPEN ENDED TERMS	c. COSATI Field/Group

18. DISTRIBUTION STATEMENT

19. SECURITY CLASS *(This Report)*
Unclassified

20. SECURITY CLASS *(This page)*
Unclassified

21. NO. OF PAGES
557

22. PRICE

EPA Form 2220-1 (9-73)

REPRODUCED BY
U.S. DEPARTMENT OF COMMERCE
NATIONAL TECHNICAL INFORMATION SERVICE
SPRINGFIELD, VA. 22161

N O T I C E

THIS DOCUMENT HAS BEEN REPRODUCED FROM THE BEST COPY FURNISHED US BY THE SPONSORING AGENCY. ALTHOUGH IT IS RECOGNIZED THAT CERTAIN PORTIONS ARE ILLEGIBLE, IT IS BEING RELEASED IN THE INTEREST OF MAKING AVAILABLE AS MUCH INFORMATION AS POSSIBLE.

EPA/600/D-89/195

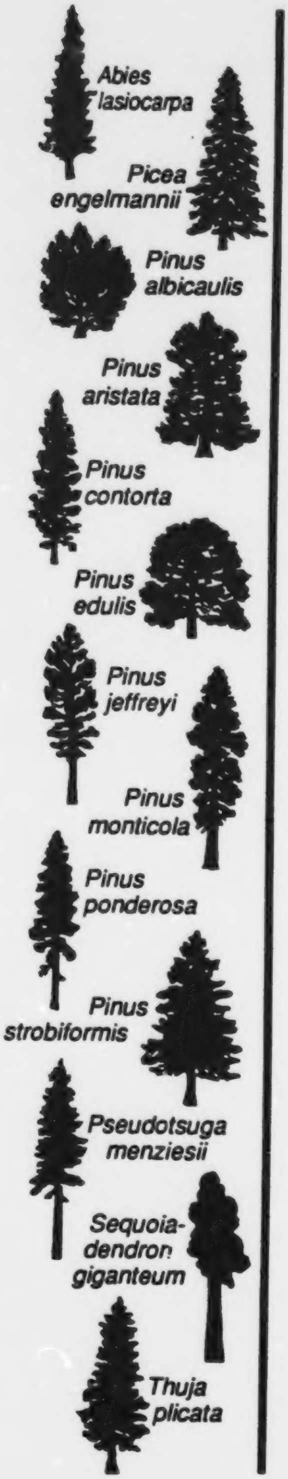
Abies lasiocarpa
Picea engelmannii
Pinus albicaulis
Pinus aristata
Pinus contorta
Pinus edulis
Pinus jeffreyi
Pinus monticola
Pinus ponderosa
Pinus strobiformis
Pseudotsuga menziesii
Sequoia-dendron giganteum
Thuja plicata

TRANSACTIONS

EFFECTS OF AIR POLLUTION ON WESTERN FORESTS

Edited by
Richard K. Olson
NSI Technology Services Corporation
U.S. EPA Environmental Research Laboratory
Corvallis, Oregon
Allen S. Lefohn
A.S.L. and Associates
Helena, Montana

Sponsored by
Air & Waste Management Association's
TE-2 Ecological Effects Committee
U.S. Environmental Protection Agency
USDA Forest Service
National Park Service
California Air Resources Board

Anaheim, California
June 1989

Air & Waste Management Association
(formerly APCA)

NOTICE

This document has been reviewed in accordance with U.S. Environmental Protection Agency policy and approved for publication. Mention of trade names or commercial products does not constitute endorsement or recommendation for use.

Effects of Air Pollution on Western Forests
(APCA *Transactions* Series, ISSN ; no.)

Includes Index

1. Air Pollution—Environmental Aspects—Western States.
2. Forests—Western.
I. Olson, Richard K. II. Lefohn, Allen S. III. Series

ISBN 1989

Copyright 1989 by Air & Waste Management Association
(Formerly APCA)

This collective work is protected by copyright. No technical paper appearing in these *Transactions* may be reproduced in any form without permission from the author(s) and from the publisher:

Air & Waste Management Association
(formerly APCA)
P.O. Box 2861
Pittsburgh, PA 15230

Table of Contents

Foreword	vii
Symposium Organizing Committee	ix
Acknowledgments	ix

CHAPTER ONE
Air Quality and Deposition: Clouds

Summertime Cloud Immersion Frequency at Elk Mountain, Wyoming	J.R. Snider and J.A. Garcia	3
Front Range Acidic Clouds and Precipitation	F. Parungo, C. Nagamoto, and B. Kopcewicz	15
Fog and Cloud Water Chemistry in Western Washington	F.A. Basabe, R.L. Edmonds, W.L. Chang, and T.V. Larson	33
Airborne Chemical Measurements in Nighttime Stratus Clouds in the Los Angeles Basin	L.W. Richards	51
Cloud Chemistry and Occurrence in the Western United States: A Synopsis of Current Information	P.S. Muir and M. Böhm	73

CHAPTER TWO
Air Quality and Deposition: Precipitation

Chemistry of Summer Cloud, Precipitation and Air at a Rocky Mountain-Top Location	D.F. Miller, R.D. Borys, and R. Graw	105
Background Concentration of Sulfate in Precipitation along the West Coast of North America	R.J. Vong	117
Analysis of a Summertime Acid Rain Event in the Sierra Nevada	C.D. Unger	137
Fog and Rain Chemistry in Northern California	S. Bicknell	147

CHAPTER THREE
Air Quality and Deposition: Gases and Particulates

Dry Deposition of Nitrate and Sulfate to Coniferous Canopies in the Rocky Mountains	H.J. Sievering, J. Braus, and J. Caine	171
Ozone Deposition and Leaf Area Index at the Pawnee National Grassland for the 1988 Growing Season	K.F. Zeller and D.L. Hazlett	177

Air Quality at a High Elevation, Remote Site in Western Canada	A.H. Legge and S.V. Krupa	193
Ozone at a Remote, High-Altitude Site in Sequoia National Park, California	B.S. Pedersen and T.A. Cahill	207
A Regional Characterization of Air Quality and Deposition in the Coniferous Forests of the Western United States	M. Böhm	221

CHAPTER FOUR
Forest Condition and Trends

Risks to California Forests due to Regional Ozone Pollution: A Data Base and Ranking of Forest Sensitivity	D.C. Peterson and C. Daly	247
Photochemical Oxidant Injury to Ponderosa (*Pinus Ponderosa* Laws.) and Jeffrey Pine (*Pinus Jeffreyi* Grev. and Balf.) in the National Parks of the Sierra Nevada of California	D.M. Duriscoe and K.W. Stolte	261
Ozone Injury to Jeffrey and Ponderosa Pines Surrounding Lake Tahoe, California and Nevada	B.S. Pedersen	279
Ozone Injury and Growth Trends of Ponderosa Pine in the Sierra Nevada	D.L. Peterson, M.J. Arbaugh, and L.J. Robinson	293
Trend of Ozone Damage to Conifer Forests between 1974 and 1988 in the San Bernardino Mountains of Southern California	P.R. Miller, J.R. McBride, S.L. Schilling, and A.P. Gomez	309
Current and Potential Threats to Biodiversity in Forests of the Lower Pacific Coast States	S. Henderson, R.K. Olson, and R.F. Noss	325
Comparisons of Aircraft and Satellite Sensors for Monitoring Air Pollution Effects on Forests	C.D. Elvidge, J.E. Vogelmann, and C.A. Fox	337
Early Detection of Air Pollution Injury to Coniferous Forests Using Remote Sensing	S.L. Ustin, B. Curtiss, S.N. Martens, and V.C. Vanderbilt	351
Use of Quality Control Procedures for Assessing Variation in Measurements of Forest Canopy Condition	S.P. Cline, W.G. Burkman and C.D. Geron	379
Analysis of Growth Trends and Variation in Conifers from Arizona and New Mexico	D.A. Graybill and M.R. Rose	395

CHAPTER FIVE
Growth and Physiological Mechanisms of Effect

Specific Leaf Weight and Other Characteristics of Ponderosa Pine as Related to Visible Ozone Injury — D.M. Ewell, L.C. Mazzu, and D.M. Duriscoe — 411

Seasonal Physiological Responses of Ozone Stressed Jeffrey Pine in Sequoia National Park, California — M.T. Patterson and P.W. Rundel — 419

Photosynthetic Response of Giant Sequoia Seedlings and Rooted Branchlets of Mature Foliage to Ozone Fumigation — N.E. Grulke, P.R. Miller, R.D. Wilborn, and S. Hahn — 429

Potential Effect of Premature Needle Loss on the Foliar Biomass and Nutrient Retention of Lodgepole Pine — A.W. Schoettle — 443

Effects of Photochemical Smog on the Growth and Physiology of Ponderosa Pine Seedlings Grown Under Nitrogen and Magnesium Deficiencies — A. Bytnerowicz and B.K. Takemoto — 455

Sensitivity of Western Conifers to SO_2 and Seasonal Interaction of Acid Fog and Ozone — W.E. Hogsett, D.T. Tingey, C. Hendricks, and D. Rossi — 469

Nutrient Effects on Responses of Willow and Alder to Ozone — C.S. Greitner and W.E. Winner — 493

CHAPTER SIX
Response of Soils to Atmospheric Deposition

The Effect of Nitrogen Accumulation and Nitrification on Soil Chemical Properties in Alder Forests — H. Van Miegroet, D.W. Cole, D. Binkley, and P. Sollins — 515

Forest Soil Sulfur Pools and SO_4^{2-} Adsorption and Desorption Capacity Following Elevated Inputs of SO_4^{2-} — R.B. Harrison, D.W. Johnson, and D.E. Todd — 529

Soil-Solution Equilibria in Lysimeter Leachates Under Red Alder — J.O. Reuss — 547

Sensitivity of Forest Soils in the Western U.S. to Acidic Deposition — D. Binkley — 561

Index of Authors — 575
Index of Subjects — 576

Foreword

The Symposium on the Effects of Air Pollution on Western Forests was held as part of a process to summarize current knowledge of air pollution and forested ecosystems in the eleven western states. The goal of the Symposium was to use this information to produce a better understanding of the biological and physical processes that occur in this area of the United States.

At first glance, the papers presented at the Symposium do not appear to present a unified view. A paper describing forests where federal ozone standards are frequently exceeded is followed by data from another region where a peak of 60 ppb is considered high. Clouds with a pH of 3.7 bathe a montane forest while an adjacent lowland forest receives only pH 5.0 rain. A forest where virtually every tree has foliar ozone damage contrasts with a forest only ten kilometers away, but on the other side of a ridge, that has no damage.

Clearly, a primary attribute of the West is diversity. Forests totalling 230 million acres range from temperate rain forest to arid pinyon-juniper; from newly regenerating clear-cuts to ancient forests. They occupy a range of climates from Mediterranean to subalpine. Management practices include wilderness, intensive harvesting, and residential development. Air pollution in forested areas, as indicated above, includes multiple pollutants and wide ranges of concentrations. Given this diversity, it is not contradictory to conclude from the papers in these *Transactions* that extensive areas of western forests are not stressed by air pollution, while at the same time large areas of western forests are being damaged by air pollution.

"Large," however, is defined differently by different observers. For example, the Los Angeles basin is surrounded by the Angeles, San Bernardino and Cleveland National Forests. These areas receive some of the heaviest pollutant loads in the United States; the studies of forest damage in the San Bernardino Mountains are well known. Because these forests constitute a small fraction of the forested area in California, this situation is often classified as atypical and essentially local in nature. In contrast, the decline of high-elevation spruce-fir forests in the eastern United States is often described as a regional and important problem with links to air pollution. Yet, the total acreage of those high elevation forests is less than the acres of forest in the three southern California National Forests.

Regardless of forest size, quantifying the effects of air pollution on western forests is difficult. Air quality data for forested areas are limited. Periodic, long-term measurements of forest growth and condition are even rarer. There are large gaps in understanding of the mechanisms through which forests respond to pollutants, whether at the biochemical, tree, stand or ecosystem level. Each of the ten *Transactions* papers addressing the topic of forest condition and growth trends makes clear that many natural and anthropogenic stresses influence forest condition, and each of these stressors, and their interactions, needs to be considered in a study of air pollution effects on forests.

Despite, or perhaps because of, these difficulties, the scientists at the Symposium have displayed admirable ingenuity in addressing this issue. The diversity of questions in the West has been met with an equally diverse set of research approaches. Dendrochronologists have used tree-ring series to provide a long-term record of tree growth that pre-dates the advent of air pollution. Satellite and airborne spectrometers are being evaluated as tools to

Preceding page blank

efficiently quantify canopy condition over large areas. Research is proceeding to determine the mechanisms of tree response to stress.

Progress in these and other areas of research will improve our ability to evaluate forest condition, but is unlikely to significantly reduce the complexity of the task. A terrestrial analog of acid neutralizing capacity that will allow forests to be classified by a single number may never be found. Suites of measurements of forest parameters and of multiple stressors will be required and will be costly. So, the question remains, is it worth the effort?

The answer must be based on both the value of the resource and the perceived level of risk. The ecological, economic, and aesthetic values of western forests are beyond question. The papers in this volume demonstrate that some western forests are presently at risk from air pollution. However, to fully answer the question we need to look into the future. A Symposium paper on biodiversity points out that global climate change, another result of air pollution, could have major deleterious impacts on western forests. Continued rapid population increases in the West (roughly 1 million people per year), the United States, and the world as a whole make it likely that total emissions of greenhouse gases and other pollutants will increase. At the same time, this increased population guarantees greater economic pressures on these forests.

The policy changes and actions needed to prevent or mitigate these impacts are beyond the scope of this discussion. A review of the Symposium papers does, however, lead to two recommendations for research in support of policy decisions. The first is that implementation of a system for long-term monitoring of forest condition in the West is essential for supporting either effects research or regulatory policies. One-time surveys cannot provide sufficient information on status and trends in forest ecosystems.

Second, monitoring needs to be supplemented by an increased ability to predict trends. Because of the inertia inherent in both forests and potential stressors such as climate change, detection of forest responses may occur too late for effective prevention or mitigation. The ability to look toward the future is critical and currently lacking.

The tasks of learning how to monitor western forests and learning to predict changes are closely related, both requiring a good understanding of how western forests function and of the processes through which atmospheric stressors influence that functioning. The papers in these *Transactions* are part of the foundation on which this future research will be built. We anticipate that the information contained within this volume will serve those scientists who are beginning to take the next steps.

Richard K. Olson
NSI Technology Services Corporation
U.S. EPA Environmental Research Laboratory
Corvallis, Oregon

Allen S. Lefohn
A.S.L. and Associates
Helena, Montana

Editors, Symposium *Transactions*

Symposium Organizing Committee

Chairman, Technical Program Committee
George M. Hidy

Symposium Chairs
Richard K. Olson
Allen S. Lefohn

Session Chairs

Margi Böhm............... NSI/U.S. EPA Environmental Research Laboratory
Air Pollution Effects on Western Forests:
Atmospheric Deposition—Clouds

Lowell Ashbaugh.. California Air Resources Board
Air Pollution Effects on Western Forests:
Atmospheric Deposition—Wet

Allen S. Lefohn... A.S.L. and Associates
Air Pollution Effects on Western Forests:
Atmospheric Deposition—Gas/Dry

Donald Graybill .... University of Arizona
Air Pollution Effects on Western Forests:
Forest Condition and Trends I

Ken Stolte... National Park Service
Air Pollution Effects on Western Forests:
Forest Condition and Trends II

Robert C. Musselman .... U.S. Forest Service
Air Pollution Effects on Western Forests:
Growth and Physiological Mechanisms

Dan Binkley .... Colorado State University
Air Pollution Effects on Western Forests:
Soil Mediated Processes

Richard K. Olson..... NSI/U.S. EPA Environmental Research Laboratory
Air Pollution Effects on Western Forests:
State of Science, Overview

Logistical Support
Janet McFayden

ACKNOWLEDGMENTS

In addition to the Symposium Organizing Committee, credit for the success of the Symposium and this *Transactions* publication is owed to many people.
Hal Englund, Director of Publications for AWMA,
oversaw production of this volume.
Over 50 reviewers worked with the authors and session chairs to ensure the quality of all the papers presented at the Symposium.
Pris Hardin, Arlene Kovash and Julie Borden handled layout
and design for the *Transactions*, while
Penny Kellar and Perry Suk provided technical editing.
Charley Peterson and Roger Blair gave their approval
and support to these projects.
The Symposium was sponsored by
the Air and Waste Management Association,
U.S. Environmental Protection Agency, USDA Forest Service,
National Park Service, and California Air Resources Board.

Chapter One

Air Quality and Deposition: Clouds

Summertime Cloud Immersion Frequency at Elk Mountain, Wyoming	J.R. Snider and J.A. Garcia	3
Front Range Acidic Clouds and Precipitation	F. Parungo, C. Nagamoto, and B. Kopcewicz	15
Fog and Cloud Water Chemistry in Western Washington	F.A. Basabe, R.L. Edmonds W.L. Chang, and T.V. Larson	33
Airborne Chemical Measurements in Nighttime Stratus Clouds in the Los Angeles Basin	L.W. Richards	51
Cloud Chemistry and Occurrence in the Western United States: A Synopsis of Current Information	P.S. Muir and M. Böhm	73

Summertime Cloud Immersion Frequency at Elk Mountain, Wyoming

J.R. Snider[1] and J.A. Garcia[2]

[1] *Department of Atmospheric Science*
University of Wyoming
Laramie, Wyoming, 82071

[2] *Department of Physics*
University of Extremadura
Badajoz, Spain

INTRODUCTION

The immersion of subalpine and alpine forests in clouds and the accompanying deposition of the chemical constituents contained within cloud water is recognized as an important vector of acid and nutrient flux to these sensitive ecosystems.[1] Few studies of cloud occurrence have been conducted in the forest areas of the northern Rocky Mountains. Auer[2] monitored the frequency of orographic clouds with bases lower than the crestlines of the Medicine Bow, the Wind River, and the Big Horn Mountains and inferred cloud immersion frequencies of approximately 30% for the winter months. Recent emphasis has been placed on the determination of cloud immersion frequencies during the growing season.[3,4] In this report we examine data from which one can infer the frequency of late spring and summer cloud immersion events at Elk Mountain, Wyoming.

EXPERIMENTAL METHODS

Elk Mountain is located at the northern end of the Medicine Bow Mountains in southeastern Wyoming (Figure 1a). The Elk Mountain Observatory (EMO) is located 0.3 km east of a short N-S running ridge (Figure 1b). Two automated weather stations, operated during the summers of 1985 and 1988, were used in this study. The locations of these stations are shown in Figure 1b. During the 1985 study, data were collected at the ridge site (3.35 km MSL) between July 25 and September 5. During May, June, July, and August 1988 data were collected by a PAM-II weather station[5] (2.50 km MSL), which was located at the base of Elk Mountain.

Data acquisition was via satellite links to receiving stations located at Colorado State University (1985 data) and at the National Center for Atmospheric Science (1988). Transmitted data consisted of temperature (T), humidity (measured as a wet bulb temperature [T_{wb}] in 1988 or as relative humidity [RH] in 1985), wind speed and direction, and the sum of the diffuse (q) and the direct (Q) solar energy components as measured by a pyranometer (1988 data only). Approximately 25% of the 1985 data were lost due to problems at the satellite receiving station,[6] and 45% to 50% of the 1988 humidity data was not retrieved because of periods when the psychrometer was not supplied with water (Table I). Fifteen minute intervals were averaged and used to evaluate the presence of clouds. Cloud immersion frequency was calculated as the number of 15-min intervals divided by the total number of intervals in each data set.

Preceding page blank

The humicap hygrometer (Met One, Inc., Model 083C-1) used during 1985 was calibrated using relative humidity standards consisting of salt solutions. These calibrations indicated that the sensor was operating within the error tolerances quoted by the manufacturer (i.e., ±5%). Given observations of that accuracy, $RH > 95\%$ was taken as an indication of cloud immersion events. Some of these high humidity events may have been associated with precipitation from higher clouds.

The temperature and the humidity data from the PAM-II station were checked twice during the summer of 1988 using a portable psychrometer. The T and T_{wb} measurements from the two devices agreed to better than ±0.5° C. The dew point temperature (T_{dp}) was derived from measurements of T and T_{wb}.

We have inferred the 1988 cloud immersion frequency by evaluating the lifted condensation level (LCL) from the following formula.[7]

$$LCL = 122 \cdot (T-T_{dp}) \qquad [1]$$

where the dew point depression ($T-T_{dp}$) is expressed in degrees centigrade. The LCL (expressed in meters above the PAM-II site) is a good estimate of cloud base elevation resulting from adiabatic lifting of air originating from the measurement level. Cloud immersion is assumed to have resulted from LCL values lower than the summit elevation. Using Equation (1), a dew point depression of less than 7° C corresponds to a LCL lower than the summit of Elk Mountain.

Measurements of $(Q + q)$ were used as a secondary criterion for indicating the presence of clouds. The output of the pyranometer was normalized by the clear-sky response (i.e., $(Q + q)_{clear}$), and two conditions were used to specify the presence of mountain-top clouds: (1) $T-T_{dp} < 7°$ C, and (2) $(Q + q)/(Q + q)_{clear} < 0.5$. Although we have limited our evaluation of the 1988 data set to the daytime hours, both the daytime and the nighttime hours were included in the calculation of the 1988 cloud immersion frequency.

The methods we used for inferring the presence of mountain-top clouds were compared with measurements of cloud base elevation using pilot balloons, and with measurements of RH and cloud liquid water at EMO.[8] These wintertime studies have shown that measurements of RH at EMO and measurements of $T-T_d$ at PAM-II are reliable predictors of mountain-top cloud immersion events.

RESULTS

Analysis of the 1985 Observations

The histogram of cloud events shown in Figure 2 demonstrates that a majority of the cloud events occurred during daylight hours. This observation indicates that radiative cooling of the air to its dew-point temperature is not a dominant mechanism of cloud formation during the summers at Elk Mountain. The morning peak may be associated with forced lifting of air, while the afternoon peak is likely to be associated with convective activity.[9] The minimum in cloud frequency near 1400 MST is consistent with our observations of wintertime clouds at EMO.

As illustrated in Figure 3, relative humidities greater than 95% were associated with three episodes. All of these periods were coincident with or preceded by the occurrence of a frontal passage (the frontal events are indicated by vertical arrows in Figure 3). The typical weather patterns associated with these fronts consisted of a weak trough at the 500 millibar level and a surface low near the

Wyoming/Montana border. Weather systems that did not produce cloud events were displaced further to the north or were associated with weaker 500 millibar flow patterns.

The data shown in Figure 3 yield an average cloud immersion frequency of 3.0% during August and parts of July and September 1985.

Analysis of the 1988 Observations

Examples of the meteorological data collected in 1988 are shown in Figures 4a, 4b, and 4c. The figures illustrate post-frontal conditions following a late season snow storm (Figure 4a), a typical fair weather period in May (Figure 4b), and a cloud event during the evening of July 18 (Figure 4c). Time intervals corresponding to dew point depressions less than 7° C are also delineated. Although the measurements of $T\text{-}T_{dp}$ indicate that nighttime cloud events occurred more frequently than daytime events, evening drainage winds (i.e., wind direction from the east) are evident in Figures 4a and 4b. Because of such nocturnal winds, the dew point depression criteria is insufficient to diagnose mountain-top cloud events. Consequently, only daytime data were analyzed.

The wind data shown in Figure 4c are an exception to the observations shown in Figures 4a and 4b. The high wind speeds observed on the evening of July 18 were associated with a frontal system that passed the PAM-II station at -1800 MST. The high wind speeds and low dew point depressions that occurred subsequent to frontal passage indicate that the mountain summit was immersed in cloud throughout the evening of July 18 and part of the following morning. This conclusion is substantiated by our observations of stratiform orographic clouds on the mountains west and east of Laramie. The 7-h duration of this nocturnal cloud immersion event was comparable to all of the daytime cloud events detected in July 1988.

The results of our calculations, along with the data recovery percentages, are tabulated in Table I. The observed minimum in cloud frequency during July 1988 is corroborated by the paucity of precipitation at Rawlins, WY (1.9 km MSL). It is evident that more than 75% of the cloud exposure occurs in May and June. A comparable percentage of the precipitation at Rawlins also occurred during these months. Observations at Mt. Werner, CO, indicate a connection between the monsoon and midsummer cloud events.[6] In contrast, most of the cloud immersion events at Elk Mountain were observed to be associated with weak cyclonic frontal systems propagating from the northeastern Pacific Ocean. This difference stems from the fact that Elk Mountain is located to the north and to the east of the continental divide (Figure 1a) and is therefore isolated from the southwesterly flow associated with the monsoonal thunderstorms.

CONCLUSIONS

Average summertime cloud immersion frequencies of 3.0% and 2.7% were deduced for 1985 and 1988, respectively. Both averages are thought to be conservative because a significant portion of the 1985 data were collected in the drier-than-normal month of August, and because the 1988 cloud frequency was evaluated only from daytime measurements. It is of interest that cyclonic frontal systems are found to coincide with the cloud immersion events at Elk Mountain. Summertime cloud immersion frequencies at Mt. Werner, CO, appear to be a factor of two larger than our observations at Elk Mountain.[6] In view of the large year-to-year variability of monthly precipitation, it is likely that cloud frequencies have similar variability. Therefore, longer term measurements will be required for obtaining representative cloud frequency data and to better evaluate how comparable Mt. Warner and Elk Mountain are. The frequencies reported here are only estimates. It is also of interest that sites in the Appalachian Mountains experience cloud immersion during 35% to 60% of the year.[10,11] These values are estimated to be at least twice those of Elk Mountain.

ACKNOWLEDGMENTS

We are indebted to John Sheaffer (Colorado State University) who supplied us with the 1985 Elk Mountain weather data and to Gerry Albright and Cathy Irwin (National Center for Atmospheric Research) who installed the PAM-II weather station.

REFERENCES

1. G.M. Lovett, W.A. Reiners, and R.K. Olson, "Cloud droplet deposition in subalpine balsam fir forests: hydrological and chemical inputs," *Science*, 218:1303 (1982).
2. A. Auer, "Wyoming orographic cloud census, 1968-1969," Report to Wyoming Natural Resources Board, State Engineer's Office, 1969, 25pp.
3. Western Conifers Research Cooperative (WCRC), "1987 Research Plan," U.S. EPA, 1987, 84pp.
4. D.F. Miller and R.D. Borys, "Characterization of cloud chemistry and frequency of canopy exposure to clouds in the Rocky Mountains," Final Report prepared for U.S. EPA, Western Conifers Research Cooperative, 1988, 98pp.
5. F.V. Brock, G.H. Saum and S.R. Semmer, "Portable automated mesonet II," *J. Atmos. Oceanic Technol.* 3:573 (1986).
6. E.R. Reiter, J.D. Sheaffer, J.E. Bossert, R.C. Fleming, W.E. Clements, J.T. Lee, S. Barr, J.A. Archuleta and D.E. Hoard, "ROMPEX 85—The Rocky Mountain Peaks Experiment 1985: Preliminary Assessment," unpublished report, Colorado State University, Department of Atmospheric Science, For Collins, CO, 1986, 17pp.
7. J.V. Iribarne and W.L. Godson, *Atmospheric Thermodynamics*, Reidel, Dorrecht, Holland, 1981, 259pp.
8. J.R. Snider, *Measurement of Sulfur Dioxide Reaction Rates in Wintertime Orographic Clouds*, University of Wyoming dissertation, 1989, 350pp.
9. B.E. Martner, *Wyoming Climate Atlas*, University of Nebraska Press, Lincoln, NE, 1986, 432pp.
10. K.L. Rancourt and J.B. Howe, "On the distribution of acidity within clouds as a function of droplet size," *Mount Washington Observatory News Bulletin*, 28:48 (1987).
11. K.J. Olszyna, J.F. Meagher and E.M. Bailey, "Gas-phase, cloud and rain-water measurements of hydrogen peroxide at a high-elevation site," *Atmos. Environ.* 22: 1699 (1988).
12. National Climatic Data Center, *Climatological Data—Wyoming*, 94:5 (1985).
13. National Climatic Data Center, *Climatological Data—Wyoming*, 97:5 (1988).

Table I. Precipitation amount and cloud frequency in southeastern Wyoming.

	May	June	July	August
Rawlins, Wy[9] average ppt. ±1σ (mm/month)	30.7(±18.0)	21.1(±16.3)	17.3(±13.7)	19.0(±14.7)
Rawlins, Wy[12] 1985 ppt. (mm/month)	25.4	26.7	16.8	2.8
Rawlins, Wy[13] 1988 ppt. (mm/month)	20.1	25.9	2.5	14.0
Data Recovery[a] from PAM-II 1988 (%)	48.9	51.2	47.0	43.9
Cloud frequency[b] at Elk Mountain 1988 (%)	5.8	2.4	0.87	1.7

[a] Data Recovery represents the percentage of the study period when the PAM-II station was operational and when the psychrometer was filled with water.

[b] Cloud frequency was calculated from the fraction of the study period given by the Data Recovery percentage. Both day and nighttime hours were included in the normalization.

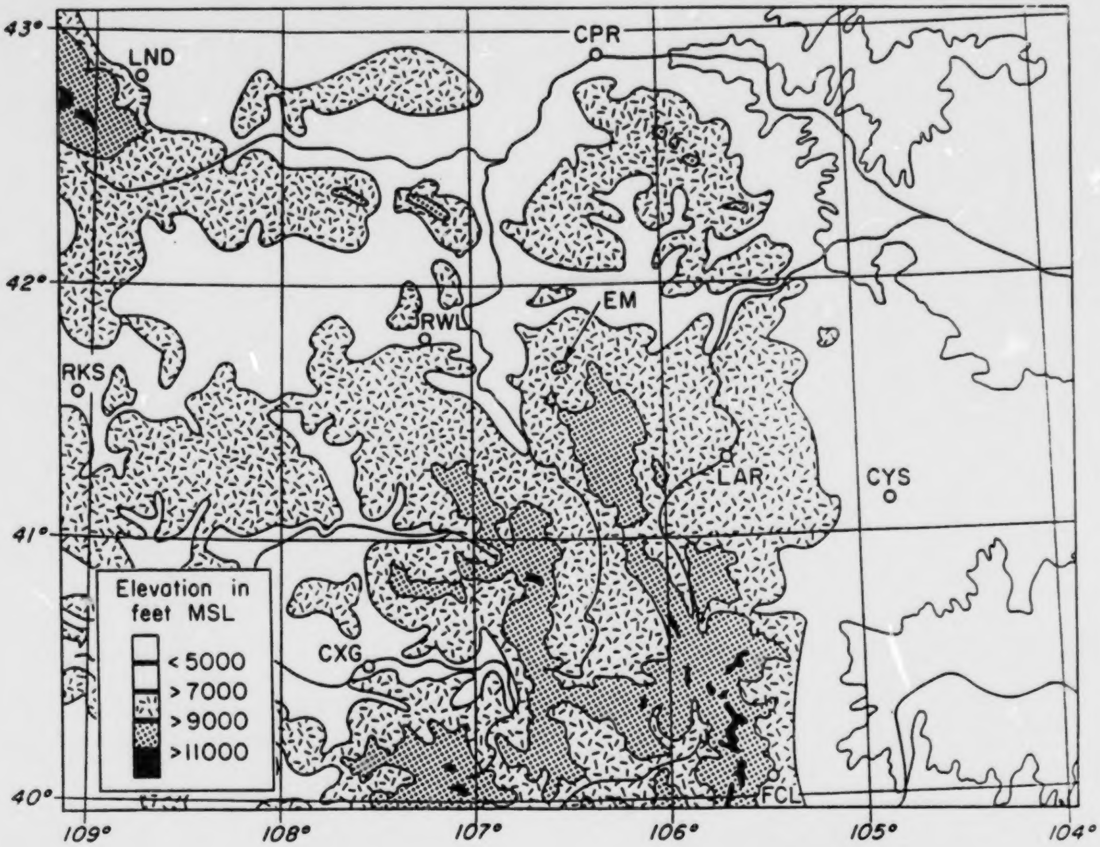
43°
42°
41°
40°
109°
108°
107°
106°
105°
104°
LND
CPR
EM
RWL
RKS
LAR
CYS
CXG
FCL
Elevation in feet MSL
< 5000
> 7000
> 9000
>11000

Figure 1a. Map illustrating the region in the vicinity of Elk Mountain (EM). The towns Craig (CXG), Fort Collins (FCL), Cheyenne (CYS), Laramie (LAR), Casper (CPR), Rawlins (RWL), Lander (LND) and Rock Springs (RKS) are labeled. The rivers (indicated by heavy lines) are the Yampa (at CXG), the South Platte (east of FCL), the Colorado (west of FCL), the Laramie (at LAR), the North Platte (east of RWL), and the Sweetwater (south of LND).

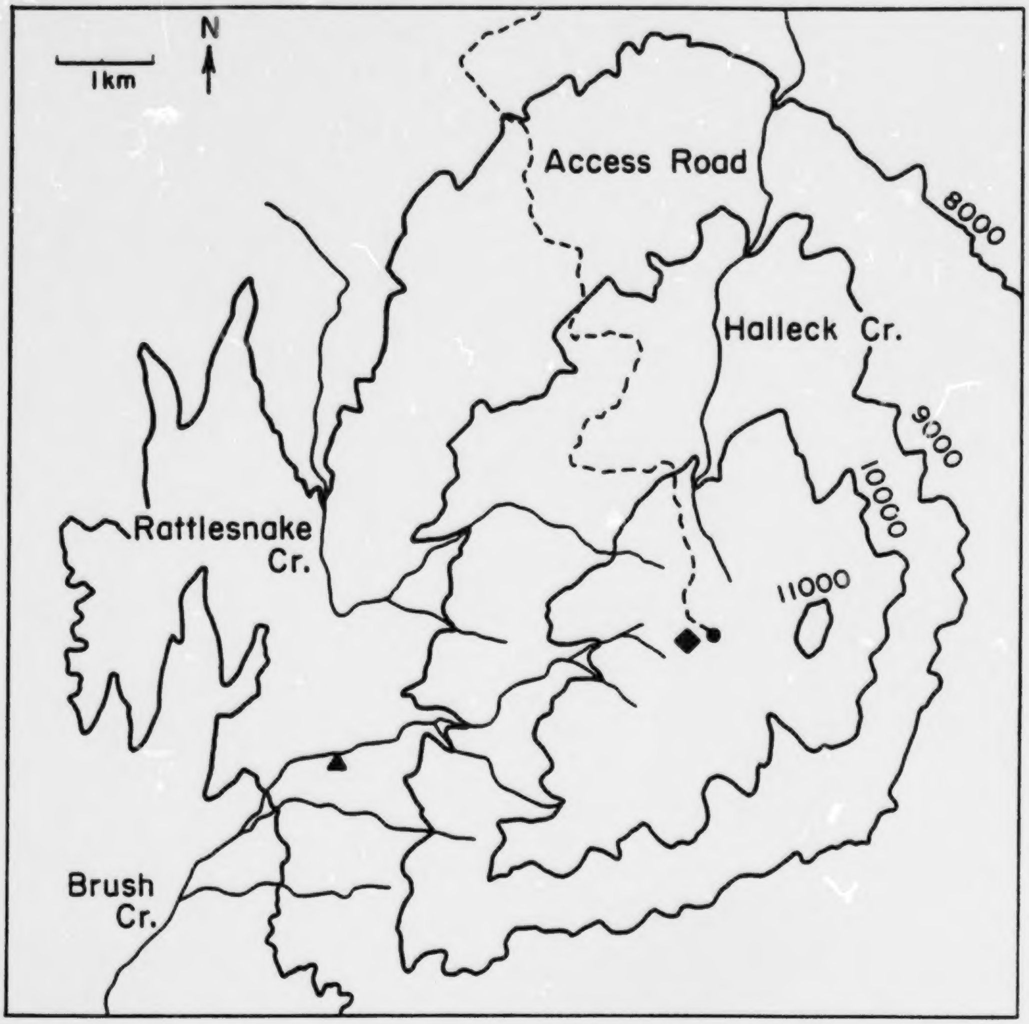
N
1km
Access Road
8000
Halleck Cr.
9000
10000
11000
Rattlesnake Cr.
Brush Cr.

Figure 1b. Detailed map illustrating the facilities at Elk Mountain. Measurements during the summer of 1985 were conducted on the ridge (◆) to the west of the Elk Mountain Observatory (●). The location of the PAM-II weather station is shown at the base of Elk Mountain (▲). Height contours are labeled in feet above sea level.

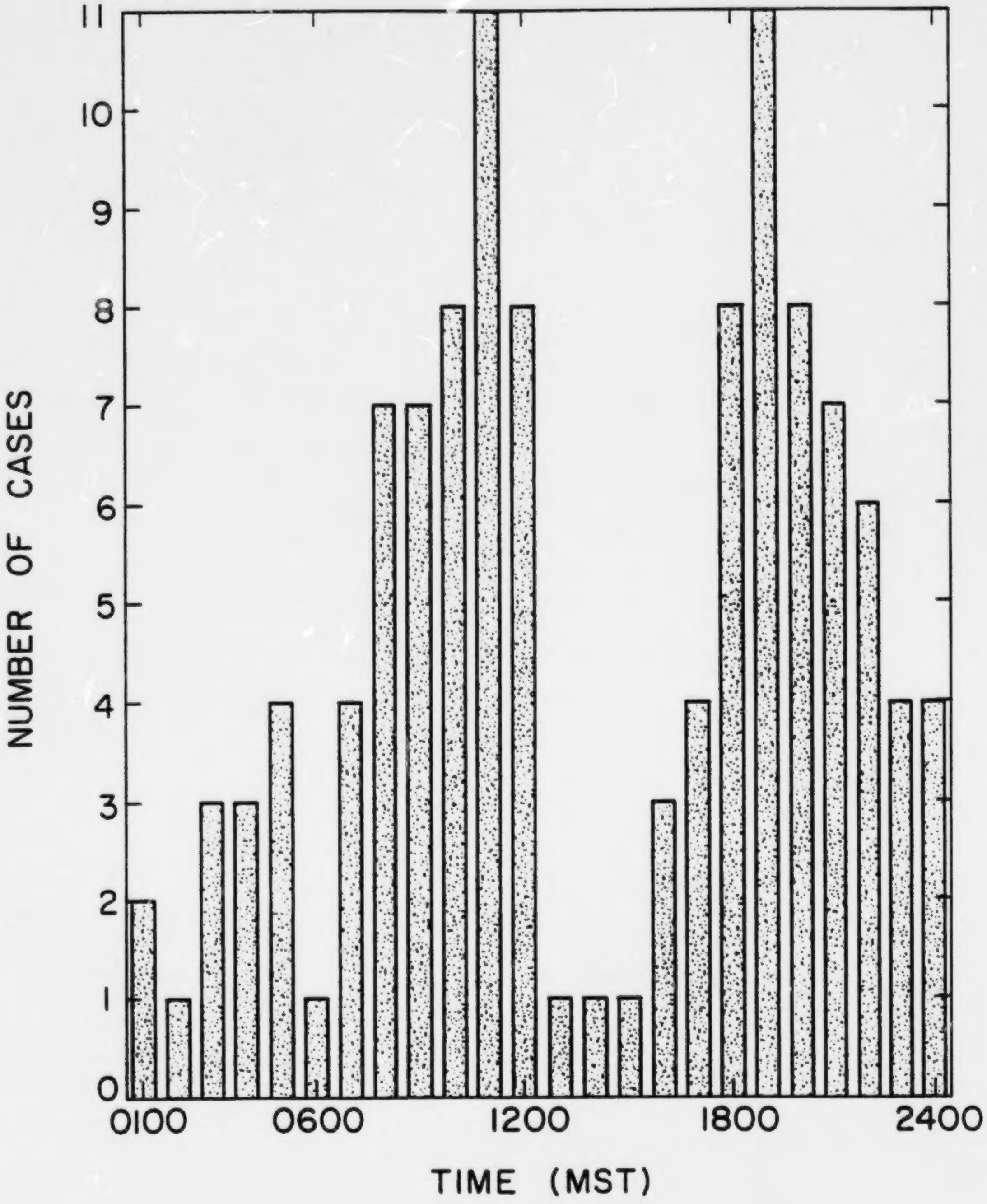

Figure 2. Histogram of cases (corresponding to 15-min averaging intervals) with RH values greater than 95%. Data were collected in the summer 1985.

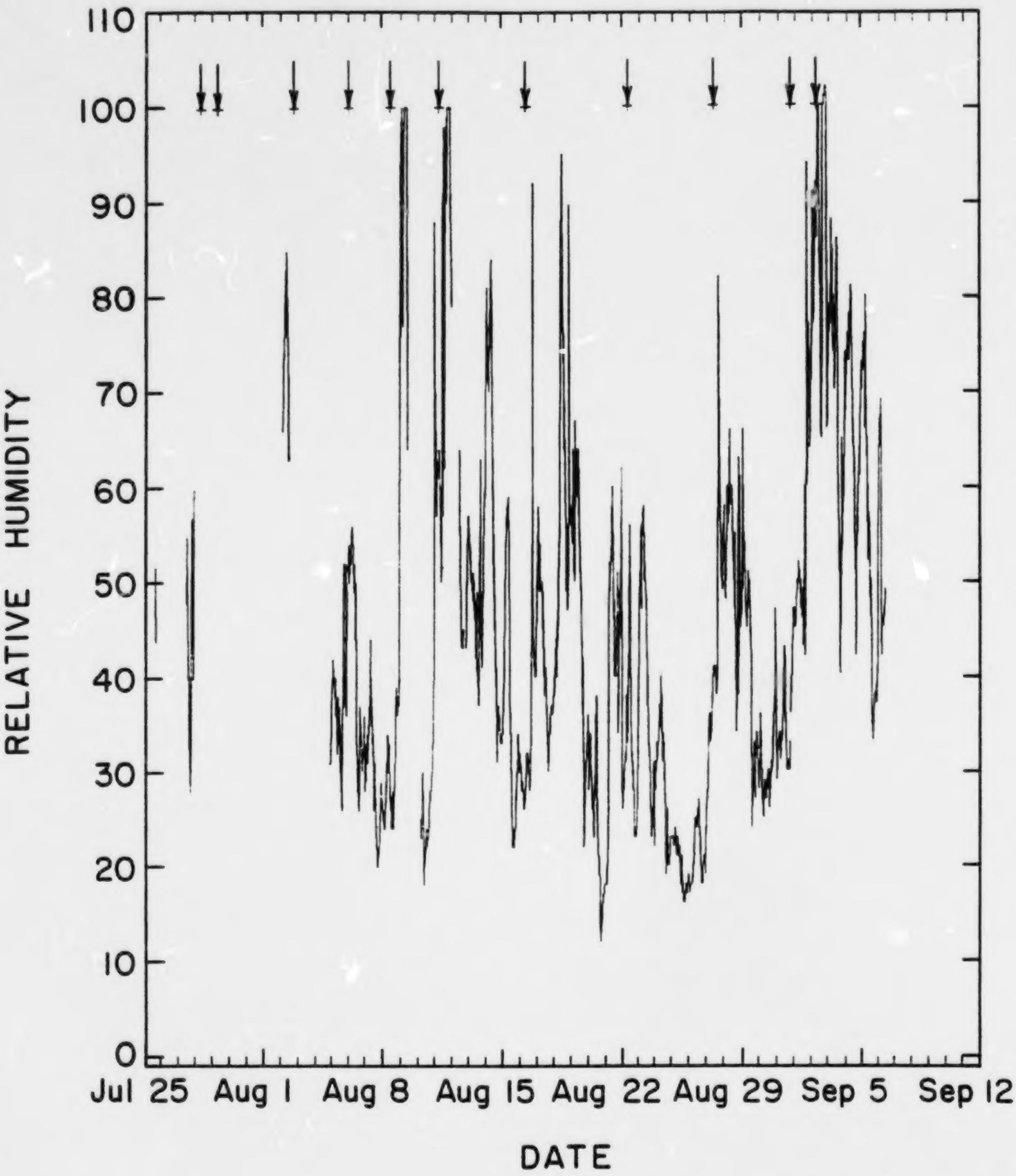

Figure 3. Time series of relative humidity during the summer of 1985. The occurrence of frontal passages are indicated by the vertical arrows at the top of the graph. Tic marks on the abscissa indicate local midnight.

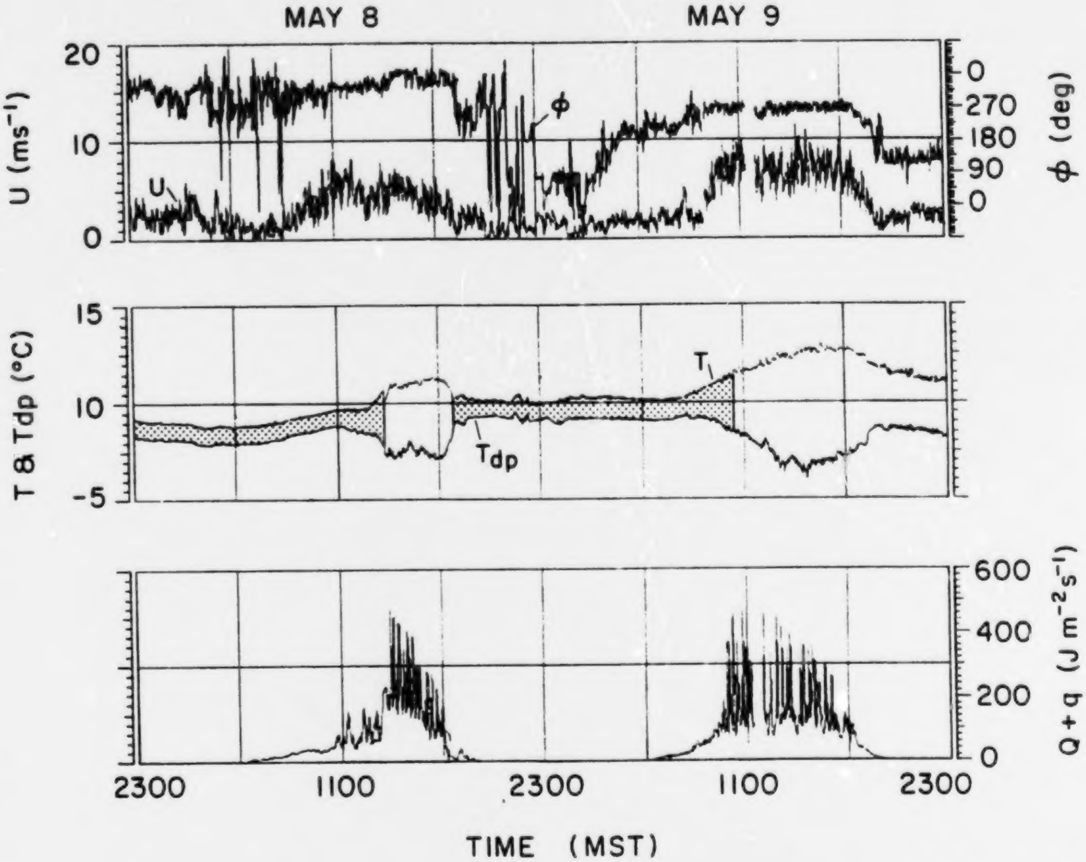

Figure 4a. Time series of wind speed (U) and wind direction (ø) (top panel), temperature (T) and dew point temperature (T_{dp}) (middle panel), and solar radiation (Q + q) (bottom panel). Data were collected at the PAM-II weather station, May 8 and 9, 1988. Dew point depressions ($T-T_{dp}$) less than 7° C are indicated by stippling.

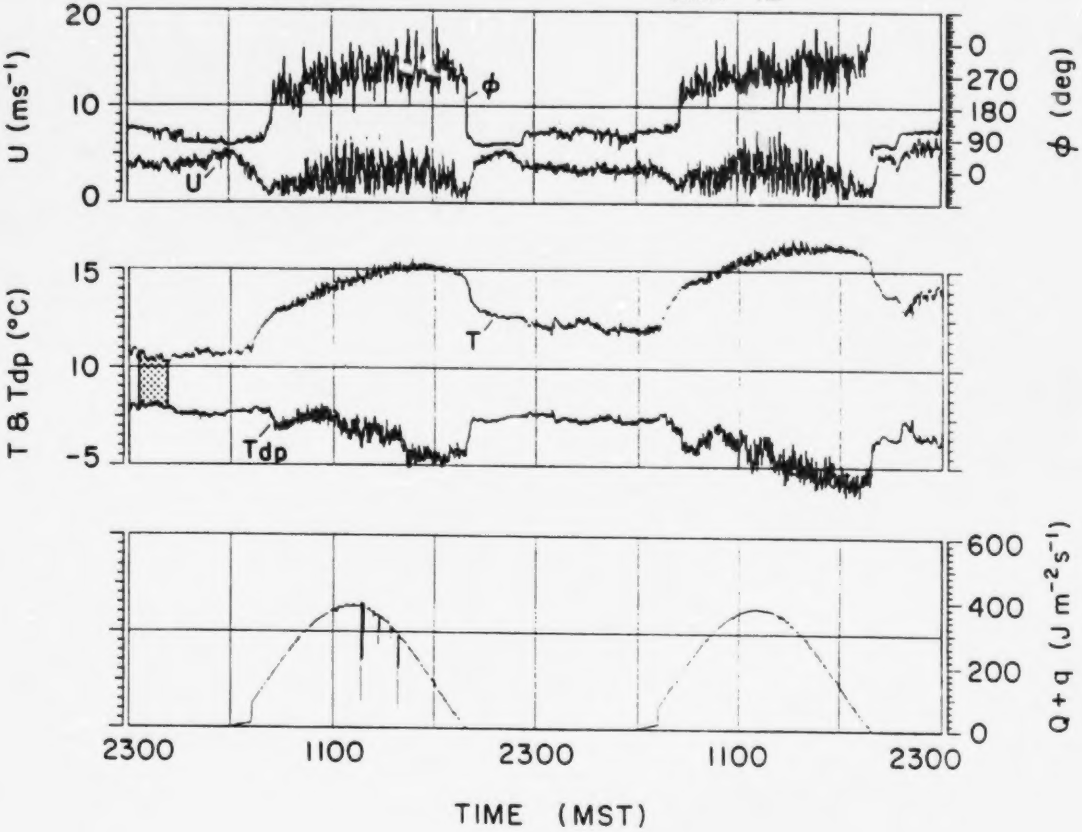

Figure 4b. Same as in Figure 4a with the exception that data were collected on May 11 and 12, 1988.

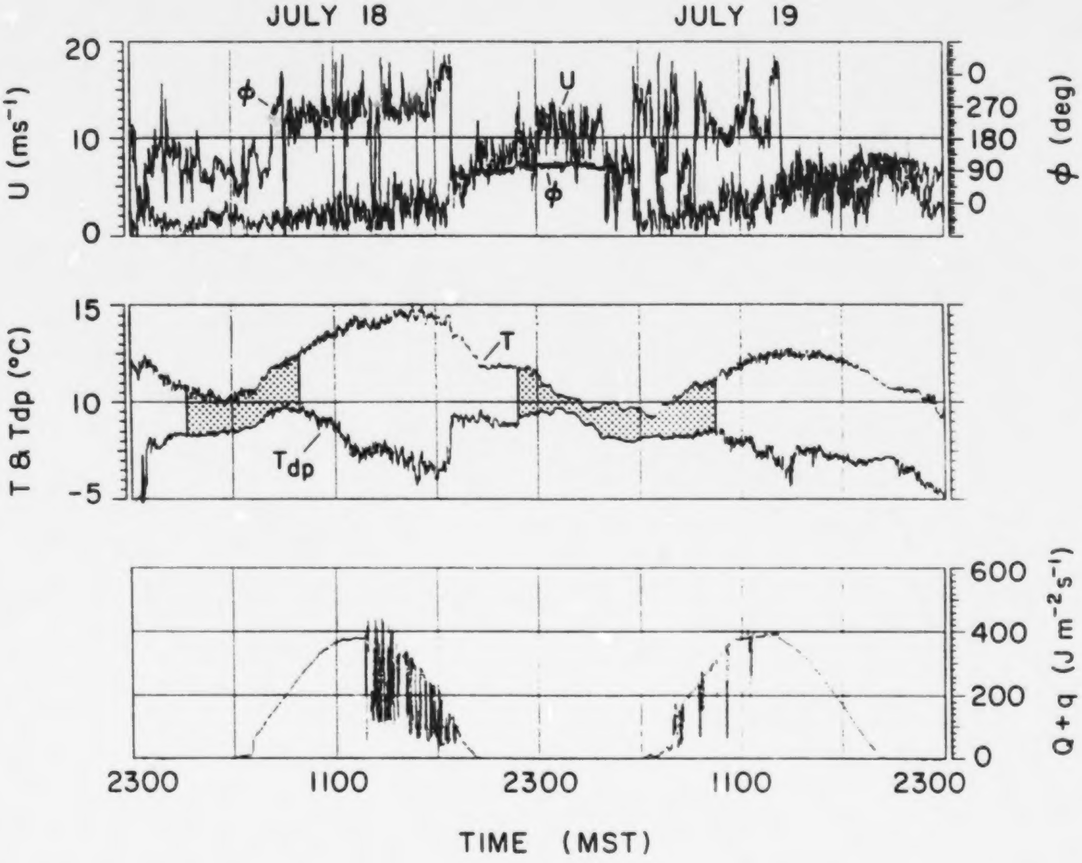

Figure 4c. Same as in Figure 4a with the exception that data were collected on July 18 and 19, 1988.

Front Range Acidic Clouds and Precipitation

Farn Parungo, Clarence Nagamoto, and Barbara Kopcewicz

Air Resources Laboratory, NOAA/ERL
Boulder, Colorado 80303

INTRODUCTION

We have investigated acidic clouds, precipitation, and air quality in the Front Range for the past decade. Our research focuses on the mechanisms of wet deposition of air pollutants and processes that incorporate pollutants into the precipitation system, from cloud condensation, to in-cloud scavenging, to below-cloud washout. The city of Denver and several smaller cities along the eastern foothills of the Rocky Mountains have a combined population of 2.5 million. The metropolitan air pollution is known as one of the worst in the nation and is often referred to as the "Denver brown cloud." The major sources are motor vehicles, space heating, power plants, oil refineries, and other industries. Besides common SO_2 and NO_x gases, particulate matter, CO, and O_3 are often present in concentrations exceeding the Primary National Ambient Air Quality Standards. The incorporation of these air pollutants into the hydrological system generally results in acidic cloud, acid rain, or acidic snow. The effect of acid deposition on local forests, lakes, and soil has caused increasing public concern. To improve our understanding of acid precipitation formation in this area, we collected samples of rain and snow, cloud drops and cloud water, cloud condensation nuclei, atmospheric aerosols, and soil to analyze the samples' chemical compositions. By comparing the chemistry of the samples, collected in the same storm system, one should be able to discern the stepwise incorporation of air pollutants into precipitation processes. However, most storms did not act as a stationary enclosed system. Thus, simultaneous or sequential samples might not represent the same air parcel. Furthermore, for aircraft safety, most cloud water samples and cloud drop replicas were collected on nonprecipitation days during nonstormy conditions. Thus, no direct temporal and spatial correspondence between chemistry of cloud water and precipitation was available. Because of these difficulties, we chose to focus our attention on the average chemical composition of all the samples in each class. We then compared these averages to investigate the general chemical modification in each process of precipitation.

METHODS OF SAMPLE COLLECTION AND ANALYSIS

Bulk Cloud Water

A cloud water collector developed by Parungo et al.[1] was installed in an aircraft to collect cloud water. The collector consisted of a stainless steel tube (1 m long and 0.6 cm in diameter) and a liquid-nitrogen cooling system. Just before the aircraft entered a warm cloud, liquid nitrogen was pumped into the tube to cool the tube surface to -10° C. Cloud drops that impacted the tube froze thereon. For most supercooled clouds, no liquid nitrogen cooling was necessary. As reported by Parungo et al.,[1] a wind tunnel test showed that the collector's efficiency was >60% for drop diameter between 2 and 50 μm with liquid water content ranging from 0.1 to 1.0 g/m^3. Laboratory tests showed freezing did not alter the pH of SO_2 or NO_2 solutions. Small pH changes (<5%) were observed for CO_2 or NO solutions. A Johnson-William Wire was used to measure liquid water content of clouds. The frozen cloud-water samples were melted in our laboratory and analyzed with an ion chromatograph (IC).

Individual Cloud Drops

An airborne cloud-drop replicator developed by Hallett[2] was used to collect cloud drops that impacted a Formvar-coated film, evaporated, and left replicas with solid residues enclosed. The sampled films were examined with a scanning electron microscope (SEM) for cloud-drop concentration and size distribution. An X-ray energy spectrometer (XES) was used to determine the elemental composition of the particles imbedded in the individual drops. Figure 1 shows examples of the micrographs of the collected cloud drops and the X-ray spectra of the particles in two drops. The peaks at certain KeV in the spectrum indicate the consisting elements. The peak heights reflect the quantity of the elements present. Because individual particles differ in matrix, quantitative analysis with this technique is not accurate. Cloud drops also were collected at ground level on the mountain slope with an impactor that replicates drops for individual drop analyses.

Cloud Condensation Nuclei

A continuous condensation nucleus counter developed by Langer[3] and modified by Rosinski et al.[4] was used to simulate cloud condensation on the ground level. Air samples containing aerosol particles were drawn into a chamber where the temperature was regulated between 10° and 20° C and supersaturation (SS) was kept at 1–2% (droplets grew very slowly to precipitable sizes if SS <1%). Cloud condensation nuclei (CCN) in the sample air stream nucleated water vapor, grew into ~50-µm-diameter droplets, and fell into a receiver at the bottom of the chamber. Gases and inactive aerosols followed the air stream, which made a right-angle turn and exited from the chamber. Cloud water samples that were nucleated by CCN and collected at the bottom of the chamber were analyzed with an IC and a pH meter.

Aerosol Samples

Bulk aerosol samples were collected on Teflon filters (Zefluor, 90-mm diameter, 1-µm pore, 99.9% collection efficiency for particles >0.3 µm). For every cubic meter of air sample, 1 mL of deionized water was used to extract the soluble aerosols. The solution simulated a cloud with liquid water content of 1 g/m^3 as described by Lazrus et al.[5] The ion concentrations and pH were measured. For precipitating clouds, LWC (Liquid Water Content) could be as high as 2 g/m^3. However, for nonprecipitating clouds, the LWC ranged between 0.1 and 1 g/m^3. To compare aerosol chemistry directly with cloud water chemistry or rain/snow chemistry, a normalized concentration should be applied in accordance with the measured cloud LWC.

Individual particle analysis was performed on Nuclepore filters that had a uniform background (47 mm diameter, 0.1 µm pore) with an SEM-XES system. Particles containing sulfate or nitrate were identified with morphological spot tests. Briefly, sulfate in a particle reacts with $BaCl_2$ that has been precoated on sampling substrate to form a characteristic hollow ring. Nitrate-containing particles react with a precoated Nitron ($C_{20}H_{16}N_4$) film to produce characteristic needles or fibers. Detailed procedures have been reported by Bigg et al.[6] and Mamane and Pena.[7]

Soil Samples

Soil samples (1 g), collected at various locations, were extracted with 100 mL of deionized water. More than 99.9% of the mass did not dissolve in water. The filtrates were analyzed with an IC and a pH meter.

Rain And Snow Samples

Bulk rain and snow samples were collected in Boulder with an automatic collector and analyzed with IC. Generally, one sample was taken for each short event. For prolonged events, one sample was taken in the morning, one in the afternoon, and one in the night. Individual snow crystals also were collected with a replicator, and the replicas were examined with an SEM for crystal sizes, structures, and riming states. The ice nuclei and scavenged particles in individual snow crystals were analyzed with an XES for elemental composition.

RESULTS AND DISCUSSION

Bulk Analyses

The bulk samples of cloud water, rain, snow, CCN solution, aerosol extract, and soil filtrate were analyzed for pH values and dominant cation and anion concentrations. Because CO_3^{2-} and organic anions were not measured, the total anion equivalence accounted for only 80–95% of the total cation equivalence in individual samples. The average ion concentrations in each class of samples are listed in Table I. Colorado lake water data were adapted from a report by Chappell et al.[8] The measurements show that the local soil and lakewater were alkaline (pH, ~8). The aerosols, which were mixtures of natural crustal dust and anthropogenic primary and secondary particulate matter, were slightly acidic (pH, ~6). The solutions of CCN collected at ground levels were also slightly acidic (pH, ~6). However, cloud-water samples that were collected in clouds were very acidic (pH, ~4). The clouds selected for investigation were generally big and thick. Liquid water contents, measured with a Johnson-William hot wire, ranged from 0.2 to 1.0 g/m^3 and averaged 0.5 g/m^3. If cloud drops consisted of only ground-level CCN and water, the pH and ion concentrations should be similar to those of the CCN solutions that simulated cloud water on the ground. The fact that genuine cloud samples had hydrogen ion concentrations two orders of magnitude greater than those of CCN and aerosols suggested that the acidity had increased tremendously during the updraft as reported by Tanner et al.[9] (1984) and after the formation of clouds, as reported by Lazrus et al.[5] and Rosinski et al.[4] This was in accordance with the measurements of SO_4^{2-} and NO_3^- concentrations in cloud-water samples that were, respectively, 3 and 34 times higher than in CCN. This indicates that most SO_4^{2-} and NO_3^- were probably incorporated by scavenging of atmospheric gases: SO_2 and HNO_3/NO_x either below clouds or in clouds.

Figure 2 shows the pH values for cloud-water samples collected in a stratiform cloud over eastern Colorado during one flight. It clearly illustrates that cloud water near the City of Denver (pH = 3.3) was more acidic than cloud water from further east (pH, 3.8–4.4). The measurements suggested that Denver air pollution contributed local acidic clouds.

Figure 3 shows the pH values for snow and rain samples collected in 1987. The results are similar to previous data[10] obtained between 1980 and 1986. Rain samples (pH, 4.79) in summer months were more acidic than snow samples (pH, 5.29) in winter months, and precipitation (pH, ~5) was less acidic than cloud water (pH, ~4). Figure 4 shows the variations of SO_4^{2-} and NO_3^- concentrations in 1987 precipitation samples. As in previous years, concentrations of SO_4^{2-} were higher in summer months than in winter months. The concentrations of NO_3^- had little discernible seasonal pattern. In prolonged storms, series (2 to 12) of sequential snow or rain samples were taken. The pH and ion concentrations fluctuated as the storms progressed. As discussed by Parungo et al.,[10] the precipitation chemistry depends not only on air and cloud chemistry but also on cloud microphysics, *exempli gratia*, precipitation rate, snow crystal structures, size and concentration, and the degree of riming. Therefore, it is important to investigate individual hydrometeors and aerosols.

Individual Aerosol Particles Analysis

The morphology of local atmospheric aerosols examined with SEM depicted irregular-shaped crustal dust, spherical flyash, Aitken nuclei (dia. < 0.2 μm), and well-structured pollen. The XES analysis showed that large particles (dia. > 1 μm) generally consisted of Si, Al, Ca, S, K, and/or Fe. The smaller particles primarily contained S, which often mixed with crustal components. The spot test on $BaCl_2$ substrate showed that 50% of the large particles were coated with a layer of SO_4^{2-} (Figure 5a) and 95% of the smaller particles contained SO_4^{2-} (Figure 5b). These hygroscopic particles are good CCN that can initiate clouds at condensation levels. The spot test on Nitron substrate showed few nitrate-containing particles (<5%) in dry air. However, when the relative humidity exceeded 70%, 80% of the particles were coated with nitrate on some occasions. Figure 5c shows the characteristic fiber morphology, indicating that nitrate reaction had taken place on the surface of a particle. Figure 5d shows an example of pollen, which appeared seasonally in the aerosols. Being hydrophobic, these particles could not serve as CCN for cloud formation.

Individual Cloud Drop Analysis

Cloud drop replicas collected with an airborne replicator were examined with an SEM. Size distributions of drop concentrations varied with time and location. Generally, in local clouds, one or more particles remained in every drop; presumably they had served as cloud condensation nuclei. The elemental compositions analyzed by XES showed that 90% of the nuclei contained Si and S, 75% contained Ca and Al, and 50% contained Fe and K. Other elements such as Mg, Zn, Ni, Mn, Pb, and Cu also appeared in a few percent of nuclei.

Figure 6a shows the cloud-drop replicas collected on the ground in a mountain town (Nederland, elevation 2.8 km) 60 km west of Denver. An orographic cloud was formed by up-slope flow from the east and persisted for hours. The individual cloud drops had pH values, measured with litmus paper, ranging from 3.5 to 4.0. Figure 6b shows an X-ray spectrum of CCN that had elemental compositions similar to those of samples collected in the aircraft. Figure 6c shows cloud drops that reacted with Nitron substrate, forming needle crystals as positive NO_3^- identification. Approximately 90% of the drops contained NO_3^-. Figure 6d shows positive SO_4^{2-} reaction with $BaCl_2$ substrate. Almost all the drops in this cloud contained SO_4^{2-}. The results indicate that the cloud drops were very acidic and highly contaminated with crustal dust, sulfate, and nitrate particles.

Individual Snow Crystal Analysis

On the basis of our observations, a schematic diagram (Figure 7) is fabricated to show the development of rain drops and snow crystals. Local cloud water is acidic (pH, ~4). Summer showers formed by coalescence of cloud drops are likely to be as acidic as cloud water. The chemistry of snow may differ from that of clouds, depending on the mechanisms of snow formation as discussed in the following.

Parungo and Weickmann[11] investigated local snow crystal growth for the past decade and observed that most snow developed by up-slope systems through condensation followed by freezing; that is, water vapor converts to liquid drops first, then freezes to frozen drops with the assistance of ice nuclei. At temperatures between -6° and -10° C and at water saturation, the frozen cloud drops are covered with a layer of quasi-liquid, which hinders diffusion growth to snow crystals but enhances conglomerating growth to graupel. Figure 8A shows the edge of a graupel specimen, the form of precipitation often found in the initial stage of a storm. Since graupel is a physical conglomeration of numerous frozen drops, the chemistry of the precipitation is similar to that of the generating clouds, which are acidic and contain high concentrations of SO_4^{2-} and NO_3^-.

At colder temperatures (-12° to -25° C), when moisture is above ice saturation but below water saturation, diffusion growth becomes the dominant mechanism in which water vapor is deposited on frozen drops and develops into hexagonal snow crystals. We have observed hexagonal columns, plates, sectors, and dendrites (crystal structures depend on temperatures and moisture fluxes) in most prolonged winter storms. Because a great number of water molecules deposited on the ice crystal during the growth, the contamination in the frozen drop is diluted. As a result, the acidity and the concentrations of ions in snowmelt samples are lower than the generating cloud-water samples. Figure 8B shows an example in which the center frozen drop contained particles and the outer diffusion-grown crystal was relatively clean.

During very cold temperatures and low humidity, we have observed snow crystals grown by the deposition mechanism in which water vapor is deposited on ice nuclei without passing through the liquid drop phase. Figure 8C shows an example of snow crystals collected at -25° C at night when ground cooling causes slight ice saturation. The ice nucleus is at the center of the crystal symmetry. Crystals like these generally have little contamination, and the pH of snowmelt is close to that of pure water.

In many orographic storm systems, the continuous updraft forms more new cloud layers. When the snow crystals fall into these layers, they capture the cloud drops and freeze them. Figure 8D shows an example of rimed crystals. The melted rimed crystal samples have the properties of both snow crystals and cloud drops. The heavier the riming, the more acidic and more contaminated the snowmelt sample. Borys et al.[12] made a similar observation in Steamboat Springs, CO.

A case study demonstrates the microphysical effect on precipitation chemistry. On January 5, 1988, up-slope flow developed a shallow orographic cloud, and snow began at noon. Graupel mixed with heavily rimed sectors was observed. The simultaneous bulk snow sample had a pH of 4.2, SO_4^{2-} of 0.92 mg/L, and NO_3^- of 4.75 mg/L. Samples collected in the evening, at night, and the next morning showed lightly rimed sectors and dendrites. The bulk snow samples all had a pH of 4.9. Concentrations were between 0.20 to 0.33 mg/L for SO_4^{2-} and between 1.55 to 1.72 mg/L for NO_3^-. In the late afternoon of January 6, when the snow was subsiding, the snow crystals were unrimed plates. The bulk snow sample had a pH of 6.0 and both SO_4^{2-} and NO_3^- concentrations were 0.10 mg/L. The case showed that precipitation chemistry depends on the development of individual hydrometeors.

Another case study demonstrates below-cloud scavenging. On February 21, 1988, a forest fire burned 200 acres of heavily wooded land in Sunshine Canyon, 10 km west of Boulder. The orange flame and brown smoke were visible in Boulder throughout the day and night. A dark cloud developed downwind east of the fire. At 10 a.m. the next day, intense snow, which had not been predicted by the weather services, was falling in Boulder but not in Denver. The snow halted the fire, and at noon precipitation stopped and left 5 cm of brownish snow on the ground. Figure 9 shows a snow crystal, collected in Boulder, that contains thousands of particles. It demonstrates that snow crystals were good collectors of atmospheric aerosols. The bulk sample had a pH of 6.7. The ion concentrations were as follows: SO_4^{2-}, 1.10 mg/L; NO_3^-, 0.82; Ca^{2+}, 5.42; Mg^{2+}, 0.51; K^+, 0.32; NH_4^+, 0.53; Na^+, 0.18; and Cl^-, 0.43. The data suggest that alkaline smoke particles were incorporated into the precipitation (soot and flyash are insoluble in water, and thus cannot be measured by IC). The clouds probably developed as a result of the fire, which heated the air mass and lifted it to condensation levels. The smoke particles may also have served as CCN to initiate the clouds and as ice nuclei to initiate the precipitation. This was probably a natural way to extinguish a forest fire and to clean up smoke in the air.

CONCLUSIONS

Our investigation has led to the following conclusions:

1. Front-range clouds are highly contaminated and very acidic (pH, ~4). The source of the acidity is Denver metropolitan air pollution. The acid clouds and fogs that very often cover the Rocky Mountain ranges and foothills can potentially damage the forests.

2. Precipitation samples (pH, ~5) show less acidity and lower SO_4^{2-} and NO_3^- concentrations than cloud-water samples. This is probably because diffusion growth dilutes the contamination.

3. Graupel formed by accretion of frozen drops is as acidic as the cloud drops. Rimed snow crystals have the combined properties of crystals and cloud drops. The heavier the riming, the more acidic the crystal, because snow crystals are generally less acidic than cloud drops.

4. Summer showers are generally more acidic and have greater concentrations of SO_4^{2-} than prolonged winter snow. In summer, photooxidation, which can convert SO_2 gas to SO_4^{2-} particles, is enhanced, and thus more SO_4^{2-} particles can serve as CCN and be incorporated into a cloud by cloudbase condensation. Summer months also produce higher concentrations of H_2O_2, which should enhance S(IV) to S(VI) conversion in the clouds. Since convective showers are developed by coalescence of clouds or melting of graupel with less diffusion growth, little dilution should occur. Therefore, the showers can be as acidic as the generating clouds.

5. Photochemical production of nitrate should also be enhanced in summer months. However, space heating in winter months may increase nitrate precursor gases (NO_x). As a result, little seasonal variation was observed.

6. Case studies demonstrated that precipitation chemistry is a function of both air chemistry and development of individual hydrometeors.

REFERENCES

1. F. Parungo, C. Nagamoto, I. Nolt, M. Mias, and E. Nickerson, "Chemical analysis of cloud water collected over Hawaii," *J. Geophys. Res.* 87:8805 (1982).

2. J. Hallett, "Measurement of size, concentration and structure of atmospheric particles by the airborne continuous particle replicator," Report AFGL-TR-76-0149, Desert Research Institute, Reno, NV, 1976, 92pp.

3. G. Langer, "Continuous condensation nucleus counter," *Proc. Internat. Conf. Cloud Physics*, Toronto, Amer. Meteor. Soc., 1968, p. 30.

4. J. Rosinski, B. Gandrud, C. Nagamoto, and F. Parungo, "Cumulative chemical composition of atmospheric cloud condensation nuclei," *J. Aerosol Sci.* 15:709 (1984).

5. A.L. Lazrus, P.L. Haagenson, G.L. Kok, B.J. Huebert, C.W. Kreitzberg, G.E. Likens, V.V. Mohnen, W.E. Wilson, and J.W. Winchester, "Acidity in air and water in a case of warm frontal precipitation," *Atmos. Environ.* 17:581 (1983).

6. E.K. Bigg, A. Ono, and T.A. William, "Chemical test for individual submicron aerosol particles," *Atmos. Environ.* 8:1 (1974).

7. Y. Mamane and R. de Pena, "A quantitative method for the detection of individual submicrometer size sulfate particles," *Atmos. Environ.* 12:68 (1978).

8. W.R. Chappell, R.R. Meglen, G.A. Swanson, L.A. Taylor, R.J. Sistko, R.B. McNelly, and R.W. Klusman, *Acidification Status of Colorado Lakes*, University of Colorado, 1985, 154pp.

9. R. Tanner, R. Kumar, and S. Johnson, "Vertical distribution of aerosol strong acid and sulfate in the atmosphere," *J. Geophys. Res.* 89:7149 (1984).

10. F. Parungo, C. Nagamoto, and R. Madel, "A study of the mechanisms of acid rain formation," *J. Atmos. Sci.* 44:3162 (1987).

11. F. Parungo and H. Weickmann, "Ice crystal growth at (-8 ± 2)° C," *J. Rech. Atmos.* 17:139 (1983).

12. R.D. Borys, P.J. Demott, and E.E. Hindman, "The significance of snow crystal and mountain-surface riming to the removal of atmospheric trace constituents from cold clouds," in *Precipitation Scavenging, Dry Deposition and Resuspension*, Vol. 1, Elsevier, New York, 1983, p. 181.

Table I. Ion concentrations (μg/g of water) and pH in samples collected in Colorado. n = number of samples; x = average concentration; σ = standard deviation; and – = insufficient data.

Statistic	Lake (n = 139)	Soil[a] (n=24)	Aerosols[b] (n = 21)	CCN (n=17)	Cloud water (n = 23)	Precipitation (n = 201)
SO_4^{2-}						
x	130	0.77	2.02	4.50	15.00	2.50
σ	624	0.30	1.31	3.22	6.0	1.60
NO_3^-						
x	–	0.48	2.68	0.22	7.41	1.83
σ		0.49	2.79	0.41	7.0	1.56
Cl^-						
x	8.10	0.28	0.59	2.4	2.40	0.47
σ	34.4	0.25	0.57	1.43	2.14	0.60
Na^+						
x	28.9	1.11	0.89	2.7	4.6	0.69
σ	102	1.03	0.99	1.34	2.7	0.50
NH_4^+						
x	–	0.28	1.98	0.92	1.90	0.86
σ		0.49	1.98	0.56	0.83	0.94
K^+						
x	3.32	0.86	0.19	–	0.92	0.19
σ	4.62	1.20	0.09		0.89	0.47
Ca^{2+}						
x	32.0	4.26	1.24	–	–	0.45
σ	49.3	2.84	0.84			0.55
Mg^{2+}						
x	21.0	0.51	0.11	–	–	0.06
σ	97.9	0.37	0.08			0.11
pH						
x	8.23	7.84	6.26	6.06	4.02	5.13
σ	0.80	1.23	0.51	0.33	0.46	0.73

[a] 1 g of soil extracted with 100 g of water.

[b] Aerosols in 1 m^3 air extracted with 1 g of water.

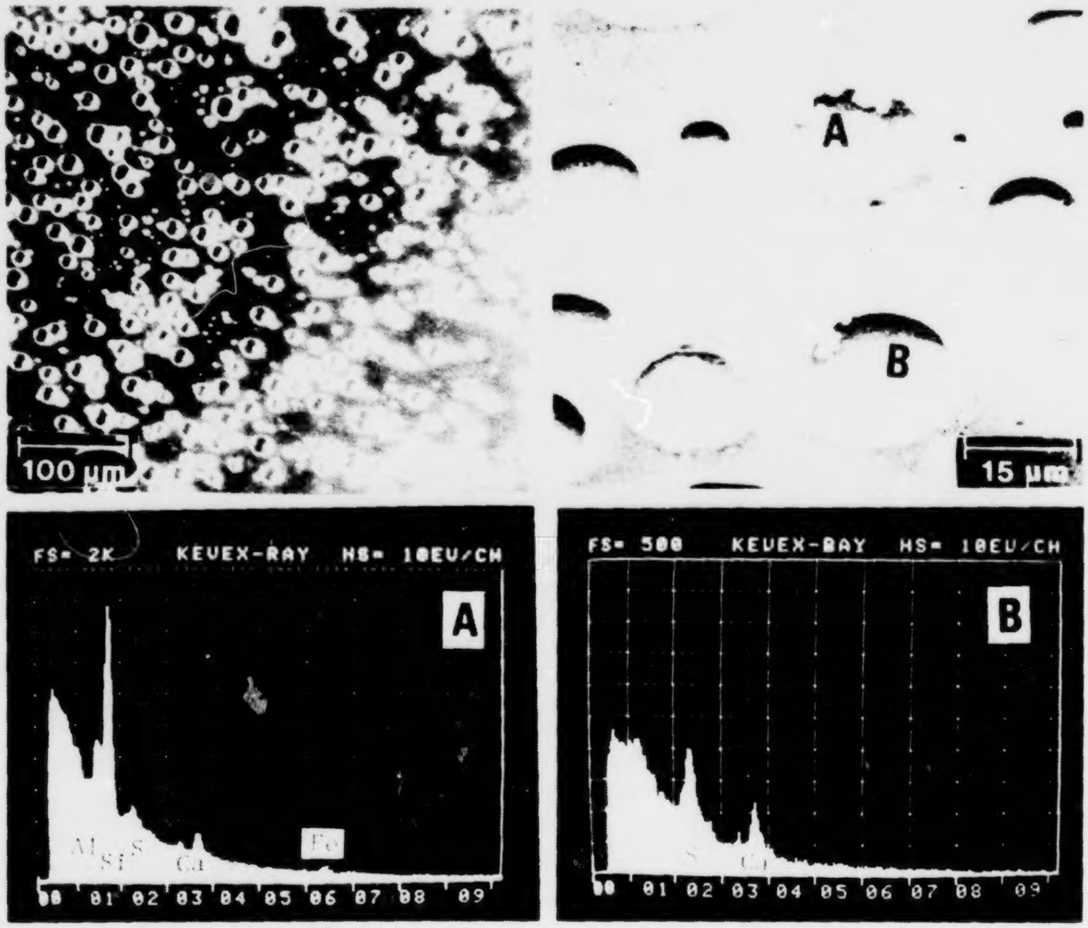

Figure 1. Micrographs of cloud drops and X-ray spectra of particles in two indicated drops.

Reproduced from best available copy.

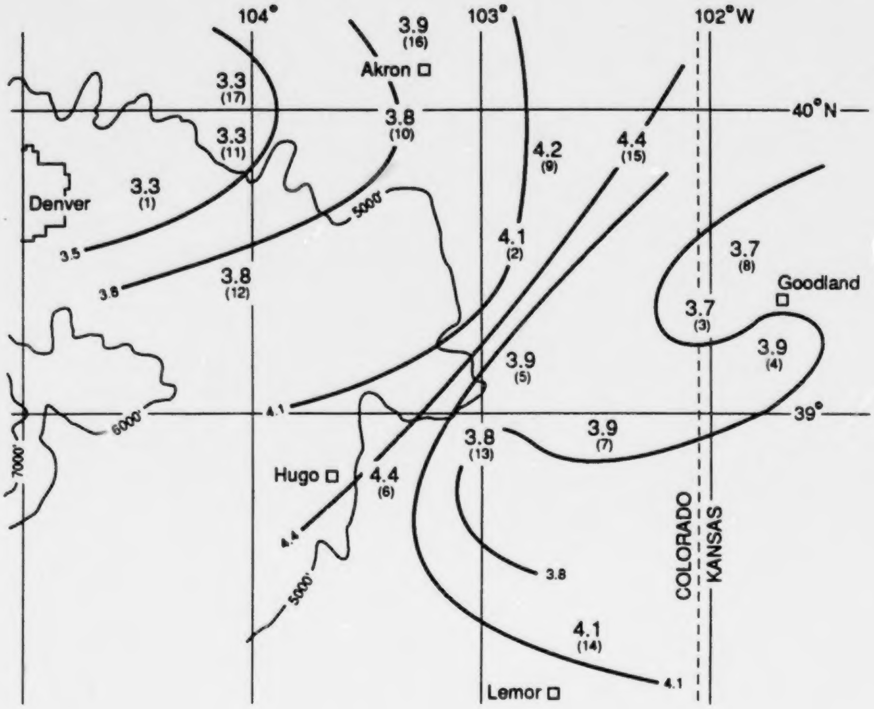
104°
3.9
(16)
103°
102°W
Akron
3.3
(17)
40°N
3.8
(10)
3.3
(11)
4.2
(9)
4.4
(15)
3.3
(1)
Denver
5000'
3.5
4.1
(2)
3.7
(8)
Goodland
3.8
3.8
(12)
3.7
(3)
3.9
(4)
3.9
(5)
6000'
4.1
39°
3.8
(13)
3.9
(7)
7000'
Hugo
4.4
(6)
4.4
COLORADO
KANSAS
3.8
5000'
4.1
(14)
4.1
Lemor

Figure 2. Cloud-water sample pH values collected at various locations. Sample sequence is indicated ( ).

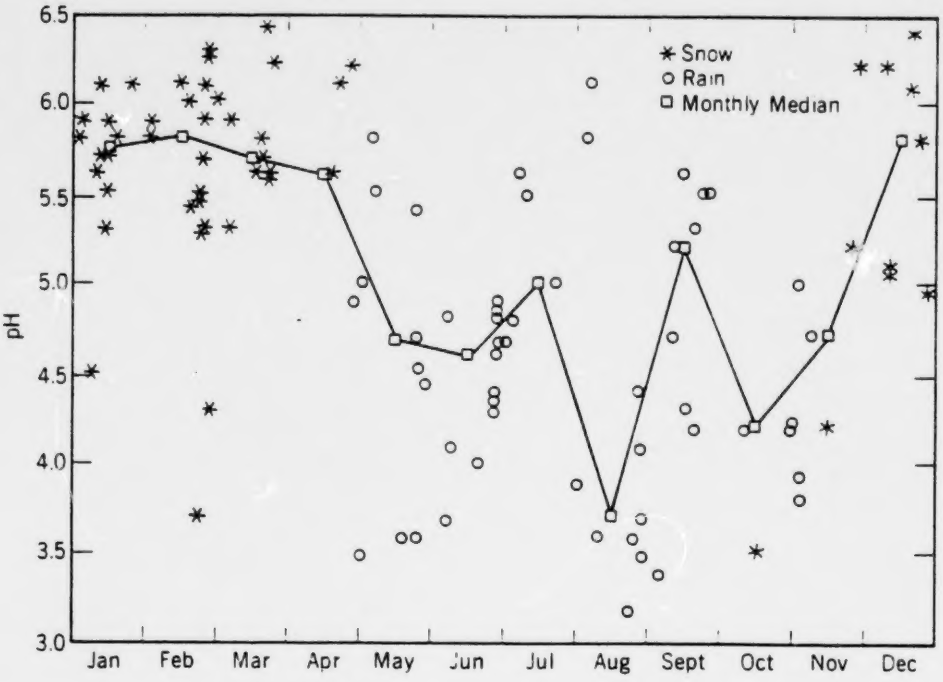

Figure 3. Snow and rain sample pH values in 1987.

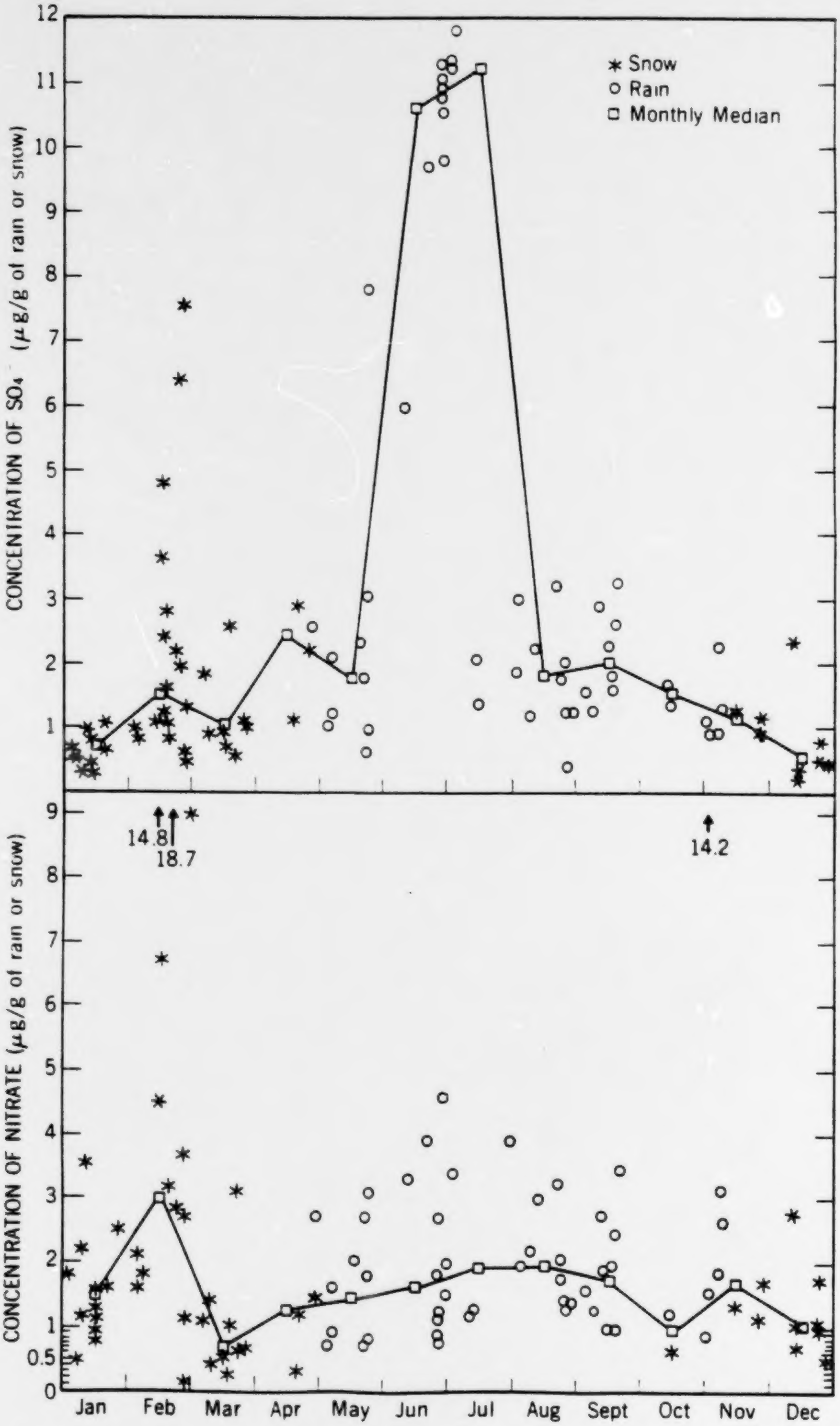

Figure 4. Concentrations of sulfate and nitrate ions in 1987 precipitation samples.

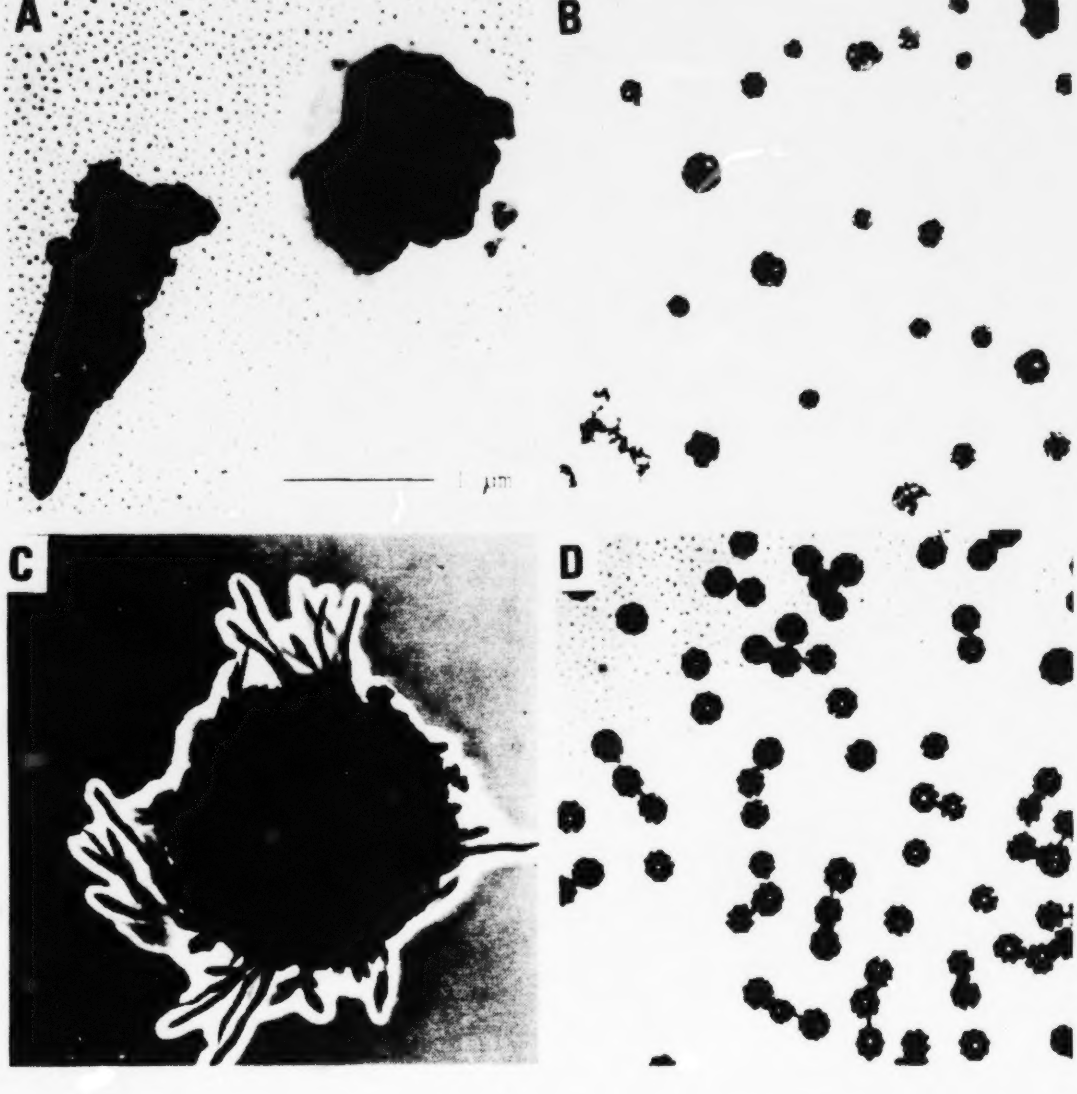

Figure 5. (A) and (B) Aerosol particles collected on $BaCl_2$-coated film. The hollow rings indicated that the particles contain SO_4^{2-}. (C) Particle collected on Nitron-coated film. The needle morphology indicates the presence of NO_3^-. (D) Pollen collected on $BaCl_2$-coated film.

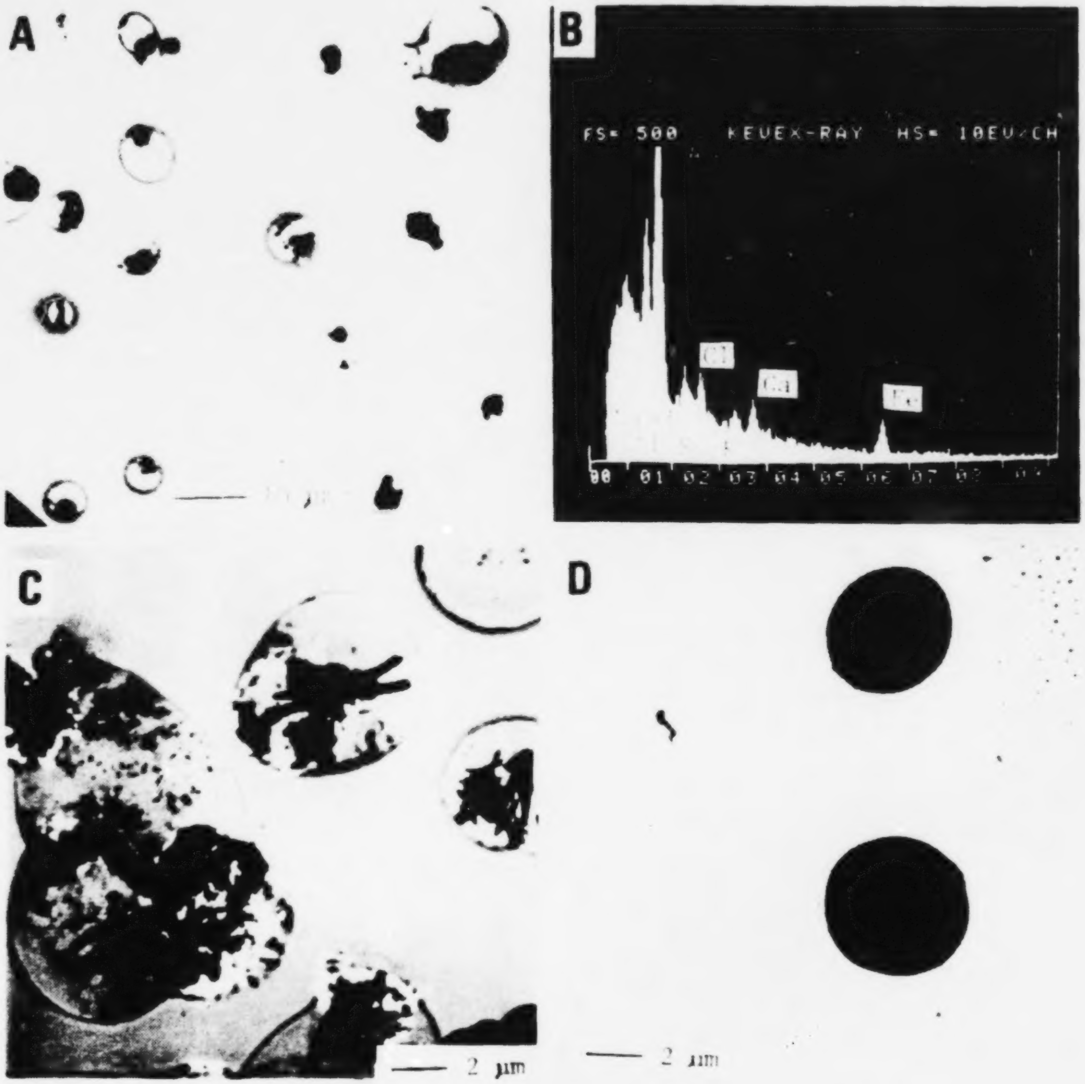
A
B
FS= 500 KEVEX-RAY HS= 10EV/CH
Cl
Ca
Fe
00 01 02 03 04 05 06 07 08
C
2 µm
D
2 µm

Figure 6. (A) Fog drops and enclosed CCN. (B) X-ray spectrum of a typical CCN. (C) Fog drops collected on Nitron-coated film indicate that most drops contained NO_3^-. (D) Fog drops collected on $BaCl_2$-coated film; hollow rings indicate drops containing SO_4^{2-}.

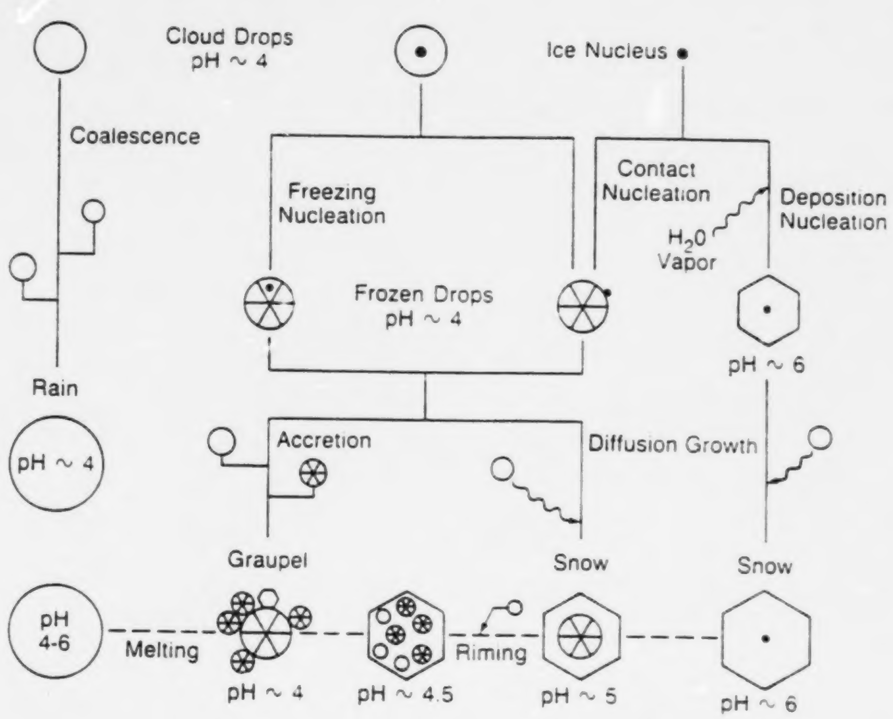
Cloud Drops
pH ~ 4
Ice Nucleus
Coalescence
Freezing
Nucleation
Contact
Nucleation
Deposition
Nucleation
H_2O
Vapor
Frozen Drops
pH ~ 4
pH ~ 6
Rain
pH ~ 4
Accretion
Diffusion Growth
Graupel
Snow
Snow
pH
4-6
Melting
Riming
pH ~ 4
pH ~ 4.5
pH ~ 5
pH ~ 6

Figure 7. Schematic diagram of hydrometeor developments.

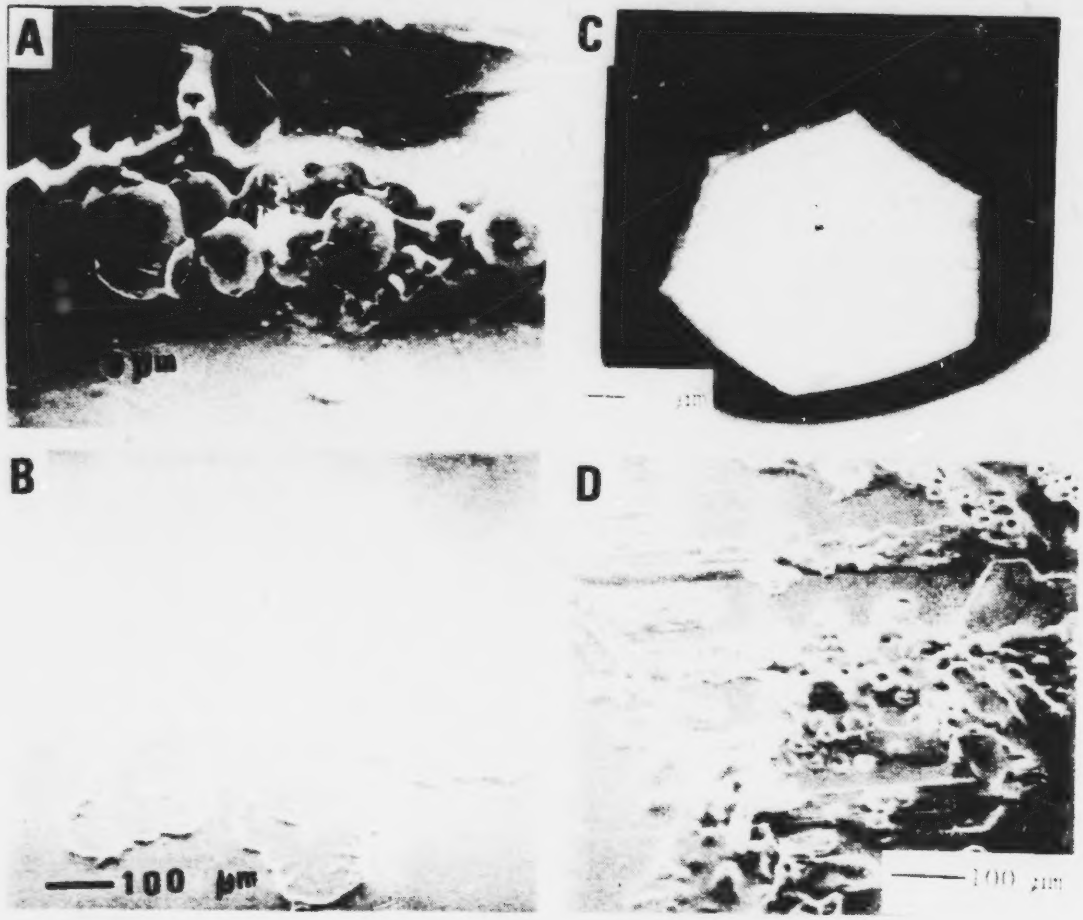

Figure 8. (A) Frozen drops at the edge of a graupel specimen. (B) Diffusion-grown ice crystal with a frozen drop at the center. (C) Deposition-grown ice crystal. (D) Snow crystal rimed with frozen drops.

Reproduced from best available copy.

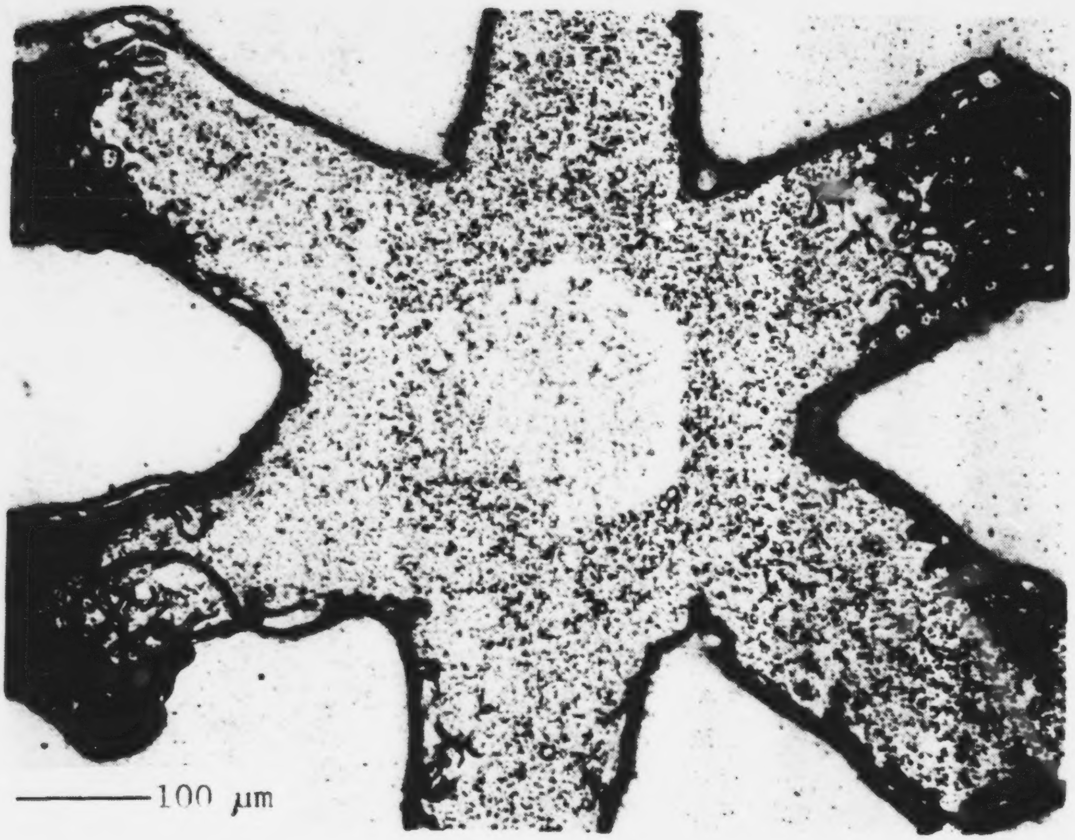

Figure 9. An example of ice crystals that collected numerous aerosol particles.

Fog and Cloudwater Chemistry in Western Washington

Felix A. Basabe,[1] Robert L. Edmonds,[1]
Wen Ling Chang,[2] and Timothy V. Larson[2]

[1] *College of Forest Resources,*
University of Washington,
Seattle, WA 98195

[2] *Department of Civil Engineering,*
University of Washington,
Seattle, WA 98195

INTRODUCTION

Acidic cloudwater deposition is a possible stressor in some forest regions, as evidenced by red spruce decline in the northeastern United States at elevations above cloud base.[1,2] In 1976, Castillo et al.[2] collected cloudwater with pH ranging from 3.5 to 5.0 at Whiteface Mtn., NY, and Van Valin et al.[3] reported mean pH values from 3.1 to 4.7 at the same site in 1987. Foliar leaching has been associated with exposure to acidic clouds that are downwind from anthropogenic sources.[2] Joslin et al.[1] found cation leaching from red spruce needles at Whitetop Mtn. in the southern Appalachians. Acid fog/clouds have also been sampled in the western United States. Waldman et al.[4] collected fog samples at a site 25 km northeast of Los Angeles and found pH levels ranging from 2.1–3.1. Low pH fog caused cation leaching from pine needles at this site.[5] Similar leaching effects were found in a controlled exposure of Douglas-fir seedlings to acidic cloudwater.[6]

In addition to pH, the potential effect of acid fog on forests is related to other factors. Red spruce seedlings showed reduced assimilation of CO_2 when exposed to sulfuric acid mist at pH 2.6, but increased assimilation with exposure to nitric acid mist at the same pH.[7] Increased N inputs, however, may not be beneficial. Excess NH_4^+ may increase cell death and decrease frost hardiness of plants, especially when the plants are exposed to strong acids.[8]

Clouds and fog are common in some montane forests of the Pacific Northwest during the growing season and at low elevations during winter and early spring. Over a six year period (1982–1987), some locations in the Washington Cascade Mountains that are downwind from major urban areas experienced 1 or more hours per day of surface clouds for 50 to 100 days during the growing season.[9] Results from a preliminary assessment of cloudwater chemical composition at Paradise Ranger Station on Mt. Rainier, WA, showed pH values ranging from 3.6 to 4.9.[10] This is up to 400 times the H^+ concentration of rainwater collected at the same location. The possibility of acidic cloud deposition in other forested areas in western Washington prompted the study described in this paper.

The objectives of this study were to: (1) characterize the chemical composition of fog and cloudwater in forested areas in western Washington; and (2) determine if site-to-site differences exist that may be due to anthropogenic factors.

Preceding page blank

METHODS

Twelve fog/cloudwater collection sites were established in western Washington in 1987 and 1988 (Figure 1, Table I). The sites represent the major forest types of western Washington, and they were chosen because of a known or potential high frequency of fog/cloud events.[9] The sites were located along a suspected pollution gradient from coastal Washington (clean site), across the Puget Sound lowlands (with anthropogenic pollutant sources), and into the Cascade Mountains. Local point sources of pollution were avoided. Active collectors were installed at four low-elevation sites to collect radiation fogwater. Active and/or passive collectors were placed at the other eight sites, located at higher elevations (450 to 1950 m).

Both collectors capture cloud droplets by impacting them onto 0.5 mm teflon monofilaments. The active collector, described by Daube et al.,[11] can collect cloudwater in stagnant to low wind events, and it excludes most raindrops at low wind speed. Under windy conditions, the active collector should be pointed into the wind for maximum efficiency; this is difficult during the gusty wind conditions that occur in high mountain areas. The passive collector is described by Falconer and Falconer.[12] Its collection efficiency is dependent on wind speed but is independent of wind direction. Raindrops are not excluded.

By definition, a cloud event began when horizontal visibility was less than 1 km. One or more hourly samples were taken for each event. Sampling was discontinued during rain or if horizontal visibility exceeded 1 km for more than 15 minutes. Prior to each event the monofilament teflon collection strands were rinsed with 100 ml distilled deionized water, and the rinse water was collected for analysis. The polyethylene sample bottles containing the samples were kept cold on site and were transported in a cooler with ice to the University of Washington laboratory as soon as possible after collection. Upon arrival, samples were weighed and pH measurements were taken on 2-5 ml aliquots at room temperature (usually within 24-h). The remaining sample was filtered through a 0.2 um Millipore filter, and then stored at 4° C until further analysis. Ammonium and anion analyses were conducted weekly, and cation analyses were conducted twice a month (Table II).

All laboratory analyses, with the exception of NH_4^+, were traceable to the National Bureau of Standards. Ten percent of the samples were reanalyzed to determine precision (Table III). The source of the relatively poor accuracy for K^+ is unknown but it is not of consequence since less than 3% of the total concentration of cations could be attributed to K^+. For all ions, each computerized data entry was checked against the original data forms for input error.

Samples were eliminated if: (1) the event had a single sample (to avoid analyzing events lasting less than one hour); (2) the ratio of total cation to anion equivalents was less than 0.5 or greater than 2.0; or (3) there was a significant calcium carbonate soil contamination (if the equivalent ratio of Ca^{2+} to the sum of Ca^{2+}, H^+, and NH_4^+ was greater than 0.2). These samples were not included in subsequent comparisons across sites. Dust contamination was a local site effect only. After data screening , only one event remained for Hurricane Ridge and Copper Ridge which excluded them from subsequent inter-site comparisons.

The hourly data were used to examine the relationships between H^+ and dominant acidic anion concentrations, and between sodium and chloride concentrations. To compare cloudwater concentrations at different sites, the event mean aqueous concentration was used. Some events had more hourly samples than others and thus would be heavily weighted in site-to-site comparisons. The arithmetic mean rather than a volume weighted mean was selected because the samplers did not collect a constant proportion of the total cloudwater volume over all events due to differences in local wind speed. Finally, vegetation exposure differences between sites are not characterized here because there is no generally accepted exposure index, such as total hours of exposure, total number of hours above a given concentration, or frequency of wetting and drying cycles at the tree surface.

RESULTS

Most cloud events at mountain sites were sampled in the summer after snowmelt, with the majority of samples collected at Stampede Pass, Cheeka Peak and Burley Mountain (Table IV). These three sites also had the longest events (longer than 15 h). With the exception of Paradise, where less than half of the events were sampled, nearly all the events that occurred at the other mountain sites were sampled. The above four sites are historically very cloudy compared to the other locations.[9]

Active and passive cloudwater collector comparison tests were conducted in August, 1988 at Cheeka Peak and Burley Mtn. The collectors did not sample the same volume of cloudwater, but there was a good relationship between collectors in chemical composition (Table V). On the basis of these results, data from active and passive samplers were combined.

Of the mountain cloud samples, 20% failed the screening procedure. Most of these samples were from Cheeka Peak and they failed because of the Ca^{2+} screening criteria. Only seven samples failed the charge balance criteria.

All samples collected from the mountain sites were acidic (pH 3.1–5.9). Figure 2 summarizes the average event mean concentration of each species at these sites. Because this figure does not have confidence limits, it should not be used to make conclusions about site-to-site differences. A one-way analysis of variance (ANOVA) was used to analyze event variability of 44 events: Cheeka Peak (13 events, 128 samples), Stampede Pass (25 events, 128 samples) and Burley Mtn. (6 events, 26 samples). The variability of H^+, NH_4^+, NO_3^-, and SO_4^{2-} in cloudwater from these three sites was significantly greater between events than within events ($p < 0.0002$).

There was no statistical relationship between concentration of any of the acidic species and sample volume, regardless of wind direction during a given event. However, using hourly sample data from Cheeka Peak, Stampede Pass, and Burley Mtn. there was a strong relationship between H^+ concentration and NO_3^- plus non-sea-salt (n.s.s.) SO_4^{2-} (Figure 3). This relationship improved if the NH_4^+ concentration was added to the H^+ concentration. Data from other high-elevation sites not shown in Figure 3 have similar relationships. In addition, there was a strong association between Na^+ and Cl^- concentrations due to the influence of sea spray (Figure 3). Using either Cl^- or Na^+ concentrations resulted in a difference of less than 1% in the sea salt correction for SO_4^{2-}.

Event means for H^+, NH_4^+, NO_3^-, and n.s.s. SO_4^{2-} for Cheeka Peak, Stampede Pass, Burley Mtn., Paradise, Sunrise, and Cascade Pass are shown in Figure 4.

Nearly all events shown occurred in the summer or early fall. Although hundreds of samples were collected at these sites, an event at one site did not usually coincide in time with an event at another site, a result consistent with records of cloud frequency at these sites.[9] Figure 4 also shows pair-wise comparisons based on a one-way ANOVA for each ionic species. Tukey's multiple comparison tests show that Cheeka Peak had significantly lower average concentrations of H^+, NH_4^+, NO_3^-, and n.s.s. SO_4^{2-} than did Stampede Pass ($p < 0.05$). In addition, cloudwater from Cheeka Peak was significantly lower in NH_4^+ than the sites southwest of the greater Seattle area, and n.s.s. SO_4^{2-} was higher at Paradise compared to Cheeka Peak and Cascade Pass ($p < 0.05$).

The extent to which air mass trajectory influences site-to-site and event-to-event variability in the mean concentration of H^+, NH_4^+, NO_3^-, and n.s.s. SO_4^{2-} was also examined using 850 mb maps and interpolated isobaric trajectories. Table VI summarizes the event means for these dominant acidic species by wind direction at Cheeka Peak and Stampede Pass. The other sites did not have a sufficient number of events to capture all wind directions. A two-way ANOVA revealed substantial effects of both site and wind direction for all four acidic species . Relatively lower concentrations of H^+, NH_4^+, NO_3^-, and n.s.s. SO_4^{2-} were observed at Cheeka Peak compared to Stampede Pass. When the winds were from the northwest concentrations of these acidic ions were higher at both locations than when the winds were from the west and southwest combined. There was an interaction between site and wind direction only for NH_4^+.

The low-elevation radiation fog sites at Everson, Marblemount, and the University of Washington operated during the winter (see Table IV). Relatively few events were collected at these sites. Figure 5 shows the mean values of the major ionic species at the low-elevation sites, including the Hoh River (sampled during the growing season). The pH values ranged from 4.1 to 7.0 at these sites. There were large amounts of NH_4^+ and small amounts of H^+ in these samples compared with the high elevation sites. Many low-elevation events consisted of single samples, most of which would not pass the ionic charge screening. Therefore, low-elevation samples were not screened prior to analysis. An unpaired t-test of event means should reveal that the average NH_4^+ concentration at low-elevation sites was higher than the average at the mountain sites ($p < 0.0001$), while H^+ concentrations were lower ($p < 0.03$).

DISCUSSION

This study represents the most complete characterization of summer and fall mountain cloud chemistry in western Washington to date, and confirms preliminary observations of relatively acidic cloudwater at Paradise Ranger Station on Mt. Rainier in 1987.[10] Cloudwater pH values less than 4.0 are relatively common in montane forests downwind from major developed areas in the Puget Sound Region of western Washington. Substantially more acidic events were observed than Weathers et al.[13] reported for Marys Peak (1249 m msl) in the Oregon coast range.

The observed ionic compositions of cloudwater are similar to those reported from California, the Midwest, and the northeastern United States.[14-17] However, the extreme pH values (<2.5) reported elsewhere in California and the northeastern United States were not found here.[15,17] Comparison of the present results to six recent studies reporting cloudwater chemical composition from the eastern and western United States is possible because the same type of cloudwater collectors were used with similar sampling protocols, and collections were made during the same time of year as the other studies.[1,3,5,13,17,18]

Substantially higher concentrations of acidic species were found at several high-elevation sites located in the Cascades southeast of Seattle than at Cheeka Peak, a relatively remote site on the Pacific coast. At Cheeka Peak and Stampede Pass, two sites with sufficient samples to analyze the relationship between species concentration and wind direction, there were significant differences for both location and wind direction, and an interaction between these two variables for NH_4^+. These results are consistent with the general location of the anthropogenic sources of NH_4^+ relative to these two sites. When the wind was from the west and southwest, there was a significantly higher concentration at Stampede Pass downwind of several urban areas than there was at Cheeka Peak, upwind of these same areas. When the wind was from the north or northwest, the upwind/downwind difference increased, suggesting that areas to the north and west of Stampede Pass were major contributors of NH_4^+ in the cloudwater.

The primary difference between the low-and high-elevation cloud and fogwater samples is that NH_4^+ was significantly higher in low-elevation radiation fog ($p < 0.0001$) and H^+ was higher in mountain clouds ($p < 0.03$). This observation is consistent with data reported from other sites in the United States.[14-17] The low-elevation sites were in areas where the locally originated radiation fog might be enriched from agricultural sources. We are not sure if the differences between the low-and high-elevation sites represent a site effect or a seasonal effect. The poor charge balance in the high pH samples collected at low elevations was probably due to high concentrations of bicarbonate ion, an ionic species that was not measured in this study.

CONCLUSIONS

Regional cloudwater chemistry in western Washington indicates anthropogenic enhancement of ionic concentrations in clouds collected downwind from developed areas in the Puget Sound. Low-elevation radiation fogwater composition was generally less acidic than mountain clouds. There was considerably more NH_4^+ in low-elevation fog compared mountain clouds. In general the mountain clouds in the Olympic Peninsula and North Cascades were less acidic than mountain clouds southeast of the greater Seattle area.

REFERENCES

1. J.D. Joslin, C. McDuffie, and P.F. Brewer, "Acidic cloud water and cation loss from red spruce foliage,"*Water, Air and Soil Pollut.* 39:355 (1988).

2. R.A. Castillo, J.E. Jiusto, and E. McLaren, "The pH and ionic composition of stratiform cloud water," *Atmos. Environ.* 17(8):1497 (1983).

3. C.C. Van Valin, D.L. Wellman, and L.P. Stearns, "Aerosol and cloudwater properties at Whiteface Mountain, New York," *Water, Air and Soil Pollut.* 34:369 (1987).

4. J.M. Waldman, J.W. Munger, D.J. Jacob, and M. R. Hoffmann, "Chemical characterization of stratus cloudwater and its role as a vector for pollutant deposition in a Los Angeles pine forest," *Tellus* 37B:91 (1985).

5. J.M. Waldman and M.R. Hoffmann, "Nutrient leaching from pine needles impacted by acid fog," *Water, Air and Soil Pollut.* 37:193 (1988).

6. D.P. Turner and D.T. Tingey, "Foliar leaching and root uptake of Ca, Mg, and K in relation to acid fog effects on conifers," *Bull. Ecol. Soc. Amer.* 69(2):324 (1988).

7. J. Jacobson and J. Lassoie, "Test of the nitrogen fertilization hypothesis of red spruce decline," Project Status Reports, Forest Response Program Annual Meeting, Feb. 22-26, 1988, Corpus Christi, TX. Volume 1:141.

8. B. Nihlgard, "The ammonium hypothesis—an additional explanation for the forest dieback in Europe," *Ambio.* 14:2 (1985).

9. F.A. Basabe, "Fog frequency in Pacific Northwest forests," Report to Western Conifers Research Cooperative, EPA, Corvallis, OR., Nov. 1988.

10. F.A. Basabe, R.L. Edmonds, and T.V. Larson, "Ozone levels and fog chemistry in forested areas in Western Washington," Proceedings, *Thirty-fifth Annual Western International Forest Disease Work Conference.*, Nanaimo, British Columbia, Aug. 18-21, 1987.

11. B. Daube, Jr., K.D. Kimball, P.A. Lamar, and K.C. Weathers, "Two new ground-level cloud water sampler designs which reduce rain contamination," *Atmos. Environ.* 21(4):893 (1987).

12. R.E. Falconer and P.D. Falconer, "Determination of cloud water acidity at a mountain observatory in the Adirondack Mountains of New York State," *J. of Geophys.* Res. 85:7465 (1980).

13. K.C. Weathers, G.E. Likens, F.H. Bormann, S.H. Bicknell, B.T. Bormann, B.C. Daube, J.S. Eaton, J.N. Galloway, W.C. Keene, K.D. Kimball, W.H. McDowell, T.G. Siccama, D. Smiley, and R.A. Tarrant, "Cloudwater Chemistry from ten sites in North America," *Environ. Sci. and Technol.* 22:1018 (1988).

14. D.J. Jacob, J.M. Waldman, J.W. Munger, and M.R. Hoffmann, "Chemical composition of fogwater collected along the California coast,"*Environ. Sci. and Technol.* 19:730 (1985).

15. R.L. Brewer, R.J. Gordon, and L.S. Shepard, "Chemistry of mist and fog from the Los Angeles urban area," *Atmos Environ.* 17(11):2267 (1983).

16. P.S. Muir, K.A. Wade, B.H. Carter, T.V. Armentano, and R.A. Pribush, "Fog chemistry at an urban midwestern site," *JAPCA* 36:1359 (1986).

17. K.D. Kimball, R. Jagels, G.A. Gordon, and K.C. Weathers, "Differences between New England coastal fog and mountain cloud water chemistry," *Water, Air and Soil Pollut.* 39:383 (1988).

18. V.A. Mohnen and J.A. Kadlecek, "Cloud chemistry research at Whiteface Mountain," *Tellus* 41(B):79 (1989).

Table 1. Site descriptions.

Site Location	Latitude/Longitude	Elevation (meters)	Vegetation type
Everson[a]	48°58.29' 122°15.65'	50	Agricultural and mixed woods
Copper Ridge[b]	48°50.50' 121°27.50'	1920	Abies lasiocarpa Tsuga mertensiana
Cascade Pass[b]	48°28.33' 121°03.50'	1644	Abies lasiocarpa Tsuga mertensiana
Marblemount[a]	48°32.50' 121°27.00'	09	Rural and mixed woods
Hoh River[a]	47°49.28' 124°02.52'	96	Rural, pasture, mixed woods
Hurricane Ridge[a]	47°55.59' 123°21.94'	1617	Abies lasiocarpa
Cheeka Peak[a,b]	48°22.50' 124°39.78'	450	Picea sitchensis Tsuga heterophylla Pseudotsuga menziesii
U of W[a]	47°38.70' 122°27.63'	15	Urban
Stampede Pass[b]	47°16.74' 121°20.53'	1217	Pinus monticola Tsuga heterophylla Abies amabilis
Sunrise[a]	46°55.00' 121°39.50'	1950	Abies lasiocarpa Pinus albicaulis
Paradise[a]	46°48.00' 121°44.00'	1646	Abies lasiocarpa, Tsuga mertensiana
Burley Mtn.[a,b]	46°24.50' 121°52.00'	1618	Abies lasiocarpa, Picea engelmannii Tsuga mertensiana

[a] Active collector used

[b] Passive collector used

Table II. Chemical analysis methods.

Ion	Instrument	Technique
Ca^{2+}, Mg^{2+}, Na^{+}, K^{+}	Jarrel Ash ICP[a]	Emission spectroscopy
Cl^{-}, NO_3^{-}, SO_4^{2-}	Dionex 2010i[a,b]	Ion exchange chromatography AS4A column (1.75 $mMHCO_3$, 1.80 mMH_2CO_3 eluent)
NH_4^{+}	Technicon II Auto analyzer[a]	Standard Technicon colorimetry(indophenol method)
H^{+}	Beckman 71[c] pH meter	Combination electrode 4.0 & 7.0 buffers

[a] Dept. of Chemistry (Bagley Hall)

[b] Forestry Soils Lab (Bloedel Hall) and Environmental Chemistry Lab (Bagley Hall)

[c] Clean Air Lab Civil Engineering (Wilcox Hall)

Table III. Data quality for 1988 cloud water samples.

Measurement	Number of Samples	Average Precision (%)[a]	Average Accuracy (%)[b]
pH	695	0.52	1.4
NH_4^{+}	669	0.84	–
Ca^{2+}	660	3.1	4.1
K^{+}	660	22.9	115.0
Mg^{2+}	660	3.9	4.1
Na^{+}	660	7.6	9.6
Cl^{-}	675	5.5	8.3
NO_3^{-}	696	4.2	3.6
SO_4^{2-}	683	4.1	6.0
Volume	700	0.0006	0.001

[a] precision = standard deviation of paired replicates expressed as a percentage of the pair mean

[b] accuracy = percent deviation from NBS standard

Table IV. Events and samples collected at 12 sites in Western Washington.

Site	Operation Period	Number of events	Number of samples
Everson	11/87-4/88	1	2
Copper Ridge	7/88-9/88	3	11
Cascade Pass	7/88-9/88	5	5
Marblemount	11/87-4/88	1	1
Hoh River	5/88-10/88	7	8
Hurricane Ridge	6/88-10/88	3	12
Cheeka Peak	4/88-12/88	42	301
U of W	12/87-12/88	3	6
Stampede Pass	6/88-10/88	45	177
Sunrise	7/88-9/88	3	9
Paradise	6/88-10/88	5	20
Burley Mtn.	7/88-9/88	9	47

Table V. Linear regression of cloudwater composition collected simultaneously by co-located active[11] and passive[12] collectors[a].

Ion[b]	Linear Regression[c]			
	Range (ueq/l)	Intercept[d] (ueq/l)	Slope (S.E.)	R^2 [e]
H^+	69-241	32.0	.93 ± .16	.92
NH_4^+	9-147	3.0	.96 ± .16	.93
NO_3^-	27-118	- 0.8	.97 ± .12	.96
SO_4^{2-}	73-295	- 0.8	.80 ± .16	.90
Cl^-	10-615	- 15.0	.84 ± .11	.95

[a] Comparison tests were conducted in August 1988 at Cheeka Peak and Burley Mtn.

[b] Event mean (ueq/l)

[c] Concentration of active = concentration of passive x slope + intercept

[d] Intercept values are not significantly different from 0 (.05 level)

Table VI. Aqueous mean concentrations of acidic species at Cheeka Peak and Stampede Pass as a function of upper level (850 mb) wind direction (N = northwest and S/W = west and southwest). Results of an analysis of variance are shown below the table for four ionic species. Under both wind directions, Cheeka Peak is upwind of Stampede Pass. The interaction location and wind direction is the difference beyween site mean concentrations as wind direction changes (the upwind/downwind difference).

		N		W/S		Totals	
Ionic Species	site	number of observations	average event mean concentration (ueq/l)	number of observations	average event mean concentration (ueq/l)	number of observvations	average event mean concentration (ueq/l)
Hydrogen Ion[a]	Cheeka Peak	10	101	7	61	17	84
	Stamp. Pass	11	187	11	138	22	162
	Total	21	146	18	108	39	128
Ammonium Ion[b]	Cheeka Peak	10	14	7	13	17	14
	Stamp. Pass	11	97	11	58	22	78
	Total	21	58	18	41	39	50
Nitrate Ion[c]	Cheeka Peak	10	42	7	24	17	34
	Stamp. Pass	11	142	11	74	22	108
	Total	21	94	18	54	39	76
Non-sea-salt Sulfate Ion[d]	Cheeka Peak	10	73	7	55	17	66
	Stamp Pass.	11	230	11	159	22	195
	Total	21	155	18	119	39	138

[a] site: $p < 0.0003$
wind: $p < 0.04$
interact: $p < 0.83$

[b] site: $p < 0.0001$
wind: $p < 0.06$
interact: $p < 0.08$

[c] site: $p < 0.0001$
wind: $p < 0.007$
interact: $p < 0.10$

[d] site: $p < 0.0001$
wind: $p < 0.06$
interact: $p < 0.25$

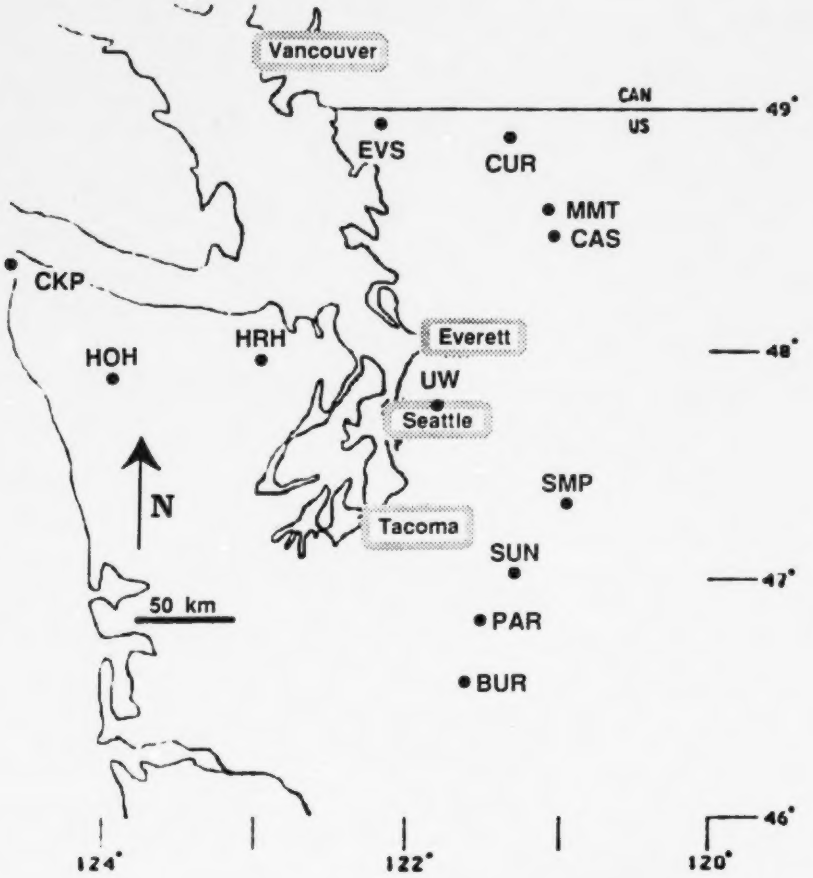
Vancouver
CAN
US
49°
EVS
CUR
MMT
CAS
CKP
HOH
HRH
Everett
48°
UW
Seattle
N
SMP
Tacoma
SUN
47°
50 km
PAR
BUR
46°
124°
122°
120°

Figure 1. Location of fog/cloudwater collection sites in western Washington (EVS=Everson, CUR=Copper Ridge lookout, MMT=Marblemount Ranger Station, CAS=Cascade Pass Ranger Station, CKP=Cheeka Peak, HOH=Hoh River, HRH=Hurricane Ridge Ranger Station, UW=University of Washington, SMP=Stampede Pass Weather Station, SUN=Sunrise Ranger Station, PAR=Paradise Ranger Station, BUR=Burley Mountain Lookout).

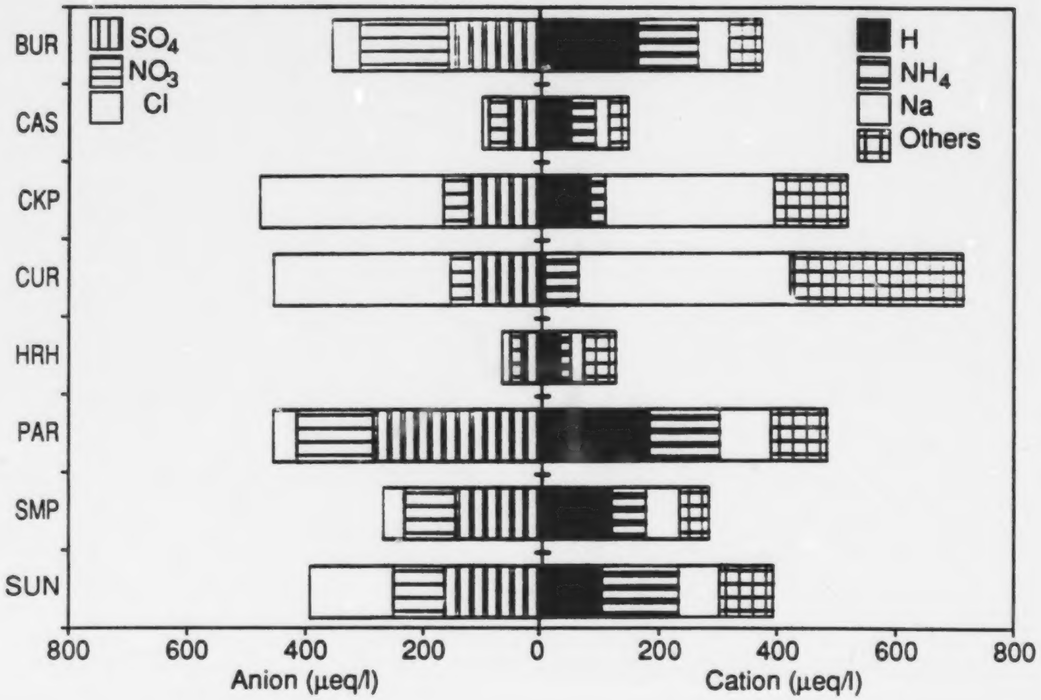

Figure 2. Averages of event mean aqueous concentrations of dominant ions in cloudwater collected from eight mountain sites in western Washington during the 1988 growing season (see Figure 1 for sampling locations).

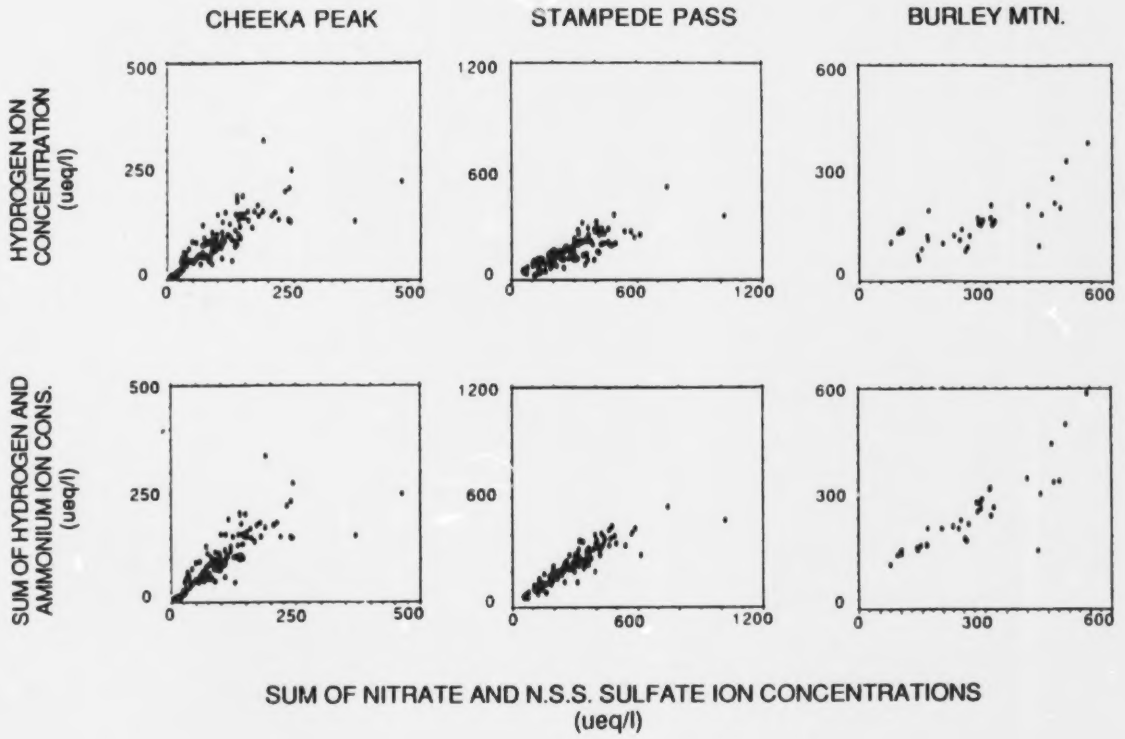

Figure 3a. Scatter plots illustrating relationships between the dominant cloudwater ions from three mountain sites in western Washington. The data are 1-h samples collected during the 1988 growing season. All relationships are significant ($p < 0.05$).

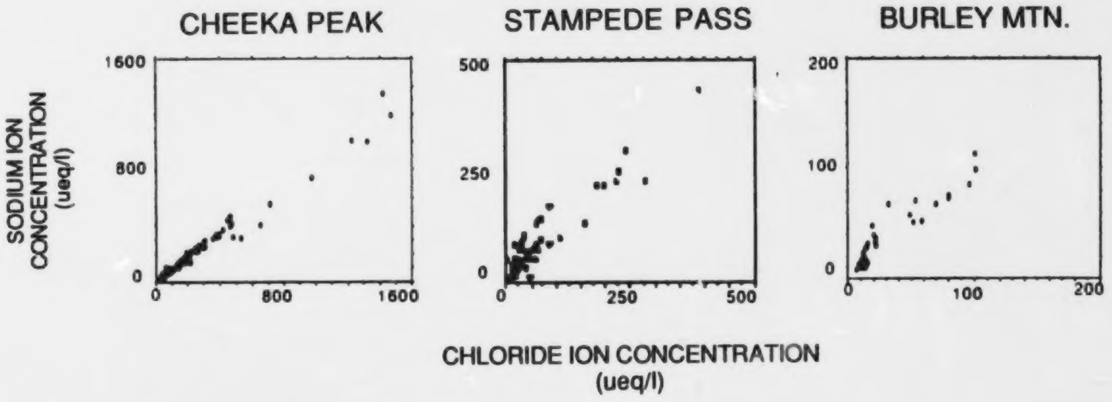

Figure 3b. Scatter plots illustrating relationships between the dominant cloudwater ions from three mountain sites in western Washington. The data are 1-h samples collected during the 1988 growing season. All relationships are significant ($p < 0.05$).

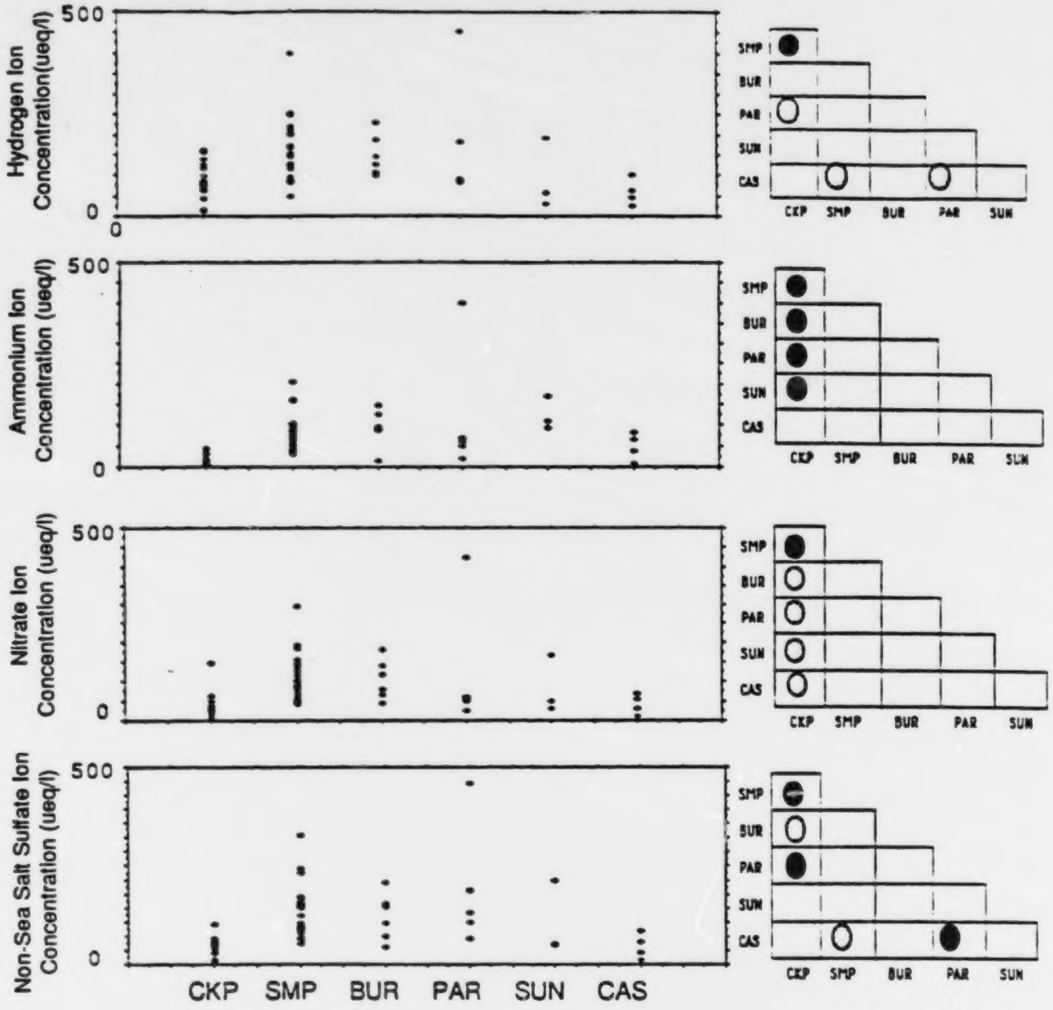

Figure 4. Event mean aqueous concentrations of the major acidic ions in cloudwater at six mountain sites. The events occurred between June 15 and Oct. 11, 1988, usually on different days at each site. Pairwise comparisons were made with Tukey's test. Differences that were significant ($p < 0.05$) are shown as dark circles to the right side of each panel.

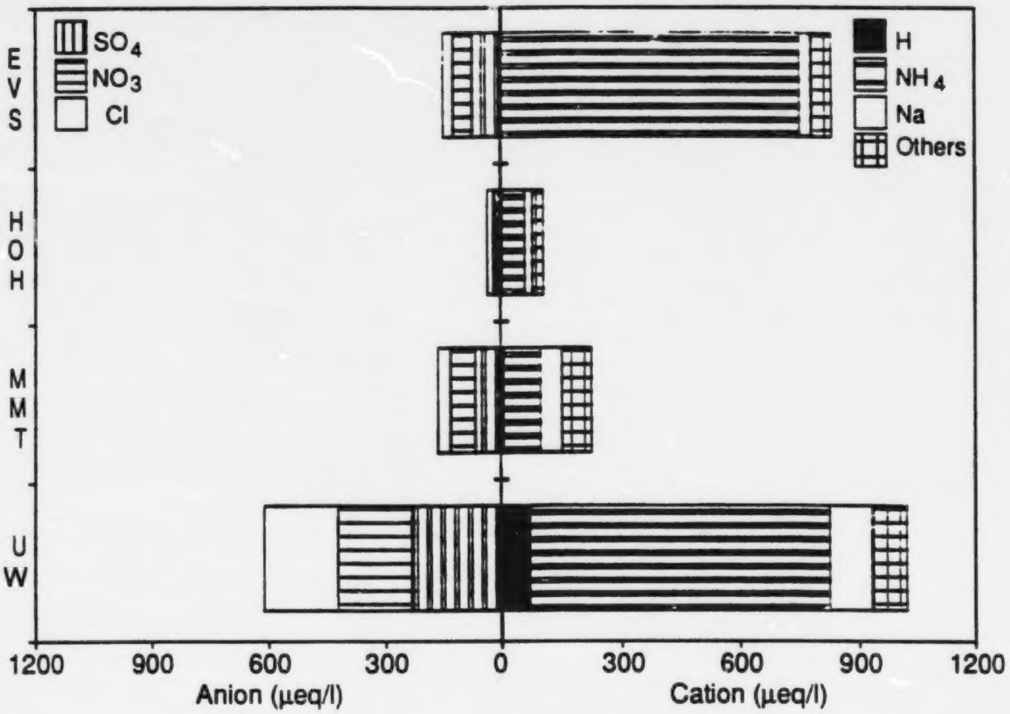

Figure 5. Average of event mean aqueous concentrations of dominant ions in fogwater collected at four low-elevation sites in western Washington during the winter and spring of 1988 (See Figure 1 for sampling locations).

Airborne Chemical Measurements in Nighttime Stratus Clouds in the Los Angeles Basin

L. Willard Richards

Sonoma Technology, Inc.
5510 Skylane Blvd., Suite 101
Santa Rosa, CA 95403-1083

INTRODUCTION

The Los Angeles Basin frequently experiences high concentrations of sulfate and nitrate in cloud-free air as well as in clouds and fogs. These species cause visibility degradation, material damage, and adverse ecological and health effects. Therefore, it is of interest to document the ambient concentrations of these species and to determine the chemical pathways primarily responsible for their formation. Many studies of the Los Angeles aerosol have been performed on the ground, both in clear air and in fogs, to characterize the aerosol composition, size distribution, and sources. A review appears in the Program Plan for the Southern California Air Quality Study.[1] These studies have indicated that liquid water in the atmosphere can enhance aerosol formation rates. During much of the year, night and morning low clouds are a routine part of the Los Angeles weather, so it is reasonable to expect that these clouds would play a significant role in the aerosol and acidity budgets. This paper reports the first systematic airborne investigation of the chemistry of these stratus clouds.

The Los Angeles Basin is a good laboratory for studies of stratus cloud chemistry because the meteorology repeats itself in a reasonably predictable pattern and the pollution levels are high enough that many species occur at concentrations well above their chemical detection limits. Clouds form along the coast in the evening, then sometimes spread inland during the night and persist for a few hours after sunrise. The cloud ceiling data from Los Angeles International (LAX) and Ontario International (ONT) Airports were reviewed, and it was found that May and June were the months with the highest frequency of suitable stratus clouds. Clouds high enough to be above the minimum altitude for instrument flight rules and covering much of the Basin occurred on about one-third of the nights and tended to occur in cycles lasting two to four days. The next best time of year was October.

It was an objective of this study to produce a data base suitable for use in computer models, and these data have been modeled by Seigneur and Wegrecki.[2]

All of the data and discussions in this paper have previously been reported to the California Air Resources Board in final reports available from the National Technical Information Service (NTIS). These reports give complete descriptions of the experimental methods and tabulate most of the data, so only the more important results are presented here. The first Final Report[3] describes results obtained in November 1981 and May 1982, the second[4] results from October and November 1983 and June 1984, and the third[5] results from May and June 1985. The first and third final reports were accompanied by data volumes,[6,7] which contain tabulations and plots of the

Preceding page blank

data. The data volumes were not submitted to NTIS. A journal article also has been prepared.[8]

EXPERIMENTAL METHODS

The experimental equipment and procedures are briefly outlined in this article and are described in detail in the reports cited above. The airborne sampling was performed with a twin-engine Beechcraft Queen Air. There were six sampling ports and manifolds for aerosol and gas sampling on the side of the fuselage over the wing and ports for two warm cloud water collectors in the top of the fuselage about 4.4 m from the nose. The probes to measure cloud liquid water content and droplet size distributions were on top of the fuselage at the nose.

Continuous Measurements

The air quality sampling instruments in the Queen Air are listed in Table I. The manifold for the nephelometer includes a cyclone to remove particles larger than about 2 μm, so the nephelometer responds to fine particles but is insensitive to cloud droplets.

Aerosol size distributions for particles between 0.1 μm and about 1 μm diameter were measured by the Active Scattering Aerosol Spectrometer Probe (ASASP-X) manufactured by Particle Measuring Systems, Inc. (PMS). Particles with diameters greater than about 2 μm were measured with the PMS Forward Scattering Spectrometer Probe (FSSP-100), which was usually locked in the 2 to 32 μm size range. The cloud liquid water content (LWC) was calculated from the FSSP data and also measured with a probe designed by King, et al.[9] and built by Sonoma Technology, Inc. (STI.)

Grab Samples

Cloud Water Samples. Two Mohnen warm cloud water collectors were used.[10,11] These were designed to collect particles larger than about 3 μm and are inefficient at collecting submicron-sized particles, and have known shortcomings.[12] One collector was equipped with a miniature pH electrode to continuously record the cloud water pH. No stabilizing reagents were added to the cloud water from this collector, and the samples were analyzed as summarized in Table II. The flow from the second cloud water collector was divided between two bottles containing stabilizing solutions for labile species. One of the bottles contained the stabilizing solution for the determination of H_2O_2, and the other was used either for the determination of sulfur (IV) or for carbonyl compounds. Immediately after collection, the cloud water samples were placed in an ice chest with a temperature near 4° C.

Filter Samples. Interstitial aerosol samples were collected on Teflon and nylon filters behind the cyclone with a 2-μm particle size cutpoint. A carbonate-impregnated filter was used to determine SO_2. A summary of the sampling and analytical methods appears in Table III, and further information is given in the Final Reports cited above.

Bubblers. Gas samples were collected at a flow rate of 1 lpm in two micro-impingers that contained 10 ml of liquid. One bubbler contained 2,4-dinitrophenylhydrazine solution, which was analyzed for formaldehyde and acetaldehyde, and the other contained 0.1 N KOH, which was analyzed for acetate as an indicator of PAN.

Hydrocarbon Canisters. Gas samples were drawn through a Teflon sampling line by a metal bellows pump into 3.2-l electropolished stainless steel canisters. The canisters were flushed before being filled and were analyzed by gas chromatography.

Flight Patterns

Airborne chemical sampling under instrument conditions in an airspace as congested as the Los Angeles Basin presents some significant logistical challenges. Flight patterns compatible with other air traffic were determined in advance and were discussed with and approved by the air traffic controllers. Before and during the flights, clearances were obtained to fly the preset patterns.

The flight patterns used to collect chemical grab samples in the June 1985 flights are shown in Figure 1. The flight tracks were calculated from LORAN data. Each sampling track was roughly perpendicular to the prevailing winds, so air masses could be approximately followed by moving from one track to the next track inland at time intervals determined by the wind velocity. The three-dimensional distribution of acidity was explored by a flight pattern consisting of a series of missed instrument landing approaches at eight airports in the Basin.

RESULTS AND CONCLUSIONS

Overview of the Observed Spatial Distributions

The spatial distributions of the concentrations of the more important chemical species are summarized first to provide a setting for the results that follow. Nearly all data were collected between 11 p.m. and dawn because the clouds form at night. At the altitude of the stratus clouds, the concentrations of most species were relatively uniform throughout the sampled regions of the Basin. The most significant exception was the H_2O_2 concentration in the cloud water, which tended to decrease with increasing distance from the coast. In contrast to the horizontal uniformity, there were typically strong vertical gradients for the concentrations of most species. Thus, nearly all grab samples were collected in a thin layer of stratus clouds whose composition did not vary much horizontally, but which was sandwiched between air masses with strong vertical composition gradients. Most grab samples were collected at altitudes between 600 and 750 m (2000 and 2500 ft) above ground level. The ground level in the inland portions of the Basin is about 300 m msl, so the sampling altitudes were typically 100 to 300 m msl higher in inland portions of the Basin than along the coast.

Profiles recorded during takeoff and landing showed that at night, the O_3 concentrations were typically near zero at ground level and increased with altitude, while the NO_x concentrations decreased with altitude. The shape of these profiles was influenced by NO emissions from mobile sources during the night. Ozone concentrations at cloud height were usually in the range between 20 and 100 ppb and typically were close to 60 ppb. Ozone concentrations became small at night only at the surface.

Figure 2 shows a sharp increase in the O_3 concentration from about 60 ppb in and below the clouds to more than 120 ppb just above the cloud tops. These data were recorded at 1:29 a.m. on June 3, 1984 above the Whittier Narrows (near the middle of the Basin). The light scattering by fine particles also increases sharply at the cloud top. Ozone concentrations were typically higher just above the clouds than in them, but there were times when the O_3 concentrations changed little at the cloud tops.

When flying at constant altitude through broken clouds, it was common to observe that the O_3 concentrations were higher out of the clouds than in, sometimes by as much as 50 ppb. In June 1984, the average difference for all data was 7 ppb. It is not known whether this observation is due to chemical or meteorological effects, but meteorological effects are more likely. It is possible that a vertical component of the wind can create regions below the cloud tops that contain trace gas concentrations similar to those found above the cloud tops.

The sulfate and nitrate concentrations and the pH in the clouds were remarkably uniform throughout the basin. This finding applies to the narrow range of altitudes at which clouds were sampled.

Lead was always observed in the cloud water samples collected offshore, indicating that these air masses contained urban emissions. No flights were intended to collect samples far enough offshore that they would be free of urban emissions. The purpose of collecting grab samples over the ocean was to characterize the air flowing into the Basin.

It was consistently observed that H_2O_2 concentrations in the cloud water tended to be higher near the coast (about 100 μM) and to be lower in the inland portions of the Basin (20 to 40 μM). The lead and elemental carbon data show that urban emissions were present in all samples. Therefore, it cannot be assumed that the H_2O_2 along the coast was advected into the basin by "background" air.

Cloud Water Composition

The average composition of the cloud water samples collected in May-June 1985 is shown in Figures 3 and 4. These pie diagrams include only species for which analyses were performed. It is likely that the great majority of the ionic species present in the clouds are included in Figure 4, but Figure 3 is distorted by the omission of nearly all organic compounds. The Los Angeles aerosol contains high concentrations of carbon species,[13] which make up about 40% of the annual average fine-particle mass.[14] Rain and fog water and snow samples collected in the Los Angeles Basin have been shown to contain significant concentrations of organic acids and measurable concentrations of a broad range of other organic species.[15-18] Therefore, it is expected that organic compounds were a significant fraction of the species in the cloud water.

Most individual cloud water samples have a composition similar to the average compositions shown in the Figures 3 and 4. At the end of the first year of sampling, the average ionic composition (in equivalents) was summarized as being:

40-50% HNO_3
20-30% $(NH_4)_2SO_4$
10-20% $NaCl$

and this generalization has remained valid each year. This recipe does not necessarily indicate that ammonium and sulfate ions are associated with each other or that their sources are related; it only indicates that the average number of equivalents of each is approximately the same.

Table IV gives the minimum, maximum, and mean concentrations observed for some of the more important species for each of the three sampling programs. The major source of variability in these data is that the maximum readings in May 1982 were observed near the Kaiser Steel Mill in Fontana, which was closed soon afterward. This closure, the shift from oil to gas for electric power generation, and other process changes caused SO_2 emissions in the Basin to decrease between 1982 and 1984.

The cloud water pH increased slightly during the years these flights were conducted, with the greatest change between 1982 and 1984. Little scatter was observed in the pH values; all samples collected in 1984 and 1985 fell in a one pH unit range. Most cloud water samples had a pH slightly greater than three.

Ion Balances. The ion balances for each collected sample are given in the Final Reports[3-5] and show a slight bias in direction expected if undetermined organic anions were present.

Hydrogen Peroxide. Hydrogen peroxide measurements were started in May 1982 when Gregory Kok came to the field to perform these analyses. In 1982, aliquots were removed for the H_2O_2 analyses immediately after the aircraft landed; but beginning in 1984, water samples were collected directly into a stabilizing solution and were analyzed as described in Table II. To determine the comparability of the two methods, both methods were used for some samples in 1984. The results are given in Figure 5 and show that measured H_2O_2 concentrations were not significantly biased by cloud water sample storage before analysis.

The mean and range of the observed H_2O_2 concentrations are reported in Table IV. The most important result from the H_2O_2 determinations is that H_2O_2 was found in every cloud water sample submitted for analysis. Thus, H_2O_2 concentrations never became small as predicted by some computer simulations.[19,20] The excess H_2O_2 has the potential to rapidly form sulfate whenever SO_2 is mixed into the clouds. The potential effect on sulfate concentrations is discussed in the following section on sulfur chemistry.

Carbonyl Compounds. The concentrations of HCHO and CH_3CHO were measured in the cloud water and in the gas phase because of their potential importance in free radical chemistry during both day and night. The means and ranges of the cloud water concentrations of these species are reported in Table IV. Betterton and Hoffmann[21] made calculations based on the Henry's Law constant that showed the cloud water concentrations of CH_3CHO were at least a factor of 100 too large to be consistent with the gas-phase data. The same analytical method was used for both the bubbler and cloud water samples, and similar results were observed in 1984[4] and 1986.[5] These data suggest that the atmospheric chemistry of CH_3CHO is not completely understood. The HCHO concentration data agreed with the Henry's Law constant of Dong and Dasgupta[22] to within a factor of two.

Trace Metals. Trace metals were measured to complete the ion balance, to determine the concentrations of catalytic metals such as iron and manganese, and to provide a tracer of urban emissions. Figure 4 shows that trace metals accounted for an average of about 31% of the cations in 1985. The role of iron and manganese is discussed in the section on sulfur chemistry.

The data for lead showed that all cloud water samples contained urban emissions, even those collected over the ocean near the coast.

Organic Species. The cloud water collectors and storage bottles were made out of plastic so that the sample collection and storage equipment would not alter the ionic or trace metal content of the water. Such equipment is not appropriate for the collection of samples to be analyzed for organic species. Funding limitations prevented collecting cloud water samples with equipment that would not alter the concentrations of organic species and performing the additional analyses required to determine the concentrations of the more important compounds. Therefore, no information is available on organic compounds other than HCHO and CH_3CHO. This is an important omission in the data.

Sulfur Chemistry

The sulfur chemistry results observed in 1981 and 1982 were significantly different from those observed in later years. In May 1982, both sulfur (IV) and H_2O_2 were found in every cloud water sample analyzed for both species. This finding was reported in a preliminary communication.[23] In contrast, sulfur (IV) was undetectable or present in only insignificant concentrations in all cloud water samples collected in 1983 through the end of sampling in 1985. In every year, H_2O_2 was found in all cloud water samples analyzed for that species. The H_2O_2 concentrations were often high enough to form significant amounts of sulfate if SO_2 were added to the clouds.

Sulfur (IV) in Cloud Water. The sulfur (IV) concentrations in the cloud water ranged from 5 to 365 µM, averaged 76 µM in 1981 and 1982, and were typically a few hundred times larger than could be explained by the observed SO_2 concentration and cloud water pH. This observation, plus the 1982 finding that sulfur (IV) and H_2O_2 were found to coexist in water samples hours after collection, suggested that the sulfur (IV) was stabilized against oxidation. Concurrent laboratory research had shown that sulfur (IV) can be stabilized against H_2O_2 oxidation by forming an adduct with HCHO.[24] Thus, the field observations could be reproduced in the laboratory.

Calculations using the equilibrium constant for the reaction of HCHO and sulfite to form hydroxymethanesulfonic acid[25] gave the result that half or less of the sulfur (IV) was in the adduct with HCHO. Reasonable values for the concentrations of CH_3CHO and other aldehydes were not great enough to explain the 1982 observations. This inconsistency has not been explained.

In the sampling done in 1983 through 1985, the gas-phase SO_2 concentration was always below the limit of detection (1 to 2 ppb), except for occasional, isolated plumes in the southeastern part of the Basin. Sulfur (IV) concentrations in the cloud water and aerosol were either at or below the limit of detection during these years.

Sulfate in Plumes. The highest observed sulfate concentrations were associated with plumes in the Fontana area in May 1982. During the night of May 21-22, cloud water concentrations of 25 and 38 $\mu g/m^3$ and aerosol concentrations of 32 and 68 $\mu g/m^3$ were observed, giving total sulfate concentrations of 57 and 106 $\mu g/m^3$. Total nitrate concentrations in the plumes ranged from 94 to 115 $\mu g/m^3$. The majority of the sulfate was collected on filters behind the 2-µm-cut cyclone, and this suggested that the sulfate formed in the plumes was in the smaller particles. No sulfate concentrations comparable to these were observed after 1982.

Sulfate from Sea Salt. A cloud water sample collected off Newport Beach between 5:45 and 6:30 a.m. on November 14, 1983, contained concentrations of Cl^-, Na^+, K^+, Ca^{2+}, and Mg^{2+} whose ratios matched those for sea salt. Those concentrations were used to estimate that 12.3 μg/ml of the observed 14.5 μg/ml sulfate in the collected water (or 1.6 $\mu g/m^3$ of the observed 1.9 $\mu g/m^3$ ambient concentration) was from sea salt.

The sodium concentrations in the samples collected in June 1984 were used to estimate the contribution of sea salt to the sulfate concentration. In general, a few percent up to 11% of the sulfate was attributed to sea salt. In most cases, the ambient concentration of sulfate in the cloud water from sea salt was estimated to be between 0.1 and 0.2 $\mu g/m^3$, and the highest value was 0.4 $\mu g/m^3$.

Sulfate Formation Pathways. The 1984 data were used to make estimates of the relative importance of three mechanisms for the oxidation of sulfur (IV) to sulfate. The dominant pathway was oxidation by H_2O_2, and for the H^+ and H_2O_2 concentrations observed in 1984, the sulfur (IV) consumption rate ranged from 0.5 to 5.0/s. The Fe and Mn concentrations in the cloud water were high enough that the second most important reaction pathway was Fe-Mn-catalyzed oxidation of sulfur (IV), and calculated consumption rates ranged from 0.4×10^{-2}/s to 1.4×10^{-2}/s (or 24 to 84%/min.). These rates may be overestimates of the true values because some of the Fe and Mn in the cloud water may have been bound in chemical compounds that are not catalytically active. For conditions typical of stratus in the Los Angeles Basin, oxidation of sulfur (IV) by O_3 consumes sulfur (IV) at a rate less than 0.1%/h, or 3×10^{-7}/s.

Seigneur and Wegrecki[2] give data for the relative importance of the dominant sulfate formation mechanisms based on their model results.

Additional Sulfate from H_2O_2. The observed H_2O_2 concentrations were in the range from 1 to 167 μM, and the mean H_2O_2 concentration in May-June 1985 was 57 μM. This H_2O_2 will oxidize SO_2 gas to sulfate in the cloud water as rapidly as the SO_2 is mixed into the clouds. Therefore, estimates were made of the amount of sulfate that would be formed if additional SO_2 were available.

H_2O_2 was measured only in the cloud water, so the Henry's Law constant reported by Hwang and Dasgupta[26] was used to estimate the gas-phase concentration. The calculated fraction of the total H_2O_2 in the cloud water ranged from 34% to 71% and had a mean of 59% in the May-June 1985 data. The additional sulfate that would be formed by this H_2O_2 if the SO_2 were made available ranged from 1 to 16 $\mu g/m^3$ and averaged 5.2 $\mu g/m^3$. The average of the percentage increases in the sulfate concentration was 65%. The tabulated data appear in a final report.[5]

These results show that the stratus clouds in Los Angeles have a significant capacity to rapidly oxidize SO_2 to sulfate. Should the SO_2 emissions again increase in the Basin, it is expected that the portions that become entrained in clouds would be rapidly oxidized to sulfate.

Nitrate Chemistry

Nitrate was the anion with the highest concentration in the cloud water. Figure 4 shows that on the average, nitrate accounted for slightly more than half of the anion equivalents in 1985. Also, the hydrogen and nitrate ion concentrations in equivalents were approximately the same. Similar results were obtained from all sampling sessions between 1981 and 1985.

The possibility of significant biases in the nitrate data should be recognized. These could be caused by the rapid transfer of HNO_3 between the gas and liquid phase on the cloud water collector rods, in the sampling ducts, or on the filters.

The measured NO_x and nitrate concentrations show that the oxidation of nitrogen oxides to nitrate was typically half to three-quarters complete in the sampled clouds, but the ratios ranged from about 20% conversion to 93% conversion. Ozone was always present in the clouds, and at night the oxidation of NO to NO_2 had always gone to completion. In most samples, the average NO_x concentration during a cloud sampling orbit was between 3 and 10 ppb, and the cloud water plus interstitial aerosol nitrate concentration was between 10 and 40 $\mu g/m^3$.

The reaction pathways by which HNO_3 is formed in the Los Angeles Basin have been investigated in a series of articles by Russell et al.[27-29] Seigneur and Wegrecki[2] compare the results of model calculations for two of the 1985 aircraft flights with the experimental data and discuss the relative importance of the nitrate formation mechanisms under the conditions of these experiments.

Flights that Followed Air Parcels

In May-June 1985, the chemical sampling flights were designed to follow air parcels to measure the change of the cloud composition with time. To accomplish this, the flight patterns shown in Figure 1 were planned to form a sequence along typical wind trajectories in areas where such flight patterns were permitted under instrument conditions. Radiosonde data were then used to determine the length of time between starting the collection of samples in each location.

Five flights that attempted to follow air parcels were made in 1985: three near Long Beach and two near Ontario. The data from all five flights were combined to determine the way the species concentrations changed with time. Except for Pb, the average concentrations of trace metals tended to decrease, the SO_4^{2-} concentration tended to remain constant, and the NO_3^- and NH_4^+ concentrations tended to increase with time. NH_4^+ showed the greatest increase. Examination of the data from the individual flights showed that the concentrations of the metals Na, K, Ca, and Mg tend to vary together as if they were controlled by the same factors. It is believed that the concentrations of these metals were controlled by meteorological processes such as vertical mixing and droplet settling.

A significant concentration trend was observed during only one flight in May-June 1985. This was on the morning of May 26, when there was enough drizzle from the clouds being sampled to cause some runoff from paved areas. The flight patterns used to collect these data are plotted in Figure 1 and are the three orbits between Pomona and Riverside. Figure 6 shows on a logarithmic scale the ambient concentrations of species in the cloud water observed during successive sampling orbits. The average concentration of Na, K, Ca, and Mg in the cloud water decreased by about a factor of two each hour. The concentrations of NO_3^- and SO_4^{2-} decreased less than that, and the NH_4^+ and Pb concentrations changed little. These data show that the settling of large droplets out of the clouds during drizzle can remove significant amounts of dissolved species.

The experiments in which air parcels were followed were designed to study formation processes, but it turned out that the effects of removal processes and vertical mixing were more apparent in the data. The experiment also was designed to provide data for model evaluation, and the results from two of these flights have been modeled by Seigneur and Wegrecki.[2] Their model includes all the processes discussed above.

Aerosol Formation

One of the more important impacts of the nighttime stratus in the Los Angeles Basin is that the clouds leave aerosol behind when they evaporate in the morning. Also, the removal processes described previously can form large aerosol particles below the clouds. These processes can account for a number of prior observations of aerosol properties in the Los Angeles Basin.

The data for the cloud water composition and cloud droplet size distribution provide enough information to estimate the size distribution and composition of the aerosol remaining after cloud evaporation. The following assumptions were used to construct these estimates:

1. All cloud droplets have a composition equal to the composition of the collected water. This assumption ignores the possibility that the smaller droplets may be more concentrated than the large droplets as suggested for example, by Levine and Schwartz.[30]

2. Only two-thirds of the nonvolatile species present in the cloud water were determined, and the aerosol had a density of 1.5 g/cm^3.

3. Neither HNO_3 nor HCl remain in the "dry" aerosol.

None of these assumptions are completely valid, but they allow estimation of the size distribution and composition of aerosol left behind. Because of the cube root in the calculation of particle diameter from mass, errors in estimates of the composition of the aerosol have a smaller impact on the estimated particle diameters.

The estimate of the concentration of undetermined species in the cloud water is highly uncertain because no attempt was made in this study to determine the total concentration of organic species. Gray et al.[14] measured the fine-particle aerosol composition at 10 sites in the Basin for the calendar year 1982 and found that carbon compounds accounted for an average of about 40% of the aerosol mass. Some carbon species, such as oil particles and some types of soots, are hydrophobic and may not be present in cloud water in proportion to their aerosol concentrations. Therefore, aerosol data provide only rough guidance for the concentrations of carbon species in the cloud water.

Some water will be retained by the aerosol.[31] No attempt was made to account for retained water, so the estimates presented here are most nearly applicable at the lower humidities which occur in the afternoons.

The cloud water contained large concentrations of HNO_3 and some chloride. For purposes of this approximate calculation, it is assumed that HNO_3 and HCl evaporate in equal proportions and that the evaporation continues until either all the hydrogen ions are gone or until all the nitrate and chloride are gone. It was almost always the case that nitrate and chloride remained in the aerosol rather than hydrogen ions, so the control strategy of decreasing the amount of ammonia available to be mixed into the clouds would decrease the aerosol concentrations remaining after cloud evaporation.

These calculations have been performed in each of the three studies and have always given similar results. Figure 7 shows the average aerosol composition by mass remaining after the evaporation of the cloud water samples whose average composition is given in Figures 3 and 4. Comparison of Figures 3 and 7 clearly shows the calculated loss of nitrate and chloride upon cloud evaporation. Ammonium nitrate is known to be volatile,[32] and evaporation of this species as the ambient temperature increases would reduce the aerosol nitrate concentrations to lower levels than shown in Figure 7.

The assumption that all cloud droplets in one sample have the same composition makes it possible to estimate the particle size distributions of the remaining aerosol from cloud droplet size distributions. Figure 8 shows three cloud droplet size distributions measured in 1982 and the estimated size distribution of the aerosol remaining after evaporation of these clouds. Figure 8 also shows sulfate size distributions measured in the Los Angeles Basin by Hering and Friedlander.[33] Those authors discuss the possibility that their Type I aerosol size distributions are formed by growth of wet aerosol particles. The data presented here show that the Type I aerosol size distributions reported by Hering and Friedlander can also be formed in significant concentrations by the evaporation of stratus clouds.

Aerosol particles near 0.5 μm in size are more effective on a mass basis in causing haze than are the smaller particles formed by dry photochemical processes. Thus, ammonium salts formed in or processed by fogs and clouds are more effective in causing haze than the same concentrations of salts formed in the absence of liquid. Furthermore, when 0.5 μm to 1.0 μm particles are present in significant concentrations, small particles can coagulate with them and thereby contribute more to the light extinction than would be possible in the absence of these particles.

Persistence of Sulfur (IV) after Cloud Evaporation

The observation in this study of sulfur (IV) in Los Angeles cloud water provides a possible explanation of earlier observations. It was noted during attempts to distinguish sulfuric acid from other sulfates in the Los Angeles Basin that about 10% of the aerosol sulfur could be volatilized as if it were sulfuric acid. However, it was not sulfuric acid because it would only partially lose this volatility upon exposure to ammonia.[34] The observation of a volatile component in the sulfur aerosol in the Los Angeles Basin appears to be the rule rather than the exception.[35-38] These observations can be explained if some of the Sulfur (IV) observed in cloud water in this study persists in the aerosol when the clouds evaporate. Sulfur (IV) has been previously detected in the aerosol in Los Angeles,[39] and nonsulfate sulfur has been detected in the Denver aerosol.[40]

ACKNOWLEDGMENTS

This work was supported by the California Air Resources Board. Douglas Lawson, Eric Fujita, and Praveen Amar each made significant contributions.

The participants in the field work upon which this paper is based are co-authors of the final reports and J. A. Anderson, D. L. Blumenthal, and J. A. McDonald played key roles in this work.

In the first year, chemical analyses were performed by William Munger, Jed Waldman, and Daniel Jacob from Michael Hoffmann's laboratory. In subsequent years, most analyses were performed by EMSI, which is now a subsidiary of Combustion Engineering. In addition, Greg Kok of NCAR performed the H_2O_2 analyses, P.K. Dasgupta of Texas Tech University performed the sulfur (IV) analyses, Daniel Grosjean gave advice on the carbonyl collection and analysis procedures, and Rei Rasmussen analyzed the hydrocarbon canisters.

Ted Smith assisted with the initial design of the study and gave meteorological advice each year. Bob Anderson performed the forecasting in 1984, and Bill Knuth operated the radiosondes and made the forecasts in 1985.

REFERENCES

1. D.L. Blumenthal, J.G. Watson, and P.T. Roberts, "Southern California Air Quality Study (SCAQS) program plan," STI Report No. 96040-708R, submitted to the California Air Resources Board, 1987.

2. C. Seigneur and A.M. Wegrecki, "Mathematical modeling of cloud water chemistry in the Los Angeles Basin," Submitted to *Atmos. Environ.*

3. L.W. Richards, J.A. Anderson, D.L. Blumenthal, S.L. Duckhorn, and J.A. McDonald, "Characterization of reactants, reaction mechanisms, and reaction products leading to extreme acid rain and acid aerosol conditions in Southern California," Final Report No. STI 83 ES-200, NTIS No. PB 83-252825, submitted to the California Air Resources Board, 1983.

4. L.W. Richards, J.A. Anderson, D.L. Blumenthal, and J.A. McDonald, "Characterization of the composition and three dimensional distribution of acidity in Southern California clouds," Final Report No. STI 90083-506, NTIS No. PB 85 223014/AS, submitted to the California Air Resources Board, 1985.

5. L.W. Richards, J.A. Anderson, N.L. Alexander, D.L. Blumenthal, W.R. Knuth, and J.A. McDonald, "Characterization of the reactants, mechanisms, and species in South Coast Air Basin cloudwater," Final Report No. STI 94120-606-12FR, NTIS No. PB 87-171229/AS, submitted to the California Air Resources Board, 1987.

6. L.W. Richards, J.A. Anderson, D.L. Blumenthal, A.A. Brandt, S.L. Duckhorn, S.Z. Hynek, J.A. McDonald, and N. Waters, "Characterization of reactants, reaction mechanisms, and reaction products leading to extreme acid rain and aerosol conditions in Southern California, Final Data Volume, November 1981 and May 1982 flights," STI Report No. STI 83 DV-0052, submitted to the California Air Resources Board, 1983.

7. L.W. Richards, J.A. Anderson, N.L. Alexander, and J.A. McDonald, "Characterization of reactants, mechanisms, and species in South Coast Air Basin cloudwater," Data Volume No. STI 94120-607-10DV. Submitted to the California Air Resources Board, October 1986.

8. L.W. Richards, "Airborne chemical measurements in nighttime stratus clouds in the Los Angeles Basin," Submitted to *Atmos. Environ.*

9. W.D King, D.A. Parkin, and R.J. Handsworth, "A hotwire liquid water device having fully calculable response characteristics," *J. App. Meteorol.* 17:1809 (1978).

10. W. Winters, A. Hogan, V. Mohnen, and S. Barnard, "ASRC airborne cloud water collection system," ASRC-SUNYA Publication No. 728, Atmospheric Sciences Research Center, SUNYA, Albany, NY, 1979.

11. V.A. Mohnen, "Cloud water collection from aircraft," *Atmos. Tech.* 12:20 (1980).

12. B.J. Huebert and D. Baumgardner, "A preliminary evaluation of the Mohnen slotted-rod cloud water collector," *Atmos. Environ.* 19:843 (1985).

13. D. Grosjean, "Particulate carbon in Los Angeles air," *Sci. Total Environ.* 32:133 (1984).

14. H.A. Gray, G.R. Cass, J.J. Huntzicker, E.K. Heyerdahl, and J.A. Rau, "Characteristics of atmospheric organic and elemental carbon particle concentrations in Los Angeles," *Environ. Sci. Tech.* 20:580 (1986).

15. K. Kawamura and I.R. Kaplan, "Organic compounds in the rainwater of Los Angeles," *Environ. Sci. Tech.* 17:497 (1983).

16. K. Kawamura and I.R. Kaplan, "Capillary gas chromatography determination of volatile organic acids in rain and fog samples," *Anal. Chem.* 56:1616 (1984).

17. K. Kawamura and I.R. Kaplan, "Biogenic and anthropogenic organic compounds in rain and snow samples collected in Southern California," *Atmos. Environ.* 20:115 (1986).

18. K. Kawamura and I.R. Kaplan, "Compositional change of organic matter in rainwater during precipitation events," *Atmos. Environ.* 20:527 (1986).

19. J.R. Young, F.W. Lurmann, and D.A. Godden, "The potential role of mobile source emissions in the fogwater chemistry of the Los Angeles Basin," Prepared for Motor Vehicle Manufacturers Association of the United States, Inc. ERT Document P-B542-001, 1983.

20. D.J. Jacob and M.R. Hoffmann, "A dynamic model for the production of H^+, NO_3^-, SO_4^{2-} in urban fog," *J. Geophys. Res.* 88:6611 (1983).

21. E.A. Betterton and M.R. Hoffmann, "Henry's law constants of some environmentally important aldehydes," *Environ. Sci. Tech.* 22:1415 (1988).

22. S. Dong and P.K. Dasgupta, "Solubility of gaseous formaldehyde in liquid water and generation of trace standard gaseous formaldehyde," *Environ. Sci. Tech.* 20:637 (1986).

23. L.W. Richards, J.A. Anderson, D.L. Blumenthal, J.A. McDonald, G.L. Kok, and A.L. Lazrus, "Hydrogen peroxide and sulfur (IV) in Los Angeles cloud water," *Atmos. Environ.* 17:911 (1983).

24. G.L. Kok, S.N. Gitlin, and A.L. Lazrus, "Kinetics of the formation and decomposition of hydroxymethanesulfonate," *J. Geophys. Res.* 91:2801 (1986).

25. P.K. Dasgupta, K.B. DeCesare, and J.C. Ullrey, "Determination of atmospheric sulfur dioxide without tetrachloromercurate(II) and the mechanism of the Schiff reaction," *Anal. Chem.* 52:1912 (1980).

26. H. Hwang and P.K. Dasgupta, "Thermodynamics of the hydrogen peroxide-water system," *Environ. Sci. Tech.* 19:255 (1985).

27. A.G. Russell, G.J. McRae, and G.R. Cass, "Mathematical modeling of the formation and transport of ammonium nitrate aerosol," *Atmos. Environ.* 17:949 (1983).

28. A.G. Russell, G.J. McRae, and G.R. Cass, "The dynamics of nitric acid production and the fate of nitrogen oxides," *Atmos. Environ.* 19:893 (1985).

29. A.G. Russell and G.R. Cass, "Verification of a mathematical model for aerosol nitrate and nitric acid formation and its use for control measure evaluation," *Atmos. Environ.* 20:2011 (1986).

30. S.Z. Levine and S.E. Schwartz, "In-cloud and below-cloud scavenging of nitric acid vapor," *Atmos. Environ.* 16:1725 (1982).

31. G. Hänel, "The properties of atmospheric aerosol particles as functions of the relative humidity at thermodynamic equilibrium with the surrounding moist air," *Adv. Geophys.* 19:74 (1976).

32. A.W. Stelson, S.K. Friedlander, and J.H. Seinfeld, "A note on the equilibrium relationship between ammonia and nitric acid and particulate ammonium nitrate," *Atmos. Environ.* 13:369 (1979).

33. S.V. Hering and S.K. Friedlander, "Origins of aerosol sulfur size distributions in the Los Angeles Basin," *Atmos. Environ.* 16:2647 (1982).

34. L.W. Richards, H.H. Wang, and A.B. Harker, "Motor vehicle sampling experiment, final report," Report No. SC592.5FR, submitted to State of California Air Resources Board, Rockwell International, 1977.

35. L.W. Richards, K.R. Johnson, and L.S. Shepard, "A comparison of sulfuric acid measurement methods," Environmental Division Paper No. 30. Presented at the 176th National Meeting of the American Chemical Society, Miami Beach, Fl, September 11-14, 1978.

36. L.W. Richards, K.R. Johnson, and L.S. Shepard, "Sulfate aerosol study, final report," Report No. AMC8000.13FR. Submitted to Coordinating Research Council, Rockwell International, 1978.

37. L.W. Richards, et al., "Los Angeles field modeling and measurement study first year final report," Submitted to U.S. Environmental Protection Agency, Rockwell International, 1979.

38. D.B. Kittelson, R. McKenzie, M. Vermeersch, F. Dorman, D. Pui, M. Linne, B. Liu, and K. Whitby, "Total sulfur aerosol concentration with an electrostatically pulsed flame photometric detector system," *Atmos. Environ.* 12:105 (1978).

39. R.J. Farber, A.A. Huang, L.D. Bregman, R.L. Mahoney, D.J. Eatough, L.D. Hansen, D.L. Blumenthal, W.S. Keifer, and D.W. Allard, "The third dimension in the Los Angeles Basin," *Sci. Total Environ.* 23:345 (1982).

40. G.T. Wolff, R.J. Countess, P.J. Groblicki, M.A. Ferman, S.H. Cadle, and J.L. Muhlbaier, "Visibility-reducing species in the Denver 'brown cloud'—II. Sources and temporal patterns," *Atmos. Environ.* 15:2485 (1981).

41. K. Fung and D. Grosjean, "Determination of nanogram amounts of carbonyls as 2,4- dinitrophenylhydrazones by high-performance liquid chromatography," *Anal. Chem.* 53:168 (1981).

42. S.M. Kunen, A.L. Lazrus, G.L. Kok, and B.J. Heikes, "Aqueous oxidation of SO_2 by hydrogen peroxide," *J. Geophys. Res.* 88:3671 (1983).

43. G.L. Kok and K. Wilson, "A derivatization technique for the determination of peroxides in precipitation," Presented at the Conference on Gas-Liquid Chemistry of Natural Water, Brookhaven National Laboratory, Upton, New York, 1984.

Table I. Air quality sampling and data recording instruments.

Parameter	Manufacturer and Model	Parameter	Manufacturer and Model
SO_2	Meloy 285	Broad Band Radiation	Eppley PSP
NO/NO_x	Monitor Labs 8440		
O_3	Monitor Labs 8410	Ultraviolet Radiation	Eppley
b_{scat}	MRI 1569	True Airspeed	J-TEC
Condensation Nuclei	Environment One Rich 100	Turbulence	MRI 1120
		Temperature	YSI/MRI
Aerosol Charge Acceptance	Washington University	Dew Point	General Eastern
Altitude	Validyne	Liquid Water Content	STI King Probe
Indicated Airspeed	Validyne	Data Logger (includes time)	MRI Data System
Position	King KX170B/HTI DVOR	Stripchart Recorder	Linear Instruments
LORAN Postion	II-Morrow	Printer	Axiom

Table II. Collection and chemical analysis of cloud water samples during 1983-1985.

Unstabilized Cloud Water
- pH
- Conductivity
- Ion chromatography: SO_4^{2-}, NO_3^-, Cl^-
- Colorimetry: NH_4^+
- Atomic absorption spectroscopy: Na, K, Ca, Mg, Fe, Mn, Pb

Cloud Water Collector with Stabilizing Solutions
- Collect in DNPH solution to determine formaldehyde and acetaldehyde[41]
- Collect in formaldehyde solution to determine sulfur (IV)[25]
- Collect in p-hydroxyphenylacetic acid solution to determine hydrogen peroxide[42,43]

Table III. Collection and chemical analysis of filter and bubbler samples during 1983-1985.

Flow (lpm)	Diam. (mm)	Filter Medium	Method and Analytes	Analytical Laboratory
Filters collected behind 2-μm-cut cyclone				
50	47	Teflon	Ion Chromatography (IC): sulfate and nitrate Colorimetry: ammonium	EMSI
		Carbonate impregnated	IC sulfate to determine sulfur dioxide	EMSI
30	47	Teflon	Replicate IC & Colorimetry on selected filters. Archive others as backup	EMSI
		Nylon	IC nitrate to determine nitric acid	EMSI
30	47	Quartz (masked to 10 mm)	Visual reflectance for elemental carbon	STI
25	25	Teflon	Archived for replicate or trace metal analysis	–
Total sample collector				
50	47	Paper Teflon Nylon	Ion Chromatography: sulfate and nitrate Colorimetry: ammonium	EMSI
Bubblers				
Bubbler sample collected at about 1 lpm with 2,4-dinitrophenylhydrazine solution for formaldehyde and acetaldehyde.[41]				EMSI
Bubbler sample collected at 1 lpm in which the air flow was passed first through water then through 0.1 N KOH. The KOH solution was analyzed for acetate as an indicator of PAN.				TTU

EMSI: Environmental Monitoring and Services, Inc. of Combustion Engineering
STI: Sonoma Technology Inc.
TTU: Texas Tech University.

Table IV. Summary of cloud water concentrations

Analyte	Time Period	Mean	Maximum	Minimum
Ambient concentrations of water species in $\mu g/m^3$				
SO_4^{2-}	May 1982	15	38	4.0
	Jun 1984	6.5	12	3.3
	May-Jun 85	11	16	3.7
NO_3^-	May 1982	36	91	7.6
	Jun 1984	17	24	7.3
	May-Jun 85	22	40	5.2
NH_4^+	May 1982	5.8	18	0.6
	Jun 1984	1.6	2.3	0.8
	May-Jun 85	3.4	7.5	0.6
Water concentrations in μM				
H_2O_2	May 1982	33	88	1
	Jun 1984	55	127	16
	May-Jun 85	57	167	12
HCHO	May 1982	37	72	6
	Jun 1984	43	73	20
	May-Jun 85	29	53	11
CH_3CHO	Jun 1984	30	55	4.8
	May-Jun 85	4.3	7.5	0.7
pH				
	May 1982	3.0	3.6	2.3
	Jun 1984	3.0	3.6	2.8
	May-Jun 85	3.4	3.8	2.9

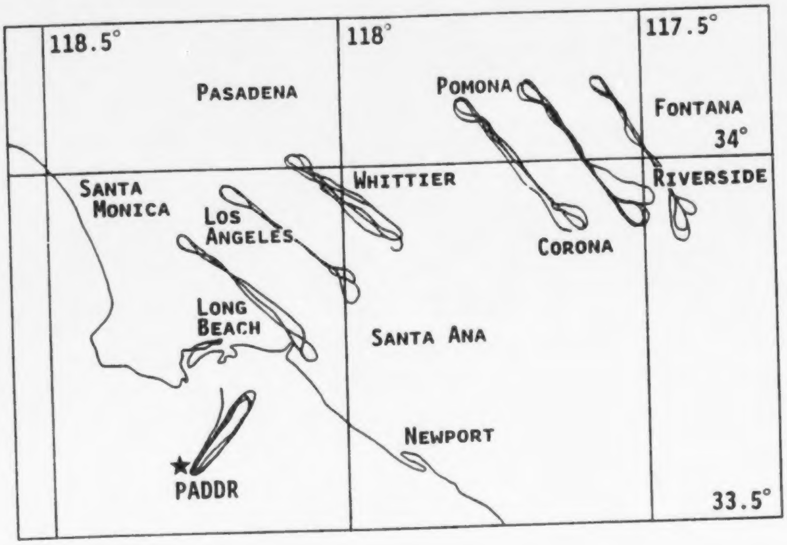
118.5°
118°
117.5°
PASADENA
POMONA
FONTANA
34°
SANTA MONICA
WHITTIER
RIVERSIDE
LOS ANGELES
CORONA
LONG BEACH
SANTA ANA
NEWPORT
PADDR
33.5°

Figure 1. Flight patterns for grab sample collection in 1985 plotted from LORAN data recorded during sampling.

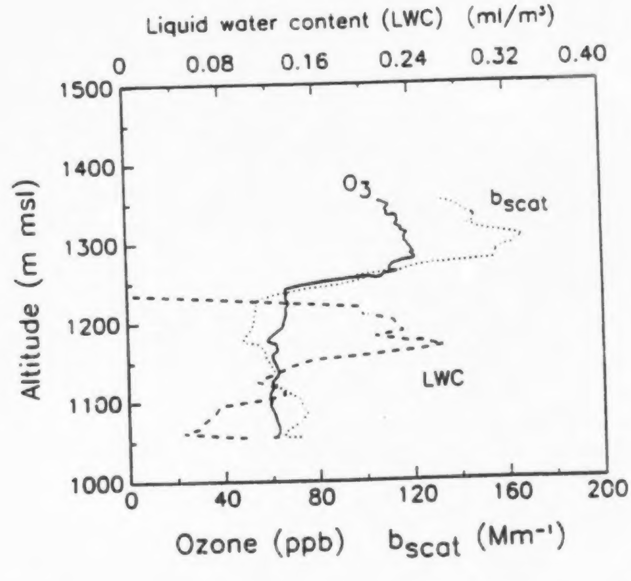

Figure 2. Vertical profiles of ozone, light scattering, and liquid water content in and above the clouds at 1:30 a.m. PDT on June 3, 1984 above the Whittier Narrows.

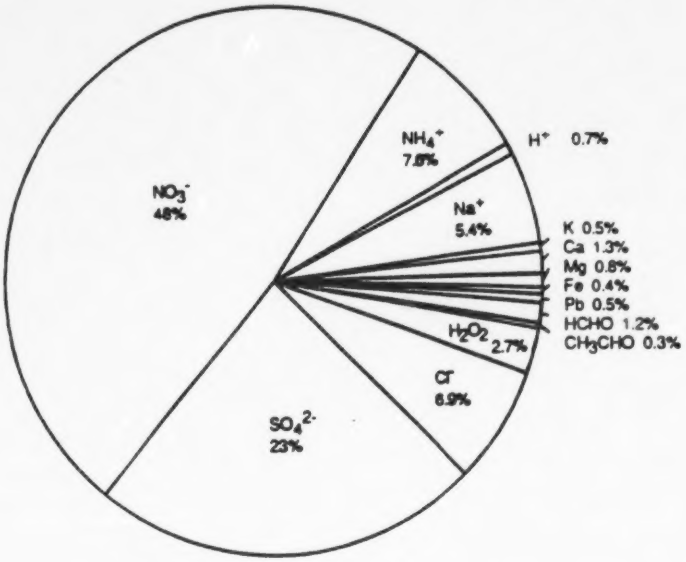

Figure 3. May-June 1985 average cloud water mass camposition. Only species for which chemical analyses were performed are included. Concentrations too small to show in the diagram are SO_3^{2-} 0.03% and Mn 0.02%.

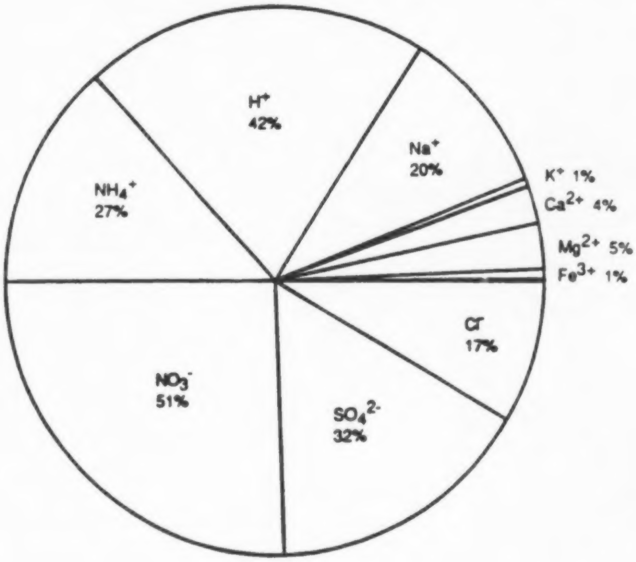

Figure 4. May-June 1985 average cloud water composition in equivalents. Only the determined ionic species are included, and the cation and anion percentages each sum to 100%. Concentrations too small to show are Pb^{2+} 0.2%, Mn^{2+} 0.04%, and HSO_3^- 0.02%.

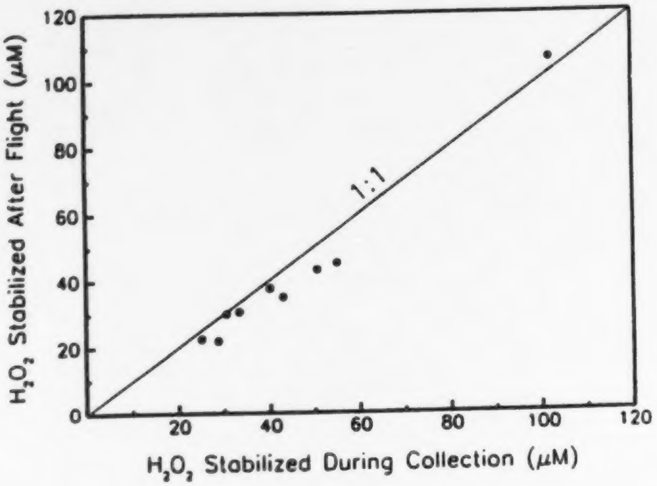

Figure 5. Comparison of cloud water H_2O_2 concentrations measured in simultaneously collected water samples with stabilization after collection and during flight.

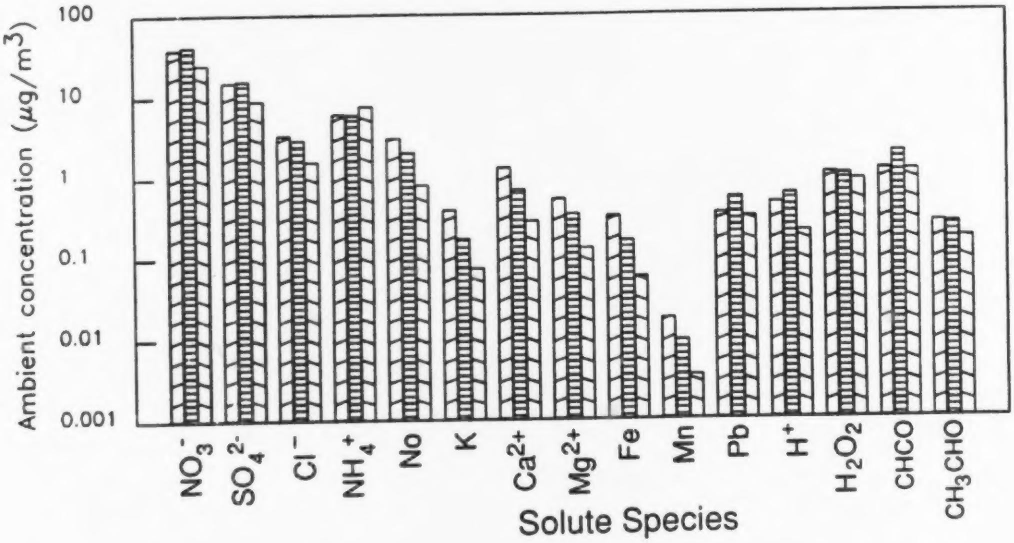

Figure 6. Ambient concentrations of species in the cloud water on a night when there was significant drizzle. The three bars show concentrations measured at 1-h intervals.

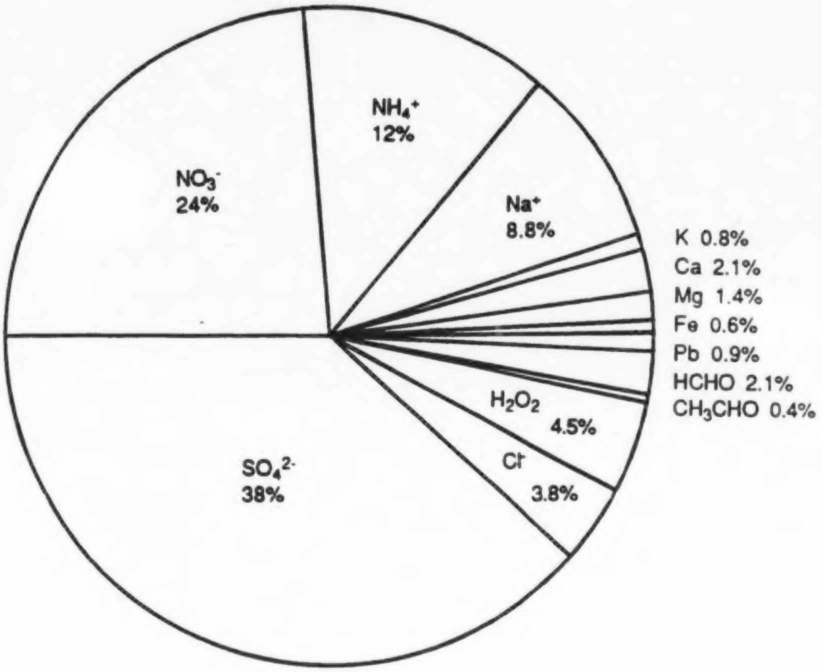

Figure 7. Calculated May–June 1985 average mass composition of the aerosol remaining after cloud evaporation. Only species determined are included. Concentrations too small to show are SO_3^{2-} 0.05%. H^+ 0.04%, and Mn 0.03%. Compare with cloud water composition in figure 3.

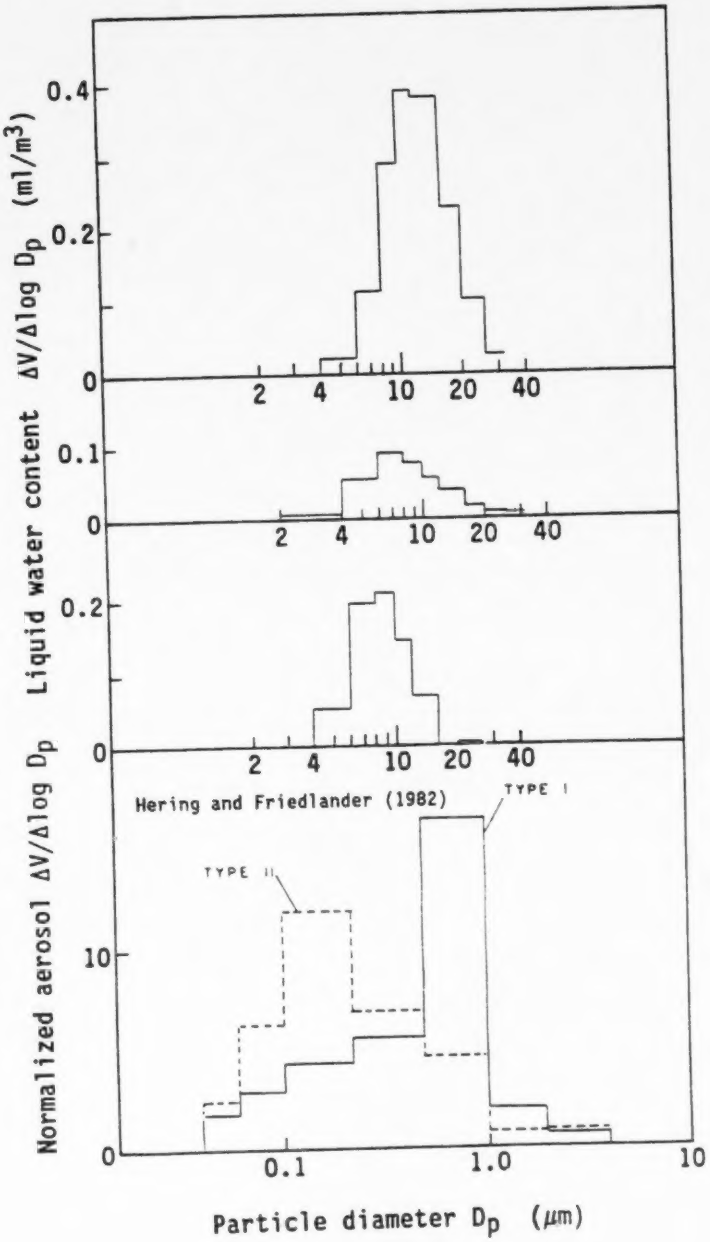

Figure 8. Comparison of calculated aerosol particle size distribution generated by cloud evaporation with size distributions experimentally measured.[33] The three upper panels show cloud droplet size distribution in μm and are displaced horizontally in the figure so the scale at the bottom gives the aerosol size distribution resulting from cloud evaporation.

Cloud Chemistry and Occurrence in the Western United States: A Synopsis of Current Information

Patricia S. Muir[1]
Margi Böhm[2]

[1] *Department of General Science,*
Room 355 Weniger Hall
Oregon State University
Corvallis, OR 97330-6505

[2] *NSI Technology Services Corporation*
U.S. EPA Environmental Research Laboratory
Western Conifers Research Cooperative
200 SW 35th Street
Corvallis, OR 97333

INTRODUCTION

In coastal and mountainous environments, the interception of cloud droplets may account for a large fraction of the moisture and chemical loading to the ecosystem.[1] Recent information implies that the chemistry of the clouds may also play an important role in the condition of the receptor ecosystems. Fog and cloud water often contain higher concentrations of inorganic ions than rain, and strongly acidic fogs and clouds have been documented at several sites in the United States and Europe, including southern California,[2-6] a suite of sites in the eastern United States ranging from Maine to Virginia,[7,8] the midwestern United States,[9] the Po Valley in Italy,[10] and the Glatt Valley in Switzerland.[11] High concentrations of potentially toxic organic compounds have also been detected in fog water (e.g., pesticide alteration products).[12] Unexplained declines in forest condition tend to increase with elevation where cloud immersion is more frequent.[13,14] Exposure of forest ecosystems to cloud water enriched with H^+ or other chemicals (e.g., nitrogen species, heavy metals, or toxic organics), in concert with additional anthropogenic (e.g., ozone) and natural stresses (e.g., drought), may contribute to these declines (op. cit.).

Many forests in the western United States are subjected to severe drought stress during the growing season. Fog and cloud events alleviate this stress by providing moisture to the system. The quantity of intercepted water is related to the area and density of the tree profile; to the degree of exposure of the trees to windblown fog or cloud; and to the frequency of occurrence, liquid water content (LWC), and duration of the fog or cloud event. For example, the annual moisture input under a forest canopy in coastal and western Oregon is 26–40% greater than in the open, because of interception of fog or non-precipitating clouds by the foliage.[15,16] Coastal fog in California is an important source of moisture to the redwood forests; in one month, the equivalent of 50–100% of the annual rain volume for the area was intercepted by the vegetation and introduced to the ecosystem by cloud-drip.[17] Similar results apply to coastal Douglas fir forests in northern California.[18] Although the accuracy of these numbers may be questioned because of outdated sampling techniques, the interception of moisture from fog and cloud obviously plays an important role in the water budget for these areas.

Western forests are efficient at trapping moisture from fog and nonprecipitating cloud; therefore, fog and cloud may provide an important contribution to the total input of chemical species to these ecosystems. Unfortunately, there are no regional programs that are studying cloud droplet interception, chemistry, and deposition in western forests. In addition, very little information is available on the frequency of occurrence and duration of cloud events in forested areas. There is a need to assess the potential for cloud interception and associated deposition of chemicals to western forests, based on the chemistry, frequency of occurrence, and duration of fog and cloud events.

This paper strives to summarize information available on the chemistry and occurrences of clouds across the western United States and to identify data and research needs. Areas most likely to be impacted are identified and the seasonal characteristics of impact are discussed. This information, together with information on western cloudwater chemistry, can provide an estimation of the potential importance of cloud interception to forests of the West. Emphasis will be placed on nonprecipitating, low-level clouds such as stratus and stratocumulus in forested areas of the conterminous United States west of 105°W. Since fog (e.g., maritime, radiation, etc.) is technically stratus cloud at ground level and since we will limit our discussion to nonprecipitating cloud types, we shall use the term "cloud" to refer to all nonprecipitating, low clouds, including fog.

MATERIALS AND METHODS

Cloudwater Chemistry

Data Description. The data on ionic composition of cloudwater used in this study were taken from published reports on cloud chemistry from the western United States. These reports presented data either as means or medians, means or medians with maximums and minimums, or as ranges. Range data were most common; thus, reports that presented only median or mean ionic concentrations were excluded. Additional criteria for the inclusion of data in our analysis were chosen to maximize the number of comparable studies:

1. Only those reports giving data on concentrations of H^+ (or pH), Na^+, Ca^{2+}, Mg^{2+}, NH_4^+, SO_4^{2-}, NO_3^-, and Cl^- were included.

2. Reports that gave data weighted by liquid water content were rare and therefore were excluded.

The final data set consists of information from sites ranging from urban and industrial (Los Angeles Basin) to remote and forested (northern California, Oregon, and Alaska) (Table I). Elevations ranged from approximately 75 meters above sea level (masl) to 1856 masl. In southern California most sampling occurred in winter (December, January, February), whereas spring or fall collections were more common at the other sites (Table I).

We used data on maximum and minimum concentrations of H^+ (as pH), Na^+, Ca^{2+}, Mg^{2+}, NH_4^+, Cl^-, SO_4^{2-}, and NO_3^- to maximize the number of published studies that we could compare. Our use of range data may disguise apparent differences in cloudwater chemistry between sites and events, but the general patterns revealed by our analyses are likely robust. While undoubtedly important in influencing cloudwater acidity, particularly in some regions of the West,[8,19] data on organic acids were not included, as few published studies report such data. Similarly, we did not include data on LWC as those data are often not measured or presented. Finally, we have not adjusted for oceanic contributions as our focus is potential impact of acid clouds on western forests regardless of ion sources.

Published cloudwater composition data that include concentration ranges for ions are of two basic types. One type gives data for sequential samples within a single cloud event, while the other addresses data spanning a series of different events. We distinguished between these in our analyses. Henceforth, we will use "event" to refer both to single cloud events and to different events for which composite data are available, but will distinguish between the two where necessary. Our data on maximum and minimum concentrations from sequential samples within a single event are the single highest and lowest concentrations, respectively, for each ion within the sequential series of samples.

Cloudwater Collectors. The clouds were sampled using either the Caltech Rotating Arm Collector[20] (RAC) or active strand collectors such as the Caltech Active Strand Cloudwater Collector[21] (CASCC) and the CWP Active Strand Collector[22] (CWP-ASC). The RAC collects cloud droplets by impaction in slots on the leading edges of a rotating Teflon-coated rod. Centrifugal force drives droplets into the collection bottles. The instrument has a 50% size cutoff of approximately 15 μm,[23] collects droplets up to 100 μm diameter efficiently, and traps about 60% of the total liquid cloudwater.[20] The active strand collectors sample cloud by impaction of the droplets on Teflon strands. Cloudwater is drawn across a bank of Teflon strands using a fan located at the rear of the collector. The coalesced droplets accumulate in a collection bottle located beneath the strands. Data from studies using two types of active strand collectors are reported in this paper. The bank of Teflon strands is vertically oriented in the CWP-ASC,[22] but inclined at an angle of 35° from vertical in the CASCC.[21] The angled strands have a higher individual collection efficiency, but the CWP-ASC has more rows of strands, resulting in similar total collection efficiencies for the two instruments.[23] The active strand collectors have a 50% size cutoff of 3.3–3.5 μm and efficiently collect droplets of 2–100 μm.[21,23]

Although the chemical composition of cloud samples can be affected by the type of collectors used,[24] samples collected by the RAC and a slightly modified CASCC did not differ significantly in concentrations of H^+, Na^+, Ca^{2+}, Mg^{2+}, NH_4^+, Cl^-, NO_3^-, or SO_4^{2-}.[25] Differences between samples collected by these two types of instruments were not greater than those between co-located RACs.[25] In addition, the differences in concentrations for H^+, NH_4^+, SO_4^{2-}, and NO_3^- were particularly small, whereas those for Ca^{2+}, Mg^{2+}, Na^+, and Cl^- were larger.[25] The samples collected using the RAC had higher concentrations of the latter ions than those collected using the modified CASCC.[25] Hence, some caution should be used when comparing concentrations of Ca^{2+}, Mg^{2+}, Na^+, and Cl^- in samples collected by the RAC and active strand collectors.

The ionic composition of samples collected with the CWP-ASC has not been compared with that from the CASCC or modified CASCC. Differences are probably small as the instruments differ mainly in residence time of the sample on the strands (shorter with the CASCC, reducing the potential for evaporation during periods of patchy cloud).[23] There are also small, but droplet size dependent, differences in collection efficiency between the two instruments for droplet diameters less than 10 μm.[23]

Cloud Occurrence

Data Description. Meteorologists have been collecting information on cloud type, base height, and degree of cloud cover for decades. However, very few observations are available for forested regions, especially over an area as large and with as much complex terrain as the West. The most complete published description of cloud occurrence in the West can be found in the *Atlas of Global Distribution of Total Cloud Cover and Cloud Type Amounts Over Land*, which was constructed using routine weather observations coded by the observers of the World Meteorological Organization (WMO).[26] The information is presented as multiyear averages by quarter (where December, January, and February comprise winter) for 5° (latitude) x 5° (longitude) grids. Observations were made four to eight times a day depending on quarter of year and grid location.[26] The frequency of occurrence (%), amount-when-present (%), average cloud amount (%), average base height, phase and amplitude of diurnal cycle, and interannual variation are presented for total cloud; low clouds such as stratus, stratocumulus, nimbostratus, cumulus, and cumulonimbus; middle clouds such as altocumulus and altostratus; and high clouds such as cirrocumulus, cirrostratus, and cirrus. Since middle and high clouds are not likely to intercept terrestrial ecosystems, only the characteristics of low clouds, particularly stratus (St) and stratocumulus (Sc), are of interest in this paper.

The western United States is covered by a 4 x 5 matrix of 5° x 5° grids. A total of 85 WMO reporting stations across the West were used to generate the cloud atlas.[26] Since the reporting stations are usually located at airports and near urban areas, the cloud atlas is probably not representative of forested and high elevation areas. However, it does provide an estimation of the condition of the atmosphere within the sphere of vision at each site. In most cases, this sphere should include at least the lower slopes of nearby mountain ranges. While mountain slopes that are above the visible cloud base are not necessarily immersed in cloud, the WMO data provide information for potential impaction at elevations above the reported mean base heights.

DATA ANALYSIS

Cloudwater Chemistry

The concentration data are expressed in µeq/l. Since the data exhibited log-normal distributions, statistical analyses were performed on log-transformed data.

Data on ionic composition of cloudwater were analyzed by principal components analysis.[27,28] (Data matrix consisted of 36 events by 16 ionic concentration variables, representing maximums and minimums for H^+, Na^+, Ca^{2+}, Mg^{2+}, NH_4^+, Cl^-, NO_3^-, SO_4^{2-}). Principal components analysis maximizes the variance extracted by a set of orthogonal components from multivariate data.[27] The components are linear combinations of variables (in our case, ionic concentrations). The technique allows for the reduction of an n-dimensional space into a few components that capture as much of the correlation structure as possible. The principal components were extracted from a matrix of correlation coefficients between the ions.

Similarities among ions were expressed using a hierarchical agglomerative cluster analysis, which groups ions according to similarity.[28] We used Ward's method as the clustering algorithm on a matrix of Euclidian distances among ions in sample space.[29] The logarithm of Wishart's objective function was used to scale the resulting dendrogram.[30]

Cloud Occurrence

Information on how often St and Sc occur during each quarter is not directly available from the Cloud Atlas. The "frequency of occurrence" category refers to percent occurrences within a cloud level rather than to the total number of observations. This category is thus of little use in determining the impact of St/Sc on terrestrial ecosystems, but rather serves to identify which of the low clouds is predominant. "Average cloud amount" (expressed as % of sky cover) is the overall average percent of the sky covered by a cloud type, including times when it was not present. Average cloud amount for each quarter was calculated using all observations for a particular hour averaged together regardless of year.[26] That is, summed across all years of record.

$$\text{Average cloud amount (\%)} = [100 * [\Sigma(c_1)]/N_1 + \ldots + 100 * [\Sigma(c_i)]/N_i]/n \qquad [1]$$

where i = hour of observation,
n = number of observations per day,
N_i = number of observations for hour i across all years,
c_i = cloud cover in eighths for hour i.[31]

Since certain clouds exhibit a systematic diurnal cycle that may not be reflected in the data set, this averaging approach is desirable because it normalizes hourly observations relative to the frequency with which those observations were made. Thus, eq. [1] minimizes the diurnal bias that would be present if the mean were constructed by averaging all observations regardless of time of day. The results from equation [1] are not biased by annual trends, since Warren et al. did not find good evidence for annual trends.[26]

An estimate of the number of days during which St/Sc cloud occurred can be obtained by assuming that $N_1 = N_2 = \ldots = N_i$ = (total # observations) / n = # observation days. Equation [1] then becomes

$$\text{Average cloud amount (\%)} = 100 * S(c_i) / N \qquad [2]$$

where N = least # observation days/year.

The maximum cloud cover possible is 8/8. If all cloud occurrences were 8/8, then $S(c_i)$ = # completely overcast days, which will, by definition, be less than the number of partially cloudy days (i.e., 1/8 through 7/8) given the same $S(c_i)$. It then follows from equation [2] that,

$$\text{Least Number of Observation Days with St/Sc} = \text{Average cloud amount (\%)} * N/100 \qquad [3]$$

We are now able to estimate the minimum number of days during which St/Sc clouds were observed for each quarter of the year.

The cloud base estimates were superimposed on eight topographical transects (Figure 1) to indicate where interception with stratus and stratocumulus cloud (excluding ground based stratus) is most likely. This information together with St/Sc cloud characteristics from the Cloud Atlas[26] (Table IIa,b,c,d) can be used to infer where, how often, and when interception with stratus and stratocumulus clouds is most likely to occur across the West.

RESULTS AND DISCUSSION

Cloudwater Chemistry

There were large ranges in cloudwater ionic concentrations within events at specific sites and also substantial differences among sites (Figure 2a,b). The samples were generally dominated by SO_4^{2-}, NO_3^-, and NH_4^+, and to a lesser extent by Cl^-, Na^+, and Ca^{2+}. Maximum nitrate concentrations were often higher at western sites in southern California and Sierra Nevada than at some sites in the eastern United States (e.g., see data for Loft Mtn., VA; Mohonk Mtn., NY; Whiteface Mtn., NY; Hubbard Brook, NH; Lakes-of-the-Clouds, NH; and Bar Harbor, ME).[7,8] The ratio of mean maximum SO_4^{2-} to mean maximum NO_3^- in western clouds was 0.7, which is lower than typically recorded for eastern sites.[7,8] Most samples from southern California were as acidic, or more so, than those from the eastern United States (mean minimum pH for southern California sites = 2.52; mean minimum pH for several eastern U.S. sites = 2.92).[8] However, the cloud samples from the more northern and remote of the western sites were generally less acidic than those from the eastern United States (mean minimum pH for clouds from Alaska,[32] Oregon,[32] Redwood National Park,[33] and Yosemite and Sequoia National Parks[19,34] = 4.48).

Differences in cloud chemistry among sites and events were revealed by the principal components analysis (Figure 2a,b, Table III). The first principal component probably represents the total dissolved ionic composition of the events. The first axis (component) explained 71% of the variance among event chemistries (Table IV). The maximum and minimum concentrations of all ions were strongly and negatively correlated with this axis (Table IV). Thus, events with higher ionic concentrations are found on the left of the first axis (Figure 2a,b). Interestingly, H^+ had the weakest correlation with the first axis. In addition, other cations such as NH_4^+, Na^+, and Ca^{2+} were usually present in higher concentrations than H^+.

The location of events on the first axis corresponds roughly to a south-north gradient in sampling sites, although the variability in cloudwater concentrations among events at specific sites can be substantial (Table III, Figures 2a,b and 3). The two extreme events were samples from Upland, California[4] and from Yosemite National Park, 13 Nov., 1988.[19] The Upland sample had a high total ionic strength, and was particularly high in NO_3^- while the Yosemite sample was much more dilute, especially with respect to NO_3^-, SO_4^{2-}, and NH_4^+ (Table III, Figure 2a,b). Not surprisingly, the most acidic and enriched cloud events were from southern California (lowest pH = 2.06, Henninger Flats[6]; highest $[NO_3^-]$ = 16,300 μeq/l, Henninger Flats[6]; and highest $[SO_4^{2-}]$ = 9,400 μeq/l, Bakersfield[35]). The least acidic and enriched cloud events were from the more northern and remote sites, although one southern California sample had the lowest acidity (minimum $[H^+]$ = 0.1 μeq/l, Bakersfield[35]; also note (Figure 2b) the unusually high maximum $[NH_4^+]$ = 13,300 μeq/l for this site). The maximum concentrations of SO_4^{2-}, NO_3^-, and NH_4^+ in the clouds of Alaska,[32] Oregon,[32] Redwood National Park[33] and Yosemite and Sequoia National Parks in California[19,34] were generally lower by one or two orders of magnitude than concentrations recorded in the southern California clouds (Figure 2a,b). Some site-site and event-event differences in ionic concentrations may have been caused by differences in LWC; unfortunately LWC data were not generally available.

The first axis corresponds well, but not perfectly, with geography (Figure 3). For example, note the unusually high concentrations observed on April 24, 1986, at Giant Forest, Sequoia National Park (Table III, Figures 2a,b and 3). The other two samples from Giant Forest were much less concentrated and are located far to the right on the first axis (Table III, Figures 2a,b and 3). For the most part, however, the similarities between different events sampled at the same site are striking; variations in chemistry are greater among different sites than between different events from the same site. Notice the closeness between the two samples from Lennox, CA, and between the two samples from Henninger Flats, CA. The latter two samples were separated by a year. The occurrence of regional-scale cloud events is suggested by the similarity in location on the first principal axis of the samples collected on April 28, 1988, at Sequoia and Yosemite National Parks (ranks by score are 12 and 13 respectively).

The samples from Oregon and Alaska are located toward the right end of the first axis, but are not the most dilute in the data set; some samples from Yosemite and Sequoia National Parks had lower overall ionic strengths (Figures 2a,b and 3). The samples from Oregon and Alaska were dominated by Na^+, Cl^-, and SO_4^{2-}, (oceanic constituents). The samples from Sequoia and Yosemite tended to be dominated by NH_4^+, NO_3^-, and SO_4^{2-}, which are usually more representative of anthropogenic influences. (Sources of sulfate may be both oceanic/natural and anthropogenic.) The samples from Redwood National Park in northern California had higher ionic strengths than those from Oregon and Alaska, but were not necessarily less concentrated than samples from Sequoia and Yosemite, despite the greater proximity of the latter to urban sources. Seasalt components (Na^+ and Cl^-) tended to be more important constituents of cloudwater from Redwood than from Sequoia and Yosemite, as would be expected with Redwood National Park's proximity to the ocean. These contributions enhanced the total ionic loading of the Redwood samples. On the other hand, anthropogenic influences were evident in higher concentrations of NO_3^- in many of the Sequoia and Yosemite samples than in the samples from Redwood.

We are unable, for the most part, to make inferences about the importance of variables such as type of cloud collector, type of cloud (e.g., maritime and radiation fog versus stratus or stratocumulus cloud), site type (urban/industrial/forest/agricultural), site elevation, or season of year as predictors of event chemistry because these factors covary with sampling areas in our data set. For example, most of the data from southern California are from urban or industrial regions at low elevations, while the more northern data are all from forested areas at relatively high elevations. However, the samples from Henninger Flats, CA are from a forested area at 870 masl, 25 km NE of the Los Angeles Civic Center.[6] These samples are similar to, but less concentrated than, the other highly enriched samples from southern California, which suggest that the proximity of the site to a large urban center is important in influencing its cloud chemistry. Henninger Flat's elevation and dilution of the polluted air mass by cleaner drainage flows down the mountain slope at night may have slight mitigating effects.

To increase our understanding of cloud deposition of chemicals to western forests, we need data from a greater diversity of western sites, seasons within sites, and types of fogs and clouds. For example, fogs (as defined by the researchers; e.g., maritime and radiation fogs) tended to be more highly enriched than clouds in our data set (Figure 4). Is this a general difference between fogs and clouds, or an artifact of our having radiation fog data primarily from urban/industrial areas and cloud data from more remote sites? Three cloud events, as opposed to fog events, (two from Henninger Flats, southern

California) were found toward the highly enriched end of the concentration gradient, suggesting that the apparent differences in ionic concentrations between fogs and clouds revealed here result, at least in part, from limitations in data availability. As another example, cloudwater sampled in the winter (December, January, February) appears to be more highly concentrated than that sampled at other times of year (Figure 4). This contrasts with rainwater results, which often are more enriched in summer than in winter.[36] Because time of year, collection site, and event type (fog vs. cloud) covary in our data set, it is impossible to determine the true seasonal patterns in cloud chemistry. More data are needed to more fully answer these and related questions.

As was indicated by the principal components analysis, correlations between different ions and between maximum and minimum concentrations of a given ion were positive, and generally large. Thus, concentrations of the ions varied in parallel between events, such that all ions were giving similar information about the ionic strength of the cloudwater. The strongest relationships were found within three groups of ions that are probably representative of three different source contributions to cloud chemistry (Figure 5):

1. Na^+, Mg^{2+}, and Cl^- from sea salt
2. Ca^{2+} and Mg^{2+} from soil dust
3. SO_4^{2-}, NO_3^- , and NH_4^+ from anthropogenic activities

Note, in particular, the similarity between NO_3^- and NH_4^+ (both for maximums and minimums), and their similarity with SO_4^{2-}. H^+ shows a relatively low similarity to the other ions, and indeed samples with high ionic strength were not necessarily high in H^+ concentration. The available published data on western cloudwater chemistry do not allow us to perform a detailed analysis of source contributions.

Most of the variation in ionic content was explained by the first principal component. The second axis accounted for about 12% of the variance in the data set, and the third axis for about 6% of the variance (Table IV). The second principal component appears to relate primarily to the range in ionic concentrations within events. Events with relatively large differences between maximums and minimums for each ion were found toward the top of the axis, and those with lower intra-ion variability were found toward the bottom of the axis. The differences in intra-ion variability among events relate largely to the period of integration of each event. Sequential samples within a single event generally had lower intra-ion variability than did those data composited from several different events (see Table I for description of data types). Thus, the number of cloudwater samples comprising each event was positively correlated with the second principal component (Pearson's $r = 0.68$). The third principal component had low explanatory power, and correlations of ions with the axis were generally weak and not readily interpretable (Table IV); the artifact identified in the second principal component may have weakened the ionic signatures in the residuals.

Thus, the variability in cloudwater chemistry among sites and events was best explained by the first principal component and by the results of the cluster analysis. These two analyses indicate that:

1. the primary axis of variability is one of total dissolved ionic concentrations,

2. ionic concentrations (including acidity) generally decrease from southern California toward more northern and remote sites.
3. concentrations of all ions are positively correlated across events.
4. ions in three source groups; anthropogenic, sea salt, and soil dust, exhibit similarities.
5. the relative importance of each source group as an influencer of cloudwater chemistry varies with study site.
6. the method of compositing data affects data comparability among studies; composites across a number of cloud events have larger intra-ion variabilities than do composites of sequential samples within one event.

There is a striking similarity between results 1, 3, and 4 and those obtained by a principal components analysis of cloud chemistry data for Sequoia National Park.[19] The first principal axis is attributed to the same source of variation; large, positive correlations between inorganic ions were also found; and the same three major source groups of ions were hypothesized. Further, there is agreement in percent variation attributed to the three principal axes. Since the data used in our analyses exhibit a larger concentration and geographic range than the data from Sequoia National Park,[19] it is remarkable that the results are so similar.

Cloud Occurrence

Regional Patterns in Cloud Occurrence. The regional patterns in ground level cloud (fog) occurrence across the United States have been described and mapped using information from airports and weather stations.[37-39] In general, the data are limited and the maps only show the relative distribution of fog in valleys.[37] The maps generally exhibit similar patterns. However, the Court and Gerston[39] map estimates frequencies of occurrence that are 20–50% higher than the others,[37,38] while using fewer stations and a longer period of record.

The number of days with ground-level cloud (fog) decreases rapidly with distance inland from the Pacific coast. For example, coastal areas annually receive fog during 60 days and the central West is exposed during fewer than 10 days. Fog frequency may be about 8% higher north of San Francisco than to the south.[37] There is a noticeable influx of coastal fog into the Willamette Valley, OR, and Puget Sound, WA, allowing the western slopes of the Cascades to be exposed to maritime and radiation fogs during an estimated 45 days per year. There is little influx of coastal fog into the Central Valley of California, although fogs (maritime and radiation) are estimated to occur 30 days/year along the western slopes of the Sierra Nevada (Stone[37] estimates the average exposure in the Sierra Nevada at less than 15 days per year). Fog is estimated to occur during 15–45 days per year in the northern Bitterroot Mountains of Idaho and Montana.

The seasonal patterns in ground level cloud (fog) occurrence are a function of the formation process, latitude, and altitude. For example, advection fog (caused by differences between the surface temperatures of air and water), as found along the Pacific coast, has a summer maximum. In Washington, the maximum occurs in August with fog during 12 days at Tatoosh Island, and in California, Pt. Conception receives most advection fog from June through September with 40 hours per month exposure.[37] On the other hand, patterns of ground level cloud (fog) formed in the Continental regime (e.g., radiation fogs) exhibit less seasonal consistency. For example, Cheyenne, WY, shows a slight maximum during May, but since fogs occur during less than 2 days for any given month, this is probably insignificant. Salt Lake City rarely experiences continental fogs, although fog can be expected to occur during 2 days in January. Fresno, CA, has a marked winter peak, with continental fogs forming during 9 days in December and January (the "Tule" radiation fog), whereas in Seattle, WA, the continental fog maximum (6 days) is in October.[37]

Limited information on cap and orographic cloud formation across the West is also available from several research projects in the Washington Cascades and the Colorado and Wyoming Rockies.[40-43] For the Washington Cascades and Olympic Mountains, only the data from the National Oceanic and Atmospheric Administration (NOAA) site at Stampede Pass (east of Seattle at 1200 masl) are considered complete enough for this report.[40] The data are 16 hourly observations per day, presented for 1982-1987. The mean number of days during which Stampede Pass is exposed to cloud does not vary much from December to June (15–25 days/month), but during the summer months there is a reduction in cloud occurrence (12–20 days/month). November seems to be the cloudiest month (28 days with cloud) at this site. These data indicate that, on average, Stampede Pass (and other similar sites in the Cascades) is exposed to cloud during more than 200 days per year. This estimate of exposure far exceeds that predicted by Stone[37] and Court and Gerston[39] and illustrates the limitation of their maps for area-specific applications.

During the winters of 1980–81 and 1983–84, the frequency of occurrence and duration of "liquid cloud" or fog in the Colorado Rockies was investigated using observations made every morning and evening by volunteers.[41,42] The results indicate that liquid clouds occur more frequently over the southern and northern Rockies than over the central Rockies, which is not surprising since the sites in the south and north are located on the primary barriers intercepting the westerlies. The frequency and duration of wintertime liquid water clouds impacting the Rockies near Steamboat Springs, CO, were studied in more detail.[42] The site was enveloped in cloud for 24% of observed time during December, 1981, and January, 1982.

Elk Mountain, an isolated peak at the north end of the Medicine Bow Range in southern Wyoming, is covered by clouds about 1 of every 3 days from November to April.[43] The base heights of these cap and orographic clouds are typically between 2600-3400 masl.

Estimation of Areas Impacted by Stratus and Stratocumulus Clouds. The average base heights for above ground St and Sc[26] are superimposed by quarter on eight topographical transects of the West to identify regions of interception (Figure 1). The regions discussed relate to the four rows of the 4 x 5 matrix of 5° x 5° grids covering the West.

Region 1 covers Washington, northern Idaho, and Montana. The predominant clouds are St/Sc in winter and cirrus during the remaining seasons (Table IIa). The areas most likely to intercept St and Sc clouds are the western slopes of the Cascades, Washington, and the Bitterroot Range, Idaho/Montana (Figure 1). (The Olympic Mountains west of Seattle are included with the Cascades.)

Region 2 includes Oregon, northern California, southern Idaho, northern Nevada, northern Utah, Wyoming, and northern Colorado. The predominant cloud types covering this area are St/Sc west of the Cascades, and high clouds such as cirrostratus, cirrocumulus, and cirrus to the east (Table IIb). The areas most likely to intercept St/Sc clouds are the western slopes of the Cascades, the western and northern slopes of the Bitterroot Range, the highest peaks of the Bighorn Mountains, and the northern Front Range, Colorado (Figure 1).

No cloud interception is anticipated over the high desert of Nevada, northern Utah, and southern Wyoming.

Region 3 is comprised of central California, Nevada, Utah, northern Arizona, Colorado, and northern New Mexico. The predominant cloud type is St/Sc west of the Sierra Nevada, and high clouds such as cirrocumulus, cirrostratus, and cirrus to the east (Table IIc). The California Coast Range, the western slopes of the Sierra Nevada, the southern, western and eastern slopes of the San Juan Mountains, the Front Range, Colorado, and the Sangre de Christo Mountains, New Mexico, are most likely to intercept St/Sc clouds (Figure 1).

Region 4 covers southern California, Arizona, and New Mexico. The predominant clouds experienced over this region are St and Sc west of the Coast Range (except during winter when cirrus clouds are more dominant), and high clouds such as cirrocumulus, cirrostratus, and cirrus to the east (Table IId). The only areas where cloud interception is anticipated are the Coast Range, California, (including San Gabriel and San Bernardino Mountains around the Los Angeles Basin) and the highest peaks of the Sacramento Mountains, New Mexico (Figure 1).

Thus, stratus and stratocumulus clouds are expected to intercept with terrestrial ecosystems in the Coast Range of Washington, Oregon, and California, the western slopes of the Cascades and the Sierra Nevada, with the peaks of the Bitterroot Range of Idaho and Montana, the Bighorn Mountains (and Wind River Range) of Wyoming, and with the San Juan Mountains and Front Range of Colorado and New Mexico.

North-South Gradients in Cloud Occurrence within Mountain Ranges. Information on the north-south gradients of cloud occurrence is available for three of the identified mountain ranges: the Cascades, the Coast Range, and the Front Range (Table II).

The frequencies of exposure to St/Sc clouds (including ground-level fog) do not vary much between the northern and southern Cascades, although the range in base heights (of above ground-level cloud) decreases from 750-900 masl in the north to 700-800 in the south (Table IIa,b). The maximum period of occurrence of St/Sc clouds is winter, when average sky cover by St/Sc is 47-49% (St/Sc occurrence during 36 days). Exposure to St/Sc clouds during spring, summer, and fall is also substantial (Table IIa,b). On average, St/Sc clouds are observed to cover in excess of 30% of the sky during all seasons of the year. This translates to expected exposure during at least 100 days/year.

There are subtle differences in frequencies of occurrence of St/Sc clouds (including ground-level fog) along the Coast Range, California, with the southern areas receiving less exposure (Table IIc,d). The average base heights of above ground-level St/Sc are slightly higher in the north. The maximum period of occurrence is summer (average sky cover by St/Sc is 34-40%, i.e., St/Sc clouds occur during at least 18-23 days), although the seasonal range is less than in the Cascades. It is estimated that, on average, the Coast Range of California is exposed to St/Sc during more than 100 days/year.

The southern portion of the Front Range consistently receives fewer occurrences of St/Sc clouds than the north, and the average base heights of above ground-level St/Sc are also consistently higher in the south (Table IIb,c). The Front Range is exposed to non-precipitating clouds more often in spring (on average, 19–27% of sky is covered with St/Sc clouds, i.e., potential exposure during, at least, 15 days). Summer exposures are low. On average, the Front Range is exposed to St/Sc during, at least, 73 days of the year.

North-South Gradients in Cloud Occurrence across the West. Although there are seemingly few north-south differences in St/Sc occurrence in the Cascades and Coast Range, there is a noticeable difference between these two areas (Table II). The season of maximum occurrence of St/Sc clouds is winter in the north (Cascades) and summer in the south (Coast Range, California). In addition, St/Sc clouds cover 25% more sky (and therefore greater potential for occurrence) in the north than in the south during winter and the converse is true for summer. Spring and fall frequencies are similar to each other as well as across the north-south gradient. The average base heights are not much different in winter (700–750 masl in the north compared to 590–650 masl in the south), but during the remainder of the year, the base heights in the Coast Range are between 200 and 310 m lower than in the Cascades.

There is also a significant difference between cloud occurrence in the Cascades (north) and the Sierra Nevada (south). St/Sc occurs twice as often in winter in the north (49% of sky cover attributed to St/Sc clouds) than in the south (22% of sky cover attributed to St/Sc clouds, i.e., exposure during 14 days); in spring and fall, the northern mountains are exposed to St/Sc three times more often than in the south; and in summer, the southern mountains rarely experience St/Sc clouds.

East of the primary western orographic barriers, we can compare the frequency of occurrence of St/Sc clouds in the Bighorn Mountains in the north with that in the San Juan Mountains in the south (Table II). There are no striking differences between these two areas, except that the average base heights are higher in the south, and there is no anticipated interception during summer in the north. In both cases, only the highest peaks will intercept St/Sc clouds, and even then, interception is probably infrequent (St/Sc clouds covered on average, 22% of the sky in winter, 16% in spring and fall, and 7% in summer).

West-East Gradients in Cloud Occurrence across the West. In the northern areas of the western U.S., there is a distinct reduction in the frequency of occurrence of St/Sc clouds between areas west versus east of the Cascades. Comparisons between the Cascades (west), Bitterroot Mountains (central), and the Bighorn Mountains (east) show that in winter, St/Sc clouds cover 9% more of the sky in the west than central regions, and 22% more in central than eastern regions. During the remainder of the year, similar average cloud cover is attributed to St/Sc in the central and eastern areas, however the western areas record 16% more sky cover in spring and fall, and 21% more in summer (Table IIa,b,c,d).

Elsewhere, similar relationships hold. For example, a comparison of frequency of occurrence of St/Sc clouds impacting the Coast Range, Sierra Nevada, San Juan Mountains, and Front Range of Colorado shows the same kind of results. The main differences are between the areas to the west and east of the primary orographic barrier (in this case, the Coast Range). The Coast Range receives 14% more St/Sc in winter, 16% more in spring and fall, and 32% more in summer than the areas to the east (Table II). Less area is probably impacted by St and Sc clouds to the east of the Cascades and the Sierra Nevada than to the west (Figure 1). In most cases, in the central West, only the highest peaks intercept the stratus and stratocumulus clouds.

In conclusion, regional estimates of total non-precipitating cloud occurrence across the West are impossible given the lack of published information on the occurrence of cap and orographic cloud. We are thus only able to comment on the frequency with which stratus and stratocumulus clouds are expected to intercept with terrestrial ecosystems in the Coast Range of Washington, Oregon, and California, the western slopes of the Cascades and Sierra Nevada, with the peaks of the Bitterroot Range of Idaho and Montana, the Wind River Range and Bighorn Mountains of Wyoming, and with the San Juan Mountains and Front Range of Colorado and New Mexico.[26,37-39]

Comparisons of cloud frequency data imply the following:

1. In winter, we anticipate 25% more St/Sc clouds along the northern Pacific Coast than in the south; the converse is true for summer. In spring and fall, the entire coast is exposed to similar amounts of St/Sc.
2. Forests along the western slopes of the Cascades are exposed to more St/Sc clouds than those along the western slopes of the Sierra Nevada; we anticipate twice the exposure in winter and three times in spring and fall.
3. Forests to the west of the Cascades and Coast Range, California are exposed to 9–14% more St/Sc clouds in winter, 16% more in spring and fall, and 21–32% more in summer than forests to the east of these primary orographic barriers.
4. The occurrence of St/Sc clouds is similar across the intermountainous area.

CONCLUSIONS

Most interception is anticipated along the Pacific coast in the Coast Range of northern California, Oregon, and Washington and along the western slopes of the Cascades. This interception is considered to be more frequent in summer in the south and winter in the north. The frequency of occurrence of stratus and stratocumulus clouds is low over the Sierra Nevada and central Western Mountains; however, total cloud interception is underestimated due to a lack of information on the frequency of occurrence of cap clouds. Cloud interception is also considered low along the eastern slopes of Wyoming, Colorado, and New Mexico. However, we need more intensive data on the frequency of occurrence, duration, and liquid water content of clouds in western forests to support conclusions on hydrological and chemical inputs to forest ecosystems from cloud interception.

The available data on cloud chemistry indicate that the regions of the western United States in which cloud interception is considered greatest are generally regions with clouds of relatively low ionic concentrations. For example, the limited data from the Coast Range (Mary's Peak, Oregon, and Redwood National Park, California) suggest that clouds in this area are less acidic than clouds to the south. There is, however, a paucity of data on cloud chemistry from most of the Coast Range in Washington, Oregon, and California, and from the western slopes of the Cascades. We need more data on cloud frequency of occurrence, duration, LWC, and chemistry from these areas in which cloud interception is considered most frequent. These data are needed for two reasons: (1) to assess more completely the potential for present impacts on forest ecosystems, and (2) to provide a baseline against which impacts of an increasing human population can be judged. Some of the nation's most productive forests are found in these areas, and any potential injurious impact on these forests should be assessed. We also need a more complete seasonal characterization of cloud chemistry in these areas. For example, cloudwater samples from Mary's Peak were collected during the summer and fall, while interception is anticipated to be most frequent in winter.

There is no information on cloudwater chemistry and occurrence for other areas of the western United States. These areas include the western and northern upper slopes of the Bitterroot Range in Idaho and Montana, as well as the Rocky Mountains.

Although cloud interception is considered low in southern California, the chemistry of the few events that do occur is so concentrated that adverse effects to vegetation may currently exist. Similarly, total deposition of ionic species intercepted by the foliage and introduced to soil systems at the northern sites may not be as inconsequential as the low concentrations lead us to believe, given the high frequency of occurrence of cloud events. However, the concentrations in the northern Cascades and Coast Range are generally too low to directly affect the forest ecosystems. Areas downwind of urban and industrial sources of air pollutants (e.g., western slopes of the Cascades east of Seattle, the Front Range west of Denver) are most likely to intercept acidic clouds and the combination of exposure and acidity may be important to forest health.

ACKNOWLEDGMENTS

We would like to acknowledge those researchers responsible for collecting and publishing the data used in this report, Bruce McCune for his assistance with the data analysis, Terralyn Vandetta for her invaluable graphic capabilities, Rene Wahl and Jane Bruce for assisting with manuscript preparation, and our reviewers for their helpful comments and suggestions. This research was supported by funds provided by the Western Conifers Research Cooperative within the joint U.S. Environmental Protection Agency–USDA Forest Service Forest Response Program. The Forest Response Program is part of the National Acid Precipitation Assessment Program. Mention of trade names or commercial products does not constitute endorsement or recommendation for use.

REFERENCES

1. O. Kerfoot, "Mist precipitation on vegetation," *For. Abstr.*, 29:8 (1968).

2. J.M. Waldman, J.W. Munger, D.J. Jacob, R.C. Flagan, J.J. Morgan, and M.R. Hoffmann, "Chemical composition of acid fog," *Science*, 218:677 (1982).

3. R.L. Brewer, E.C. Ellis, R.J. Gordon, and L.S. Shepard, "Chemistry of mist and fog from the Los Angeles urban area," *Atmos. Environ.*, 17:2267 (1983).

4. J.W. Munger, D.J. Jacob, J.M. Waldman, and M.R. Hoffmann, "Fogwater chemistry in an urban atmosphere," *J. Geophys. Res.*, 88(C9):5109 (1983).

5. D.J. Jacob, J.M. Waldman, J.W. Munger, and M.R. Hoffmann, "Chemical composition of fogwater collected along the California coast," *Environ. Sci. Technol.*, 19:730 (1985).

6. J.M. Waldman, J.W. Munger, D.J. Jacob, and M.R. Hoffmann, "Chemical characterization of stratus cloudwater and its role as a vector for pollutant deposition in a Los Angeles pine forest," *Tellus*, 37B:91 (1985).
7. V.A. Mohnen, and J.A. Kadlecek, "Cloud chemistry research at Whiteface Mountain," *Tellus*, 41B:79 (1989).

8. K.C. Weathers, G.E. Likens, F.H. Bormann, S.H. Bicknell, B.T. Bormann, B.C. Daube Jr., J.S. Eaton, J.N. Galloway, W.C. Keene, K.D. Kimball, W.H. McDowell, T.G. Siccama, D. Smiley, and R.A. Tarrant, "Cloudwater chemistry from ten sites in North America," *Environ. Sci. Technol.*, 22:1018 (1988).

9. P.S. Muir, K.A. Wade, B.H. Carter, T.V. Armentano, and R.A. Pribush, "Fog chemistry at an urban midwestern site," *JAPCA* 36(12):1359 (1986).

10. S. Fuzzi, G. Orsi, and M. Mariotti, "Radiation fog liquid water acidity at a field station in the Po Valley," *J. Aerosol Science*, 14:135 (1983).

11. C.A. Johnson, L. Sigg, and J. Zobrist, "Case studies on the chemical composition of fogwater: the influence of local gaseous emissions," *Atmos. Environ.*, 21(11):2365 (1987).

12. D.E. Glotfelty, J.N. Seiber, and L.A. Liljedahl, "Pesticides in fog," *Nature*, 325:602 (1987).

13. P. Schütt and E.B. Cowling, "Waldsterben, a general decline of forests in Central Europe: symptoms, development, and possible causes," *Plant Disease*, 69(7):548 (1985).

14. B.I. Chevone and S.N. Linzon, "Tree decline in North America," *Environ. Pollut.*, 50:87 (1988).

15. L.A. Isaac, "Fog drip and rain interception in coastal forests," USDA Forest Service Res. Note No. 34, Pacific Northwest Forest and Range Experiment Station, Portland, OR.

16. D.R. Harr, "Fog drip in the Bull Run municipal watershed Oregon," *Water Resour. Bull.*, American Water Resources Association, 18(5):785 (1982).

17. G.T. Oberlander, "Summer fog precipitation on the San Francisco peninsula," *Ecology*, 37:851 (1956).

18. H.D. Azevedo and D.L. Morgan, "Fog precipitation in coastal California forests," *Ecology*, 55:1135 (1974).

19. M.R. Hoffmann, J.L. Collett, and B.C. Daube, "Characterization of cloud chemistry and frequency of canopy exposure to clouds in the Sierra Nevada Mountains," Draft Final Report, California Air Resources Board, Sacramento, CA., Contract No. a6-185-32, 1989.

20. D.J. Jacob, R.T. Wang, and R.C. Flagan, "Fogwater collector design and characterization," *Environ. Sci. Technol.*, 18:827 (1984).

21. B. Daube, Jr., R.C. Flagan, and M.R. Hoffmann, "Active Cloudwater Collector," U.S. Patent No. 4,697,462, 1987.

22. B. Daube, Jr., K.D. Kimball, P.A. Lamar, and K.C. Weathers, "Two new ground-level cloud water sampler designs which reduce rain contamination," *Atmos. Environ.*, 21(4):893 (1987).
23. B. Daube, Jr., W.M. Keck Laboratories, California Institute of Technology, Pasadena, CA, private communication, 1989.

24. S.V. Hering, D.L. Blumenthal, R.L. Brewer, A. Gertler, M.R. Hoffmann, J.A. Kadlecek, and K. Pettus, "Field intercomparison of five types of fogwater collectors," *Environ. Sci. Technol.*, 21:654 (1987).

25. D.J. Jacob, J.M. Waldman, M. Haghi, M.R. Hoffmann, and R.C. Flagan, "Instrument to collect fogwater for chemical analysis," *Rev. Sci. Instrum.*, 56(6):1291 (1985).

26. S.G. Warren, C.J. Hahn, J. London, R.M. Chervin, and R.L. Jenne, "Global Distribution of Total Cloud Cover, and Cloud Type Amounts Over Land," U.S. Dept. of Energy, DOE/ER/60085-H1, 1986.

27. B.G. Tabachnick and L.S. Fidell, *Using Multivariate Statistics*, Harper and Row, NY, 1983.

28. B. McCune, "Multivariate Analysis on the PC-ORD System," Holcomb Research Institute, Butler University, Indianapolis, IN, HRI Report No. 75 (1987).

29. J.H. Ward, Jr., "Hierarchial grouping to optimize an objective function," *J. Amer. Statist. Assoc.*, 58:236 (1969).

30. Wishart's objective function (D. Wishart, "An algorithm for hierarchial classifications," *Biometrics*, March:165, 1969).

31. Cloud cover is described in eighths of sky covered with a particular cloud type (0/8–clear, 4/8–half the sky is covered, 8/8–completely overcast).

32. B.T. Bormann, R.F. Tarrant, M.H. McClellan, and T. Savage, "Chemistry of rain and cloud water at remote sites in Alaska and Oregon," *J. Environ. Qual.*, (in press).

33. S.H. Bicknell, "North coast cloud water project," in C. Biles (Ed.) Proceedings of the Conference on Natural Resources and Environmental Systems, Humbolt State Univ., Arcata, CA, 1987.

34. J. Collett, Jr., B. Daube, Jr., J.W. Munger, and M.R. Hoffmann, "Cloudwater chemistry in Sequoia National Park," *Atmos. Environ.* (in press).

35. D.J. Jacob, J.M. Waldman, J.W. Munger, and M.R. Hoffmann, "A field investigation of physical and chemical mechanisms affecting pollutant concentration in fog droplets," *Tellus*, 36B:272 (1984).

36. National Atmospheric Deposition Program, "NADP/NTN Annual Data Summary," Available from Program Coordinator, NADP/NTN, Natural Resource Ecology Laboratory, Colorado State University, Fort Collins, 1987.

37. R.G. Stone. "Fog in the United States and adjacent regions." *Geographical Review*. 26(1):111 (1936).

38. "Climate and Man." *Yearbook of Agriculture*. USDA. 1941 p. 737.

39. A. Court and R.D. Gerston. "Fog frequency in the United States." *The Geographical Review*. 56:543 (1966).

40. F.A. Basabe. "Fog frequency in Pacific Northwest forests." Report 7B1068NASA. Available from Program Director. Western Conifers Research Cooperative. EPA-CERL. Corvallis. OR.

41. E.E. Hindman. R.D. Borys. and P.J. DeMott. "Hydrometeorological significance of rime ice deposits in the Colorado Rockies." *Water Resour. Bull.* American Water Resources Association. 19(4):619 (1983).

42. E.E. Hindman. "Characteristics of supercooled liquid water in clouds at mountaintop sites in the Colorado Rockies." *J. Climate and Applied Meteorology*. 25:1271 (1986).

43. M.K. Politovich and G. Vali. "Observations of liquid water in orographic clouds over Elk Mountain." *J. Atmospheric Sciences*. 40(5):1300 (1983).

Table I. Sources of data on western cloudwater chemistry.

Study Area	Altitude (m)	Description	Season[a]	Type[b]	Collector[c]	Data[d]
Douglas Is., AK[32]	800	forest	summer/fall	cloud	CWP-ASC	2
Mary's Peak, OR[32]	1245	forest	summer/fall	cloud	CWP-ASC	2
Redwood NP, CA[33]	305	forest	unknown	fog	CWP-ASC	2
Giant Forest, Sequoia NP[34]	1856	forest	spring/fall	cloud	CASCC	1
Lower Kaweah, Sequoia NP[19]	1856	forest	spring/summer	cloud	CASCC	1
Turtleback Dome, Yosemite NP[19]	1590	forest	spring/fall	cloud	CASCC	1
Bakersfield, CA[35]	130	urban	winter	fog	RAC	2
Pasadena, CA[4]	150	urban	winter	fog	RAC	1
Lennox, CA[4]	75	industrial	winter	fog	RAC	1
Oildale, CA[4]	130	industrial	winter	fog	RAC	1
Upland, CA	320	urban	spring	fog	RAC	1
Bakersfield, CA[2]	130	urban	winter	fog	RAC	1
Henninger Flats, CA[6]	870	forest	spring/summer	cloud	RAC	2

[a] Seasons:
Winter = Dec, Jan, Feb
Spring = March, April, May
Summer = June, July, Aug
Fall = Sept, Oct, Nov

[b] Cloud type:
fog = formed at or near ground
cloud = orographic or cap cloud

[c] Cloudwater collector:
CWP = CWP Active Strand Collector
CASCC = Caltech Active Strand Cloudwater Collector
RAC = Rotating Arm collector

[d] Data type:
1 = maxs and mins from sequential samples within one event
2 = maxs and mins across several events

Table IIa. Cloud characteristics for those areas (45-50° N) where stratus and stratocumulus interception is anticipated.

	western slopes of Cascades, WA				Bitterroot Mtns, ID/MT			
Cloud Characteristics	winter	spring	summer	fall	winter	spring	summer	fall
most freq occ cloud	stratus	cirrus	cirrus	cirrus	stratus	cirrus	cirrus	cirrus
most freq occ low cloud	stratus	stratus	stratus	stratus	stratus	stratus	cumulus	stratus
freq occ of St/Sc (%)[a]	66	48	41	50	60	40	20	40
base height St/Sc (masl)	750	900	850	800	2500	2700	2800	2600
min # days with St/Sc	36	26	20	25	23	15	6	14
av. cloud amount (%)[b]	49	33	28	34	40	25	11	25

[a] % of observed low clouds identified as stratus or statocumulus

[b] expressed as % cloud cover

Table IIb. Cloud characteristics for those areas (40-45° N) where stratus and stratocumulus interception is anticipated.

	western slopes of Cascades, OR				Bitterroot Mtns, ID			
Cloud Characteristics	winter	spring	summer	fall	winter	spring	summer	fall
most freq occ cloud	stratus	stratus	stratus	stratus	cirrus	cirrus	cirrus	cirrus
most freq occ low cloud	stratus	stratus	stratus	stratus	stratus	stratus	stratus	stratus
freq occ of St/Sc (%)	58	50	39	48	50	33	15	30
base height St/Sc (masl)	700	800	750	730	2400	2600	2700	2500
min # days with St/Sc	20	18	13	16	18	11	4	10
average cloud amount (%)	47	38	29	38	38	22	8	21

	Bighorn Mtns, WY/MT				northern Front Range, CO			
Cloud Characteristics	winter	spring	summer	fall	winter	spring	summer	fall
most freq occ cloud	cirrus	cirrus	cirrus	cirrus	cirrus	cirrus	cirrus	cirrus
most freq occ low cloud	stratus	stratus	clear	stratus	stratus	stratus	cumulus	stratus
freq occ of St/Sc (%)	35	35	15	28	30	35	16	28
base height St/Sc (masl)	2700	2600	no int	2650	2400	2400	2600	2500
min # days with St/Sc	12	14	5	12	11	15	5	11
average cloud amount (%)	16	21	7	16	22	27	10	22

Table IIc. Cloud characteristics for those areas (35-40° N) where stratus and stratocumulus interception is anticipated.

	Coast Range of northern CA				Sierra Nevada			
Cloud Characteristics	winter	spring	summer	fall	winter	spring	summer	fall
most freq occ cloud	stratus	stratus	stratus	stratus	cirrus	cirrus	cirrus	cirrus
most freq occ low cloud	stratus	stratus	stratus	stratus	stratus	cumulus	clear	clear
freq occ of St/Sc (%)	46	43	53	44	34	19	5	15
base height St/Sc (masl)	650	610	430	550	1200	1400	1500	1300
min # days with St/Sc	18	17	18	15	14	8	2	6
average cloud amount (%)	36	32	40	32	22	11	2	8

	San Juan Mountains, CO				southern Front Range, CO			
Cloud Characteristics	winter	spring	summer	fall	winter	spring	summer	fall
most freq occ cloud	cirrus	cirrus	cirrus	cirrus	cirrus	cirrus	cirrus	cirrus
most freq occ low cloud	stratus	stratus	cumulus	stratus	stratus	stratus	cumulus	stratus
freq occ of St/Sc (%)	35	30	18	28	30	30	13	25
base height St/Sc (masl)	3000	3500	3900	3200	3000	2800	2900	2700
min # days with St/Sc	8	7	3	7	10	14	5	10
average cloud amount (%)	22	16	8	16	16	19	7	16

	Sangre de Christo Mountains, NM			
Cloud Characteristics	winter	spring	summer	fall
most freq occ cloud	cirrus	cirrus	cirrus	cirrus
most freq occ low cloud	stratus	stratus	cumulus	stratus
freq occ of St/Sc (%)	32	30	15	27
base height St/Sc (masl)	3100	3550	3750	3250
min # days with St/Sc	9	8	4	7
average cloud cover (%)	19	17	8	16

Table IId. Cloud characteristics for those areas (30-35° N) where stratus and stratocumulus interception is anticipated.

	Coast Range of southern CA				Sacramento Mountains, NM			
Cloud Characteristics	winter	spring	summer	fall	winter	spring	summer	fall
most freq occ cloud	cirrus	stratus	stratus	stratus	cirrus	cirrus	cirrus	cirrus
most freq occ low cloud	stratus	stratus	stratus	stratus	stratus	clear	cumulus	stratus
freq occ of St/Sc (%)	31	48	51	43	23	19	12	24
base height St/Sc (masl)	590	590	450	520	1800	no int	no int	1900
min # days with St/Sc	14	23	23	19	16	13	6	16
average cloud amount (%)	21	34	34	29	18	13	7	18

Table III. Rank order of cloud events along the first principal component axis together with study area, date the sample was collected, and citation. Position on first principal component (fpc) axis is illustrated in Figures 2, 3, and 4. Rank orders increase from left to right on x-axis.

Rank by score on fpc axis	Site	Date	Citation
1	Upland, CA (Los Angeles Basin)	05/14/82	4
2	Bakersfield, CA (San Joaquin Valley)	01/14/82	2
3	Oildale, CA (San Joaquin Valley)	01/14/82	4
4	Pasadena, CA (Los Angeles Basin)	11/23-24/81	4
5	Lennox, CA (Los Angeles Basin)	12/07-08/81	4
6	Lennox, CA	12/18-19/81	4
7	Henninger Flats, CA (Los Angeles Basin)	05-06/83	6
8	Henninger Flats, CA	06/82	6
9	Giant Forest, Sequoia NP, CA (Sierra Nevada)	04/24/86	34
10	Bakersfield, CA	12/82-01/83	35
11	Lower Kaweah, Sequoia NP, CA (Sierra Nevada)	06/5/88	19
12	Lower Kaweah, Sequoia NP, CA	04/28/88	19
13	Turtleback Dome, Yosemite NP, CA (Sierra Nevada)	04/28/88	19
14	Giant Forest, Sequoia NP, CA	05/03/86	34
15	Turtleback Dome, Yosemite NP, CA	05/12-13/88	19
16	Redwood NP, CA (Coast Range)	1984-1985	33
17	Lower Kaweah, Sequoia NP, CA	09/20/88	19
18	Lower Kaweah, Sequoia NP, CA	05/17/88	19
19	Turtleback Dome, Yosemite NP, CA	04/30/88	19
20	Lower Kaweah, Sequoia NP, CA	10/28-29/87	19
21	Turtleback Dome, Yosemite NP, CA	04/23/88	19
22	Lower Kaweah, Sequoia NP, CA	11/14/87	19
23	Turtleback Dome, Yosemite NP, CA	05/29/88	19
24	Douglas Island, AK (Coastal)	07-09/84 & 97-09/85	32
25	Lower Kaweah, Sequoia NP, CA	11/02/87	19
26	Lower Kaweah, Sequoia NP, CA	10/31/87	19
27	Turtleback Dome, Yosemite NP, CA	11/16/88	19
28	Turtleback Dome, Yosemite NP, CA	05/17/88	19
29	Mary's Peak, OR (Coast Range)	06/29-11/01/85	32
30	Lower Kaweah, Sequoia NP, CA	10/22/87	19
31	Lower Kaweah, Sequoia NP, CA	11/01/87	19
32	Turtleback Dome, Yosemite NP, CA	04/14/88	19
33	Turtleback Dome, Yosemite NP, CA	05/28/88	19
34	Lower Kaweah, Sequoia NP, CA	11/17/87	19
35	Giant Forest, Sequoia NP, CA	10/21/85	34
36	Turtleback Dome, Yosemite NP, CA	11/13/88	19

Table IV. Pearson's r correlation of ionic concentrations with the principal components axis (n=36).

	Axis 1	Axis 2	Axis 3
% of Variance Explained	71.4	11.8	6.31
Min H^+	0.785	-0.360	0.225
Max H^+	0.561	0.345	-0.047
Max Na^+	-0.822	0.452	0.272
Min Na^+	-0.821	-0.211	0.489
Max NH_4^+	-0.906	0.032	-0.344
Min NH_4^+	-0.808	-0.433	-0.330
Max Ca^{2+}	-0.892	0.297	-0.005
Min Ca^{2+}	-0.858	-0.414	0.154
Max Mg^{2+}	-0.860	0.445	0.173
Min Mg^{2+}	-0.814	-0.378	0.342
Max SO_4^{2-}	-0.935	0.257	-0.152
Min SO_4^{2-}	-0.928	-0.261	-0.082
Max NO_3^-	-0.924	0.092	-0.311
Min NO_3^-	-0.880	-0.372	-0.244
Max Cl^-	-0.798	0.546	0.102
Min Cl^-	-0.854	-0.168	0.221

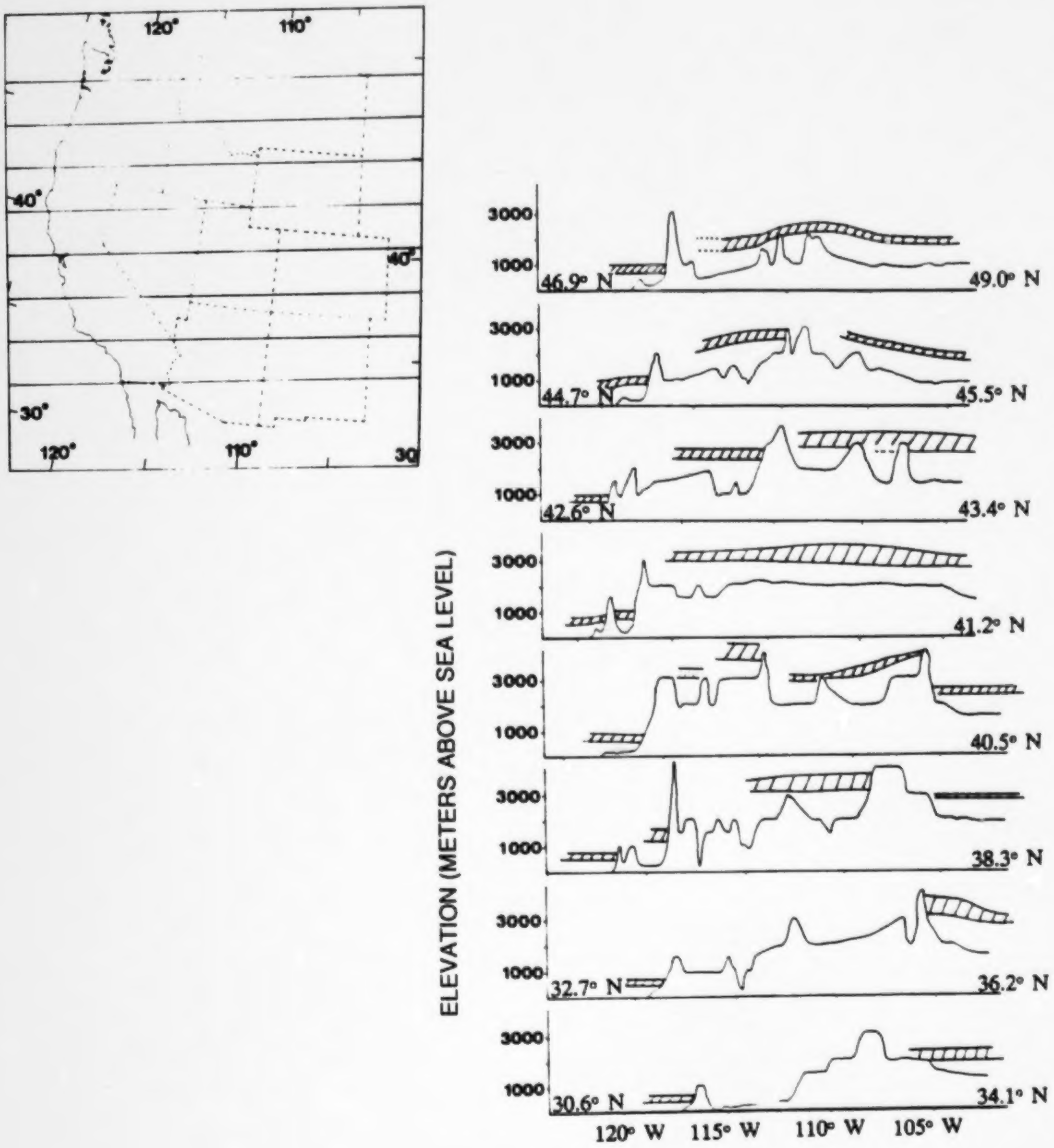

Figure 1. West-east transects across the western United States showing elevational variations in the range of mean base height for above ground stratus and stratocumulus clouds. Insert illustrates location of transects. Range of base heights is estimated for quarters of the year where winter is defined as December, January and February. "Regions" referred to in the text relate to the transects by latitude, where 45°–50° N = Region 1; 40°–45° N = Region 2; 35°–40° N = Region 3; 30°–35° N = Region 4.

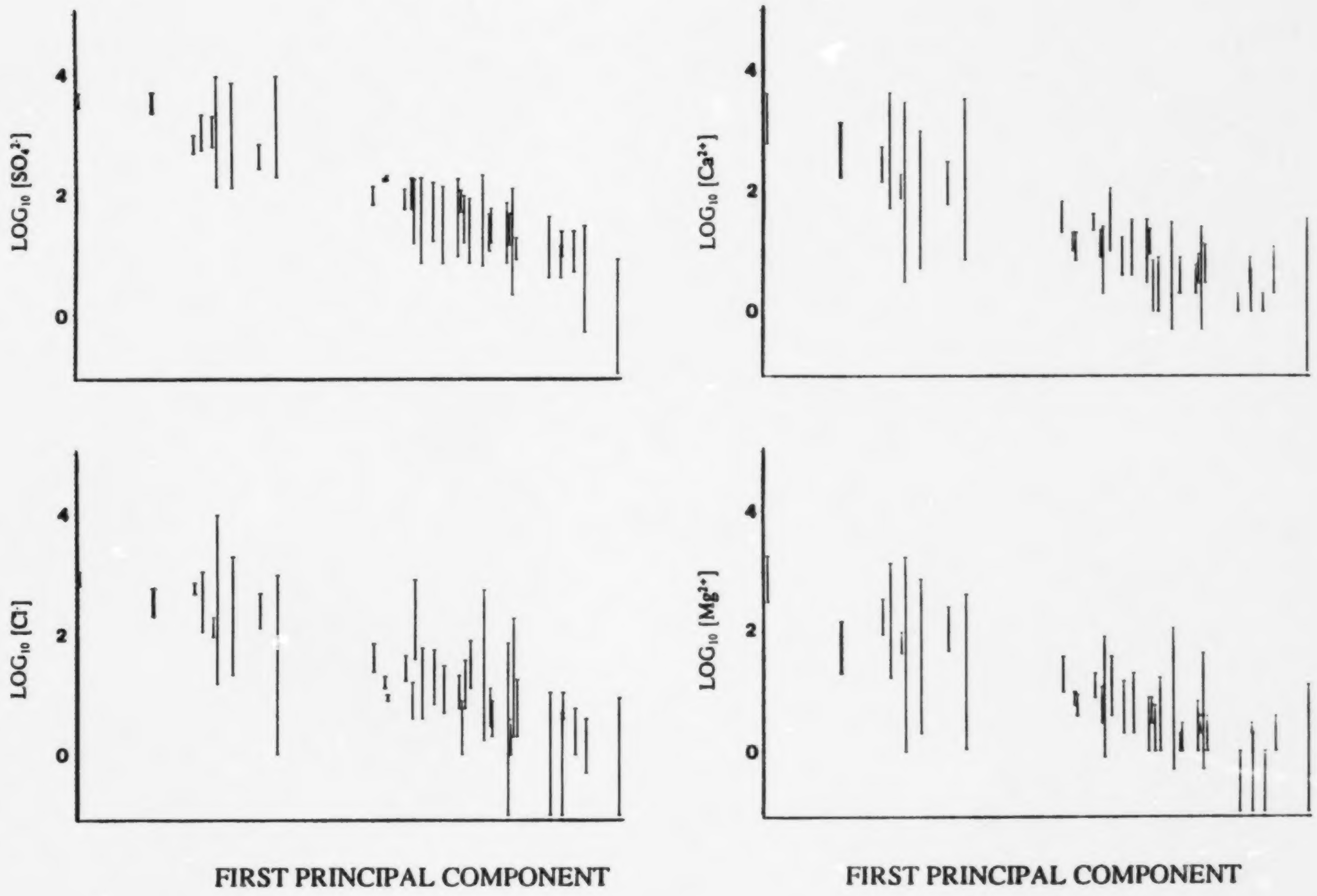

Figure 2a. Ranges ($\log_{10}$) of ion concentrations (μeq/l) for each cloud event (n = 36). Order on x-axis corresponds to the score by event for the first principal component. The site, sampling period, and citation are listed in Table III.

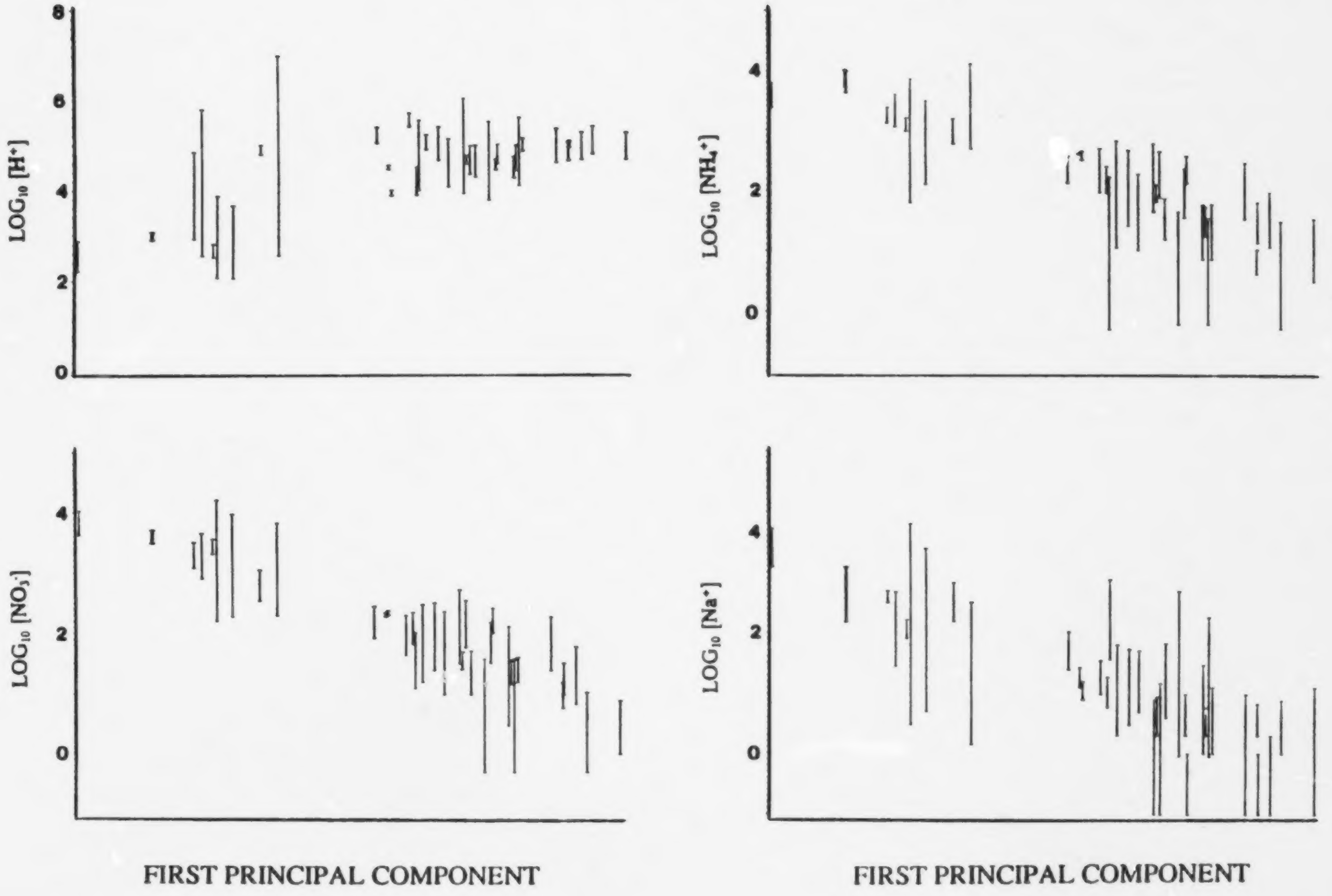

Figure 2b. Ranges ($\log_{10}$) of ion concentrations (μeq/l) for each cloud event (n = 36). Order on x-axis corresponds to the score by event for the first principal component. The site, sampling period, and citation are listed in Table III.

Table V. Comparison between the air concentrations and cloud concentrations of NO_3^- and SO_4^{2-} at Mt. Werner, Colorado.

	Cloud Aqueous Conc. (µmol/l)	Cloud Air Conc.[a] (µg/m^3)	Clear Air Conc. (µg/m^3)
NO_3^-	96.6	0.56	0.17
SO_4^{2-}	81.0	0.72	0.81
HNO_3^-			0.27
SO_2			0.82[b]

[a] Concentrations of cloud species in air volume units.

[b] 1.23 as sulfate.

Table VI. Estimates of NO_3^- and SO_4^{2-} deposition fluxes at Mt. Werner, Colorado relative to the processes of precipitation, occult deposition, and dry deposition.

	Estimates of Deposition Fluxes (kg/ha/y)	
Deposition Process	NO_3^-	SO_4^{2-}
Precipitation	8.8	12.3
Occult	5.3	6.9
Dry	1.25[a]	0.57[b]

[a] Components are HNO_3, 1.20 kg/ha/y; particulate nitrate, 0.05 kg/ha/y.

[b] Components are SO_2 as sulfate, 0.31 kg/ha/y; particulate sulfate, 0.26.

Table IV. Summary of clear air data

Date on	Date off	ET (h)	Ambient Concentrations			
			NO_3^- (µg/m^3)	SO_4^{2-} (µg/m^3)	HNO_3 (µg/m^3)	SO_2 (µg/m^3)
5/22/87	5/29/87	143	0.77	1.32	0.10	0.18
5/29/87	6/05/87	164	0.16	0.61	0.29	0.43
6/05/87	6/13/87	127	-	0.68	0.00	0.04
6/13/87	6/22/87	214	0.05	0.64	0.22	0.06
6/22/87	6/26/87	168	0.09	0.64	0.37	1.87
6/29/87	7/07/87	188	0.44	1.13	0.25	0.95
7/07/87	7/14/87	116	0.57	0.61	0.00	1.03
7/14/87	7/21/87	173	0.33	1.12	0.38	0.89
7/21/87	7/30/87	212	0.00	0.95	0.33	0.40
7/30/87	8/07/87	189	0.01	0.68	0.33	1.66
8/07/87	8/16/87	212	0.10	0.72	0.33	0.38
8/16/87	8/23/87	171	0.06	0.86	0.34	1.80
8/24/87	8/31/87	128	0.00	0.78	0.38	0.87
8/31/87	9/08/87	189	0.05	0.93	0.34	1.10
9/08/87	9/16/87	198	0.11	0.76	0.45	1.88
9/16/87	9/23/87	148	0.00	0.54	0.28	1.11
9/23/87	9/29/87	144	0.01	0.79	0.30	1.07
Average concentrations			0.17	0.81	0.27	0.82

Table I. Volume-weighted chemical composition of cloud water for four selected events at Mt. Werner, Colorado.

	LWC (g/m^3)	Aqueous Concentrations ($\mu eq/l$)										
Event		H^+	Na^+	K^+	NH_4^+	Ca^{2+}	Mg^{2+}	Cl^-	NO_3^-	SO_4^{2-}	CHO_2^-	$CH_3CO_2^-$
1 6/09/87	0.09	92.5	3.8	1.6	65.5	4.6	2.1	10.2	33.6	61.6	20.5	9.3
2 7/11/87	0.06	20.1	9.9	15.0	83.0	6.8	2.3	9.4	37.4	76.7	17.4	12.7
3 7/31/87	0.13	44.7	5.2	3.5	61.7	3.5	1.8	5.3	53.6	88.3	24.5	11.4
4 8/24/87	0.12	106.0	8.5	5.4	36.3	1.7	0.5	5.6	38.2	83.2	5.5	4.9

Table II. Comparison of anion concentrations of cloud and precipitation during a change in the flow from southwesterly to easterly.

	Anion Concentrations ($\mu eq/l$)			
	Southwesterly Flow		Easterly Flow	
Anions	Cloud	Precip	Cloud	Precip
NO_3^-	37.4	6.1	13.0	2.2
SO_4^{2-}	76.7	6.0	10.7	3.8
HCO_2^- and $CH_3CO_2^-$	30.1	3.5	23.0	0.7

Table III. Comparison of chemical composition of cloud water and precipitation at Mt. Werner, Colorado.

	Aqueous Concentrations ($\mu eq/l$)										
	H^+	Na^+	K^+	NH_4^+	Ca^{2+}	Mg^{2+}	Cl^-	NO_3^-	SO_4^{2-}	CHO_2^-	$CH_3CO_2^-$
Cloud–events	84.2	6.7	5.1	55.5	3.5	1.4	7.5	39.1	76.0	14.7	8.7
Precip–events	33.3	2.3	2.2	4.7	3.7	0.6	5.7	20.9	48.5	1.3	0.56
Cloud/precip ratio	2.5	2.9	2.3	11.8	0.9	2.3	1.3	1.9	1.9	11.3	15.5
Cloud–totals	216	6.9	5.1	56.8	3.1	1.3	10.5	96.6	162	12.7	7.7
Precip–totals	49.5	2.2	1.1	8.5	11.5	1.7	4.6	16.0	29.1	2.2	0.87
Cloud/precip ratio	4.3	3.1	4.6	6.6	0.3	0.7	2.2	6.0	5.5	5.7	8.8

10. D.F. Miller and R.D. Borys, "Characterization of cloud chemistry and frequency of canopy exposure to clouds in the Rocky Mountains," Final Report prepared for the U.S. Environmental Protection Agency, Western Conifers Research Cooperative, Corvallis, OR, 1988.

11. D.W. Fehey, et al., "Reactive nitrogen species in the troposphere: Measurements of NO, NO_2, HNO_3, particulate nitrate, peroxyacetyl nitrate, O_3, and total reactive odd nitrogen at Niwot Ridge, CO," *J. Geophys. Res.*, 91:9781 (1986).

12. D.F. Miller. "SO_2 Measurements in the National Parks," Final Report prepared for the National Park Service, Air Quality Division, Denver, CO, 1988.

13. J.R. Young, "Data inventory report for the Chevron baseline visibility study, Clear Creek Properties, CO," Doc. P-B220. ERT, Inc., Camarillo, CA, 1982.

14. R.D. Borys, K.A. Rahn, and D.H. Lowenthal, "Contributions of smelters and other sources to pollution sulfate at a mountaintop site in northwestern Colorado. Submitted to *Nature* (1988).

15. V. Mohnen, Atmospheric Science Research Center, SUNY, Albany, NY, personal communication, 1988.

16. G.M. Lovett and W.A. Reiners, "Cloud water: An important vector of atmospheric deposition," in *Precipitation Scavenging, Dry Deposition and Resuspension*, Vol. 1. H.R. Pruppacher, R.G. Semonin, and W.G. Slinn Eds., Elsevier Science, New York, NY, 1983, p. 171.

17. E.E. Hindman, "Characteristics of supercooled liquid water in clouds at mountaintop sites in the Colorado Rockies," *J. Climate Appl. Meteor.*, 25:1271 (1986).

18. J.R. Young, E.C. Ellis, and G.M. Hidy, "Deposition of air-borne acidifiers in the western environment," *J. Environ. Quality*, 17:1 (1988).

deposition processes. Estimates of the dry deposition flux for these species are an order of magnitude less than the estimates of wet deposition fluxes.

ACKNOWLEDGMENTS

We would like to acknowledge the valuable assistance of Wanda Brachaczek, Judith Chow, Nancy Granata, Penny Ragland, and John Watson. We also thank the U.S. Forest Service, the Steamboat Ski Corporation and the Colorado State University for their cooperation.

The research was supported by funds provided by the Western Conifers Research Cooperative within the joint U.S. Environmental Protection Agency-USDA Forest Service Forest Response Program. The Forest Response Program is part of the National Acid Precipitation Assessment Program. This paper has not been subject to EPA or Forest Service review and should not be construed to represent the policies of either Agency.

REFERENCES

1. P.D. Falconer, "Cloud chemistry and meteorological research at Whiteface Mountain: Summer 1980," ASRC Publication 806, State University of New York, Albany, NY, 1981.

2. U. Katz and D.F. Miller, "Development and evaluation of cloud water collectors," Final Report to the Coordinating Research Council, Atlanta, GA, 1984.

3. P.H. Daum, T.J. Kelly, S.E. Schwartz, and L. Newman, "Measurements of the chemical composition of stratiform clouds," *Atmos. Environ.*, 18:2671 (1984).

4. J. Kadlecek, S. McLaren, N. Carmarota, V. Mohnen, and J. Wilson, "Cloud water chemistry at Whiteface Mountain," in *Precipitation Scavenging, Dry Deposition and Resuspension*. H.R. Pruppacher, R.G. Semonin, and W.G. Slinn, Eds., Elsevier Science, New York, NY, 1983, p. 103.

5. P. Roth, C. Blanchard, J. Harte, H. Michaels, and M.T. El-Ashry, "The American West's acid rain test," Res. Rep. 1. World Resour. Inst., Washington, DC, 1985.

6. U.S. Environmental Protection Agency, "Total alkalinity of surface waters-a map of the western region," EPA-600/D-85-219 (1986).

7. U. Katz, "A droplet impactor to collect liquid water from laboratory clouds for chemical analysis," Communications a la VIII^{eme} Conference Internationale sur la Physique des nauges, Clermont-Ferrand, France, 1980, p. 696.

8. W.C. Kenne and J.N. Galloway, "Organic acidity in precipitation of North America," *Atmos. Environ.*, 18:2491 (1984).

9. S.P. Cline, "Quality Assurance Audit Report". U.S. EPA Environmental Research Laboratory, Corvallis, OR, 1988.

average concentrations of HNO_3 and particulate nitrate in clear air, one would expect to find a total nitrate concentration of 0.44 µg/m^3 in clouds, assuming unity scavenging and no enrichment process. The average cloud concentration of 0.56 µg/m^3 is only slightly greater than the expected value. For total sulfate, the picture is somewhat different. The concentration of sulfate in the clouds was comparable to the concentration of particulate sulfate alone in clear air. This suggests that little SO_2 absorbed into cloud had converted to sulfate.

Estimates of Deposition Fluxes

The response of high-elevation forests to air pollutants relates to both exposure and deposition. Exposure to extreme concentrations of soluble ions is thought to occur during cycles of cloud impaction followed by evaporation. High concentrations of ozone and other oxidants at such times likely exacerbate the acidic effects. These conditions, we are told,[15] are more prevalent in the East than the West. Precipitation, on the other hand, tends to bathe the forests with weakly acidic solutions and contributes mainly to the cumulative effects of deposition. Airborne species that are dry deposited would seem to contribute to both exposure and cumulative deposition. The present study was not designed specifically to investigate either of these phenomena. We can, however, make a crude assessment of the relative magnitude of species flux to the forest canopy by the processes of "occult" (i.e., cloud) deposition, precipitation, and dry deposition.

Measured fluxes of precipitation at the Storm Peak Laboratory were computed for the case studies described previously when the precipitation rate exceeded 0.3 mm/h. Cloud water flux was estimated using a model[16] that incorporates collection efficiency for forests. Several important assumptions and approximations were needed in applying the model to conditions at Mt. Werner (for details see reference 10). From that application, we estimated that the cloud water flux to the forest canopy relative to the precipitation flux averaged 20% during periods of simultaneous cloud and precipitation. Taking into consideration the periods of cloud interception alone and precipitation alone reduced to 10% the estimate of cloud water flux relative to that of precipitation. On the basis of an annual deposition analysis, 10% is probably a conservative fraction because, under winter conditions at Storm Peak, precipitation rarely occurs without clouds impacting the mountain.[17]

Using the 10% estimate, the nitrate and sulfate concentrations from Table III, and the assumption that the annual precipitation at Storm Peak is 89 cm, the annual wet deposition fluxes for nitrate and sulfate are given in Table VI. Estimates of the annual dry deposition fluxes for those species are also entered there. Those fluxes were calculated from the average air concentrations (Table V) and the following deposition velocities: (1) fine-particle sulfate and nitrate, 0.1 cm/s, (2) nitric acid, 1.4 cm/s, and (3) sulfur dioxide, 0.08 cm/s.

Direct comparisons of these deposition fluxes with existing data can be made only for precipitation. From the average of three NADP/NTN/UAPSP sites in rural Colorado in 1984,[18] the nitrate precipitation flux was 5.2 kg/ha/y and the sulfate flux was 5.3 kg/ha/y. The higher precipitation fluxes computed in Table VI would be consistent with a larger annual precipitation rate at the higher elevation of Storm Peak Laboratory.

It is apparent from Table VI that the effective deposition fluxes for nitrate and sulfate, as well as for several other soluble species, on average at this high-elevation site, are of comparable magnitude for the precipitation and occult concentrations were less than 0.1 μg/m^3. During the other 14 weekly intervals, the HNO_3 concentration ranged between 0.22 and 0.45 μg/m^3. The average concentration for the summer was estimated at 0.28 μg/m^3.

The summer-averaged concentration of particulate sulfate was 0.81 μg/m^3, and weekly averages ranged between 0.61 and 1.32 μg/m^3. The summer-averaged concentration of vapor-phase SO_2 was 0.82 μg/m^3, and weekly averages ranged between 0.04 and 1.88 μg/m^3.

It is of interest to compare these estimated concentrations of sulfur and nitrogen species with other reported values. Fehey et al.[11] reported the concentrations of several NO_x/NO_y species measured at Niwot Ridge, Colorado during the summer and fall of 1984. That site is similar in longitude and elevation to that of Mt. Werner, but Niwot Ridge is about five miles east of the continental divide and is occasionally subject to the intrusion of urban pollution from the Front Range. The average HNO_3 concentration measured at Niwot Ridge was approximately 100 ppt (0.26 μg/m^3), which compares well with the average concentration of 0.28 μg/m^3 observed at Storm Peak Laboratory. The average concentration of particulate nitrate at Niwot Ridge was about 0.1 μg/m^3, somewhat less than the average concentration of 0.17 μg/m^3 observed at our site. Overall, the similarity is close.

There are fewer data available for comparing the SO_2 and sulfate concentrations in the area. A recent report[12] on SO_2 concentrations in National Parks gives an annual average SO_2 concentration of 1.3 μg/m^3 for six remote parks in the western United States. An annual mean SO_2 concentration of 0.83 μg/m^3 was reported for Arches National Park in Utah, the Park closest to Storm Peak, Colorado. The average concentration during the summer at Mt. Werner was 0.82 μg/m^3.

Young[13] reported that the mean concentration of fine particulate sulfate at Clear Creek, CO, was 1.1 μg/m^3, in comparison with an average of 0.81 μg/m^3 observed at Mt. Werner, CO. An average sulfate concentration of 0.34 μg/m^3 was measured in the winter at this site.[14] Thus, our clear air measurements of SO_2 and sulfate compare closely with other measures of these species in remote areas of Colorado.

It is also of interest to compare the concentration of nitrate and sulfate species observed in clear air with the concentrations observed in clouds. This presumably provides some insights about the efficiency of clouds in scavenging these airborne species and the possible tendency of becoming enriched by either accumulation or oxidation processes. Ideally, one would measure the species concentrations of the interstitial air while sampling the cloud drops. We were not equipped to do that. Alternatively, we sampled clear air when neither cloud nor precipitation was present (about 92% of the total time). Therefore, our comparison of the composition of clear air and cloudy air involves different air masses and possibly different sources of pollution. The results are given in Table V, where the average concentration of all cloud samples are compared with the summer-averaged clear-air concentrations. The concentrations of cloud species in air-volume units was computed using the liquid-water content of cloud.

Because nitric acid is so highly soluble in water, HNO_3 vapor is always assumed to be totally absorbed by cloud whenever the chance arises. Thus, based on the this cold front was the cleanest precipitation collected in the study. At the very end of the event, cloud water became too cold to sample with the Katz collector.

As the summer progressed and the thermally derived low-pressure system built in the west, conditions for monsoonal flow began to develop. Under these conditions, air rises as it is heated over the continent and is replaced at low levels with moist, cool air from oceanic areas. In the Great Basin, the moisture originates from the Gulf of California and/or the Pacific Ocean west of Baja. The moist air flows northward, is heated from below and forms large areas of cloudiness with imbedded thunderstorms. This was the type of weather that spawned the events of July 31 and August 23-25 at Storm Peak Laboratory.

In general, the monsoonal flow resulted in significantly higher liquid water content in cloud than had previous storms. The cloud event in August was the most persistent of the 1987 summer season. Rain accompanied the cloud event throughout August 23 and from noon until midnight on the 24th. Cloud persisted through much of the 25th without precipitation. During a 2-h period on that day, the concentrations of nitrate and sulfate in cloud reached the extremes of 563 and 589 µeq/l, respectively, with a LWC of 0.12 g/m^3.

A number of precipitation events occurred when clouds were well above the elevation of Mt. Werner. These were sampled in the interest of obtaining a complete picture of the chemical composition of precipitation during the study period. There were several instances in May, June, and July when precipitation was in the form of snow, and the supercooled cloud that was present could not be sampled with the cloud collector.

Table III compares the chemical composition of precipitation and cloud water at the Storm Peak Laboratory. All concentration data in Table III are volume-weighted averages. The set of data at the top of Table III compares the chemistry during the four events discussed previously where cloud and precipitation were simultaneously present. In those instances, the largest differences in concentrations between cloud water and precipitation were for NH_4^+ and the organic acids.

The bottom set of data in Table III compares the chemical composition between the total sampling of clouds and precipitation over the entire study period. In this comparison, the disparity in concentration of "acidic species" between cloud and precipitation is larger than that for the case studies. The cloud events in August had the most influence on this spread. For the species NH_4^+, NO_3^-, SO_4^{2-}, CHO_2^- and $CH_3CO_2^-$, the clouds were more concentrated than precipitation by factors of five to eight. In contrast, we found Ca^{2+} to be more concentrated in precipitation than in clouds.

As described in Section 2, a filter-pack system was used to integrate air samples during periods when there was neither cloud nor precipitation. From these collections, weekly estimates were made of the ambient concentrations of particulate nitrates and sulfates and gaseous HNO_3 and SO_2. Those estimated concentrations, in units of micrograms per cubic meter, are presented in Table IV.

The mean concentration of particulate nitrate during the study was 0.17 $\mu g/m^3$ and varied between zero and 0.77 $\mu g/m^3$. (The uncertainty in the particulate nitrate data was large.) For 3 of 17 weeks, the vapor-phase HNO_3

indicate the presence of cloud. The threshold of observed cloud corresponded to a b_{scat} value of 0.8/km, a nominal meteorological range of 4.9 km.

Field data were acquired with a Campbell Scientific 21X data logger as 5-min averages.

Quality Assurance

Quality assurance was an integral part of this study. A Quality Assurance Project Plan (QA Plan 701.1) was submitted independently to the U.S. EPA and implemented throughout the course of work. The Plan was structured according to guidelines in the "Quality Assurance Implementation Plan for the Forest Response Program," which was issued by the U.S. EPA Corvallis Environmental Research Laboratory (April 1986). Independent field audits were conducted by the U.S. EPA. A quality assurance audit report for the study has been filed.[9]

RESULTS AND DISCUSSION

Frequency of Exposure

Clouds enveloped the Storm Peak Laboratory on 32 of the 133 days of the investigation. This cloud condition represented 5.7% of the total study period. Precipitation was recorded on 50 days, but the total hours of precipitation represented only 2.5% of the total period. There were approximately 100 h when the mountain was immersed in cloud with no precipitation. Fifty-four samples of cloud and 59 samples of precipitation were chemically analyzed.

Based on a historical analysis of summertime precipitation records near Steamboat Springs, it was concluded that the 1987 summer was normal, and the frequency and duration of cloud events were judged to be representative of the area.[10]

Chemical Composition of Cloud, Precipitation, and Air

There were four major cloud events during the summer study which collectively accounted for 67% of all cloud water sampled. Table I summarizes the average volume-weighted concentrations of soluble species of each cloud event. The first important event began on the evening of June 8 as moisture moved in from the southwest. Cloud dissipated by midnight, but a more persistent cloud cover developed around 0700 the next morning and lasted throughout the day. This cloud was associated with a frontal passage and a wind shift to the west/northwest. During the event of June 9, the concentrations of sulfate and nitrate in both cloud and precipitation increased with time. This observation is opposite the trend observed most frequently in the East.[2]

The event beginning July 11 involved an approaching cold front from the northwest with moisture from the southwest overrunning the front. As the front progressed, winds became light and northeasterly. This flow pattern is typical for cold-front passage at the site, as cold, dense Canadian air with high pressure behind the front is advected down the plains on the east side of the Rockies and is forced over the continental divide. This transition in flow brought marked changes in the composition of cloud and precipitation. Table II compares nitrate, sulfate, and the organic acids for the two synoptic conditions. Cloud associated with easterly flow had one-third the concentration of nitrate and one-seventh the concentration of sulfate compared to cloud from the southwest. With respect to nitrate and sulfate, the snow that came with

Sample Collections

The sampling of cloud drops for chemical analysis is subject to contamination from other airborne particles and hydrometeors. Katz[7] developed and tested a new cloud-water collector to overcome such problems. A subsequent version adapted specifically for stationary field work[2] was used to collect cloud water in this study. In this configuration, cloud drops accelerate in three jet streams and impact on Teflon rollers. The rotation of the impaction zone and the convergence of drops upon a contacting roller minimizes reentrainment and evaporation. A unique feature of the instrument is a continuous readout of the sample volume, which translates to a direct measure of the liquid water content (LWC) of cloud. A measure of the LWC is necessary to determine cloud deposition flux and to any interpretation of cloud chemistry that relates to species concentrations in precipitation or clear air. Clouds were generally sampled over 30-min periods. If cloud LWC was unusually low, longer integration periods were allowed to provide sufficient volumes of water (10 to 15 ml) for chemical analysis.

Rain and snow were sampled with an Aerochem Metrics wet/dry collector. Samples were obtained on an event basis. More frequent collections were made if the site was simultaneously in cloud.

When neither cloud nor precipitation was present, clear air was sampled for particles and gases using a filter-pack system. A Teflon prefilter captured total particles, and a quartz-fiber backup filter impregnated with K_2CO_3 and glycerin captured acidic gases. Each integrated sampling period was seven days minus the time of wet events.

Sample Disposition and Analysis

Cloud and precipitation samples were logged in by volume and weight. A 300-µl aliquot was taken immediately and analyzed for pH with an Altech meter and Lazar micro pH probe. The remaining sample was split into two aliquots; one was doped with a drop of 0.1% chloroform solution to prevent degradation of organic acids.[8] All samples were kept refrigerated.

After exposure, Teflon filters were extracted with 5 ml of deionized water in an ultrasonic bath. Quartz filters were extracted with 5 ml of 1% H_2O_2 solution. The purpose of the peroxide was to convert adsorbed SO_2 to sulfate.

A Dionex Series 4000i ion chromatograph was used for the analysis of inorganic ions: Na^+, NH_4^+, K^+, Cl^-, NO_3^- and SO_4^{2-} and organic ions: HCO_3^- and $CH_3CO_2^-$. Formate and acetate were resolved using a sodium borate eluent and a Dionex AS4A separation column. Calcium and magnesium were analyzed by atomic absorption spectroscopy.

Field Measurements

Precipitation amount and rate were measured with a Sierra tipping bucket gauge (Campbell Scientific Model RG 2501), which was calibrated in units of 0.01" per tip. Temperature and relative humidity were measured with a combined probe (R.M. Young Model 207). Wind speed and direction were measured with a R.M. Young Wind Sentry Model 03001-5.

An integrating nephelometer (MRI Model 2050B) was used to monitor relative changes in forward light scattering. It was empirically calibrated onsite to

Chemistry of Summer Cloud, Precipitation and Air at a Rocky Mountain-Top Location

David F. Miller[1]
Randolph D. Borys[1]
Richard Graw[2]

[1] *Desert Research Institute*
PO Box 60220
Reno, NV 89506

[2] *Enecotech, Inc.,*
1801 Broadway
Denver, CO 80202

INTRODUCTION

Some high-elevation forests in the United States are at risk because of change in their environment. It is hypothesized that the decline of spruce-fir forests in the East may be related to the additional exposure to, or deposition of, acidic species brought about by the interception of cloud water. The efficient scavenging of gases and particles in the cloud-forming process and the aqueous-phase reactions that ensue can lead to an enrichment of potentially harmful species in clouds. The analysis of cloud water samples from the top of Whiteface Mountain, NY, has shown much larger concentrations of hydrogen, sulfate and nitrate ions in cloud drops compared to the concentrations in raindrops falling from the same cloud.[1,2] Therefore, mountainous forests that are frequently submersed in cloud may be exposed to higher doses of acidity than forests at lower elevation.

Previous cloud chemistry studies in the United States have been conducted primarily in the East[3] and in the Appalachian Mountains,[4] where acidic air pollutants are most abundant. While the air in the West is generally cleaner than in the East, the mountain ranges and associated ecosystems of the West may be more vulnerable to damage than those of the East.[5] The added susceptibility relates to thinner soils, faster run-off from steeper terrain and higher barriers to intercept moisture. Furthermore, the thousands of lakes associated with the alpine and subalpine ecosystems of the West are characterized by low alkalinities (i.e., poor acid neutralizing capacities).[6]

This paper summarizes a study of cloud and precipitation chemistry at a high-elevation site in the Rocky Mountains during the summer of 1987. Measurements of the chemical composition of clear air were also made in an attempt to address a broader question of the relative magnitudes of wet, dry, and "occult" deposition of acids in the Rockies.

FIELD SITE AND MEASUREMENT METHODS

Field Site

The study was conducted at the Storm Peak Laboratory, elevation 3220 m MSL, on the west summit of Mt. Werner (40°27'N, 106°44'W). The location is six miles east of the town of Steamboat Springs in the Park Range of northwestern Colorado.

Preceding page blank

Chapter Two

Air Quality and Deposition: Precipitation

Chemistry of Summer Cloud, Precipitation and Air at a Rocky Mountain-Top Location	D.F. Miller, R.D. Borys, and R. Graw	105
Background Concentration of Sulfate in Precipitation along the West Coast of North America	R.J. Vong	117
Analysis of a Summertime Acid Rain Event in the Sierra Nevada	C.D. Unger	137
Fog and Rain Chemistry in Northern California	S. Bicknell	147

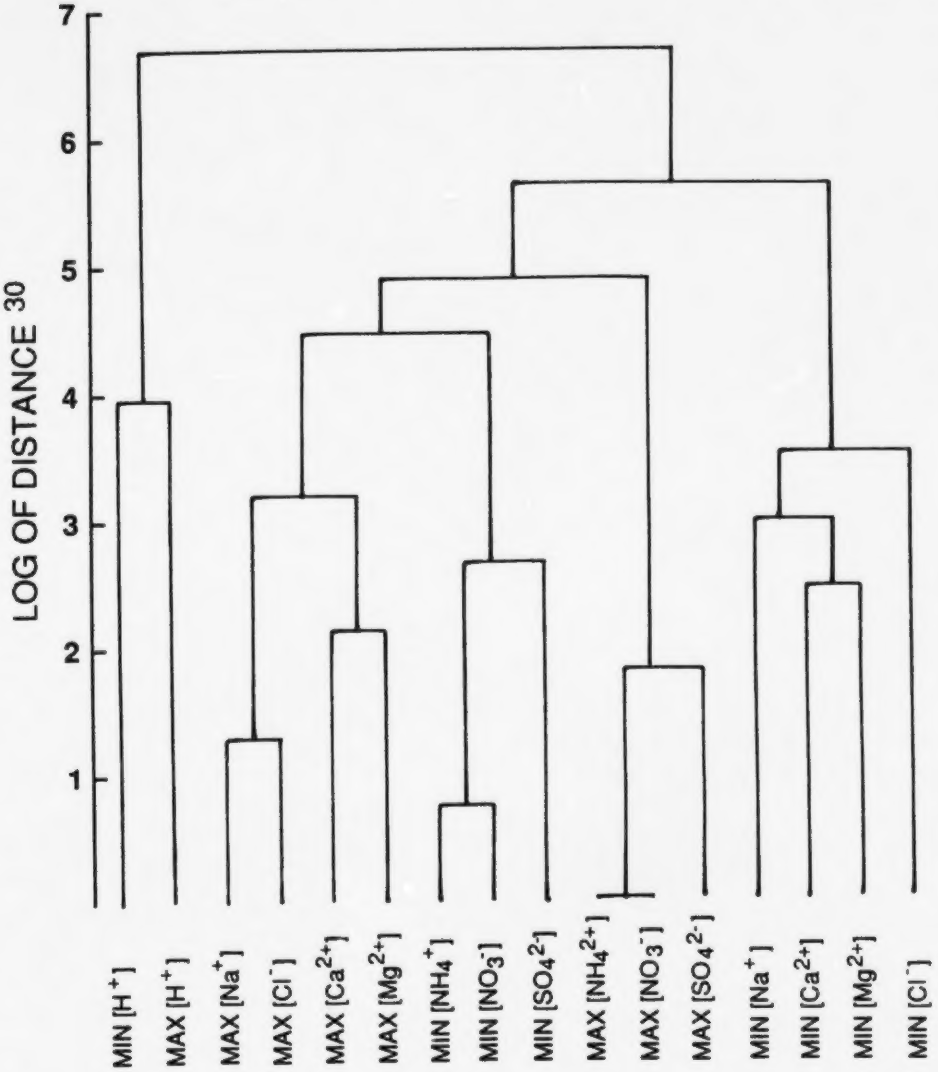

Figure 5. Dendrogram showing relationships among ions identified by cluster analysis.

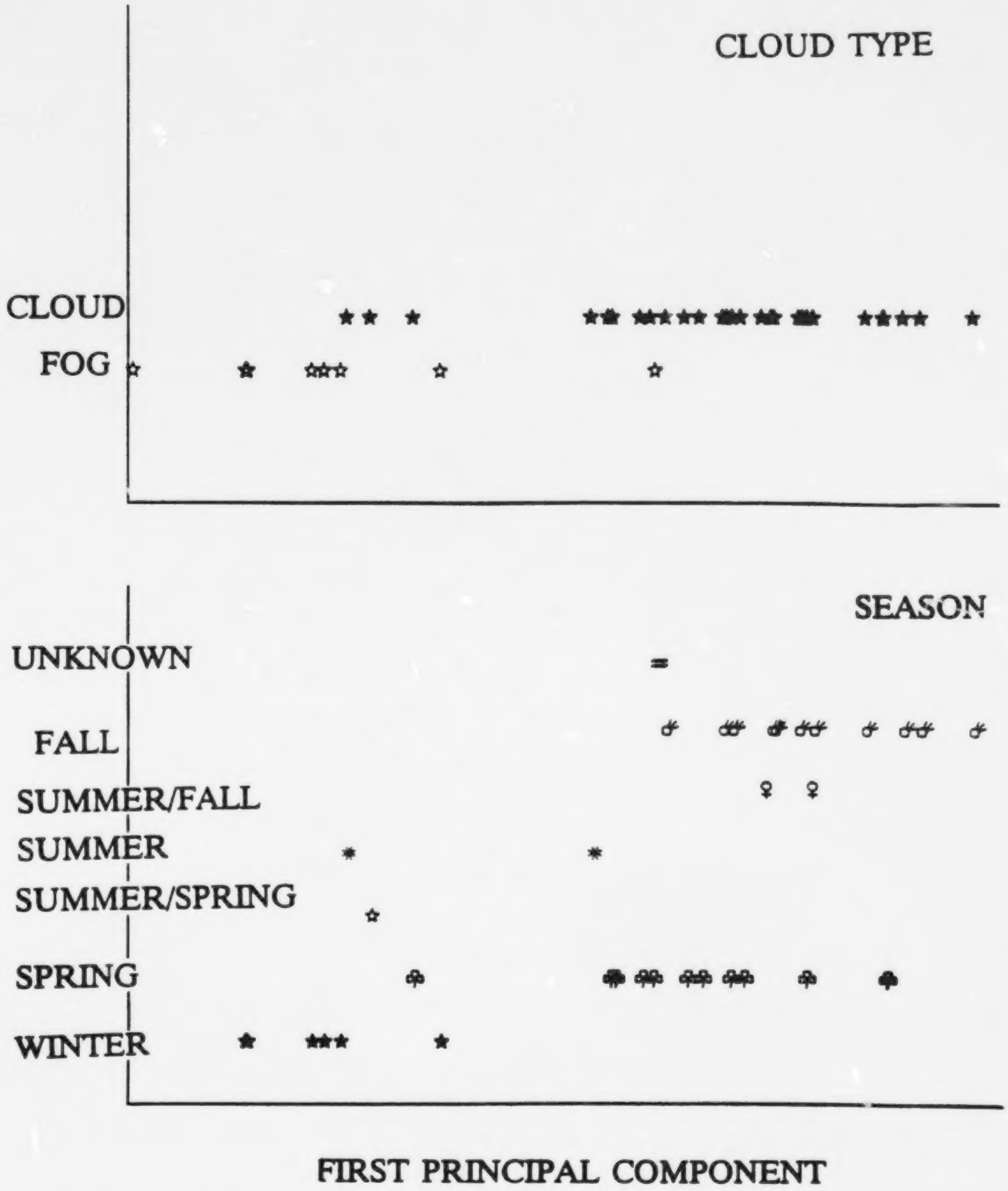

Figure 4. Overlay of cloud type and season for each cloud event (n = 36). Order on x-axis corresponds to score by event for the first principal component. The site, sampling period, and citation are listed in Table III.

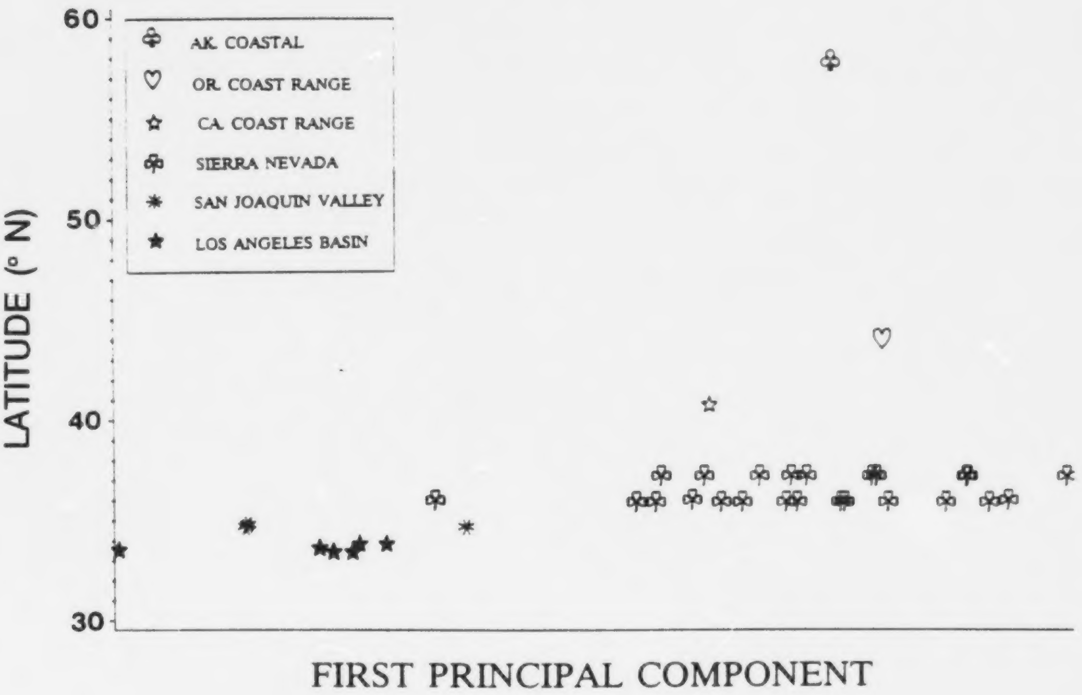

Figure 3. Relationship between geographic position (latitude) of sites where cloudwater sampling occurred and score by event for the first principal component (n = 36). The site, sampling period, and citation are listed in Table III.

Background Concentration of Sulfate in Precipitation along the West Coast of North America

Richard J. Vong

Department of Atmospheric Sciences
Oregon State University
and
U.S. EPA Environmental Research Lab
200 S.W. 35th Street
Corvallis, OR 97333

INTRODUCTION

In recent years research on the atmospheric chemistry of remote areas has increased. This work has led to the identification of important natural sources of acidic and basic emissions and to a better understanding of the transformation, transport, and deposition of sulfate from the remote atmosphere. It is useful to determine typical values for precipitation chemistry from marine air masses approaching the west coast of the United States and Canada to establish a reference point for comparison with urban and industrial areas.

Background concentrations are most commonly measured at sites remote from anthropogenic sources, although sites at great distances may not represent a useful background for some distant region. It is necessary to define carefully the meaning of background relative to the region of interest.[1] While marine background and continental background sites may be influenced by different mixes of chemical compounds,[2] sulfate is nearly always an important or dominant component such that marine background sulfate concentrations are useful for comparison with more polluted areas. Data sets from several sites monitored for multiple years are considered appropriate because averaging over time and space helps reduce variability associated with meteorology and sources, respectively.

To separate natural and anthropogenic sources, one of the following definitions of "background" concentration might be appropriate:

1. The lowest concentrations of pollutants observed in the Northern Hemisphere.
2. The average concentrations that would occur if natural emissions were distributed uniformly over the Northern Hemisphere.
3. The average concentrations expected if anthropogenic sources did not exist.

Any definition of background must be qualified not only with regard to location but also to meteorology. For example, at a clean site such as the Mauna Loa observatory in Hawaii (at 3400 m elevation), the study of carbon dioxide and aerosol data indicates three different background regimes, one observable during upslope winds and the other two observed with downslope winds.[3] At low-elevation sites along the west coast of North America, a similar difference has been observed in onshore marine air masses and offshore moving continental air masses.[4,5]

Preceding page blank

The elevation of the Mauna Loa site points out several important aspects of defining background from remote site measurements. The acid-base species available in pre-cloud air, precipitation amount, and scavenging efficiency must be considered when high-elevation samples are considered for use in defining a background. Thus, measurements made at a nearby remote site that is at a much higher elevation or where the precipitation is dominated by snowfall would not be appropriate for estimation of background in lower elevation regions.

A recent review of global background aerosol and precipitation chemistry suggested that remote locations in the Northern Hemisphere had higher sulfate concentrations than the Southern Hemisphere.[6] However, the west coast of North America has very clean precipitation relative to the rest of the continent,[7-10] and it is cleaner than the Northern Hemisphere background concentrations presented by Schwartz.[6] This is supported by event sampling[11,12] on the coast of Washington state which suggests that rain associated with onshore air flow is similar to rain falling at low altitudes in other remote, mid-latitude marine settings, including Southern Hemisphere sites.[13-21]

If low trace metal concentrations such as Pb, Cd, Cu, Zn, and As are used as the criteria, the cleanest precipitation on the earth falls in Antarctica, the South Pacific Ocean, and Greenland.[22-24] Precipitation along the west coast of North America has low concentrations (<1 ppb) of trace metals.[12,25-29]

A summary of the chemical composition of rainwater measured at remote sites is given in Table I. At remote marine sites, the dominant anion in precipitation should be sulfate.[30] Methane sulfonic acid (CH_3SO_3H or MSA) has been detected in marine precipitation and may be an indicator of marine origin of the sulfate species.[31,32] At remote continental sites, organic acids can be important components of the total anion concentrations[2] especially formate and acetate.[33,34] The important cations are H^+ and NH_4^+. If these data are representative, they suggest a preliminary estimate of background SO_4^{2-} concentration of about 5 ueq/L, NO_3^- of 3 ueq/L, formate of 1 ueq/L, and ammonium of 2 ueq/L, resulting in a pH close to 5.

Most of the measurements made in remote locations are either in the Southern Hemisphere or are of such short duration that their representativeness is uncertain. A reference point from Northern Hemisphere, mid-latitude precipitation chemistry data is needed for comparison to U.S. and Canadian values for urban and industrial areas. Thus, we analyzed data collected at coastal sites in British Columbia, Washington State, and Oregon to define a background value of rainwater sulfate concentration for the west coast of North America. Before performing this data analysis, we evaluate factors controlling the chemistry of precipitation in remote, marine locations: natural sources and scavenging of gases and aerosol by clouds and precipitation. Within this context a background definition can be provided that will be a useful reference point for evaluating an ecosystem departure from the conditions associated with remote areas with similar characteristics.

Physics and Chemistry of Remote Precipitation

The acidity of precipitation is determined dynamically by a titration of the acidic (e.g. CO_2, SO_2, H_2SO_4, HNO_3, HCOOH) by basic (e.g., NH_3 and $CaCO_3$), forming materials in air and in atmospheric liquid water. Thus, "background" sulfate concentration cannot be described only by the pH in the absence of local or anthropogenic sulfate; it must also include information regarding ammonia and other important acid-base species.[39]

Sulfate in the cloud water solution, for example, will increase in proportion to the sulfuric acid (H_2SO_4) added to the system, but the presence of basic materials, such as ammonia, means that the H^+ will not increase in proportion to the amount of H_2SO_4 added.[40] This inherent non-linearity between H^+ and SO_4^{2-} in weakly buffered rainwater means that pH is not, by itself, sufficient to characterize the acid-base chemistry of precipitation.

Ultimately, the H^+ availability in precipitation is determined by the emissions of acids and bases into the air mass, production of acids in the air or clouds, transfer of preexisting acidic and basic aerosol and gaseous species into the cloud water, and oxidation of aqueous organic acids to CO_2.

The primary acid-base components influencing precipitation chemistry in marine air masses moving onshore in remote locations are sulfuric acid, nitric acid, formic acid, methanesulfonic acid, ammonia, calcium carbonate, and, with a small effect, sea salt.[35]

One important source of rainwater solute in marine air is seawater droplets,[17,18] which are produced when air bubbles burst at the sea surface. When these droplets evaporate, aerosol particles are formed. The sea salt contains many species besides sodium and chloride in a sufficiently constant composition so that the fraction of those species attributable to sea salt usually can be subtracted from the measured values. Thus sulfate and calcium often are expressed as "excess" (i.e., the amount not associated with sea salt).[6,18]

The primary source of sulfuric acid in remote marine air is expected to be the oxidation of $(CH_3)_2S$ (dimethylsulfide or DMS), with sulfur dioxide (SO_2) as an intermediate compound. DMS is excreted by certain marine phytoplankton.[38]

The precursors of most acid-base species in precipitation are introduced into the atmosphere as gases. They are removed from the atmosphere by dissolution in atmospheric water (cloud-water or rain), absorption directly at the earth's (or ocean) surface, or by oxidation and physical transformation to aerosol or cloud particles. Particles created by gas-to-particle conversion generally will be less than 1 μm in diameter and will remain airborne with a potential lifetime of about two days.[41,42] Northern Hemisphere background sulfate aerosol concentrations are frequently about 0.2 to 0.5 $\mu gm/m^3$.[6]

Although gas-phase emission and conversion may be an important consideration in agricultural or industrialized areas, it is expected that along the west coast of North America the concentrations of background gases will be small.[43] Preexisting aerosol and the atmospheric liquid water content should be enough to approximate the acid-base character of the cloud and rain water.[30]

Solid phase precipitation forms by vapor deposition onto ice nuclei, which generally are not soluble. The snow crystal thus may contain very little sulfate. Solid-phase precipitation and rain that is melted snow potentially are chemically different and more dilute than rain[44]; elevation may have a large effect on the composition of precipitation. As elevation increases, temperature decreases, and precipitation formation increasingly involves snow-flake growth by vapor deposition. This results in a decrease in the concentration of the solutes compared to scavenging by liquid phase hydrometeors.[44]

METHODS

Data for the west coast of North America were obtained from the Atmospheric Environment Service of Canada and the U.S. Acid Deposition System (ADS). Data for five sites in British Columbia, Washington, and Oregon were screened for internal consistency and evidence of anthropogenic or continental influences. Histograms of the sulfate data (with and without screening and seasalt corrections) were used to compare sites and define background concentrations.

Other stations were not used in this study because the site locations were judged less likely to produce results that could be described as background. For example, the site in Denali National Park, Alaska, was not included because of possible influences from Anchorage area emissions and its inland, high-elevation location. Coastal sites in California also display higher concentrations of SO_4^{2-}, NO_3^-, NH_4^+, Ca^{2+}, and H^+,[45] presumably due to influences from anthropogenic emission sources. Polluted air transported to the west off the California coast could influence marine sites during subsequent onshore flow.

Data selection

Precipitation chemistry data from sites in the Canadian Network for Sampling Precipitation (CANSAP), the U.S. National Atmospheric Deposition Program (NADP), and the British Columbia Ministry of Environment[46] were examined for their usefulness in this analysis. After a preliminary review, only long-term data from five sites, three in the USA and two in Canada, were used in this study.

The results for the following coastal sites located at Port Hardy and Terrace, British Columbia (1980–83), Alsea Guard Station (1980–85) and Schmidt Farm (1980–83), Oregon, and Hoh River, Washington (1980–85), were used. Their specific locations are as follows:

> Hoh River, also called Olympic National Park, in northwestern Washington, latitude 47° 52'N, longitude 123° 55'W, NADP network.
>
> Alsea, in Siuslaw National Forest, NW of Eugene, Oregon, latitude 44° 23'N, longitude 123° 37'W, NADP network.
>
> Schmidt Farm, also called Hyslop, near Albany, Oregon, latitude 44° 38'N, longitude 123° 13'W, NADP network.
>
> Port Hardy, on Vancouver Island, Canada, latitude 50° 28'N, longitude 127° 22'W, CANSAP network.
>
> Terrace, in Northwestern British Columbia, latitude 54° 28'N, longitude 128° 35'W, B.C. Ministry of Environmental network.

The sampling records for these five sites were examined and found to be without serious gaps, and analytical procedures were determined to be constant throughout the period of interest. The analytical errors in SO_4^{2-}, NO_3^-, Ca^{2+}, NH_4^+, and H^+ are believed to be small enough to allow a precise and accurate evaluation of background values in the concentration ranges presented in Tables I and IV.[47,48] The H^+ concentrations for these sites likely represent a minimum value (maximum pH) because unpreserved precipitation samples are subject to biodegradation.[33,34,49] Vong[32] collected rainwater on the Washington coast and found increases of about 0.1 pH unit for unpreserved rainwater samples compared to samples that had been refrigerated and chloroformed.

Data Screening

A series of screening tests were applied to the data to eliminate samples that might not be valid or representative of background conditions. As a preliminary step, samples were eliminated when the field-site operator reported obvious problems with the sample's quality or the sample was recorded as snow. The screening was designed to be conservative in the sense that a sample would be rejected only if it was clearly unsuitable. Three subsets of data were formed: a "minimally screened" set where only screening steps one and two (see below) were applied to ensure sample integrity, a second set where sea salt corrections were applied to the sulfate concentrations of samples in the "minimally screened" data set, and third a "fully screened" set where samples with suspected continental or anthropogenic influence were eliminated and seasalt corrections were applied to the sulfate and calcium data.

In the first screening step, a charge balance was calculated as the absolute value of the difference between anions (Cl^-, NO_3^-, SO_4^{2-}) and cations (Na^+, Mg^{2+}, K^+, Ca^{2+}, NH_4^+, H^+) divided by the sum of anions and cations. To pass this screening step, a sample was required to have less than a 40% charge balance error; this resulted in samples surviving the entire four-step screening procedure with a mean charge balance error of 7% (about 5 ueq/L).

In the second screening step, sampling efficiency (comparison of rain gauge depth with sample volume) and sea salt (Cl^-/Na^+) ratios were utilized to identify additional samples of questionable integrity. At marine sites it is important to correctly evaluate sodium concentration if sulfate correction for sea salt is applied to determine "excess sulfate." Rainwater collected within several hundred kilometers of the ocean generally has the same Cl^-/Na^+ ratio as bulk seawater.[18,32,45,50] "Excess (or non-sea-salt) sulfate" concentrations are determined by calculating the concentration of sulfate that would have occurred if all the sodium in the sample were derived from sea salt, and then subtracting that amount from (analytical) "total sulfate" concentration. The correction is applied by subtracting 0.117 ueq/L [SO_4^{2-}] for every ueq/L [Na^+] in the sample. "Excess sulfate" and total sulfate are compared in Figure 2.

Poor sampling efficiency (rain collected by the sampler compared to rain collected by a rain gauge) could indicate problems with the sampler operation. A factor of two deviation in sampler efficiency was allowed; data used in the analysis had an efficiency greater than 50% or less than 200%. A sample also was required to be within a factor of two of the expected Cl^-/Na^+ ratio (1.8 by mass)[18,51] Screening based on the Cl^-/Na^+ ratio was not performed if the Na^+ concentration was relatively small (Na^+ <40 ueq/L), because the sea salt correction for sulfate would be small. Screening steps 1 and 2 constitute checks for sample integrity.

Few sampling sites at mid-latitude locations in North America are always isolated from anthropogenic emissions sources; aerosol concentrations were much lower along the coast of Washington during onshore flow than when air trajectories had passed over continental areas.[4] Precipitation concentrations at Bermuda vary considerably depending upon air trajectory.[52] Rain along the west coast generally occurs under southwest flow from the Pacific[53]; most precipitation samples would be collected during onshore flow.[11] It would be desirable to identify rain samples collected during offshore flow or during onshore flow with a past overland trajectory. A meteorological analysis cannot provide this information because of the weekly and monthly sampling intervals. Later we present a principal component analysis of the "minimally screened" rainwater data to indicate that continental and anthropogenic sources are still influencing some samples in that data subset.

Screening steps 3 and 4 identify samples with evidence of a period of continental residence for the air mass. Studies that analyzed precipitation chemistry in very isolated locations[13,36] or that selected 'clean' air trajectories[11,12,32,39] suggested upper limits for three components of background precipitation: nitrate, ammonia, and calcium (all indicative of terrestrial emission sources). These criteria were derived from Northern Hemisphere sampling,[11] but they are consistent with Southern Hemisphere data.[13,14]

Application of screening step 3 to the data from the west coast of North America asks: what are the sulfate concentrations in rainwater samples that have nitrate concentrations (an 'anthropogenic tracer') in the same range as that of clean rainwater collected elsewhere? The levels for screening are defined from Vong et al.,[11,12] Quinn et al.,[39] (samples always contained less than 5 ueq/L each of nitrate and ammonium ion), Galloway and Gaudry[36] and Galloway et al.[14] (NO_3^- concentrations were less than 5 ueq/L, 95% confidence; NH_4^+ was less than 5 ueq/L).

Calcium, especially as calcium carbonate, is a major earth mineral and may be evidence of contamination by wind-blown dust. However, calcium is also a significant component of seawater.[17,51] Therefore, "excess calcium" ($Caxs^{2+}$) is calculated to remove the seasalt contribution (Ca^{2+} - 0.0378 * Na^+ for mg/L units). In screening step 4, rainwater samples with NH_4^+ greater than 5 ueq/L (see above) or with more than 10 ueq/L $Caxs^{2+}$ were removed from the data. Most remote rainwater samples have excess calcium less than 10 ueq/L.[13] This definition for background sulfate concentration is based on an indirect indicator of marine air trajectories, that is, samples with $Caxs^{2+}$, NO_3^- and NH_4^+ concentrations less than screening levels derived from experiments in which only 'clean air' was sampled.

RESULTS

The effect of the screening procedure was investigated by tracking the number of samples surviving each of the four screening steps. Sulfate concentrations were compared with and without the final two steps of screening and with and without the correction for seasalt sulfate. Mean concentrations for five species key to the acid-base chemistry are presented as well as a multivariate analysis used to identify correlations between the variables in the "minimally screened" data.

Effects of Screening

A total of 385 rainwater samples survived the four-step screening procedure, which represented 62% of the 617 rain samples chemically analyzed by the NADP and CANSAP laboratories for these five sites. As seen in Table II, the largest number of samples were eliminated due to the sea-salt-sampler efficiency ratios at the Hoh (30 samples eliminated/219 total samples), Terrace (15/46), and Schmidt (39/125) sites. At the Alsea (31/180) and Schmidt (37/125) sites, a number of samples were dropped due to nitrate concentration but at Pt. Hardy the greatest number of samples (7/47) were dropped due to the NH_4^+ and Ca^{2+} screening step. For most sites relatively few samples were eliminated due to the last screening step (excess calcium or ammonium). Overall, 15% of the samples were eliminated due to nitrate screening but only 6% were eliminated at the northern three sites (British Columbia and Washington).

Estimates of Background

For purposes of this paper, background sulfate concentration in rainwater was defined as a range of values observed in weekly or monthly samples collected at the most remote, low elevation sites on the west coast of North America (after eliminating sea salt contributions). The measurement sites selected for analysis were upwind of population and industrial centers, and it was possible to identify, and exclude, individual measurements that appeared to be influenced by anthropogenic sources. For reasons stated earlier, this definition also excludes measurements taken during precipitation in the form of snow. Five sites that met the above criteria, two in British Columbia, Canada, one in Washington, and two in Oregon were selected for analysis. There is no *a priori* reason to believe that these sites are different with respect to observed background sulfate values.

Following selection of these sites, the aqueous concentration of sulfate in rainwater, rather than the deposition rate of sulfate via rain, was selected as the appropriate variable. This decision was based partly on the fact that the concentration of sulfate does not display a significant correlation with weekly precipitation amount at these marine sites. The total amount of rain in a year varies among the five coastal sites and varies considerably between the coast and any inland region of interest (as much as a factor of three). It is rainwater sulfate concentration rather than sulfate wet deposition that is a common characteristic of these five coastal sites. The removal of sulfate species from the air is a relatively inefficient mechanism; a correspondingly large atmospheric residual amount of sulfur is not removed in any given rain event over spatial scales of 100 km.[54] Therefore, if deposition were chosen, geographic variability in the amount of rain between the background reference point and any inland regions becomes the single most important determinant of any comparison of sulfate deposition rate. The choice of sulfate concentration in rainwater, rather than deposition rate, eliminates this potential rainfall bias.

Based on the above approach, the sulfate concentration measurements at the five sites were screened to require internal consistencies of sample volume to rain gauge measurements, ionic balance, and a sodium-to-chloride ratio similar to seawater. Histograms of the "fully screened and minimally screened" data for one site are presented in Figure 2. The Schmidt, OR, site is presented to illustrate the effect of screening on the data for the site that had the largest fraction of samples fail screening step 3. The location of the Schmidt, OR, site is further inland than the other sites analyzed here; more frequent continental influence (see Table II) is not surprising. Histograms for the other four sites are presented elsewhere.[47]

A principal component analysis of the "minimally screened" data for the five sites demonstrated that sea salt was the predominant source of chemical variability (see Table III). Therefore, the sulfate correction using sodium ion concentration as an index of sea salt was necessary to remove sea salt contributions to total sulfate. Additional sources were weakly indicated, with the suggestion of a soil-derived or combustion factor (PC#2). Unfortunately, no tracers of marine excess sulfate (such as MSA) were available for this analysis.

Figure 2 shows the original total sulfate histograms (solid) for the Schmidt site and the "excess sulfate" histograms (cross-hatched) resulting from this correction. A substantial number of the high sulfate observations (20 ueq/L) were associated with high seasalt levels. Because the sea salt sulfate is largely contained in large aerosol (dia. >1 μm), this portion of the background aerosol would be quickly removed as an air mass moves inland and is not useful as a reference point for inland areas. Histograms for the other sites were similar.[47]

The sea salt correction alone is not adequate for the analysis of background sulfate concentrations. It is required that no known anthropogenic sources should influence the measurements. To this end, the screening criteria described as steps 3 and 4 were established based on source information gained from principal component analysis (Table III, PC#2) and knowledge of precipitation chemistry for event samples at remote locations. The nitrate and ammonium ion restriction was based on the ocean not being a significant source of these ions, whereas the excess calcium screening criteria reduced the influence of crustal material.

Figure 2 shows the excess sulfate frequency distribution after this final screening procedure as the "fully screened" value. The high values (>20 ueq/L) in the minimally screened data (steps 1 and 2) are virtually eliminated from the fully screened data. Shifts in the distributions for the other four sites also occurred with seasalt corrections and full screening.

These distributions provide the concentration values expected for "background" sulfate from weekly to monthly sampling intervals. The distributions reflect the influence of a widely distributed, sub-micrometer sulfate aerosol and its influence on coastal, lowland rainwater.[11,30,55] Using the Junge equation[18] with fine sulfate aerosol concentrations of 0.2 to 0.4 $\mu g/m^3$ appropriate for remote areas,[6] nucleation scavenging efficiencies of 0.8 to 1.0[11,56] and cloud liquid water contents of 0.5 to 1.0 g/m^3,[11,30,57,58] one would expect background rainwater sulfate concentrations to vary between 3 and 16 ueq/L. This aerosol is expected to influence rainwater chemistry in a similar way at these sites as it does at the downwind region of interest, absent the effects of altitude mentioned above.

Support for this notion of a widely distributed sulfate aerosol is noted when one compares the excess sulfate distributions for rainwater at each of the five sites with the average distribution for all five sites; their similarity suggests a general widespread background concentration that is relatively invariant over space along the west coast of North America when multi-annual averaging periods are considered. This finding is consistent with the widespread distribution of the likely emission source: production of DMS by biological activity in upwelling areas of the ocean and over the open ocean.[35,38]

Figure 3 presents two versions of the frequency distribution of "fully screened excess" sulfate for all five sites (the data were summarized both by weighting each site equally [solid] or by weighting by the number of samples collected [cross-hatched]). The two presentations are very similar, with about 86% of the samples having excess sulfate between 2 and 12 ueq/L and a few samples with concentrations between 14 and 22 ueq/L. This results in mean or median values lower than Schwartz's[6] estimate of a mean background precipitation sulfate concentration of 10-15 ueq/L for the Northern Hemisphere. The data analyzed here are entirely consistent with Schwartz's background sulfate aerosol data and nucleation scavenging theory, which predicts 3-16 ueq/L background sulfate for rain. Schwartz's rainwater data were primarily from

Bermuda and the Arctic but his aerosol data covered a much larger portion of the Northern Hemisphere. Clearly, the Pacific Coast of Washington, Oregon, and British Columbia experiences very clean rain.

The sulfate ion concentrations shown in Figure 3 are the best estimate of the background sulfate in rainwater on the west coast of North America. A distribution is more appropriate than a single value because the background is expected to vary over time with variation in emission sources and meteorology. It is emphasized that this distribution is applicable over an annual averaging period with a one-week to one-month sampling time.

Table IV presents the chemical composition for the "fully screened" data set (i.e., after screening steps 1-4). Neglecting seasalt, sulfate is the dominant anion in rainwater while hydrogen ion (mean = 5 ueq/L) is usually the most important cation for these samples. Nitrate (mean = 1 ueq/L) is present at levels less than 50% of excess sulfate concentration. Ammonium was always very low (<2 ueq/L) at these coastal sites. No data were available for organic anions. These results are consistent with our preliminary estimate of 5 ueq/L for excess sulfate in background rainwater. The mean pH of 5.3 is slightly higher than the value of 5.0 predicted from event sampling, possibly because of slightly higher levels of cations such as $Caxs^{2+}$ (mean = 2 ueq/L), especially at the Alsea and Terrace sites. The weekly/monthly sampling intervals underestimate H^+ because of biodegradation of organic acids; the 'true' pH for these sites would be below 5.3 (see above).

It is interesting to note the fairly large differences in weekly precipitation amount (mean/range = 1) between the five sites in contrast to the relatively consistent values for rainwater sulfate concentrations (mean/range = 0.6). The wet deposition of excess sulfate is directly related to precipitation amount in background locations but is relatively independent of sulfate concentration. This is consistent with the concept of concentration rather than deposition as the most representitive characteristic of background rainwater composition along the west coast of North America.

The sulfate concentrations reported here are useful as an estimate of background along the west coast of North America as a reference point with which to compare data from industrial and urban areas. Sulfate should be a more useful characteristic of background than pH because excess sulfate is a conservative tracer whereas H^+ is easily removed from the system by addition of bases such as soil dust or ammonia. A comparison of background with industrial/urban precipitation composition was conducted by Galloway et al.[14] using remote data that was collected mostly in the Southern Hemisphere or distant from continental land masses. Our analysis indicates that their comparison holds true when mid-latitude, Northern Hemisphere precipitation composition is used as the reference value.

It is not known at this time how far inland the air masses are influenced by the marine sulfate aerosol; given a lifetime of about two days for sub-micrometer sulfate aerosol, this background concentration would be expected to persist on the order of a few hundred kilometers. Naturally occurring terrestrial emissions could add to marine excess sulfate, and scavenging processes could alter the incoming marine air before reaching urban/industrial areas. Therefore, it is important to distinguish this reference value (2-12 ueq/L excess sulfate) from the actual contribution of the marine aerosol farther inland or the sum of all natural contributions, both of which are unknown at this time.

CONCLUSIONS

The description of the acid-base chemistry of precipitation and mechanisms of precipitation formation imply that any useful interpretation of precipitation measurements must consider those perspectives. Data derived from rain must be separated from data derived from snow measurements. For the purposes of this report, "background" sulfate was defined as the range of concentration in weekly or monthly samples of rain collected over multi-annual periods at remote sites, upwind of urbanized areas, with the further requirement that data with evidence of possible anthropogenic source contamination be excluded.

In the marine air masses studied in this report, sulfate was the dominant ion in the acid-base balance; other ions were present but were less important in a charge balance sense. The screening techniques appear to have been successful in defining a useful reference value for excess sulfate whose spatial consistency reflects a widespread sulfate aerosol oceanic source and whose temporal variation is consistent with the concept of nucleation scavenging of that sulfate aerosol by liquid water. Since this background sulfate is only slowly removed by rainfall, the region of non-sea-salt, marine sulfate influence may extend approximately several hundred kilometers downwind from the west coast of North America.

Values obtained from several long-term record sites along the west coast of North America were mutually consistent and suggest a background excess sulfate concentration in the range of 2 to 12 ueq/L for most weekly and monthly samples. The distribution has a mode of approximately 8 ueq/L with a mean of 5.5 ueq/L for 3 to 5 years data at each of five sites. The average measured pH of this rainwater was 5.3, but actual pH values are likely to be slightly lower than the measured values due to changes in sample composition between collection and chemical analysis.

ACKNOWLEDGMENTS

This work was supported by the Forest Response Program of NAPAP through cooperative agreement #CR815714-01 between Oregon State University and EPA ERL-Corvallis. Data analysis had previously been performed under a grant from the Atmospheric Environment Service of Canada to Cirrus Consultants, Vancouver, B.C.[47] I thank Bob Charlson and Tim Larson for valuable discussions.

REFERENCES

1. P.W. Summers, "Regional Background Atmospheric Sulphate Levels in Canada:Preliminary Estimates and Implications for Control Strategies," Atmos. Environ. Service of Canada Report, Downsview, ONT, 1985.

2. W.N. Keene and J.N. Galloway, "The biogeochemical cycling of formic and acetic acids through the troposphere: an overview of current understanding," *Tellus* 40BP:322 (1988).

3. G.E. Shaw, "Transport of Asian Desert aerosols to the Hawaiian Islands," *J. Applied Met.* 19:1254 (1980).

4. T.D. Fox and J.D. Ludwick, "Lead concentrations associated with 1000 mb back trajectories at Quillayute, Washington," *Atmos. Environ.* 10:799 (1976).

5. J.D. Ludwick, T.D. Fox, and S.R. Garcia, "Elemental concentrations of northern hemispheric air at Quillayute, Washington," *Atmos. Environ.* 11:1083 (1978).

6. S.E. Schwartz, "Are global cloud albedo and climate controlled by marine phytoplankton?" *Nature* 336:441 (1988).

7. R.J. Vong and T.V. Larson, "A Critical Review of Acid Deposition Research in the Pacific Northwest," Seattle, WA:Puget Power and Light Co. Research Project 1983-1, Final Report, 1983.

8. S. Nikleva, "Acid Rain on the West Coast of British Columbia," Report 8305-4 PAES, Atmospheric Environment Service, Vancouver, B.C., 1983.

9. R.J. Vong, T.V. Larson, D.S. Covert, and A.P. Waggoner, "Measurement and modeling of Western Washington precipitation chemistry," *Water, Air and Soil Pollution*, 26:71 (1985).

10. C.F. Powers and D.L. Rambo, "A review of precipitation chemistry in the western USA," *Environ. Monitor. Assess.*, 1:93 (1981).

11. R.J. Vong, H.C. Hansson, D.S. Covert, and R.J. Charlson, "Acid rain: simultaneous observations of a natural marine background and its acidic aerosol precursor," *Geophys. Res. Lett.* 14, 4:338 (1988).

12. R.J. Vong, H.C. Hansson, H.B. Ross, D.S. Covert, and R.J. Charlson, "Northeastern Pacific submicrometer aerosol and rainwater composition: a multivariate analysis," *J. Geophys.Res.* 93, D2:1625 (1988).

13. J.N. Galloway, G.E. Likens, W.C. Keene, and J.M. Miller, "The Composition of Precipitation in Remote Areas of the World," *J. Geophys. Res.* 87:8871 (1982).

14. J.N. Galloway, G.E. Likens, and M.E. Hawley, "Acid precipitation: natural versus anthropogenic components," *Science* 226:829 (1984).

15. E. Eriksson, "The chemical composition of Hawaiian rain," *Tellus* 9:509 (1957).

16. C.E. Junge, "The concentration of nitrate and ammonium in rain water over the United States," *Trans. Amer. Geophys. Union*, 39:241 (1958).

17. C.E. Junge and R.T. Werby, "The concentration of chloride, sodium, potassium, calcium, and sulfate in rain water over the United States," *J. Meteorology*, 15:417 (1958b).

18. C.E. Junge, *Air Chemistry and Radioactivity*, Academic Press, New York, 1963.

19. U. Dayan, J.M. Miller, W.C. Keene, and J.N. Galloway, "An analysis of precipitation chemistry from Alaska," *Atmos. Environ.* 19:651 (1985).

20. G.E. Likens, W.C. Keene, J.M. Miller, and J.N. Galloway, "Chemistry of precipitation from a remote terrestrial site in Australia," *J. Geophys.Res.* 92:13299 (1987).

21. J.M. Miller and A.M. Yoshinaga, "The pH of Hawaiian precipitation, a preliminary report," *Geophys. Res. Lett.* 8:779 (1981).

22. M.R. Legrand and J.R. Delmas, "The ionic balance of Antarctic snow:a 10-year detailed record," *Atmos. Environ.* 18, 9:1867 (1984).

23. J.N. Galloway, J.D. Thornton, S.A. Norton, H.L. Volchok, and R.A.N. McLean, "Trace metals in precipitation, a review and assessment," *Atmos. Environ.* 16:1677 (1982).

24. C.I. Davidson, W.D. Goold, T.P. Mathison, G.B. Wiersma, K.W. Brown, and M.T. Reilly, "Airborne trace elements in Great Smoky Mtn, Olympic, and Glacier National Parks," *Environ. Sci. Tech.* 19:27 (1985).

25. L.A. Rancitelli and R.W. Perkins, "Trace element concentrations in the troposphere and lower stratosphere," *J. Geophys. Res.* 75:3055 (1970).

26. T.M. Tanner, L.A. Rancitelli, and W.A. Haller, "Multielemental analysis of natural waters by neutron activation techniques,"*Water, Air, and Soil Poll.*, 1:132 (1971).

27. R.R. McLaren, "Lower Mainland and South Coast B.C. Precipitation Chemistry Data," Report PAES 85-2, Atmospheric Environment Service Pacific Region, Vancouver, B.C., 1985.

28. R.R. McLaren, "Lower Mainland Precipitation Chemistry Data," Report PAES 82-4, Atmospheric Environment Service Pacific Region, Vancouver, B.C., 1982.

29. R.R. McLaren, "Sampling of Snowpacks for Chemical Analysis in Southwestern British Columbia," Report PAES 82-3, Atmospheric Environment Service Pacific Region, Vancouver, B.C., 1982.

30. R.J. Charlson and H. Rodhe, "Factors controlling the acidity of natural rainwater," *Nature* 295:683 (1982).

31. E.S. Saltzman, D.L. Savoie, R.G. Zika, and J.M Prospero, "Methane sulfonic acid in the marine atmosphere," *J. Geophys. Res.* 88, C15, 10897 (1983).

32. R.J. Vong, "Simultaneous Observations of Rainwater and Aerosol Chemistry at a Remote Mid-Latitude Site," PhD Dissertation, University of Washington, Seattle, WA., 1985.

33. W.C. Keene, J.N. Galloway, and J.D. Holden,"Measurement of Weak Organic Acidity in Precipitation from Remote Areas of the World," *J. Geophys. Res.*, 88:5122 (1983).

34. W.C. Keene, R.J. Galloway, and J.D. Holden, "Organic Acidity in Precipitation for Remote Areas of the World," Proc. 3rd Nat. Sympos. on Recent Advances in Measurement of Pollutants in Ambient Air and Stationary Sources, USEPA, RTP, NC. (1983).

35. J.N. Galloway, "The deposition of sulfur and nitrogen in the remote atmosphere," in *The Bio-geochemical Cycling of Sulphur and Nitrogen in the Remote Atmosphere: NATO Advanced Research Workshop*, J.N. Galloway, R.J. Charlson, M.O. Andreae, H. Rodhe, Eds., D. Reidel Publishing Co., Dordrecht, 1985.

36. J.H. Galloway and A. Gaudry, "The composition of precipitation on Amsterdam Island, Indian Ocean," *Atmos. Environ.* 18:2649 (1984).

37. R. Arimoto, R.A. Duce, B.J. Ray, and C.K. Unni, "Atmospheric trace elements at Enewetok Atoll, 2. Transport to the ocean by wet and dry deposition," *J. Geophys. Res.* 90:2391 (1985).

38. M.O. Andreae and H. Raemdonck, "Dimethylsulfide in the surface ocean and marine atmosphere: a global perspective," *Science* 221:744 (1983).

39. P.K Quinn, R.J. Charlson, and T.S. Bates, "Simultaneous observations of ammonia in the atmosphere and ocean," *Nature* 335:336 (1988).

40. R.J. Vong and R.J. Charlson, "The pH of a cloud or rain drop: a computer based solution for a six component system," *J. Chem. Educ.* 62:141 (1985).

41. H.R. Pruppacher and J.D. Klett, *Microphysics of Clouds and Precipitation*, D. Reidel Publ., Boston, 1980.

42. H. Rodhe and J. Grandell, "On the removal time of aerosol particles from the atmosphere by precipitation scavenging," *Tellus* 24, 5:442 (1972).

43. M.O. Andreae, H. Berresheim, T.W. Andreae, M.A. Kritz, T.S. Bates, and J.T. Merrill, "MSA, sulfate, and SO_2 in air over the eastern portion of the North Pacific," *J. Atmos.Chem.* 6:149 (1988).

44. B.C. Scott, "Sulfate Washout in Winter Storms," *J. Applied Met.*, 20:619 (1981).

45. J.H. Gibson, "NADP/NTN annual data summary, precipitation chemistry in the United States," Colorado State University, Ft.Collins, CO, 1987.

46. W. Sandberg, "Precipitation Monitoring Reports for Aggassiz, Kitimat, Pender, Sechelt, Squamish, Smithers, and Victoria," British Columbia Ministry of the Environment, Victoria, B.C., 1985.

47. P.G. Sagert, M.G. Ruby, B. Fane, J.L. Frazer, R.J. Charlson, L.C. Duncan, T.V. Larson, and R.J. Vong, "Background Concentrations of Sulphate in Precipitation along the British Columbia Coast," Report PAES-86-1, Atmos.Environ.Service of Canada, Vancouver, B.C., 1986.

48. D.L. Sisterson, B.E. Wurfel, and B.M. Lesht, "Chemical Differences Between Event and Weekly Precipitation Samples in Northeastern Illinois," *Atmos. Environ.* 19:1453 (1985).

49. W.N. Keene and J.N. Galloway, *Atmos.Environ.* 18:2491 (1984).

50. L. Granat and R. Soderlund, "Atmospheric Deposition Due to Long and Short Distance Sources," University of Stockholm, Dept. of Meteorology, Report AC-32, Stockholm, Sweden, 1975.

51. H.D. Holland, *The Chemistry of the Atmosphere and Oceans*, John Wiley and Sons, New York, 1978.

52. J.L Moody and J.N. Galloway, "Quantifying the relationship between atmospheric transport and the chemical composition of precipitation on Bermuda," *Tellus* 40B, 463 (1988).

53. J.E. Overland and B.A. Walter, "Marine weather of the inland waters of western Washington," NOAA report EML-44, Nat. Ocean. and Atmos. Admin., Seattle,WA, 1983.

54. R.J. Vong, L. Moseholm, D.S. Covert, P. Sampson, J. O'Loughlin, M. Stevenson, R.J. Charlson, W.H. Zoller, and T.V. Larson, "Changes in rainwater acidity associated with closure of a copper smelter," *J. Geophys. Res.* 93, D6:7169 (1988).

55. D. Savoie, "Nitrate and non-sea-salt sulfate aerosols over major ocean regions of the world ocean: concentrations, sources, and fluxes," PhD thesis, University of Miami, Miami, FL, 1984.

56. J.B. Jensen and R.J. Charlson, "On the efficiency of nucleation scavenging," *Tellus* 36B, 5:367 (1984).

57. P.V. Hobbs and P.O.G. Persson, "The mesoscale and microscale organization of clouds and precipitation in mid-latitude cyclones, V. The substructure of narrow cold frontal rainbands," *J. Atmos. Sci.* 39:295 (1982).

58. P.Y. Wang and P.V. Hobbs, "The mesoscale and microscale structure and organization of clouds and precipitation in mid-latitude cyclones, X. Wavelike rainbands in occlusion," *J. Atmos. Sci.* 40:1959 (1983).

Table I: Chemical composition of rainwater collected at remote sites [ueq/L].

	Lake Ozette WA[11,12]	Amsterdam Island[13]	Poker Flat Alaska [35]	Katherine Australia [33,34,36].	Enewetok Atoll[37]
H^+	5.2	8.8	11.0	16.6	-
SO_4^{2-}	15.2	29.2	7.2	6.3	-
$SO_4(xs)^{2-}$	5.8	4.9	7.1	5.5	5.8
Na^+	78.8	206.5	1.0	7.0	48.
Cl^-	98.2	237.7	2.6	11.8	57.
Br	-	-	-	-	0.1
Mg^{2+}	18.3	45.9	0.2	2.0	14.
NO_3^-	2.5	1.3	1.9	4.3	-
NH_4^+	2.3	1.8	1.1	2.0	-
K^+	3.0	4.4	0.6	0.9	1.
Ca^{2+}	3.8	8.6	0.1	2.5	2.5
RCOOH	0.97	2.2		0.6-53.0	-
MSA	0.07	-	-	-	-
Ratio[a]:NH_4^+ /$SO_4(xs)^{2-}$	0.4	0.4	0.2	0.4	-

[a] Ratio as [ueq/L / ueq/L]

Table II. Number of samples remaining after each step of the screening.

	Alsea 1980-85	Schmidt 1980-83	Hoh 1980-85	Pt.Hardy 1980-83	Terrace 1980-84
N	180	125	219	47	46
N1	177	122	212	46	45
N2	164	83	182	42	30
N3	133	46	167	38	30
N4	128	35	162	31	29

Number of samples surviving four successive screening steps:

N =Number of rain samples chemically analyzed by the network.

N1 =Number within 40% of charge balance (passed step 1).

N2 =Number with sea-salt ratio and sampler efficiency between 50-200% (passed step 2).

N3 =Number with NO_3^- < 5 ueq/L (passed step 3).

N4 =Number with both $Caxs^{2+}$ < 10 ueq/L and NH_4^+ < 5 ueq/L (passed step 4).

Table III: Principal component analysis of the "minimally screened" data (i.e.- after screening steps 1 and 2):

	Alsea	Schmidt	Hoh	Pt. Hardy	Terrace	All Sites
PC#1	Na^+,Cl^-,Mg^{2+}	Na^+,Cl^-,Mg^{2+}	Na^+,Cl^-,Mg^{2+}	Na^+,Cl^-,Mg^{2+}	Na^+,Cl^-	Na^+,Cl^-,Mg^{2+}
PC#2	$Caxs^{2+}$ SO_4xs^{2-}	$Caxs^{2+}$ H+	H+ SO_4xs^{2-} NO_3^-	NH4+ NO_3^-	$Caxs^{2+}$ Mg^{2+}	H+ SO_4xs^{2-} $Caxs^{2+}$

SO_4xs^{2-} and $Caxs^{2+}$ have been corrected for sea salt, see text.

Table IV: Precipitation composition for five sites along the west coast of North America ("fully screened data," i.e., after screening steps 1-4) [ueq/L] (volume-weighted mean).

	Alsea OR	Schmidt OR	Hoh WA	Pt.Hardy B.C.	Terrace B.C.	All Five[a]
Rainfall [mm/wk]	48.3	44.1	73.2	46.7	28.5	48.1
Charge Bal	0.05	0.08	0.07	0.07	0.19	0.07
Cl^-/Na^+	1.8	2.2	2.5	1.7	2.1	2.1
N	128	35	162	31	29	385
Na^+	45.0	13.0	24.0	66.0	5.4	34.0
SO_4xs^{2-}	5.5	5.0	4.4	6.4	7.8	5.5
NO_3^-	1.7	2.5	1.4	1.4	0.6	1.4
H^+	3.6	3.2	3.7	8.3	7.5	5.1
NH_4^+	1.4	2.0	1.4	0.7	0.4	1.2
$Caxs^{2+}$	3.8	2.0	1.3	3.4	4.1	2.2

[a] All= precipitation-weighted mean of all samples for the five sites.

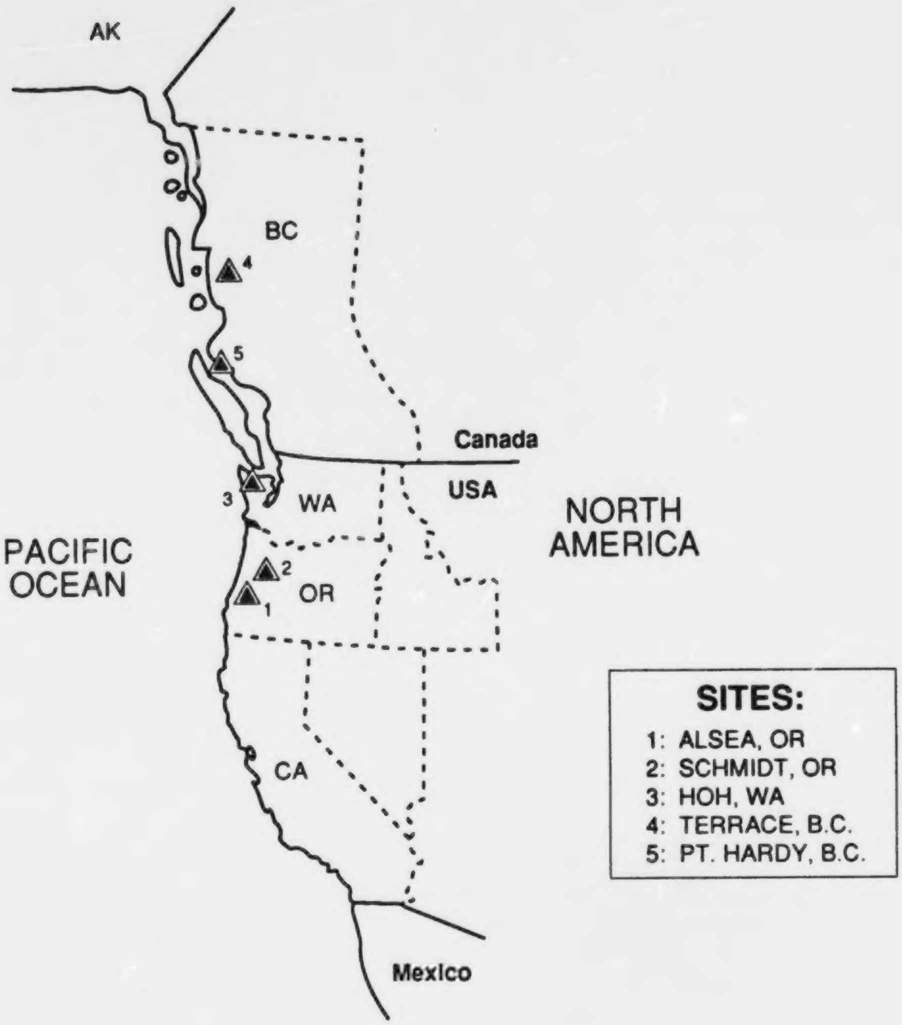
AK
BC
4
5
Canada
USA
3
WA
2
OR
1
CA
Mexico
PACIFIC OCEAN
NORTH AMERICA
SITES:
1: ALSEA, OR
2: SCHMIDT, OR
3: HOH, WA
4: TERRACE, B.C.
5: PT. HARDY, B.C.

Figure 1. Rainwater collection sites used in the analysis of background sulfate.

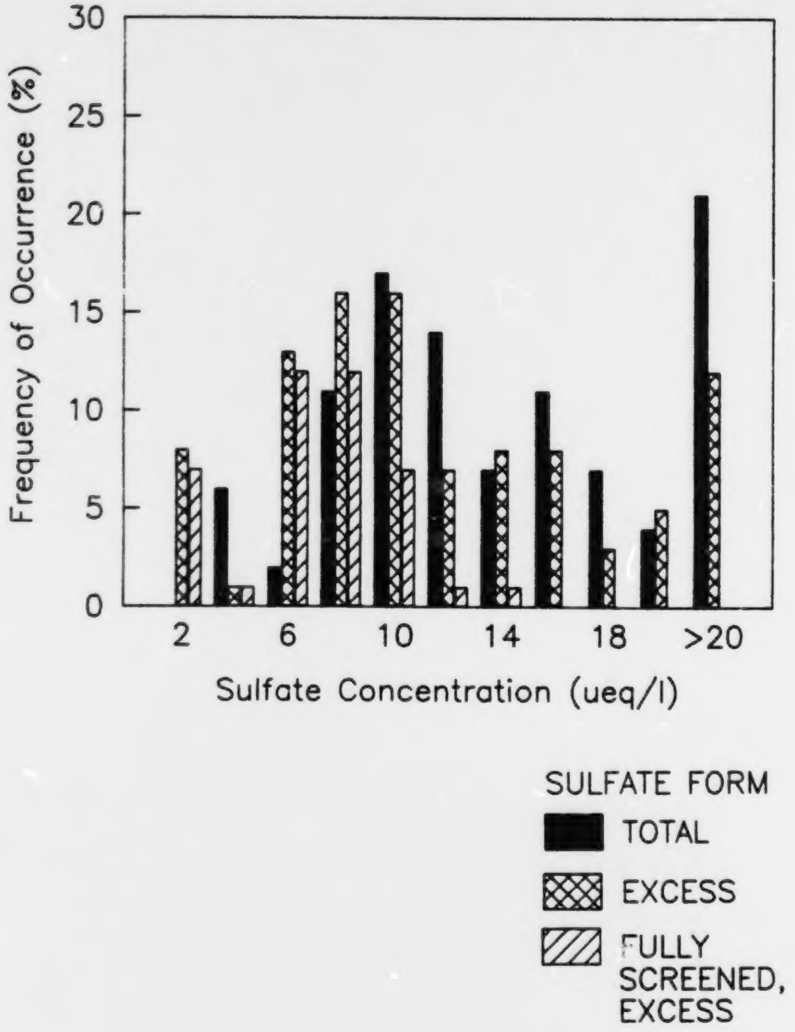

Figure 2. Schmidt, Oregon site: total and excess sulfate.

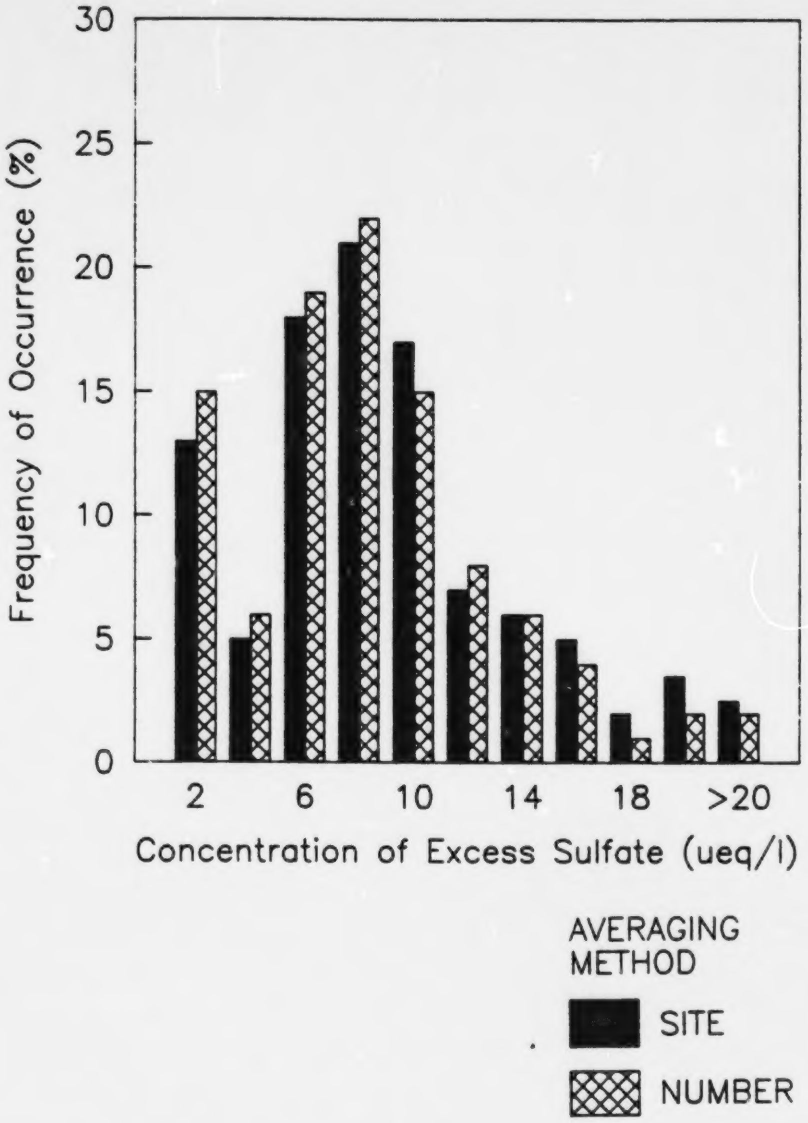

Figure 3. Excess sulfate concentration for all stations.

Analysis of a Summertime Acid Rain Event in the Sierra Nevada

Charles D. Unger

Crocker Nuclear Laboratory
University of California, Davis
Davis, CA 95616

INTRODUCTION

From July through September the western United States experiences a seasonal shift in weather that produces a pronounced change in wind patterns and precipitation. The affected area extends from the Rocky Mountains to California; the western edge of the area is recurrently the Sierra Nevada. During this period, pulses of warm, moist air of subtropical origin move northward, accompanied by extensive thunderstorm activity.

An acid rain event occurred at Emerald Lake in the Sierra Nevada on July 17-20, 1984.[1] The site is located in Sequoia National Park at 2800 m elevation, southeast of Fresno. The event was characterized with relatively high levels of acidity in the rainwater (pH of 4.25) and significant amounts of rain (4.5 cm); therefore the acid deposition was large. The nitrate ion concentration was 35.3 micro-equivalents/L and the sulfate ion concentrations were 23.8 micro-equivalents/L in the rainwater. Using these values, the nitrate ion flux was 985 kg/km^2 and the sulfate flux was 102.8 kg/km^2. This paper includes analyses of meteorological conditions during July 17-20, 1984, when airborne pollutants from emissions in Northern Mexico, Arizona, and the Colorado River basin may have been transported northward within a moist airmass and contributed to rainfall acidity at Emerald Lake.

Other acid rain events, with pH values between 4.65 and 4.85, were monitored during the summers of 1984-1985.[1] Therefore, the acid precipitation above was not an isolated event. However, other rainfall events had less acidity and rainfall. We analyzed the rainfall event with the highest acidic flux.

Thunderstorms are thermodynamic entities in which the potential energy of atmospheric instability and the latent heat of condensation are rapidly converted into kinetic energy with strong (and occasionally destructive) winds and violent vertical air currents. These forces can produce torrential rain, hail, lightning, and thunder. An ample supply of moist, unstable air is necessary to maintain the storm. Acid rain precursors and other pollutants in the entrained air are contained in the falling raindrops, forming acid rain. Thunderstorms may be viewed as gigantic vacuum cleaners that remove pollutants from the atmosphere and deposit them on the earth's surface in rainwater.

ANALYSIS

Meteorological charts for July 17-20, 1984, were used to identify source areas of acid rain precursors. Radar charts (Figure 1) indicate an extensive band of thunderstorms extending through New Mexico, Arizona, Nevada, and the Sierra Nevada. Radar tops were reported between 35,000-42,000 ft and contour intensities indicated moderate to heavy rates of rainfall in some thunderstorm cells through California. Thunderstorm cells were moving northward at 10-15 knots in the Emerald Lake area.

A satellite picture in the visual bandwidth (Figure 2) indicated a cyclonic circulation over Baja, CA, and significant cloud masses over western Arizona, southern California, and the Sierra Nevada. A satellite picture in the infrared bandwidths (Figure 3) provided information on cloud height; the higher, colder clouds are shown in white, and the lower, warmer clouds are in darker tones. Significant cloud masses extending to high altitudes, frequently associated with thunderstorm activity, were observed over the Sierra Nevada. The satellite chart depicting the water vapor content (Figure 4) indicated cyclonic transport of a moist airmass with high water content to the Sierra Nevada.

Vertical wind shear occurs when thunderstorms extend to high altitudes. Therefore, pollutants entrained in the rainwater at Emerald Lake arrived from different source areas at different altitudes. Surface and 500 mb charts (about 5800 m) for July 16 and July 19 are shown in Figures 5 and 6. A high pressure cell at 500 mb moved from northern California to Northern Arizona between July 16-19, causing the winds aloft to veer from easterly to southeasterly to southwesterly at Emerald Lake during this period. Back trajectory analysis to Emerald Lake using 500 mb charts indicate transport over north-central Mexico, southern Arizona, and the Colorado River Basin (Figure 5). Significant emissions of acid rain precursors occur along this trajectory, including emissions from copper smelters in Arizona and northern Mexico and from the Mojave Generating Station, a coal fired power plant located on the Colorado River near Needles. Sulfur dioxide emissions from this plant averaged 138 tons per day during July 17-20, 1984. (Data supplied by plant operator). Furthermore, high ambient fine sulfur aerosol concentrations have been documented[2] along this trajectory (Figure 7).

Back trajectory analysis at 850 mb (about 1500 m) is quite different from the 500 mb trajectory and indicates transport over California from the southwest (Figure 6). Significant emissions of acid rain precursors occur in the San Joaquin Valley along this trajectory. Average sulfur dioxide emissions in Kern County in 1985 were 50 tons per day. Wind velocities (calculated from the upper wind charts) averaged 5.3 mph in the 72 hrs before arrival at Emerald Lake at 850 mb (transport distance 380 miles) and 10.7 mph (transport distance 770 miles) at 500 mb.

INTERPRETATION AND DISCUSSION

Both the thunderstorm moisture and acid rain precursors were transported to the Sierra Nevada from other areas. The meteorological analyses above provide abundant evidence of moisture of subtropical origin being transported northward through northwest Mexico, Arizona, and the Colorado River basin. We hypothesize that emissions of acid rain precursors from these areas were also transported north in the moist airmass and contributed to rainfall acidity in the Sierra Nevada.

Significant emissions of acid rain precursors also occur in the San Joaquin Valley. However, the necessary data are not available in this study for a quantitative determination of source contributions to total rainwater acidity at Emerald Lake. Suggested resources to make this determination in future research include improved analyses of both dissolved and undissolved elements in water samples. Element concentration can provide signatures for emissions sources, especially if they can be detected at low concentrations. For example, selenium is frequently found in emissions from coal combustion. Such research is currently being conducted at Crocker Nuclear Laboratory, University of California, Davis.

SUMMARY AND CONCLUSIONS

Regional transport of acid rain precursors has been studied and documented in the eastern United States. The analyses of meteorological data in this report suggest that California may also be affected by regional pollutant transport when southeasterly winds-aloft transport both moisture and pollutants into the Sierra Nevada during the summer season. Additional research is needed to quantify the relative contributions of local and long-distance sources to rainfall acidity.

REFERENCES

1. J.M. Melack, R. Jellison, and G. Dana, "Chemical and Biological Survey of Lakes and Streams Located in the Emerald Lake Watershed, Sequoia National Park," University of California, Santa Barbara, CA. Final report submitted to California Air Resources Board, Sacramento, CA, February 1987.

2. T.A. Cahill, R.A. Eldred, P.J. Feeney, and L.K. Wilkinson, "Particulate Monitoring and Data Analysis for the National Park Service, 1982-1985," Air Quality Group, University of California, Davis, CA. March 1988.

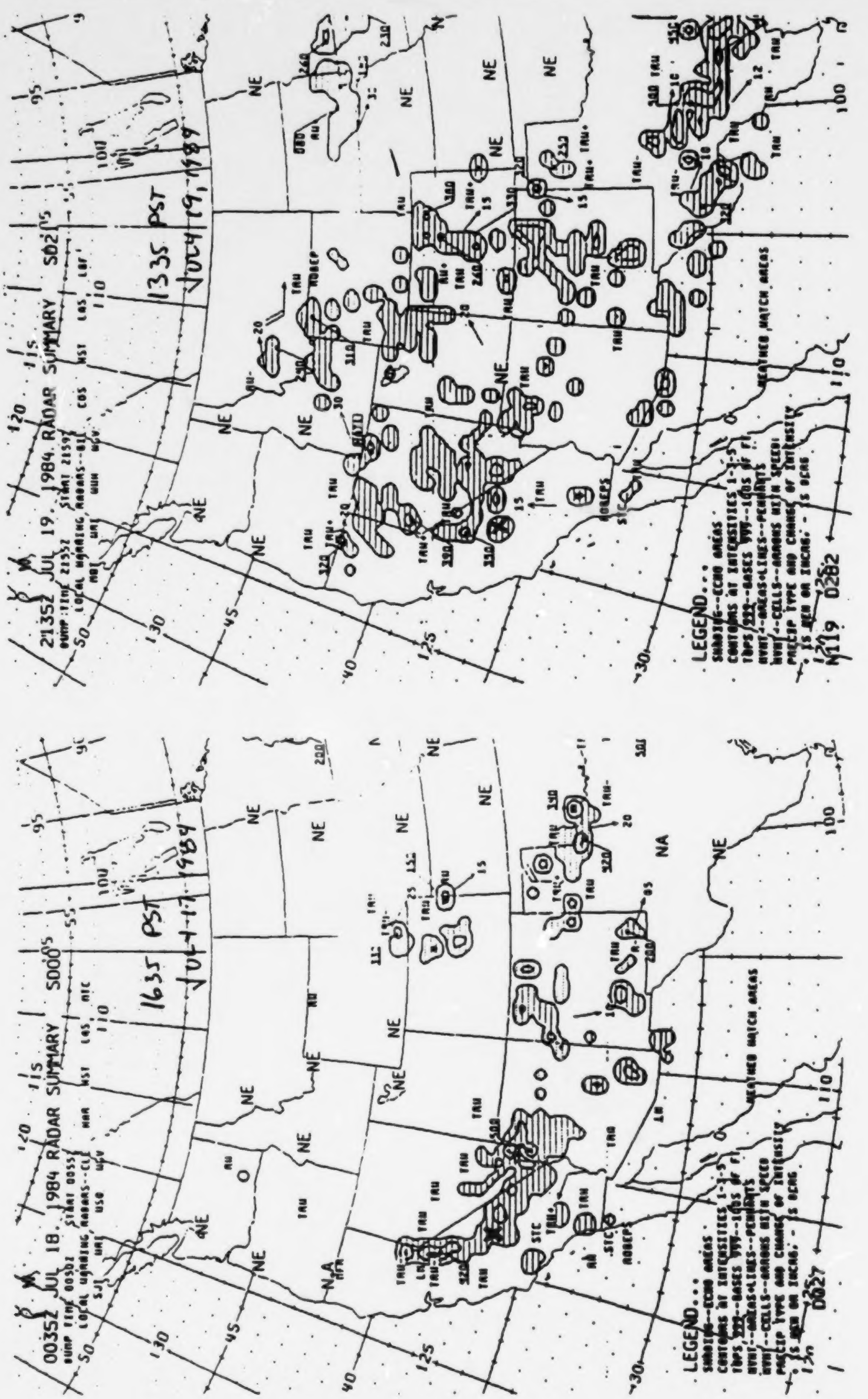
00352 JUL 18 1984 RADAR SUMMARY
1635 PST JULY 17, 1984
21352 JUL 19 1984 RADAR SUMMARY
1335 PST JULY 19, 1984
LEGEND...
NE
TRW

Figure 1. Radar summaries for July 17 and 19, 1984. The location of Emerald Lake is marked by an "X."

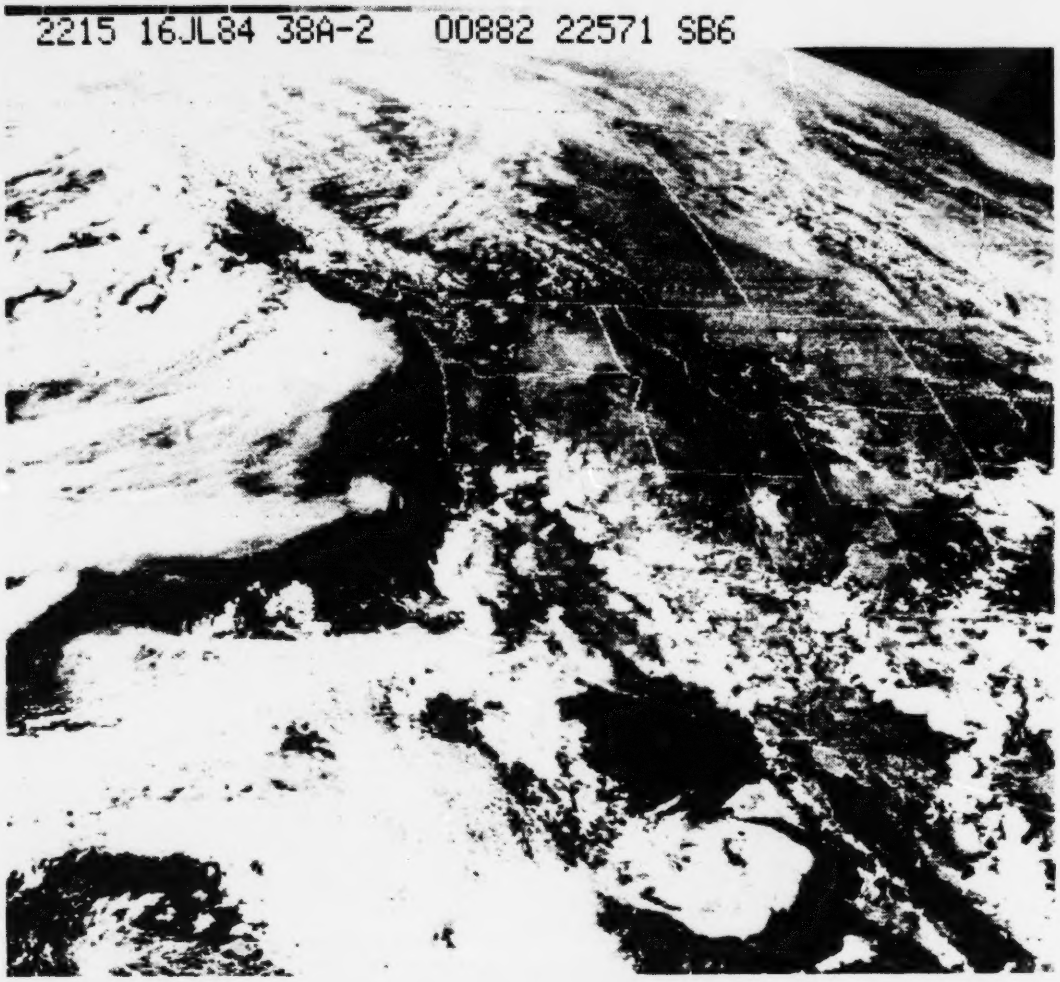
2215 16JL84 38A-2 00882 22571 SB6

Figure 2. Satellite picture, July 16, 1984. Visual bandwidth 0.4-0.6 microns.

Reproduced from best available copy.

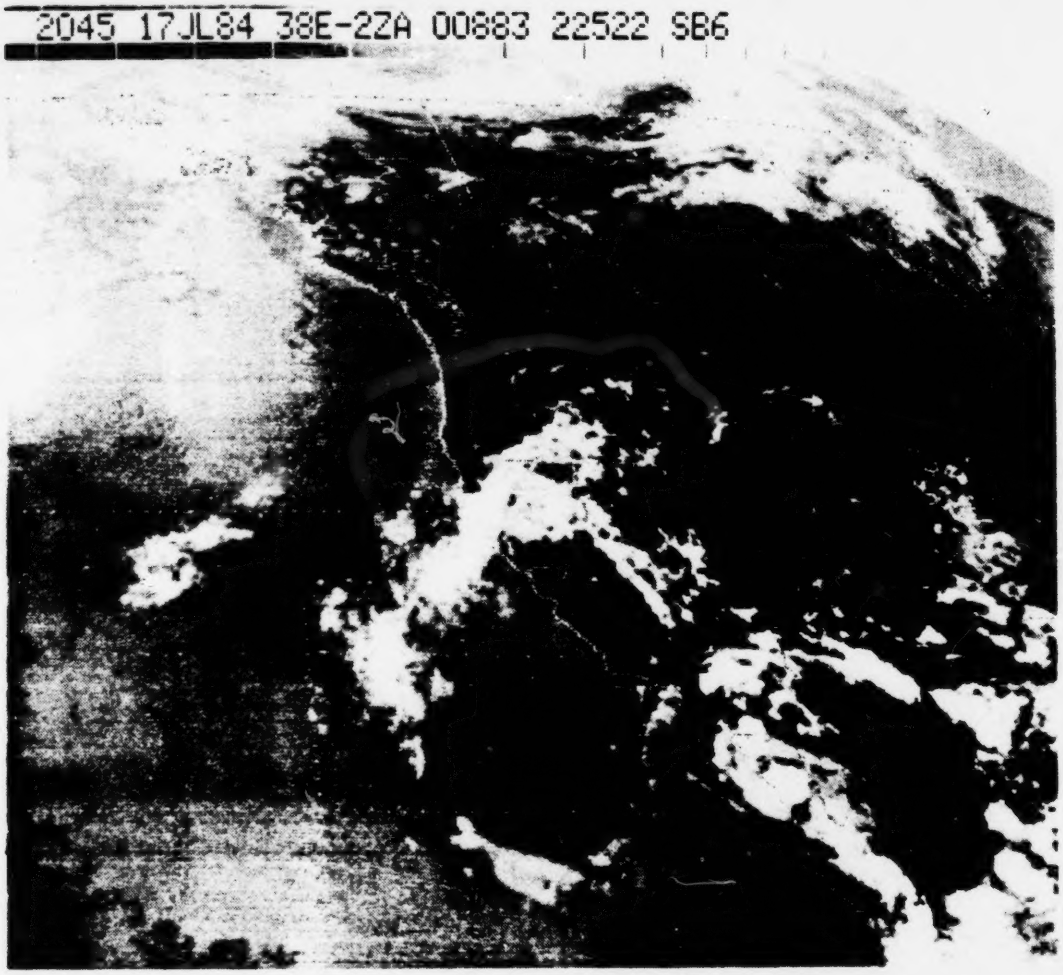
2045 17JL84 38E-2ZA 00883 22522 SB6

Figure 3. Satellite picture, July 17, 1984. Infra-red bandwidth 1.1 microns.

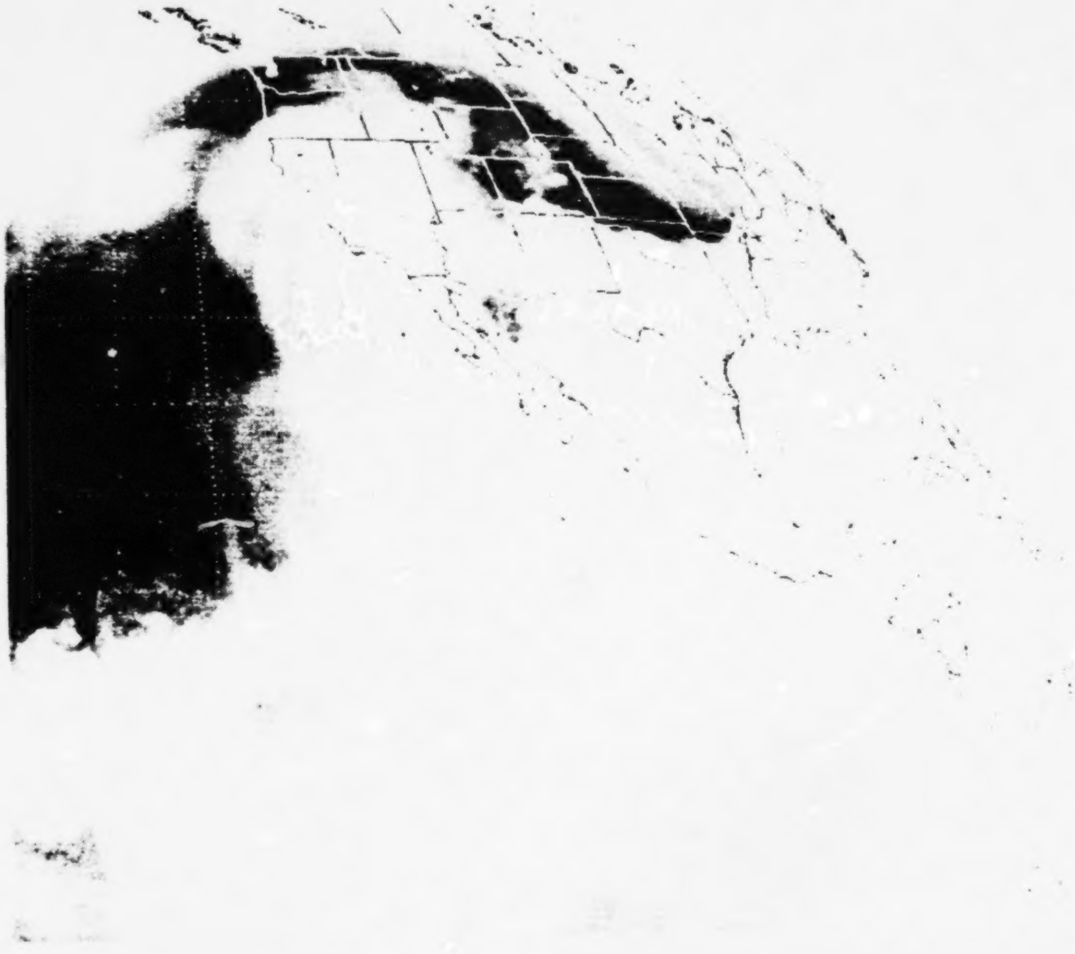

Figure 4. Satellite picture, July 17, 1984. Water vapor bandwidth 6.7 microns.

Reproduced from best available copy.

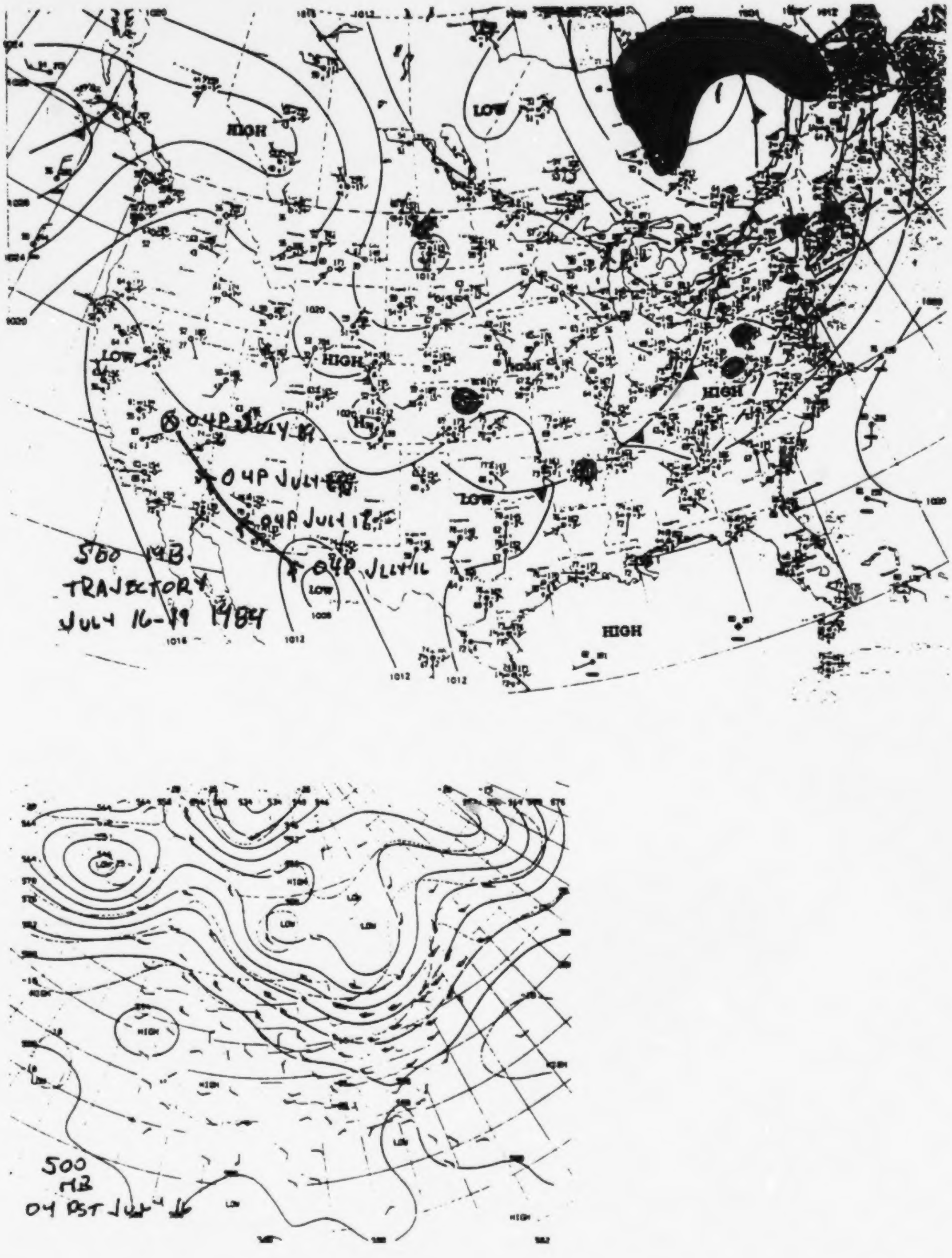
HIGH
LOW
HIGH
LOW
HIGH
H
LOW
HIGH
LOW
HIGH
04P JULY 19
04P JULY
04P JULY 18
04P JULY 16
500 MB
TRAJECTORY
JULY 16-19 1984
1020
1012
1024
1016
1008
500
MB
04 PST JULY
HIGH
LOW
LOW
LOW
HIGH
LOW
HIGH

Figure 5. Surface and 500 mb charts, July 6, 1984. The 500 mb trajectory (19,000 ft) to Emerald Lake (July 16-19) is shown on surface chart.

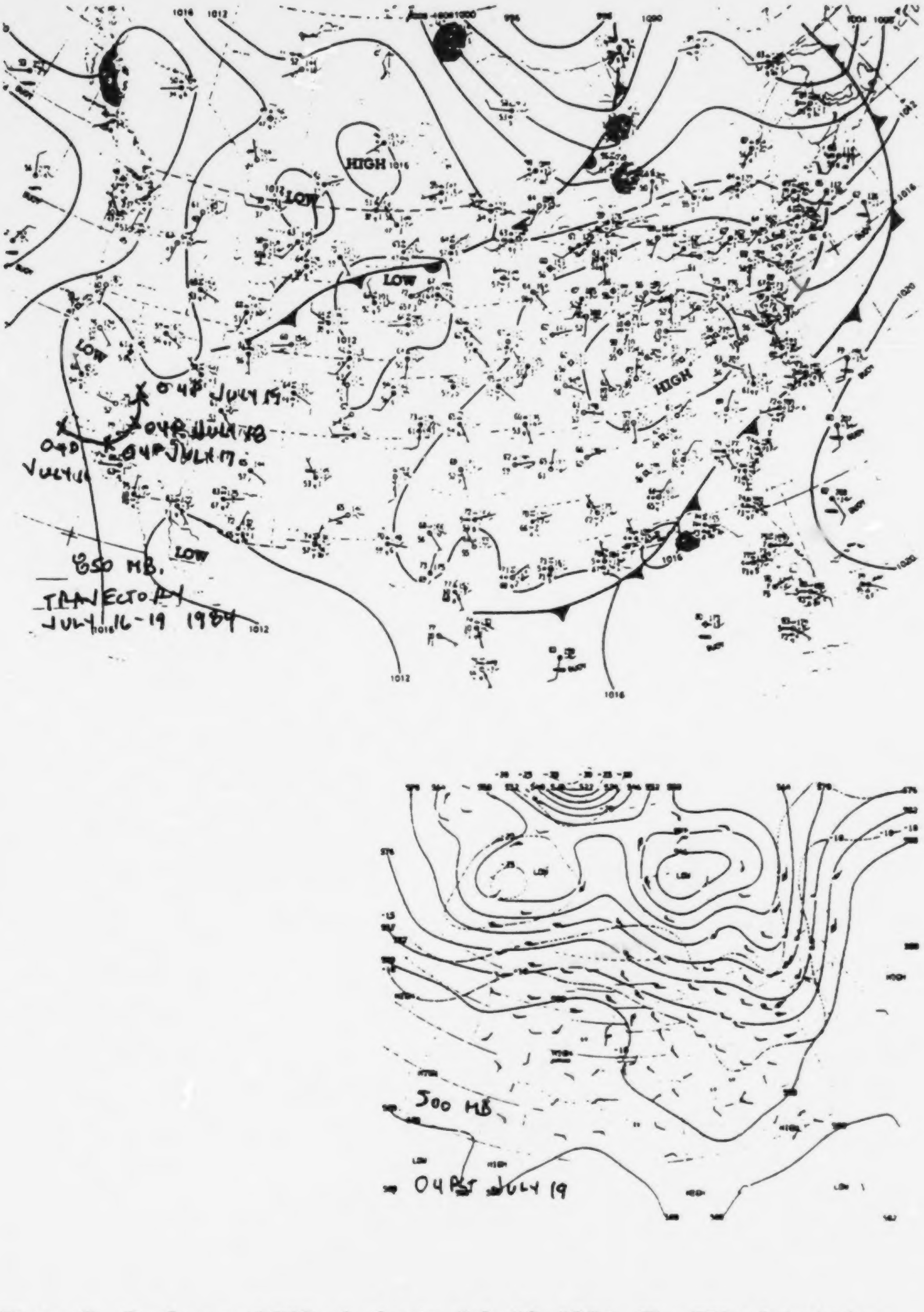
LOW
HIGH
LOW
LOW
HIGH
LOW
04P JULY 19
04P JULY 18
04P JULY 17
04P JULY 16
850 MB.
TRAJECTORY
JULY 16-19 1984
500 MB
04PST JULY 19

Figure 6. Surface and 500 mb charts, July 19, 1984. The 850 mb trajectory (5,000 ft) to Emerald Lake (July 16-19) is shown on surface chart.

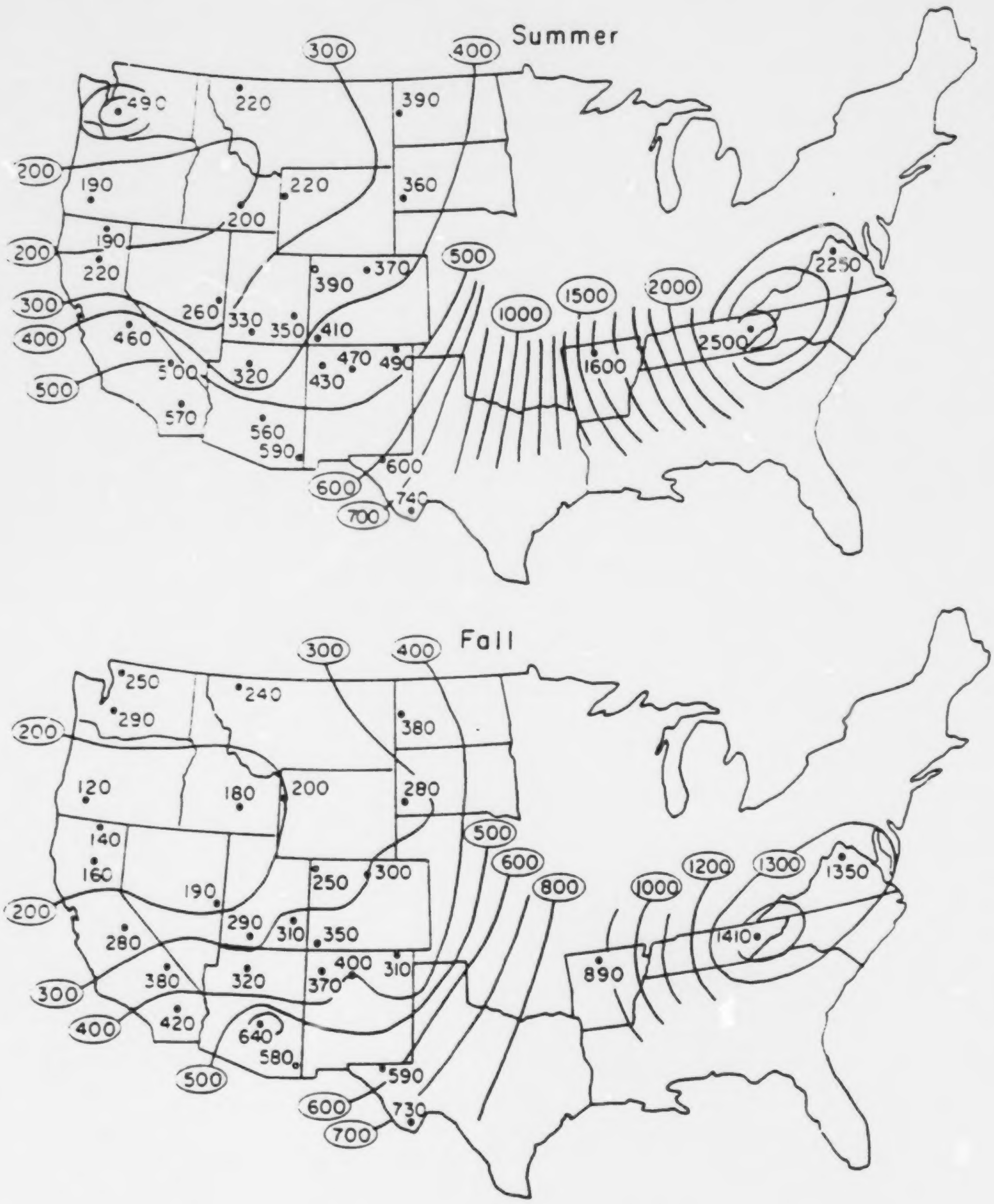
Summer
300
400
490
220
390
200
190
220
360
200
190
200
220
500
370
390
1500
2000
2250
300
400
260
330
350
410
1000
460
470
490
2500
1600
500
500
320
430
570
560
590
600
600
740
700
Fall
300
400
250
240
290
380
200
120
180
200
280
140
500
600
160
800
1200
1300
1350
1000
190
250
300
200
290
310
350
1410
280
400
310
890
300
380
320
370
400
420
640
580
500
590
600
730
700

Figure 7. Contour maps of fine sulfur concentrations in ng/m^3 for summer and fall, June 1982 to February 1985. (Source: Particulate Monitoring and Data Analysis for the National Park Service, 1982–1985.)

Fog and Rain Chemistry in Northern California

Susan H. Bicknell

Forestry Department
Humboldt State University
Arcata, California 95521

INTRODUCTION

Acid precipitation is a recognized problem in Scandinavia and other parts of Europe, the eastern United States, and southern California.[1] Acidic clouds and fog (ground-based clouds) have been reported in more regions than acid rain.[2,3] Many studies have concentrated on urban areas and the health implications of inhaling acid fog.[4-7] A few studies have examined cloud chemistry in more remote regions.[8-11] The role of ground-based clouds as vectors for introducing nutrients and pollutants into forest ecosystems has received less attention.[12-14,2] One of the earliest studies of fog chemistry associated with nutrient inputs to forests was conducted in coastal redwood forests of California.[15]

Cloud studies, especially those in coastal California, have been conducted with the objective of characterizing a few cloud events, rather than with characterizing the clouds on the average for a specific location. In order to characterize the chemistry of clouds at a particular location, we must be able to compare chemical concentrations of one site with those of another site. Small sample sizes at individual sites and studies that move the collector from site to site in pursuit of clouds preclude intersite comparisons. The early results of this study indicated that although early samples showed no significant differences among sites, the addition of more samples lent statistical evidence of significant differences.

The objective of this study was to characterize the chemistry of ground-based clouds and rain at three northern California coastal locations. This study was part of the Cloud Water Project (CWP).[2,3] The major goal of the CWP was to collect chemical data on cloud and rain using standardized protocols and to compare inter- and intrasite differences across a wide geographical range. One of the early conclusions of the CWP was that inter- and intrasite comparisons were enhanced by large sample sizes. Cloud chemistry, as indicated by the Cloud Water Project, was not normally distributed for any ion. Central tendency (e.g., mean, median) was difficult to discern because of the range of variability encountered. The following study showed that three things happened when more samples were collected at three California sites. First, the central tendency became stronger and more easily discerned (means and medians became more alike). Second, the extreme values measured were similar to previous extreme values, reducing the suspicion that the first extreme values were outliers, or worse, contaminations. Third, significant differences among sites became statistically detectable.

EXPERIMENTAL METHODS

Ground-based clouds and rain were sampled at three sites in redwood (*Sequoia sempervirens* D. Don. Endl.) forests in coastal California. The three sites were located in Redwood National Park in Orick, California, Arcata City Forest in

Arcata, California, and Redwood Regional Park in Oakland, California (Figure 1). Their site characteristics are summarized in Table I. The Redwood National Park site was the most removed from urban pollution sources. It was located 2 km east of Highway 101, approximately 10 km south of the nearest town, Orick. There were no industrial activities within 50 km of the collecting site. The Arcata City Forest site was located within the city limits of the town of Arcata, population approximately 8,000. Highway 101 passed within 4 km of the site, and heavy forest products industrial activities, including pulp mills, were located 2 km to the NW and less than 10 km to the SW. The Oakland site was within the East Bay Regional Parks, which are bordered on the west by the cities of Oakland and Berkeley. This site was expected to have a higher level of air pollution than the other two sites.

Sampling protocol has been previously reported.[2] Rain was collected in bulk precipitation collectors uncovered only during an event. Ground-based clouds were sampled at 1.5 m above the ground in CWP active cloud water collectors.[16] A fan in the rear of the cloud water collector drew water droplet-laden air into the collector through a ventral opening and across a removable cartridge of Teflon strands. Water droplets impacted on the strands and dripped into a polyethylene bottle. The intent of the study was to use a standard 5 h sampling period. In practice, many events were shorter than 5 h while others exceeded 5 h due to overnight collections. The actual sampling time was usually determined by practical considerations such as the onset and cessation of the event, as well as nighttime driving conditions during cloud events. Since the collectors were manually operated, operator availability was also a limitation.

Coastal northern California experiences long, rainless summers punctuated by frequent low coastal clouds and rainy winters when ground-based clouds are rare. Therefore, the conditions limited most cloud samples to the summer months when ground-based clouds were common. Rain samples were likewise mostly limited to the winter rainy season. Rain clouds were generally much higher than the sites, and therefore were precluded from cloud water sampling. Although radiation fog was a common occurrence along the flat portions of the northern California coast, it was rare at the elevations and locations of the three sampling sites. The cloud samples collected at these sites were ground-based clouds arising from onshore movement of marine air. In contrast, the rain samples were from storms originating many miles off shore that transported clouds and rain to the three sites. Sampling at Redwood National Park ran from August 2, 1984 through April 15, 1986. Arcata City Forest sampling occurred from July 22, 1986 until October 19, 1987. Oakland samples were collected between July 25, 1986 and April 29, 1987.

Samples were retrieved after 5 h of collection time, at the end of the event (if earlier), or within 20 h after the beginning of the event (if operator access was limiting). Hydrogen ion concentration was recorded for two 10 ml aliquots of the sample within 2 h of retrieval. A combination electrode pH meter was calibrated with standards at 4.00 and 7.00 at 20° C. Calibration was checked for each sample measured. If the two samples were not within 0.1 pH unit, a third aliquot was analyzed. If more than 50 ml of the sample remained, it was packaged for shipment to the analytical laboratory for chemical analysis. Samples from Redwood National Park were sent to the Institute of Ecosystem Studies (IES) in Millbrook, New York. Samples from Arcata and Oakland were analyzed at the Cooperative Chemical Analytical Laboratory at Oregon State University Department of Forest Sciences (OSU). Analytical techniques used at

IES have been reported.[2] At OSU, NH_4^+, Cl^-, NO_3^- and SO_4^{2-} were measured with a Technicon II autoanalyzer using Technicon standard techniques. K^+, Na^+, Ca^{2+}, and Mg^{2+} levels were obtained with a Perkin Elmer 5000 Atomic Absorption Spectrophometer (flame atomization). If sample volumes permitted, pH was recorded a second time at the lab using a combination electrode calibrated at 4.00 and 7.00 at room temperature. All samples were refrigerated or frozen between retrieval and analysis, except during shipment. Data from samples containing insects or excessive particulates were discarded. Analytical accuracy was checked with blind duplicates and solutions of known strengths.

Summary statistics were calculated without volume weighting because the samples were not collected in a manner related to deposition rates. Linear regression was applied to samples where pH measurements were obtained both in the field and in the lab to test the accuracy of the field measurements. The chemical concentrations for rain and clouds from the three sites were compared using Kruskal-Wallis nonparametric 1-way analysis of variance. Comparisons within sites by season and by year were made using Mann-Whitney tests. Non-seasalt SO_4^{2-} was calculated as recommended by Keene et al.[17] Ion balances were determined for all samples in which all principal ions were measured according to the formulas provided by Weathers et al.[2]

RESULTS

Field H^+ and lab H^+ were very strongly correlated (Figure 2). The regression equation was only slightly different from a 1:1 ratio ($x = 1.06y - 0.077$) ($r^2 = 0.85$). The probability that these two measures were not related was less than 0.0001. Since a much larger sample size is achieved using the field pH values instead of the lab pH values, only field pH is reported here (Tables II and III). Field pH values were slightly more acidic that lab values. Biological activity in the sample reduced acidity over time.

Ground-based cloud was more acidic and contained higher median concentrations of all ions than rain (Table IV). The physics of droplet size predicted that the smaller droplets of ground-based cloud would have higher solution concentrations than large rain droplets.[6] In addition, California coastal ground-based clouds are characteristically associated with stagnant air patterns where local pollutants accumulate over several days. California rain storms, on the other hand, occur under unstable conditions where clean air masses cross the Pacific from great distances and arrive at the coast bringing relatively uncontaminated clouds and rain. Seasonal fluctuations in pollutant supply may also play a role. The difference between cloud and rain chemistry was greater than differences accountable by different seasons, different sampling years, or different sites. Seasonal differences were less significant and of a smaller magnitude. For example, summer rain at Arcata had three times more SO_4^{2-} than winter rain (Table IV.). The ratio of SO_4^{2-} in cloud to rain at Arcata was over 14. Significant differences between sampling years were also not as pronounced. There were no significant differences between 1984 and 1985 in cloud chemistry at Redwood National Park. At Arcata, clouds contained 4.8 times higher median concentrations of NO_3^- in 1987 than in 1986. The ratio of NO_3^- in cloud to rain at Arcata was 88.0. Differences among sites were only slightly more pronounced than differences within sites by season and year. The following two sections outline the intersite comparisons.

Chapter Three

Air Quality and Deposition: Gases and Particulates

Dry Deposition of Nitrate and Sulfate to Coniferous Canopies in the Rocky Mountains	H.J. Sievering, J. Braus, and J. Caine	171
Ozone Deposition and Leaf Area Index at the Pawnee National Grassland for the 1988 Growing Season	K.F. Zeller and D.L. Hazlett	177
Air Quality at a High Elevation, Remote Site in Western Canada	A.H. Legge and S.V. Krupa	193
Ozone at a Remote, High-Altitude Site in Sequoia National Park, California	B.S. Pedersen and T.A. Cahill	207
A Regional Characterization of Air Quality and Deposition in the Coniferous Forests of the Western United States	M. Böhm	221

Preceding page blank

170

Preceding page blank

Dry Deposition of Nitrate and Sulfate to Coniferous Canopies in the Rocky Mountains

H. Sievering,[1] J. Braus[1]
and
J. Caine[2]

[1] *Environmental Sciences Program*
University of Colorado at Denver
1200 Larimer St., Denver, CO 80202
and Air Quality Group/GMCC
National Oceanic and Atmospheric Administration

[2] *Mountain Research Station*
University of Colorado at Boulder

INTRODUCTION

Dry deposition (DD) fluxes to deciduous and coniferous canopies have been measured in parts of the United States, Canada, and Europe by using several methods. Among these methods are air filtration sampling,[1] micrometeorological measurements,[2,3] the throughfall/incident technique,[4-6] and the needle- or leaf-washing technique.[7-9] Whereas the majority of studies cited have concentrated on deciduous canopies, increasing attention is being directed toward potentially more sensitive coniferous trees. This study employed both the throughfall/incident and needle-washing techniques on a coniferous canopy to determine dry deposition fluxes. Estimates of DD and canopy exchange (CE) were calculated and compared with those obtained through application of the Lovett and Lindberg[5] multiple regression algorithm to throughfall/incident data.

EXPERIMENTAL METHODS

Sampling was performed in a predominantly lodgepole pine (*Pinus contorta* ssp. *latifolia Engelm.*) forest (elev. 10,000 ft = 3048 m) on Niwot Ridge in the Rocky Mountains. The site lies about 80 km northwest and 40 km northwest of Denver and Boulder, CO, respectively. The period of sampling extended from June 19 to August 3, 1987, and May 20 to August 2, 1988.

Wet Deposition—Throughfall/Incident Sampling

Throughfall and incident precipitation were collected in Aerochem-Metric wet/dry sampler buckets lined with plastic bags that tested clean for nitrate (NO_3^-) and sulfate (SO_4^{2-}). The incident wet/dry sampler, located in a clearing, was separated from the throughfall wet/dry sampler by a distance of about 30 m. Following each rain event, debris (such as needles and cones) was removed from the sample with Teflon tweezers. The sample was then transferred to linear polyethylene collector bottles and transported approximately 800 m to the University of Colorado Mountain Research Station (MRS) laboratory where it was refrigerated until chemical analyses could be performed. The samples were analyzed using ion chromatography for NO_3^-, SO_4^{2-} and, if a sufficient volume was collected within a very short time of the event, for ammonium (NH_4).

Three bulk precipitation collectors, placed adjacent to the throughfall wet/dry sampler and at the same level as the sampler's wet bucket, were used to quantify the spatial variability of precipitation fluxes beneath the canopy. A bulk collector consisted of a linear polyethylene funnel to which was attached a length of Teflon tubing. A linear polyethylene collector bottle was fastened to the end of the Teflon tubing. The bulk sample, which drained through the tubing into the bottle, was cleaned of debris with Teflon tweezers although, in 1988, Teflon screens eliminated most of this debris. The bulk sample bottles were capped and then transported to a refrigerator in the MRS lab. These samples were also analyzed by ion chromatography for NO_3^-, SO_4^{2-} and, when possible, for NH_4.

Dry Deposition—Needle Wash Sampling

Needle-washing was conducted 1.5 m from the throughfall wet/dry sampler under the lodgepole pine canopy. Lodgepole pine needles occur in bundles of two, have a half circle cross-sectional shape, and average 3.5 cm in length.

During 1987 sampling, two natural branchlets and one surrogate branchlet were washed following each rain event. One additional surrogate branchlet and one Teflon-coated natural branchlet were added during 1988 sampling. Each branchlet was dipped into a linear polyethylene bottle containing 500 ml of deionized (DI) water and washed for 8 min followed by an additional 2-min wash in a second 500 ml DI water bottle. It was found after repeated trials of varying wash durations that an 8-min wash followed by a 2-min wash removed the dry-deposited particulates from the needles without extracting the species of interest from within the needles themselves.

As was the case for the throughfall, incident and bulk samples, the needle-wash samples were transported to the MRS lab and stored in a refrigerator until ion chromatography analysis was performed for NO_3^- and SO_4^{2-}. This entire procedure was repeated before the next rainfall. A total of 28 such antecedent periods were sampled during 1988, along with numerous needle-wash samples after rain events in 1987 and 1988.

A Belfort wetness indicator also was positioned under the lodgepole pine canopy near the needle-wash branchlets and throughfall wet/dry sampler. The wetness indicator charted the duration of canopy wetness. From this record, the time in hours that lapsed between needle washes and between throughfall events was determined. This time was then used in dry deposition flux calculations.

RESULTS AND DISCUSSION

The concentration of NO_3^- in incident precipitation determined by automated wet/dry sampling at the MRS 10,000 ft site was 1.1 and 1.98 mg/L in 1987 and 1988, respectively; for SO_4^{2-} it was 0.75 and 1.51 mg/L, respectively. These values are the same or slightly below the NO_3^- and SO_4^{2-} concentrations determined from an NADP sampler at 11,600 ft on top of Niwot Ridge. For comparison, the NO_3^- concentrations are about half those observed in central Europe, whereas the SO_4^{2-} concentrations are less than half those observed in central Europe.[4] It is also interesting that ion concentrations obtained from summer 1987 samples (June 23–August 3) were substantially higher than those from summer 1988 samples (May 24–August 2) while the amount of precipitation for summer 1988 was 9.1 L vs. 6.7 L for summer 1987.

Throughfall precipitation (T) concentrations of NO_3^- and SO_4^{2-} observed using automated wet/dry sampling were two to three times higher than incident precipitation (I) values. During the 1987 sampling, I was only 29% and 55% of T for NO_3^- and SO_4^{2-}, respectively. During 1988 sampling, I was only 40% and 56% of T for NO_3^- and SO_4^{2-}, respectively. These numbers suggest that dry deposition, often estimated by T-I, constitutes 60-70% of NO_3^- total deposition to the conifer canopy and about 45% of the total deposition for SO_4^{2-}.

Of course, the more correct statement of T-I is given by

$$T - I = DD + CE \qquad [1]$$

where DD is the dry deposition of an ionic constituent and CE is canopy exchange for that constituent during a precipitation event. Since the conifer canopy is not a passive collection surface, the CE term may be non-negligible. There are three physical/chemical exchange mechanisms that may be active at the conifer canopy. The first mechanism is exudation (E), the movement of ions from the interior of conifer needles to their surfaces during dry periods; the second is leaching (L), similar movement of ions but during precipitation (wetted surface) periods; the third is retention (R) of dry- or wet-deposited ions by the interior of needles. Generally, canopy exchange is given by $L - R + E$.

Lovett and Lindberg[5] have proposed that a multiple linear regression formulation may be used to determine the relative magnitude of DD and CE. They suggest

$$T - I = b_1 A + b_2 P \qquad [2]$$

where A is the antecedent period, the time between the end of the rain event and beginning of the next rain event, and P is the amount of precipitation during rain events. This formulation forces any contribution from exudation into the b_1A term so that Lovett and Lindberg implicitly assume $CE = L - R$, that is, $E = 0$, and thus CE occurs only during the rain event. Further, each precipitation event is assumed to wash the canopy thoroughly and completely of particulate matter SO_4^{2-} and NO_3^- deposited during the antecedent period, A.

Although these assumptions may apply to the Oak Ridge, TN, deciduous forest setting in which Lovett and Lindberg have obtained fairly good results, not all of them may apply to the drier, coniferous forest setting at Niwot Ridge nor elsewhere in the Rocky Mountain region of the United States. We have found that precipitation events cannot be assumed to thoroughly wash the canopy. In fact, 2–4 mm rains often do not produce a throughfall sample. To address this concern, Lovett and Lindberg's regression formulation was modified somewhat in that we have observed that use of throughfall volume (TV) is to be preferred over P in equation 2. The two summer data periods produced a total of 10 events for regression analysis. The percentages of total NO_3^- and SO_4^{2-} deposition due to I, DD, and CE to the conifer canopy determined using equation 2, but with TV replacing P, are shown in Table I. Note that the p values are quite significant (i.e., $p < 0.025$) except for DD of SO_4^{2-}.

The fact that the outcome of multiple regression for DD of SO_4^{2-} is not significant may be largely due to the variability of throughfall rain beneath the canopy. The three bulk throughfall samplers indicated that NO_3^- varied under the canopy by ±10-20%, whereas for SO_4^{2-} it varied by ±35-50%. Considering these natural, canopy-induced uncertainties, the regression results may be considered very good indeed. The needle-wash results partially substantiate the separation of DD and CE obtained by regression.[3] In analyzing these results, we make the assumption that the difference in observed NO_3^- or SO_4^{2-} concentrations between an exposed natural branchlet and a Teflon-coated branchlet is due to CE. On an event basis, leaching and exudation enhanced the dry deposition of NO_3^- on washed conifer branchlets by up to 35%; retention caused up to a 25% reduction. Also on an event basis, leaching and exudation enhanced dry deposition of SO_4^{2-} by about 30%; retention often caused more than a 10% reduction in dry deposition. These results are based on 20 at least two-day-long needle-wash sampling periods during June 12–August 12, 1988. The average ratio of natural branchlet to Teflon-coated branchlet NO_3^- and SO_4^{2-} concentrations across the 20 needle-wash sampling periods suggests that CE as a percentage of CE + DD falls in the range -15.8% to +15.4% for NO_3^- and -4.4% to +31.4% for SO_4^{2-}, both at 90% confidence. Even though CE may not contribute significantly on an average basis, its needle-wash-estimated contribution relative to DD is better identified by the event data. Thus, the needle-wash sampling qualitatively confirms the Table I multiple regression view that CE must be considered in the identification of dry and wet deposition of NO_3^- and SO_4^{2-} when using the throughfall/incident approach.[3]

We shall consider that DD is conservatively obtained by the regression approach since the 1987 needle-wash results[3] indicate that CE may be somewhat less than shown in Table I. Thus, the DD values in Table I may be underestimates. Even so, the 25–50% DD for NO_3^- and 10–35% DD for SO_4^{2-} as a percentage of total beneath canopy deposition constitute very significant inputs of these ions to the conifers of the Niwot Ridge forested area. Table II presents the magnitude, in milligrams per square meter of ground area per day, of NO_3^- and SO_4^{2-} for wet deposition (incident precipitation) and DD (after subtracting canopy exchange) in each of the 1987 and 1988 summers. For NO_3^- we may conclude that DD contributes as much or more than wet deposition to its total input at conifer forested areas of the Niwot Ridge area. For SO_4^{2-} we conclude that DD is less important than wet deposition, though it must clearly be considered to establish total atmospheric inputs. The results obtained at Niwot Ridge would appear to be applicable, in a qualitative sense, to canopies throughout the Colorado Front Range. The approximate doubling, 1988 vs. 1987, for both wet and dry deposition of NO_3^- and of SO_4^{2-} is especially interesting. We plan to continue our Niwot Ridge summertime sampling as well as perform a correlation study of NO_3^- and SO_4^{2-} deposition with meteorological factors to better understand the large differences found in 1987 and 1988.

ACKNOWLEDGMENTS

We would like to thank the University of Colorado at Denver, Office of Research and the National Science Foundation Long-Term Ecological Research (LTER) Program for financial support. We also thank the Mountain Research Station staff for their logistical support throughout the past three years.

REFERENCES

1. W.R. Pierson, W.W. Brachaczek, S.M. Japar, G.R. Cass, and P.A. Solomon, "Dry deposition and dew chemistry in Claremont, California, during the 1985 Nitrogen Species Methods Comparison Study," *Atmos. Environ.* 22:1657 (1988).

2. B.B. Hicks and M.L. Wesley, "Turbulent transfer processes to a surface and interactions with vegetation," in *Atmospheric Sulfur Deposition*, D.S. Shriner, C.R. Richmond, and S.E. Lindberg, Eds., Ann Arbor Science, Ann Arbor, MI, 1980.

3. H. Sievering and J. Braus, "Dry deposition of nitrate and sulfate to Rocky Mountain coniferous canopies by direct and indirect measurement," submitted to *Atmos. Environ.*, 1989.

4. K.D. Höfken, F.X. Meixner, and D.H. Ehhalt, "Deposition of atmospheric trace constituents onto different natural surfaces," in *Precipitation Scavenging, Dry Deposition, and Resuspension*, H.R. Pruppacher, R.G. Semonin, and W.G.N. Slinn, Eds., Elsevier Press, New York, NY, 1983, p. 825.

5. G.M. Lovett and S. E. Lindberg, "Dry deposition and canopy exchange in a mixed oak forest as determined by analysis of throughfall," *J. Appl. Ecol.*, 21:1013 (1984).

6. B. Freedman and U. Prage, "Ambient bulk deposition, throughfall, and stemflow in a variety of forest stands in Nova Scotia," *Can. J. For. Res.* 16:854 (1986).

7. J.M. Dasch, "Measurement of dry deposition to a pine canopy," GMR Research Publication GMR-5153, Detroit, MI, 1985.

8. S.E. Lindberg and G.M. Lovett, "Field measurements of particle dry deposition rates to foliage and inert surfaces in a forest canopy," *Environ. Sci. Tech.*, 19:238 (1985).

9. J.E. Sickles, W.D. Bach, and L.L. Spiller, "Comparison of several techniques for determining dry deposition flux," in *Precipitation Scavenging, Dry Deposition, and Resuspension*, H.R. Pruppacher, R.G. Semonin, and W.G.N. Slinn, Eds., Elsevier Press, New York, NY, 1983, p. 1979.

Table I. Percentage of nitrate (NO_3) and sulfate (SO_4) total deposition beneath a conifer canopy due to incident precipitation (I), dry depositio (DD), and canopy exchange (CE) at the 10,000' Niwot Ridge, CO, site for the 1987 and 1988 summers. Determined by use of a multiple-regression approach.

	NO_3^- Loading, % of Total	SO_4^{2-} Loading, % of Total
I	35	55
DD	25-50 (0.01)[a]	10-35 (0.17)[a]
CE	15-30 (0.02)[a]	20-35 (0.02)[a]

[a] Numbers in parentheses are p values. The probability is that the stated percentage may actually be zero.

Table II. Wet (incident) and median dry-deposited canopy loadings of nitrate (NO_3) and sulfate (SO_4), in mg per sq meter of ground area per day, to conifer forested areas in Niwot Ridge during the summers of 1987 and 1988.

	Summer 1987 mg/m^2/day		Summer 1988 mg/m^2/day	
	NO_3	SO_4	NO_3	SO_4
Wet	1.8	1.3	4.7	3.9
Median Dry	2.3	0.8	4.6	1.2

Ozone Deposition and Leaf Area Index at the Pawnee National Grassland for the 1988 Growing Season

Karl F. Zeller[1]
Donald L. Hazlett[2]

[1] U.S. Forest Service
Rocky Mountain Forest and Range Experiment Station
240 West Prospect
Ft. Collins, CO 80526

[2] Range Science Department and Natural Resource Ecology Laboratory
Colorado State University
Ft. Collins, CO 80523

INTRODUCTION

The dry deposition of ozone and sulfur and nitrogen compounds are the focus of several large research programs currently underway across the United States. To perfect the techniques necessary to measure total deposition effects in ecological studies of forested watersheds, the USFS has established an eddy correlation deposition research facility. Located about 50 km northeast of Fort Collins, CO, the Pawnee site was established in July 1986, at the Central Plains Experimental Range (CPER) in shortgrass steppe vegetation. The concept was to begin dry deposition measurements over simple terrain, gain experience and understanding, then adapt the technology to more complex situations. A major goal for establishing the site was to provide eddy correlation dry deposition measurements, a micrometeorological technique considered capable of providing true deposition, concurrent with data from other methods for determining dry deposition. Such candidate methods include filter pac systems, eddy accumulators, and box measurements.

Eddy correlation measurements at the USFS Pawnee site have been taken continuously since May 1987. A detailed report[1] describes the Pawnee site eddy correlation system, mathematical procedures to reduce data uncertainty and correct errors, initial data results, and descriptions of the fast-response chemical sensors required for the technique.

Essentially, the result of an eddy correlation measurement is the vertical flux of some measurable quantity. In the case of ozone, or any other downward-moving quantity, the measured flux is the deposition. Fluxes of ozone, nitrogen oxides, momentum, moisture, and heat have all been measured at the Pawnee site. If the flux of a quantity is divided by its mean, a deposition velocity for the quantity in question can be obtained.

Leaf area index, soil moisture and precipitation were also measured at the Pawnee site during the 1988 growing season in support of the deposition research.[2] Leaf area index (LAI) is an attribute of plant communities that indicates cover, influences water use via transpiration, enables comparisons of light utilization among communities and, if measured throughout the growing season, can indicate seasonal growth patterns. A main predictor of the amount of leaf area produced is the balance between precipitation and evapotranspiration. In semiarid grasslands, evaporation is high relative to precipitation, and leaf area indices are usually less than one.[3]

Variations in growth patterns among plant species or groups of plant species in the same community can indicate different adaptations to climatic fluctuations and/or to resource availability patterns. Therefore, comparisons of leaf area development patterns among species or species groups are a means of measuring when and if differences in growth patterns occur. Of special interest in this regard is the hypothesis that ozone deposition possibly affects, or is affected by, plant growth in shortgrass steppe vegetation. No efforts have previously been made to compare the pattern of leaf area development with patterns of ozone deposition. This paper presents ozone deposition and LAI measurements. It compares precipitation, soil water and ozone deposition with patterns of leaf area development.

EXPERIMENTAL METHODS

Ozone

Eddy correlation dry deposition (flux) data collection at the Pawnee site requires interfacing sensitive micrometeorological and chemical sensors with real-time data processing. Data were collected at approximately 17 hertz and summarized for half-hour averaging periods. The eddy deviations of ozone, c', and vector wind component deviations are multiplied or correlated together, averaged over the half-hour sampling period, then rotated perpendicular to the mean wind vector for that sampling period, to obtain the vertical flux, F_c (equation 1). This method is described by McMillen.[4]

$$F_c = \overline{w'c'} \qquad [1]$$

Where:

F_c = The vertical flux of c in units of either parts per billion • meters/second (ppb • m/sec) or micrograms per square meter per second;

$c' = c - \bar{c}$. Ozone concentration which is the instantaneous deviation between the instantaneous concentration, c (ppb), and the average concentration, $\bar{c}$ (ppb);

$w' = w - \bar{w}$, the vertical wind component in m/sec analogous to c'.

Equation 1 is the essence of the eddy correlation measurement. Certain meteorological and terrain conditions must be satisfied to obtain valid flux measurements. Simply, the terrain should be relatively flat and the variations in the meteorological and chemical parameters measured should be statistically stationary. These requirements were considered in the analyses reported here.

Eddy correlation data were collected and processed in real time using a personal computer equipped with an analogue-to-digital data acquisition card. The program used to collect and process the data has been adapted from a similar flux data collection program developed by McMillen.[4] The measurements must be made with instruments having fast time response characteristics. In practice, in order to capture the flux within the structure of atmospheric turbulence, the chemical sensor detecting ozone should be able to measure changes in concentration for time periods less than a second. The ozone sensor used at the Pawnee site is based on the chemiluminescent ambient air monitoring technique. It is a prototype instrument that was developed at Denver University.[5]

The eddy correlation half-hour data summaries are assembled, processed and stored in 1-week data blocks that span Tuesday to Tuesday, corresponding to the protocols of other wet and dry deposition programs. The ozone deposition data for comparisons with LAI in this paper were obtained by integrating measured ozone flux with respect to time for the closest 8 weeks of validated data associated with the corresponding LAI measurements. A single representative deposition value for the week was then obtained by averaging the weekly integrated data.

Leaf Area Index

Leaf area index (LAI), the ratio between the amount of leaf area and the amount of ground surface area, was measured eight times at both a grazed and an ungrazed location adjacent to the Pawnee site during the 1988 growing season. Except for two determinations in June, LAI was determined once a month from April 13 to October 1. Each LAI was determined by the nondestructive point-quadrat technique of Warren-Wilson[6] using a frame with 5 cm intervals between pins. The number of vegetation contacts per pin when a rod was passed through the canopy at 32.5° angle from the horizontal was recorded. Each total LAI value is based on 500 to 600 pin executions. The average number of contacts per pin was multiplied by coefficients to obtain a LAI value. Although Warren-Wilson recommended using 3 pin angles, Knight[7] compared LAI results from only the 32.5° angle and found a maximum error of only 5% of the LAI value. Knight's equation was used in this study:

$$\mathrm{LAI} = 0.87 f_{32.5} \qquad [2]$$

Where: $f_{32.5}$ = the average number of contacts per pin for the 32.5° angle.

Pin contacts with canopy plant material were identified as dead or live plant tissue. Dead tissue contacts were further categorized as "old dead," from previous growing seasons, or "current year dead." Live tissue contacts were hits with green plant tissue whether the plant part was leaf, stem or reproductive. Live hits were categorized as C-4 grasses, C-3 graminoids (i.e., grasses and sedges) and total green leaf area. Although life-forms for cacti, forbs and shrubs were recorded, they were not used in this paper. Each category of canopy contact was entered into equation 2 for LAI determinations.

An advantage of LAI determinations by the point-quadrat technique over biomass harvesting, especially when growth patterns of C-3 (cold season) and C-4 (warm season) plants are of interest, is that the same plants can be sampled each date and thereby reduce error associated with spatial variation in the proportion of C-3 and C-4 plants. To assure sampling the same areas, two lines were permanently marked at each study site. Permanent line end-points were established by randomly selecting two locations at each site. From one end-point a 15 m line was run north and from the other location a 15 m line was run west. Along each line two parallel transects (2 m apart) were read by moving the point-quadrat frame along the line twice, once facing in one direction and the second time facing in the opposite direction. Therefore, a total of four transect lines were measured for each site and date. For each transect 150 pins were run (125 in April) for a total of 600 pins (500 in April) per LAI determination. Data from each transect were kept separate for statistical comparisons.

Leaf area indices were determined for two plant communities that were on level terrain. These study sites were on loam soil, adjacent to the instrument shelter that housed the instrumentation to determine ozone deposition. One site was within a 6-ha exclosure protected from grazing since 1968. The other was a grazed site located just outside the exclosure area in a pasture that has been moderately grazed; 1988 grazing began in June. Both loam sites were dominated by *B. gracilis.*

The C-3 graminoids (grasses and sedges) encountered during the study were *Agropyron smithii* Rydb., *Carex eleocharis* Bailey, *Sitanion hystrix* and *Stipa comata* Trin. & Rupr. The C-4 grasses encountered were *Aristida purpurea* Nutt., *Bouteloua gracilis*, and *Sporobolus cryptandrus* (Torr). A. Gray. Shrubs encountered were *Artemisia frigida* Willd, *Chrysothamnus nauseosus* (Pall). Britt., *Eriogonum effusum* Nutt., and *Gutierrezia sarothrae* (Pursh) Britt. & Rusby. Forbs included *Allium textile* A. Nels. & Macbr., *Cryptantha minima* Rydb., *Cymopterus montanus* T. & G., *Lepidium densiflorum* Schrad., *Leucocrinum montanum* Nutt., *Sphaeralcea coccinea* (Pursh) Rydb., *Thelesperma filifolium* (Hook). A. Gray, and *Tradescantia occidentalis* (Britt). Smyth. All the above listed shrubs and forbs have C-3 photosynthetic pathways. The cactus species at all sites was *Opuntia polyacantha* Haw., the only species in this study with a CAM photosynthetic pathway.

Soil water content was measured by the neutron scattering method (Troxler model 1257) at 30, 45, 60 and 75 cm depths (Figure 1). This method estimates soil water content in a spherical area approximately 20 cm around the measurement point. Therefore, in this study the soil water content was not estimated for the top 10 cm of soil nor at depths greater than 95 cm. The volumetric soil water amounts were determined by a calibration equation developed by comparing probe counts with gravimetric soil water contents at 210 measurement points (correlation coef., $r = 0.87$).

RESULTS

Ozone Data

Ozone data for the week starting Tuesday, June 7, 1988 (Julian day 159) are presented in this section. This week was selected to demonstrate the variability of ozone and its flux as well as the difficulty in determining a single representative deposition value from a week of data. It represents one of the highest ozone deposition weeks. All data have been calibrated and edited and invalid data have been culled. Figure 2 presents the half-hour average ozone concentration in parts per billion (ppb). Note the highest concentration for the week was 88 ppb, at 05:30 p.m. Mountain Standard Time on June 10th (Julian day 162).

The ozone flux data have not been corrected nor adjusted for sensor time response, temperature and moisture fluxes, sample volume averaging, or sonic anemometer shadowing (Figure 3). These corrections[1] can be substantial (they averaged +48% for the week of June 7, Figure 3). The above corrections are accounted for in the diurnal calculations presented below and in the integrated ozone deposition data used to compare with LAI data. Note the diurnal nature of the ozone deposition values in Figure 3; these data result in deposition velocities that also vary diurnally between 0.0 at night and peak values of 0.9 cm/sec during the day. Typical mid-afternoon deposition velocities are around 0.5 cm/sec, however.

The ozone flux data for each week associated with a LAI measurement were integrated and assembled diurnally. Figure 4 presents diurnal, half-hour average fluxes measured for the week June 7 to June 14, 1988 (Julian days 159 to 166). The diurnal nature of ozone deposition is evident. The data in Figure 4 are in turn averaged over the 24-hour period to obtain an overall average flux value used to compare with the LAI measurements. During the week shown in Figure 4, the Pawnee site experienced a total of about 130,000 micrograms of ozone deposition per square meter. This relates to an average flux of about 19,000 micrograms per square meter per day, or about 390 micrograms per square meter per half-hour for the week. Table I gives the corresponding half-hour ozone deposition results for the remaining week periods associated with the LAI data.

A comparison of ozone concentration to ozone deposition is of interest because the proportionality between the two is the so-called deposition velocity (V_d). A representative V_d for the period June 5-14, 1988, is the slope (0.37 cm/sec) of the linear regression line shown in Figure 5. Other weeks investigated had similar slopes and y-intercepts. The scatter in Figure 5 is mostly diurnal.

Leaf Area Index

Green leaf area peaked during July at both the grazed and ungrazed loam sites, while production of leaf area was greatest during May (Figures 6 and 7, and Table I). May was also the month of greatest soil water loss (Figure I). The LAI of C-3 and C-4 graminoids were plotted separately (graphs B in Figures 6 and 7) to determine if different water use efficiencies or ozone deposition translated to differences in peak growth activity. The LAI of C-4 grasses was similar at both study sites. The leaf area of C-4 grasses surpassed that of C-3 graminoids during May at the ungrazed site. Amounts of C-3 leaf area were so low at the grazed site, however, that the leaf area of C-4 species at this site was always greater than that of C-3 graminoids.

Total, C-3, and C-4 leaf area development responded to rainfall. Following a 40 mm precipitation event on July 7 (Figure 1), both sites had a large resurgence in soil water content. Following this event, senescence of green leaf tissue accelerated while green leaf area increased by only a small amount (see shaded areas in Figures 6 and 7). After attaining maximum leaf area, soil-stored water was essentially depleted at all sites and the water supply became more dependent on unpredictable thunderstorm events. Grazing may have reduced standing dead biomass and altered the relative abundance of certain species. Nevertheless, the total leaf area of C-4 grasses was similar at the grazed and ungrazed sites.

Ozone and Leaf Area Index

The time-integrated ozone deposition data are presented as positive number in Table I and in the figures presented in this section to make comparisons with LAI data easier to follow. Linear regressions were run on each LAI category verses ozone deposition. Since LAI measured and ozone deposition were not on the same date, the ozone deposition data were linearly extrapolated to the LAI measurement dates for analyses. The extrapolated values are listed separately in Table I. Maximum ozone deposition values of the order 370 micrograms per meter square per half-hour were associated with LAI determinations of about 0.6. The best correlation coefficients (bottom row Table I) were (1) ozone deposition and total ungrazed LAI (0.89) and (2) ozone deposition with ungrazed C-3 LAI (0.89). The worst correlation coefficients were (1) ozone deposition and total ungrazed green LAI (0.62) and (2) ungrazed

C-4 LAI (0.62). The normalized ungrazed total LAI, the normalized ungrazed total green LAI, and the normalized ozone deposition versus Julian day, all peak from May to July as shown in Figure 8. Figure 9 is a plot of the extrapolated ozone deposition data versus: grazed total green LAI, grazed total (green and total dead) LAI, ungrazed total green LAI, and ungrazed total LAI. In each category there is a trend of higher values of ozone deposition with higher LAI values.

SUMMARY AND CONCLUSIONS

Seasonal patterns of leaf area development and ozone deposition, along with precipitation and soil water amounts, were compared at a shortgrass steppe site in Colorado (the Pawnee site). Emphasis was on possible relationships between LAI and ozone deposition. Leaf area indices of old standing dead, live green, C-3 graminoids, and C-4 grasses were determined. Soil water was measured by a neutron probe for 30–75 cm depths. Maximum leaf area indices of total green material ranged from 0.35–0.40, with the C-4 grasses constituting 58-74% and C-3 grasses 9–36% of these amounts. Although ozone deposition is diurnal, time-integrated patterns of ozone deposition were somewhat correlated with LAI measurements, which might be expected since surface resistance is related to canopy behavior. Averaged ozone deposition values determined by eddy correlation ranged from 260 to 390 micrograms per square meter per half-hour period averaged over week periods during the 1988 growing season; corresponding LAI determinations ranged from about 0.1 to 0.6.

The measured relationship between ozone deposition and leaf area development suggests that whatever factors are controlling LAI are also influencing ozone deposition. This is the first attempt we know of to relate actual measured ozone deposition to measured LAI. More research is in order: if the aerodynamic resistance contribution to the measured flux were removed, the remaining contributions of stomatal, cuticular and surface resistances would perhaps correlate better with LAI; also of interest are questions relating similar deposition and concentration measurements to plant effects at various locations and elevations.[8] If ozone in the lower boundary layer is truly a detriment, and if there is a link between LAI and ozone deposition, then can we, or should we, look to agricultural and other areas with high leaf area production as a sink for unwanted ozone?

ACKNOWLEDGMENTS

This research was funded by the Shortgrass-Steppe Long-Term Ecological Research Program (National Science Foundation grant BSR-8114822), the USFS Rocky Mountain Forest and Range Experiment Station Dry Deposition Project, Ft. Collins, CO and by EPA/USFS IAG No. DW-12933093-01-0.

REFERENCES

1. K. Zeller, W. Massman, D. Stocker, D.G. Fox, D. Stedman, and D. Hazlett, "Initial results from the Pawnee eddy correlation system for dry acid deposition research," USDA FS/RMFRES Res. Paper RM-282, Jan. 1989, 32pp.

2. D.L. Hazlett, "Leaf area development in four plant communities of the Colorado steppe," submitted to *Ecology*, January, 1989.

3. F.I. Woodward, *Climate and Plant Distribution*, Cambridge University Press, 1987, 174pp.

4. R.T. McMillen, "A basic program for eddy correlation in non-simple terrain," NOAA Tech. Memo ERL ARL-147 ATDD, Oak Ridge, TN, 1986, 32pp.

5. J.D. Ray, D.H. Stedman, and G.J. Wendel, "Fast chemiluminescent method for measurement of ambient ozone," *Analyt. Chem.* 58:598 (1986).

6. J. Warren-Wilson, "Estimation of foliage denseness and foliage angle by inclined point quadrats," *Aust. J. Bot.* 11:95 (1963).

7. D.H. Knight, "Leaf area dynamics of a shortgrass prairie in Colorado," *Ecology* 54:891 (1973).

8. A.S. Lefohn, A.S.L. Assoc., Helena, MT, private communication, 1989.

Table I. Leaf Area Index and Ozone Deposition Data

	Ungrazed				Grazed				Ozone Flux[a]	
LAI date (Julian Day)	Total live+ dead	Total Green	C-4	C-3	Total live+ dead	Total Green	C-4	C-3	Measured Flux	Extra-polated Flux[b]
(68)									262	
Apr 7 (98)	0.45	0.045	0.002	0.017	0.24	0.056	0.005	0.007		304
(103)									311	
May 5 (126)	0.44	0.125	0.029	0.046	0.32	0.152	0.059	0.015		330
(138)									341	
Jun 1 (153)	0.64	0.384	0.193	0.080	0.50	0.339	0.206	0.028		377
(159)									392	
Jun 23 (175)	0.61	0.370	0.212	0.070	0.49	0.312	0.196	0.029		387
(180)									386	
(187)									371	
Jul 13 (195)	0.58	0.396	0.258	0.078	0.50	0.348	0.260	0.004		361
(201)									353	
Aug 8 (221)	0.49	0.325	0.241	0.042	0.47	0.328	0.213	0.016		324
Sep 9 (253)	0.41	0.133	0.055	0.023	0.26	0.107	0.039	0.004		279
(264)									263	
Oct 2 (276)	0.43	0.158	0.088	0.025	0.29	0.126	0.080	0.000		246
LAI vs. Ozone Correlation Coefficient	0..89	0.62	0.62	0.89	0.82	0.77	0.70	0.81		

[a] Ozone flux units: micrograms/square meter/half hour

[b] Linear extrapolation of measured ozone flux with time.

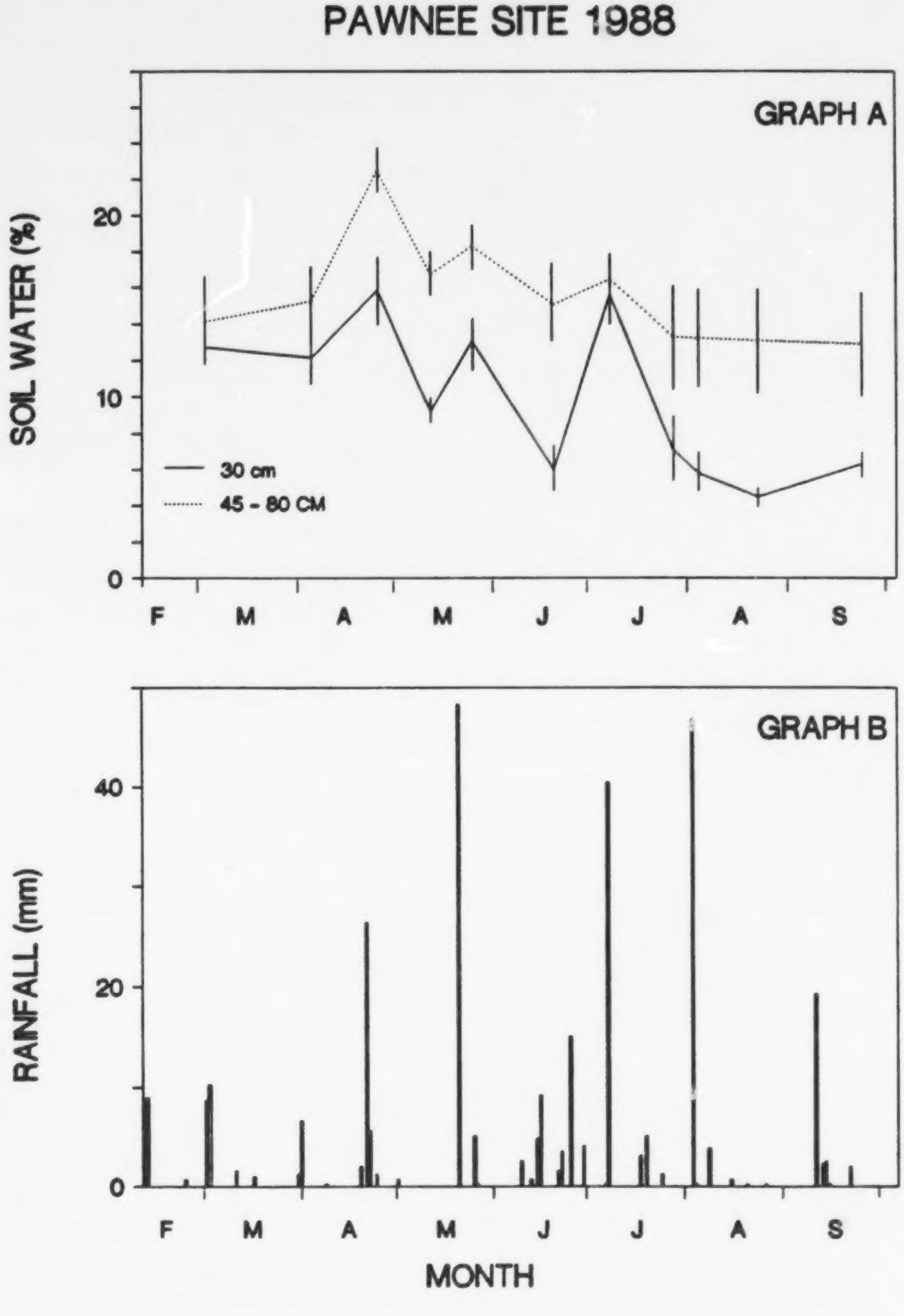

Figure 1. Graph A: Pawnee site soil water for the 1988 growing season.
Graph B: Pawnee site precipitation for the 1988 growing season.

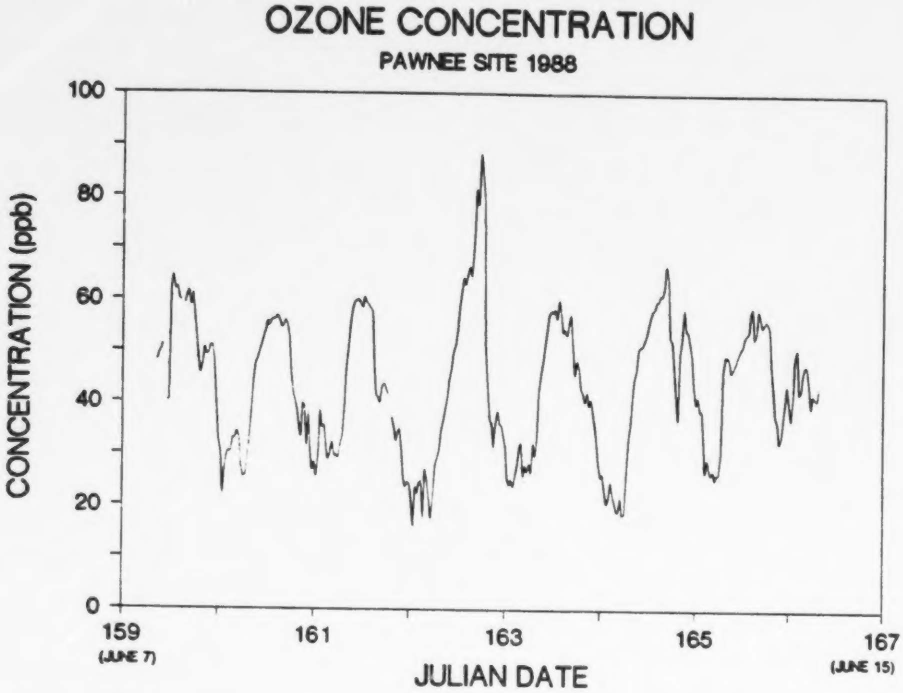

Figure 2. Half-hour ozone concentration for the period June 7-14, 1988.

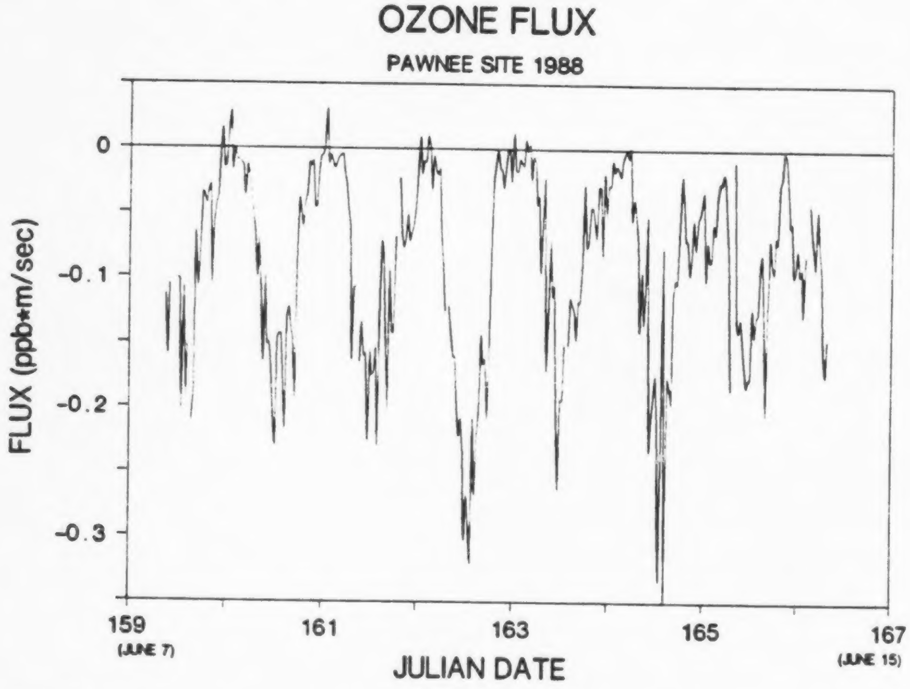

Figure 3. Ozone flux (deposition) for the period June 7-14, 1988. A negative value indicates flux in the downward vertical direction.

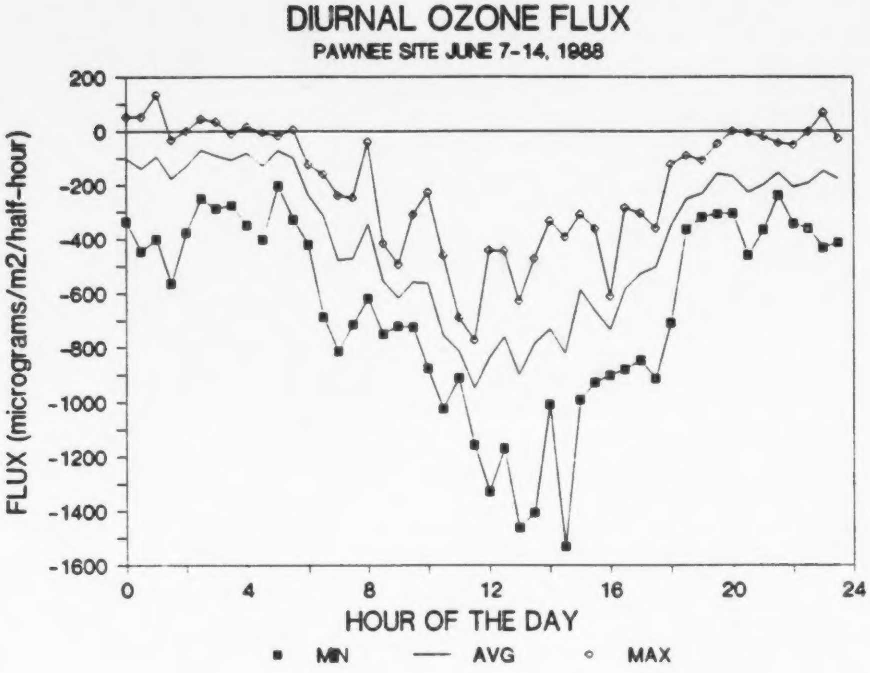

Figure 4. Maximum, average, and minimum diurnal ozone flux for the period June 7-14, 1988. Flux units (ppb m/sec, fig. 3) have been converted to micrograms/m^2/half-hour for convenience in integrating the date. Points represent the mean maximum, average or minimum flux for each hour over the period June 7-14. Negative values indicate downward flux.

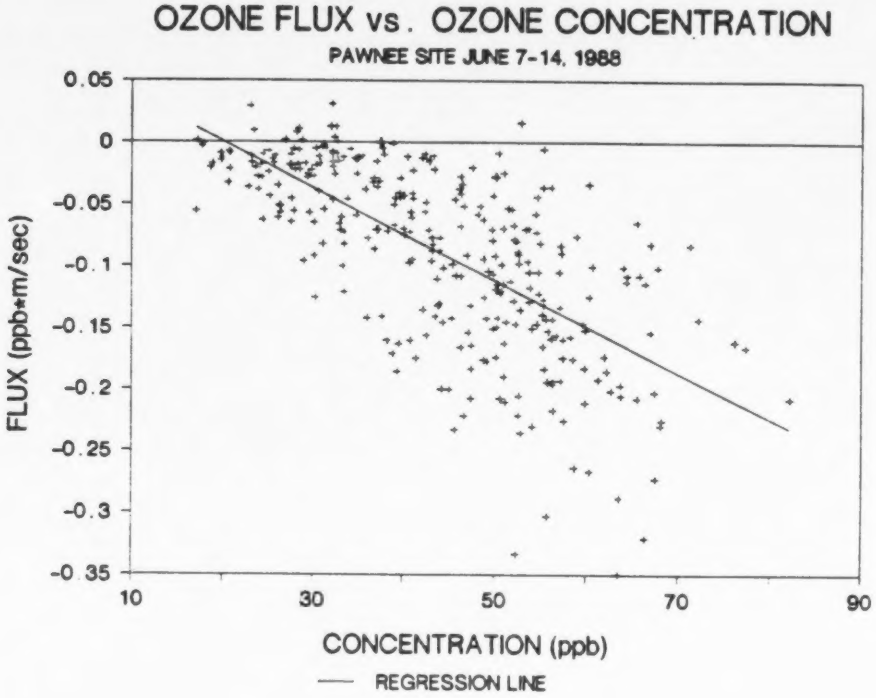

Figure 5. Ozone concentration versus ozone flux for the period June 7-14, 1988. The solid line is the regression y = -0.00374x + 0.0757 (correlation coefficient 0.67).

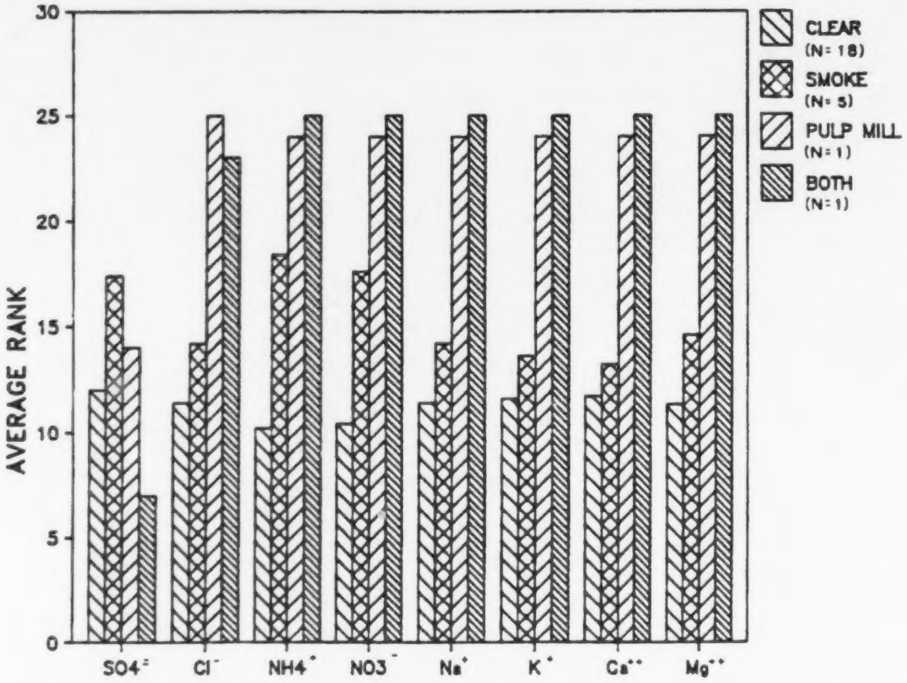

Figure 10. Average rank of cloud events at Arcata grouped by air pollution conditions. High rank indicated high concentrations. The sample size (n =) includes samples that were analyzed for all principal ions and differs from the text.

Cloud Chemistry

The three sites were more alike than different in cloud water chemistry. Acidity of cloud water did not differ significantly among the three sites. Median pH at Redwood National Park was 4.32; Arcata was 4.14 and Oakland was 4.05. Sulfate (total) was significantly more abundant in ground-based clouds at Redwood National Park than at Arcata or Oakland (P = 0.0075) (Figure 3). This difference may be a result of greater exposure to sea salt since the Redwood National Park site is closest to the ocean. However, the non-seasalt fraction of SO_4^{2-} was still significantly higher for Redwood National Park than for the other two sites. The fact that these samples were collected in different years must be considered as a possible partial explanation.

Potassium levels were significantly higher in clouds at Arcata than at the other two sites (P = 0.0004) (Figure 4). The most likely source of K^+ at Arcata was wood smoke from slash burning and forest fires. The Arcata City Forest is a commercial forest in the midst of millions of hectares of commercial forest holdings. Slash burning occurred extensively in the fall of 1986 and 1987, and forest fires were extensive in the coast ranges east of the site in fall 1987. The Redwood National Park site was surrounded by public lands where slash burning was precluded and where no forest fires occurred during the collection period. The Oakland site was in a largely unforested region of the state. More comments will be given to the role of smoke at Arcata in a later section.

Rain Chemistry

Oakland rain was less acidic than rain collected at Arcata and Redwood National Park (P = 0.0013) (Figure 5). Median pH was 4.95 at Redwood National Park, 4.99 at Arcata, and 5.25 at Oakland. Redwood National Park rain had 2 and 3 times the concentration of total SO_4^{2-} of Oakland and Arcata respectively (P = 0.0012) (Figure 6). Non-seasalt SO_4^{2-} was about 3 and 4 times as high at Redwood National Park as at Oakland and Arcata, respectively. Whereas Arcata had higher levels of K^+ in clouds, Oakland rain had 2 and 4 times the K^+ of Redwood National Park and Arcata (P = 0.0018) (Figure 7). This higher level of K^+ in winter rains at Oakland may be a result of a local contribution of smoke from urban wood-burning home-heating stoves.

Oakland rain had 5 and 16 times the median concentrations of NH_4^+ of Arcata and Redwood National Park (Figure 8). This higher level of NH_4^+ may account at least in part for the more basic pH of Oakland rain. We would expect rain collected from an urban area to have higher levels of nitrogenous ions than more remote areas. Median values of NO_3^- were higher at Oakland than at Arcata or Redwood National Park. Kruskal-Wallis 1-way analysis of variance indicated that Oakland ranked the highest for NO_3^- levels in rain (P = 0.0002) (Figure 9). The mean values for NO_3^- suggested that Redwood National Park had the higher levels. This was an instance in which the mean of a non-normally distributed population gave misleading evidence.

Arcata Extreme Events

Local air pollution events at Arcata were easily discernible. The most common wind direction is from the northwest. These winds carry relatively clean marine air. Pacific storm fronts are infrequently preceded by 24 to 48 hours of winds from the southwest. These winds carry a strong smell from pulp mills located to the southwest of Arcata. Field observation by smell at the Arcata site was sufficient to detect these events. Wind direction at the site was not a good indication of these events because of the influence of hilly topography on the wind. Smoke from forest wildfires in the fall of 1987 and from commercial slash burning in the fall of 1986 and spring of 1987 was also easily detected by both smell and haze at the site in Arcata. In a few instances, these air pollution events were coincident with the formation of ground-based clouds in the morning and evening. The Arcata cloud events were divided into four groups based on air pollution conditions at Arcata 1 km west of the site for the 24 h preceding a collection: (1) no apparent smells or haze (clear)-28 samples, (2) forest fire slash smoke smell or haze-5 samples, (3) pulp mill smell and haze-2 samples, (4) both forest fire smoke and pulp mill smell-1 sample. These conditions were documented by field notes of observations of the site operator. Significant differences among these four groups were detected only for pH. The samples collected under smoky conditions were the most acidic ($P < 0.01$, Kruskal-Wallis). The relative rankings of the four groups indicated that smoke and haze conditions at Arcata are associated with the highest fog concentrations of the principal ions (Figure 10).

Comparison of Cloud and Rain Chemistry with Other Studies

At least five other studies have reported cloud chemistry for locations along the California coast.[5,6,15,18,19] With one exception, these studies concentrated on southern urban areas. All of these studies sampled relatively few events at many sites rather than concentrated on many events at a few sites. The earliest study reported five cloud samples from coastal Humboldt County only about 50 km south of the Arcata study site, and provided the most directly comparable conditions to the Redwood National Park site. The cloud chemistry reported for Arcata, Redwood National Park and Oakland is within the range of values established by these previous studies. The larger sample size reported for these three sites enabled a better understanding of the central tendency of cloud chemistry at each location. Furthermore, a larger sample size also showed the recurrence of extreme events in many cases (Figures 3-9).

Ion balances (Table II and III) confirm findings by other authors that this group of ions does not tell the whole story for precipitation chemistry in the West.[5] Ion balances are generally large and positive, especially for cloud water in Arcata and Oakland. Organic acids may account for part of this imbalance.[2]

The NO_3^-/SO_4^{2-} ratio calculated from the data presented here ranges from 0.17 to 0.27 for clouds and from 0.05 to 0.43 for rain. These ratios are at the low end of the range reported in the literature for clouds and rain in California.[21,20,5,6,18,19] These ratios are partially a result of high SO_4^{2-} values. Sulfate levels may be correlated with industrial forestry operations such as pulp mills. This does not explain, however, why Redwood National Park which is remote from such operations, should have the highest levels, rather than Arcata, which is relatively near pulp mills.

The difference between cloud and rain chemistry suggests the importance of clouds as vectors for nutrients as well as pollutants into coastal ecosystems. Measurements of deposition rates of cloud water to forest canopies would enable the use of these data in the calculation of nutrient and pollutant fluxes.

CONCLUSIONS

Relatively large sample sizes enabled detection of statistically significant differences among and within sites in cloud and rain chemistry. The largest and most significant differences were between cloud and rain chemistry.

Differences among the sites were less prominent and less common, and seasonal and annual variations were least common. Chemical concentrations in cloud water at the more remote sites were more similar to Oakland than might be expected. Oakland showed higher levels of nitrogenous ions, as would be expected from the higher density of vehicular traffic in the Bay Area. High values of sulfate at Redwood National Park are not yet explained. High values of potassium at Arcata are likely to be the result of forest fires and commercial forest slash burning in the region. Although North Coast cloud chemistry is not as clean as that reported for remote sites,[9,2] it is not as polluted as that reported for some sites in the eastern United States or in southern coastal California.

ACKNOWLEDGMENTS

This project was funded by a grant to F.H. Bormann of Yale University and G.E. Likens of the Institute of Ecosystem Studies of the New York Botanical Garden from the Andrew Mellon Foundation. Additional sources of funding for this project included United States EPA, McIntire-Stennis Administration, and East Bay Regional Parks. Analytical data were provided in 1984–85 by the Institute of Ecosystem Studies and in 1986–87 by the Cooperative Chemical Analytical Laboratory of Oregon State University, Department of Forest Science, and USDA Forest Service. The National Park Service (Redwood National Park), East Bay Regional Parks, the city of Oakland, and the town of Arcata provided cooperation and permission for site location. K.C. Weathers was Project Coordinator for the first two years. Susanne Lemcke, Julie Philips, Scott Liston, Don Bicknell, and Dorothy Walker were field assistants.

REFERENCES

1. V.A. Mohnen, "The challenge of acid rain," *Sci. Am.* 259(2):30 (1988).

2. K.C. Weathers, G.E. Likens, F.H. Bormann, S.H. Bicknell, B.T. Bormann, B.C. Daube, Jr., J.S. Eaton, J.N. Galloway, W.C. Keene, K.D. Kimball, W.H. McDowell, T.G. Siccama, D. Smiley, and R.A. Tarrant, "Cloudwater chemistry from ten sites in North America," *Environ. Sci. Tech.* 22:1018 (1988).

3. K.C. Weathers, G.E. Likens, F.H. Bormann, J.S. Eaton, W.B. Bowden, J.L. Anderson, D.A. Cass, J.N. Galloway, W.S. Keene, K.D. Kimball, P. Huth, and D. Smiley, "A regional acidic cloud/fog event in the eastern United States," *Nature* 319:657 (1986).

4. W.J. Deal, "The quantity of acid in acid fog," *JAPCA* 33(7):691 (1983).

5. J.M. Waldman, J.W. Munger, D.J. Jacob, R.C. Flagan, J.J. Morgan, and M.R. Hoffman, "Chemical composition of acid fog," *Science* 218:677 (1982).

6. R.L. Brewer, R.J. Gordon, L.S. Sheppard, and E.C. Ellis, "Chemistry of mist and fog from the Los Angeles Urban area," *Atmos. Environ.* 17(11):2267 (1983).

7. P.S. Muir, K.A. Wade, B.H. Carter, T.V. Armentano, and R.A Pribush, "Fog chemistry at an urban midwestern site," *JAPCA* 36(12):1359 (1986).

8. T. Sherbatskoy and M. Bliss, "Occurrence of acidic rain and cloud water in high elevation ecosystems in the Green Mountains of Vermont," *Transactions of the Air Pollution Control Association Specialty Conference on The Meteorology of Acid Deposition*, P.J. Samson, Ed., Hartford, CT, 1983.

9. F. Parungo, C. Nagamoto, I. Nolt, M. Dias, and E. Nickerson, "Chemical analysis of cloud water collected over Hawaii," *J. Geophys. Res.* 87(C11):8805 (1982).

10. R.E. Falconer and P.D. Falconer, "Determination of cloud water acidity at a mountain observatory in the Adirondack Mountains of New York State," *J. Geophys. Res.* 85(C12):7465 (1980).

11. G.J. Dollard, M.H. Unsworth, and H.J. Harve, "Pollutant transfer in upland occult precipitation," *Nature* 302:241 (1983).

12. G.M. Lovett, W.A. Reiners, and R.K. Olson, "Cloud droplet deposition in subalpine balsam fir forests: Hydrological and chemical inputs," *Science* 218:1303 (1982).

13. G.M. Lovett, "Rates and mechanisms of cloud water deposition to a subalpine balsam fir forest," *Atmos. Environ.* 18(2):361 (1984).

14. G.M. Lovett and W.A. Reiners, "Canopy structure and cloud water deposition in subalpine coniferous forests," *Tellus* 38B:319 (1983).

15 J. Azevedo and D.L. Morgan, "Fog precipitation in coastal California forests," *Ecology* 55:1135 (1974).

16. B.C. Daube, Jr., K.D. Kimball, P.D. Lamar, and K.C. Weathers, "Characteristics of an active cloud water collector," *Atmos. Environ.* (1987).

17. W.C. Keene, A.A.P. Pszenny, J.N. Galloway, and M.E. Hawley, "Seasalt corrections and interpretation of constituent ratios in marine precipitation," *J. Geophys. Res.* 91:6647 (1986).

18. E.J. Mack, U. Katz, C.W. Rogers, D.W. Gaucher, K.R. Piech, C.K. Akers, and R.J. Pilie, "An investigation of the meteorology, physics, and chemistry of marine boundary layer processes," *Calspan Report No. CJ-6017-M-1, Project Sea Fog Fifth Annual Summary Report*, Calspan Corporation, Buffalo, New York, 1977.

19. D.J. Jacob, J.M. Waldman, J.W. Munger, and M.R. Hoffmann, "Chemical composition of Fogwater Collected along the California Coast," *Environ. Sci. Tech.* 19(8):730 (1985).

20. J.P. Cook and H. Le, *California Acid Deposition Data July 1984-June 1987*, California Air Resources Board, August, 1988.

21. J.C. McColl, L.K. Monette, and D.S. Bush, "Chemical characteristics of wet and dry atmospheric fallout in Northern California," *J. Environ. Qual.* 11(4):585 (1982).

Table I. Site Characteristics.

Site	Latitude Longitude	Elevation (meters, mean sea level)	Distance to Salt Water	Dominant Vegetation
Orick	41° 15' 124° 02'	287 M msl	2 km	*Sequoia sempervirens* *Picea sitchensis* *Alnus oregona*
Arcata	40° 55' 124° 05'	275 M msl	10 km	*Sequoia sempervirens* *Pseudotsuga menziesii* *Alnus oregona*
Oakland	37° 49' 122° 10'	450 M msl	11 km	*Sequoia sempervirens*

Table IIa. Chemical content of cloud water at Redwood National Park. Concentrations are in microequivalents per liter.

Ion	N	Mean	SD	Min	25-%tile	Median	75-%tile	Max
Ca^{2+}	16	16.6	14.04	4.0	6.0	11.2	23.0	50.0
Mg^{2+}	14	43.8	49.34	1.6	13.2	23.0	57.6	164.5
K^+	15	11.0	6.86	2.6	5.4	9.5***	13.8	28.1
Na^+	15	244.2	241.31	37.0	72.2	127.9	365.4	772.1
NH_4^+	14	92.0	56.01	.6	43.8	108.9	138.6	168.0
H^+	22	74.0	73.01	5.6	15.8	47.4	112.2	251.2
SO_4^{2-} (Total)	16	156.0	95.19	29.1	78.1	144.7**	233.2	349.8
SO_4^{2-} (Excess)	14	123.7	67.66	22.3	55.7	135.7***	174.4	231.6
NO_3^-	16	45.6	29.36	12.6	19.4	32.6	73.8	104.8
Cl^-	15	275.1	263.71	38.4	92.0	141.0	361.0	839.1
Ion Balance	13	-4.5						

The following symbols are used in Tables II-III to indicate the probability that a significant difference does not exist among the three sites for the indicated variable:

$*0.05 \geq P > 0.01$
$**0.01 \geq P > 0.001$
$***P \leq 0.001$

Table IIb. Chemical content of cloud water at Arcata City Forest. Concentrations are inmicroequivalents per liter.

Ion	N	Mean	SD	Min	25-%tile	Median	75-%tile	Max
Ca^{2+}	25	48.0	104.35	3.5	12.5	17.0	25.0	461.6
Mg^{2+}	25	70.2	157.32	3.9	9.6	17.9	40.8	612.9
K^+	25	24.8	26.50	6.9	11.8	16.4^{***}	24.6	113.5
Na^+	25	339.1	753.22	18.3	65.7	96.6	139.2	2838.2
NH_4^+	25	167.1	173.78	31.3	80.4	102.1	197.9	921.1
H^+	35	107.6	102.05	3.0	38.0	72.4	154.9	489.8
SO_4^{2-} (Total)	25	72.5	41.00	9.5	48.1	64.3^{**}	102.0	180.7
SO_4^{2-} (Excess)	25	56.7	41.95	0.0	27.8	49.5^{**}	77.5	177.6
NO_3^-	25	29.5	40.72	1.0	5.5	17.6	30.5	178.5
Cl^-	25	157.5	144.59	34.4	57.0	105.2	193.8	533.1
Ion Balance	23	72.8						

The following symbols are used in Tables II-III to indicate the probability that a significant difference does not exist among the three sites for the indicated variable:

$^{*}0.05 \geq P > 0.01$
$^{**}0.01 \geq P > 0.001$
$^{***}P \leq 0.001$

Table IIc. Chemical content of cloud water at Oakland. Concentrations are in microequivalents per liter.

Ion	N	Mean	SD	Min	25-%tile	Median	75-%tile	Max
Ca^{2+}	12	19.0	11.78	6.5	9.5	17.0	25.0	46.4
Mg^{2+}	12	18.9	14.58	6.3	8.0	13.4	30.0	43.2
K^+	12	8.9	2.33	6.1	7.2	8.3^{***}	10.1	13.0
Na^+	12	62.2	58.79	14.8	19.1	33.1	100.3	167.0
NH_4^+	12	171.5	54.09	103.6	124.9	168.9	219.6	251.2
H^+	23	130.3	126.82	25.1	63.1	89.1	141.3	562.3
SO_4^{2-} (Total)	12	76.4	25.54	50.2	57.8	70.4^{**}	86.1	136.0
SO_4^{2-} (Excess)	12	68.8	22.26	47.9	53.4	66.3^{**}	71.4	128.5
NO_3^-	12	18.5	14.51	3.6	5.8	11.9	31.0	47.0
Cl^-	12	94.5	79.42	27.6	32.9	51.8	178.3	222.3
Ion Balance	12	78.7						

The following symbols are used in Tables II-III to indicate the probability that a significant difference does not exist among the three sites for the indicated variable:

$^{*}0.05 \geq P > 0.01$
$^{**}0.01 \geq P > 0.001$
$^{***}P \leq 0.001$

Table IIIa. Chemical content of rain at Redwood National Park. Concentrations are in microequivalents per liter.

Ion	N	Mean	SD	Min	25-%tile	Median	75-%tile	Max
Ca^{2+}	30	3.6	2.95	0.0	1.5	2.5	5.5	11.0
Mg^{2+}	30	9.2	11.62	0.0	1.6	4.1	12.3	39.5
K^{+}	29	2.7	2.24	0.5	1.0	2.3^{**}	3.6	9.5
Na^{+}	30	45.2	60.22	1.7	7.0	19.1	61.8	243.6
NH_4^{+}	30	1.4	2.19	0.0	0.0	0.3^{***}	1.1	7.8
H^{+}	59	21.1	26.88	4.0	5.6	11.2^{**}	22.4	141.3
SO_4^{2-} (Total)	32	12.1	11.69	0.6	4.2	8.3^{*}	16.7	58.3
SO_4^{2-} (Excess)	30	6.1	5.29	0.4	3.3	4.4	7.9	27.0
NO_3^{-}	32	5.3	13.26	0.0	0.7	1.8^{***}	4.4	75.0
Cl^{-}	30	49.0	57.80	1.7	9.0	21.9	76.4	197.4
Ion Balance	29	29.1						

The following symbols are used in Tables II-III to indicate the probability that a significant difference does not exist among the three sites for the indicated variable:

$^{*}0.05 \geq P > 0.01$
$^{**}0.01 \geq P > 0.001$
$^{***}P \leq 0.001$

Table IIIb. Chemical content of rain at Arcata. Concentrations are in microequivalents per liter.

Ion	N	Mean	SD	Min	25-%tile	Median	75-%tile	Max
Ca^{2+}	20	4.7	8.57	0.0	0.7	2.0	4.0	38.4
Mg^{2+}	20	7.2	11.37	0.2	1.2	3.1	8.7	50.3
K^{+}	20	1.7	1.74	0.3	0.5	1.3^{**}	1.8	7.4
Na^{+}	20	29.1	49.48	0.9	4.3	13.9	29.8	220.1
NH_4^{+}	20	2.2	3.36	0.0	0.3	1.0^{***}	2.3	13.9
H^{+}	30	20.9	40.39	1.2	4.4	10.2^{*}	18.2	213.8
SO_4^{2-} (Total)	20	3.7	3.82	0.0	0.0	4.4^{*}	5.5	14.4
SO_4^{2-} (Excess)	20	1.4	1.83	0.0	0.0	0.0	3.2	4.7
NO_3^{-}	20	1.1	2.62	0.0	0.1	0.2^{**}	1.1	12.0
Cl^{-}	20	39.6	52.98	8.8	12.1	23.2	43.7	244.0
Ion Balance	20	9.9						

The following symbols are used in Tables II-III to indicate the probability that a significant difference does not exist among the three sites for the indicated variable:

$^{*}0.05 \geq P > 0.01$
$^{**}0.01 \geq P > 0.001$
$^{***}P \leq 0.001$

Table IIIc. Chemical content of rain at Oakland (Redwood Regional Park). Concentrations are in microequivalents per liter.

Ion	N	Mean	SD	Min	25-%tile	Median	75-%tile	Max
Ca^{2+}	17	7.2	6.41	1.5	3.5	4.5	8.5	22.0
Mg^{2+}	17	6.5	5.45	1.1	2.0	5.9	9.0	20.8
K^+	17	7.3	8.49	0.8	1.5	4.6^{**}	7.9	33.5
Na^+	17	27.9	3.50	4.3	9.1	20.4	45.2	93.5
NH_4^+	17	10.1	10.74	2.1	2.9	4.9^{***}	12.5	39.7
H^+	19	6.1	3.81	1.1	3.2	5.6^{*}	7.9	12.6
SO_4^{2-} (Total)	17	5.0	3.81	0.0	0.0	5.3^{*}	6.5	12.2
SO_4^{2-} (Excess)	17	2.4	2.43	0.0	0.0	1.4	4.3	6.6
NO_3^-	17	3.1	2.61	0.6	1.1	2.3^{***}	4.0	8.8
Cl^-	17	29.5	21.06	10.3	14.3	19.8	41.7	91.1
Ion Balance	17	51.5						

The following symbols are used in Tables II-III to indicate the probability that a significant difference does not exist among the three sites for the indicated variable:

$^{*}0.05 \geq P > 0.01$
$^{**}0.01 \geq P > 0.001$
$^{***}P \leq 0.001$

Table IV. Ratio of cloud to rain median concentrations of ions.

	Redwood National Park	Arcata City Forest	Oakland (Redwood Park)
Ca^{2+}	4.5^{***}	8.5^{***}	3.8^{**}
Mg^{2+}	5.6^{***}	5.8^{***}	5.9^{**}
K^+	4.1^{***}	12.6^{***}	1.8^{*}
Na^+	6.7^{***}	6.9^{***}	1.6
NH_4^+	363.0^{***}	102.1^{***}	34.5^{***}
H^+	4.2^{***}	7.1^{***}	15.9^{***}
SO_4^{2-} (Total)	17.4^{***}	14.6^{***}	13.3^{***}
SO_4^{2-} (Excess)	30.8^{**}	--^{a***}	47.4^{***}
NO_3^-	18.1^{***}	88.0^{***}	5.2^{***}
Cl^-	6.4^{***}	4.5^{***}	2.6^{**}

[a] The median for rain was 0.0, therefore no ratio could be obtained.

The following symbols are used to indicate the probability that a significant difference does not exist between cloud and rain concentrations for the ions indicated based on Mann-Whitney comparison:

$^{*}0.05 \geq P > 0.01$
$^{**}0.01 \geq P > 0.001$
$^{***}P \leq 0.001$

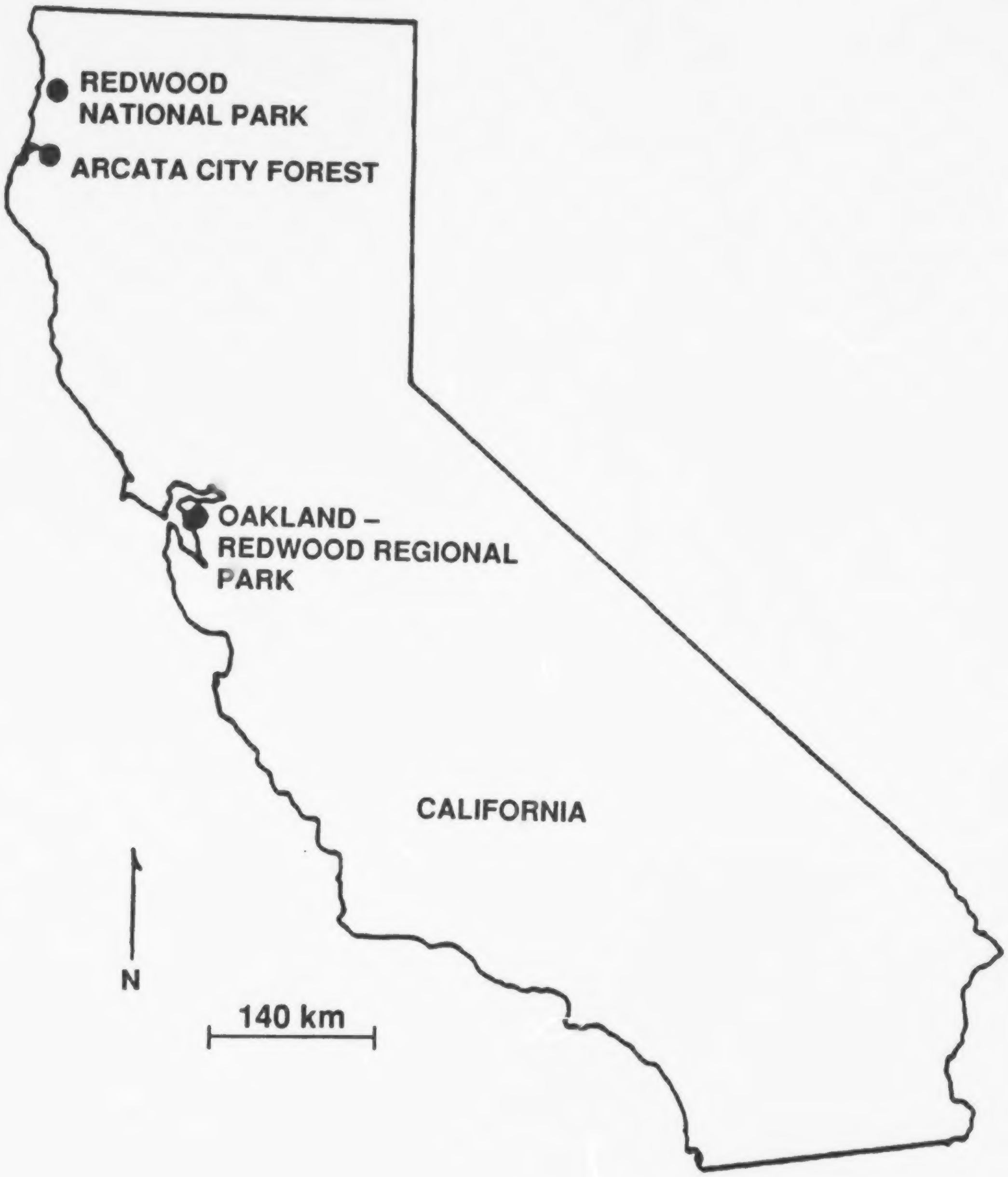
REDWOOD
NATIONAL PARK
ARCATA CITY FOREST
OAKLAND –
REDWOOD REGIONAL
PARK
CALIFORNIA
N
140 km

Figure 1. Three sampling locations in coastal California.

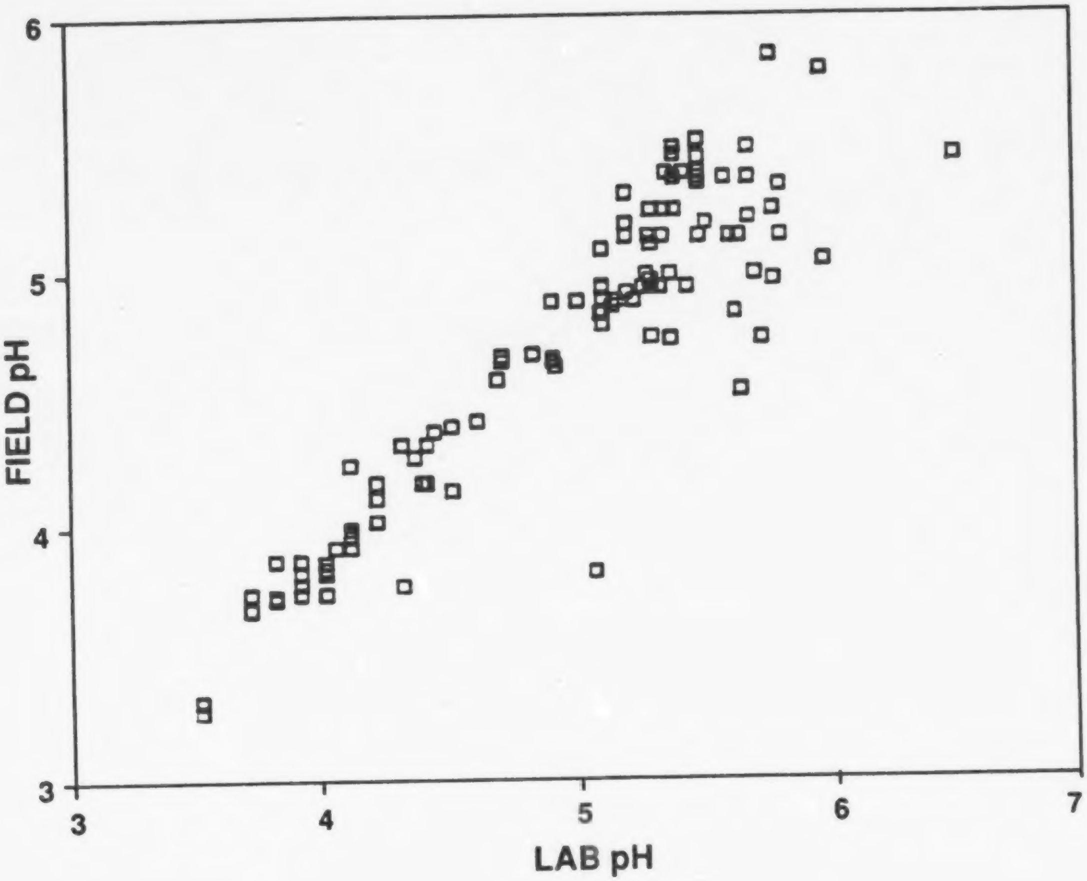

Figure 2. Relationship between pH recorded at the site (field) and at the laboratory (IES and OSU).

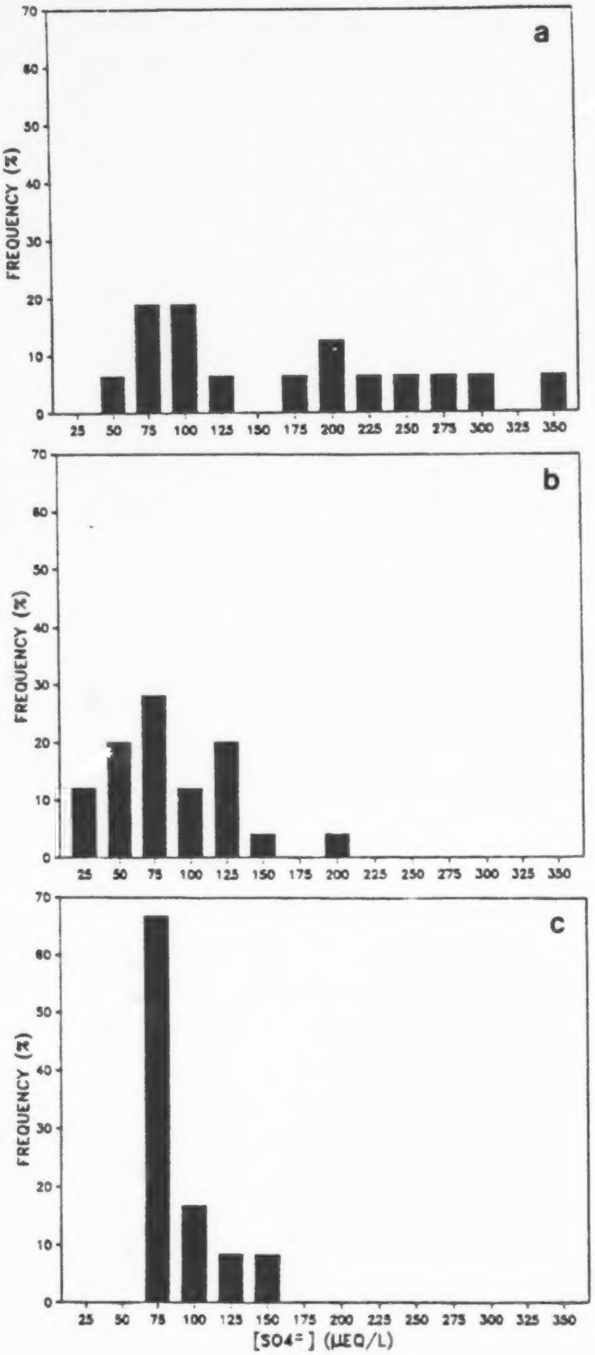

Figure 3. Frequency distribution for total SO_4^{2-} in clouds at (a) Redwood National Park, (b) Arcata, and (c) Oakland. Redwood National Park had significantly more sulfate ($P < 0.01$).

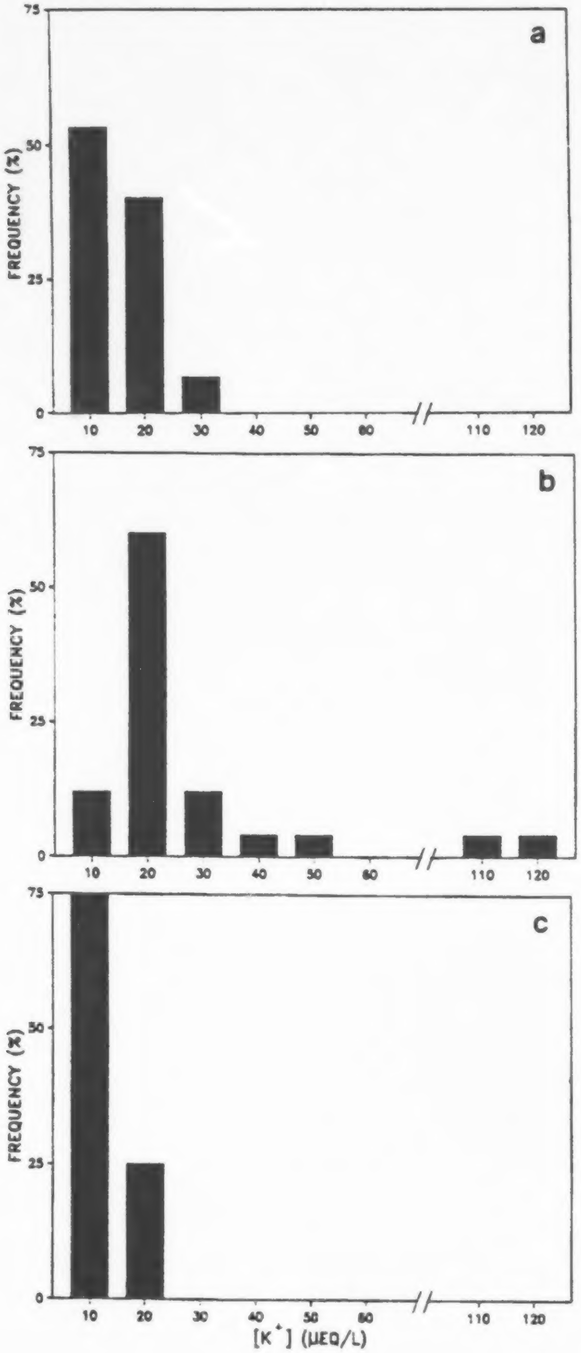

Figure 4. Frequency distributions for K$^+$ in clouds at (a) Redwood National Park, (b) Arcata, and (c) Oakland. Arcata clouds had more K$^+$ ($P < 0.001$).

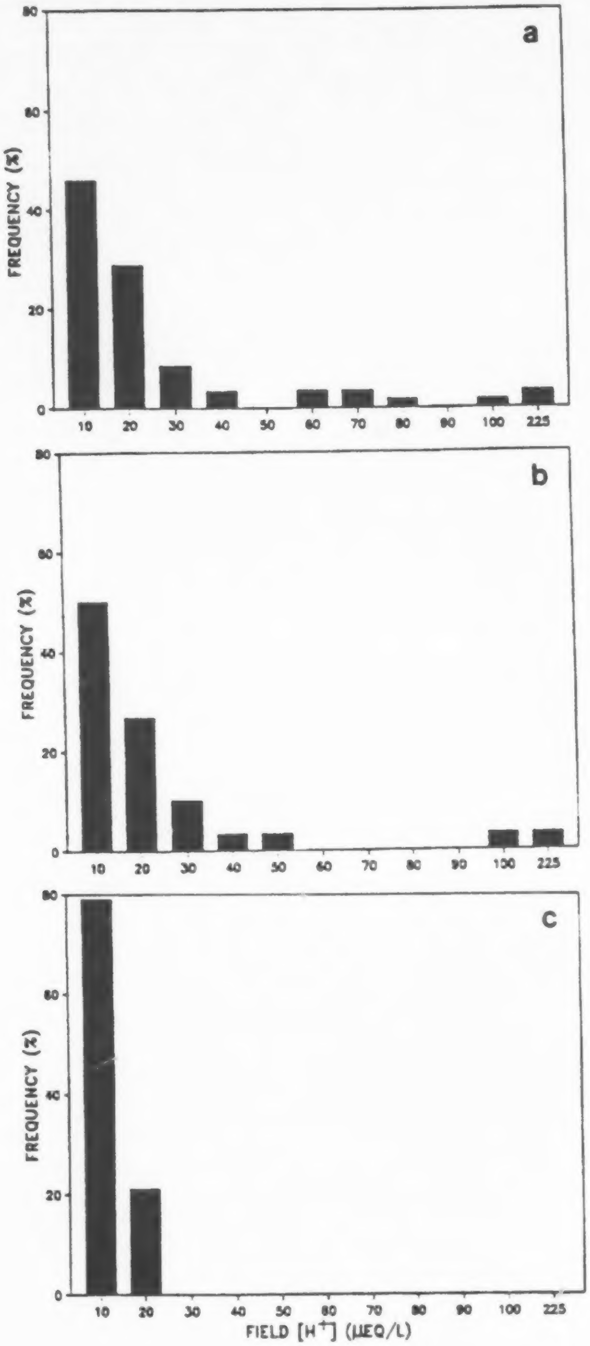

Figure 5. Frequency distribution for H^+ in rain at (a) Redwood National Park, (b) Arcata, and (c) Oakland. Oakland rain was least acidic ($P < 0.01$).

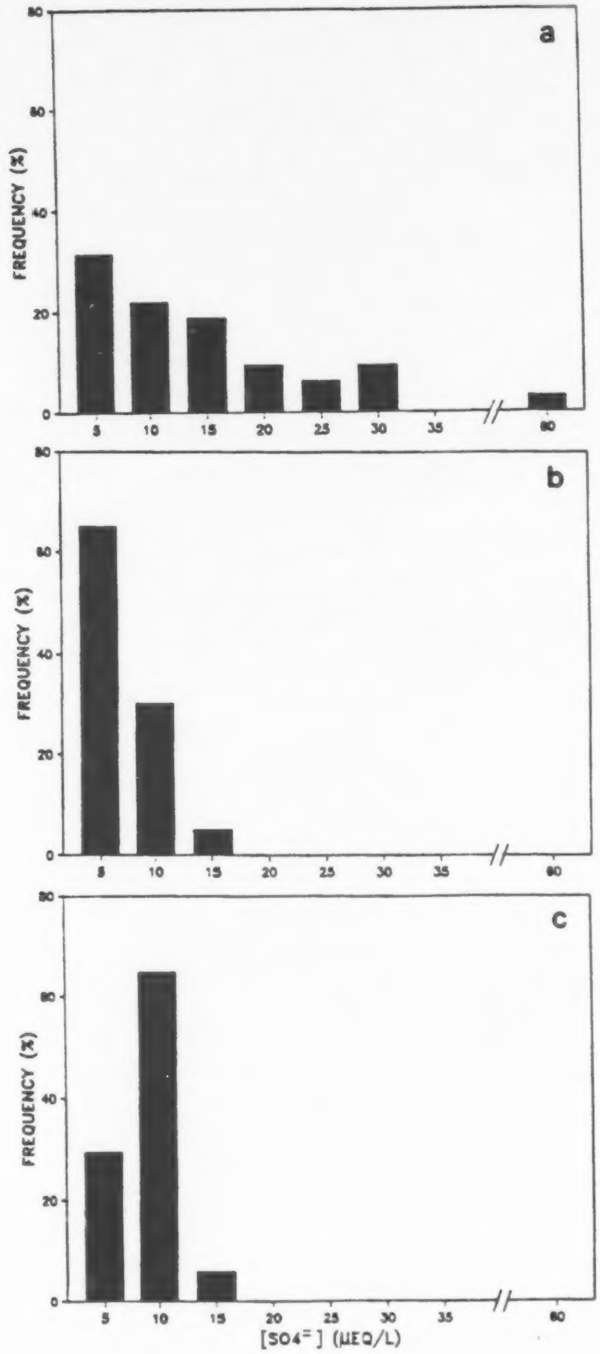

Figure 6. Frequency distribution for SO_4^{2-} in rain at (a) Redwood National Park, (b) Arcata, and (c) Oakland. Redwood National Park had more sulfate ($P < 0.01$).

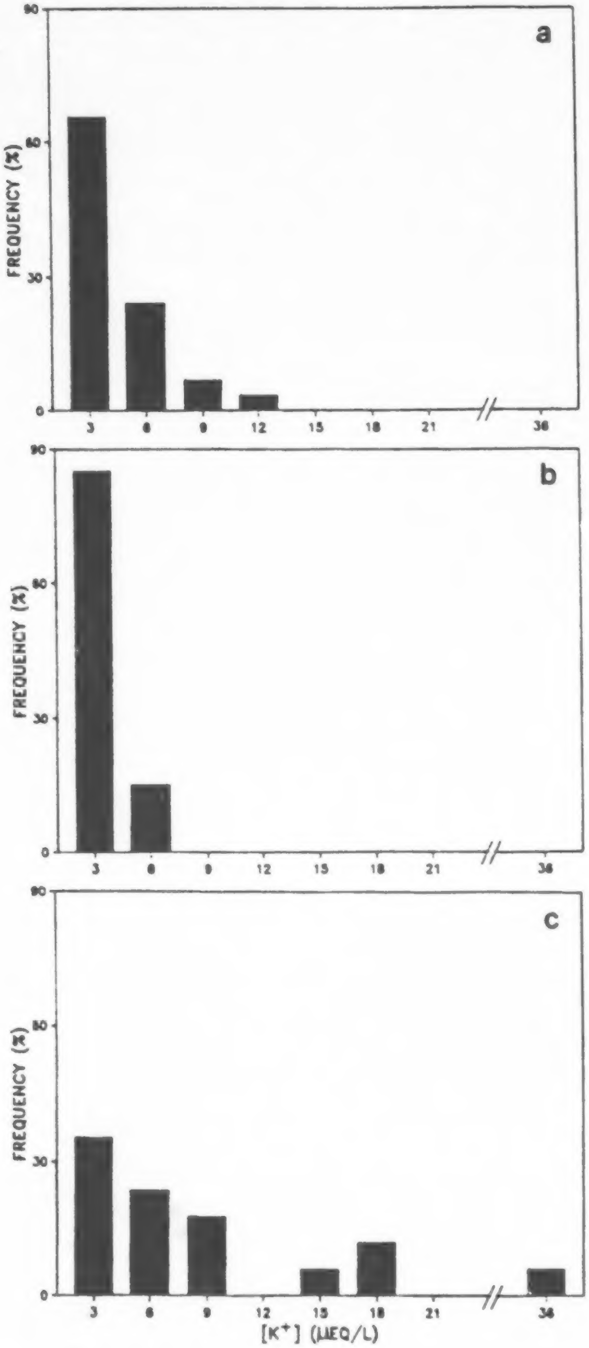

Figure 7. Frequency distributions for K^+ in rain at (a) Redwood National Park, (b) Arcata, and (c) Oakland. Oakland rain had significantly more K^+ ($P < 0.01$).

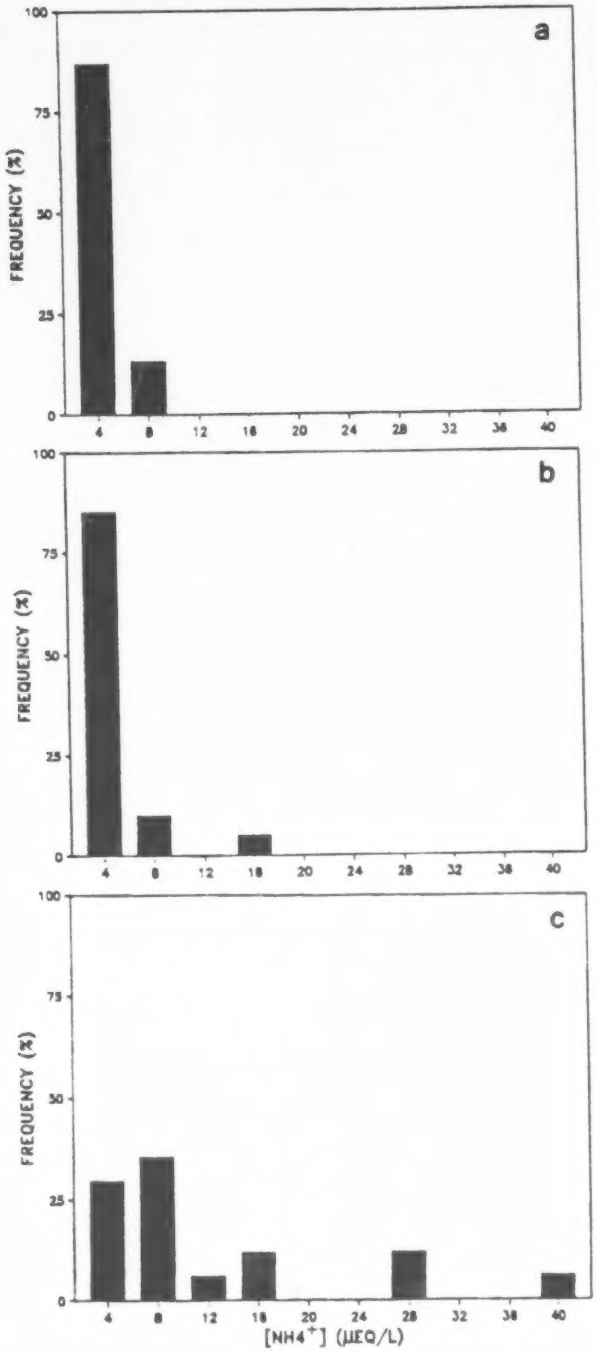

Figure 8. Frequency distributions for NH_4^+ in rain at (a) Redwood National Park, (b) Arcata, and (c) Oakland. Oakland had more NH_4^+ in rain than the other two sites ($P < 0.001$).

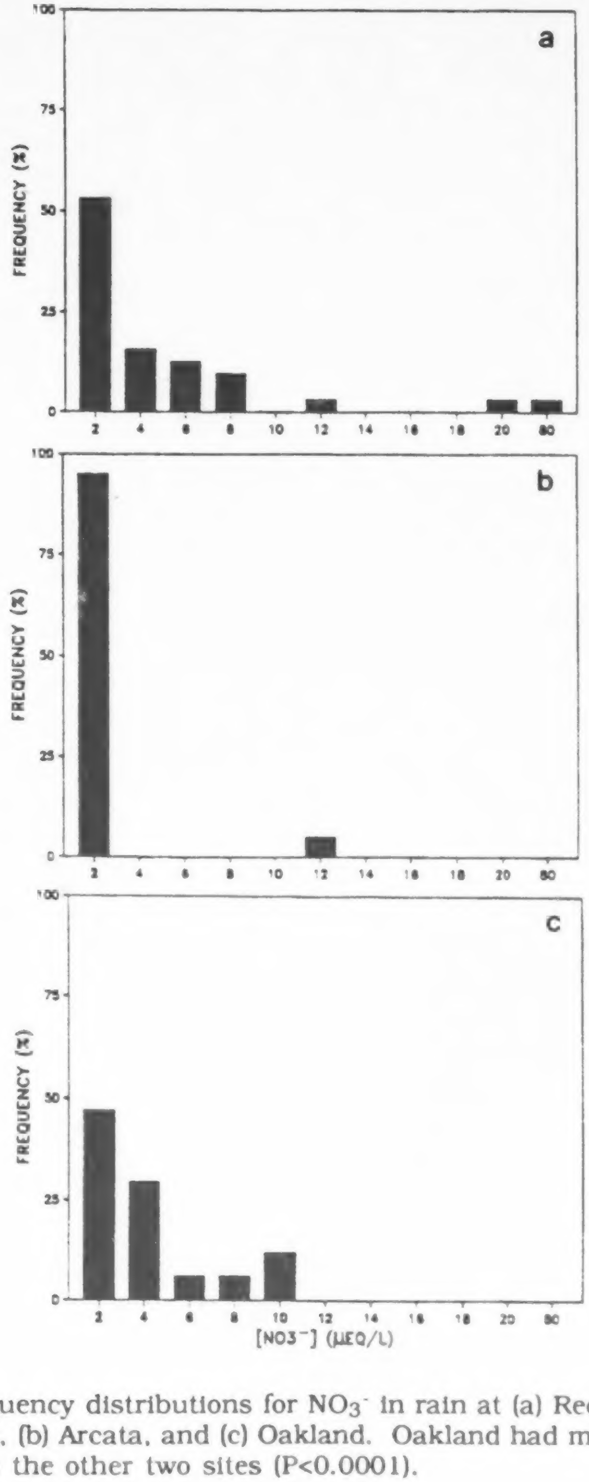

Figure 9. Frequency distributions for NO_3^- in rain at (a) Redwood National Park, (b) Arcata, and (c) Oakland. Oakland had more NO_3^- in rain than the other two sites ($P<0.0001$).

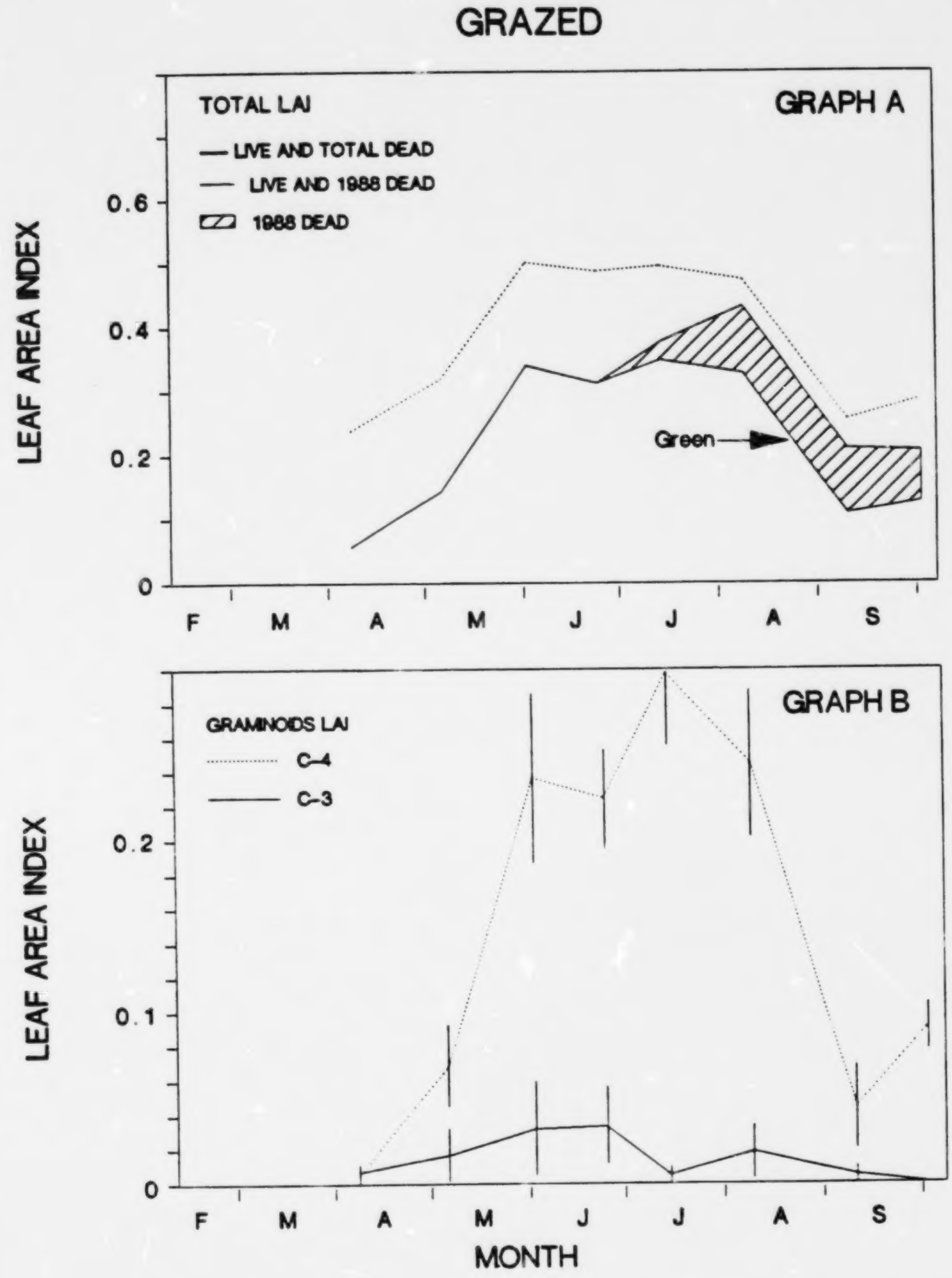

Figure 6. Graph A: Grazed site LAI for: total (live + 1988 dead + previous season's dead); 1988 (live + dead); and 1988 live.
Graph B: Grazed site LAI for live C-3 and C-4 graminoids.

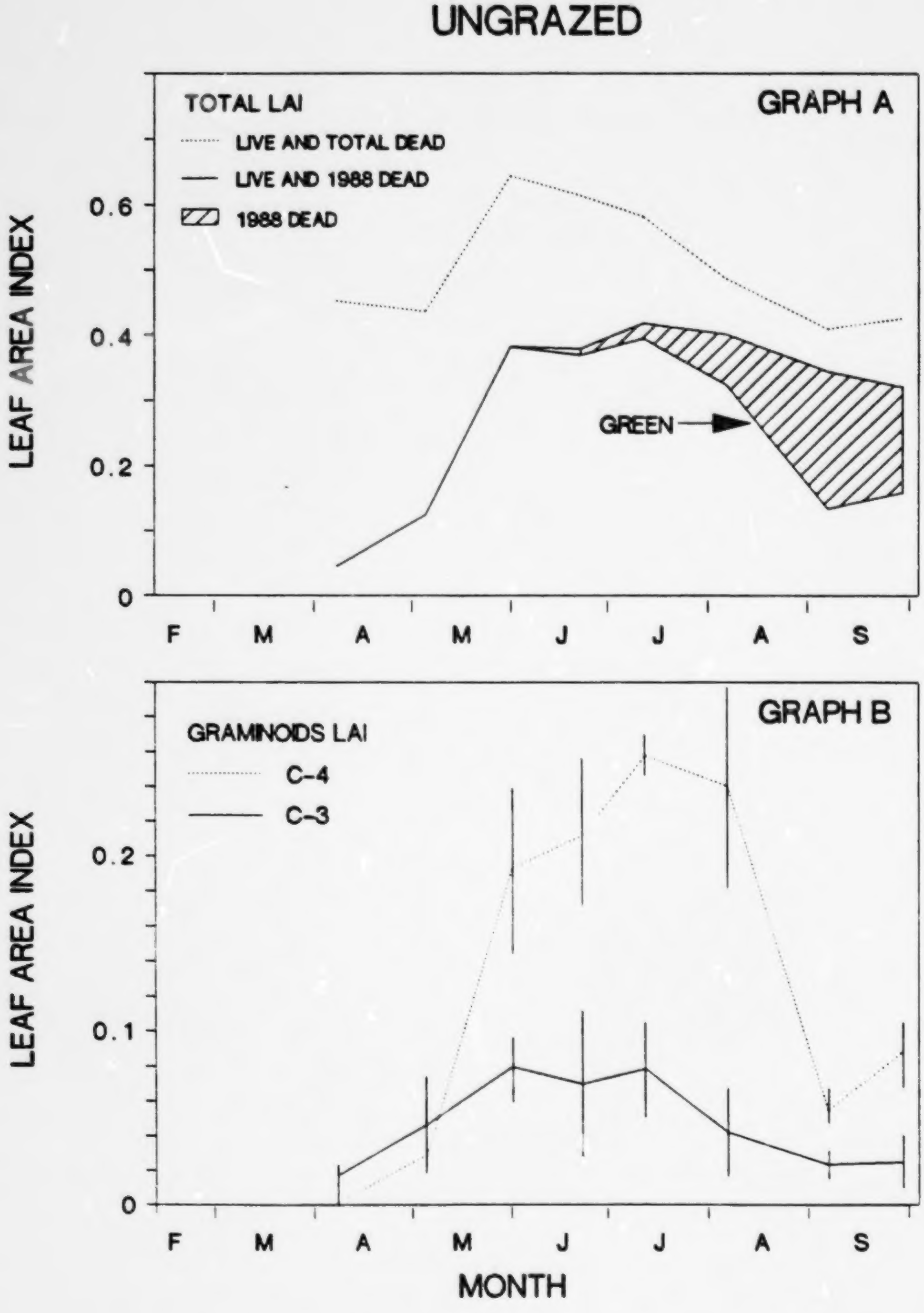

Figure 7. Graph A: Grazed site LAI for: total (live + 1988 dead + previous season's dead); 1988 (live + dead); and 1988 live.
Graph B: Grazed site LAI for live C-3 and C-4 graminoids.

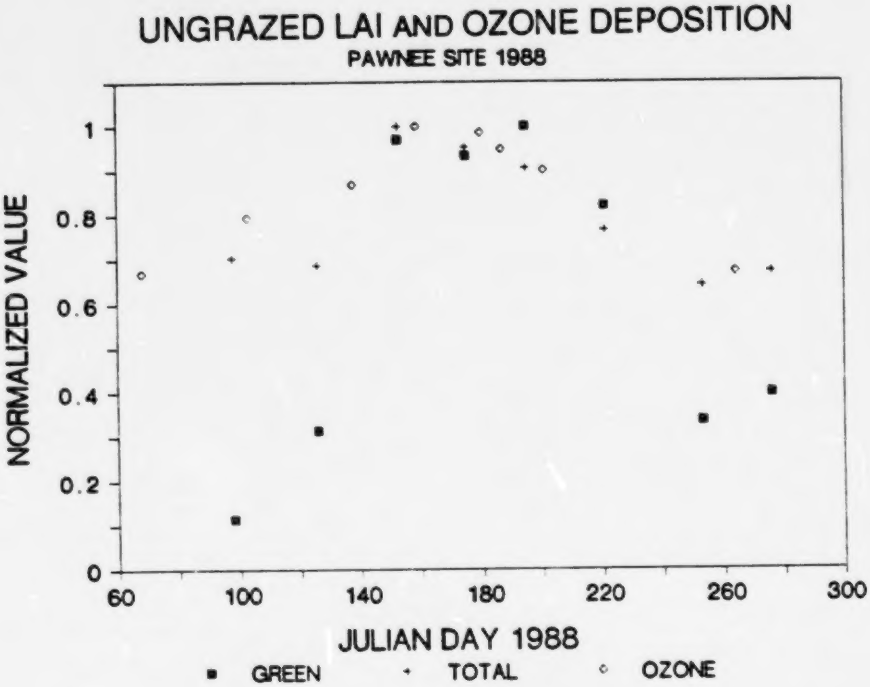

Figure 8. Normalized ungrazed total LAI (green only), normalized ungrazed total LAI (green + all dead) and normalized time integrated ozone deposition versus Julian day. Note ozone deposition is plotted as a positive value for comparison purposes.

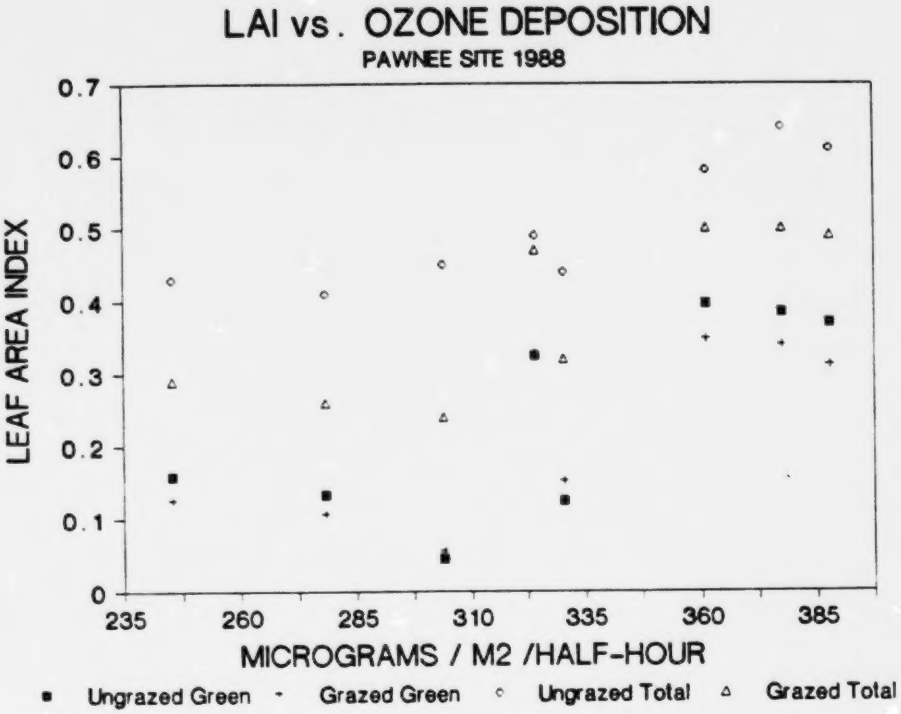

Figure 9. Extrapolated time integrated ozone deposition (plotted as a positive value) versus ungrazed green LAI, grazed green LAI, ungrazed total LAI (green + all dead) and grazed total LAI (green + all dead) for the Pawnee site 1988 growing season.

Air Quality at a High Elevation, Remote Site in Western Canada

Allan H. Legge[1]
Sagar V. Krupa[2]

[1] *Kananaskis Centre for Environmental Research*
University of Calgary
Calgary, Alberta

[2] *Department of Plant Pathology*
University of Minnesota
St. Paul, Minnesota

INTRODUCTION

Certain chemical constituents (e.g., photochemical oxidants) occur naturally in the troposphere, the background air quality. From a mechanistic sense, background air quality is defined as that monitored at remote sites. While there is some question as to whether any location on the earth is truly untouched by human activities in some way, we refer to the atmosphere in such remote areas as natural troposphere.[1] The background concentrations of "trace gases" in this "clean" troposphere are essentially determined by the competitive physical, chemical, and biological processes.[2] The chemistry of the clean troposphere and the mathematical simulation of the relevant physical and chemical processes have been extensively reviewed.[3-11]

A great deal of emphasis is presently being directed to an increased understanding of the characteristics of the "natural troposphere" and evaluating its role in the assessment of the ecological impacts of air pollutant stress.

Within the framework of the Alberta Government-Industry Acidic Deposition Research Program (AG-I-ADRP) in evaluating the present and potential effects of acidic and acidifying air pollutants (sulphur and nitrogen oxides) on selected environmental components within Alberta, a background air quality monitoring station was established at Fortress Mountain, Alberta (Table I, Figure 1), and many quality parameters were quantified and characterized there over a 24-month period (1985–87).

MATERIALS AND METHODS

A summary of the characteristics of the background air quality monitoring station is provided in Table I. Similarly Table II provides a summary of the environmental variables measured and the corresponding methodologies used.[12]

RESULTS AND DISCUSSION

Automated Measurements of Gaseous Air Pollutants

The pollutant concentrations were initially evaluated for their frequency distributions. Such distributions did not fit a "normal" or "log-normal" frequency distribution. They were best described by the distribution functions of the Weibull family.[12]

An example of the Weibull distribution consists of

$$P_x(x) = c\,a^{-1}\{(x-\xi_0)/a\}^{c-1}e^{-[(x-\xi_0)/a]^c} \qquad (\xi_0 < x)$$

where c is the shape, a is the scale, and ξ_0 is the location of the distribution.

At Fortress Mountain >99% of the 10-min mean values of all pollutant concentrations measured by automated methods (with the exception of O_3 and CO_2) were below the minimum detection limit for the appropriate methodology used in each case. Therefore, in the case of primary pollutants (exception of CO_2), a stochastic Weibull probability generator was used to substitute all values below the minimum detection limit with values predicted by the probability generator. The unbias and robustness of the probability generator was tested prior to its application.[12]

Table III provides a comparison of mean hourly pollutant concentrations at Fortress Mountain (1985–87) with values published in the literature for remote and rural locations.[12] The mean hourly concentrations at Fortress Mountain for SO_2, NO_2, and O_3 were below or nearly equal to the concentrations reported for remote sites. The concentrations of other pollutants were within the range reported for rural sites. The relatively high values for H_2S and NO were most likely due to the mathematical artifacts caused by the very high number of observations below the detection limits of the methodologies used (>99% over the two year period), which were substituted by the values derived through the Weibull probability generator. Nevertheless, the Fortress Mountain site may be considered representative of an acceptable background air quality site for Alberta and possibly for northwestern North America.

As opposed to the smoothened pollutant statistics, the range and percentiles of pollutant concentrations, both 10-min and 1-h, varied between the two monitoring years (1985–86 vs. 1986–87). This is to be expected due to the stochasticity and variability in the climatology at any given site between years.

The computation of long-term means also tends to mask the underlying pollutant episodicity. At the Fortress Mountain site, while the hourly mean O_3 concentrations ranged from 40.9 ppb during 1985–86 to 45.8 ppb during 1986-87, corresponding maximum concentrations ranged from 70.9 to 129.4 ppb. These high O_3 concentrations were associated with episodes on two or more consecutive days (Table IV) each time from April 15 to June 30, 1987.[12] Such O_3 episodes were observed on 14 of the 45 days examined. The importance of these types of pollutant episodes in the context of vegetation effects has been previously discussed in detail.[13-15]

Unusually large, site specific O_3 episodes have been previously reported for other high elevation air quality monitoring sites.[16] The occurrence of these episodes have been attributed to stratospheric intrusion; NO_x-NMOC (non-methane organic carbon)-CO chemistry; long-range transport or their combination.[1]

The characteristics of the O_3 episodes at Fortress Mountain were not consistent with the known characteristics of stratospheric intrusion. Five general characteristics of these episodes at Fortress Mountain are:

1. O_3 episodes generally occurred over two or more consecutive days. During these episodes, highest daily maxima occurred both during daylight and nighttime hours. These patterns were not consistent with known characteristics of stratospheric intrusion. Stratospheric intrusions are often characterized by relatively rapid changes in the O_3 concentration with peaks occurring at times not expected from photochemical processes. For example, the data for Zugspitze, West Germany, showed a maximum 1 hour average O_3 concentration of 196 ppb at midnight on January 8, 1975.[17] Such high O_3 concentrations were not observed in the region surrounding Zugspitze on the previous day.

   While O_3 data were not available for the region surrounding Fortress Mountain, the type of phenomenon observed at Zugspitze should result in the modification of the daily O_3 profile. There were no distinct differences in the daily O_3 profile of episode versus nonepisode days at Fortress Mountain.

2. If there was stratospheric intrusion, it should result in some dilution of tropospheric NO and NO_2. This was not the case at Fortress Mountain.

3. Lower stratospheric air is known to be virtually free of moisture. Thus, its intrusion into the troposphere should result in a reduction in the relative humidity. This was not the case at Fortress Mountain when episode and nonepisode days were compared.

4. According to Viezee et al.[18] aircraft measurements of four stratospheric O_3 intrusion events suggest that half of the O_3 mass injected into the upper troposphere by these events is likely mixed and diluted into the troposphere above the 3 km elevation. The Fortress Mountain monitoring site was located at a 2.1 km elevation. Viezee et al. suggested that ground-level elevated concentrations of O_3 due to stratospheric intrusions occur less than 1% of the time. At Fortress Mountain O_3 episodes were observed on 30% of the 45 days examined.

5. At Fortress Mountain the highest O_3 concentrations were observed both in 1986 and 1987 during months with the highest net solar radiation. The decay of water molecules and photochemical scavenging of O_3 were considered to be unimportant in the region due to the lack of any major sources.

Data are available that strongly suggest ground-level impacts of stratospheric intrusion are infrequent and do not generally lead to O_3 concentrations exceeding 100 ppb.[1] Thus, long-range transport of photochemical oxidant precursors from urban areas is well known: for example, long-range transport from western Europe has been postulated to be primarily responsible for some of the elevated ozone concentrations observed in Norway.[19,20] In this context, Liu et al.[21] point out that the photochemical life time expected for O_3 is fairly long (~10 days).

In order to determine whether long-range transport of O_3 and/or its precursors can explain the occurrence of O_3 episodes at Fortress Mountain, air mass trajectory analysis was performed for both episode and nonepisode days based on an isobaric model.[22] Examples of boundary layer air trajectories in 3-h time steps are shown for specific days of high or low O_3 concentrations measured at Fortress Mountain (Figures 1 and 2). All sub-figures are labelled with the ending time of the trajectory at Fortress Mountain, and the average 1-h O_3 concentration for that time. Of the 14 O_3-episode days examined, the trajectories showed a variety of directions and speeds of air movement. Although the trajectories did not indicate that a single unique condition caused high O_3 concentrations, it was possible to suggest source areas for the air mass.

It should be recognized, however, that the trajectories are estimates based upon observed and forecasted wind fields and may contain significant errors, especially during times of rapidly changing flow conditions. Furthermore, they represent the air flow only in the lower layers (lowest 500 m) of the atmosphere. In mountainous regions, as at Fortress, there are likely to be local variations in air flow not accounted for by the large-scale wind analyses. Thus, the trajectories should be interpreted as an estimate of the general direction and speed of air masses arriving at Fortress.

Taken as a group, these results indicated that the high O_3 concentrations at Fortress Mountain were generally associated with air masses from the west and southwest.

Because of the elevation of the Fortress Mountain monitoring site (2103 m MSL), air movement at altitudes above the boundary layer was also considered in the analysis of air mass trajectories. For two cases of high ozone concentrations at Fortress Mountain (May 13, and May 30, 1987, Figure 1) trajectories were calculated from LFM wind data for the 700 millibar level (approximately 3000 m above sea level). These higher altitude trajectories confirmed that general air movement during these periods was from British Columbia and northwestern Washington state to Fortress Mountain.

From the preceding discussion it appeared highly probable that the O_3 episodes at Fortress Mountain were mainly caused by long range transport. Local photochemistry appeared to be unimportant since the 10 min NO_2 concentrations were below the detection limit during >99% of the monitored time and the correlation coefficients (r) between NO_2 : NO versus O_3 were <0.02 independent of the class of O_3 concentrations (<50.0 ppb; 50.1–90.0 ppb or >90.1 ppb) used in the statistical analysis.

Integrated Measurements of Gaseous and Fine Particulate Pollutants

Using a serial annular denuder-filter pack system (KAPS Sampler) 48-h integrated samples of SO_2, HNO_2, HNO_3, NH_3 and fine particle SO_4^{2-} and NO_3^- were collected at Fortress Mountain. These samples were analyzed by the appropriate method described in Table II. A summary statistic of the observed concentrations of the various chemical constituents are presented in Table V. The mean value for the SO_2 concentration measured by the denuder method (2.0 µg/m^3 SO_4^{2-} value converted to SO_2, 1.33 µg/m^3 or 0.51 ppb) was much higher than the mean of the 10-min values (0.16 ppb) reported with the continuous monitoring method (Table III). This was most likely because >99% of the observations were below the minimum detection limit (4 ppb); the continuous monitoring method and the Weibull probability generator most likely did not provide precise enough values to substitute missing values. The mean values of all other pollutants were in the low end of the range for typical ambient concentrations (Table VI). These results substantiate the previous conclusion that the Fortress Mountain site may be considered as a background site for many air pollutants, with the exception of O_3 .

Chemistry of Daily Rain

About April through October in each of the two years, rain samples were collected as 0.32 cm sequentially incremental fractions of each rain event using a refrigerated sampler.[24] The chemical analyses of these samples were conducted according to the procedures described in Table II.

In this paper, only summary statistics on averaged daily (24 h) precipitation chemistry are presented in Table VII. The mean pH of rain at Fortress Mountain (4.73) was quite comparable to the mean values (pH 4.78–4.96) reported in the literature for five remote sites.[25] While the mean SO_4^{2-} concentration at Fortress Mountain (22.8 µeq/l) was comparable to the remote sites (2.9–36.3 µeq/l), the mean NO_3^- concentrations at Fortress Mountain (13.2 µeq/l) were much higher than for the remote sites (1.7–5.5 µeq/l). Nevertheless, the correlation coefficients (r), between H^+ and SO_4^{2-} and H^+ and NO_3^- were very low at Fortress Mountain (0.13 and 0.18 respectively). In this case, higher r values for SO_4^{2-} were obtained with K^+ (0.73), Mg^{2+} (0.69), Ca^{2+} (0.63), and NH_4^+ (0.58). Similarly higher r values for NO_3^- were obtained with NH_4^+ (0.68), K^+ (0.64), Mg^{2+} (0.61), and Ca^{2+} (0.50). These results suggest that a major portion of rain SO_4^{2-} and NO_3^- at Fortress Mountain was not associated with free acidity, and the rain chemistry at that site was governed by well aged air masses. These conclusions were substantiated by additional statistical analysis, Principal Component Analysis.

Based on the results obtained with cation-anion balance, it appeared highly probable that the free acidity of rain at the Fortress Mountain site was most likely due to H^+ associated with anions not quantified in the present study (e.g., organic acids). Based on measurements and indirect calculations, organic acids may contribute 16–35% or more of the free acidity in precipitation of North America.[26,27]

CONCLUSIONS

Mean concentrations of several pollutants (SO_2, NO, and NO_2) measured at the Fortress Mountain, Alberta site were representative of true present day other remote and/or rural sites. Mean O_3 concentration was also within this range. However, hourly O_3 concentrations exceeded the Alberta Air Quality Objective (1-h concentration of 0.08 ppm) over 250 hours during the spring and early summer of 1987. Given the remote location of Fortress Mountain, the occurrence of these high O_3 concentrations and their characteristics were examined for their basis. While stratospheric intrusion and local photochemistry were considered, it was concluded that the O_3 episodes were due to long-range transport. The environmental impacts of these O_3 episodes are yet to be evaluated. Relative to welfare effects, plant species are considered to be most sensitive to O_3. Thus, the episodic peak concentrations of O_3 and their impacts on high elevation plant communities are of some concern.

The mean concentrations of HNO_2, HNO_3, SO_4^{2-} and NO_3^- measured at Fortress Mountain were at the lower end of the scale of known mean concentrations of such pollutants. Similarly, while the mean pH of rain at Fortress Mountain was 4.73, neither SO_4^{2-} nor NO_3^- correlated well with the free acidity. The H^+ appeared to be associated with molecular species such as the organic acids.

In the final analysis, because detailed resolution of data on many air pollutants are available for Fortress Mountain, such information can be used to understand air pollutant exposure dynamics at a background site and ecosystem behavior. With the exception of episodic O_3, Fortress Mountain can be considered as a true background site.

ACKNOWLEDGMENTS

The research described in this paper was part of a much larger effort sponsored by the Alberta Government-Industry Acidic Deposition Research Program. The authors would like to convey their deepest appreciation to the Program Members Committee for initiating and supporting the effort. Appreciation is also conveyed to many colleagues who participated in the research work, in particular Eric Peake, Mel Strosher, George McVehil, Miloslav Nosal, and Martin Hansen.

REFERENCES

1. B.J. Finlayson-Pitts and J.N. Pitts, *Atmospheric Chemistry: Fundamentals and Experimental Techniques*, John Wiley and Sons, New York, 1986, p. 1098.

2. K.L. Demerjian, "Atmospheric chemistry of ozone and nitrogen oxides," in *Air Pollutants and Their Effects on the Terrestrial Ecosystem*, A.H. Legge and S.V. Krupa, Eds., John Wiley and Sons, New York, 1986, p. 105.

3. W.L. Chameides and J.C. Walker, "A photochemical theory of tropospheric ozone," *J. Geophys. Res.* 78:8751 (1973).

4. W.L. Chameides and J.C. Walker, "A time-dependent photochemical model for ozone near the ground," *J. Geophys. Res.* 81:413 (1976).

5. P.J. Crutzen, "Photochemical reactions by and influencing ozone in the troposphere," *Tellus* 26:47 (1974).

6. J. Fishman and P.J. Crutzen, "A numerical study of tropospheric photochemistry using a one-dimensional model," *J. Geophys. Res.* 82:5897 (1977).

7. H. Levy, II, "Normal atmosphere: Large radical and formaldehyde concentrations predicted," *Science* 173:141 (1971).

8. J.A. Logan, "Nitrogen oxides in the troposphere: Global and regional budgets," *J. Geophys. Res.* 88:10,785 (1983).

9. J.A. Logan, M.J. Prather, S.C. Wofsy, and M.B. McElroy, "Tropospheric chemistry: A global perspective," *J. Geophys. Res.* 86:7210 (1981).

10. D.H. Stedman and R.E. Shetter, "The global budget of atmospheric nitrogen species," *Adv. Environ. Sci. Tech.* 12:411 (1983).

11. R.W. Stewart, S. Hameed, and J.P. Pinto, "Photochemistry of tropospheric ozone," *J. Geophys. Res.* 82:3134 (1977).

12. A.H. Legge and S.V. Krupa (Eds.), "Acidic Deposition: Oxides of Sulphur and Nitrogen," Lewis Publishers Inc. Chelsea, Michigan (In press), 1989.

13. S. Krupa and R.N. Kickert, "An analysis of numerical models of air pollutant exposure and vegetation response," *Environ. Pollut.* 44:127 (1987).

14. A.S. Lefohn and V.C. Runeckles, "Establishing standards to protect vegetation—Ozone exposure/dose considerations," *Atmos. Environ.* 21:561 (1987).

15. W.E. Hogsett, D.T. Tingey and E.H. Lee, "Ozone exposure indices: Concepts for development and evaluation of their use," in *Assessment of crop loss from air pollutants*, W.W. Heck, O.C. Taylor, and D.T. Tingey, Eds., Elsevier Applied Science, London, 1988, p. 552.

16. U.S. Environmental Protection Agency, Air Quality Criteria for Ozone and Other Photochemical Oxidants, Volume II, Research Triangle Park, NC: U.S. Environmental Protection Agency, Environmental Criteria and Assessment Office, EPA Report No. EPA-600/8-84-020, 1984.

17. H.B. Singh, F.L. Ludwig, and W.B. Johnson, "Tropospheric ozone: Concentrations and variabilities in clean remote atmospheres," *Atmos. Environ.* 12:2185 (1978).

18. W. Viezee, W.B. Johnson, and H.B. Singh, "Stratospheric ozone in the lower troposphere-II, Assessment of downwind flux and ground-level impact," *Atmos. Environ.* 17:1979 (1983).

19. J. Schjoldager, B. Sivertsen, and J.E. Hanssen, "On the occurrence of photochemical oxidants at high latitudes," *Atmos. Environ.* 12:2461 (1978).

20. J. Schjoldager, "Ambient ozone measurements in Norway, 1975–1979," *JAPCA* 31:1187 (1981).

21. S.C. Liu, D. Kley, M. McFarland, J.D. Mahlman, and H. Levy II, "On the origin of tropospheric ozone," *J. Geophys. Res.* 85(C12):7546 (1980).

22. J.L. Heffter, Air resources laboratory's atmospheric transport and dispersion model (ARL-ATDM), NOAA Tech. Memo. ERL-81, 1980.

23. M.R. Coscio, G.C. Pratt, and S.V. Krupa, "An automated refrigerated, sequential precipitation sampler," *Atmos. Environ.* 16:1939 (1982).

24. J.N. Galloway, G.E. Likens, W.C. Keene, and J.M. Miller, "The composition of precipitation in remote areas of the world," *J. Geophys. Res.* 87:8771 (1982).

25. W.C. Keene and J.N. Galloway, "Organic acidity in precipitation of North America," *Atmos. Environ.* 18:2491 (1984).

26. S.V. Krupa, J.P. Lodge, Jr., M. Nosal, and G.E. McVehil, "Characteristics of aerosol and rain chemistry in North Central U.S.A.," in *Acidic Rain: Scientific and Technical Advances*, R. Perry, R.M. Harrison, J.N.B. Bell, and J.N. Lester, Eds., Selper Ltd., London, 1987, p. 121.

27. R.K. Stevens, Review of methods to measure chemical species that contribute to acid dry deposition, in *Proceedings: Methods for Acidic Deposition Measurement*, EPA Report 600/9-86/014, 1986, p. 10.

Table I. Description of the sampling site at Fortress Mountain, Alberta.

Site Name:	Fortress Mountain
Coordinates:	50°49'40" 115°12'20"
Elevation:	2103 m MSL
Site Description:	
a) Location:	The monitoring site is located on the northernmost edge of a ridge at the treeline, paralleling the Kananaskis River valley, which has a southwest to northeast orientation.
b) Access:	Access to the Fortress site from Calgary is via the TransCanada Highway west, and south on Highway 40 to the Fortress Junction.
c) Topography:	Elevation of the valley floor, ridge, and mountain peaks of the surrounding area are approximately 1200, 2100, and 3000 m, respectively.
d) Vegetation:	The monitoring site lies within the subalpine and alpine ecoregions. The vegetation in this area is sparse. The more common vegetation components of the two ecoregions consist of lodgepole pine (secondary succession by Engelman spruce) within the sub-alpine region and low growing shrubs, fescue grass, and Phyllodoce communities, within the alpine region.
e) Sources:	Summer: human activity is low, mainly hiking and camping. Winter: human activity is much higher due to the large number of skiers.
f) Snowfall:	x 263.7 mm ± 97.2 mm/y
g) Rainfall:	x 319.3 mm ± 85.3 mm/y
h) Soil:	Brunisolic soils are most abundant in this region. In some areas, soils are poorly developed due to harsh alpine environment.
i) Emissions:	Total NO_x and SO_2 emissions within these two ecoregions are 2.6 and 4.2 t/d, respectively. Percentage of the total area of Alberta occupied by these two ecoregions is 6.3%.

Table II. Summary of air quality and meteorology measurement methodology.

Measurement Category and Parameter	Measurement Method	Time Period of Data Resolution
1. Gases		
a) Near Continuous		
H_2S	Flame photometry	2 min.
SO_2	Flame photometry	2 min.
NO_x (NO, NO_2)	Chemiluminescence	2 min.
O_3	UV photometry	2 min.
CO_2	IR absorption	2 min.
b) Instantaneous		
COS	Gas chromatography*	
CS_2	Gas chromatography	
H_2S	Gas chromatography	
SO_2	Gas chromatography	
c) Integrated		
SO_2	Annular denuder + IC**	24 h or 48 h
HNO_3 (vapour)	Annular denuder + IC	24 h or 48 h
HNO_2 (vapour)	Annular denuder + IC	24 h or 48 h
NH_3	Annular denuder + colorimetry	24 h or 48 h
NMHC[a]	Gas chromatography*	1 h
2. Particulate Matter (Integrated)		
SO_4^{2-}	Annular denuder/filter + IC	24 h or 48 h
NO_3^-	Annular denuder/filter + IC	24 h or 48 h
NH_4^+	Annular denuder/filter + colorimetry	24 h or 48 h
Cations (24 ions)	Dichot filter + XRF**	48 h or 96 h
3. Precipitation (rain only) [SO_4^{2-}, NO_3^-, Cl^-, Ca^{2+}, Mg^{2+}, Na^+, K^+, NH_4^+, H^+]	Automated, refrigerated sequential sampler + IC + AA + colorimetry	32 mm sequential, samples of individual rain events
4. Meteorology (10 m) (Surface)		
Wind direction	Wind vane	2 min.
Wind speed	Anemometer	2 min.
Air temperature	Thermistors	2 min.
Dew Point	Dew cell	2 min.
Barometric pressure	Analog output barometer	2 min.
Radiation	Pyrradiometer	2 min.
Rain	Tipping bucket	–

* Identity of individual substances was confirmed by mass spectrometry.

** IC = Ion chromatography; XRF = x-ray fluorescence spectroscopy; AA = Atomic absorption spectroscopy.

[a] Non-methane hydrocarbons.

Table III. A comparison of mean hourly pollutant concentrations at Fortress Mountain (1985-87) with values published in the literature for remote and rural locations. All concentrations in ppb.

Pollutant	Remote Locations	Fortress Mountain	Rural Locations
SO_2	< 1.0	0.16	1.0-30
H_2S	0.05 - 0.10	0.55	-
NO	< 0.05	0.52	0.05 -20
NO_2	< 1.0	1.2	1.0-20
O_3	< 50	43	20-80
CO_2	346*	346*	-

Typical range of concentrations at Fortress Mountain were: SO_2 0.00–14.8; H_2S 0.10–0.57; NO 0.00–7.2; NO_2 0.10–13.0; O_3 2.8–122.4; CO_2 312–381.*

* ppm

For details and literature regarding the pollutant concentrations in remote and rural locations, the reader is referred to Legge and Krupa.[12]

Table IV. Characteristics of representative O_3 episode versus non-episode days at Fortress Mountain, 1987.

Episode			Nonepisode		
Date	Highest x Hourly O_3 (ppb)	Hour	Date	Highest x Hourly O_3 (ppb)	Hour
Apr 24	93.5	1800	Apr 23	66.5	0300
Apr 25	89.3	0100	Apr 28	68.1	1300
Apr 26	86.8	1200	Apr 29	63.5	2400
May 12	105.8	2400	May 05	81.1	2400
May 13	122.4	0100	May 10	72.6	0100
May 25	113.4	2200	May 21	63.2	0400
May 26	101.1	0100	Jun 04	67.6	1500
May 27	108.3	1200	Jun 08	69.7	0200
May 28	107.6	2000	Jun 09	49.2	2400
May 29	107.3	1000	Jun 11	56.4	2400
May 30	110.3	0400	Jun 13	66.0	1700
May 31	100.3	1100	Jun 16	68.8	1400
Jun 06	102.7	0800	Jun 22	52.8	0100
Jun 07	91.4	0100	Jun 30	53.3	0700

Table V. Summary statistics of integrated (annular denuder - filter pack) 48-hr measurements of gaseous and fine particulate pollutants at Fortress Mountain during 1985-87.

		Concentration µg/m^3					
Pollutant	(n)	Mean	S.D.	Median	70%	99%	Range
HNO_2	137	0.05	0.06	0.03	0.05	0.44	0.005–0.46
HNO_3	154	0.31	0.32	0.25	0.33	2.30	0.0005–3.50
SO_2	154	1.33	2.61	0.50	1.09	18.30	0.0003–18.30
NH_3	154	0.26	0.15	0.26	0.32	0.91	0.04–1.30
NO_3^-	149	0.13	0.09	0.11	0.14	0.59	0.02 –0.66
SO_4^{2-}	146	0.51	0.37	0.45	0.66	1.90	0.05 –2.00

Table VI. Typical ambient concentrations of chemical species related to acidic dry deposition.[23]

Pollutant	Range of Concentrations (mg/m^3)
SO_2	0.20–30
HNO_2	0.20–2.0
HNO_3	0.10–15
NH_3	0.10–20
NO_3^- (fine particle)	0.10–10
SO_4^{2-} (fine particle)	0.20–40

Table VII. Summary statistics of daily precipitation chemistry at Fortress Mountain. Sampling period: approximately April-October, 1986 and 1987. Ion concentrations in µeq/L.

							Range	
Ion	(n)	Mean	S.D.	Median	75%	95%	Min.	Max.
H^+	50	18.4	15.8	17.0	28.3	54.7	.09	72.4
Cl^-	37	3.7	2.4	2.8	5.1	9.5	1.00	10.3
NO_3^-	52	13.2	7.8	10.8	15.8	30.6	3.3	42.4
SO_4^{2-}	52	22.8	14.1	19.0	30.2	54.3	5.6	63.3
Ca^{2+}	40	30.4	24.7	22.3	39.1	90.6	2.2	100.2
Mg^{2+}	40	6.1	6.2	4.1	9.6	22.3	1.1	26.5
Na^+	40	4.6	6.3	2.1	4.8	23.9	1.3	23.4
K^+	31	1.4	1.4	.90	2.0	5.0	.28	6.8
NH_4^+	45	20.3	14.1	17.4	29.2	47.2	1.6	49.5

Median pH 4.77; Mean pH 4.73 and this value should be viewed with caution since it was derived from non-normally distributed data.

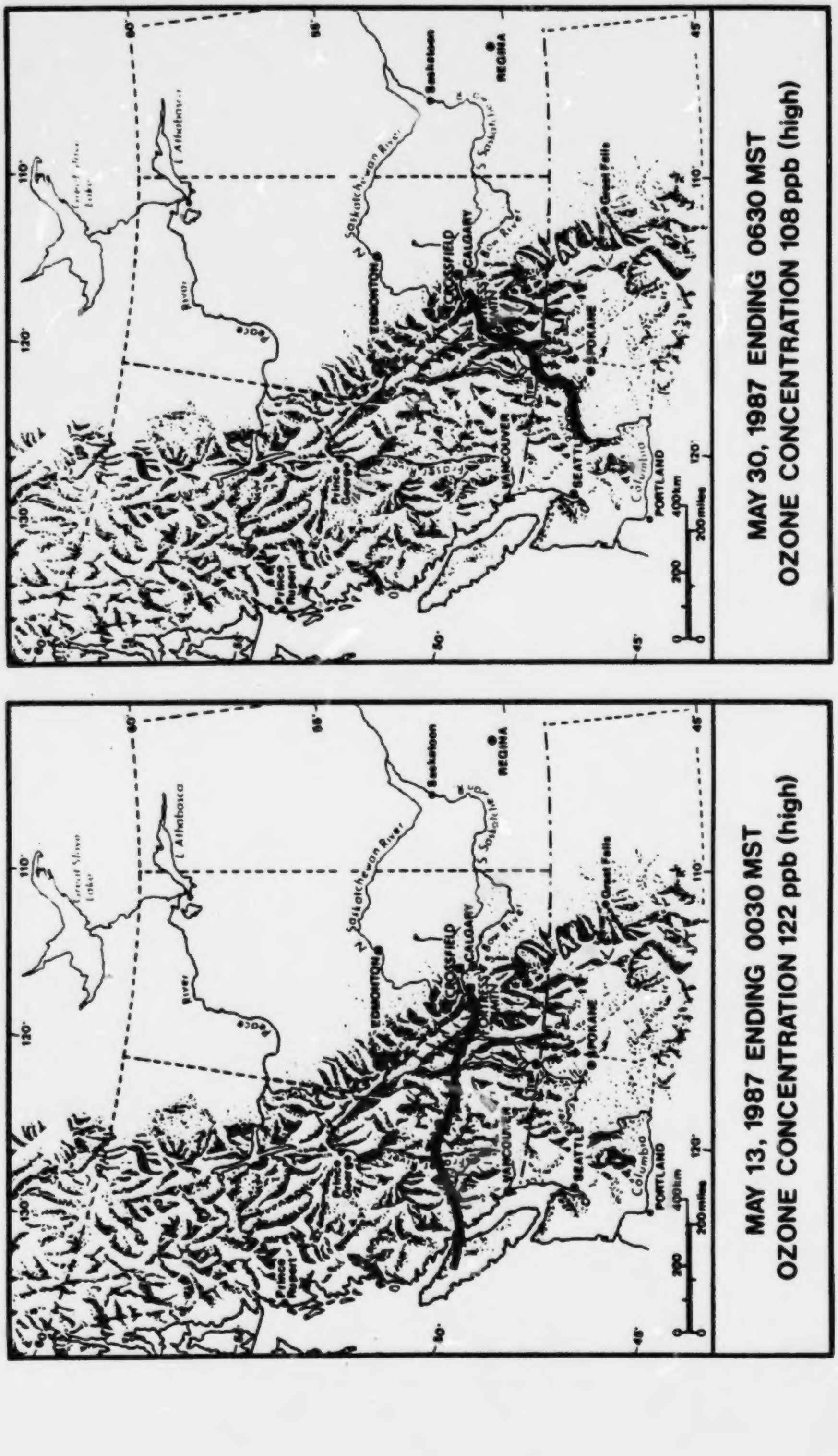
MAY 13, 1987 ENDING 0030 MST
OZONE CONCENTRATION 122 ppb (high)

MAY 30, 1987 ENDING 0630 MST
OZONE CONCENTRATION 108 ppb (high)

60°
55°
50°
45°
130°
120°
110°
Great Slave Lake
L Athabasca
Peace
River
N Saskatchewan River
S Saskatchewan River
Bow River
EDMONTON
CROSSFIELD
CALGARY
Saskatoon
REGINA
Prince Rupert
Prince George
VANCOUVER
SEATTLE
PORTLAND
SPOKANE
Great Falls
Columbia
400km
200miles
200

Figure 1. Trajectories for the air masses arriving at Fortress Mountain on two days with high O_3 concentrations. The individual arrows represent 3-h steps in travel time of the air masses.

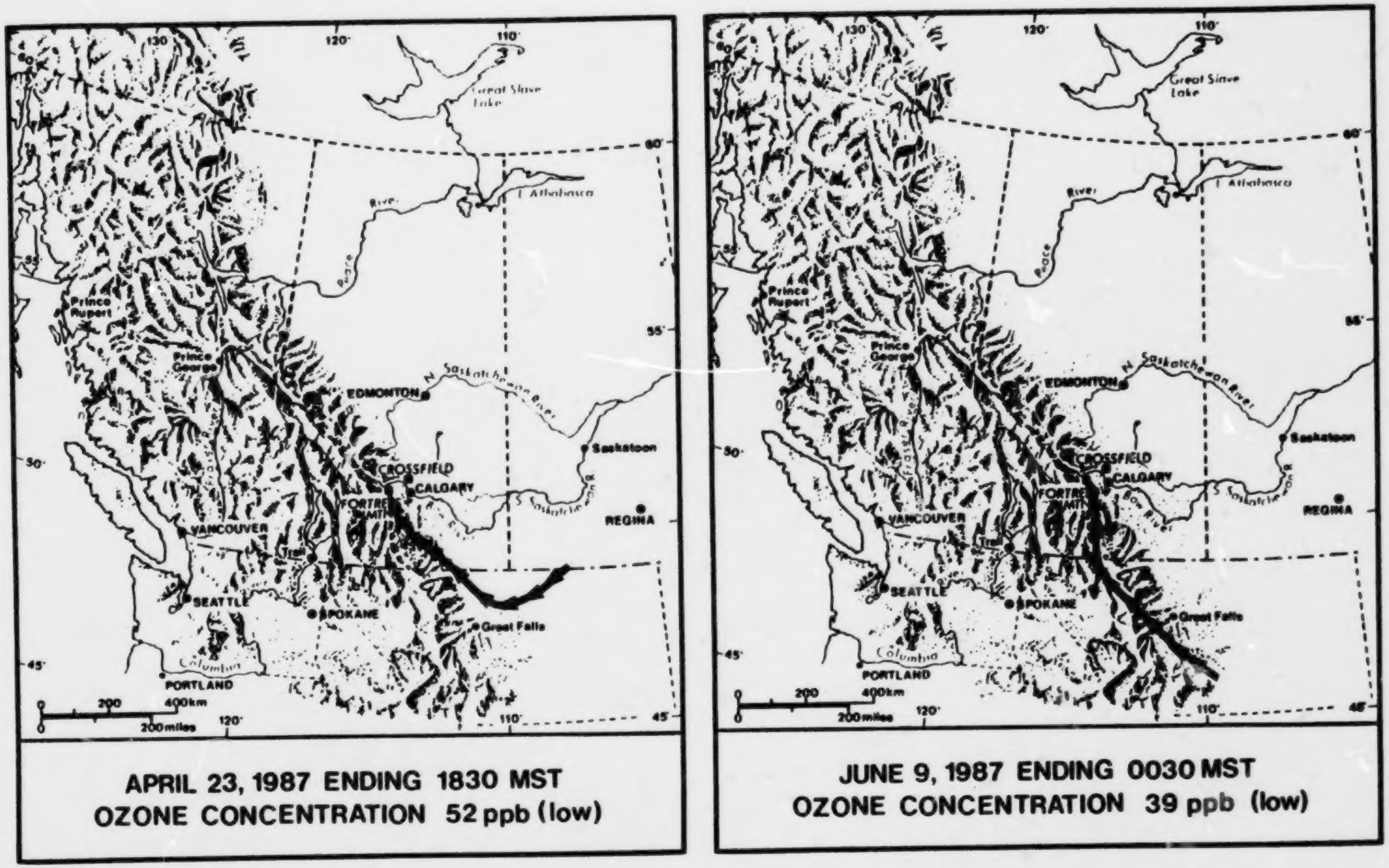

APRIL 23, 1987 ENDING 1830 MST
OZONE CONCENTRATION 52 ppb (low)

JUNE 9, 1987 ENDING 0030 MST
OZONE CONCENTRATION 39 ppb (low)

130°
120°
110°
60°
55°
50°
45°
Great Slave Lake
L. Athabasca
Peace River
Prince Rupert
Prince George
EDMONTON
N. Saskatchewan River
Saskatoon
CROSSFIELD
CALGARY
FORTRESS
S. Saskatchewan
REGINA
VANCOUVER
SEATTLE
SPOKANE
Great Falls
Columbia
PORTLAND
200
400km
200miles

Figure 2. Trajectories for the air masses arriving at Fortress Mountain on two days with low O_3 concentrations. The individual arrows represent 3-h steps in travel time of the air masses.

Ozone at a Remote, High-Altitude Site in Sequoia National Park, California

Brian S. Pedersen[1]
Thomas A. Cahill[2]

[1] *Department of General Science*
Oregon State University
Corvallis, OR 97331

[2] *Crocker Laboratory*
University of California
Davis, CA 95616

INTRODUCTION

Sequoia National Park, located in the Sierra Nevada mountains east of California's San Joaquin Valley, is significantly impacted by ozone. Ozone concentrations measured at two sites in the park regularly exceed California's 0.09 ppm ozone standard. A National Park Service study found visible foliar ozone injury on 39% of the ponderosa and Jeffrey pines in Sequoia and neighboring Kings Canyon National Parks.[1]

This paper describes ozone concentration measurements made near Emerald Lake, Sequoia National Park, during summer, 1987. The monitoring site, located approximately 1 km north of the lake at an elevation of 2740 m, is in a designated wilderness area. A solar-powered ozone monitor was operated nearly continuously at the site between July 27 and September 24. The Emerald Lake ozone results are compared to ozone measurements from Lower Kaweah, Ash Mountain, and Visalia (Figure 1). Lower Kaweah (1920 m elevation) and Ash Mountain (610 m) are both located in the same river drainage as the Emerald Lake site. Visalia (100 m) is an urban site located in the San Joaquin Valley approximately 70 km WSW of Emerald lake. The ozone monitors at these three sites are operated under standard U.S. Environmental Protection Agency protocols.[2,3]

Because of difficulties associated with operating at a remote, high-altitude site, there is substantial uncertainty associated with the absolute ozone concentrations measured. The relative ozone concentrations, however, provide information on the transport of ozone to Emerald Lake. The factors that contributed to the uncertainty are detailed below, following a description of the ozone monitoring instrumentation.

METHODS

Instrumentation

The location of the monitoring site imposed significant constraints on our choice of ozone monitor and associated instrumentation. No power was available at the site. Site access was by trail or helicopter only, and helicopter operation was limited to before and after the summer visitor season. Further, the equipment had to have only a minimal visual impact on the landscape. Consequently, it was not possible to employ standard ozone monitoring instrumentation and protocols.

We chose an ozone monitor designed for industrial hygiene applications. This CSI 2000 chemiluminescent-type monitor is portable (10 kg), uses 12 VDC electricity, and has been designated by the U.S. Environmental Protection Agency as an ozone reference method.[4] The monitor requires only 10% of the power of UV photometric-type monitors (comparison based on Dasibi model 1003AH), and unlike conventional UV photometric-type monitors, is designed to operate over a wide-range of temperatures (10–40° C). The CSI monitor does require a supply of reaction gas. However, a Q-size gas cylinder (40 kg) is sufficient for approximately 3 months of continuous monitoring.

Power was provided by four photovoltaic panels (ARCO, M75) with a combined area and peak output of 1.6 m^2 and 188 W. A regulator (Bobier Electronics, Sunselector Junior) controlled the charging of four deep discharge-type batteries rated at 105 amp-hours each (GNB, ST154). This system provided power for the ozone monitor, data logger, meteorological instruments, and other air pollution instrumentation. A much smaller system would be capable of powering the ozone monitor and related equipment alone. A data logger (Omnidata International, Easylogger) recorded the ozone concentrations and the ozone monitor's sample air flow rate, internal fault indicator, cabinet temperature, and the supply voltage from the solar power system. This logger also supported the meteorological instruments and other samplers. Data were stored on EPROM packs that were replaced weekly by a field technician, mailed back to the laboratory; and the data downloaded to a microcomputer. The operation of the ozone monitor, data logger, and other equipment was checked thoroughly by the technician at least once per week.

The monitoring site was an open, rocky bench in a glacial valley with widely scattered small trees and shrubs. The ozone monitor intake was located 1.5 m above the ground.

Calibration

The ozone monitor was calibrated in Sacramento, CA, by California Air Resources Board (CARB) technicians with a transfer ozone standard before and after operation of the monitor at Emerald Lake. These calibrations included comparisons at local atmospheric pressure (15 m elevation), as well as low pressure comparisons using a simple high-altitude simulation system. This system (Figure 2) was designed so the ozone monitor would experience reduced pressure at its intake and exhaust ports. A valve between the ozone source and monitor reduced the pressure at the monitor's inlet, and a pump regulated by a vacuum regulator (Conoflow) maintained reduced pressure at the monitor's outlet. The vacuum regulator manufacturer claims control to within a pressure of 0.5 cm water. Calibrated gauges indicated the pressure at the inlet and outlet. By iteratively adjusting the valve and vacuum regulator, we could obtain the same pressure at both ports and simulate any altitude's pressure. As a check on the performance of the high-altitude simulation system, the monitor was operated next to the ozone monitor at Lower Kaweah for 38 h after the monitoring at Emerald Lake was completed. The Lower Kaweah ozone monitor is calibrated regularly by the CARB. Because the ozone monitor was subjected to a wide range of temperatures, we also performed an experiment to test the manufacturer's claim of temperature insensitivity.

The above evaluations revealed three major problems with the ozone monitor's calibration. First, a substantial drift in the monitor's span occurred between calibrations by the CARB (span is the slope of the linear function relating the ozone monitor's voltage output to ppm ozone). Second, our simple high-altitude simulation did not properly simulate reduced atmospheric pressure.

And third, the monitor was found to be more sensitive to temperature than expected.

The monitor's zero point drifted only a negligible amount between calibrations; it never differed from zero by more than 0.001-ppm ozone (Figure 3). The CSI monitor had a very linear response to ozone during all CARB calibrations, $r^2 > 0.999$ (two zero and three span points per calibration). The coefficient of determination between the co-located CSI monitor and Lower Kaweah monitor was $r^2 = 0.72$ (38 pairs of hourly mean measurements; 0.033–0.075-ppm ozone concentration range).

The middle three lines in Figure 3 are results for calibrations at Sacramento pressure. The line marked "pre-calibration" is the result from the CARB calibration prior to operation at Emerald Lake; the two lines marked "post-calibration" are the results from calibrations after monitoring had concluded. Immediately prior to the pre-calibration, a new intake filter was installed at the ozone monitor's inlet, and the filter was treated with an airstream with a high ozone concentration. The purpose of this treatment is to allow ozone to react with any reactive material in the new filter. The first post-calibration was made with the filter that had been used during the entire monitoring period at Emerald Lake; the second post-calibration was made with a new, treated filter. As shown in the figure, a 70% span change occurred between the pre-calibration (span = 0.17 ppm/V) and post-calibration (span = 0.29 ppm/V) with the same filter. Once the filter was replaced and treated (span = 0.18 ppm/V), the difference was negligible. This strongly suggests that the cause of the span change was a dirty intake filter. A dirty filter acts as an ozone "scrubber," decreasing the sensitivity of the monitor and causing an underestimation of ozone concentration. We did not change this filter in the field because it is necessary to treat a new filter with ozone and no ozone source was available on site. (An experiment showed that a new untreated filter gave the same results as a used one so changing the filter without ozone treatment is not sufficient to prevent ozone scrubbing.)

The results of the monitor's internal span test does not contradict the hypothesis that the intake filter was responsible for the span change. This test could indicate if a span change occurred due to a problem within the monitor. The span test is performed by stopping the sample pump and turning on a constant-output light source within the reaction chamber. This check was performed at least weekly while the monitor was operating at Emerald Lake, during the course of the calibrations in Sacramento, and during the comparison at the Lower Kaweah site. The changes in the test results over time were not sufficient to account for the difference in pre- and post-calibrations: the range of span values was 16% of the mean value.

The span test data also provide information on how well the monitor survived being transported to and from the Emerald Lake site. The pre- and post-calibration results do not necessarily indicate how the monitor functioned at Emerald Lake because changes may have occurred during transportation of the monitor. Our only means of assessing whether any span changes occurred is from the monitor's span test. The small changes measured suggest, but do not prove, that the ozone monitor's performance at Emerald Lake was not substantially different than during the Sacramento calibrations.

Figure 3 shows the results of the comparison between the CSI monitor and the ozone monitor at Lower Kaweah (bottom line), as well as a calibration performed at Sacramento using the high-altitude simulation system adjusted for Lower Kaweah's pressure (top line). Both tests were made after monitoring at Emerald Lake was completed and with the used intake filter. The simulation system did not properly simulate high-altitude: the span measured with the simulation system (0.58 ppm/V) differed substantially from that determined at Lower Kaweah (0.13 ppm/V). When operating with the high-altitude simulation system, the monitor was much less sensitive to ozone than at Lower Kaweah. This suggests that air was entering the ozone monitor through internal leaks during calibrations with the high-altitude simulation system because the monitor's internal plumbing was placed under partial vacuum by the high-altitude simulation system. High-altitude calibrations with this monitor must be performed either at high altitude or using a vacuum chamber large enough to hold the entire monitor.

Without a high-altitude calibration, the only method to determine the monitor's calibration at Emerald Lake's elevation is to extrapolate from the calibrations at Sacramento and Lower Kaweah. One line was fit to logarithmically transformed span data from the CARB post-calibration (used filter) and the Lower Kaweah comparison (two data points). Assuming that span is a logarithmic function of elevation is equivalent to assuming it is a linear function of atmospheric pressure. A line with the same slope was fit through the logarithmically transformed span data point obtained during the CARB pre-calibration (new, treated intake filter). Both lines were extrapolated to Emerald Lake's elevation to give a span range corresponding to the pre- and post-calibration results: 0.06–0.10 ppm/V.

Ozone monitor cabinet temperatures ranged between 18 and 42° C over the course of the operating period at Emerald Lake. Above 40° C, the monitor automatically shuts off. This occurred initially for a few hours each day until a thermostatically controlled fan was installed in the monitor's cabinet to provide cooling. Even with the fan, however, diurnal temperature swings of 15° C occurred. Because we were concerned about the validity of the monitor manufacturer's claim of only limited span change with temperature, we tested the temperature response in the laboratory. The monitor was placed in a cabinet in which we could adjust the temperature and connected to a constant ozone source monitored by another, calibrated ozone monitor. The results showed a 19% span change between 26 and 40° C (several hours were allowed for the monitor to equilibrate at each temperature). This contrasts with the 8% change claimed by the manufacturer for this temperature change. Furthermore, this test indicated a hysteretic effect that prevents us from simply correcting ozone readings based on the measured monitor cabinet temperature.

The temperature effect on the monitor's calibration requires that the span range be increased to 0.05–0.10 ppm/V. This is the range applied to the Emerald Lake data presented below. This range may not completely encompass the variations in span that occurred, however, and the results presented below should be viewed with caution.

RESULTS

The ozone monitor operated continuously except for midday hours during much of August when the ozone monitor cabinet temperature exceeded 40° C and during a 5-day period in September (8/16–21) because of an operator error.

The peak ozone concentration measured at Emerald Lake during the summer was 0.03-0.06 ppm; the minimum was 0.005-0.01 ppm. Ozone concentrations for the four sites are summarized in Table I. Twenty-four-hour mean ozone concentrations were highest at Ash Mountain, followed by Lower Kaweah, Visalia, and Emerald Lake. The mean concentration for Emerald Lake, 0.017-0.033 ppm, is biased low because most missing data occurred during afternoons when concentrations were likely to be higher than average. The number of hours during which the California ozone standard was exceeded at each site followed the same order as mean ozone concentrations; no exceedance hours were observed at Emerald Lake.

The Emerald Lake ozone data provide no indication that a drift in span associated with a buildup of contamination on the intake filter had occurred during the summer. A linear least-squares line fit to 24-h mean ozone concentrations from Emerald Lake, Lower Kaweah, and Ash Mountain indicated a slight declining trend in ozone concentrations over the course of the summer at all three sites. However, the decline at Emerald Lake was less than at the other two sites, the opposite of what we would expect if the intake filter was responsible for the observed span change and if the ozone concentration trends over the course of the summer at the three sites were similar.

Mean daily ozone concentrations at the four sites are presented by hour in Figure 4. Note that only the high span value has been used for the Emerald Lake data. The diurnal ozone concentration cycle is apparent for all four sites even though the curves represent 60-day means. The amplitude of the diurnal concentration cycle was greatest at Visalia and least at Emerald Lake. This figure clearly shows the phase-differences in the diurnal cycles of the four sites. The mean times of maximum and minimum ozone concentration are listed in Table II. The hour when the diurnal maxima and minima occurred during the summer was within a 3-h period except at Visalia where the variation was greater. Note that maximum and minimum ozone levels were generally reached progressively later each day as site elevation increased.

Mean hourly wind direction and speed at Emerald Lake are shown in Figure 5. The curves are based on data from the ozone monitoring site for the week July 29-August 5, and are representative since winds were very regular throughout the summer. Winds typically began to change from up-valley to down-valley at 1900 (all times are PST), and began to reverse again at 0900. The peak in the diurnal ozone cycle at Emerald Lake occurred at approximately the same time as the decline in up-valley winds. Similarly, the minimum in the diurnal ozone cycle occurred just after the return of up-valley winds.

There is correspondence in ozone concentrations between the four sites. One measure of this correspondence is the coincidence of peak ozone concentration days during the summer. Table III shows the day number of the four highest ozone peaks at Emerald Lake and the corresponding ranking for the other three sites. The four highest ozone concentration days at Emerald Lake were among the six highest days at Lower Kaweah and Ash Mountain. There was less peak correspondence between Emerald Lake and Visalia.

Another measure of correspondence is the coefficient of determination (r^2) for paired hourly ozone data from two sites. Because the coefficient of determination between two sinusoidal waves that are not in phase is a function of the phase angle, we have "shifted" all the data so the time of maximum concentration is the same. The times of maximum concentration given in Table II were used for this purpose. This shifting reduces the effect of phase-shift on the r^2 values so meaningful comparisons may be made. Table IV shows r^2 values for four site pairs. Each comparison is based on at least 1000 pairs of hourly mean concentrations. A strong correspondence was found between Lower Kaweah and Ash Mountain ozone concentrations ($r^2 = 0.65$). A moderate correspondence was found for Lower Kaweah and Visalia ($r^2 = 0.35$) and for lower Kaweah and Emerald Lake ($r^2 = 0.31$). There was little correspondence between Emerald Lake and Visalia ($r^2 = 0.16$).

DISCUSSION

Because of the effect of temperature on the ozone monitor's span, we must be cautious in making conclusions about the nature of the diurnal ozone concentration cycle at Emerald Lake. However, in our laboratory test of temperature's effect on the ozone monitor, we found span changes of less than 20% associated with temperature changes covering most of the range encountered in the field. The daily maximum ozone concentration at Emerald Lake was frequently twice the daily minimum so the temperature effect alone could not explain the diurnal cycle observed. However, the temperature effect may have had an impact on the timing of the diurnal maxima and minima, yet we wouldn't expect this to cause a substantial phase shift in the diurnal pattern.

Our measurements of the diurnal ozone concentration cycle support the hypothesis that ozone is transported from the San Joaquin Valley up the Sierra Nevada slope each day by valley winds.[5,6] Three findings lend support to this hypothesis. First, the connection between the time of ozone maxima and minima at Emerald Lake, and the change in wind speed and direction, show that up-slope, valley winds carry a higher concentration of ozone than down-slope, mountain winds. Second, ozone concentrations at Emerald Lake peaked at 1900 on average during the summer, after solar insolation had declined. This suggests that the ozone found at Emerald Lake is not produced locally. Third, the 2-h lag between the peak daily ozone concentrations at Lower Kaweah and Emerald Lake is consistent with valley winds with a mean speed of 2 m/s transporting ozone the 15-km distance separating the sites. (Such a calculation is not appropriate for the distances between the other sites. Visalia is not the ozone source area. And Lower Kaweah is located at the western edge of a high bluff so ozone transport to Lower Kaweah is not topographically confined to the valley where Ash Mountain is located.) Transport of ozone to Emerald Lake implies that ozone concentrations at Emerald Lake are higher than background levels.

There appears to be a weaker correspondence between the ozone concentrations at Emerald Lake and Lower Kaweah than between Ash Mountain and Lower Kaweah. This does not appear to be due simply to the proximity of the sites since they are nearly equidistant, and the difference in elevation between Emerald Lake and Lower Kaweah is less than between Ash Mountain and Lower Kaweah. One explanation for the difference in correspondence is that it is related to the problems with the ozone monitor. Alternatively, it could be a real effect for which we propose three possible explanations. First, valley winds are not perfect pollutant conveyors. Pollutant concentrations would be expected to decline with distance from the source region (San Joaquin Valley) due to surface deposition and mixing with air above. Second, Emerald Lake may be at the edge of the "reach" of the valley winds. The ability of the valley winds to transport pollutants is determined by the distance from pollution sources, the speed of the valley winds, and the number of hours each day when the valley winds occur. These factors limit the distance that valley winds can carry pollutants each day, and it is possible that Emerald Lake is close to this maximum distance. A third possible explanation is that increased boundary-layer mixing due to convective activity at higher elevations dilutes the ozone that is transported there. This may be particularly true for the area surrounding Emerald Lake because the area is rocky with only sparse vegetation. There is potential for much more surface heating near Emerald Lake than over the heavily forested ground at lower elevations.

CONCLUSIONS

While the quality of the Emerald Lake ozone data is questionable due to problems with the monitor's calibration, several conclusions can be tentatively made. Ozone concentrations at Emerald Lake are not as high as at Lower Kaweah or Ash Mountain, where the California ozone standard is regularly exceeded. Even our upper estimate of the peak ozone concentration at Emerald Lake during the monitoring period (0.06 ppm) is significantly less than the California ozone standard. The timing of the diurnal ozone concentration maxima and minima at the four sites, and the correspondence between the diurnal wind and ozone concentration cycles at Emerald Lake indicate that ozone is being transported to Emerald Lake from lower elevations. This implies that the Emerald Lake area is experiencing ozone concentrations higher than background levels. We hope that our results will not be considered conclusive evidence that ozone concentrations at Emerald Lake are well below current standards and that future ozone measurements will be made to verify our findings.

Because of the substantial evidence for injury to forest vegetation by ozone in Sequoia National Park (and other critical resource areas) there is a need for ozone monitoring in remote areas where forests are located. As indicated in this report, however, remote ozone monitoring is a difficult task. Our experience clearly shows the need for thorough laboratory evaluation of ozone monitors prior to their use for remote monitoring. It is important that provision be made for frequent on-site calibration, as done at standard ozone monitoring stations, even at the expense of a larger solar power system. Research is under way on alternative ozone monitoring techniques that are potentially more suitable for remote use than chemiluminescent or UV-photometric monitors.[7,8] The performance of these alternatives should also be carefully evaluated under field conditions.

ACKNOWLEDGMENTS

This project was funded by the California Air Resources Board under contract #A5-180-32. We gratefully acknowledge the efforts of the many individuals from the California Air Resources Board, National Park Service, and University of California, Davis, who contributed to this project. Susan Asam prepared the figures. Drs. Patricia Muir and Bruce McCune, and anonymous reviewers provided helpful comments on the manuscript.

REFERENCES

1. D.M. Duriscoe, "Cruise survey of western yellow pine (*Pinus ponderosa* and *P. Jeffreyi*) for oxidant air pollution injury in Sequoia and Kings Canyon National Parks, California," National Park Service, Denver, CO, 1987.

2. D. Shimp, California Air Resources Board, Sacramento, CA, private communication, 1989.

3. R. Hebner, National Park Service, Boulder, CO, private communication, 1989.

4. CSI, "Operation and Service Manual for CSI Series 2000 Ozone Monitors," Austin, TX, 1978.

5. S. Duckworth and D. Crowe, "Ozone patterns on the Western Sierra Slope," California Air Resources Board, Sacramento, CA, 1979.

6. P.R. Miller, M.H. McCutchan, and H.P. Milligan, "Oxidant air pollution in the Central Valley, Sierra Nevada foothills, and Mineral King valley of California," *Atmos. Environ.* 6:623 (1972).

7. M. Flores, National Park Service, Boulder, CO, private communication, 1988.

8. D. Cronn and M.J. Campbell, "The development and testing of a passive ozone monitor for outdoor monitoring using dry chemiluminescence," in: *Forest Response Program Annual Meeting, Project Status Reports, Vol. 11, Atmospheric Impacts Research Program*, North Carolina State University, Raleigh, NC, 1988.

Table I. Ozone statistics summary.[a]

Site	Elevation (m)	24-h Mean Concentration (ppm)	California Standard Exceedance Hours[b]	Data Hours
Emerald Lake	2740	0.017-0.033	0	1156
Lower Kaweah	1920	0.068	123	1405
Ash Mountain	610	0.080	320	1364
Visalia	100	0.050	118	1295

[a] Data are for days #207-266 (July 27, 1987–September 24, 1987). Total hours = 1440.

[b] California ozone standard: > 0.09 ppm hourly average.

Table II. Time of maximum and minimum ozone concentration at four sites.[a]

Site	Mean Hour of Maximum Ozone Concentration	Mean Hour of Minimum Ozone Concentration
Emerald Lake	1900	1000
Lower Kaweah	1700	0800
Ash Mountain	1800	0600-0700
Visalia	1500	0500

[a] Data are for days #207-266 (July 27, 1987–September 24, 1987). All times PST.

Table III. Ozone peak concentration day correspondence.

Day # (Date)	Peak concentration day rankings Emerald Lake	Lower Kaweah	Ash Mountain	Visalia
229 (8/18)	1	3	6	[a]
228 (8/17)	2	4	5	[a]
237 (8/26)	3	5[b]	3	[a]
216 (8/5)	4	2	3	1[b]

Data are for days #207-266 (July 27, 1987–September 24, 1987).

[a] indicates day not among six highest peaks.

[b] indicates two peaks with same concentration tied for ranking.

Table IV. Paired ozone concentration data correspondence.[a]

Monitoring Sites	r^2	Observations
Lower Kaweah/Ash Mountain	0.65	1328
Lower Kaweah/Visalia	0.35	1262
Lower Kaweah/Emerald Lake	0.31	1124
Emerald Lake/Visalia	0.16	1031

[a] Data are for days #207-266 (July 27, 1987–September 24, 1987). Total possible hours = 1440.

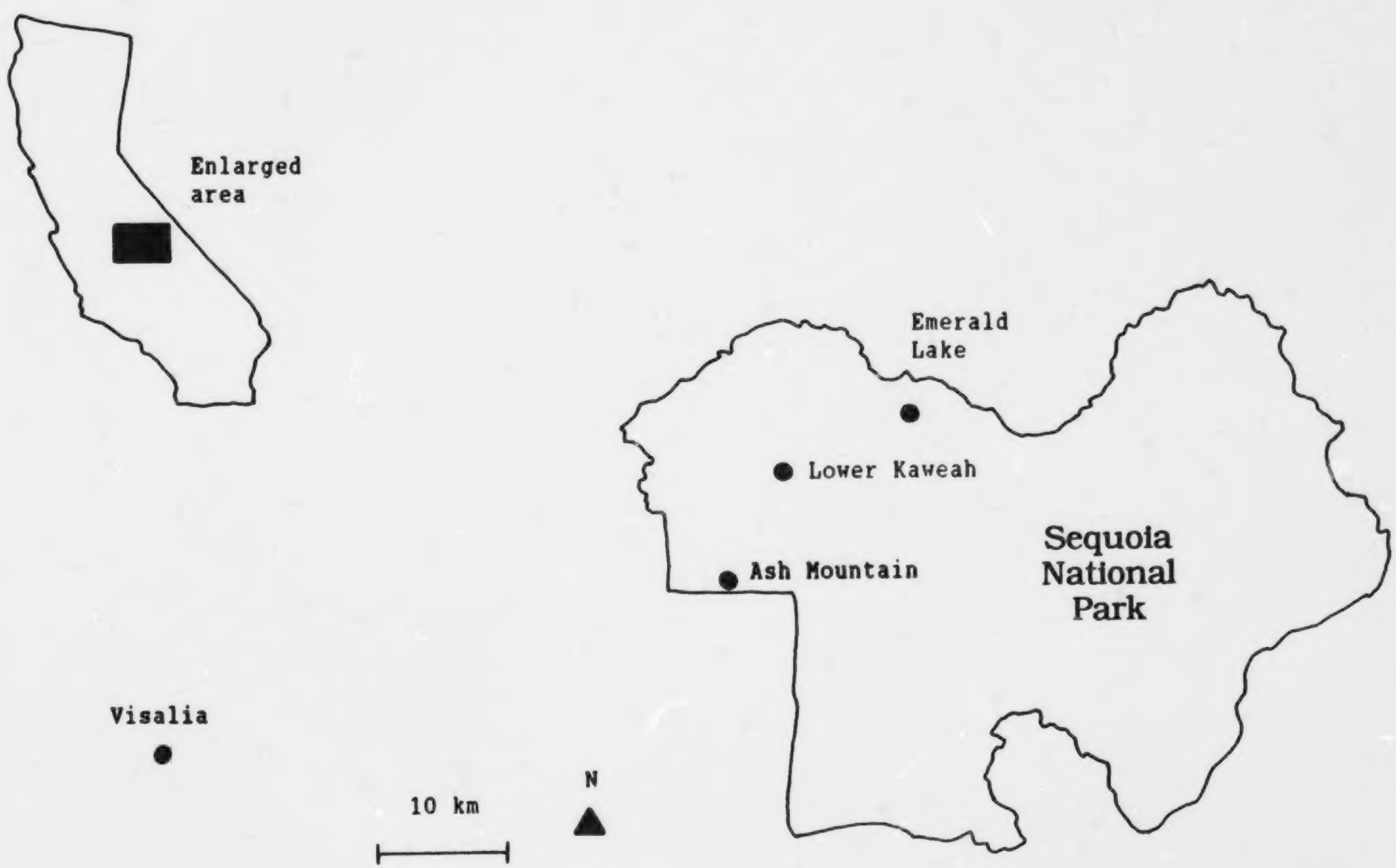
Enlarged
area
Emerald
Lake
Lower Kaweah
Ash Mountain
Sequoia
National
Park
Visalia
10 km
N

Figure 1. Map of ozone monitoring sites and Sequoia National Park.

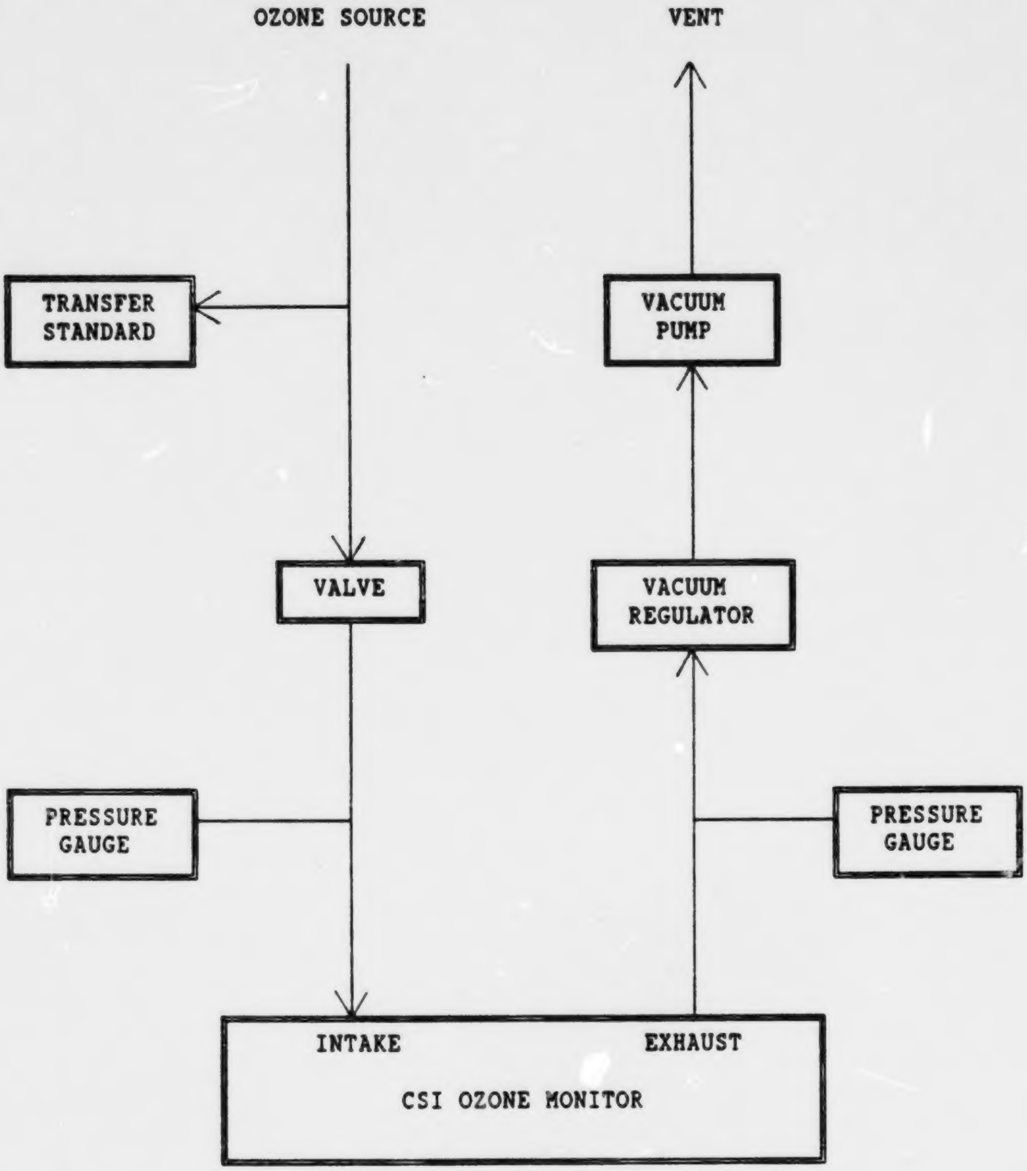
OZONE SOURCE
VENT
TRANSFER STANDARD
VACUUM PUMP
VALVE
VACUUM REGULATOR
PRESSURE GAUGE
PRESSURE GAUGE
INTAKE
EXHAUST
CSI OZONE MONITOR

Figure 2. High-altitude simulation system.

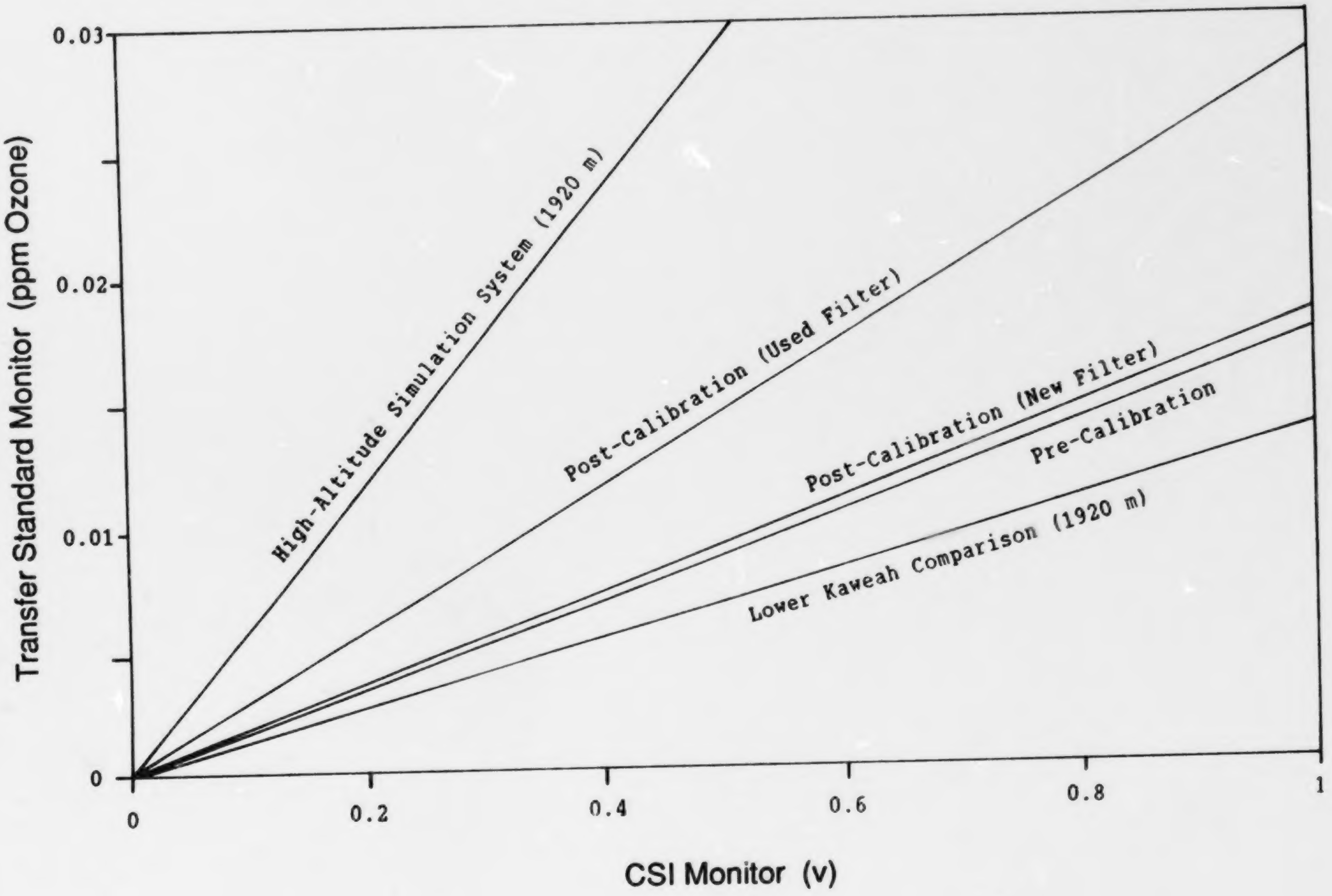

Figure 3. Results of ozone monitor calibrations.

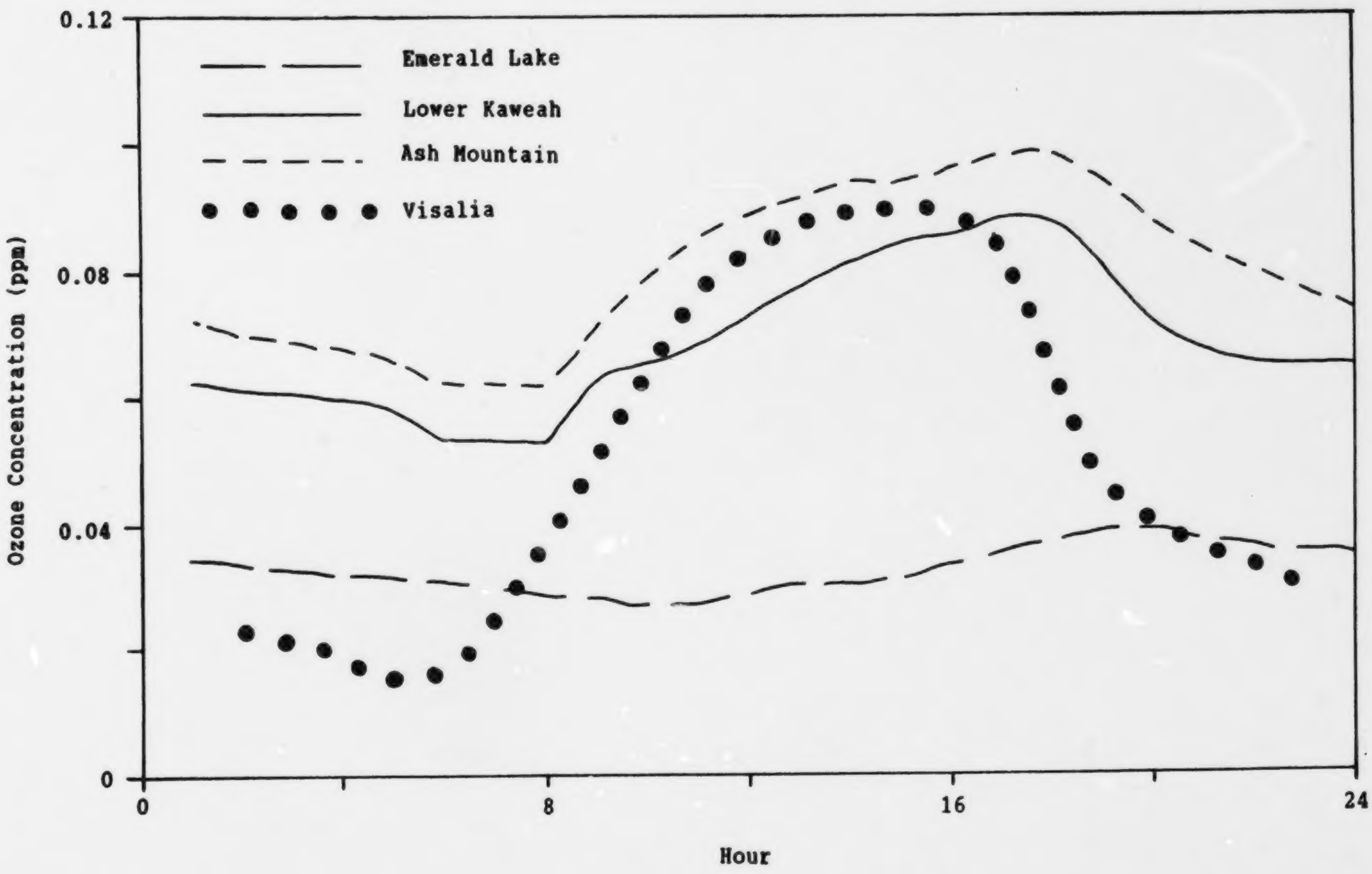

Figure 4. Mean hourly ozone concentrations at four sites (times are PST). The curves are based on data for days #207-266 (July 27 through September 24, 1987). The high span value has been used for the Emerald Lake Data.

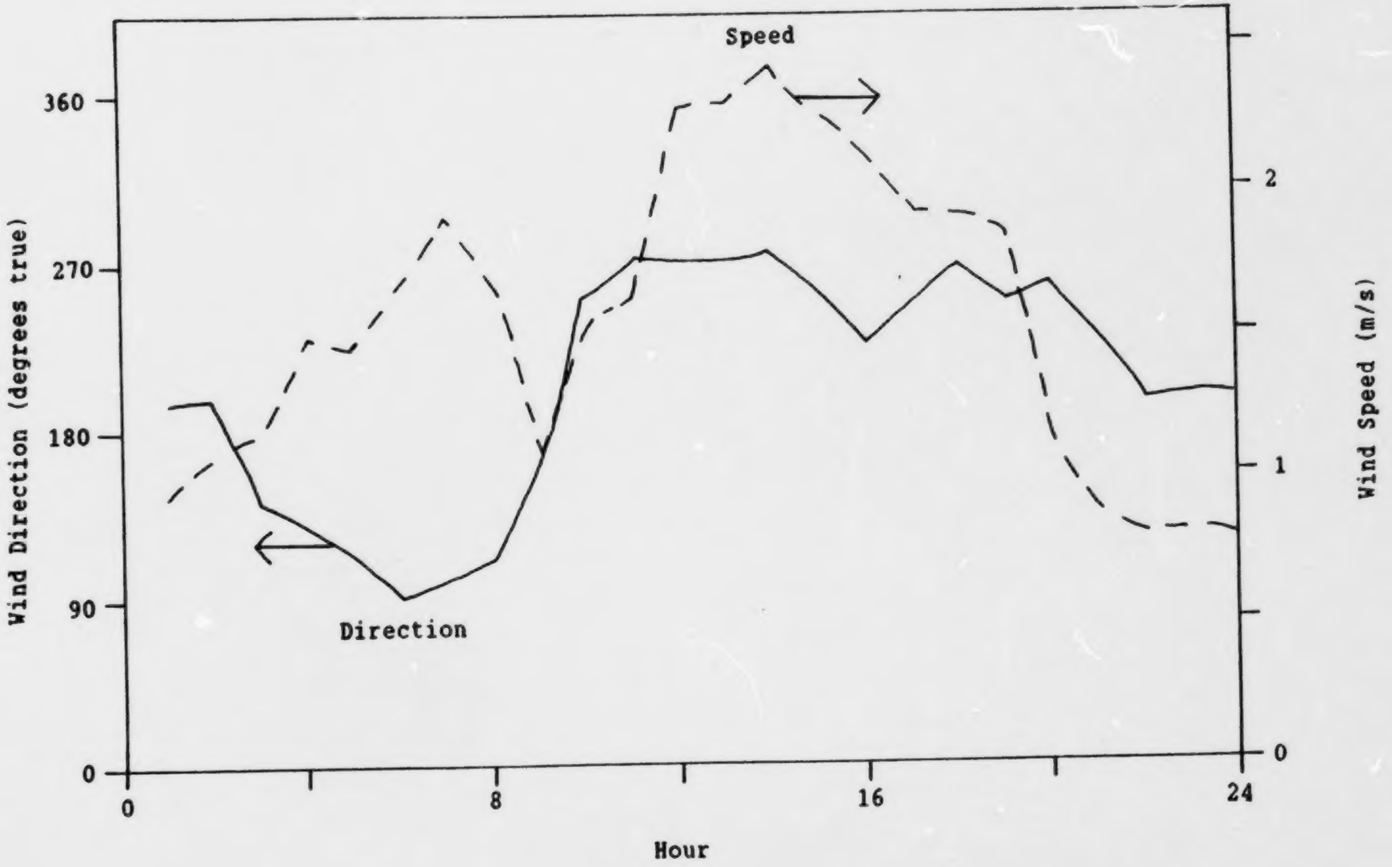

Figure 5. Mean hourly wind direction and speed at Emerald Lake (times are PST). The curves are based on data from the ozone monitoring site for days #209-216 (July 29 through August 5, 1987). Upslope winds are westerly (270 degrees) and downslope winds are easterly (90 degrees).

A Regional Characterization of Air Quality and Deposition in the Coniferous Forests of the Western United States

Margi Böhm

NSI Technology Services Corporation
U.S. EPA Environmental Research Laboratory
Western Conifers Research Cooperative
200 SW 35 Street
Corvallis, OR 97333

INTRODUCTION

Subsequent to their discovery and documentation in Scandinavia and northeastern North America, acid deposition and gaseous pollution episodes have been reported at several locations in the western United States, i.e., the eleven states west of 105° W. Acid precipitation is widespread in California and has been documented in the Los Angeles Basin, San Francisco Bay, the San Joaquin Valley, and the Sierra Nevada.[1-3] Southern and Central California have received particular attention especially with respect to ozone,[4] cloudwater concentrations,[5-9] deposition loadings,[10-12] and haze.[13] Observations of acid precipitation and of sensitive high mountain watersheds showing signs of acidification have been noted in Colorado.[14-16] Reports describing air pollution in the Pacific Northwest[17,18] and the central and southwestern states[13,19-24] are becoming more frequent.

This paper presents a characterization of emissions, ambient concentrations, and deposition of pollutants in the western United States with emphasis on areas covered by coniferous forests. The primary pollutants of concern are sulfur dioxide (SO_2) and nitrogen dioxide (NO_2); and the secondary pollutants discussed are ozone (O_3) and the concentration and deposition of acidic species in rain, snow, and cloudwater.

MATERIALS AND METHODS

Emissions

Estimates of emissions and the locations of point sources were obtained from the 1985 National Acid Precipitation Assessment Program (NAPAP) Interim Assessment and emissions database (1985 NAPAP National Emissions Data System, NEDS).[25] The emission data are estimates of the quantity of emissions and the activity of the source during 1985.

Ambient Gas Concentrations

Hourly concentrations of ambient SO_2, NO_2, and O_3 are monitored at state level. Most of these data are available from the EPA Aerometric Information Retrieval System (AIRS). To limit uncertainties associated with nonstandard calibration techniques prior to EPA standardization in 1979, the study period started on January 1, 1980. Months with less than 500 sampling hours were excluded from the analysis.

Rain and Snow

Weekly composite precipitation samples have been collected in the West since 1978 by the National Atmospheric Deposition Program/National Trends

Network (NADP/NTN). The data were screened using the NADP/NTN flagging system to identify samples that were contaminated (bulk deposition or bird droppings), that represented sampling periods longer than 8 days, that were collected using nonstandard sampling procedures, or for which there were no field or laboratory data. Confidence in the deposition loading estimates is not as high as that for the chemical concentrations because the quality of the precipitation amount data is not known. Consequently, actual loadings are usually under-estimated, especially when precipitation amounts are not available or sampler efficiency is low.[26] Although sample integrity can be compromised by using a weekly composite sampling period, and ionic concentrations may be underestimated,[27-29] I believe that the concentration data are generally more accurate than the deposition data. Thus, deposition of ions across the West will not be discussed in as much detail as ionic concentration of precipitation.

Cloud

Some information on cloud chemistry and frequency of occurrence in the West is available from the published literature, a summary of which is presented by Muir and Böhm.[30] There are no regional programs (such as the eastern Mountain Cloud Chemistry Project) studying cloud chemistry and deposition to western forests. In addition, there is little information on the frequency of occurrence and duration of cloud events in forested areas.

Site Selection

A siting criterion of ≤20 km from the boundaries of coniferous forests was applied to select the sites used in this analysis. These sites were identified using 1:2,500,000 ecoregion maps.[31,32] Although ecoregions represent many different factors besides vegetation type, the areas identified as typically covered with coniferous forests correlate well with those depicted on the 1:3,168,000 Natural Vegetation Map[33] and 1:7,500,000 Major Forest Types Map.[34] A total of 24 sulfur dioxide (SO_2), 20 nitrogen dioxide, 58 ozone (O_3), and 44 wet deposition sites were selected. To illustrate the most important spatial and temporal characteristics of air pollution regimes in and around western coniferous forests, the data from a subset of ten SO_2, nine O_3, and eleven NADP/NTN wet deposition sites (choice based on geographic location, period of record, and data capture) will be discussed in this paper (Table I, Figure 1).

DATA ANALYSIS

Ambient Gas Concentrations

Monthly fractiles[35] (expressed as cumulative percent of total observed hours) were used to describe the occurrence of SO_2 and O_3 within 20 km of coniferous forests. Generally, SO_2 concentrations were low, and consequently no further analysis of the data was performed. Since O_3 does occur at levels that may be detrimental to vegetation (hourly values >60 ppb),[36] seasonal and spatial patterns in hourly O_3 concentrations were further investigated using median and worst diurnal traces for each month. Worst day is defined as that with the highest maximum value following the hypothesis that peak O_3 concentrations cause damage to vegetation.[37-39] Interannual variation was estimated from the number of hours per year O_3 concentrations exceeded 80 ppb.

Nitrogen oxides are rapidly oxidized in the atmosphere and do not occur in concentrations high enough to negatively effect western forests. Secondary pollutants, such as peroxyacetyl nitrate (PAN) and aerosol nitrate may play a more important role in receptor areas far removed from NO_2 sources. Unfortunately, there is a paucity of regional data on PAN and aerosol nitrate across the West, and consequently the study of deposition of nitrogen to forest ecosystems is limited, in this paper, to that deposited during precipitation events.

Wet Deposition

The weekly sampling period adopted by NADP/NTN prevented a detailed analysis of the frequency and duration of wet deposition as recommended by Hogsett et al.[35] The spatial patterns in precipitation chemistry are discussed using descriptive statistics for sulfate, nitrate, and hydrogen ion concentrations and deposition. The temporal patterns were approximated using weekly sulfate concentration data, to which a Fourier series (detrended with a class variable that addresses annual variations) is fitted using least-squares regression. The curves presented have been tested for goodness of fit by week and year and are superimposed on the weekly minimum, 25th percentile, 75th percentile, and maximum values for the period of record.

RESULTS AND DISCUSSION

Sulfur Dioxide (SO_2)

Thresholds reported for direct foliar injury to plants from 1-h exposures to SO_2 range between 500 and 2500 ppb for sensitive species.[40,41] Long-term thresholds have proven more difficult to estimate.[41] There is some evidence that annual average concentrations as low as 10–20 ppb, together with occasional peaks of 40–80 ppb, can reduce tree growth.[42]

Emission Patterns. Sulfur dioxide is emitted into the atmosphere during anthropogenic activities such as the combustion of fossil fuels, smelting of ores, manufacturing of steel, and refining of petroleum. Sulfur dioxide is also emitted naturally from sources such as fumaroles and volcanoes. Geothermal activity in North America is concentrated in Alaska, the western contiguous United States, and Mexico, and therefore natural SO_2 emissions may play an important but sporadic role in the West.[25] For example, the Mount St. Helens eruptions between 1980 and 1982 contributed an estimated 0.34 million metric tons of SO_2 to the atmosphere, more than the annual contribution from man-made sources in the states of Washington and Oregon.

Anthropogenic sources of SO_2 are scattered across the eleven western states, although major point sources are primarily located in Arizona, New Mexico, Colorado, Wyoming, Montana, and Washington (Figure 2). Total SO_2 emissions by state for 1985 are estimated between 0.04 and 0.59 million metric tons/year.[25] Interestingly, California has the second highest estimated emissions despite the absence of sources emitting more than 500 metric tons SO_2 per year (Figure 2).

In 1985, the estimated total SO_2 emissions for the West were 2.15 million tons, 10% of the national estimate.[25] With the exception of Arizona, the western states generally have SO_2 emission densities less than 1.50 metric tons/km^2,[43] although orographic/meteorological conditions in many of the source areas may prevent dispersion of plumes and localized pockets of high ambient SO_2 levels probably exist.

Regional trends in SO_2 emissions imply that the Western situation has not changed much during the past decade.[25] These results do not reflect the situation at a state level. SO_2 emissions increased between 1980-1986 by an estimated 25% in Idaho and by 10.5% in Wyoming, remained unchanged in Oregon and Colorado, and decreased slightly elsewhere.[25]

Sulfur dioxide emissions in the West are expected to stabilize at between 2.0-2.2 million tons/year by 1990.[44,45] After 1990, increasing emissions from stationary fuel combustion sources should outweigh the continuing decline in smelter emissions, resulting in a gradual increase in SO_2 emissions by the year 2000. These projections are approximate since emissions from several large smelters in northwestern Mexico are expected to increase through the 1990s and may influence SO_2 levels in Arizona and New Mexico.[45]

Ambient Concentrations. Data from ten of the twenty-four SO_2 sites identified within 20 km of coniferous forests are discussed (Table I). The period of operation of these sites is important, especially in areas where large SO_2 sources have since been shut down. The following discussion serves to identify potential exposure conditions in and around certain coniferous forests by providing an overview of the levels of ambient SO_2 concentrations ($[SO_2]$) that have recently been experienced in the West. An analysis of point source close-downs and the influence on $[SO_2]$ is not included in the scope of this paper.

The lowest ambient $[SO_2]$ were measured at Apache Sitgreaves NF, AZ (1982-1986); San Bernardino, CA (1980-1981, 1983-1984); and Albuquerque, NM (1980-1986), where levels greater than 10 ppb were rarely encountered (Figure 3). Concentrations at Olympic NP, WA (1980-1986) are also generally low; $[SO_2] > 30$ ppb occurred during less than 5% of measured hours per month. On the other hand, Greenlee County, AZ (1980-1984); Shoshone County, ID (1980-1983); Kellogg, ID (1980-1981); and Anaconda Deer Lodge, MT (1981), were often exposed to high $[SO_2]$. At Greenlee County, the seasonal maxima occur during winter (November-January) when SO_2 concentrations exceeded 80 ppb during 20% of the measured hours per month; high summertime exposures were also frequent ($[SO_2] > 80$ ppb during 10% of measured hours per month). Anaconda Deer Lodge, MT, was exposed to $[SO_2] > 80$ ppb during at least 15% of measured hours during the winter and early summer months, whereas Kellogg showed a summer maximum of 17% of measured hours per month (August-October), and springtime sub-maximum with $[SO_2] > 80$ ppb during 10% of measured hours per month.

The remaining sites were usually exposed to $[SO_2] < 40$ ppb. Denver, CO (1980-1986); King County, WA (1980-1986); Burbank, CA (1980-1986); and Bountiful, UT (1980-1986) recorded more frequent occurrences of the higher concentrations during winter. At Bellingham, WA, (1983-1986) and Miami, AZ (1980-1986), $[SO_2]$ were less than 30 ppb with a small maximum in summer.

A comparison between ambient $[SO_2]$ and the locations of point sources illustrates the local nature of this pollutant. Sites reasonably close to SO_2 sources with emissions greater than 100 metric tons/year (Bellingham and King County, WA; Burbank, CA; Denver, CO; Bountiful, UT; and Miami, AZ) recorded ambient $[SO_2] > 20$ ppb during all the months of the year. On the other hand, San Bernardino, CA; Apache Sitgreaves NF, AZ; and Albuquerque, NM are also located near to sources, but high ambient $[SO_2]$ were rarely measured.

Nitrogen Dioxide (NO_2)

Nitrogen dioxide does not occur in concentrations high enough to be phytotoxic to vegetation. However, as NO_2 is a precursor of O_3, it is appropriate to discuss the emission patterns of this pollutant.

Emission Patterns. Transportation (primarily highway vehicles) is the major source of anthropogenic nitrogen oxides (NO_x) in the West.[44] Consequently, large emissions occur in and around cities, with fewer sources in rural and remote areas, except around large point sources.

The 11 western states emitted an estimated 3.01 million metric tons of NO_x in 1985, 15.8% of the national total.[25] The highest emissions (estimated at 1.11 million metric tons/1985) were for California (second only to Texas on a national scale), with Oregon and Idaho (0.21 and 0.08 million metric tons/1985 respectively) having the lowest emissions in the West.[25] The largest emission densities are found in and around the major cities such as Los Angeles, San Francisco, Puget Sound (Seattle-Tacoma), Salt Lake City, Las Vegas, Phoenix, Albuquerque, and Denver.[43]

Regionally, NO_x emissions in the West decreased slightly between 1980 and 1985.[25] At state level, Arizona, Colorado, and Wyoming show larger estimates for 1985 than for 1980 (increased power plant emissions) as did Montana and Nevada (increased emissions from power plants and highway vehicles), whereas California, Oregon, and Washington show decreases. Nitrogen oxide emissions are expected to remain constant through the 1980s as further controls are placed on mobile sources; but after 1990, a gradual increase in emissions is projected.[45]

Ozone (O_3)

Ozone is a secondary pollutant created in the presence of nitrogen oxides, volatile organic compounds (hydrocarbons), and sunlight. The major source areas for O_3 are therefore related to those for NO_x and hydrocarbons. Since ultraviolet light energy is required to drive the photochemical reactions, O_3 concentrations fluctuate both seasonally and with latitude.

Ozone is the only regionally dispersed pollutant known to injure foliage and cause tree mortality.[46] Adverse effects can start occurring at concentrations above 60 ppb,[36] however, effects generally manifest themselves during short exposures to concentrations greater than 80 ppb.[37]

Ambient Concentrations. Data from nine of the fifty-eight O_3 sites identified within 20 km of coniferous forests are presented (Table I). The following discussion serves to identify potential exposure conditions in and around certain coniferous forests by providing an overview of the levels of ambient O_3 concentrations that have been experienced recently in the West.

The lowest hourly O_3 concentrations were recorded at Olympic NP, WA, where levels never exceeded 60 ppb (Figure 4). Sites such as South Lake Tahoe, CA, Mammoth Lakes, CA, Apache Sitgreaves NF, AZ, and Albuquerque, NM, were exposed to $60 < [O_3] < 80$ ppb during the summer months (Figure 4). Exposure to O_3 at Albuquerque occurred in summer (April–September), when such concentrations were observed during 2–10% of measured hours per month. Ozone concentrations increased between March and August at Apache Sitgreaves NF, with 5–25% of measured hours recording values between

60 and 80 ppb. The O_3 season in the Sierra Nevada extended from March-November, with concentrations between 60 and 80 ppb occuring 2-25% of measured hours per month at South Lake Tahoe, and 2-30% of measured hours per month at Mammoth Lakes.

Hourly $[O_3] > 100$ ppb were measured at King County, WA, Boulder, CO, Bountiful, UT, and Lake Gregory, CA (Figure 4). Concentrations in this range were recorded during mid-summer (June-August) for 5% of measured hours per month, except at Lake Gregory. The San Bernardino Mountains (Lake Gregory) are exposed to hourly O_3 concentrations in excess of 100 ppb all year round, with frequencies of occurrence of 1-2% of measured hours in winter and 10% in summer.

Most of the sites show increased O_3 levels in summer, with maximum exposure during June, July, and August. The exceptions are Olympic NP where hourly concentrations never exceeded 60 ppb, and the sites in Arizona (Flagstaff and Apache Sitgreaves NF) where higher concentrations occurred during May. Boulder, CO; Bountiful, UT; Lake Gregory, Mammoth Lakes, and South Lake Tahoe, CA recorded elevated O_3 concentrations (>80 ppb) at least once a month. Of these, Bountiful and Lake Gregory were exposed to hourly $[O_3] > 120$ ppb during at least 6 of the 12 months.

Seasonal and diurnal trends in $[O_3]$ were further investigated using monthly median and worst diurnal patterns for Lake Gregory, Mammoth Lakes, and South Lake Tahoe, CA, and King County, WA. The magnitude of elevated $[O_3]$ at Lake Gregory is remarkable and serves to illustrate the consequences of urbanization in a poorly ventilated valley (Figures 5 and 6). Ozone concentrations peak late in the afternoon at Lake Gregory, implying long range transport (Figure 5). Mammoth Lakes and South Lake Tahoe, although located close to urban settlements, show less diurnal variation than Lake Gregory and King County; a pattern usually expected for remote, high elevation sites[47] (Figure 5). King County exhibits a diurnal pattern characteristic of an urban site with $[O_3]$ reaching the minimum detection limit of the monitoring instrument (5-10 ppb) during the night and early morning hours (Figure 5).

Ozone concentrations at Lake Gregory have a distinct seasonal pattern, with marked increases during the summer (Figure 5). The Sierra Nevada sites show very little seasonality in $[O_3]$, although winter concentrations are lower than those in summer (Figure 5). The seasonal pattern in O_3 at King County does not exhibit marked changes in concentration, but rather in diurnal cycle, with O_3 formation occurring earlier in summer than winter (Figure 5). These seasonal patterns illustrate the influence of solar energy in the presence of an abundant (Los Angeles Basin) and limited (King County) supply of O_3 precursors.

The median monthly diurnal patterns of $[O_3]$ measured at Mammoth Lakes and South Lake Tahoe do not show depletion of O_3 during the night and early morning hours, as would be expected for sites measuring locally generated O_3 (e.g., compare the graphs with that for King County in Figure 5). Thus, although the urban centers of Mammoth Lakes and South Lake Tahoe probably generate many of the O_3 precursors, there is evidence to suggest that either additional O_3 is being transported to these areas, or the background levels are of the order of 30-40 ppb. Similar results have been documented in Alberta, Canada.[47]

The worst O_3 days on record, again, illustrate the extreme situation in the San Bernardino Mountains (Figure 6). The worst days are similar at Mammoth Lakes, South Lake Tahoe, and King County, although ML and SLT are exposed to longer periods of elevated levels than King County.

The number of hours per year that $[O_3] > 80$ ppb does not vary much from year to year at Lake Gregory, South Lake Tahoe, or King County (Table II). Furthermore, any trend is not consistent across the three sites and, therefore, it is suspected that any interannual variation in $[O_3]$ is a function of erratic climatic conditions. Similar results have been found in southern California.[48]

Acid Precipitation

The chemical species responsible for depressing the pH of rainwater are secondary pollutants, derived primarily from the oxidation of sulfur and nitrogen oxides. The rate of oxidation and the transport of the primary and secondary pollutants determines the areas where acid deposition is most likely to occur. Eleven NADP/NTN sites within 20 km of coniferous forests and with six years or more of data are used to illustrate the spatial and temporal patterns of acid precipitation across the western United States.

Precipitation Chemistry—Concentration. The ionic concentrations of precipitation in the West are generally 15-25% of eastern values. Mean weekly concentrations of sulfate range between 5.11-26.17 μmol/L, 2.52-66.11 μmol/L for nitrate, and 3.56-33.19 μmol/L for hydrogen ions. The 75th percentile for sulfate concentrations ranges between 6-24 μmol/L, 3-60 μmol/L for nitrate, and 4-24 μmol/L for hydrogen ions (Table IIIa). Extreme concentrations such as 350 μmol/L sulfate, 917 μmol/L nitrate, and 645 μmol/L of hydrogen ions have been recorded at a forested site north of Los Angeles (Table IIIa). Extreme values of these orders of magnitude are infrequent, site specific, and usually associated with small precipitation amounts, but should not be ignored since chemical inputs at such high levels may be toxic to forest ecosystems.

The chemical composition of precipitation across the West exhibits a spatial pattern related, not surprisingly, to the proximity of the site to pollution sources (Table IIIa, Figures 1,2). Sites removed from anthropogenic sulfur emission sources (e.g., Hoh River, WA; H.J. Andrews Forest, OR; Yosemite NP, CA; Headquarters, ID; Glacier NP, MT) have lower mean and peak sulfate concentrations (weekly mean 5-7 μmol/L) than sites in close proximity or downwind of paper/pulp mills (e.g., Alsea Forest, OR, 8.6 μmol/L), fossil fuel refineries, and power plants (e.g., San Gabriel Mountains—Tanbark Flat, CA, 26 μmol/L; and the Front Range, CO where weekly mean $[SO_4^{2-}]$ ranges between 15-20 μmol/L).

The relationship between nitrate concentrations and proximity to urban/industrial complexes is even more pronounced (Table IIIa, Figures 1,2). Hoh River and Alsea Forest have very low nitrate concentrations (2.5 and 4 μmol/L respectively); slightly higher values (6-9 μmol/L) are recorded at H.J. Andrews Forest, Headquarters, and Glacier National Park, which are located near reasonably large cities. Much higher concentrations (weekly mean $[NO_3^-]$ between 16-66 μmol/L) are found at sites downwind of large urban complexes such as Central California Valley (Yosemite and Sequoia NP), Los Angeles Basin (Tanbark Flat), and the Front Range (Manitou, CO; Alamosa, CO; and Bandelier NM, NM).

The spatial pattern in acidity (hydrogen ion concentration) is similar to that for sulfate and nitrate. Although the northern sites exhibit similar mean hydrogen ion concentrations (weekly mean [H^+] around 3-5 μmol/L), Alsea Forest, Yosemite NP and Sequoia NP, and Headquarters have recorded peak acidities [H^+] > 60 μmol/L, twice that at the other northern sites. On average, the Front range receives precipitation with twice the acidity (mean [H^+]– 10 μmol/L) as the northern sites; and although the peak values are of the same order of magnitude, the Front range sites are more often exposed to elevated acidities (as illustrated by a difference of 2 in the 75th percentiles in Table IIIa). The precipitation sampled close to a large urban area (Tanbark Flat, 35 km north of downtown Los Angeles, CA) is 3-6 times more acidic than that recorded at other NADP/NTN sites in the West.

Seasonal patterns in precipitation chemistry across the West are illustrated using [SO_4^{2-}] (Figure 7). There is a general increase in sulfate concentrations during the summer (possibly related to lower volume events) and a decrease during winter, although at more remote sites, this pattern is not easily discernable. The range in concentration is generally lower during winter than during summer, possibly related to seasonal patterns in occurrence, form (snow versus rain), and origin of air masses. Similar results have been noted at Sequoia NP, CA,[12] and in Colorado.[14,15]

Precipitation Chemistry–Deposition. Annual wet-deposition estimates for sulfate, nitrate, and hydrogen ions are generally 15-25% of eastern values (e.g., in 1986,[26] deposition estimates across the West were 2-9 kg/Ha, SO_4^{2-}; 1-5 kg/Ha, NO_3^-; and 0.03-0.1 kg/Ha, H^+). Deposition of nitrate follows similar spatial patterns to concentration (Table IIIb), with areas in close proximity to urban/industrial centers recording higher loadings. Patterns in sulfate deposition are more complex, possibly a consequence of the marine influence at remote sites such as Hoh River, Alsea Forest, and H.J. Andrews Forest in conjunction with the high precipitation amounts recorded in these areas.

Temporal patterns in deposition are related to seasonal patterns in precipitation. In general, most deposition to forested areas in the West occurs during the winter in the form of snow.

Elevational Effects. High elevation ecosystems are considered more sensitive to anthropogenically modified precipitation chemistry than low elevation ecosystems.[49] A preliminary analysis of weekly composite sulfate concentrations for 12 NADP/NTN sites in six study areas in the Colorado and Wyoming Rockies showed that [SO_4^{2-}] in snow were consistently lower than those in rain. Snow samples collected at lower elevations contained greater concentrations of sulfate relative to higher elevations. A similar relationship for rain was not well established.[50] Contrary to these results for weekly composite samples, increases in the acidity of precipitation *events* with elevation have been noted in New Mexico[51] and Scotland.[52]

Unfortunately, such results cannot be generalized and assumed to be the case in other areas. Elevational gradients are affected by a complex interaction of orographic features, mesoscale and local meteorology, distance from upwind pollution sources, as well as the seasonal variations in precipitation form, pollution emissions, and meteorology. Further research is required to identify the relationships between acid deposition and elevation.

Cloud

A recent survey of the published literature on cloud chemistry and frequency of occurrence in the West has been presented by Muir and Böhm.[30] A précis of their results is presented.

Interception of nonprecipitating (stratus and stratocumulus) clouds across the West is greatest along the Pacific coast, in the Coast Range of northern California, Oregon, and Washington and along the western slopes of the Cascades. Interception is more frequent in the south in summer and in the north in winter. The frequency of occurrence of stratus and stratocumulus clouds is low over the Sierra Nevada and central Western Mountains, although total cloud interception is probably underestimated due to a lack of information on the frequency of occurrence of cap clouds. Cloud Interception of stratus and stratocumulus cloud is also considered to be low along the eastern slopes of Wyoming, Colorado, and New Mexico.

Western cloud events exhibit a large range of concentrations, e.g., $[NO_3^+]$—16,000 μmol/L and $[SO_4^{2-}]$—4,500 μmol/L have been recorded. Samples from southern California are generally more acidic than those from the northern sites (mean minimum pHs = 2.52 and 4.48, respectively). Southern California samples tend to be dominated by SO_4^{2-}, NO_3^-, and NH_4^+, whereas samples from Alaska, Oregon, and northern California are mainly influenced by sea-salt and marine constituents (Na^+, Cl^-, and SO_4^{2-}). Concentrations of all ions in western cloudwater are positively correlated, but correlations are strongest between ions that result primarily from one of three source groups: sea salt, soil dust, and anthropogenic sources of sulfur and nitrogen.

CONCLUSIONS

Although estimated total SO_2 emissions in the West are 10% of the national estimate, pockets of high ambient $[SO_2]$ were found. For example, forests near Greenlee, AZ, Kellogg and Shoshone, ID, and Anaconda Deer Lodge, MT, were frequently exposed to $[SO_2] > 80$ ppb during the early 1980s. Indeed, SO_2-induced damage has been recorded in Montana.[53] A detailed study of the air pollution meteorology of the areas around the major SO_2 sources is required to estimate the total forest area potentially impacted by SO_2 in the West.

Nitrogen dioxide is not likely to cause damage to terrestrial ecosystems at current levels. However, since NO_x is a precursor of O_3, PAN, and nitrates, the magnitudes of emissions in areas close to forests (such as southern and central California, the Front Range of Colorado, and the Cascades of Washington) are of concern, especially since emissions are projected to gradually increase.

Ozone levels in and near forested areas are greatest downwind of large urban and industrial centers. Ponderosa and Jeffrey pine forests surrounding the Los Angeles Basin exhibit foliar damage directly related to O_3,[4] and evidence of growth reduction in Jeffrey pine has been recorded in the southern Sierra Nevada.[54,55] Comparisons of the fractiles and diurnal patterns of O_3 in these areas with those for other sites across the West indicate that O_3 levels in and near the forests of Utah and Arizona, the northern Front Range, and the western slopes of the northern Cascades are probably exposed to similar levels of O_3 (although for shorter periods of time) as those of the western slopes of the central Sierra Nevada. These levels may be debilitating to local forest species. More O_3 data in forested areas are required to accurately assess the potential for O_3 damage in areas other than southern California.

In general, concentrations and deposition of sulfate, nitrate, and hydrogen ions in precipitation events are about 15-25% of eastern values, although extreme events can occur. Urban and industrial areas seem to elevate concentrations of sulfate and nitrate by a factor of 2–6. Temporal patterns show highest concentrations during the spring, summer, and fall.

It is uncertain if acid precipitation increases or decreases with elevation. Since many high-elevation areas across the West have shallow, poorly buffered soils[49] and lakes with low alkalinity values,[3] more information on the relationship between elevation and acid precipitation in western forests is required.

The available data on cloud chemistry indicate that the regions of the western United States in which cloud interception is greatest generally have low ionic strengths. Even though cloud interception is low in southern California, the chemistry of the few events sampled is so concentrated that adverse effects to terrestrial ecosystems may occur. Similarly, total deposition of ionic species intercepted by the foliage and introduced to soil systems at the northern sites may not be inconsequential.

Generally, it is concluded that regional air pollution levels are low across the West but that local airsheds can be highly polluted. The forests most susceptible to atmospheric stresses are those downwind of major urban and industrial complexes. Forests potentially threatened by current levels of air pollution are identified as being in the San Gabriel and San Bernardino Mountains, southern Sierra Nevada, Central Utah and Arizona, the Front Range of Colorado, and the western slopes of the Cascades in Washington.

Finally, it is concluded that the paucity of regional data describing air quality, meteorology, and physiological characteristics of western forests makes it difficult to describe regionally the impact of man on air quality and deposition in and around the coniferous forests of the West.

ACKNOWLEDGMENTS

I would like to acknowledge Terralyn Vandetta for her invaluable programming skills and my reviewers for their helpful comments and suggestions. The SO_2 and O_3 fractile data were provided by Al Lefohn, A.S.& L. Associates, Helena, Montana. This research was supported by funds provided by the Western Conifers Research Cooperative within the joint U.S. Environmental Protection Agency—USDA Forest Service Forest Response Program. The Forest Response Program is part of the National Acid Precipitation Assessment Program.

REFERENCES

1. D.R. Lawson and J.G. Wendt, "Acid deposition in California," SAE Technical Paper 821246, 1982.

2. J.G. McColl, "A survey of acid precipitation in Northern California (Final Report)," CARB, Contract A7-149-30, Sacramento, CA, 1980.

3. J.M. Melack, J.L. Stoddard, and C.A. Ochs, "Major ion chemistry and sensitivity to acid precipitation of Sierra Nevada Lakes," *Water Resources Res.* 21:27 (1985).

4. P.R. Miller, O.C. Taylor, and M.P. Poe, "Spatial variation of summer ozone concentrations in the San Bernardino Mountains," Proceedings of the 79th Annual APCA Meetings, Minneapolis, MN, 1986.

5. J.M. Waldman, J.W. Munger, D.J. Jacob, R.C. Flagan, J.J. Morgan, and M.R. Hoffmann, "Chemical composition of acid fog," *Science*, 218:677 (1982).

6. R.L. Brewer, E.C. Ellis, R.J. Gordon, and L.S. Shepard, "Chemistry of mist and fog from the Los Angeles urban area," *Atmos. Environ.*,17:2267 (1983).

7. J.W. Munger, D.J. Jacob, J.M. Waldman, and M.R. Hoffmann, "Fogwater chemistry in an urban atmosphere," *J. Geophys. Res.*, 88(C9):5109 (1983).

8. D.J. Jacob, J.M. Waldman, J.W. Munger, and M.R. Hoffmann, "Chemical composition of fogwater along the California coast," *Environ., Sci., and Technol.*, 19:730 (1985).

9. J.M. Waldman, J.W. Munger, D.J. Jacob, and M.R. Hoffmann, "Chemical characterization of stratus cloudwater and its role as a vector for pollutant deposition in a Los Angeles pine forest," *Tellus*, 37B:91 (1984).

10. R.L. Leonard and C.R. Goldman, "Some measurements of the pH and chemistry at Davis and Lake Tahoe, California," *Water, Air, Soil Pollut.*, 15:153 (1981).

11. H.M. Liljestrand and J.J. Morgan, "Spatial variations of acid precipitation in southern California," *Environ. Sci. Technol.*, 15(3):333 (1981).

12. T.J. Stohlgren and D.J. Parsons, "Variation of wet deposition chemistry in Sequoia National Park, California," *Atmos. Environ.*, 21(6):1369 (1987).

13. E.S. Macias and J.O. Zwicker, "Regional haze case studies in the southwestern US–I. Aerosol chemistry composition," *Atmos. Environ.*, 15(10/11):1971 (1981).

14. C.T. Nagamoto, F. Parungo, R. Reinking, R. Pueschel, and T. Gerish, "Acid clouds and precipitation in eastern Colorado," *Atmos. Environ.*, 17(6):1073 (1983).

15. J. Harte, G.P. Lockett, R.A. Schneider, H. Micheals, and C. Blanchard, "Acid precipitation and surface water vulnerability on the western slope of the High Colorado Rockies," *Water, Air, and Soil Pollut.*, 25:313 (1985).

16. M.J. Reddy, T.D. Liebermann, J.C. Jelinski, and N. Caine, "Variation in pH during summer storms near the continental divide in central Colorado, U.S.A.," *Arctic Alpine Res.*, 17(1):79 (1985).

17. G.A. McBean and S. Nikleva, "Composition of snow in Pacific coastal mountains," *Atmos. Environ.*, 20(6):1161 (1986).

18. R.L. Edmonds and F.A. Basabe, "Ozone concentrations in Douglas fir forests in western Washington," Submitted to *Can. J. For. Res.*, 1988.

19. G.A. Dawson, "Ionic composition of rain during sixteen convective showers," *Atmos. Environ.*, 12:1991 (1978).

20. R.G. Flocchini, T.A. Cahill, L.L. Ashbaugh, and R.A. Eldred, "Seasonal behavior of particulate matter at three rural Utah sites," *Atmos. Environ.*, 15:315 (1981).

21. R.G. Flocchini, T.A. Cahill, M.L. Pitchford, R.A. Eldred, P.J. Feeney, and L.L. Ashbaugh, "Characterization of particles in the arid west," *Atmos. Environ.*, 15(10/11):2017 (1981).

22. W.P. Linak and T.W. Peterson, "Visibility-pollutant relationships in southern Arizona – II. A winter/summer field study," *Atmos. Environ.*, 17(9):1811 (1983).

23. J.J. Messer, "Geochemically alkaline snowpack in northern Utah mountains in spring of 1982," *Atmos. Environ.*, 17(5):1051 (1983).

24. E. Thomas and P.R. Buseck, "Characterization of a rural aerosol from eastern Arizona," *Atmos. Environ.*, 17(11):2299 (1983).

25. M. Placet and D.G. Streets, "NAPAP Interim Assessment, The causes and effects of acid precipitation, Volume II. Emissions and Control," NAPAP Headquarters, Washington DC, 1987.

26. National Atmospheric Deposition Program, "NADP/NTN Annual Data Summary: Precipitation chemistry in the United States, 1986," available from Program Coordinator, NADP/NTN Coordination Office, Natural Resource Ecology Laboratory, Colorado State University, Fort Collins, CO 80523, 1987.

27. R.G. De Pena, K.C. Walker, L. Lebowitz, and J.G. Micka, "Wet deposition monitoring–effect of sampling period," *Atmos. Environ.*, 19(1):151 (1985).

28. J.N. Galloway and G.E. Likens, "Calibration of collection procedures for the determination of precipitation chemistry," *Water, Air, Soil Pollut.*, 6(2/3):241 (1976).

29. J.N. Galloway and G.E. Likens, "The collection of precipitation for chemical analysis," *Tellus*, 30:72 (1978).

30. P.S. Muir and M. Böhm, "Cloud chemistry in the western United States: A synopsis of current information," Proceedings of the 82nd Annual APCA Meetings, Anaheim, CA, 1989.

31. Ecoregions of the Conterminous United States, J.M. Omernik, and A.L. Gallant, U.S. Government Printing Office, 1986, 1:2,500,000, 36" x 36", colored, English.

32. J.M. Omernik, "Ecoregions of the Conterminous United States," *Annals Assoc. Amer. Geographers*, 77(1):118 (1987).

33. Potential Natural Vegetation of the Conterminous United States, A.W. Kuchler, American Geographical Society (Special Publication # 36), Broadway, 156th Street, New York, NY 100032, (1975), 1:3,168,000, colored, English.

34. National Atlas of the United States of America, USDI, Geological Survey, Map "Major Forest Types, 1:7,500,00," Compiled from information from the US Forest Service, 1967, p. 154.

35. W.E. Hogsett, D. Olszyk, D.P. Ormrod, G.E. Taylor, and D.T. Tingey, "Air pollution exposure systems and experimental protocols: Volume 1: A review and evaluation of performance," EPA 600/3-87/037a, Environmental Research Laboratory, Office of Research and Development, Corvallis, OR 97333, September 1987.

36. E.J. Pell, "The impact of ozone on the bioenergetics of plant systems," in *Air Pollution Effects on Plant Growth*, M. Dugger, Ed., American Chemical Society, ASC Symposium Series, Washington, DC, 3:106 (1974).

37. O.C. Taylor, Ed., "Oxidant air pollution effects on a western coniferous forest ecosystem," Task B Report, University of California Air Pollution Research Center, Riverside, CA, 1973.

38. A.S. Lefohn, "A comparison of ambient ozone exposures for selected nonurban sites," *Proceedings of the 77th Annual APCA Meeting*, San Francisco, CA, June 1984.

39. A.S. Lefohn and C.K. Jones, "The characterizing of ozone and sulfur dioxide air quality data for assessing possible vegetation effects," *JAPCA*, 36(10):1123 (1986).

40. W.W. Heck and C.S. Brandt, "Effects on vegetation: Native, crops, forests," Chapter 4 in *Air Pollution*, Third Edition, A.C. Stern (Ed.), Academic Press, New York, 1977.

41. S.B. McLaughlin, "SO_2, vegetation effects and the air quality standard: Limits of interpretation and application," A Speciality Conference on the Proposed SO_x and Particulate Standard, Atlanta, GA (APCA) 1981.

42. F. Last and P. Rennie, "Forest changes expert meeting no. 3," Stockholm Conference on Acidification of the Environment, June 20-30, 1982 (Swedish Ministry of the Environment) 1982.

43. L.R. Chinkin, D.A. Latimer, and L.A. Mahoney, "Western States Acid Deposition Project, Volume 2: A review of emission inventories needed to regulate acid deposition in the western United States," Final Report SYSAPP-87/072, Western Governors' Association, Denver, CO, 1987, 148pp.

44. G.M. Hidy and J.R. Young, "Acid deposition and the West, a scientific assessment," ERT Document No. P-D572-503, March 1986.

45. J.R. Young, E.C. Ellis, and G.M. Hidy, "Deposition of air-borne acidifiers in the western environment," *J. Environ. Qual.*, 17(1):1 (1988).

46. J.N. Woodman, "Pollution induced injury to North American forests: Facts and suspicions," *Tree Physiol.*, 3:1 (1987).

47. A.H. Legge, *The present and potential effects of acidic and acidifying air pollutants on Alberta's environment. Critical Point I, 1988*, Prepared for the Acid Deposition Research Program by the Kananaskis Centre for Environmental Research, The University of Calgary, Calgary, Alberta, ADRP-B-16-88, ISBN 0-921625-23-5, 1988, 75pp.

48. H.M. Walker, "Ten-year ozone trends in California and Texas," *JAPCA*, 35(9):903 (1985).

49. M.T El-Ashry, "Study shows mountain ecosystems may be especially sensitive to acid deposition," *Ambio*, 14131:174 (1985).

50. W.G. Warren, M. Böhm, and D. Link, "Statistical methodology for exploring elevational differences in precipitation chemistry," Proceedings of the 82nd Annual APCA Meetings, Anaheim, CA, 1989.

51. C.J. Popp and A. Long, "Acidic effects in Western North America—Trends, sources, and altitude effects in New Mexico, 1979–1985," *Water, Air, Soil Pollut.*, 30:125 (1986).

52. D. Fowler, J.N. Cape, I.D. Leith, T.W. Choularton, M.J. Gay, and A. Jones, "The influence of altitude on rainfall composition at Great Dun Fell," *Atmos. Environ.*, 22(7):1355 (1988).

53. C.E. Carlson, "Sulfur damage to Douglas-fir near a pulp and paper mill in western Montana," Report 74-13, USDA-USFS Northern Region, Missoula, MT, 1974.

54. D.L. Peterson, M.J. Arbaugh, V.A. Wakefield, and P.R. Miller, "Evidence of growth reduction in ozone-injured Jeffrey pine (*Pinus jeffrey* Grev. and Balf.) in Sequoia and Kings Canyon National Parks," *JAPCA*, 37:906 (1987).

55. D.L. Peterson and M.J. Arbaugh, "An evaluation of the effects of ozone injury on radial growth of ponderosa pine (*Pinus ponderosa*) in the southern Sierra Nevada," *JAPCA*, 38(7):921 (1988).

Table I. Descriptions of pollutants measured and period of record by site. (Site numbers refer to Figure 1. NP—National Park, NF—National Forest, and NM—National Monument.)

Site #	Name	State	Pollutant	(period of record)
1	Bellingham	WA	SO_2	(83-86)
2	Olympic NP	WA	SO_2	(80-86);
			O_3	(82-86)
3	Hoh River	WA	Precipitation	(80-87)
4	King County	WA	SO_2	(80-86);
			O_3	(80-86)
5	Alsea Forest	OR	Precipitation	(79-87)
6	H.J. Andrews Forest	OR	Precipitation	(80-87)
7	South Lake Tahoe	CA	O_3	(81,84-86)
8	Yosemite NP	CA	Precipitation	(81-87)
9	Mammoth Lakes	CA	O_3	(84-86)
10	Sequoia NP	CA	Precipitation	(80-87)
11	Santa Barbara County	CA	O_3	(80-86)
12	Tanbark Flat	CA	Precipitation	(82-87)
13	Burbank	CA	SO_2	(80-86)
14	Lake Gregory	CA	O_3	(80-86)
15	San Bernardino County	CA	SO_2	(80-81,83-84)
16	Shoshone County	ID	SO_2	(80-83)
17	Kellogg	ID	SO_2	(80-81)
18	Headquarters	ID	Precipitation	(82-87)
19	Glacier NP	MT	Precipitation	(80-87)
20	Anaconda Deer Lodge	MT	SO_2	(80)
21	Bountiful	UT	SO_2	(80-86);
			O_3	(80-86)
22	Boulder	CO	O_3	(81-86)
23	Denver	CO	SO_2	(80-86)
24	Manitou	CO	Precipitation	(78-87)
25	Alamosa	CO	Precipitation	(80-87)
26	Bandelier Nat. Mon.	NM	Precipitation	(82-87)
27	Albuquerque	NM	SO_2	(80-86)
28	Flagstaff	AZ	O_3	(81-85)
29	Apache Sitgreaves NP	AZ	SO_2	(82-86);
			O_3	(80-83)
30	Miami	AZ	SO_2	(80-84)

Table II. Number of hours/year (percent) that hourly $[O_3] > 80$ ppb at Lake Gregory, South Lake Tahoe, and King County. Site number refers to Figure 1.

#	Site Name	Year							
		80	81	82	83	84	85	86	87
14	Lake Gregory	19.1	21.6	20.2	19.0	21.4	20.1	20.0	13.6
7	S. Lake Tahoe	0.5	0.6	0.1	0.0	0.1	0.2	0.3	0.6
4	King County	0.1	0.9	0.2	0.3	0.1	0.5	0.8	0.5

Table IIIa. Minimum, 25th percentile, arithmetic mean, 75th percentile, and maximum weekly concentration statistics for sulfate, nitrate, and hydrogen ions (μmol/L) in precipitation. Site numbers refer to Figure 1.

				Sulfate			
#	Site Name	N	Min	25th	Mean	75th	Max
3	Hoh River	273	0.16	2.39	5.60	6.14	66.42
6	H.J. Andrews	285	0.16	2.19	5.74	5.73	72.87
5	Alsea Forest	271	0.16	3.85	8.64	8.54	179.57
18	Headquarters	145	0.16	2.29	5.11	5.52	35.19
19	Glacier NP	257	0.16	3.64	7.27	9.68	61.52
24	Manitou	280	0.52	6.77	15.93	19.36	192.27
25	Alamosa	210	0.16	7.29	20.05	23.73	171.24
26	Bandelier NM	189	0.52	6.77	14.85	18.74	91.61
8	Yosemite NP	134	0.52	2.19	6.27	9.79	51.53
10	Sequoia NP	167	0.52	2.81	8.85	9.99	100.66
12	Tanbark Flat	130	0.52	4.58	26.17	21.97	359.14

				Nitrate			
#	Site Name	N	Min	25th	Mean	75th	Max
3	Hoh River	273	0.16	0.65	2.52	2.26	83.88
6	H.J. Andrews	285	0.16	1.45	5.97	5.65	120.65
5	Alsea Forest	271	0.16	1.13	3.93	4.03	85.65
18	Headquarters	145	0.16	3.39	8.89	10.00	60.81
19	Glacier NP	257	0.16	4.52	9.06	11.29	78.71
24	Manitou	280	0.16	12.58	26.83	33.71	270.82
25	Alamosa	210	0.24	7.42	17.95	24.36	117.75
26	Bandelier NM	189	0.16	8.23	19.61	23.55	158.72
8	Yosemite NP	134	0.16	3.55	16.55	24.36	200.98
10	Sequoia NP	167	0.16	3.55	20.36	25.81	125.97
12	Tanbark Flat	130	0.24	9.03	66.11	60.97	917.47

				Hydrogen Ion			
#	Site Name	N	Min	25th	Mean	75th	Max
3	Hoh River	281	0.08	2.24	4.07	4.68	26.92
6	H.J. Andrews	294	0.03	2.45	4.60	5.25	35.48
5	Alsea Forest	274	0.08	2.14	4.13	4.57	67.61
18	Headquarters	150	0.10	2.45	5.50	5.89	112.20
19	Glacier NP	260	0.03	2.82	4.10	6.24	8.32
24	Manitou	295	0.04	1.74	10.77	15.85	66.07
25	Alamosa	223	0.02	0.47	3.56	3.02	52.48
26	Bandelier NM	193	0.07	2.19	9.05	12.30	79.43
8	Yosemite NP	144	0.06	1.82	5.04	5.13	67.61
10	Sequoia NP	178	0.03	1.45	5.30	5.50	64.57
12	Tanbark Flat	135	0.12	3.89	33.19	23.99	645.65

Table IIIb. Minimum, 25th percentile, arithmetic mean, 75th percentile, and maximum weekly deposition statistics for sulfate, nitrate, and hydrogen ions (mg/m^2) in precipitation. Site numbers refer to Figure 1.

					Sulfate		
#	Site Name	N	Min	25th	Mean	75th	Max
3	Hoh River	273	0.00	3.62	21.74	31.85	161.16
6	H.J. Andrews	285	0.16	3.50	13.24	17.09	72.46
5	Alsea Forest	271	0.00	4.15	18.41	26.06	141.02
18	Headquarters	143	0.003	2.32	6.73	9.32	26.98
19	Glacier NP	257	0.002	3.11	5.10	11.05	48.01
24	Manitou	280	0.05	2.21	11.91	16.84	65.34
25	Alamosa	210	0.003	2.18	7.19	9.71	36.24
26	Bandelier NM	189	0.19	3.02	11.21	15.76	62.16
8	Yosemite NP	133	0.02	2.97	11.61	13.31	72.44
10	Sequoia NP	166	0.58	3.54	14.05	17.53	203.87
12	Tanbark Flat	130	0.09	5.38	19.68	31.43	92.41

					Nitrate		
#	Site Name	N	Min	25th	Mean	75th	Max
3	Hoh River	273	0.004	0.89	5.00	7.29	29.00
6	H.J. Andrews	285	0.004	2.06	6.01	8.92	28.03
5	Alsea Forest	271	0.002	0.71	4.17	6.01	26.96
18	Headquarters	143	0.004	2.01	6.95	11.05	24.46
19	Glacier NP	257	0.001	2.70	6.18	8.61	33.78
24	Manitou	280	0.00	3.01	13.26	19.28	78.87
25	Alamosa	210	0.003	1.37	4.88	7.23	23.59
26	Bandelier NM	189	0.002	2.14	9.53	14.34	45.55
8	Yosemite NP	133	0.09	3.86	14.43	22.07	118.90
10	Sequoia NP	166	0.11	5.55	17.01	18.56	161.64
12	Tanbark Flat	130	0.002	9.29	28.49	40.81	106.59

					Hydrogen Ion		
#	Site Name	N	Min	25th	Mean	75th	Max
3	Hoh River	281	E-5	0.03	0.25	0.37	1.62
6	H.J. Andrews	294	7E-6	0.03	0.19	0.28	1.09
5	Alsea Forest	274	2E-5	0.02	0.14	0.21	1.02
18	Headquarters	148	23-5	0.02	0.10	0.15	0.45
19	Glacier NP	260	4E-7	0.02	0.11	0.15	0.82
24	Manitou	295	2E-6	0.004	0.13	0.16	1.22
25	Alamosa	223	7E-7	0.001	0.02	0.02	0.38
26	Bandelier NM	193	1E-5	0.01	0.11	0.16	0.91
8	Yosemite NP	143	4E-6	0.01	0.15	0.20	1.03
10	Sequoia NP	177	2E-6	0.01	0.16	0.19	2.50
12	Tanbark Flat	135	1E-5	0.02	0.32	0.52	1.79

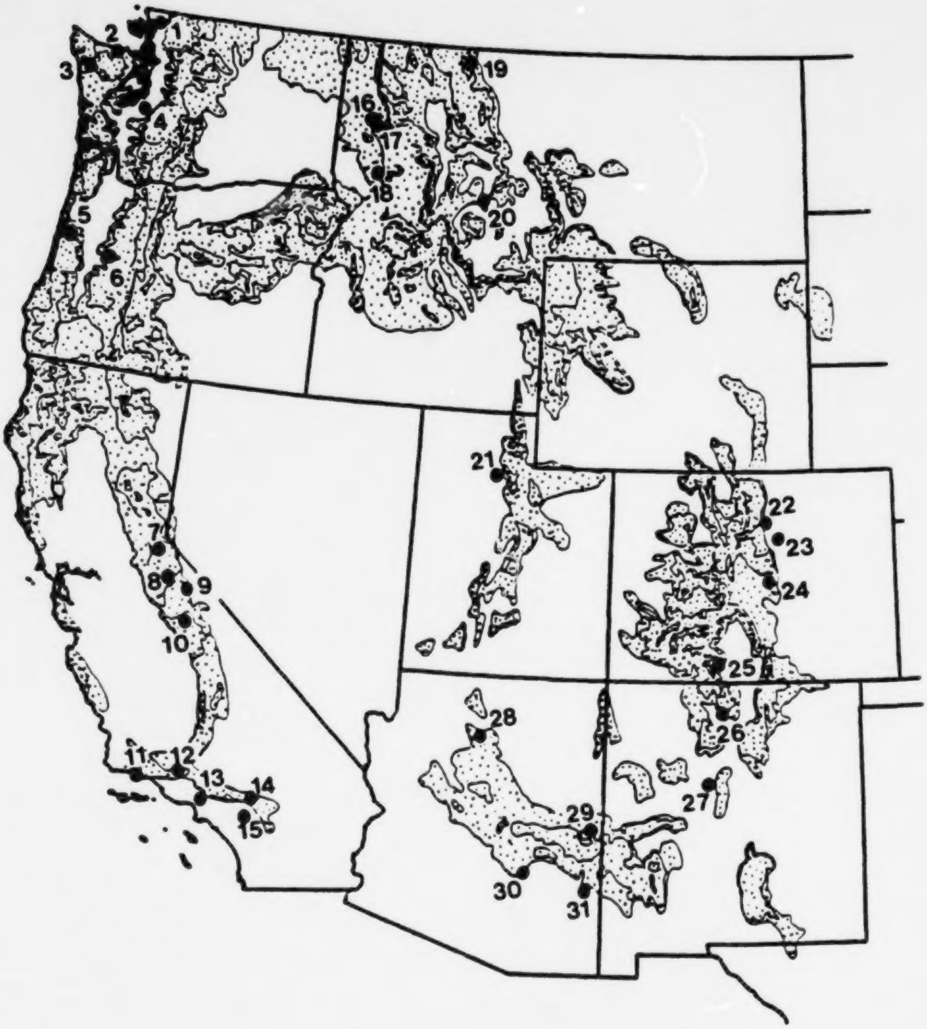
1
2
3
4
5
6
7
8
9
10
11
12
13
14
15
16
17
18
19
20
21
22
23
24
25
26
27
28
29
30
31

Figure 1. Locations of SO_2, O_3, and acidic precipitation monitoring sites within 20 km of coniferous forest ecoregions (shaded).[31] The site information is presented in Table I.

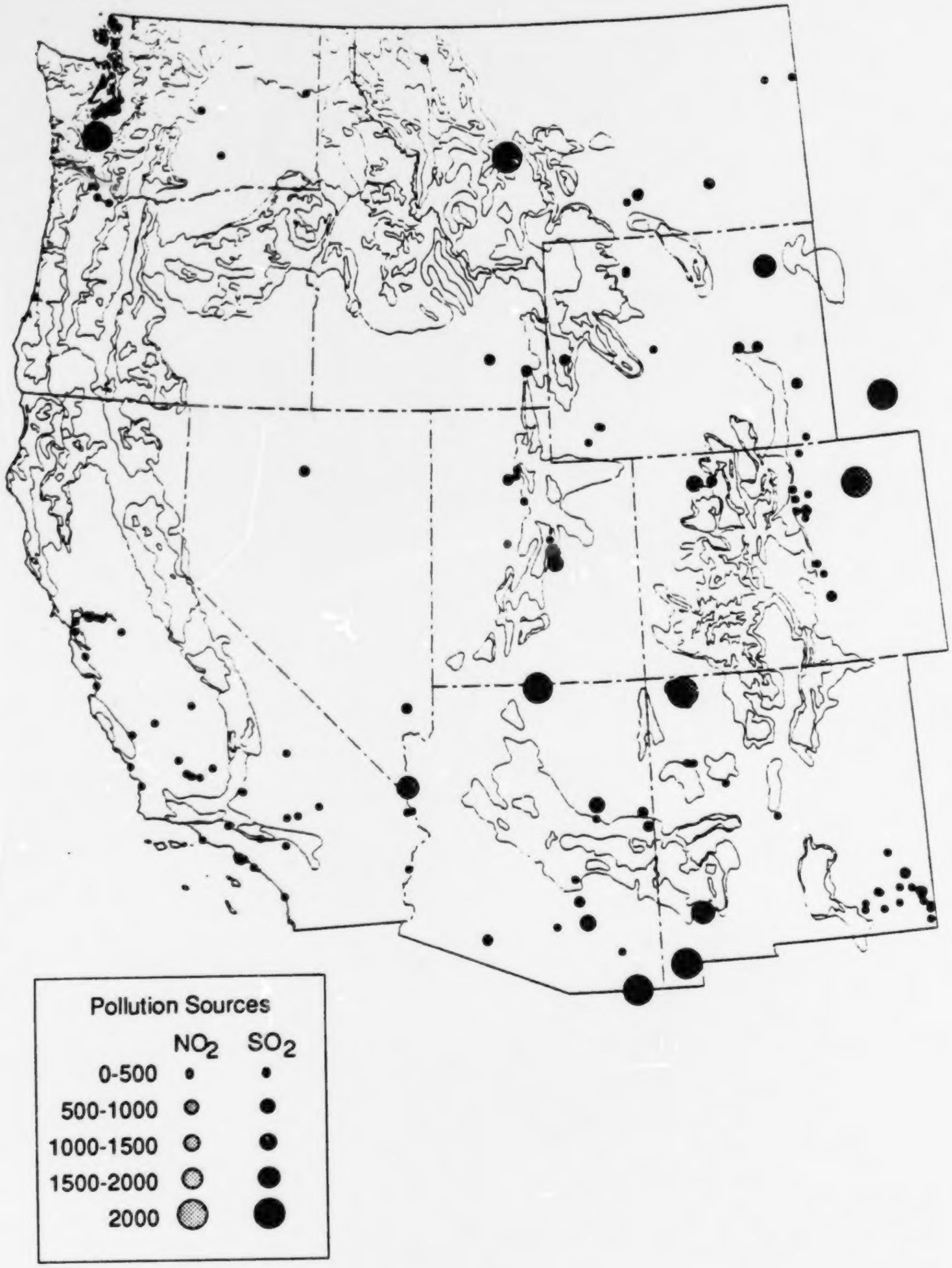
Pollution Sources
NO2 SO2
0-500
500-1000
1000-1500
1500-2000
2000

Figure 2. Point sources of SO_2 and NO_2 emitting more than 100 metric tons per year. Emission estimates are for 1985 (NEDS).

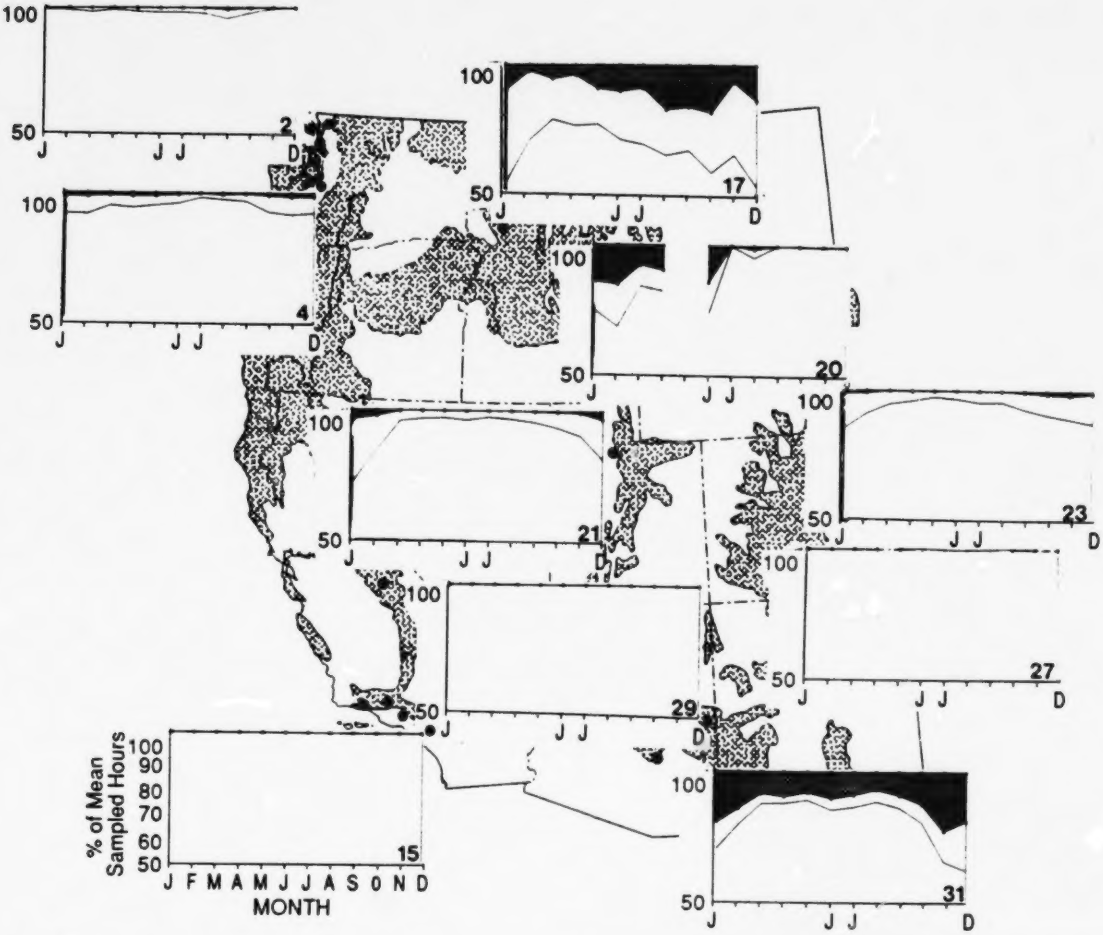

Figure 3. Spatial and temporal patterns in ambient [SO_2] using cumulative mean monthly fractiles expressed as percent of total observed hours. The shaded areas illustrate the percent of hours per month during which [SO_2] > 80 ppb, the middle zone relates to the percent of hours per month with 30 < [SO_2] < 80 ppb, and the remaining area represents the percent hours per month for which [SO_2] < 30 ppb. (For explanation of numbers, see Table I).

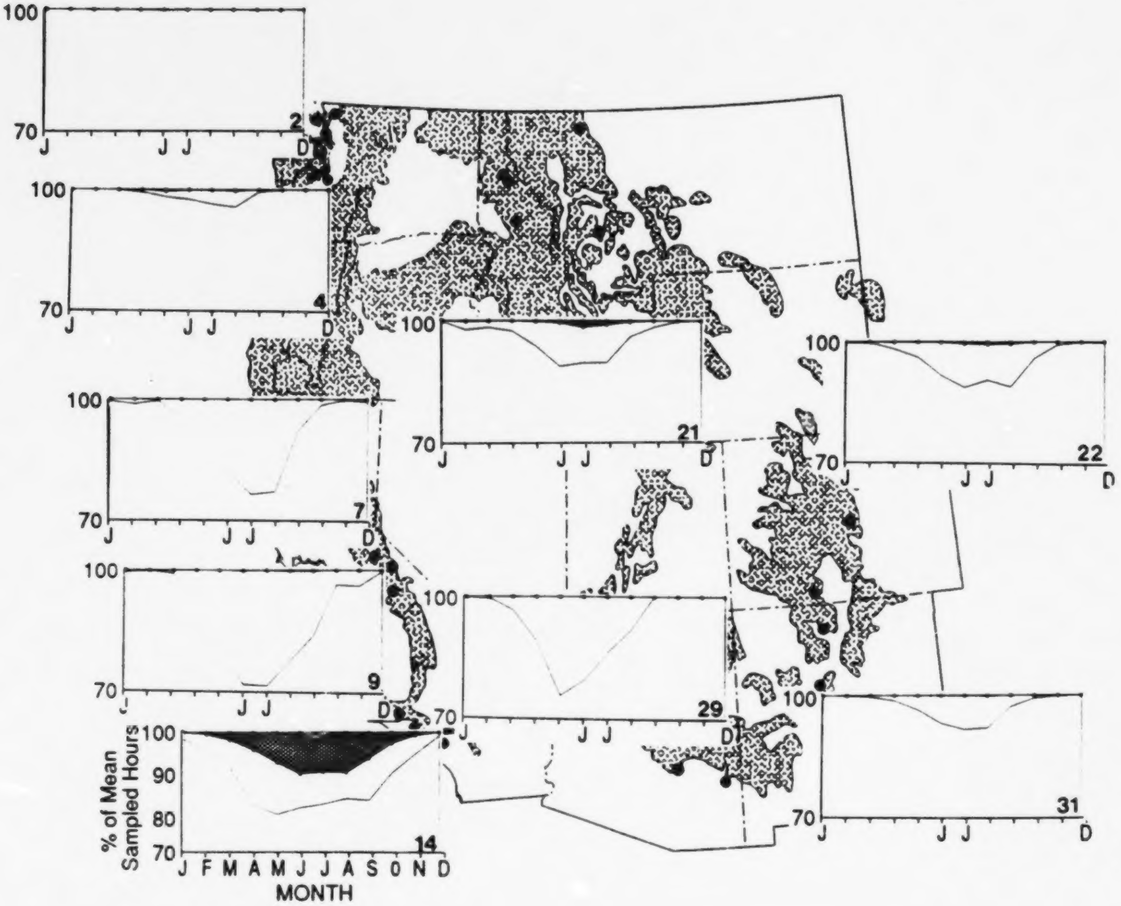
100
70
J
J J
D
2
4
7
9
14
21
22
29
31
% of Mean Sampled Hours
90
80
J F M A M J J A S O N D
MONTH

Figure 4. Spatial and temporal patterns in ambient [O_3] using cumulative mean monthly fractiles expressed as percent of total observed hours. The shaded areas illustrate the percent of hours per month during which [O_3] > 100 ppb, the middle zone relates to the percent of hours per month with 60 < [O_3] < 100 ppb, and the remaining area represents the percent hours per month for which [O_3] < 60 ppb. (For explanation of numbers, see Table I).

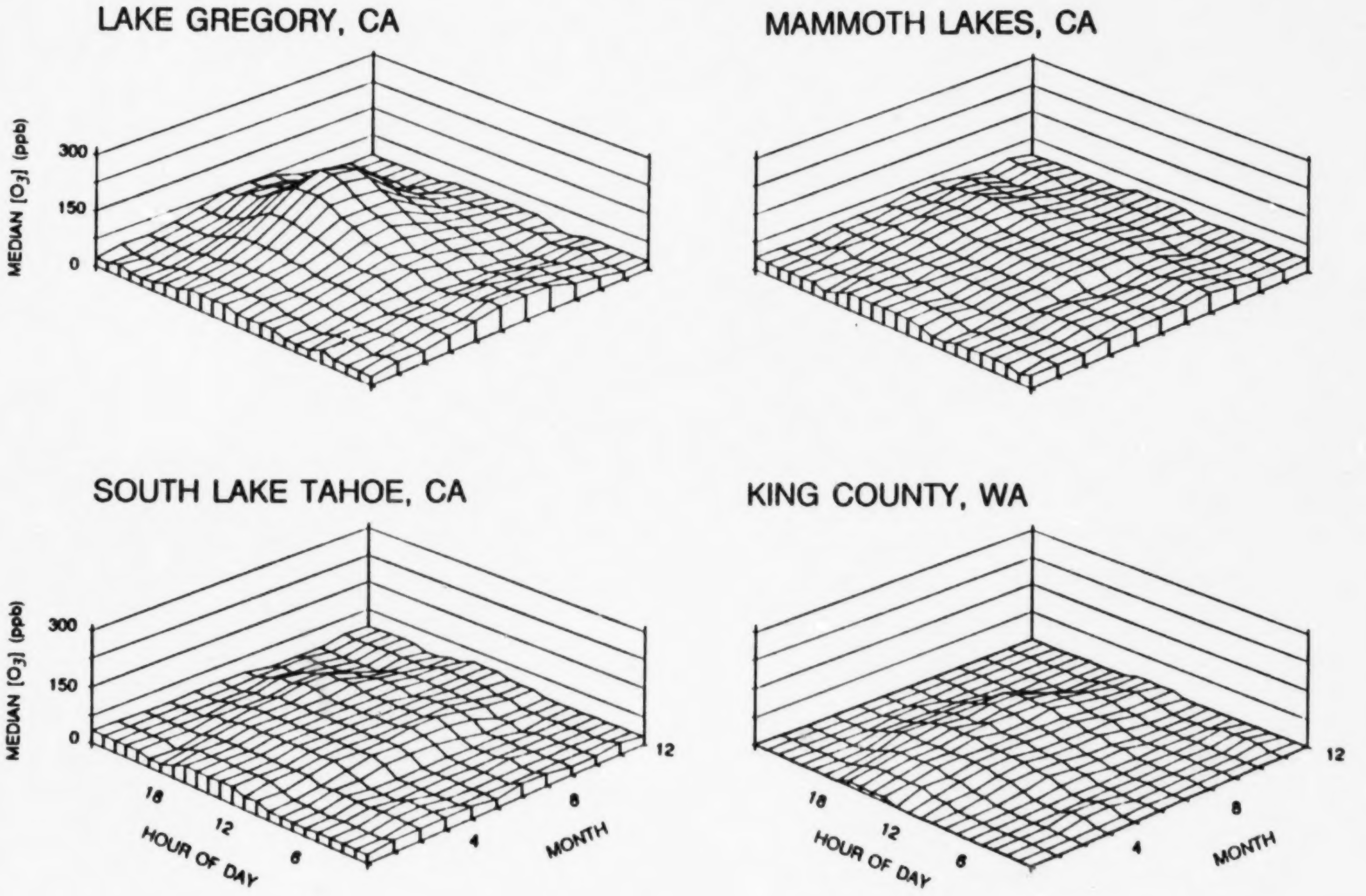

Figure 5. Median diurnal pattern in ambient [O_3] (ppb) by month for Lake Gregory, CA, Mammoth Lakes, CA, South Lake Tahoe, CA, and King County, WA.

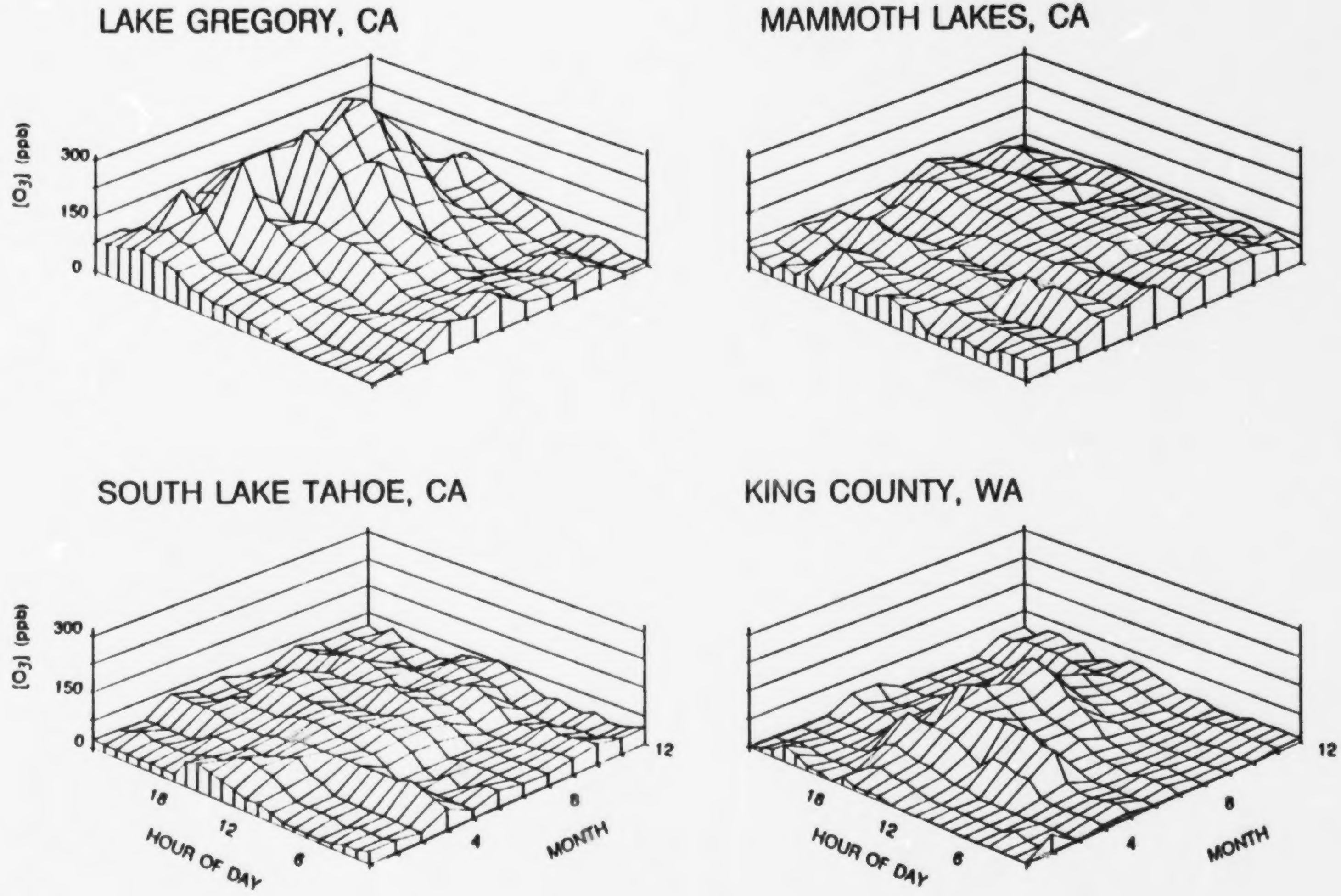

Figure 6. Diurnal patterns for the worst O_3 day (ppb) on record by month for Lake Gregory, CA, Mammoth Lakes, CA, South Lake Tahoe, CA, and King County, WA. Worst day is defined as that with the highest peak concentration.

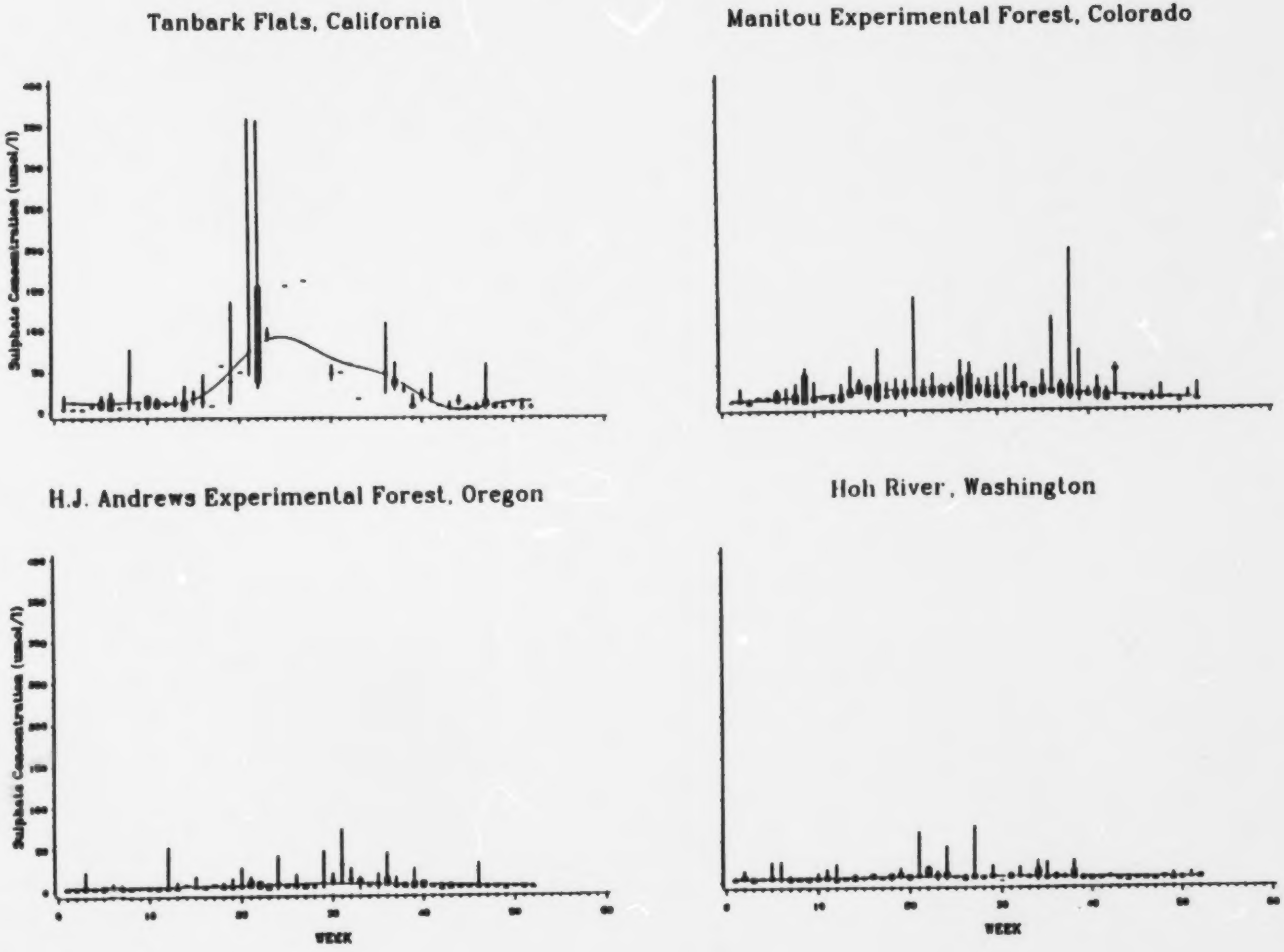

Figure 7. Seasonal patterns in sulfate concentrations in precipitation across the West as described by a Fourier series fitted to the data using least squares regression. The curve is superimposed on the weekly minimum, 25th percentile, 75th percentile, and maxiumum values for the period of record.

Chapter Four

Forest Condition and Trends

Risks to California Forests due to Regional Ozone Pollution: A Data Base and Ranking of Forest Sensitivity	D.C. Peterson and C. Daly	247
Photochemical Oxidant Injury to Ponderosa (*Pinus Ponderosa* Laws.) and Jeffrey Pine (*Pinus Jeffreyi* Grev. and Balf.) in the National Parks of the Sierra Nevada of California	D.M. Duriscoe and K.W. Stolte	261
Ozone Injury to Jeffrey and Ponderosa Pines Surrounding Lake Tahoe, California and Nevada	B.S. Pedersen	279
Ozone Injury and Growth Trends of Ponderosa Pine in the Sierra Nevada	D.L. Peterson, M.J. Arbaugh, and L.J. Robinson	293
Trend of Ozone Damage to Conifer Forests Between 1974 and 1988 in the San Bernardino Mountains of Southern California	P.R. Miller, J.R. McBride, S.L. Schilling, and A.P. Gomez	309
Current and Potential Threats to Biodiversity in Forests of the Lower Pacific Coast States	S. Henderson, R.K. Olson, and R.F. Noss	325
Comparisons of Aircraft and Satellite Sensors for Monitoring Air Pollution Effects on Forests	C.D. Elvidge, J.E. Vogelmann, and C.A. Fox.	337
Early Detection of Air Pollution Injury to Coniferous Forests Using Remote Sensing	S.L. Ustin, B. Curtiss, S.N. Martens, and V.C. Vanderbilt	351
Use of Quality Control Procedures for Assessing Variation in Measurements of Forest Canopy Condition	S.P. Cline, W.G. Burkman and C. D. Geron	379
Analysis of Growth Trends and Variation in Conifers from Arizona and New Mexico	D.A. Graybill and M.R. Rose	395

Risks to California Forests due to Regional Ozone Pollution: A Data Base and Ranking of Forest Sensitivity

Donald C. Peterson, Jr.[1]
Chris Daly[2]

[1] *RCG/Hagler, Bailly, Inc.*
P.O. Drawer O
Boulder, CO

[2] *Systems Applications, Inc.*
101 Lucas Valley Road
San Rafael, CA

INTRODUCTION

Recent declines in growth and vigor, and elevated mortality of forest trees in California have generated increased concern that these changes have been caused by air pollution. The current consensus of the forest-science community is that ozone and other oxidants are influencing the structure and productivity of forest ecosystems in California and in other regions of the United States. However, the magnitude of ozone effects on tree species and forest ecosystems is poorly defined and the exposures producing such effects have not been adequately characterized.

This paper reports a study designed to estimate risks to California forests and forest resources caused by ambient ozone concentrations and to develop a data base of forest resources for use in future analyses by the California Air Resources Board.[1] Three principal research tasks were performed:

1. A data base was constructed of forested resources in California. This data base contains 91 variables describing forest resources in 3,500 forest grid cells. Each grid cell covers approximately 30,000 acres. Data on forest tree species volume, ownership, elevation, soil type, watershed, recreation, and interpolated ozone concentrations are included in the data base.

2. The sensitivity of California forest tree species to ozone was evaluated. While ozone-caused tree injury has been described for specific locations in California, the complexity of this injury has prevented a quantitative characterization of forest tree/ecosystem response to elevated ozone concentrations. This task developed ozone sensitivity rankings for California forest tree species based on available literature and the expert judgment of Dr. Joseph McBride of the University of California at Berkeley and Dr. Paul Miller of the USDA Forest Service and the University of California at Riverside.

3. A risk assessment was performed. Using data contained in the data base and sensitivity rankings established in Task 2, this task evaluated the ozone caused risk to forest resources in California. These results are summarized by ownership category, watershed, county, air basin, and national forest.

Preceding page blank

STUDY METHODS

Forest Resources Data Base

The forests resources data base is a geographically-based archive that provides quantitative information concerning California's forests and related resources. The data base was developed by RCG/Hagler, Bailly, Inc., and Systems Applications, Inc., and currently resides at the California Air Resources Board. Data intended for many different uses and stored in many different formats by a variety of public agencies have been combined to create this archive. A primary source of information for the data base is the Forest and Range Resources Assessment (FRRAP) data base recently created by the California Department of Forestry.[2]

Additional data were gathered from numerous state, federal, and private sources. Ozone monitoring data were obtained from the U.S. Environmental Protection Agency, the California Air Resources Board, and the USDA Forest Service. Data used to calculate timber volume for national forest lands were obtained from timber inventories archived by the USDA Forest Service, Region 5, Timber Plans and Silviculture Division. Recreational use data for national forests in California were obtained from the Recreational Information Management System. Recreational data for California State Parks were acquired from the California Department of Parks and Recreation in Sacramento. Other recreation data were collected from the National Park Service, the Bureau of Land Management, the California Department of Fish and Game, the Army Corps of Engineers, and the Pacific Gas and Electric Company.

The data base is organized on a geodetic grid system with a common origin at 32 N (north latitude) and 125 W (west longitude). The grid contains 8,800 grid cells, each being 0.125 degree latitude by 0.100 degree longitude. However, only about 3,500 cells fall within California's boundaries, and only these are archived in the data base. Average cell size is about 30,000 acres.

Areas in California that contain forest resources are of primary interest in future economic and risk analyses of forest response to air pollutants; areas that do not contain forest resources are of secondary interest. Therefore, grid cells representing unforested areas are covered by a less detailed "basic" data record, while those in forested areas are covered by an "extended" data record.

All grid cells in the data base have a header record and a basic data record (Table I). The header record serves as a geographic locator for the cell. The basic data record provides information on cell area and elevation, vegetative cover, soil type, hydrologic drainages, land ownership, and ozone concentrations. Forested cells have the header record and the extended data record, which includes the basic data record plus data on timber volume and recreational use.

Distributions of Wildlife Habitat Relationship (WHR) cover type, soil series and watershed indicators were supplied by U.C. Berkeley from the FRRAP data base.[3] For each of these variables, the five highest ranking cover types in terms of area covered are reported for each cell, along with the percentage of the cell's area covered by each. The WHR classification scheme describes land use and vegetation cover in 40 categories. The level of aggregation present in WHR coding allows for the resolution of major forest types such as ponderosa pine, Douglas-fir, and redwood as well as non-forest types such as urban-agriculture, grassland, desert scrub, and alpine tundra vegetation.

Ozone concentrations are reported as four statistics: 7-, 9-, 12-, and 24-hour means averaged over the growing season. The use of the mean statistic for ozone exposure has been widely questioned in the published literature. While the relationship of tree or forest response to seasonal mean ozone concentrations is poorly defined and some research has indicated that forest tree response to ozone is influenced by peak rather than mean exposures, the selection of the appropriate exposure index or profile remains a focus of considerable debate. Because the purpose of the risk analysis was to provide a preliminary assessment based on currently available data, seasonal mean statistics were used to characterize ozone exposures across the state. These concentrations were not used to predict specific tree responses, but only to indicate the relative magnitude of ozone exposures across forested grid cells.

The statistics represent ozone conditions during the period 1977–81. This period was chosen to make maximum use of USDA Forest Service monitoring data that were collected in the southern Sierra during the late 1970s; many of these stations are not operating at present.[4] By using data from these stations, we were able to obtain a better representation of ozone concentrations in forested areas than if we used more recent, but less complete data. Locations of ozone monitoring stations used in kriging ozone concentration are shown in Figure 1.

Hourly ozone data for the analysis were obtained on magnetic tape from the ARB and on hard copy from the USDA Forest Service. The Forest Service data, totaling about 97,000 hours from seven sites, were double-entered by keypunch operators. Many of the 147 ARB sites could not be used in the analysis because site information (i.e., location and elevation) was not available. About a dozen sites had incorrect information, but they were subsequently corrected using updated information provided by the ARB project officer.

The data were first reduced by computing the 7-, 9-, 12-, and 24-hour means and variances for each day. A mean and variance were calculated for a day only if at least two-thirds of the hours had valid data. The length of the growing season was determined by the elevation and latitude of the forested grid cells. Depending on these factors, the growing season ranged from 7 months (April through October) to 4 months (June through September).

The means and variances for each day were then averaged to estimate a growing season average and a standard deviation at each of the stations for all years during the period 1977–81. Stations having less than two-thirds of the growing season days present in the 1977–81 period were not included in the analysis.

The spatial density of ozone monitoring stations is much higher in urban areas than in rural areas. The regions of most importance to this study are the higher elevation rural areas. Available techniques for reducing the sampling bias depend on the process used to select stations for interpolation. Three options for station selection were

1. selecting the highest elevation stations
2. selecting the stations with the most data and
3. selecting stations with the highest ozone concentrations.

Selecting stations on the basis of elevation seemed most plausible, as most forests are located at moderate elevations. The selection process involved searching along rows and columns If two stations were found within two grid cells of one another, the lower station was omitted. This procedure ensured that stations at higher elevations, where presumably more forest coverage would be present, would remain in the data set. The two grid cell sphere of influence seemed to work quite well. After the selection process, the data set consisted of 104 stations scattered relatively uniformly throughout California. Further reduction either by searching along diagonals or by increasing the distance of separation leaves too few stations and also eliminates some of the Forest Service high elevation sites.

The 7-, 9-, 12-, and 24-h growing season statistics were interpolated using the same kriging methodology described in Lefohn et al.[5] The computer software used in that study was obtained from Peter Knudsen of the Montana School of Mines and was applied in the present analysis. The station average concentrations were used to estimate a variogram, which describes how the variance in the difference between two stations changes with increasing separation distance. The parameters of an analytic model built into the software were fitted to the observed variogram data by eye and by trial and error. A regression analysis was performed on the average concentrations as a function of the station elevation; no statistically significant systematic relation of ozone concentration with elevation was found. Average concentrations were kriged at each grid cell in the database with the assumption that the stations resided on a flat surface.

Quality assurance was conducted through several procedures. Tables of average concentrations were inspected to assure that 24-h averages were less than 7-, 9-, or 12-h averages. In remote areas it is possible for the kriging approach to produce unreliable concentrations when forced to extrapolate, but no such problem was found. The concentration fields were plotted and visually inspected. The 12-h average concentration fields appear similar to those hand drawn by Thompson and Olszyk[6] for 1984. Distinguishing features such as the minimum over the San Francisco Bay area, a maximum in the South Coast Air Basin and the tongue of elevated concentrations extending into the lower San Joaquin Valley are reproduced accurately.

Forest Tree Species Sensitivity to Ozone

Tree species sensitivity to ozone damage was evaluated for use in the forest risk assessment. Results of this evaluation are contained in Peterson et al., and are available from the California Air Resources Board.[1] Evaluations were based on available literature and the expert judgment of the investigators, Dr. Joseph McBride of the University of California at Berkeley and Dr. Paul Miller of the USDA Forest Service and the University of California at Riverside.

Tree species were assigned to one of four sensitivity classes: tolerant, intermediate, sensitive, and no available information based on current literature. Sensitivity was assessed taking into account growth decrement and foliar injury as well as field, chamber, and laboratory experiments. Sensitivity rankings are not necessarily based on ozone exposures that are closely related to ambient air quality. However, they provide an assessment of relative sensitivity to ozone based on the currently available scientific information and the expert judgment of scientists familiar with ozone-caused forest injury in California.

Risk Assessment

Risk estimates are based on data contained in the forest data base and on the estimated sensitivity of California tree species to ozone. While the current

Preceding page blank

consensus in the forest science community is that ozone is influencing tree health in specific regions in California, surveys have concentrated on areas south of Lake Tahoe in the Sierra Nevada. Therefore, it is not possible to state with certainty how wide spread ozone injury is in California forests.

In lieu of a rigorous answer to the above issue, the risk assessment provides an assessment of California forest sensitivities and estimated exposures to ozone. Information on forest tree sensitivity and ozone exposure were coupled with information contained in the data base to provide a preliminary assessment of ozone-caused risk to forested resources in California and to guide future policy decisions and research. Four separate forest risk measures were developed:

Class 1: Highest Risk—high ozone exposure and high forest tree vulnerability
Class 2: High Risk—currently low ozone exposure but high vulnerability
Class 3: Low Risk—high ozone exposure but low vulnerability
Class 4: Lowest Risk—low ozone exposure and low vulnerability

Forest vulnerability in a cell was estimated as a function of species composition and volume as well as tree species sensitivity to ozone. Vulnerability was estimated in four steps for each cell containing both ozone and forest volume data.

First, scaled abundance values for tree species by grid cell were calculated by:

$$A_i = \frac{B_i}{a} \qquad [1]$$

Where:

A = the scaled abundance species or species group i
B_i = the volume for species or species group i
a = the area of the grid cell

Note that cell volume estimates (B) are available in the data base for the five most common tree species in a grid cell. Hence, cell volume estimates do not reflect species volumes that were not present in the top five species groups.

After scaled abundance values were calculated for each reported species, maximum abundance factors were calculated for species volume estimates. These were derived by summing the reported species volume estimates within each cell in the data base, and dividing total volume estimates for each cell by the cell's estimated area. Scaled abundance values were assigned to one of three abundance classes and assigned a ranked abundance ($A_{r(i)}$) based on their position in the distribution. Ranked abundance was 3 for the upper third of the distribution, 2 for the middle third, and 1 for the lower third of the distribution.

Ranked abundance values provide a simple measure of the abundance of a given species per unit area in a grid cell relative to other species and grid cells. This allows for simple and consistent comparisons of abundance across species and cells in the data base.

Vulnerability of the forest grid cells was estimated by multiplying ranked abundance and sensitivity for each species present in the cell and summing them, then dividing by the number of species groups for which ozone sensitivity had been ranked:

$$V = \frac{\sum_{i=1}^{n} A_{r(i)} S_i}{m} \qquad [2]$$

Where:

V = the vulnerability of the forest

$A_{r(i)}$ = the ranked abundance of species i (1 = lower $\frac{1}{3}$, 2 = middle $\frac{1}{3}$, 3 = upper $\frac{1}{3}$ of the distribution of tree species ranked abundance)

S_i = the sensitivity of species i (1 = tolerant, 2 = intermediate, 3 = sensitive)

m = the number of species/species groups for which ozone sensitivity has been ranked

Species not ranked for ozone sensitivity were assigned a value of zero for the variable S in equation 2. Therefore, the presence of unranked species groups did not enter into the calculation of cell vulnerability. Forest vulnerability, as estimated in equation 2, can range from 0 to 9. A value of 9 would depict forest tree species most vulnerable to ozone and would occur when all ranked species within a heavily forested grid cell were classified as sensitive to ozone. A value of 0 would indicate that no information on species sensitivity is available in that cell. A low, nonzero value occurs when sensitive species are not abundant.

To implement the risk ranking categories introduced above, vulnerability rankings were separated into two classes. Cells with vulnerability values found in the lower 50 percent of the distribution of cell vulnerabilities were classified as "low vulnerability" cells. Cells with vulnerability values found in the upper half of the distribution were assigned "high vulnerability" values.

The threshold separating low and high ozone exposures was based on the ARB report *Effect of Ozone on Vegetation and Possible Alternative Ambient Air Quality Standards*[7] and the modeled ambient 12-hour ozone concentrations in the data base.

This report compared four different seasonal 12-h ozone standards on the basis of their ability to protect vegetation from adverse effects due to ozone. The four concentrations ranged from a high 3-month, 12-h mean of 6 pphm concentration to a low 3-month, 12-h mean of 4 pphm. The report concluded that the 6 pphm concentration "is not very protective of vegetation." The 5 pphm concentration was considered "slightly protective of vegetation [although it was recognized that it would not] significantly protect natural vegetation such as the forest trees of the Sierra Nevada and Southern California." 4.5 pphm was recognized to provide "some protection for forest trees."

A total of 1,509 cells in the data base have records for seasonal 12-h ozone concentrations. These records range from a low of 1.58 pphm to a maximum value of 9.72 pphm. The mid-point of the distribution is 45.3 pphm. The first and third quartiles are 3.44 pphm and 4.97 pphm, respectively. The mean concentration of 4.5 pphm had a cumulative percent of 58.3, indicating that approximately 42% of the cells had higher 12-h seasonal mean ozone values. 5.0 pphm had a cumulative percent of 75.5, indicating that approximately 25% of the cells had higher 12-h seasonal mean ozone values. 5.5 pphm had a cumulative percent of 84.8, with approximately 15% of the cells having higher ozone values. Risk analyses were performed with three different ozone threshold values. These values are 4.5 pphm, 5.0 pphm, and 5.5 pphm 12-h seasonal averages.

The four point risk ranking enables investigators and policy makers to identify those forested areas at different levels of risk due to ozone concentrations. The data used to create these risk indices are more finely resolved than simple "high" and "low" estimates. However, a simple, clearly defined risk index is both more understandable and more easily justified, giving uncertainties in the existing data, when used in subsequent decision-making and research planning procedures.

RESULTS

Results of the risk analysis were presented in Peterson et al.[1] at five different levels:

- state-wide
- ARB air basin
- county
- ownership category
- National Forest

Only the state-wide results are presented in this paper.

The total number of cells in the highest risk category (Category 1) ranged from 339 when the lowest ozone threshold (4.5 pphm) was used to 112 when the highest threshold (5.5 pphm) was used. These results are summarized in Table II, along with summaries for the remaining risk categories and the middle, or 5.0 pphm scenario.

In the 4.5 pphm scenario, forested cells were classified as highest risk (21.5%), high risk (30%), low risk (21.4%), and lowest risk (27.1%). Under the 5.0 pphm scenario, the percentage of cells in the sum of the highest and high risk categories remained the same, but the percentage of cells in the highest risk category declined to 13.1 percent. As expected, the percentage of cells in the low risk category declined, and the percentage of cells in the lowest risk category increased. In the 5.5 pphm scenario, the shift of cells out of the high ozone risk categories is even more emphatic, with only approximately 16% of the cells remaining in risk categories 1 and 3.

Figures 2, 3, and 4 map the distribution of risk categories over California by grid cell for each of the three ozone scenarios. Figure 3 represents the statewide distribution of ozone-caused forest risk, assuming the 5.0 pphm ozone scenario. In this scenario, northern California is generally represented as being at "high" and "lowest" risk. These categories denote lower ozone exposure, coupled with higher and lower cell vulnerability values, respectively. Numerous cells in the central and southern Sierras are classified as being at "highest" risk, meaning that cells were exposed to high ozone concentrations and that they possessed high vulnerability values. Cell vulnerability is a function of species sensitivity and abundance. Forested cells in southern California are shown as being exposed to high ozone concentrations, but because of their lower species volume estimates, they were assigned lower ranked abundance values, resulting in a "low" risk classification.

CONCLUSIONS

This study is unique in the scope of its coverage and detail. No previous study has evaluated the risk of ozone to so many California tree species, covered such a wide geographic area, and such a variety of forest resources. Data base development relied on available secondary information provided by the USDA Forest Service, the Forest and Rangeland Resources Assessment Program, the U.S. Department of the Interior, and other governmental and private sources. Data provided by these sources were incorporated into the data base without performing exhaustive quality assurance and verification.

This reliance on secondary data is not the major source of uncertainty. Estimated ozone concentrations in forested grid cells are based on 1977–81 ozone monitoring data and have very wide margins of error. In addition, knowledge of forest injury due to ozone is extremely limited and uncertain. The results of the risk analysis should, therefore, be interpreted as broad approximations. By defining four separate risk categories for forested grid cells, we have avoided making overly precise judgments of risk and have provided researchers with a useful taxonomy of forest risk due to ozone concentrations.

ACKNOWLEDGMENTS

Work reported in this paper was performed for the California Air Resources Board under contract No. A6-049-32 by RCG/Hagler, Bailly, Inc. with the assistance of Systems Applications, Inc.

REFERENCES

1. D.C. Peterson, R.D. Rowe, J.K. Sueher, C. Daly, G. Moore, and S. Hayes, "Risks to California forests due to regional air pollution," prepared for the Research Division, California Air Resources Board by RCG/Hagler, Bailly, Inc., Boulder, CO, 1988.

2. Forest and Rangeland Resources Assessment Program, *California's Forests and Rangelands: Growing Conflict over Changing Uses*, California Department of Forestry and Fire Protection, Sacramento, CA, 1988, 348pp.

3. L. Davis, University of California, Berkeley, private communication, 1988.

4. G. Moore, Systems Applications, Inc., San Rafael, CA, private communication, 1988.

5. A.S. Lefohn, H.P Kundsen, J.A. Logan, J. Simpson, and C. Bhumralkar, "An evaluation of the kriging method to predict 7-h seasonal mean ozone concentrations for estimating crop losses," *JAPCA* 37:595 (1987).

6. C.R. Thompson and D.M. Olsyzk, "Crop loss from air pollutants assessment program, interim report," prepared by Statewide Air Pollution Research Center, Riverside, CA, 1986.

7. California Air Resources Board, "Effects of ozone on vegetation and possible alternative ambient air quality standards," technical support document, Research Division, Sacramento, CA, 1987.

Table I. Variable categories in the header, basic, and extended data records.

Variable	Units
Header	
Grid locator	x,y
Latitude/longitude of Cell Center	deg.
Air basin indicator	–
County code distribution	–
Basic Data	
Area of cell	acres
Average elevation of cell	meters
WHR cover type distribution (up to 5)	–
Soil series distriubtion (up to 5)	–
Watershed distribution (up to 5)	–
Ownership distribution	–
Ozone concentrations (24-, 12-, 9-, and 7-hour Averages over growing season	pphm
Extended Data	
Timber volume by species– USDA Forest Service (top 5 species)	1000s ft^3
Timber volume by species group– other lands (top 5 species groups)	1000s ft^3
Recreational usage total for each reporting agency 1981-1985 (1 total for each agency; up to 7 agencies)	user-days/yr
Recreational usage totals for USDA Forest Service lands, broken down by 5 activity classes, 1985 only (5 totals)	user-days/yr

Table II. Distribution of risk categories by ozone risk scenario (ozone expressed as 12-h seasonal means).

Ozone (pphm)	Risk	Frequency	Percent	Cumulative Frequency	Cumulative Percent
4.5					
	1	339	21.5	339	21.5
	2	474	30.0	813	51.5
	3	338	21.4	1151	72.9
	4	427	27.1	1578	100.0
5.0					
	1	206	13.1	206	13.1
	2	607	38.5	813	51.5
	3	194	12.3	1007	63.8
	4	571	36.2	1578	100.0
5.5					
	1	112	7.1	112	7.1
	2	701	44.4	813	51.5
	3	146	9.3	959	60.8
	4	619	39.2	1578	100.0

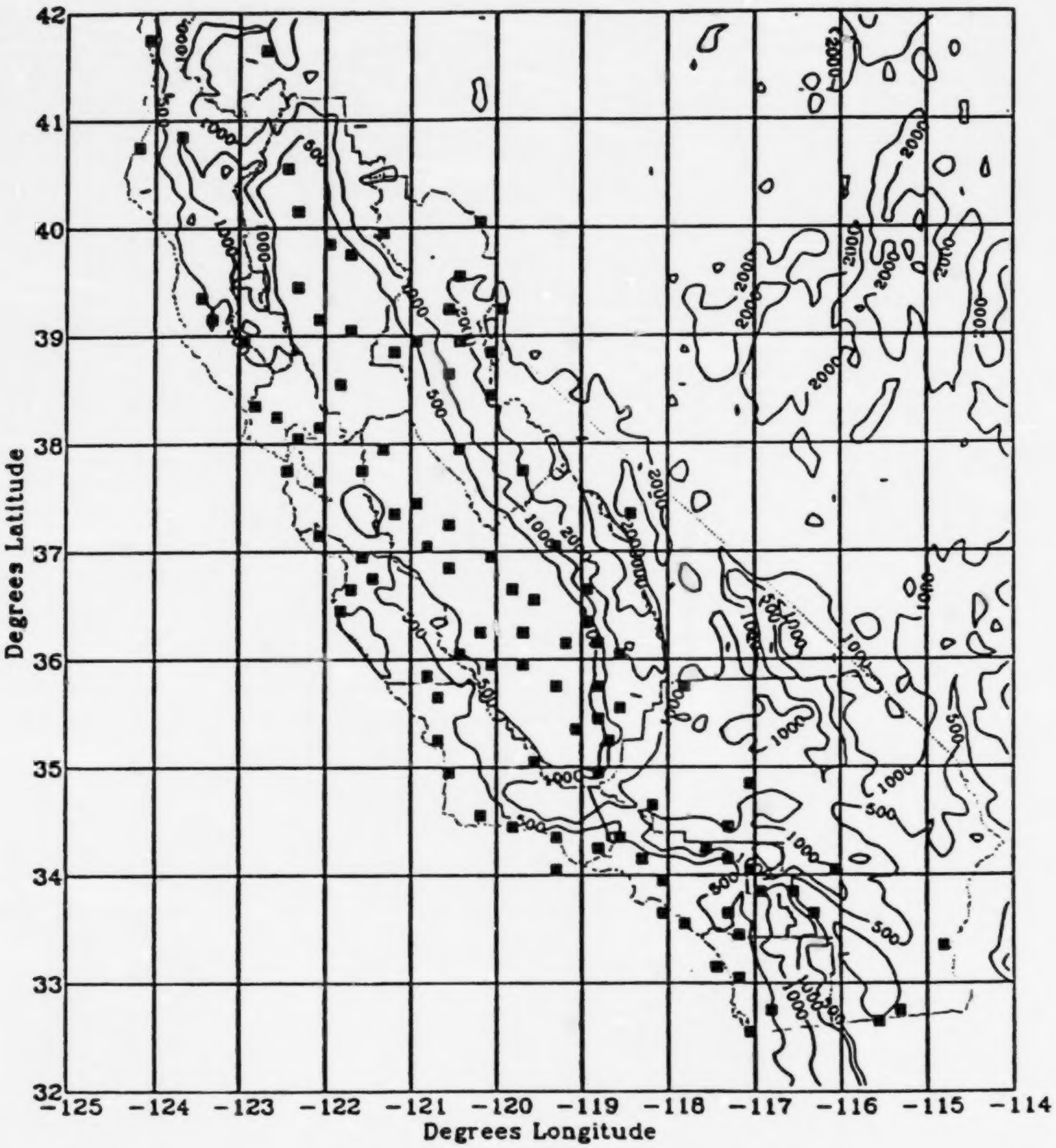

Degrees Latitude
Degrees Longitude
42
41
40
39
38
37
36
35
34
33
32
−125
−124
−123
−122
−121
−120
−119
−118
−117
−116
−115
−114
500
1000
2000

Figure 1. Locations of ozone monitoring stations used in the kriging procedure. The grid cells encompassing the coordinates of the stations are shaded. Contours represent elevation, expressed in meters.

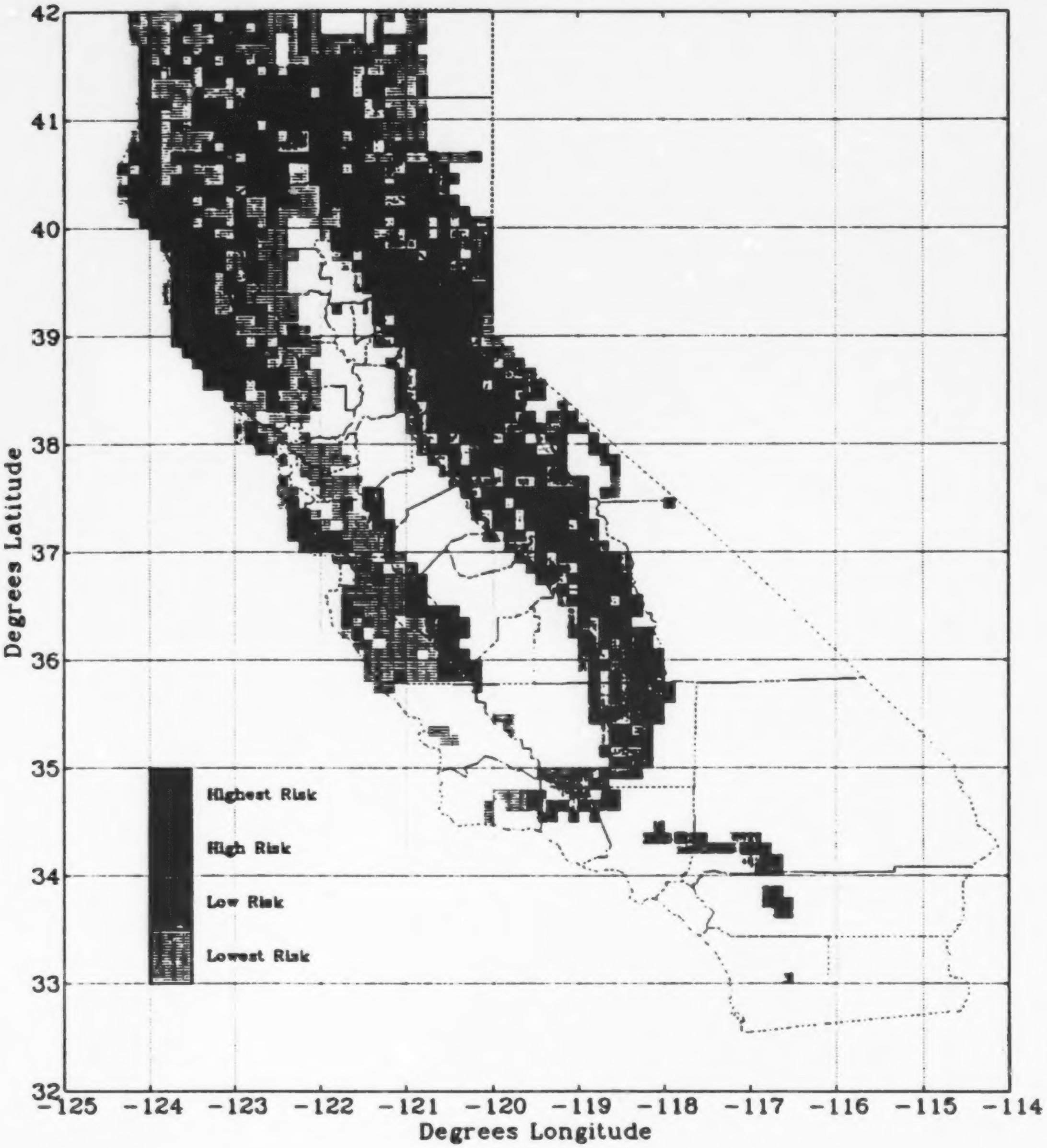
Highest Risk
High Risk
Low Risk
Lowest Risk
Degrees Latitude
Degrees Longitude
42
41
40
39
38
37
36
35
34
33
32
−125
−124
−123
−122
−121
−120
−119
−118
−117
−116
−115
−114

Figure 2. Statewide distribution of forest risk categories assuming 4.5 pphm ozone scenario.

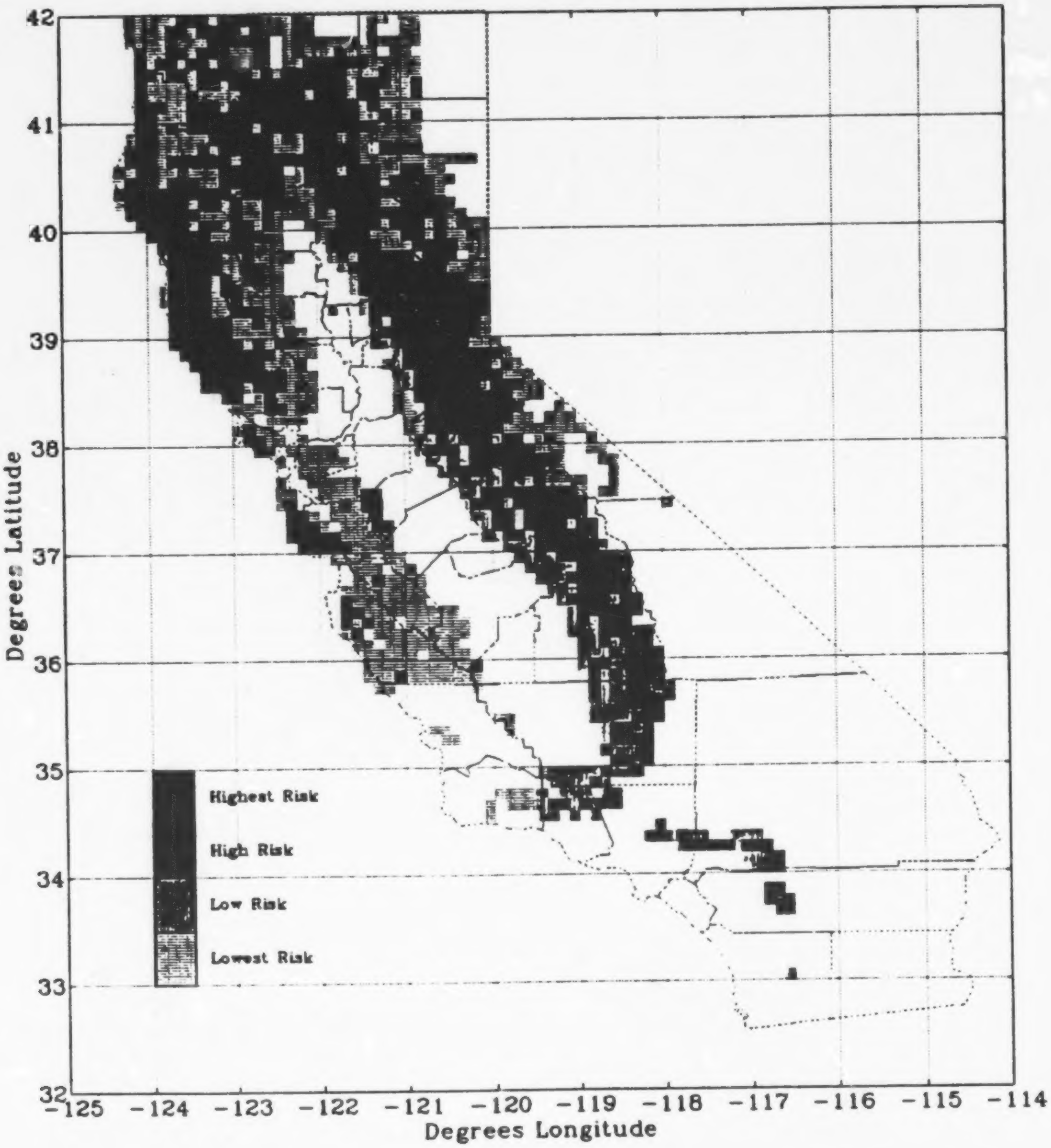
42
41
40
39
38
37
36
35
34
33
32
Degrees Latitude
-125
-124
-123
-122
-121
-120
-119
-118
-117
-116
-115
-114
Degrees Longitude
Highest Risk
High Risk
Low Risk
Lowest Risk

Figure 3. Statewide distribution of forest risk categories assuming 5.0 pphm ozone scenario.

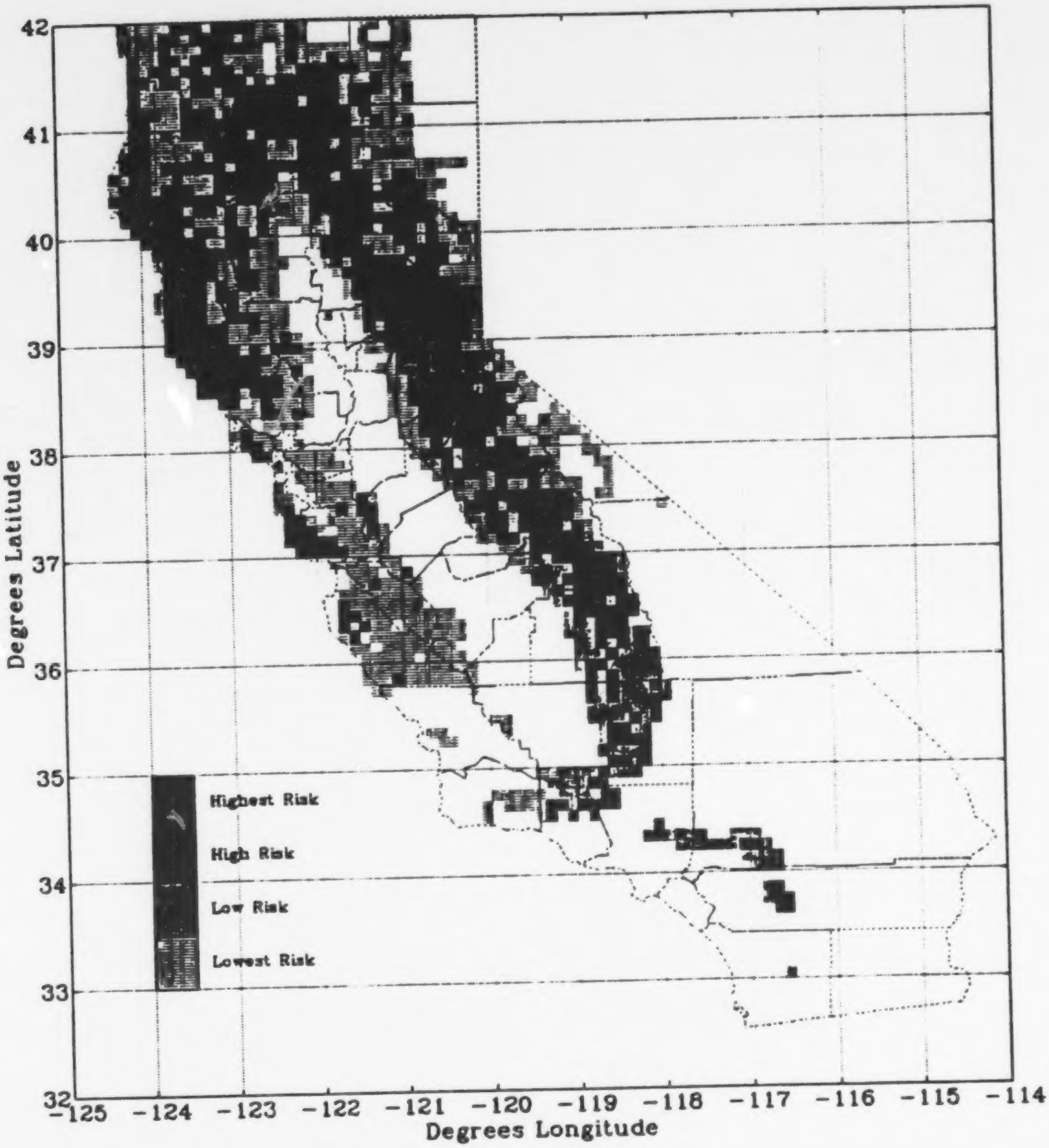
Highest Risk
High Risk
Low Risk
Lowest Risk
Degrees Latitude
42
41
40
39
38
37
36
35
34
33
32
-125
-124
-123
-122
-121
-120
-119
-118
-117
-116
-115
-114
Degrees Longitude

Figure 4. Statewide distribution of forest risk categories assuming 5.5 pphm ozone scenario.

Photochemical Oxidant Injury to Ponderosa Pine (*Pinus ponderosa* Laws.) and Jeffrey Pine (*Pinus Jeffreyi* Grev. and Balf.) in the National Parks of the Sierra Nevada of California

Daniel M. Duriscoe[1]
Kenneth W. Stolte[2]

[1] *Eridanus Research Associates*
42403 Sierra Drive
Three Rivers, CA 93271

[2] *U. S. Department of Interior*
National Park Service, Air Quality Division
12795 W. Alameda Drive
Lakewood, CO 80225

INTRODUCTION

Western yellow pines, including ponderosa pine (*Pinus ponderosa* Laws.) and Jeffrey pine (*Pinus jeffreyi* Grev. and Balf.), are important tree species in the mixed coniferous forest of the Sierra Nevada of California. Ponderosa pine dominates forest stands on xeric, sunny sites between 600 and 1800 meters in elevation (2000 to 6000 feet) in the northern part of the range and between 1200 and 2150 meters (4000 and 7000 feet) in the south. Jeffrey pine occurs on drier, rockier sites between 1500 and 2500 meters (5000 and 8000 feet) and is occasionally found at elevations up to 3300 meters (10,000 feet) in the southern part of the range. These species exhibit a known sensitivity to atmospheric photochemical oxidant (primarily ozone) pollution.[1] The symptoms of ozone stress include visible injury to the foliage, consisting of a chlorotic mottle beginning at the tips of the needles and premature needle abscission.[2] Ozone injury to the foliage of these species in the Sierra Nevada of California was documented as early as 1971.[3] In 1975, monitoring of visible injury on yellow pines was initiated on National Forest lands of the western Sierra Nevada and has continued to the present.[4-7] This monitoring effort has shown that the percentage of pines in plots with chlorotic mottle has increased from about 20% in 1977 to about 55% in 1988 in the Sierra and Sequoia National Forests and that the severity of injury also has increased.[8]

In 1980, the staff of Sequoia and Kings Canyon National Parks began to establish a network of 54 yellow pine plots to monitor oxidant air pollution injury using methods patterned after the Forest Service surveys.[9,10] These methods are referred to as the FPM (Forest Pest Management) method. The survey was completed in 1982, and it indicated that 36% of the trees sampled exhibited symptoms of chlorotic mottle. A portion of these plots in areas bordering the San Joaquin Valley where the incidence and severity of visible injury symptoms was greatest were reevaluated in 1984[11] and in 1985[12] by using methods developed by the National Park Service.[13]

These permanent plots have served to locate and mark trees for long-term monitoring and assessment of temporal trends in oxidant air pollution effects. Although plots have been located in nearly all areas of mixed conifer forests within the national park boundaries, inferences regarding spatial trends and population-wide effects have been difficult to make because the systematic design used for locating the plots may have produced a sample of individuals that may not be representative of the population as a whole.[8] In 1986, a cruise survey of ponderosa and Jeffrey pines in Sequoia, Kings Canyon, and Yosemite National Parks was conducted using a sampling design that included a large number of sample points randomly located throughout the mixed coniferous forest. The objective of this survey was to assess the extent and severity of oxidant visible injury to yellow pines on a population-wide basis and to identify geographic variation in oxidant pollution effects, including the percentage of trees showing any signs of injury, the magnitude of injury severity, and the identification of areas where injury is particularly severe or noticeably absent.

Study Area

The national parks of the Sierra Nevada include Sequoia, Kings Canyon, and Yosemite (Figure 1). They range in elevation from 300 to 4400 meters (1000 to 14,494 feet) and include several forest types. The geographic extent of the Sierran mixed coniferous forest (sugar pine, ponderosa pine, Jeffrey pine, white fir, red fir, and giant sequoia) was identified from existing vegetation type maps. The elevational range of the mixed conifer forest is from 900 to 2400 meters (3000 to 8000 feet). Ponderosa and Jeffrey pines occur throughout this area on more xeric sites. Sequoia and Kings Canyon National Parks are contiguous and are treated as one unit in this paper.

METHODS

Sampling Design

Permanent Plots. Methods of locating permanent monitoring plots as well as individual trees within plots in Sequoia and Kings Canyon National Parks have been described in previous papers.[5,9] Plots were located at 1000-ft elevation contour intervals along road and trails between 4000 and 8000 ft. Ten trees were selected systematically for inclusion in each plot. This paper presents data from 28 of the 54 plots that were reevaluated in 1984-85. These 28 plots are located near the San Joaquin Valley and represent the areas of the parks that experience the greatest ozone injury. Statistics on incidence and severity of injury therefore may not be compared directly to the cruise survey of 1986.

Cruise Survey. The cruise survey invoked an areally stratified random sampling design. A grid 3.2 km (2.0 miles) square with a north-south orientation was placed over a map of the area of occurrence of yellow pines in each of the three national parks. Only squares that contained some portion of mapped western yellow pine type accessible by road or trail were used. A random point was located on the road or trail network and used as the sample point. Two hundred and thirty-one sample points were identified in this manner on the map. After field checking each point, 208 were found to actually be in the yellow pine type.

At each sample point, trees were selected systematically. A random compass bearing was obtained, and a circular plot of 20-m radius was swept out in a clockwise direction using the random bearing as a starting point. The first 15 pruneable pines (with lowest branches within 7 m of the ground) encountered falling within the area swept out were utilized as sample trees. If the circle was closed without sampling 15 trees, the 15 closest to the sample point were then chosen regardless of compass bearing. Trees with a diameter at breast height (dbh) of less than 5 cm were not used. Two hundred and eight points, 98 in Sequoia and Kings Canyon (1470 trees) and 110 in Yosemite (1650), were evaluated during the summer of 1986.

Ozone Injury Evaluation

Permanent Plots. The 1980-82 plot work in Sequoia and Kings Canyon used the FPM method of injury evaluation. The FPM system is a count of the number of annual whorls of foliage on a branch that are free of chlorotic mottle, ranging from 0 to 4 (trees with more than four whorls free of chlorotic mottle are often rated as 4^+, but count the same as trees rated 4 in data analysis). Thus, lower scores in the FPM system indicate more severe injury than higher scores. A minimum of three branches were pruned at random from the lower crown of each tree and examined by hand for chlorotic mottle. A representative branch was selected for recording data on a particular tree.

In 1984, the National Park Service Air Quality Division (AQD) devised a more comprehensive method of pine plot evaluation.[13] Each annual whorl was scored by visually estimating the percentage of chlorotic mottle covering the surface of the needles. Other abiotic and biotic foliar injuries were also rated in a similar manner. Additionally, the modal needle length to the nearest centimeter and an estimate of the percent of fascicle retention based on the appearance of abscission scars were recorded. Data were recorded for each whorl of five branches pruned from the lower crown of each tree. Tree level data were derived by averaging percentages for all whorls and all permanent plots. The AQD method was used in the 1984 and 1985 evaluations of permanent plots. Results presented in this paper utilize the FPM system of scoring; the 1984-85 evaluations have been converted from AQD to FPM scores so that they may be directly compared with the 1980-82 evaluations.

Cruise Survey. The cruise surveys in 1986 used a 0 to 3 scale for estimates of chlorotic mottle cover, where zero represented no visible injury, 1 = 1% to 10% chlorotic mottle, 2 = 11% to 30% chlorotic mottle, and 3 = 31% to 100% chlorotic mottle coverage of the total needle surface area on a particular needle whorl. This scale approximates a square root transformation of percentage foliar injury data, which is appropriate for visible injury measurements of this type in areas with slight injury.[12,14] Foliage of different ages (needle whorls on branches) were evaluated separately. The score for an individual tree was calculated by taking the average of all whorl scores. The method of branch selection followed the FPM method (a representative branch selected from a minimum of three). The scoring of individual whorls also allowed the computation of tree scores using the FPM system. FPM scores are presented in the analysis for the purpose of comparison with previous work.

Analytical Methods

Data on incidence and severity of injury from permanent plots were aggregated for each evaluation period and the means compared using paired t-tests. Bivariate linear regression was utilized in an analysis of trends in ozone injury with elevation. An analysis of the residuals from these regressions was done to test for departures from normality for both incidence and severity data. No serious departures from normality were observed. The response of needle retention to severity of chlorotic mottle was examined using bivariate linear regression with needle whorl retention as the dependent variable.

RESULTS AND DISCUSSION

Permanent Plots

In Sequoia and Kings Canyon National Parks, the initial 1980-82 evaluation of ozone injury in ponderosa and Jeffrey pine plots indicated that the greatest injury (foliage chlorotic mottle) occurred along the west side of Sequoia Park, principally in the North, Middle, and Marble forks of the Kaweah River bordering the San Joaquin Valley.[9] Subsequent reevaluations of 28 permanent plots in these areas of greatest injury in 1984–85 showed an increase in the amount of foliar injury on plot trees and an increase in the percentage of trees injured in each plot (Table I). Twenty two of the plots had increased foliar injury, four had an improved foliar condition, and two had no change in foliar injury. Twenty four of the plots had an increased number of trees with injury, and four plots showed no change in the number of trees injured (Table 1). The mean FPM plot scores dropped (injury increased) from 2.8 in 1980-82 to 2.4 in 1984–85 ($t = 3.98$; $p = <0.001$). The mean percentage of trees injured in plots increased from 47% in 1980–82 to 79% in 1984–85 ($t = -8.13$; $p = <0.001$). There was a general increase in foliar injury on injured trees and an increase in the percentage of trees with injury in plots in the South Fork of the Kings River in Kings Canyon National Park, and in the North, Marble, East, and South Fork of the Kaweah River in Sequoia National Park. Only four plots in the Middle Fork of the Kaweah River showed any improvement in foliage condition (Table I). There was, however, a general increase in the percentage of trees injured in plots in this drainage. The increase in foliar injury was especially severe in the plot at Swale Camp, near Grant Grove in Kings Canyon National Park, where injury increased from a FPM score of 2.7 in 1980–82 to 0.9 in 1984–85. This indicates that ozone foliar injury was observed mostly on fourth or older whorls in 1980–82, and in 1984–85 had progressed, at the branch level, to the second or older whorls. The percentage of trees injured in this plot increased from 50 to 100% (Table I).

The increase in injury in most of the river drainages in Sequoia and Kings Canyon National Parks indicates either an increase in ozone dose due to increased ambient ozone concentrations in those drainages, increased sensitivity of the species to ozone, or differences in observor quantification of injury. While differences in observor scoring could be expected to produce some variability in the data, the large increases in injury are greater than one would expect from trained observer bias. Since the observers who conducted either the 1984 or 1985 plot reevaluations also participated in the 1980–82 plot evaluations, observer bias is not believed to be a significant factor in the increased injury scores. There is currently insufficient monitoring of either ambient ozone levels or environmental variables in the western river drainages of these parks to determine the causal agent of the injury increase. Ozone monitoring in the coniferous zones of Sequoia and Kings Canyon is currently limited to one ozone monitor in the Marble Fork of the Kaweah River at approximately 1800 m in elevation. Ambient ozone levels at this site typically exhibit a diurnal pattern with hourly averages frequently peaking at 0.08–0.10 ppm but seldom exceeding the National Ambient Air Quality Standard (NAAQS) of 0.12 ppm per hour. In 1988, there was only one NAAQS exceedence of ozone in Sequoia National Park.[15] The similarity in the degree of foliar injury (Table I) in river drainages of Sequoia and Kings Canyon suggests that other forks of the Kaweah River may be subjected to ambient ozone levels similar to those observed in the Marble Fork of the Kaweah. The NAAQS for ozone does not appear to protect sensitive yellow pine genotypes in Sequoia National Park from injury.

The severity of foliar injury and the percentage of trees injured in each plot was observed to decrease as elevation increased. Figure 2 shows a significant relationship between FPM plot scores and elevation for both 1980-82 ($p < 0.001$; $r = 0.58$) and 1984-85 ($p = 0.005$; $r = 0.51$). Although the correlations are weak, they do indicate an apparent trend of decreasing ozone injury with elevation. Other studies evaluating ozone injury on ponderosa and

Jeffrey pines in the Sierra Nevada also have observed the greatest foliar injury at lower elevation sites.[6,16] The similarity of the slopes of both lines suggests that the increase in severity of injury between 1980–82 and 1984–85 was consistent at all elevations. A similar trend was noted for the correlation of percentage of trees injured and elevation (Figure 3). There was a significant correlation between the percentage of trees injured in 1980-82 ($p = 0.036$; $r = -0.40$) and in 1984–85 ($p = 0.011$; $r = -0.47$) with elevation. The slopes of both correlations are similar and indicate a trend of decreasing percentage of trees injured per plot with elevation. The substantial upward displacement of the 1984–85 slope emphasizes the increase in percent trees injured between 1980–82 and 1984–85. The similarity in the slopes for 1980–82 and 1984–85 suggests that the increases in percentage of trees injured occurred consistently at all elevations.

Cruise Survey

Of the 3120 trees observed on a population-wide basis in Sequoia, Kings Canyon, and Yosemite National Parks in 1986, 1053 or 33.75% were found to have some evidence of ozone mottle on the foliage. The average FPM score of all trees observed was 3.45; the average injury found in the population as a whole was very slight. The range of tree scores, however, encompassed the entire range of possible scores from 0 (severe injury) to 4 (no injury) indicating that some trees within the population were severely injured. Ponderosa pines comprised 32.1% of the sample (1001 trees), while Jeffrey pines made up 67.9% (2119 trees). The mean ozone injury score for ponderosa pines indicated that they were more severely injured than Jeffrey pine (3.09 for ponderosa, 3.62 for Jeffrey).

Ozone injury to pines was observed to be more severe in Sequoia and Kings Canyon National Parks (average score 3.35) than in Yosemite National Park (average score 3.54). An independent-sample t-test of these two means showed a significant difference at $p < 0.001$. Trees with chlorotic mottle comprised 39.0% of the total sample in Sequoia and Kings Canyon (574 out of 1470) and 29.0% (479 out of 1650) in Yosemite. In each of the two park areas, ponderosa pines exhibited greater foliar injury than Jeffreys.

The geographic variation in ozone injury to pines within each park area was estimated by calculating average point scores from individual tree data for each of the 208 points sampled. In Sequoia and Kings Canyon, 80 out of 98 points (81.6%) contained at least one tree with chlorotic mottle symptoms; in Yosemite the ratio was 99 out of 110 (90.0%). This indicates that ozone pollution has reached nearly every area of pine forest in these national parks in sufficient amounts to produce foliar injury. Maps of the sampled points showing the relative severity of ozone injury reveal the geographic distribution of ozone effects (Figures 4 and 5). The only areas where ozone injury was not observed in Sequoia and Kings Canyon National Parks are in the headwaters of the Kern and Kings Rivers, particularly the upper Kern River basin (Figure 4). The western portion of the Kaweah River Basin contained the largest number of points with relatively more severe injury. In Yosemite (Figure 5), the west-to-east trend of decreasing ozone injury was also observed, though not as obvious. Sample points with the most severe average scores were near Crystal Cave in the Kaweah basin at an elevation of 1550 m in Sequoia-Kings (0.8—severe, indicating an average of less than one healthy needle whorl retained and trees with generally poor crown condition) and near Wawona in Yosemite at the southern end of the park at an elevation of 1650 m (1.67—moderate).

Ozone chlorotic mottle and needle retention have been shown to be closely related in yellow pines.[17] An analysis of the number of annual whorls retained by the sampled trees revealed a relationship between needle retention and ozone injury. Trees were stratified by species in this analysis to minimize genetic and elevational effects. Table II displays the means for this variable by species, among injured and uninjured trees within each species class, and by park area. The hypothesis that yellow pines with ozone mottle symptoms also have poorer needle retention than uninjured trees was tested using a t-test of the mean number of whorls retained for injured and uninjured trees. In all cases the average number of whorls retained by injured trees was significantly less than uninjured trees ($p < 0.001$). These results suggest premature needle abscission resulting from exposure to ozone pollution. A thinning of tree crowns has occurred on a population-wide level in the ponderosa and Jeffrey pine stands of the national parks of the Sierra Nevada. Several trees were found with only the current year's growth being the one moderately healthy whorl; the remainder of the foliage had either abscised or was severely afflicted with chlorotic mottle, which drastically reduces photosynthetic capability.[18] Whorl abscission was observed to be more severe in Sequoia and Kings Canyon National Parks than in Yosemite; branches sampled from injured Jeffrey pines retained an average of 1.33 fewer whorls than uninjured trees. A regression analysis was performed for each species in Sequoia and Kings Canyon National Parks with ozone injury (FPM score) as the independent variable and needle retention as the dependent variable. The results (Figure 6) indicate strong correlations for both species ($r = 0.86$ for ponderosa pines and 0.75 for Jeffrey pines); trees with more severe injury appear to hold fewer needle whorls. The slope of the ponderosa pine regression line is nearly equal to one, and the Y-intercept 1.58 suggests that a good linear model for needle abscission is that ponderosa pines will drop needles in a given whorl in the season following the appearance of chlorotic mottle symptoms on that whorl. For example, the model predicts that a tree with a FPM score of 2 (two-year-old needles, whorl 3, with chlorotic mottle) will retain 3.5 annual whorls (two-year-old needles, whorl 3, plus half of the three-year-old needles, whorl 4) at the time of the evaluation (usually August–September). The remaining three-year-old needles, whorl 4, will abscise by the following spring. The sparsity of data points in the severe and very severe injury categories should be noted, however, and the model may fail at higher injury levels. The slope of the Jeffrey pine regression line is steeper, suggesting that this species responds to ozone pollution stress by dropping older needles more readily than ponderosa pines. However, a Y-intercept of 0.2 (implying that a Jeffrey pine with chlorotic mottle on the current year's foliage would only possess two tenths of the current year's growth by September) and the shape of the scatter of points suggest a nonlinear relationship for this species in this study.

The relationship between ozone injury and elevation suggested by the permanent plot data discussed above for Sequoia and Kings Canyon National Parks was confirmed by the cruise survey data. The correlation was strongest in the Kaweah River Basin of Sequoia National Park (Figure 7); linear regression of mean FPM point scores with elevation produced a significant result ($r = 0.71$, $p < 0.001$). Higher point scores (meaning less injury) were found at higher elevations than at lower elevations.

CONCLUSIONS

The permanent plots indicate a significant increase in the degree of foliar injury and percentage of trees injured between 1980–82 and 1984–85. The causal agent of the increase in injury cannot be defined. Observations describing ozone injury with elevation from both the plots and the cruise survey indicate a trend of decreasing injury with increasing elevation. Visible ozone injury in the form of chlorotic mottle was found on ponderosa and Jeffrey pines in nearly every area of their occurrence in Sequoia, Kings Canyon, and Yosemite National Parks during the 1986 cruise survey. Although the overall injury was slight, areas of moderate injury were found, and about one third of all trees sampled showed some ozone chlorotic mottle symptoms. Based on the results of this survey, the upper portion of the Kern River basin in Sequoia National Park is the only area that may be considered free of ozone air pollution injury to pines. Jeffrey and ponderosa pines with visible ozone injury had poorer needle retention than uninjured trees. Several trees with only one moderately healthy whorl—the current year's growth—were found; the remainder of the foliage had either abscised or was severely afflicted with chlorotic mottle, which drastically reduces photosynthetic capability. These trees, growing in areas of high atmospheric ozone concentrations, are under considerable stress as a result of their sensitivity to the pollutant. If ozone concentrations continue at their present level or increase, these individuals will either die or continue to decline. The NAAQS for ozone does not appear to be adequate for protecting yellow pines in Sequoia National Park from injury.

ACKNOWLEDGMENTS

The authors wish to acknowledge the advice and guidance of Paul R. Miller of the U.S. Forest Service over the many years of field work and data collection that are represented in this paper. Doug Wallner of the National Park Service performed the 1984 field evaluation in Sequoia and Kings Canyon National Parks.

The cruise survey could not have been completed without the tireless effort of Mona Selph of Eridanus Research Associates. Others who assisted include Sylvia Haultain-Tweed, Tom Warner, Linda Mazzu, Patti Haggerty, Tom Nichols, David Parsons, David Graber, Harold Werner, Jan van Wagtendonk, and Teri Grosse. A portion of this work was funded by the Air Quality Division, National Park Service, U.S. Department of the Interior, under contract number CX-0001-4-0058.

REFERENCES

1. J.R. Parmeter, Jr., R.V. Bega, and T. Neff, "Chlorotic decline of ponderosa pine in southern California," *Plant Dis. Rep.* 46:269 (1963).

2. P.R. Miller, J.R. Parmeter, Jr., O.C. Taylor, and E.A. Cardiff, "Ozone injury to the foliage of *Pinus ponderosa*," *Phytopath.* 53:1072 (1963).

3. P.R. Miller and A.A. Millecan, "Extent of oxidant air pollution damage to some pines and other conifers in California," *Plant Dis. Rep.* 55(6):555 (1971).

4. W.T. Williams, M. Brady, and S.C. Willison, "Air pollution damage to the forests of the Sierra Nevada Mountains of California," *JAPCA* 27(3):230 (1977).

5. J. Pronos, D.R. Vogler, and R.S. Smith, Jr., "An evaluation of ozone injury to pines in the southern Sierra Nevada," Report No. 78-1, USDA Forest Service, Forest Insect and Disease Management, San Francisoc, CA 1978, 13pp.

6. J. Allison, "Evaluation of ozone injury in the Stanislaus National Forest," Report No. 82-07, USDA Forest Service, Forest Pest Management, San Francisco, CA, 1982, 7pp.

7. W.T. Williams and J.A. Williams, "Effects of oxidant air pollution on needle health and annual ring width in a ponderosa pine forest," *Environ. Cons.* 13(3):229 (1986).

8. J. Pronos, USDA Forest Service, Sonora, CA, private communication, 1989.

9. T.E. Warner, D.W. Wallner, and D.R. Vogler, "Ozone injury to ponderosa and Jeffrey pines in Sequoia-Kings Canyon National Parks," in *Proceedings of the First Biennial Conference of Research in California's National Parks*, Davis, CA, 1983, p. 1.

10. D.W. Wallner and M. Fong, "An analysis of ozone injury to ponderosa and Jeffrey pines in Sequoia and Kings Canyon National Parks," Final Survey Results. Unpublished Research Brief, USDI National Park Service, Sequoia and Kings Canyon National Parks, Three Rivers, CA, 1982, 15pp.

11. D.W. Wallner, USDI National Park Service, Fredericksburg, PA, unpublished data, 1984.

12. D.M. Duriscoe, "Evaluation of ozone injury to selected tree species in Sequoia and Kings Canyon National Parks, 1987 Survey Results," Holcomb Research Institute, Butler University, Indianapolis, IN, 1987, 216pp.

13. K.W. Stolte and J.P. Bennett, "Standardized procedures for establishing permanent pine plots and evaluating pollution injury on pines," USDI National Park Service, Air Quality Division, Lakewood, CO, 1984, 9pp.

14. P.S. Muir and B. McCune, "Index construction for foliar symptoms of air pollution injury," *Plant Dis.*, 71(6):558 (1987).

15. M.I. Flores, USDI National Park Service, Air Quality Division, Lakewood, CO, unpublished data, 1989.

16. J. Pronos and D.R. Vogler, "Assessment of ozone injury to pines in the southern Sierra Nevada, 1979/1980," Report No. 81-20, USDA Forest Service, Forest Pest Management, Pacific Southwest Region, 1982, 13pp.

17. P.R. Miller and R.E. Van Doren, "Ponderosa and Jeffrey pine foliage retention indicates ozone dose response," in *Proceedings of the Symposium on Dynamics and Management of Mediterranean-Type Ecosystems, June 22-26, 1981, San Diego, CA*, General Technical Report PSW-58, USDA Forest Service, Pacific Southwest Forest and Range Experiment Station, 1982, 621pp.

18. M.T. Patterson and P.W. Rundel, "Ozone impacts on the photosynthetic capacity of Jeffrey pine in Sequoia National Park," Draft Final Report, Project PX-0001-7-1152, National Park Service, Air Quality Division, Lakewood, CO, 1989, 34pp.

Table Ia. Percentage of ozone injured trees and FPM ozone injury rating in ponderosa and Jeffrey pine permanent plots in Sequoia and Kings Canyon National Parks from 1980 to 1985.

Drainage/Plot No. /Plot Name		Percent Trees Injured				FPM^a Score			
	Elev. (m)	'80-82	'84-85^b	Delta	'80-85 Mean	FPM '80-82	FPM '84-85	Delta	'80-85 Mean
South Fork Kings									
(7) Sheep Creek	1524	20	100	+80	60	3.5	2.3	-1.2	2.9
(10) Swale	1829	50	100	+50	75	2.7	0.9	-1.8	1.8
North Fork Kaweah									
(4) Little Baldy	2134	70	100	+30	85	2.6	1.6	-1.0	2.1
(12) Crystal Cave	1524	60	95	+35	78	1.9	0.9	-1.0	1.4
(13) Little Baldy	2438	30	60	+30	45	3.4	2.9	-0.5	3.2
(15) Quail Flat	2134	90	100	+10	90	2.6	1.6	-1.0	2.1
(20) Redwood Mtn.	1829	30	70	+40	50	3.1	2.6	-0.5	2.9
(22) Redwood Mtn.	2134	30	70	+40	50	3.7	3.0	-0.7	3.4
(44) Stony Creek	2438	40	80	+40	60	3.1	3.0	-0.1	3.1
Marble Fork Kaweah									
(1) Wolverton	2134	50	100	+50	75	2.8	2.6	-0.2	2.7
(2) Red Fir	2134	20	60	+40	40	3.5	3.1	-0.4	3.3
(3) Sawanee Creek	2134	20	60	+40	40	3.6	2.8	-0.8	3.2
(9) Triple Divide Peak	2134	10	50	+40	30	3.6	3.4	-0.2	3.5
Middle Fork Kaweah									
(16) High Sierra Trail	2438	60	80	+20	70	2.7	2.2	-0.5	2.5
(17) High Sierra Trail	2134	20	80	+60	50	3.6	2.5	-1.1	3.1
(33) Redwood Meadow	1829	60	60	0	60	2.3	2.7	+0.4	2.5
(34) Redwood Meadow	1829	60	70	+10	65	2.7	3.1	+0.4	2.9
(35) Redwood Meadow	1829	70	70	0	70	2.5	3.2	+0.7	2.9
(36) Bear Paw	1829	50	90	+40	70	2.6	2.6	0	2.6
(37) Cliff Creek	1829	70	80	+10	75	2.0	2.5	+0.5	2.3
(38) Morro Creek Trail	1829	60	80	+20	70	2.3	2.3	0	2.3

[a] Forest Pest Management method (10-tree plots) 1980–82 and 1984.

[b] Plots evaluated once or twice in period 1984–85.

Table Ib. Percentage of ozone injured trees and FPM ozone injury rating in ponderosa and Jeffrey pine permanent plots in Sequoia and Kings Canyon National Parks from 1980 to 1985.

Drainage/Plot No. /Plot Name		Percent Trees Injured				FPM[a] Score			
	Elev. (m)	'80-82	'84-85[b]	Delta	'80-85 Mean	FPM '80-82	FPM '84-85	Delta	'80-85 Mean
East Fork Kaweah									
(11) Camp Conifer	1829	30	60	+30	45	3.2	3.0	-0.2	3.1
(14) Atwell Mill	1829	30	80	+50	55	3.0	2.3	-0.7	2.7
(21) Oriole Lake	1524	100	100	0	100	1.2	1.1	-0.1	1.2
(31) Clover Creek	2438	30	50	+20	40	3.5	3.1	-0.4	3.3
South Fork Kaweah									
(32) Hockett & Garfield	2438	0	60	+60	30	4.0	3.4	-0.6	3.7
(51) South Fork	1524	60	95	+35	78	2.3	1.6	-0.7	2.0
(53) Bennett Creek	1829	100	100	0	100	1.1	0.9	-0.2	1.0
mean	1981	47.1	78.6	+34.0	62.7	2.8	2.4	-0.43	2.6
s.d.	293	26.1	17.1	+24.2	19.3	0.7	0.8	0.56	0.7
n	28	28	28	28	28	28	28	28	28

[a] Forest Pest Management method (10-tree plots) 1980–82 and 1984.

[b] Plots evaluated once or twice in period 1984–85.

Table II. Comparison of number of whorls retained on injured and uninjured trees in each park area.

	Number of Whorls Retained			Independent Sample T-Test		
Tree Group	Mean	Std. Dev.	Cases	Student's T	Degrees of Freedom	2-Tailed Prob.
All Park Areas						
Ponderosa				11.24	999	<0.001
Injured	3.72	1.00	418			
Uninjured	4.52	1.16	583			
Jeffrey				14.28	2117	<0.001
Injured	4.67	1.33	635			
Uninjured	5.73	1.65	1484			
Sequoia and Kings Canyon						
Ponderosa				10.65	460	<0.001
Injured	3.84	1.11	235			
Uninjured	5.02	1.27	227			
Jeffrey				13.06	1006	<0.001
Injured	4.78	1.34	339			
Uninjured	6.11	1.62	669			
Yosemite						
Ponderosa				7.68	537	<0.001
Injured	3.59	0.85	183			
Uninjured	4.21	0.97	356			
Jeffrey				8.29	1109	<0.001
Injured	4.55	1.31	296			
Uninjured	5.42	1.62	815			

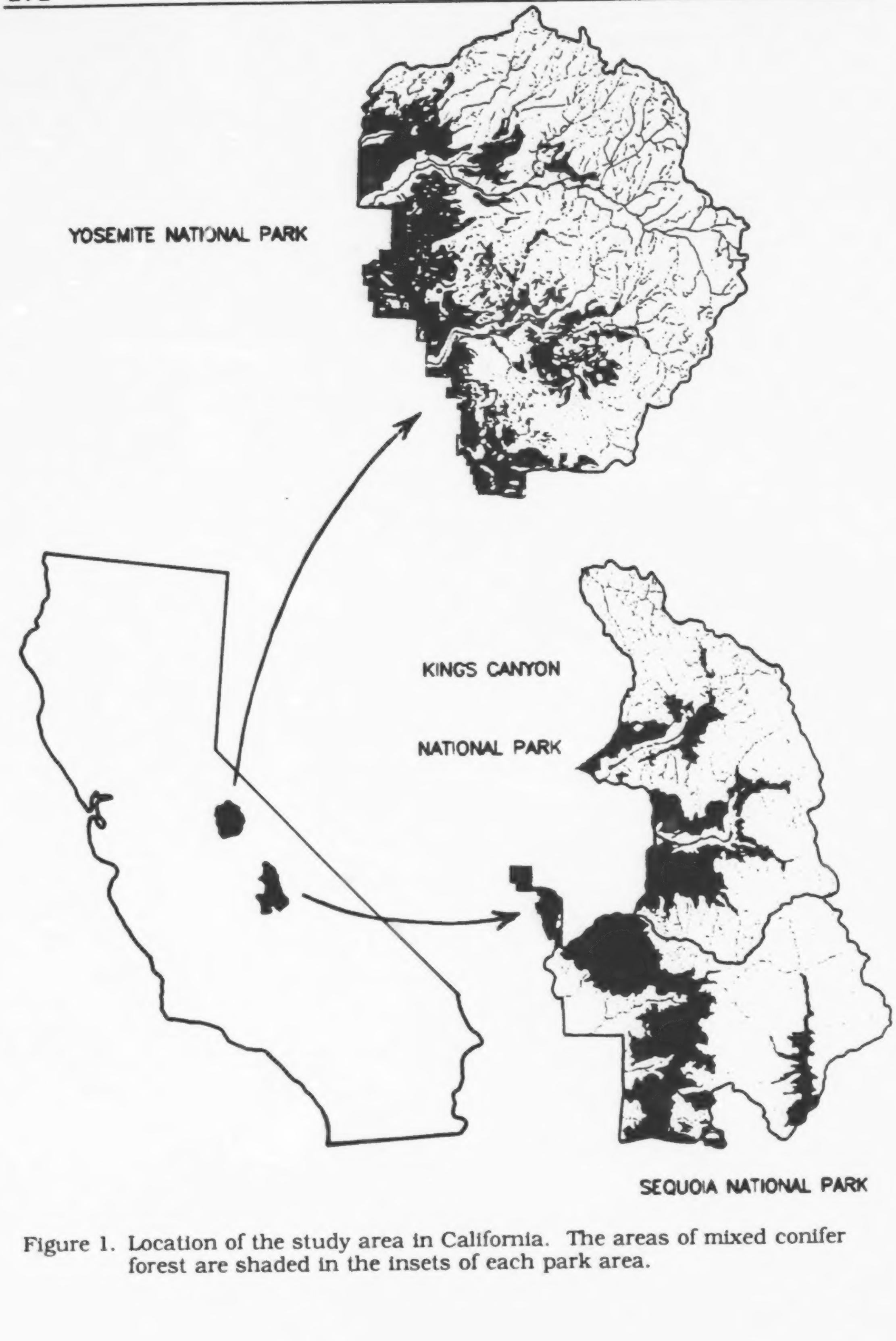
YOSEMITE NATIONAL PARK
KINGS CANYON
NATIONAL PARK
SEQUOIA NATIONAL PARK

Figure 1. Location of the study area in California. The areas of mixed conifer forest are shaded in the insets of each park area.

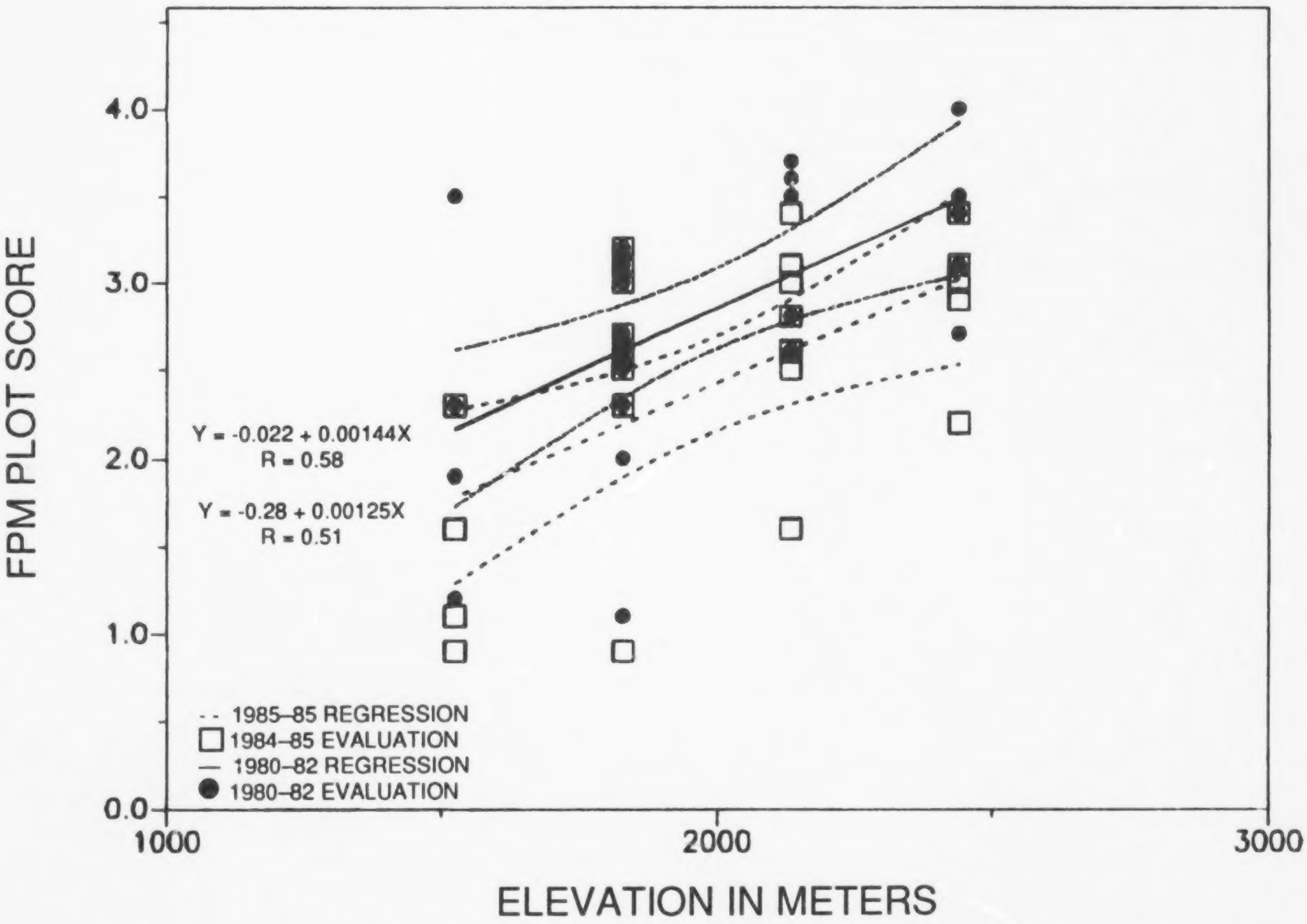

Figure 2. Scatter plot and regression lines of FPM scores in permanent pine plots in Sequoia and Kings Canyon National Parks for 1980–82 and 1984–85.

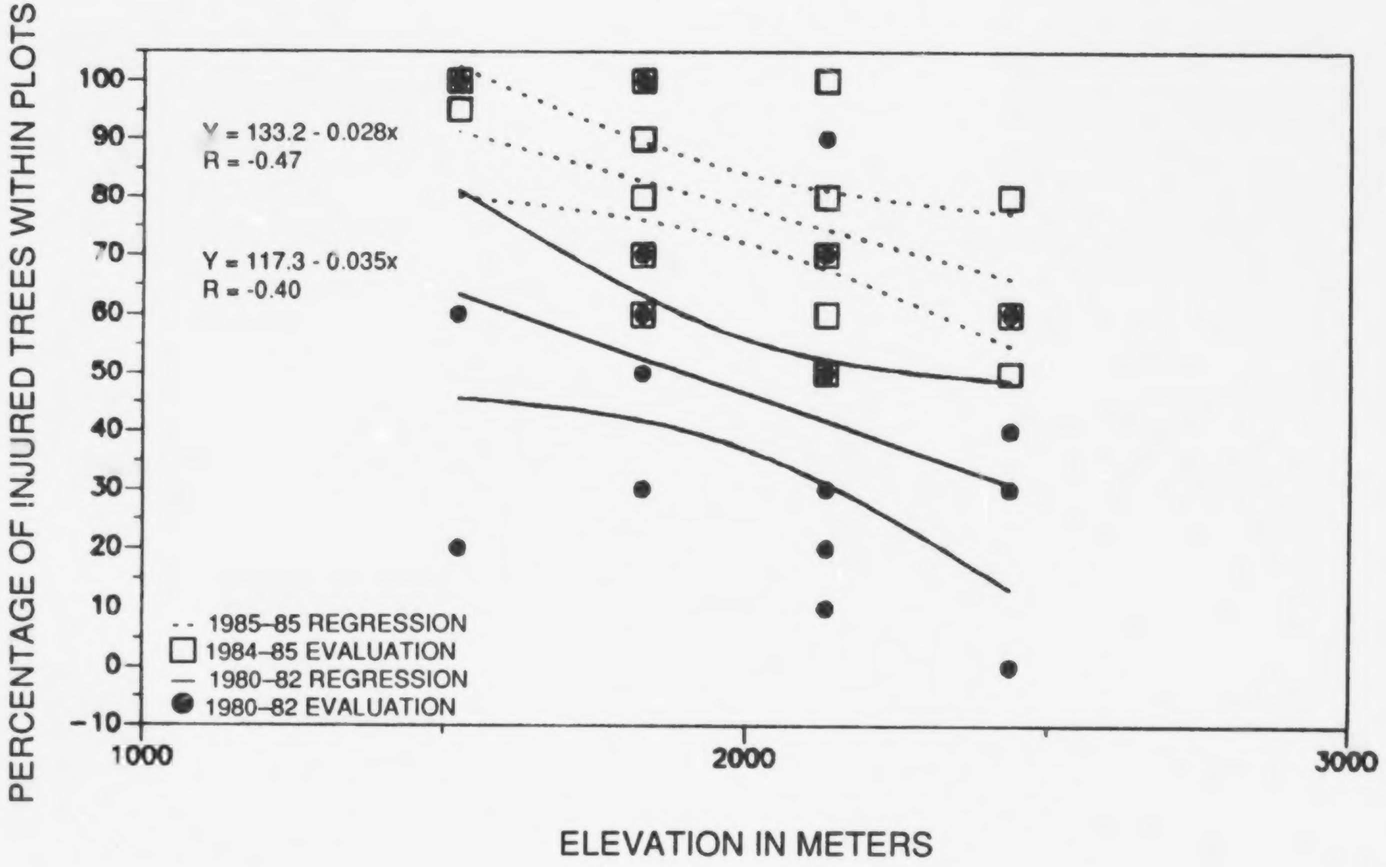

Figure 3. Scatter plot and regression lines of the percentage of trees with injury in permanent pine plots in Sequoia and Kings Canyon National Parks for the two evaluation periods.

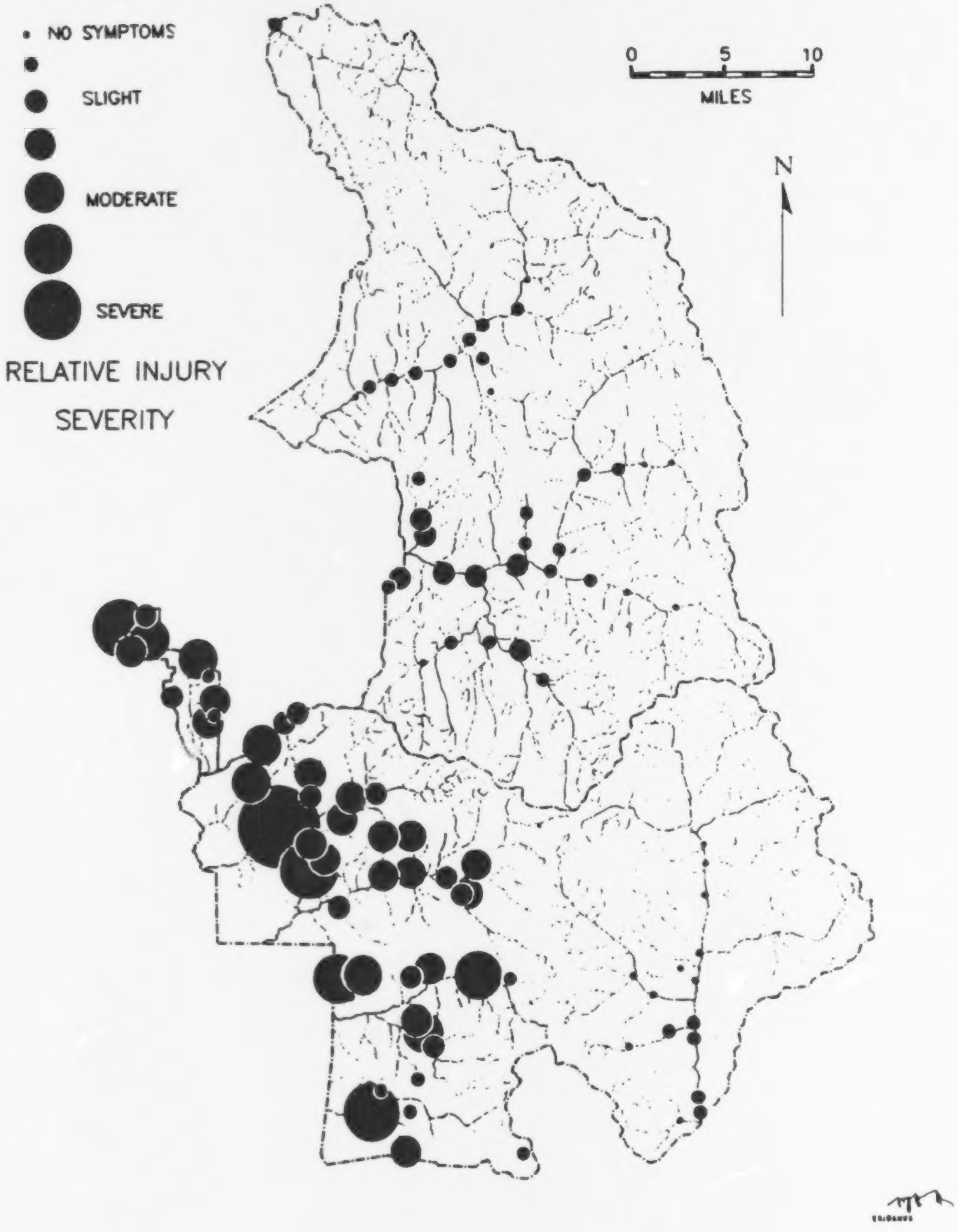
NO SYMPTOMS
SLIGHT
MODERATE
SEVERE
RELATIVE INJURY SEVERITY
0 5 10
MILES
N

Figure 4 Map showing the relative severity of foliage ozone injury found at each of 98 sample points in Sequoia and Kings Canyon National Parks in 1986. The most severe injury occurred along the western border of the mixed conifer zone.

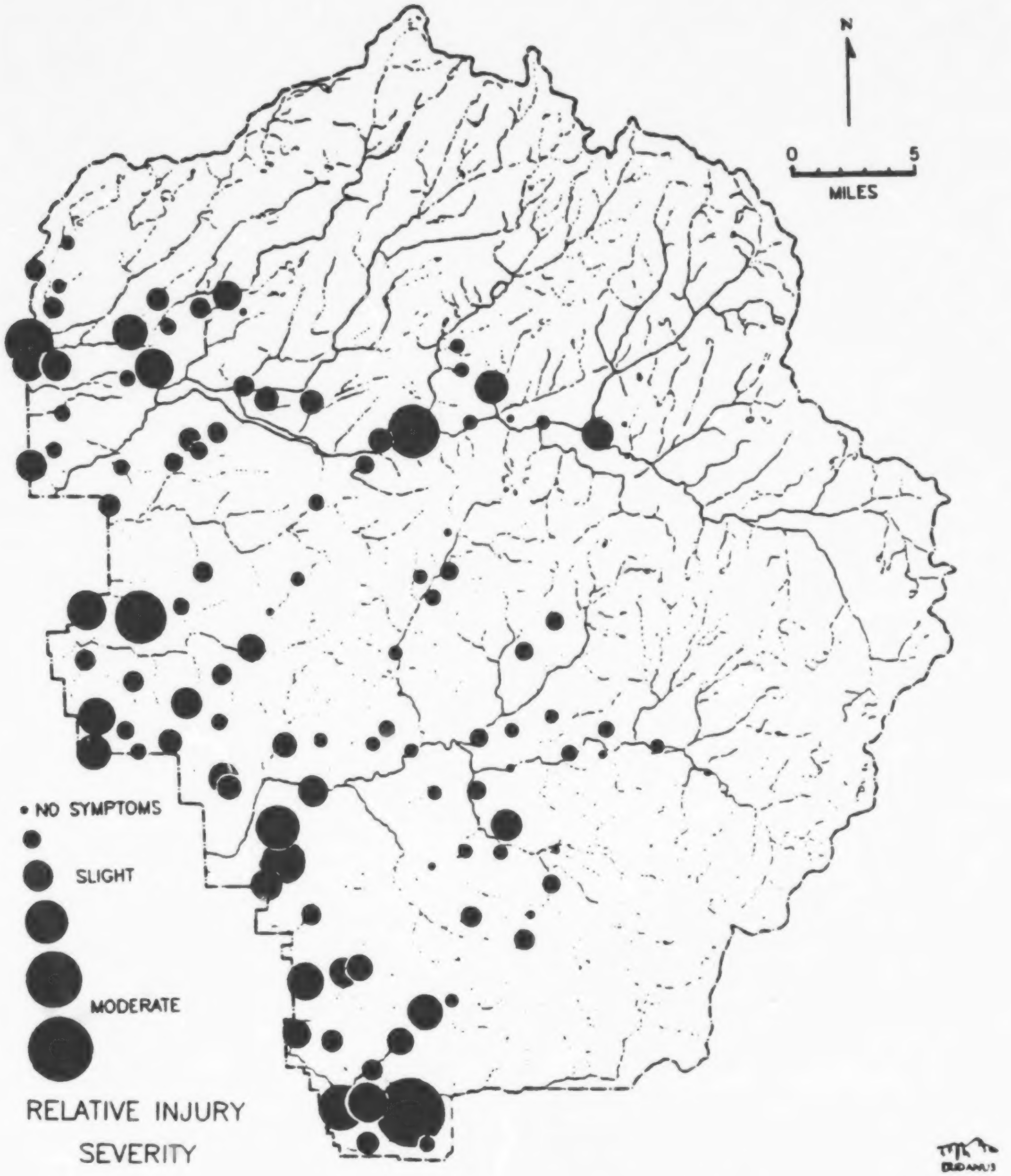
N
0
5
MILES
• NO SYMPTOMS
SLIGHT
MODERATE
RELATIVE INJURY
SEVERITY

Figure 5. Map showing the relative severity of foliar ozone injury found at each of 110 sample points in Yosemite National Park in 1986. The most severe injury occurred along the western border of the park.

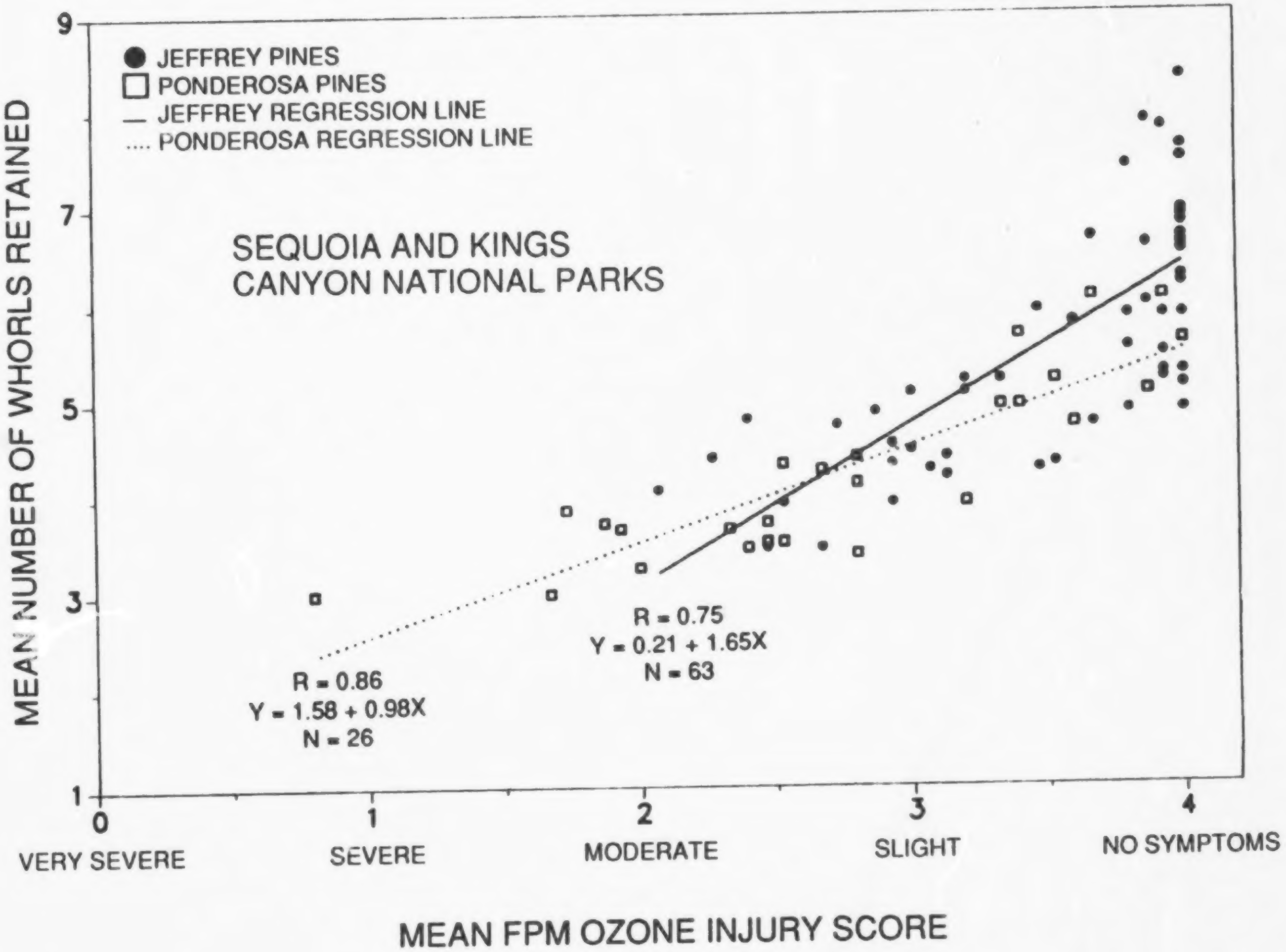

Figure 6. Scatter plot and regression lines of the relationship between mean number of annual needle whorls retained on ponderosa and Jeffrey pines observed in 1986 at each of 98 sample points in Sequoia and Kings Canyon national Parks and ozone injury severity as measured by FPM scores.

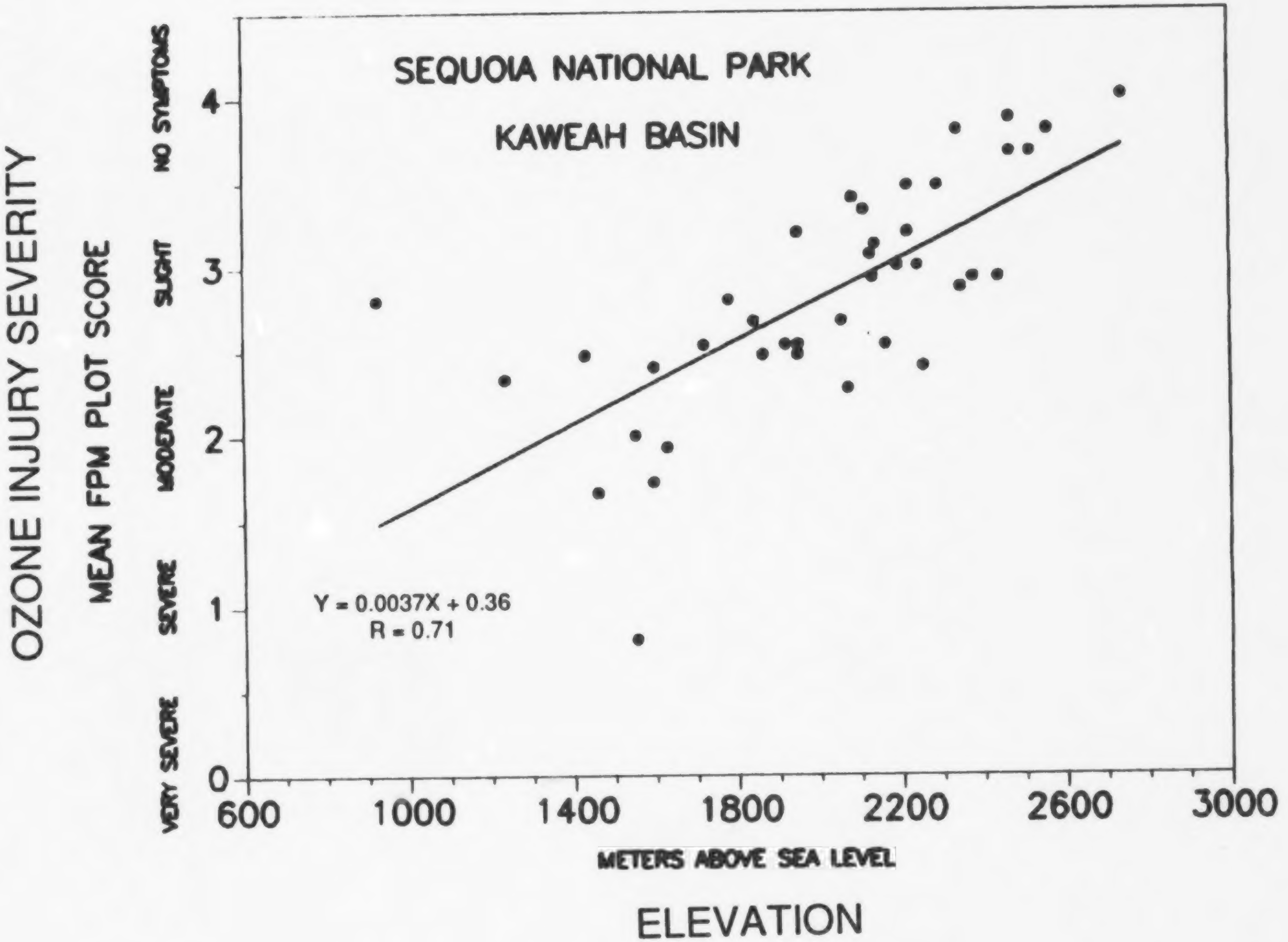

Figure 7. Relationship of ozone injury severity (mean FPM score of 15 trees at each sample point) and elevation observed in 1986 in the Kaweah River Basin of Sequoia National Park illustrated by a scatter plot and regression line.

Ozone Injury to Jeffrey and Ponderosa Pines Surrounding Lake Tahoe, California and Nevada

Brian S. Pedersen

Department of General Science
Oregon State University
Corvallis, OR 97331

INTRODUCTION

Ozone injury to forest trees is widespread in California. Foliar injury has been observed in southern California, the San Francisco Bay area, and the Sierra Nevada.[1] This report describes the first formal survey for foliar ozone injury to Jeffrey pines (*Pinus Jeffreyi* Grev. and Balf.) and ponderosa pines (*P. ponderosa* Laws.) surrounding Lake Tahoe. Ozone concentrations in the Lake Tahoe area and possible sources of this ozone are also discussed.

Ozone has been shown to decrease tree photosynthesis[2] and growth[3] and to increase susceptibility to pathogen attack.[4] Jeffrey pine, a major forest tree in the Lake Tahoe area, and the less commonly observed ponderosa pine, are among the most sensitive of California's forest trees to ozone injury.[5] One manifestation of ozone injury to these pines is a characteristic chlorotic mottling of foliage. This injury is the basis of ozone injury survey methods employed by the USDA Forest Service (FS)[6] and National Park Service (NPS).[7]

Lake Tahoe (Figure 1) straddles the California/Nevada border, east of the Sierra Nevada crest, at an elevation of 1900 m. High mountains, up to 3300 m, surround the lake forming a deep basin. The area of the basin is 1300 km^2, and approximately one-third of this area is lake surface. Most of the land within the basin is National Forest land, managed by the Lake Tahoe Basin Management Unit. The basin is a populated area with developed areas nearly surrounding the lake. The lake attracts a substantial number of tourists both in summer and winter.

In the late 1970s personnel from the FS and the State of California conducted a brief survey for foliar ozone injury on pines south of Lake Tahoe. They found evidence of injury at two sites.[8] In 1986, I surveyed twelve sites around the southern half of the lake and found injury at five. Following this preliminary survey, the detailed survey described in this report was conducted to meet three goals: (1) to determine the geographical distribution of ozone injury around Lake Tahoe, (2) to evaluate the severity of this ozone injury and compare it to the injury observed elsewhere in the Sierra Nevada, and (3) to establish permanent survey plots that could be re-examined in the future.

METHODS

The FS and NPS standard survey methods[6,7] were employed for different components of the Tahoe survey with slight modifications. However, all results in this paper are presented in terms of the FS scoring system. Results obtained by the NPS method were converted to the FS scoring system.

FS Scoring System

Each branch examined from a survey tree is assigned an ozone injury score equal to the age of the youngest whorl with ozone injury (a whorl is a single year's growth of foliage). The age of the youngest whorl with injury is a measure of the injury severity; the younger the affected foliage, the more severe the injury. A score of 0 is assigned if ozone injury is found on the current year's needles, 1 if injury is found on needles that are 1 year old, and so on. The maximum score assigned is 4; injury on older foliage is ignored. Note that the lower the branch score, the more severe the ozone injury. The score assigned to each tree is the lowest branch score from that tree. A tree with a score of 4 is considered to have no injury, 3 is slight injury, 2 is moderate injury, 1 is severe injury, and 0 is very severe injury. The score for the plot as a whole is the mean of the scores of the trees on that plot. These numerical plot scores are placed in the same categories as the tree scores based on the plot score rounded down to the nearest integer value. For example, a plot with a score of 3.7 is considered to have slight injury.

For the Tahoe survey this scoring system was modified slightly to include injury on foliage 4 years old or older, which is neglected by the FS system. Trees with such injury are grouped as having very slight injury and this scoring system is referred to as the modified FS scoring system. The very slight category was treated as no injury for the purpose of calculating the plot scores, however, to permit comparison to the results of FS surveys elsewhere in the Sierra Nevada.

Tahoe Survey

Field work was conducted during late August, September, and October 1987. A consultant with experience conducting ozone injury surveys in California's National Parks (Dan Duriscoe, Eridanus Research Associates, Kaweah, CA) was hired to train field personnel. This training was conducted for 5 days in the Lake Tahoe basin. The field personnel's injury evaluations were also verified in the field by Dr. John Pronos (USDA Forest Service, San Francisco, CA).

With very few exceptions, the pines surveyed were second-growth trees less than 100 years old. The sites ranged from very open stands to nearly closed canopies, and included pure Jeffrey pine, Jeffrey and ponderosa pine, and more diverse stands. Associated tree species included white fir (*Abies concolor* [Gord. & Glend.] Lindl.), incense-cedar (*Calocedrus decurrens* [Torr.] Florin.), sugar pine (*Pinus Lambertiana* Dougl.), and lodgepole pine (*P. contorta* Dougl.)

The injury survey was divided into two components: an in-basin survey, within the Lake Tahoe basin, and a less detailed survey of the area surrounding the Lake Tahoe basin. The in-basin survey was further divided into permanent plot and cruise subcomponents.

In-Basin Survey. The 24 in-basin survey sites were chosen at random. Each section (1 mi^2) within the basin was assigned an integer, and 24 of these integers were randomly selected. The survey plots were located at the point nearest the center of the selected sections that were (1) on National Forest, or California or Nevada State Park lands; (2) along dirt roads shown on the U.S. Geographical Survey topographical maps (7.5 minute series); (3) distant from developments; and (4) included pines. For each permanent plot a total of 15 pines, Jeffrey and/or ponderosa, were selected by the NPS method's proscribed, systematic procedure[7] and were tagged. Only trees larger than

10 cm DBH (diameter at breast height) and with accessible foliage (within 10 m of the ground) were chosen. Five branches from all around the lower portion of the canopy of each tree were examined. The percentage of needle area with chlorotic ozone mottle on each whorl was recorded, as was the presence of biotic and other abiotic injuries. The length of needles on each whorl was measured. Tree parameters, including DBH, live crown ratio, canopy position, and bole injuries were noted. Site data, including slope, aspect, elevation, and associated species were also recorded.

The cruise subcomponent of the in-basin survey consisted of evaluating an additional 25 pines at each site. The 25 pines nearest the permanent plot trees were selected, and three branches from each tree were evaluated by the FS scoring system only. These trees were not selected systematically or tagged, and no other data were recorded.

Surrounding Area Survey. This component of the survey focused on the area east of the Sierra Nevada crest but outside the Lake Tahoe basin. The FS has already conducted surveys in the National Forests west of the Lake Tahoe basin. Sixteen sites were chosen to represent the survey area. The sites were chosen for the presence of Jeffrey and/or ponderosa pines and for their accessibility. All but one of the sites was in the Toiyabe National Forest (the exception was in a county park in Nevada). At 15 of the sites, ten trees were selected and three branches evaluated by the FS scoring system. Accessible, adjacent trees distant from any developments were selected for evaluation. These trees were not selected systematically or tagged, and no other data were recorded. The sixteenth site was treated as a plot within the Lake Tahoe basin. This plot was a practice plot used during the training of field personnel. Because all work was supervised by the training consultant the results from this plot are accurate.

RESULTS AND DISCUSSION

In-Basin Survey

The results of the permanent plot subcomponent are shown in Table I. Of the 360 trees surveyed, 105 (29.2%) had foliar ozone injury. Half of these trees, 52, are considered injured by the FS scoring system. No trees with very severe injury were found, 1 (0.3%) had severe injury, 18 (5.0%) had moderate injury, 33 (9.2%) had slight injury, and 53 (14.7%) had very slight injury. Only three of the 24 plots had no trees with any injury symptoms. Seven plots had a FS plot score of no injury; the other 17 plots fell within the slight injury category. The lowest plot score (greatest injury) was 3.27; 80.0% of the pines at this site (plot 10) had ozone injury.

Figure 2 shows the location of each of the 24 plots and indicates the plot scores. Injury was observed throughout the basin. The three sites with the most severe injury were southwest of the lake.

The relationship between plot score and plot elevation is shown in Figure 3. Although plots with FS scores of no injury are found throughout the elevation range, the plots with greater injury are concentrated at lower elevations. Note, however, that the highest elevation plot (plot 6) had a score of slight injury.

Less injury was found on the 25 additional trees examined at each plot (cruise subcomponent). Of the 600 trees, 19.5% had injury as opposed to 29.2% of the tagged trees.

Surrounding Area Survey

The results of the survey of the area surrounding the Lake Tahoe basin are shown in Table II. The lowest plot score (greatest injury) was 3.00 (plot 36), which is lower than the lowest score within the basin (3.27). An equal number of the 16 plots had plot scores of slight and no injury. Of the 190 trees, 21.6% had injury, less than the 29.2% for the tagged trees within the basin. One of the trees had severe injury, 7 (3.7%) had moderate injury, 16 (8.4%) had slight injury, and 17 (8.9%) had very slight injury. The plot locations and scores are shown in Figure 4. Injury was found to the east and southeast of the basin; no injury was observed to the northwest.

Comparison to Injury on the West Slope of the Sierra Nevada

A comparison of the results of the Tahoe survey to the survey findings of the FS in five Sierra Nevada National Forests[6,9,10] indicates that the severity of ozone injury to Jeffrey and ponderosa pines increases with decreasing latitude in the Sierra Nevada (Table IIIa). The Tahoe and Eldorado National Forests are located to the west of the Lake Tahoe basin, the Stanislaus to the southwest, and the Sequoia and Sierra to the south (the Tahoe and Eldorado include parts of the Lake Tahoe basin; however, the surveys conducted in these National Forests did not include any sites in the basin). Note that data for the Sierra and Sequoia National Forests are lumped, and the survey was completed during a 2-year period. The wide range of survey dates (1979–1987) may be a factor in the apparent trend with latitude.

This comparison does not place the ozone injury observed at Lake Tahoe in proper perspective, however, because the FS surveys included trees at elevations as low as 600 m and near ozone source areas. Another comparison (Table IIIb) includes only sites above 1900 m, the elevation of Lake Tahoe. This elevation range includes data from all of the in-basin sites and most of the surrounding area sites. Although plots scored as moderately or severely injured were found only in the FS surveys, the percentage of sites above 1900 m with injury in the Lake Tahoe basin and surrounding area is greater than in the two National Forests directly west of Lake Tahoe (Tahoe and Eldorado). One implication of this finding is that it is unlikely that the source of ozone impacting trees around Lake Tahoe is to the west of the lake since trees to the west are not as frequently injured. However, the range of survey dates may also be a factor here.

Ozone Concentration Data

There are currently only three ozone monitors operating in the Lake Tahoe basin, all in the heavily developed South Lake Tahoe area. Two are operated by the California Air Resources Board (CARB), the other by the State of Nevada. During 1987, the maximum ozone concentration at the California sites was 0.09 ppm.[11] This does not exceed the California ozone standard (>0.09 ppm). The California standard has been exceeded for only three hours during the period 1980 to 1987 at these two stations. However, the annual mean ozone concentrations measured are high, 0.037 and 0.038 ppm during 1987. These mean concentrations are higher than annual mean concentrations at most Los Angeles basin monitoring sites. Such high mean concentrations are typical of high elevation sites.[11]

There is only limited ozone concentration data from other locations in the Lake Tahoe basin. The CARB operated an ozone monitor at Incline Village, a heavily developed area on the northeast shore of the lake, during the late 1970s.[11] These data suggest that ozone levels at the north end of the lake were equivalent to those at the south end. Two mobile air quality monitoring stations were operated by the CARB at nine sites around Lake Tahoe for two to four 1-week periods during summer of 1973.[12] The sites included both developed and relatively undeveloped areas. The results indicate that ozone levels are fairly uniform around the Lake. An exception is one site at the northwest end of the Lake, Tahoe City, where ozone concentrations were substantially higher than at South Lake Tahoe. But since the monitoring period was only one week it should not be concluded that ozone levels at Tahoe City are normally higher than at South Lake Tahoe.

All of the ozone monitoring measurements were made at or near lake level. The only data available from a higher elevation site, Echo Summit (elevation 2250 m), suggest that ozone concentrations there are less than at South Lake Tahoe.[13] During July 1983, the mean maximum daily concentration was 0.042 ppm at Echo Summit and 0.058 and 0.062 ppm at the two South Lake Tahoe ozone monitors. The possibility exists, however, that ozone levels may be higher at intermediate or other high elevation sites.

Ozone Exposure/Injury Response Relationship

The FS has monitored ozone concentrations near some of its survey sites in the National Forests near Lake Tahoe.[10] These data permit a comparison of the ozone exposure/ozone injury response relationship observed around Lake Tahoe and in the National Forests to the west (Table IV). The ozone data shown are for June to September. The mean daily maximum hour ozone concentration was the only statistic published by the FS; it is not known if this statistic best represents the potential for ozone injury to pines. The survey data are shown as the range of ozone injury plot scores for the plots nearest the ozone monitors. The data indicate that the exposure/response relationship found by the FS and during our survey are consistent. Ozone levels at the FS monitoring sites were slightly higher than in the Lake Tahoe basin but so was the level of ozone injury observed.

Ozone Sources

There are four possible sources for the ozone observed in the Lake Tahoe basin: (1) transport from the urban Sacramento area 140 km WSW of the lake, (2) transport from the urban Reno and Carson City areas, (3) anthropogenic production within the Lake Tahoe basin, and (4) natural background sources (stratospheric intrusion and/or biogenic production). Only the question of transport from the Sacramento area has been studied carefully. During the summer of 1978, the CARB conducted a study but found no evidence of transport over the Sierra Nevada crest from Sacramento.[14] This concurs with our finding that pines west of Lake Tahoe were less injured than pines within the basin. Transport from the Reno or Carson City areas is not likely because the prevailing winds carry pollution from Reno and Carson City away from Lake Tahoe.[15] There is substantial emission of ozone precursors related to automobile use within the basin. The 1979 estimated vehicle travel in the Lake Tahoe basin during August was 1.7 million miles per day.[16] Good conditions for ozone production exist within the deep basin: high ultraviolet light levels are available because of the basin's elevation. While natural ozone sources no doubt contribute to ozone levels in the basin, ozone concentrations are probably elevated substantially above background levels by human activities within the basin.

CONCLUSIONS

Jeffrey and ponderosa pines in the Lake Tahoe basin and surrounding area are affected by ozone. Of the 1150 pines at 40 sites examined during this survey, 263 trees (22.9%) at 30 sites (75.0%) had foliar ozone injury. Injury was widely distributed within the basin and was also observed outside the basin. The plots within the basin with greatest injury were located at lower elevations. More pines surveyed around Lake Tahoe had ozone injury than pines surveyed at comparable elevations to the west of Lake Tahoe. The ozone exposure/injury response relationship found during this survey is comparable to that found by the FS during their surveys. The severity of ozone injury around Lake Tahoe was less than in the southern Sierra Nevada.

There were no exceedances of the California ozone standard at sites monitored in the Lake Tahoe basin during 1987; however, the mean ozone concentrations there are high. Past ozone measurements within the basin indicate that ozone concentrations are fairly uniform around the lake. Ozone levels at one higher elevation site were lower than at the lake-level sites. The evidence suggests that the ozone found in the Lake Tahoe basin is not transported there from urban source areas to the east or west. It appears likely that emissions within the basin elevate ozone concentrations above background levels.

The injury survey findings and ozone concentration data indicate that the California and federal ozone standards do not protect sensitive forest trees from injury by ozone.

ACKNOWLEDGMENTS

This study was funded by generous gifts to the University of California, Davis by Mr. and Mrs. Martin B. Johnston, Reno, NV, and Mr. James McClatchy, Tiburon, CA. Susan Asam provided valuable assistance in the field and prepared the figures. Dr. Bruce McCune, and reviewers Drs. Joe McBride, Paul Miller, and John Pronos provided helpful comments on the manuscript.

REFERENCES

1. California Air Resources Board, "Effects of ozone on vegetation and possible alternative ambient air quality standards," Technical Support Document, Sacramento, CA, 1987.

2. P.B. Reich and R.G. Amundson, "Ambient levels of ozone reduce net photosynthesis in tree and crop species," *Science* 230:566 (1985).

3. D.L. Peterson, M.J. Arbaugh, V.A. Wakefield, and P.R. Miller, "Evidence of growth reduction in ozone-injured Jeffrey pine (*Pinus jeffreyi* Grev. and Balf.) in Sequoia and Kings Canyon National Parks, " *JAPCA* 37:906 (1987).

4. P.R. Miller, "Ozone effects in the San Bernardino National Forest," in *Air Pollution and the Productivity of the Forest, Proceedings of the Symposium, Izaak Walton League of America*, D.D. Davis, A.A. Millen, and L. Dochinger, Eds., Arlington, VA., 1988.

5. P.R. Miller, G.J. Longbotham, and C.R. Longbotham, "Sensitivity of selected western conifers to ozone," *Plant Dis.* 67:1113 (1983).

6. J. Pronos and D.R. Vogler, "Assessment of ozone injury to pines in the southern Sierra Nevada, 1979/1980," Report No. 81-20, USDA Forest Service, San Francisco, CA, 1981.

7. K.W. Stolte and J.P. Bennett, "Standardized procedures for establishing permanent pine plots and evaluating pollution injury on pines," National Park Service, Denver, CO, 1986.

8. W.L. Freeman, Jr., "Ozone injury to pines near South Lake Tahoe," USDA Forest Service, San Francisco, CA, 1979.

9. J.R. Allison, "An evaluation of ozone injury to pines on the Eldorado National Forest," Report No. 84-16, USDA Forest Service, San Francisco, CA, 1984.

10. J.R. Allison, "An evaluation of ozone injury to pines on the Tahoe National Forest," Report No. 84-30, USDA Forest Service, San Francisco, CA, 1984.

11. California Air Resources Board, "Air Quality Data," Volumes VIII-XIX, Sacramento, CA., 1978-87.

12. California Air Resources Board, "Air Quality in the Tahoe basin," Sacramento, CA, 1974.

13. K. Pinkerman, California Department of Transportation, Sacramento, CA, personal communication, 1987.

14. S. Duckworth and D. Crowe, "Ozone patterns on the western Sierra slope," California Air Resources Board, Sacramento, CA, 1979.

15. T.P. Hayes, J.J.R. Kinney, and N.J.M. Wheeler, "California surface wind climatology," California Air Resources Board, Sacramento, CA, 1984.

16. Tahoe Regional Planning Agency, "1982 Air Quality Plan for the Lake Tahoe Basin," South Lake Tahoe, CA, 1982.

Table I. Results of Permanent Plot Subcomponent of In-Basin Survey.

				# Trees by Modified FS Tree Score				
Plot	Elev. (m)	FS Plot Score	Total # Injured Trees	Severe	Moderate	Slight	Very Slight	No Injury
1	1940	4.00	3				3	12
2	2000	3.33	10		3	4	3	5
3	2100	3.80	5		1	1	3	10
4	1980	3.87	2		1		1	13
5	1950	3.53	7		2	3	2	8
6	2260	3.87	5			2	3	10
7	1930	4.00	0					15
8	1980	3.73	4		1	2	1	11
9	1940	3.67	7		1	3	3	8
10	1900	3.27	12		3	5	4	3
11	2050	4.00	0					15
12	2090	4.00	3				3	12
13	1940	3.60	3	1	1	1		12
14	2200	3.87	2		1		1	13
15	2220	4.00	1				1	14
16	1930	3.93	1			1		14
17	1980	4.00	0					15
18	2090	3.87	5		1		4	10
19	2050	3.80	5			3	2	10
20	2150	3.87	5			2	3	10
21	2010	3.73	8			4	4	7
22	2070	3.87	5		1		4	10
23	2000	4.00	4				4	11
24	1980	3.60	8		2	2	4	7
Total			105	1	18	33	53	255
Percent			29.2	0.3	5.0	9.2	14.7	70.8

Table II. Results of Surrounding Area Survey.

				# Trees by Modified FS Tree Score				
Plot	Elev. (m)	FS Plot Score	Total # Injured Trees	Severe	Moderate	Slight	Very Slight	No Injury
25	2380	3.95	4		1		3	36[a]
26	2160	4.00	0					10
27	2210	4.00	0					10
28	1860	3.40	9		1	4	4	1
29	2480	4.00	0					10
30	1840	3.60	6		1	2	3	4
31	1800	3.90	4			1	3	6
32	1840	3.30	4	1	1	2		6
33	1540	3.90	1			1		9
34	1920	4.00	0					10
35	1520	3.80	5			2	3	5
36	2030	3.00	8		3	4	1	2
37	1650	4.00	0					10
38	1780	4.00	0					10
39	1770	4.00	0					10
40	1840	4.00	0					10
Total			41	1	7	16	17	149
Percent			21.6	0.5	3.7	8.4	8.9	78.4

[a] Plot 25 has 40 pines; all others have 10.

Table IIIa. Comparison to Ozone Injury on the West Slope of the Sierra Nevada.

	% Plots by FS Plot Score				
Location and Survey Year	Severe	Moderate	Slight	No Injury	# Trees Surveyed
Lake Tahoe Basin ('87)			71	29	360
Tahoe Surrounding Area ('87)			50	50	190
Tahoe NF ('83)[a]		11	46	43	370
Eldorado NF ('82)		10	40	50	300
Stanislaus NF ('81)		15	67	18	460
Sierra/Sequoia NF ('79/'80)	17	17	45	21	520

[a] National Forests are listed in order from north to south.

Table IIIb. Comparison to Injury on the West Slope of the Sierra Nevada above 1900 m.

	% Plots >1900 m by FS Plot Score				
Location and Survey Year	Severe	Moderate	Slight	No Injury	# Trees Surveyed
Lake Tahoe basin ('87)			71	29	360
Tahoe Surrounding Area ('87)			50	50	130
Tahoe N.F. ('83)[a]		11	11	78	90
Eldorado N.F. ('82)			33	67	60
Sierra/Sequoia N.F. ('79/'80)	3	13	55	29	310

[a] National Forests are listed in order from north to south.

Table IV. Ozone Exposure/Injury Response Relationship.

Ozone Monitor Site and Measurement Year	Mean Daily Maximum Hour (ppm)[a]	Range of FS Plot Scores Near Ozone Monitor Site and Survey Year
Lake Tahoe basin:		
Bijou ('86)	0.060	No Injury–Slight ('87)
Tahoe ('86)	0.061	No Injury–Slight ('87)
Tahoe NF.		
Foresthill ('83)	0.068	Slight ('83)
Eldorado NF:		
Georgetown ('82)	0.073	Slight–Moderate ('82)
Stanislaus NF:		
Arnold ('82)	0.066	Slight–Moderate ('81)

[a] Ozone data are for June - September only

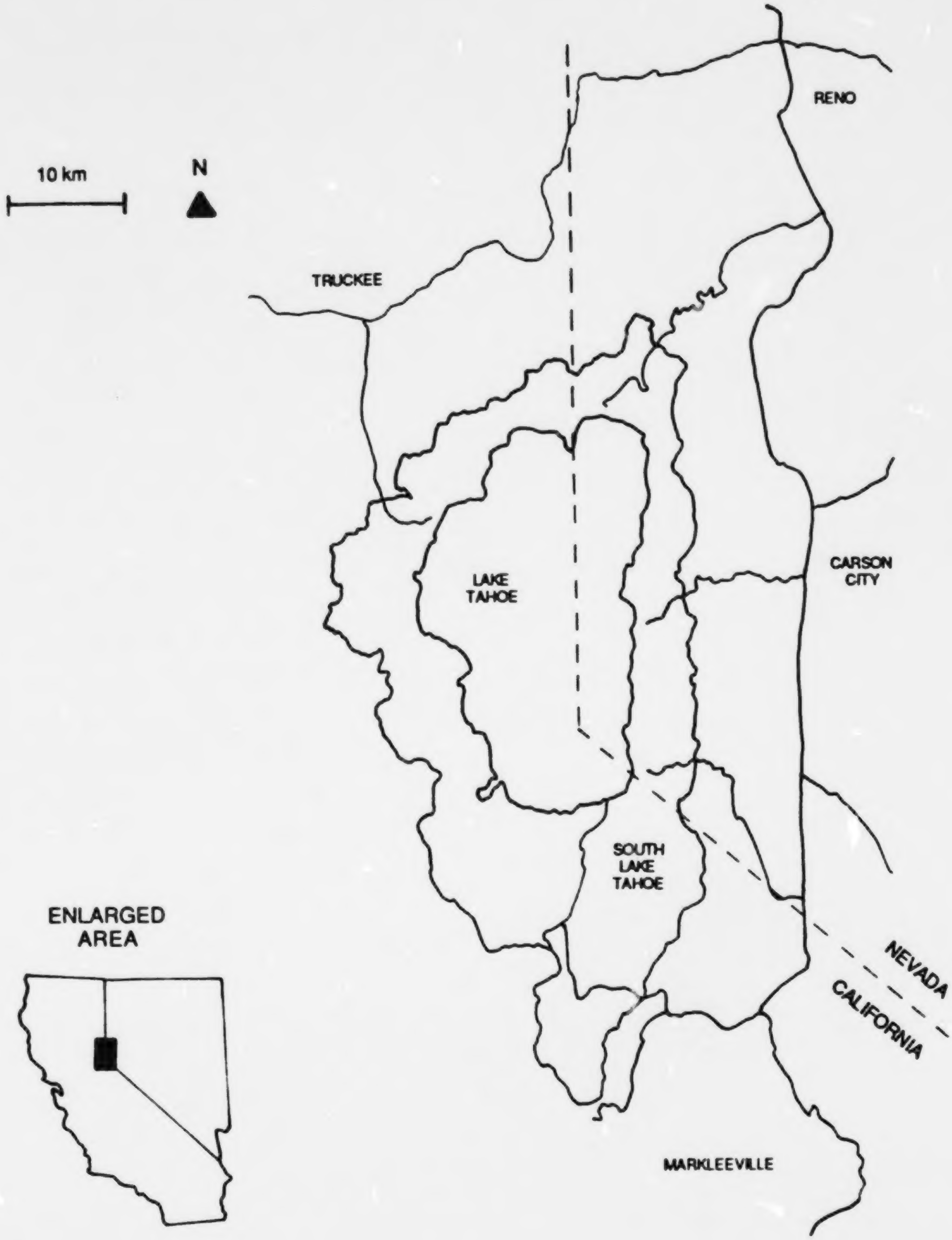
RENO
10 km
N
TRUCKEE
LAKE TAHOE
CARSON CITY
SOUTH LAKE TAHOE
ENLARGED AREA
NEVADA
CALIFORNIA
MARKLEEVILLE

Figure 1. Map of the Lake Tahoe basin showing the lake perimeter and the surrounding basin boundary. Major highways and cities are also shown.

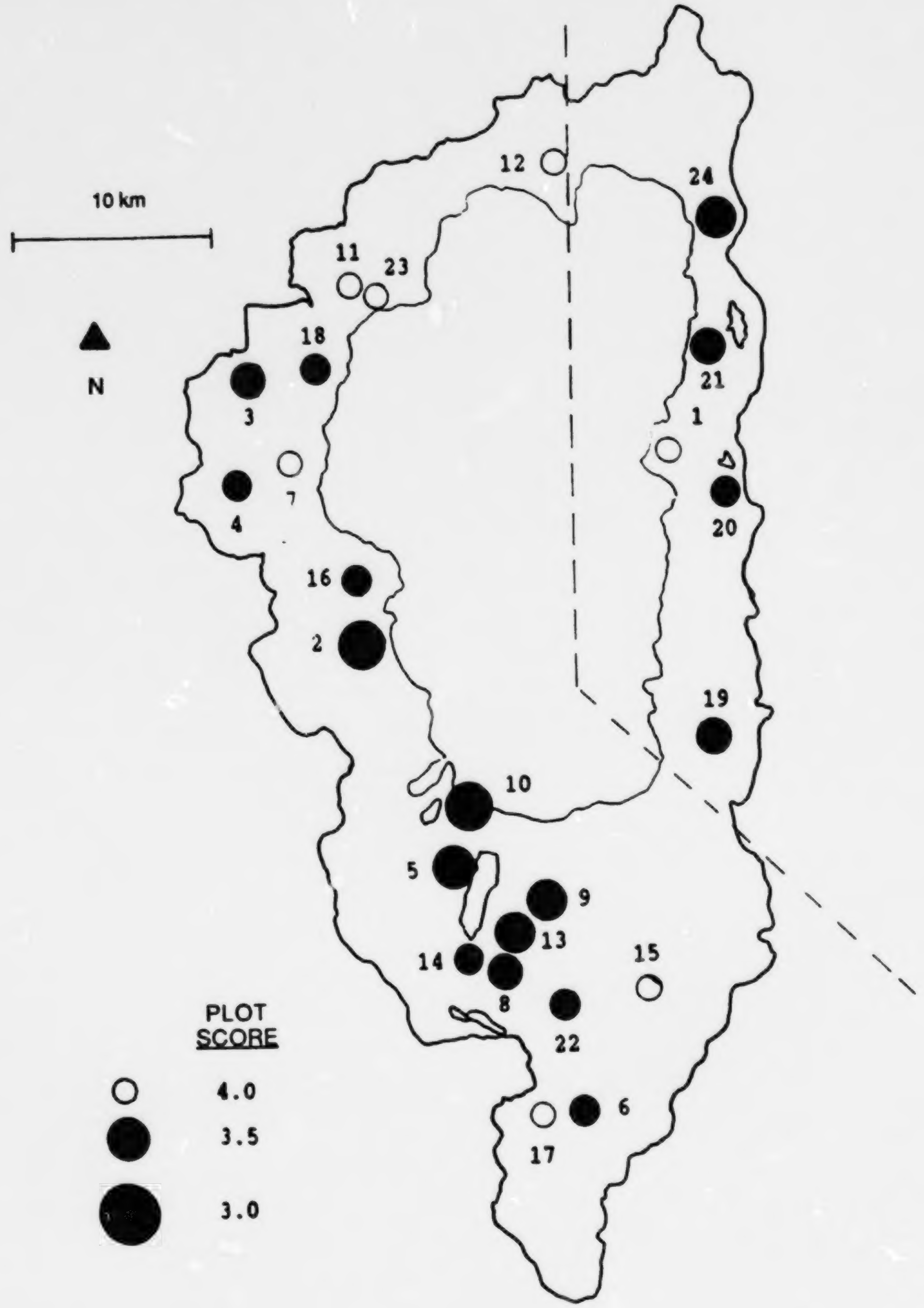
10 km
N
12
24
11
23
18
3
21
1
7
4
20
16
2
19
10
5
9
13
14
15
8
22
6
17
PLOT
SCORE
4.0
3.5
3.0

Figure 2. Results of the in-basin ozone injury survey. Open circles indicate plots with no ozone injury (FS scoring system). The area of the closed circles is proportional to the plot's injury severity. Plot numbers are shown.

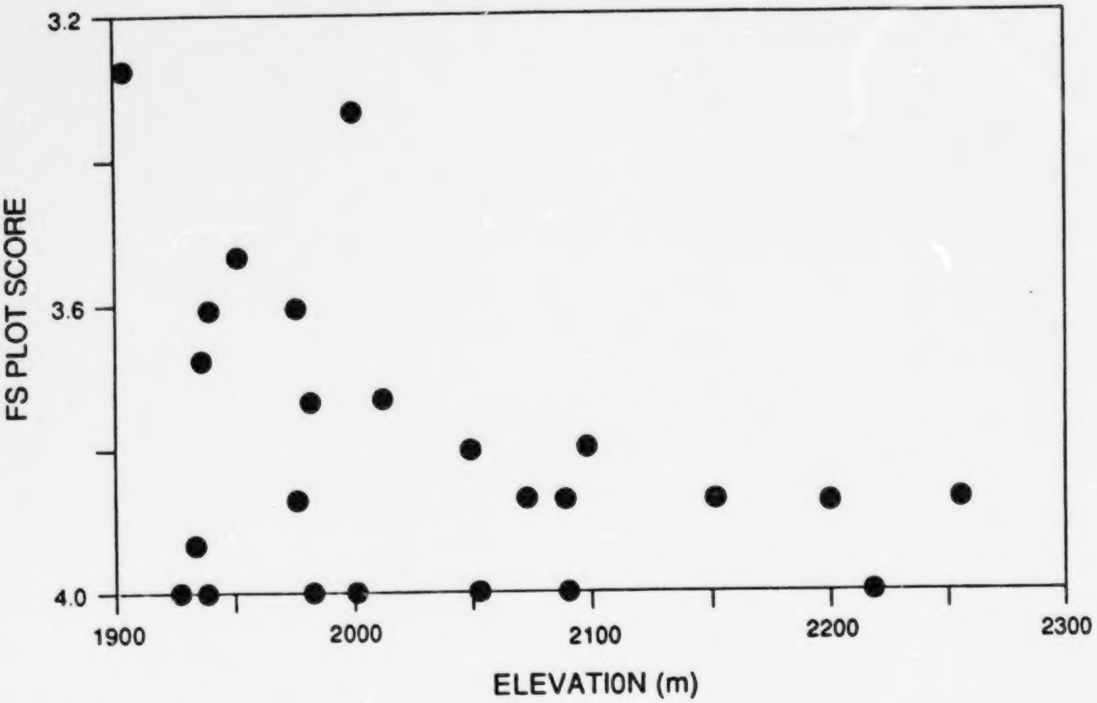

Figure 3. Ozone injury plot score vs. plot elevation. The ordinate has been inverted so higher points represent greater ozone injury

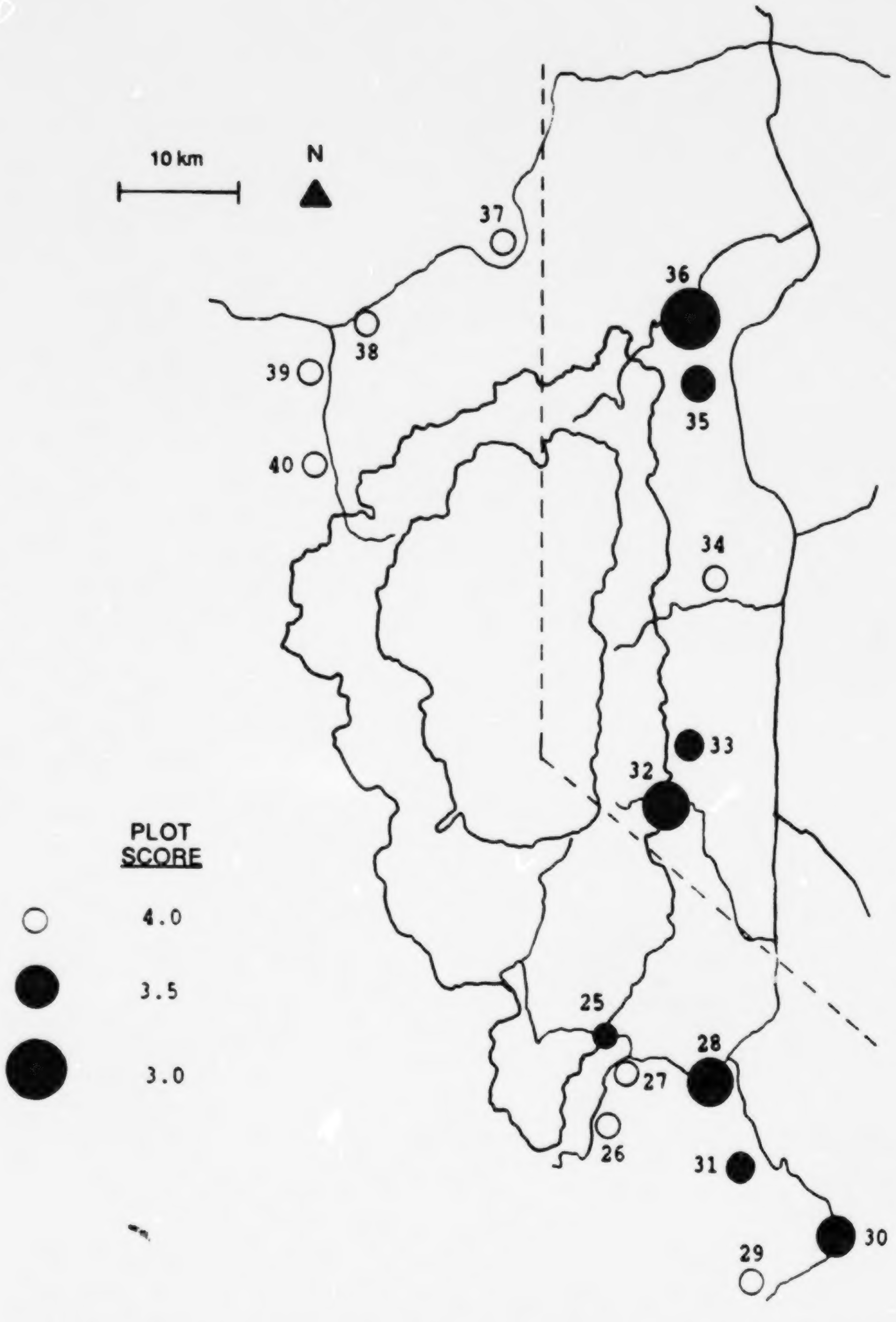
10 km
N
37
36
38
39
40
35
34
33
32
PLOT SCORE
○ 4.0
● 3.5
● 3.0
25
28
27
26
31
30
29

Figure 4. Results of the surrounding area ozone injury survey. Open circles indicate plots with no ozone injury (FS scoring system). The area of the closed circles is proportional to the plot's injury severity. Plot numbers are shown.

Ozone Injury and Growth Trends of Ponderosa Pine in the Sierra Nevada

David L. Peterson
Michael J. Arbaugh
Lindsay J. Robinson

USDA Forest Service
Riverside, California 92507

INTRODUCTION

Ozone monitoring data from the Sierra Nevada and locations to the west indicate that ozone concentrations are abnormally high in much of the range.[1] Nitrogen oxides and hydrocarbons produced from the combustion of fossil fuels in urban and industrial areas of the Central Valley and the San Francisco Bay region are photochemically oxidized and transported eastward. Exposure is highest on the west side of the range facing the Central Valley and low in the interior. There is a gradient of ozone exposure, with highest concentrations in the south and lowest in the north.

It has been previously documented that ozone concentrations are high enough to induce injury to pines in an area 500 km long from north to south. Ozone injury is visually observed as abnormally low needle retention and a characteristic chlorotic mottling. Previous studies indicate that there have been growth reductions in Jeffrey pine (*Pinus jeffreyi*) in areas of the southern Sierra Nevada with high ozone exposure and injury,[2] although a similar study failed to find growth reductions in open-grown ponderosa pine (*P. ponderosa*) from nearby stands.[3] These studies had a restricted geographic scope and a relatively small sample size.

Ponderosa pine is a dominant species of the mixed conifer forest ecosystem of the Sierra Nevada and one of the most sensitive species to ozone in North America. We expanded the geographic range of sampling in the Sierra to include a greater area of stands with potential exposure to elevated levels of ozone. Trees were cored in mixed conifer forest stands throughout the range, and needle injury was measured. Dendroecological analysis was used to evaluate temporal and spatial patterns of basal area growth, as well as factors related to local and regional growth trends.

METHODS

Sampling was conducted in five National Forests (NF) and two National Parks (NP) in the Sierra Nevada with documented symptoms of visible pollutant injury: Tahoe NF, Eldorado NF, Stanislaus NF, Yosemite NP, Sierra NF, Sequoia-Kings Canyon NP, and Sequoia NF (from north to south). Four stands in areas with ozone injury symptoms (symptomatic) and four stands in areas without injury (asymptomatic) were identified in each Forest and Park. Only mature mixed conifer forest stands with ponderosa pines greater than 50 years old were sampled.

Trees were sampled during July and August of 1987. Twenty-four ponderosa pines were sampled in each stand. Only dominant, codominant, and intermediate trees were included. Crown condition was recorded as needle chlorosis and number of years of needles retained, based on a sample of five branches from the lower crown of each tree. Chlorosis rating was based on ozone injury of the three most recent years of needles.[4]

Two cores were extracted from each sample tree at dbh. Cores were taken at the cross-slope sides of each tree and stored in straws until processed. Cores were mounted in wood blocks with glue and sanded until individual tracheids were visible under the microscope. Ring widths were measured with an incremental measuring machine equipped with a television camera and monitor and linked with a digital encoder interfaced with a microcomputer. Measurements were included in the database only if cores could be accurately crossdated. Time series of ring widths were converted to time series of annual basal area increments prior to statistical analysis.

The primary analysis was conducted using the Kalman filter.[5,6] The Kalman filter is a recursive procedure using the state-space formulation of a linear system that allows parameters to be nonstationary with time. A simple version of this filter is the random walk formulation. It is commonly expressed as two equations:

$$Y_t = F_t A_t + e_t, \quad e_t \sim \text{iid } N(0, \sigma^2 R_t) \qquad [1]$$

$$a_t = a_{t-1} + h_t, \quad h_t \sim \text{iid } N(0, \sigma Q_t) \qquad [2]$$

where Y is a column vector of observations representing the dependent variable values with time index t. The predictor variable values comprise the matrix F, and the state space-vector a_t stochastically varies as a random walk (equation 2). The disturbances are assumed to be iid normally distributed with constant variance. R_t and Q_t are matrices such that $\sigma^2 Q_t$ and $\sigma^2 R_t$ are covariance matrices.

The specific model used for the analysis was

$$B_t = a_o(t) + a_1(t)B_{t-1} + a_2(t)B_{t-2} + e_t \qquad [3]$$

where B is the individual series measurement transformed to basal area, and $a_o(t)$ is the long term growth trend associated with age, stand dynamics and other gradual environmental influences. $a_1(t)$ and $a_2(t)$ are the parameters associated with the persistence of growth changes contained in prior tree growth and climatic fluctuations. e_t is constrained to be independently distributed random variables. $a_i(t)$ is assumed to be time dependent.

An AR model was chosen as the basic model to insure that the resulting errors would be uncorrelated and identically distributed. This was important for conducting an analysis using the Kalman filter technique. A second-order process was chosen based on the results of a trial analysis of two sites. The basal area series were detrended using the smoothing spline,[7] and the residual series were fit with the appropriate AR(k) model. The majority of the series were adequately fitted with an AR(2) model. A minority of the series were adequately fitted with AR(1) or AR(3) models.

For this application, the parameter vector was chosen as

$$A_t = A_{t-1}+H_t, \qquad H_t \sim \text{iid } N(0,Q_t). \tag{4}$$

$$A_t = \begin{vmatrix} a_{0,2} \\ a_{1,t} \\ a_{2,t} \end{vmatrix} \tag{5}$$

This assumption of parameter variability through time is the simplest allowed by the Kalman filter (unless parameter stationarity is assumed). It has been previously used on the residual series (e_t and u_t).[8,9] It is appropriate for situations in which the parameter change between time intervals is 5% or less (i.e., when the parameters are changing slowly).[10] This restriction may not always be appropriate for dendroecological analysis without modification of the filter.

The observation error variance parameter R_t is a univariate constant for all t. The innovation error covariance matrix Q_t is of the form:

$$Q_t = \begin{vmatrix} q_{0,t} & 0 & 0 \\ 0 & q_{1,t} & 0 \\ 0 & 0 & q_{2,t} \end{vmatrix} \tag{6}$$

The q_is are not assumed to be time invariant for the model formulation used in this analysis, although the innovation errors are assumed to vary independently through time.

Estimates of s^2, r_t, and Q_t were estimated prior to the Kalman filter analysis. s^2 was estimated using ordinary least-squares (OLS) regression for the AR(2) model. This resulted in a block estimate assuming the constant parameters.

R_t and Q_t were estimated using a cumulative residual approach.[11,12] In this approach, the r_t and $q_{i,t}$ are considered to be the normalized residual variation not explained by the parameters when r_t and $q_{i,t}$ are set to zero. This approach also assumes $q_{i,t} = q_{j,t}$. It has the advantage of allowing these parameters to be constant or vary with time, thereby allowing the filter more flexibility to respond to abrupt parameter changes than is usually allowed by the random walk assumption.

Estimates for s^2, r_t, and Q_t were initially calculated using all observations. This was found to be adequate for most series. Refined estimates were calculated for r_t and Q_t by allowing them to vary with time. At least 10 years were used in all cases to estimate these parameters at each time t. This resulted in adequate residual properties for the model for all series fitted.

The standard filtering and smoothing equations[12] were coded into a SAS/IML program. The resulting program was used on individual core series for each tree. The appropriateness of the model for the individual series was judged based on residual statistics. Normality and autocorrelation were tested, and partial autocorrelation functions were obtained. Residual autocorrelation was judged to be the most serious model inadequacy. Low probabilities for the normal test were accepted in some cases if the residuals were sufficiently symmetric.

Confidence intervals were formed with the null hypothesis of parameter stationarity. This is equivalent to assuming $Q_t = 0$. Kalman filter estimates then become equal to those obtained in ordinary least-squares regression.[13] OLS regression theory results were used to construct 95% confidence intervals for each model parameter estimate.

Model results were interpreted separately for each tree. Interpretation was based primarily on the parameter a_0, because it was the parameter most indicative of a trend component. A growth trend change was defined to be a point at which $a_{0,t}$ estimates changed such that a significant trend resulted. A trend was defined as a consistent direction of parameter increase or decrease of 10 years or more that exceeded the 95% confidence interval bounds for parameter stationarity. Corresponding changes in $a_{1,t}$ and $a_{2,t}$ were used as supporting evidence. The initial 20 years of a series were not used due to the uncertainty of the filter convergence. Series without significant departures from the stationarity hypothesis, or that displayed growth patterns without clear trends, were considered to have no change.

The approximate date and direction of the growth change were recorded for those series that had identifiable growth patterns. Growth changes were recorded as an increase, no change, or a decrease in growth trend for each tree. Results were compiled by site and expressed as frequencies of increase and decrease per decade.

A significant decline was defined as a frequency of declines observed for a specific site that had high significance when tested against the distribution of asymptomatic sites without pollutant exposure for the same time period, or against that same site prior to the onset of elevated ozone exposure. The influence of historical and spatial dissimilarities was minimized by using these criteria. Two time periods were selected to represent segments of time prior to (1921-1950), and including (1951-1980), the effects of ozone on trees in the Sierra Nevada.

Data were arranged in contingency table form, and Chi-square tests were performed to determine significant differences between the frequency of declines for symptomatic and asymptomatic trees for the recent period (1951-1980), and between the frequency of declines in the past (1921-1950) and recent periods. The null hypotheses of independence of time and symptoms ($p = 0.156$), of homogeneity of times for symptomatic plots ($p = 0.222$), and homogeneity of symptoms for the recent time ($p = 0.218$) were tested.

Differences in trend frequencies (number of decreases minus number of increases per decade) were calculated for all sites. Frequencies of positive and negative trend changes were summed across time by site for each of the two time periods used for comparison. The net frequencies for recent asymptomatic sites were observed to fit a Gaussian distribution (Shapiro-Wilks test, $p = 0.965$). Past symptomatic site net frequencies were also fitted to a Gaussian distribution (Shapiro-Wilks test, $p = 0.373$). Significance levels for the present differences of trend change were calculated for all symptomatic sites.

RESULTS AND DISCUSSION

Ponderosa pine comprised more than 50% of the basal area in all but seven stands, with basal area ranging from 27 to 86 m^2/ha in symptomatic stands and 40 to 163 m^2/ha in asymptomatic stands. Tree age varied widely, although most trees were more than 80 years old. This is typical of many areas of the Sierra Nevada where logging was prevalent in the early 1900s, and new stands regenerated after clearcuts or partial cuts. An asymptomatic site in Sequoia NF was eliminated from the analysis because its time series of ring widths was not long enough for the statistical procedure used in this study.

Needle retention and level of ozone chlorosis are indicators of current tree vigor that are related to elevated ozone exposure. There were substantial differences in needle retention between symptomatic and asymptomatic sites throughout the Sierra Nevada. Symptomatic southern Sierra sites had relatively low needle retention, and needle retention was surprisingly low at some northerly sites (Table I). Needle retention at symptomatic sites was generally less than at asymptomatic sites, with the exception of Tahoe NF, the most northerly location.

Chlorotic injury was absent from nearly all trees at asymptomatic sites, which justifies the use of the asymptomatic classification. Ozone injury was highest for symptomatic sites in the southern Sierra, primarily in Sequoia NF, Sequoia-Kings Canyon NP, and Sierra NF (Fig. 1). Chlorosis was much less common for the four northernmost areas. Injury was rare in current year needles, moderate in 1-year-old needles, and common in 2-year-old needles at the southern sites. The highest levels of injury were measured in Sequoia-Kings Canyon NP. Most 2-year-old needles had some chlorosis, with 50% of needles in this age in injury class 2 (6–25% chlorosis) and a large percentage in the higher injury classes. More than 50% of 1-year-old needles had chlorotic injury as well. Injury levels for Sequoia NF and Sierra NF were comparable to those in the Parks for 2-year-old needles, but less severe for 1-year-old needles. There was a small amount of injury observed at Yosemite NP. The more northern locations had little injury.

The overall pattern indicates that ozone injury to needles is most severe in the southern Sierra and least severe in the north. This corresponds well to the south-to-north (high-to-low) gradient of ozone exposure[1] and corroborates survey data of crown condition collected by the USDA Forest Service and USDI National Park Service. This injury is striking in the southern half of the study area, which is approximately 250 km long. This level of widespread injury has been documented in only two other areas of the world, the Los Angeles Basin and outside Mexico City.

Loss of needles and damage to mesophyll of existing needles both lead to a reduction in photosynthesis. However, damage occurs primarily in the less productive older needles, so a large amount of needle biomass can be removed with a relatively small reduction in photosynthesis. The relationship of crown injury to physiological effects and carbon allocation over a long period of time is unknown, and natural variation makes it difficult to directly correlate crown condition with tree growth. It must also be noted that crown condition is the current status of the tree only, and may not reflect its past history.

Increases and decreases in basal area growth were noted by decade for each tree and summarized by site. There were temporal and spatial variations in growth patterns for both symptomatic and asymptomatic sites, although there were clearly some regional signals that appeared throughout most of the Sierra Nevada. Half of the symptomatic sites and all but six of the asymptomatic sites had trees with growth decreases during the 1920s. This was a period of low precipitation, and the year 1924 was an especially bad drought year that shows up in tree ring chronologies throughout the West. Low precipitation may have been responsible for the growth decreases during this decade. In contrast, the 1930s were a period of growth increases for nearly half of the symptomatic sites and all but six of the asymptomatic sites. Precipitation was relatively high during the second half of this decade, and may have been responsible for the large number of growth increases.

Tree growth patterns after 1950 are of special interest to this study because of potential impacts of air pollution during this period. Most symptomatic and asymptomatic sites had trees with growth decreases during the 1950s or 1960s, although the percentage of trees with decreases at a particular site never exceeded 25% in a given decade (Figures 2 and 3). Many sites also had substantial growth increases since 1950, with a large number of trees with increased growth (up to 60%) at several sites. Twenty symptomatic sites had at least some trees with growth decreases, with seven sites having greater than 20% of trees with decreases and one site greater than 40% (Figure 2). Growth increases tended to exceed growth decreases, however. Twenty-three sites had trees with increases, 12 of these with greater than 20% of trees with increases and 6 with greater than 40%.

Most asymptomatic sites had both growth decreases (21 sites) and increases (24 sites) as well (Figure 3). The number of trees with growth increases approximately balanced the number of growth decreases, with the exception of some of the central Sierra sites. In general, asymptomatic sites had a greater number of trees with growth reductions relative to growth increases than symptomatic sites.

Tree growth patterns indicate that there was not a large scale regional reduction in tree growth since 1950. Rather, there were several patterns of increases and decreases throughout the Sierra Nevada. A few sites deserve additional analysis because they have reduced growth since 1950, which means that they may potentially have been affected by air pollution. It is possible that stress from ozone injury has been great enough to affect tree growth in some areas, although this reduction is not a widespread response. It is important to identify such a phenomenon even if it occurs in a small region.

The growth changes discussed above relate to general patterns only. We therefore identified symptomatic sites with recent (since 1950) growth changes that may have significance relative to decreases at asymptomatic sites and to past decreases at symptomatic sites, as determined by the statistical method previously described. Results of this analysis are summarized in Tables II and III.

Although there is no evidence of widespread regional growth decreases during recent years, a few symptomatic sites had growth decreases that appear to be significant (Tables II and III). Symptomatic sites in Sequoia-Kings Canyon NP had relatively low P values compared to other forest locations in terms of both number of decreases (Table II) and number of net decreases (Table III). One site in Sequoia NF, one in Yosemite NP, and two in the Tahoe NF had low P values.

Symptomatic sites in the southern Sierra with recent growth decreases are located in areas known to have high levels of ozone exposure and ozone injury. All of the Sequoia-Kings Canyon NP symptomatic sites and one of the Sequoia NF sites have trees with reduced growth during each decade since 1940. These symptomatic sites in the southern Sierra are the ones that would most likely have reduced growth associated with ozone injury, although it is difficult to demonstrate a cause-and-effect relationship. A poor relationship between precipitation and growth decreases in symptomatic Sequoia-Kings Canyon NP sites suggests that nonclimatic factors such as air pollution stress may have affected tree growth.[14] Yosemite NP had less ozone injury than more southerly locations, although there was considerable damage to 2-year-old needles. Recent growth decreases at one of the Yosemite NP sites may therefore also be related to ozone injury, although the evidence is less convincing.

Growth reductions at two of the symptomatic Tahoe NF sites are difficult to explain. Ozone exposure and injury are low in this area, and there were few observable symptoms of disease or insect damage that may have contributed to the growth reduction. Local resource management personnel had no explanations for this recent change in growth patterns.

These analyses were designed to examine nonclimatic effects on long-term growth trends to the greatest extent possible. Symptomatic trees, that is, those trees most likely to have impacts from elevated ozone exposure, were compared to all trees from asymptomatic sites, as well as to past symptomatic tree growth. The effect of climate and other environmental factors that may differ from north to south and west to east (e.g., a west-to-east precipitation gradient) were therefore integrated in hypothesis testing. The analysis was subjective, although recent growth decreases determined in this manner have a high probability of being real and unrelated to climatic differences. It may never be possible to determine a cause-and-effect relationship between ozone exposure and tree growth in the Sierra Nevada because of the lack of long-term ozone concentration data, particularly at mountain locations.

CONCLUSIONS

This study is the largest investigation of regional tree growth for a tree species in the western United States. There is a high degree of variation in the symptomatic injury and tree growth data, although some regional patterns are apparent. These patterns can be determined only by looking at the data for each individual tree, because significant trends can otherwise be lost through aggregation and averaging procedures.

Symptomatic injury data clearly indicate a gradient of ozone-induced injury, with greatest injury in the southern Sierra Nevada and lowest injury in the north. This corresponds to patterns of ozone exposure in the mixed conifer forest on the western slopes of the range. The levels of injury recorded in this and other studies[15] indicate that there is a high level of pollutant stress on a regional basis. Crown condition should be monitored in this area as a measure of tree vigor even if growth trends are inconclusive, because it has been shown that chronic injury has led to changes in community structure at other mixed conifer forest sites.[16]

Results of basal area growth analysis were more difficult to interpret. There were clearly strong regional growth signals during this century, particularly in the 1920s and 1930s. These trends appeared to be related to precipitation, which has been shown to be the most significant factor related to tree growth in the Sierra Nevada.[1,2] Symptomatic sites in the southern Sierra Nevada have a general trend of growth decreases since 1950 in an area with a relatively high level of ozone exposure and injury. This suggests that nonclimatic factors such as air pollution may have affected growth in the Parks. We believe that it is quite likely that ozone injury has played a role in the stress complex that produced growth reductions in this area.

ACKNOWLEDGMENTS

We thank George Pollock and Darren Anderson for their assistance with all aspects of this study. Helpful comments on the manuscript were provided by Edward Cook, Thomas Swetnam, and Paul Van Deusen. We are grateful to personnel of the USDA Forest Service and USDI National Park Service for their cooperation. Research was partially supported by funds provided by the Western Conifers Research Cooperative within the joint U.S. Environmental Protection Agency-USDA Forest Service Forest Response Program. The Forest Response Program is part of the National Acid Precipitation Assessment Program. This paper has not been subject to EPA policy review and should not be construed to represent the policies of either agency.

REFERENCES

1. "California Air Quality Data," vol. 19, California Air Resources Board, Aerometric Data Division, Sacramento, CA, 1987.

2. D.L. Peterson and M.J. Arbaugh, "Growth patterns of ozone-injured ponderosa pine (*Pinus ponderosa*) in the southern Sierra Nevada," *JAPCA* 38:921 (1988).

3. D.L. Peterson, M.J. Arbaugh, V.A. Wakefield, and P.R. Miller, "Evidence of growth reduction in ozone-stressed Jeffrey pine (*Pinus jeffreyi* Grev. and Balf.) in Sequoia and Kings Canyon National Parks," *JAPCA* 37:906 (1987).

4. P.S. Muir and T.V. Armentano, "Evaluating oxidant injury to foliage of *Pinus ponderosa*:a comparison of methods," *Can. J. For. Res.* 18:498 (1988).

5. R.E. Kalman, "A new approach to linear filtering and prediction problems," *Trans. ASME J. Basic Engrg.* (ser. D) 82:35 (1960).

6. R.E. Kalman and R.S. Bucy, "New results in linear filtering and prediction problems," *Trans. ASME J. Basic Engrg.* (ser. D) 83:95 (1961).

7. E.R. Cook and R.L. Holmes, "User's manual for program ARSTAN," Univ. Arizona, Tucson, AZ, 1985.

8. H. Visser, J. Molenaar, "Kalman filter analysis in dendroclimatology," *Biometrics* 44:929 (1988).

9. P.C. Van Deusen, "Some applications of the Kalman filter to tree-ring analysis," in *Proceedings of the International Symposium on Ecological Aspects of Tree-Ring Analysis*, Lamont-Doherty Geological Observatory, Columbia Univ., Palisades, NY, 1987, p. 566.

10. P.C. Young, *Recursive Estimation and Time-Series Analysis: an Introduction*, Springer-Verlag, New York, NY, 1984.

11. A.H. Jazwinski, *Stochastic Processes and Filtering Theory*, Academic Press, New York, NY, 1970.

12. R.J. Bennett, *Spatial Time-Series: Analysis, Forecasting and Control*, Pion, London, UK, 1979.

13. P.W. Otter, "The discrete Kalman filter applied to linear regression models: statistical considerations and an application," *Statistica Neerlandica* 32:41 (1978).

14. D.L. Peterson, M.J. Arbaugh, and L.J. Robinson, "The effects of ozone stress on tree growth and vigor in the Sierra Nevada of California, USA," in *Proceedings of the IUFRO Symposium on Air Pollution and Forest Decline*, IUFRO, Interlaken, Switzerland (in press).

15. J. Pronos and D.R. Vogler, "Assessment of ozone injury to pines in the southern Sierra Nevada, 1979/1980," *USDA For. Serv. Pac. SW Region Forest Pest Manage. Rep.* 81-20, 1981.

16. P.R. Miller, "Ozone effects in the San Bernardino National Forest," in *Proceedings of the Workshop on Air Pollution and the Productivity of the Forest*, Izaak Walton League of America, Arlington, 1983, VA, p. 161.

Table I. Mean number of years of needles retained (± 1 SD) by trees from symptomatic and asymptomatic sites. Data should be compared with all other data in the table, not just within each row.

Forest	Site	Symptomatic	Asymptomatic
Tahoe NF	1	4.5 (0.6)	4.3 (0.5)
	2	4.4 (0.6)	4.8 (0.5)
	3	4.6 (0.5)	4.9 (0.6)
	4	4.3 (0.5)	4.8 (0.5)
Eldorado NF	1	3.0 (0.3)	4.5 (0.5)
	2	3.0 (0.2)	4.4 (0.6)
	3	3.7 (0.5)	4.0 (0.4)
	4	2.9 (0.4)	3.9 (1.2)
Stanislaus NF	1	2.6 (0.5)	4.8 (0.4)
	2	2.8 (0.4)	4.7 (0.5)
	3	3.6 (0.5)	4.3 (0.5)
	4	3.4 (0.5)	4.9 (0.3)
Yosemite NP	1	4.1 (0.2)	4.5 (0.2)
	2	3.9 (0.3)	4.8 (0.6)
	3	4.0 (0.2)	4.2 (0.4)
	4	4.0 (0.3)	4.3 (0.4)
Sierra NF	1	3.0 (0.2)	4.8 (0.6)
	2	3.4 (0.6)	4.6 (0.5)
	3	3.0 (0.2)	4.1 (0.3)
	4	3.0 (0.3)	4.4 (0.5)
Sequoia-Kings Canyon NP	1	3.2 (0.9)	4.0 (0.4)
	2	3.4 (0.5)	3.4 (0.6)
	3	3.4 (1.3)	3.2 (0.6)
	4	3.2 (0.7)	4.8 (0.4)
Sequoia NF	1	3.4 (0.5)	4.9 (0.2)
	2	3.6 (0.6)	5.0 (0.4)
	3	3.4 (0.6)	5.0 (0.5)
	4	3.4 (0.5)	–

Table II. Significance levels for the observed number of declines in symptomatic sites in recent years using the null hypotheses of no difference from: (1) the number of decreases in asymptomatic sites in recent years, and (2) the number of decreases in symptomatic sites from past years. The alternate hypotheses were both that the number of decreases was greater for the symptomatic sites in recent years. The empirical cumulative mass functions were used as distributions for the significance tests.

Forest	Site	P (x>X) Hypothesis 1	 Hypothesis 2
Tahoe NF	1	0.67	0.79
	2	0.64	0.75
	3	0.04	0.18
	4	0.11	0.25
Eldorado NF	1	1.00	1.00
	2	1.00	1.00
	3	0.59	0.75
	4	0.63	0.79
Stanislaus NF	1	1.00	1.00
	2	0.63	0.79
	3	0.75	0.79
	4	0.30	0.61
Yosemite NP	1	0.15	0.32
	2	0.59	0.75
	3	1.00	1.00
	4	0.33	0.64
Sierra NF	1	0.74	0.79
	2	1.00	1.00
	3	0.74	0.79
	4	1.00	1.00
Sequoia-Kings Canyon NP	1	0.19	0.25
	2	0.04	0.11
	3	0.19	0.29
	4	0.30	0.50
Sequoia NF	1	1.00	1.00
	2	1.00	1.00
	3	0.59	0.71
	4	0.15	0.25

Table III. Significance levels for the observed number of net growth decreases (decreases minus increases) in symptomatic sites in recent years using the null hypotheses of no difference from: (1) the number of net decreases in asymptomatic sites in recent years, and (2) the number of changes in symptomatic sites from past years. The alternate hypotheses were both that the number of net decreases was greater for the symptomatic sites in recent years. The distribution under the null hypotheses was assumed to be the student's t distribution with 26 and 27 df for hypotheses 1 and 2, respectively.

Forest	Site	P (x>X)	
		Hypothesis 1	Hypothesis 2
Tahoe NF	1	0.95	0.81
	2	1.00	0.99
	3	0.04	0.07
	4	0.03	0.05
Eldorado NF	1	0.60	0.45
	2	0.91	0.74
	3	0.90	0.73
	4	0.60	0.45
Stanislaus NF	1	0.95	0.81
	2	1.00	0.94
	3	0.48	0.79
	4	0.26	0.23
Yosemite NP	1	0.07	0.09
	2	0.48	0.31
	3	0.48	0.37
	4	0.21	0.20
Sierra NF	1	0.99	0.93
	2	0.99	0.93
	3	0.48	0.37
	4	1.00	0.99
Sequoia-Kings Canyon NP	1	0.36	0.29
	2	0.04	0.07
	3	0.68	0.51
	4	0.38	0.31
Sequoia NF	1	0.62	0.46
	2	0.91	0.71
	3	0.99	0.95
	4	0.05	0.08

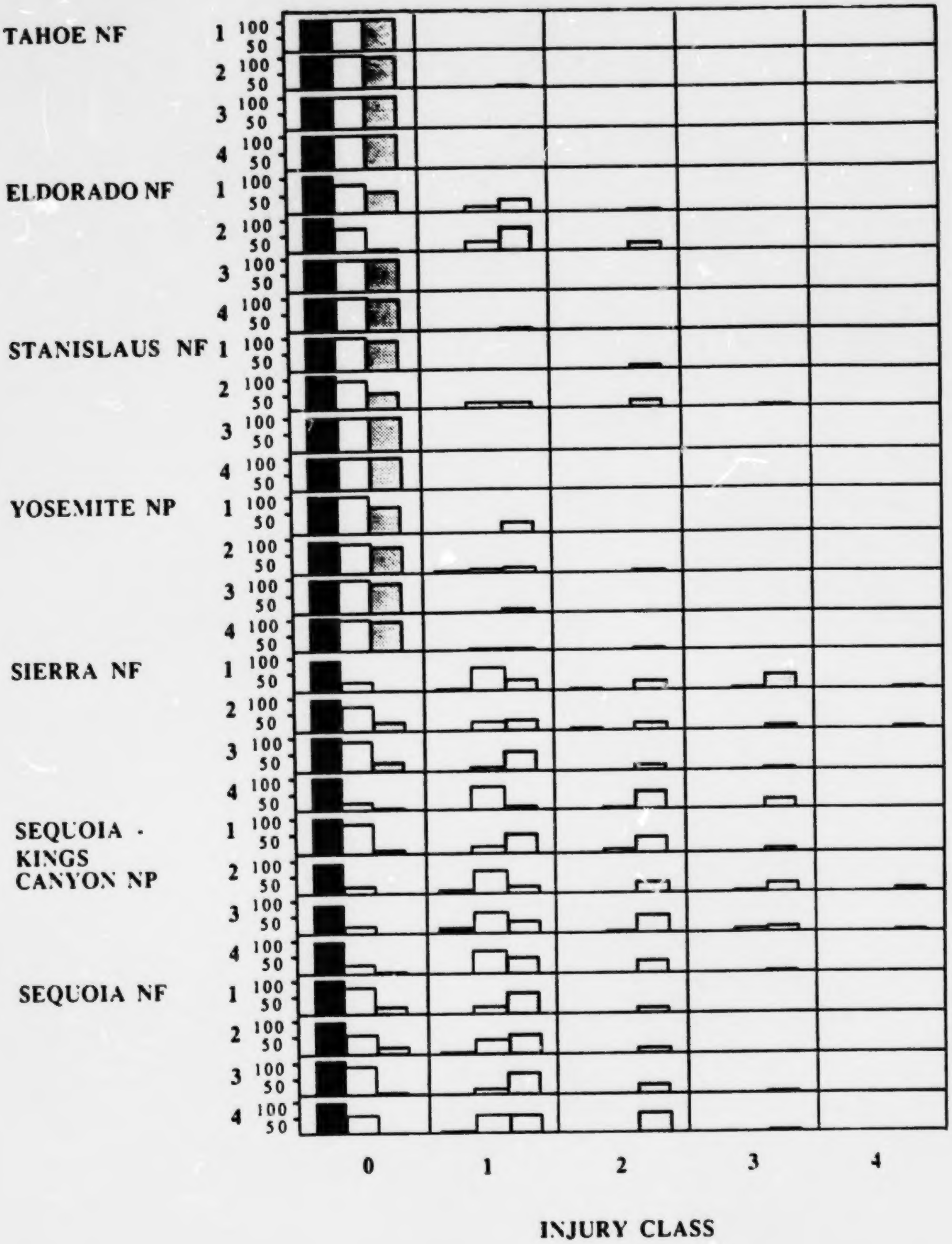

Figure 1. Percent of sample trees with ozone-caused chlorosis injury in each stand. Injury is indicated for current year (solid bar), 1-year-old (open bar), and 2-year-old (stippled bar) needles. Injury classes indicate percent chlorosis in needles as follows: 0 is 0%, 1 is 1-5%, 2 is 6-25%, 3 is 26-50%, 4 is 51-75%.

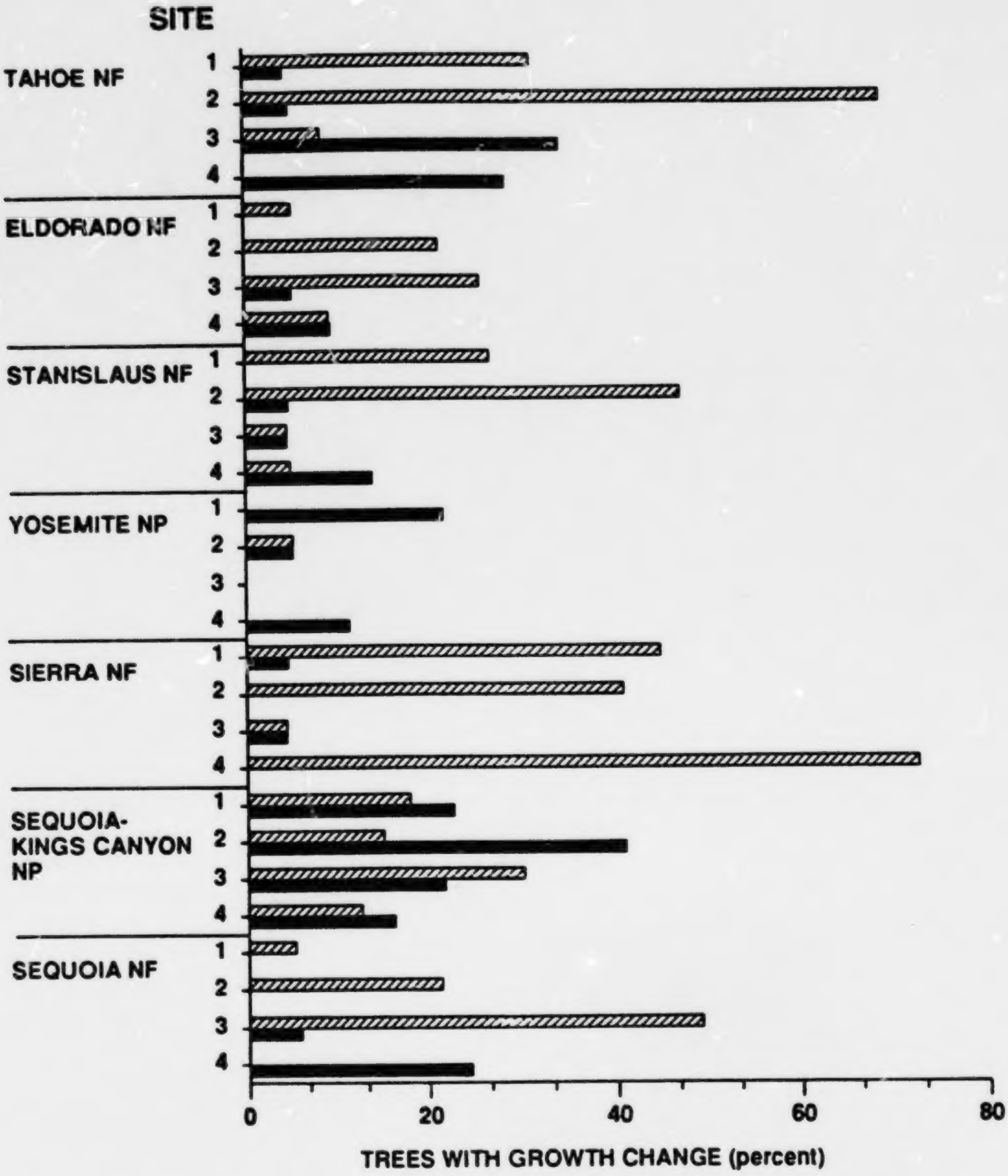

Figure 2. Percent of trees in each symptomatic site with growth decreases (solid bar) and increases (stippled bar) since 1950 as determined by Kalman filter analysis.

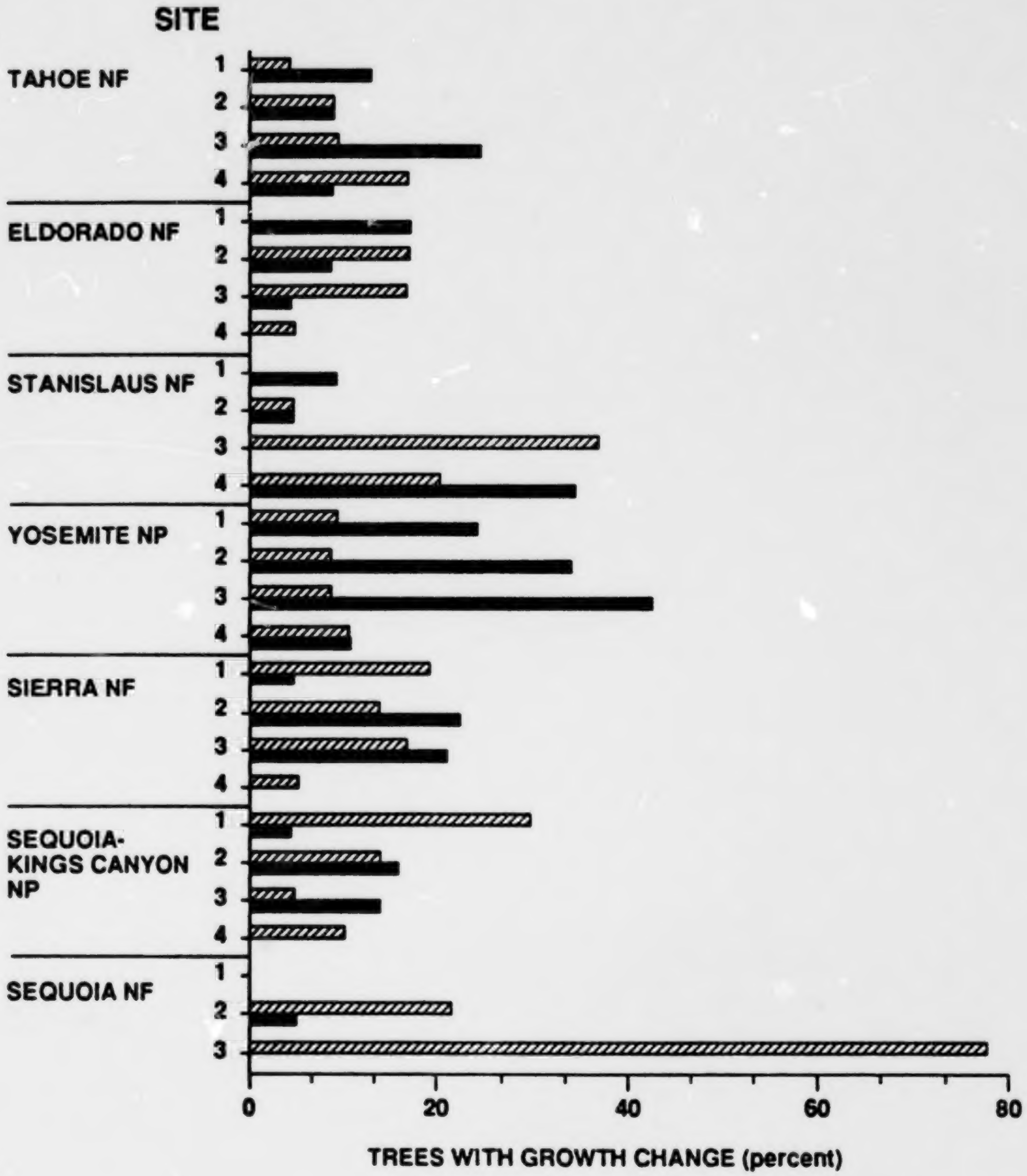

Figure 3. Percent of trees in each asymptomatic site with growth decreases (solid bar) and increases (stippled bar) since 1950 as determined by Kalman filter analysis.

Trend of Ozone Damage to Conifer Forests between 1974 and 1988 in the San Bernardino Mountains of Southern California

Paul R. Miller[1]
Joe R. McBride[2]
Susan L. Schilling[1]
Anthony P. Gomez[1]

[1] *Pacific Southwest Forest and Range Experiment Station*
USDA Forest Service
4955 Canyon Crest Drive
Riverside, CA 92507

[2] *Department of Forestry and Conservation*
Mulford Hall
University of California, Berkeley
Berkeley, CA 94720

INTRODUCTION

From 1974 to 1978 the chronic symptoms of ozone damage to ponderosa pine (*Pinus ponderosa* Laws.) and Jeffrey pine (*Pinus jeffreyi* Grev. and Balf.) were measured annually at forest plots exposed to different levels of ozone as a result of their varying distances downwind from the urban ozone source area.[1] The chronic symptoms of ozone damage to the ponderosa and Jeffrey pines in these plots were similar to symptoms observed with seedlings of these species in fumigation studies that showed their ozone sensitivities to be very similar.[2] Ponderosa and Jeffrey pine were represented in forest stands across the entire length of the San Bernardino National Forest study area and this enabled the periodic observation of changes in response to different ozone exposures. Between 1974 and 1978, the level of chronic ozone injury to crowns of ponderosa and Jeffrey pines, expressed as an ozone injury index, did not improve.[1] In a limited survey of only six plots, representing the most severe levels of chronic ozone injury to ponderosa pine, the mortality between 1973 and 1983 was 55% for seedlings (0 to 9 years), 68% for saplings and poles (10 to 49 years), 33% for young mature trees (50 to 99 years), and 14% for mature trees (>100 years).[3]

We examined the changes of crown injury and associated stem growth of different size classes of ponderosa and Jeffrey pines at intervals between 1974 and 1988 at 15 plots not disturbed by logging. These observations excluded all plot trees that were alive for only a part of the entire period of observation. Stand-level attributes, including changes in density and species composition due to tree mortality and recruitment of new seedlings, were recorded. However, these data will be the subject of another report. The observations were for the intervals 1974 to 1978, 1979 to 1983, and 1984 to 1988 during which departures of ozone and precipitation from the 1974 to 1987 means were examined at monthly intervals. Changes of stem growth were examined in relation to the ozone injury index and the available soil moisture at plots.

Preceding page blank

EXPERIMENTAL METHODS

The Study Area

The study area includes the San Bernardino Mountains, which form part of the northern and eastern boundaries of the California South Coast Air Basin. Transport of ozone-polluted air from the southwest to the northeast and east across the forested mountain barrier results in a gradient of decreasing ozone concentrations.[4] Forest vegetation plots were established at intervals in the west-to-east direction across the mountain area at sites with uneven age stands of ponderosa and/or Jeffrey pines and associated species (Figure 1). The major criterion was the presence of a sufficient number of pines with diameters at breast height (dbh) > 29.9 cm so that 50 were available in a plot 30 m wide and not more than 400 m long. Plot locations started at the lower elevational range of the forest (1500 m), and some were located as high as 2320 m (Table I). Companion trees of all species were included in the data set if they were greater than 10 cm dbh. Tree location was recorded as distance from the beginning of the plot and distance left or right from the center line.

Measuring Crown Injury and Stem Growth

At the end of the growing season from 1974 to 1978, and in 1988,the level of chronic injury to crowns of ponderosa and Jeffrey pines was estimated visually for trees of all crown competition classes. One observer was responsible for all visual estimates. Whenever possible, the estimations of needle whorl number and needle condition were determined by holding branches close enough for detailed inspection. On large trees, with branches out of reach, wide-field, 7 x 30 binoculars were used to scan upper and lower crowns. The number of annual needle whorls present on branches of the upper and lower crown, the condition of each needle whorl, needle length, and branch mortality were described by a numerical code:

Portion of Crown	Attribute	Numerical Code
Upper half	Number of needle whorls	Count:1,2,3,etc
	Condition of each whorl	
	Green, healthy	4
	Chlorotic mottle	2
	Brown, dead	0
	Needle length	
	Average length	1
	Shorter than average for the site	0
Lower half	(Repeat the measurements described above and estimate branch mortality)	
	Branch mortality	
	Normal mortality	1
	Excessive mortality for the position of the crown in the stand	0

The numbers were added to obtain an ozone injury index. For example, a tree with three annual needle whorls in both upper and lower crown, where the two youngest whorls were both rated as 4 and the older whorls each as 2, and the needle length and branch mortality were normal for the site, or position of the tree, the sum would be 29 (3+3+4+4+2+4+4+2+1+1+1 = 29). The literal meaning of different score ranges was as follows: 0 to 8 = very severe injury, 9 to 14 = severe, 15 to 21 = moderate, 22 to 28 = slight, 29 to 35 = very slight, and > 36 = no visible symptoms of ozone damage.

To determine changes of stem growth, tree diameters were measured with a steel tape to the nearest 0.1 cm in 1974, 1978, 1983, and 1988. Increases in stem area were computed from the diameter difference between times of measurement. The ozone injury index was not recorded in 1983 at the time stems were measured because a new observer was needed, but there was not enough time for training.

Monitoring Ozone and Precipitation

During the 1974 to 1978 period of intensive study, three ozone monitoring stations utilizing ultraviolet ozone photometers were operated in the study area at Camp Paivika (CP), Sky Forest (SF),and Barton Flats (BF) (Figure 1). In 1978, the San Bernardino County Air Pollution Control District established a permanent ozone monitoring site at Lake Gregory (Figure 1). The record from this station for the 1978 to 1987 period was available from the EPA Aerometric Information Retrieval System (AIRS), and the South Coast Air Quality Management District. The data from the permanent locations and from short periods of sampling at the vegetation plots with battery-powered total oxidant meters made it possible to estimate the ozone concentrations to be expected at each vegetation plot in relation to Lake Gregory (Table I).[4]

Total precipitation storage gauges were established at each plot during the 1974 to 1978 period to determine plot-to-plot differences in annual precipitation. A published record of precipitation at Lake Arrowhead (Figure 1) was available for the entire period of the study (Table I). This record was used to represent year to year changes in the study area. Available water content of soils down to 90-cm depth was determined from moist and oven-dried weights of soil samples taken at intervals during the growing season at each of the plots (Table I).[5]

RESULTS

The tree condition trends, as measured by the ozone injury index, suggested that tree condition has improved since about 1978 in all but those plots exposed to the highest ozone concentrations. This improvement coincided with lower hourly average and lower monthly maximum ozone concentrations of recent years during which annual precipitation has been generally lower than average. Stem growth response was generally related to the ozone injury index within a plot, but comparisons of differences between plots showed that available water content of soils and precipitation amount was more important than ozone injury index.

Overview of Plot Attributes and the 1988 Ozone Injury Index

Several additional characteristics of the experimental plots are summarized in Table I. Forest plots were arranged in order of increasing ozone injury index (increasing health) in 1988. As plot elevation increased from 1525 to 2320 m the precipitation generally decreased. The lower elevation plots have ponderosa pine only. In the 1900- to 2135-m range, the plots had a mixture of ponderosa and Jeffrey pines; and above 2160 m, the plots had Jeffrey pine only. Where the mixture of species was present (GVC, BF, DL, and CAO), the injury scores indicated ponderosa pine response to be quite similar to Jeffrey pine. At BF and DL the ponderosa injury index was higher (less injury), whereas at CAO and GVC the Jeffrey injury index was higher. These index values averaged 27.4 for ponderosa and 26.7 for Jeffrey. This similarity supported the requirements of our experimental design, i.e., to have stands of forest vegetation with species of similar ozone sensitivity across the entire study area. The available soil water (percent by weight in the 0-to-90 cm zone) varied widely among plots (Table I).[5]

Year-to-Year Trends of Precipitation and Ozone

The annual precipitation for each of the 14 years between 1973 and 1987 was expressed as the October through September sum where the precipitation year was defined by the October in which it began (Table II). Departures from the monthly means of the entire study period were calculated for the three intervals after which stem growth was measured, i.e., 1974 to 1978, 1979 to 1983, and 1984 to 1988 (Figure 2). The first period was about average, the second was definitely the most moist, and the last period was the driest. The last 5-year period was marked by slightly higher than average precipitation during October, November, and December but much lower than average precipitation in the January to March period immediately preceding the new growing season.

The 24-h average ozone concentrations and the average of monthly ozone maximum concentrations for May through October of the 1974 to 1987 period generally showed a gradual decline in recent years (Table II). The calculated departures from the long-term mean during each of the three observation intervals, for both the 24-h average and the averages of monthly maximum concentrations, showed higher than average concentrations during the 1974 to 1978 period, about average concentrations during 1979 to 1983, and below average levels during the 1984 to 1988 period (Figure 3). During the most recent period, the monthly maximum values decreased more than the 24-h average; early summer months exhibited slightly smaller decreases than the mid-to-late summer months.

Temporal and Spatial Trends of Chronic Ozone Injury

The crown injury to ponderosa and Jeffrey pines, expressed as the ozone injury index, was observed in 1974, 1978, and 1988. The first examination of the ozone injury index employed the paired t-test to compare index values between observation dates when data from all plots were aggregated. Computations were based on individual tree scores and not plot averages. In effect, this addresses the question: Have there been any significant changes in the ozone injury index reflected by all trees in the region of the study plots? Three stem diameter classes were examined separately to determine whether trees of different sizes (ages) responded differently to chronic ozone exposure (Table III). The observations show statistically significant improvements in all size classes between 1978 and 1988, but not between 1974 and 1978 except for Jeffrey pines greater than 60 cm dbh that were generally located in the zone of lowest ozone exposure. The 1978–1988 improvement and the decrease of ozone concentrations during this period (Figure 3) suggested a definite link between these two variables.

In Figures 4a and 4b the plots are presented (left to right) in the general order of their increasing distance from the western boundary of the study area. The ozone injury indexes increased with increasing distance. However, an examination of data from individual plots at CP and BP showed no improvement in ozone injury index (Figure 4a). Both plots received the highest ozone doses because they are located at the extreme west end of the study area. Other ponderosa and Jeffrey pine plots showed definite trends of continuing improvement of ozone injury index with the exception of Jeffrey pines at BL and BF (Figure 4b). Tree diameter class did not appear to have any definite relationship to crown injury at any particular plot, although the aggregated data of all plots (Table III) suggested that trees greater than 60 cm dbh may have improved more than smaller size classes.

Temporal and Spatial Trends of Stem Growth

Two patterns of growth response emerged. (1) In many plots the growth of all size classes improved, even in the drier 1983-1988 period; during the 1979 to 1983 period, which received more precipitation, the growth was greatest in many plots (Figures 5a,5b). (2) Growth did not improve at a few plots, particularly BP where the ozone injury index was also lower, Figure 5a. Growth apparently varied independently from ozone injury index when compared from plot-to-plot. For example, trees with the highest ozone index at HV grew less than those at CP and BP, which had low ozone injury indexes. When 1988 indexes were regressed with 1983-1988 growth for the entire group of plots, the relationship was actually negative with R = 0.310 (decreasing growth with increasing crown health). Thus, other variables, including available soil water content, competition from companion trees and understory plants, and other site characteristics masked the contribution of the improved ozone injury index in determining stem growth.

Available water content was suspected to be one of the most important variables. It varied considerably from plot to plot in the 0-90 cm layer of soil (Table I); therefore, regressions were tested between growth during the 1979 to 1983 and 1984 to 1988 periods and available water content (%) at 13 of the 15 plots, Figure 6. The regressions were R = 0.63 for 1979 to 1983, and R = 0.67 for 1984 to 1988. Even though these relationships are not high, they provide the best support now available for an explanation of plot-to-plot differences in stem growth.

The effect of ozone injury index on growth, in relation to soil water availability, can be better understood when examined on a plot-by-plot basis. For example, the regression of ponderosa pine growth at Barton Flats to the ozone injury index was R = 0.66 for both the moist 1979 to 1983 period and the dry 1984 to 1988 period, Figure 7. Therefore, the effect of the ozone injury index was apparent in this example and within other plots as well. Available water content at the Barton Flats plot was 21 %, a value at the upper end of the range of observed values (Table I). Water availability was not the most important limiting factor.

DISCUSSION

The changes of crown condition, as indicated by the ozone injury index of ponderosa and Jeffrey pines, indicated improvements of crown condition which were related to distance from the area source of ozone pollution and with a general decrease of ozone levels in the San Bernardino Mountains during recent years. These results supported the usefulness of this measurement for assessing changes of chronic ozone injury to ponderosa and Jeffrey pines. In this situation, the use of an index permits the gathering of several associated measures of chronic injury in the field and offers the advantage of the simultaneous use of all variables in the data analysis phase.[6]

The sources of variance in tree growth trends are numerous, including temperature, insolation, essential nutrients, competition with neighboring trees, logging activities, precipitation and soil moisture holding capacity (available water content), among others.[7] We have not attempted to construct a complex multivariate model to examine the relative importance of these variables in this situation because the data base was insufficient for most variables. Instead, we have attempted to understand chronic ozone injury (ozone injury index) and its relationship to winter precipitation (and available soil water content) because the latter was known to be one of the most important variables influencing stem growth.[8,9] Of the two variables, available soil water exercised a more profound influence on growth than the mean ozone injury index in plot-to-plot comparisons. In single plots, however, the range of ozone injury index values for individual trees had an unmistakeable influence on accumulated stem growth because the index was a surrogate for a quantitative measure of photosynthetically active surface area (total needle surface area).

At the plot labeled SCR the available water in the 0-to-90 cm profile was only 8 %, the lowest of all the plots. In 1974, when average ozone concentrations were higher than in recent years, SCR had the lowest crown injury index and the lowest growth. SCR had an intermediate ozone exposure level (0.08 ppm, 24-h average) during the 1974 to 1978 period (Table I). The low injury index and stem growth at SCR demonstrated the result of the combined effects of soil water deficiency and ozone stress. Most of the Jeffrey pine plots, e.g., BL, HB, and HV, had soils with low available water content. Therefore, if in one's imagination the experimental area were rotated 180° so the east end received the highest ozone exposure, then the impact of ozone on the study area as a whole might be more serious than in the present situation. The prominent influence of soil water availability makes it necessary to assess this variable before locating plots for long-term monitoring.

Finally, the average ozone levels (0.07 to 0.08 ppm, 24-h average, May to October, (Table II)), during the last 5 years at Lake Gregory, which is less than 2 mi away from both CP and BP, may represent the ozone dose that is sufficient to induce continuing tree decline among ponderosa pines at these plots which exhibit a long history of chronic ozone injury.

CONCLUSIONS

This study was limited to the examination of ponderosa and Jeffrey pines as indicators of changes in exposure to ozone over both time and space. Favorable changes in ozone air quality in recent years coincided with visible improvement of crown condition at most forest monitoring plots in the San Bernardino Mountains. Continued progress in pollution abatement will be required to prevent a return to more severe levels of damage to forest and wilderness resources in the mountains of southern California.

REFERENCES

1. P.R. Miller, O.C. Taylor, and R.G. Wilhour, "Oxidant air pollution effects on a mixed conifer forest ecosystem," U.S. EPA Environ. Res. Brief, EPA-600/D-82-278, 1982.

2. P.R. Miller, G.J. Longbotham, and C.R. Longbotham, "Sensitivity of selected western conifers to ozone," *Plant Disease* 67:1113 (1983).

3. J.R. McBride, P.R. Miller, and R. Laven, "Effects of oxidant air pollution on succession in the mixed conifer forest type of southern California," in *Proc. Effects of air pollution on forest ecosystems.* The Acid Rain Found., St. Paul, MN, 1985, p. 157.

4. P.R. Miller, O.C. Taylor, and M.P. Poe, "Spatial variation of summer ozone concentrations in the San Bernardino Mountains," Paper 86-39.2, Proceedings of the 79th Annual APCA Meetings, Minneapolis, MN, 1986.

5. O.C. Taylor, Ed., "Photochemical oxidant air pollution effects on a mixed conifer forest ecosystem, Final Report," U.S. EPA, Ecological Res. Ser., EPA-600/3-8-002, 1980.

6. P.S. Muir and B. McCune, "Index construction for foliar symptoms of air pollution injury," *Phytopathology* 71:558 (1987).

7. H.C. Fritts, *Tree Rings and Climate*, Academic Press, New York, NY, 1976.

8. G.T. Ferrell, "Weather, logging, and tree growth associated with fir engraver attack scars in white fir," USDA Forest Service Res. Paper, PSW-92, Berkeley, CA, 1973.

9. D.L. Peterson, M.J. Arbaugh, V.A. Wakefield, and P.R. Miller, "Evidence for growth reduction in ozone-injured Jeffrey pine (*Pinus jeffreyi* Grev. and Balf.) in Sequoia and Kings Canyon National Parks," *JAPCA* 37:908 (1987).

Table I. Physical and vegetational properties of 15 forest plots for monitoring long-term changes resulting from chronic ozone exposure.

Plot Name	Elevation (m)	Estimated Ozone Dose 24-h Av. May–Oct. from 1974–1978 Record (ppm)	Average Precipitation 1973–77 (cm)	Available Soil Water Top 90 cm (%)	Total Trees Ponderosa/Jeffrey (Number)	Average Ozone Injury Index in 1988 Ponderosa/Jeffrey
CP	1600	0.11	78	18	79/0	13.0/0
BP	1525	0.09	105	17	51/0	15.2/0
SF	1705	0.10	109	19	98/0	17.2/0
SCR	1830	0.08	70	8	40/0	18.2/0
COO	1900	0.09	103	12	54/0	18.7/0
DW	1725	0.10	90	15	70/0	19.8/0
UCC	1610	0.10	90	13	62/0	21.9/0
CA	1830	0.09	114	ND	45/0	22.5/0
GVC	1950	0.07	99	10	34/26	24.8/26.9
BF	1900	0.07	61	21	114/40	26.1/24.0
DL	1900	0.07	95	D	16/37	27.7/22.4
CAO	2135	0.06	82	15	12/51	31.6/33.6
BL	2320	0.07	90	12	0/123	0/35.9
HB	2160	0.05	56	10	0/114	0/43.6
HV	2225	0.05	52	9	0/147	0/51.3

Table II. Annual precipitation at Lake Arrowhead 1973 to 1987. May through October 24-hr average and monthly ozone maximum average at Sky Forest or Camp Paivika for 1974 to 1978, and for Lake Gregory from 1979 to 1987.

	Precipitation	Ozone	
Year	Total October to September (in)	24-h Average May to October (ppm)	Average of Monthly Maximum Conc. May to October (ppm)
1973	28.0	–	–
1974	29.0	0.100	0.350
1975	37.1	0.098	0.320
1976	25.7	0.075	0.285
1977	78.8	0.084	0.273
1978	47.6	0.088	0.308
1979	66.7	0.089	0.318
1980	19.8	0.070	0.256
1981	46.3	0.076	0.266
1982	71.6	0.071	0.240
1983	25.1	0.074	0.240
1984	34.0	0.076	0.263
1985	50.8	0.070	0.236
1986	23.7	0.072	0.230
1987	39.5	0.069	0.228
Mean	41.6	0.080	0.274

Table III. Changes in ozone injury index of all ponderosa and Jeffrey pines in fifteen plots between 1974 and 1987, without regard to the different ozone doses characteristic of each plot, thereby emphasizing the general trends of tree condition in the San Bernardino National Forest at three observation times. The paired t-test shows significant improvements in canopy condition between 1978 to1987. Calculations were based on individual tree scores, not plot averages.

	Stem Diameter Classes (cm)								
		10-20.9			30.0-59.9			> 60	
Year	N	Mean/ Diff.	P	N	Mean/ Diff.	P	N	Mean/ Diff.	P
Ponderosa Pine[*]									
1974	209	17.57		274	17.45		173	16.00	
74-78	209	-1.28	0.001	274	-0.88	0.01	172	+0.419	0.36
1978	209	16.29		274	16.57		172	16.40	
78-88	209	+3.36	0.00	274	+3.25	0.00	172	+4.24	0.00
1988	209	19.66		274	19.82		173	20.60	
Jeffrey Pine[**]									
1974	274	40.53		175	33.16		96	26.56	
74-78	274	+1.39	0.021	175	+1.10	0.08	96	+2.82	0.00
1978	274	41.92		176	34.27		96	29.39	
78-88	274	+1.38	0.03	176	+2.93	0.00	96	+3.40	0.00
1988	274	43.30		176	37.20		96	32.78	
Ponderosa and Jeffrey Pines[***]									
1974	483	30.60		449	23.6		269	19.80	
74-78	483	+0.23	0.54	449	-0.11	0.73	268	+1.28	0.002
1978	483	30.80		450	23.5		268	21.05	
78-88	483	+2.24	0.00	450	+3.12	0.00	268	+3.94	0.00
1988	483	33.1		450	26.60		269	24.97	

[*] Includes ponderosa pines at 11 plots:(CP, COO, SF, SCR, BP, DW, UCC, CA, GVC, BF, CAO)

[**] Includes Jeffrey pines at 7 plots:(GVC, BF, CAO, DL, BL, HB, HV)

[***] PP and JP at 15 plots:(CP, COO, SF, SCR, BP, DW, UCC, CA, GVC, BF, CAO, DL, BL, HV, HB)

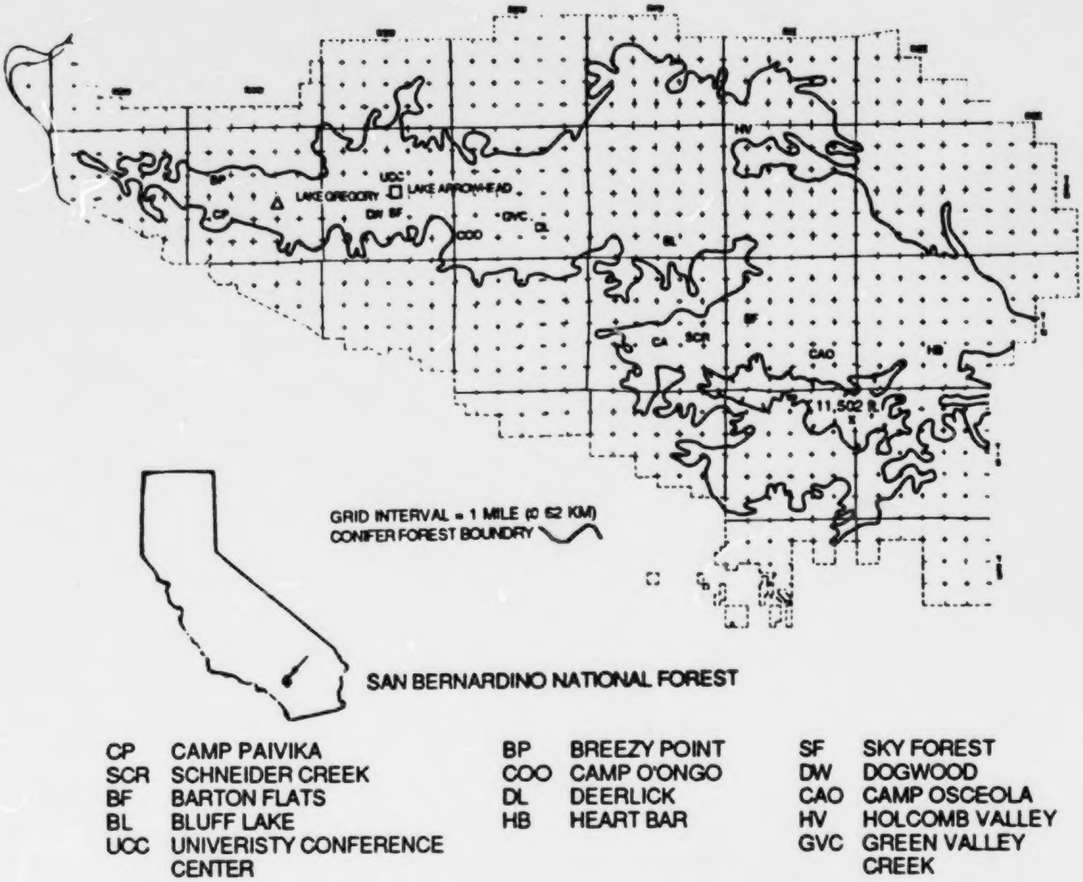
BP
LAKE GREGORY
UCC
LAKE ARROWHEAD
CP
DW SF
GVC
DL
COO
BL
HV
BF
CA
SCR
CAO
HB
11,502 ft.
GRID INTERVAL = 1 MILE (0.62 KM)
CONIFER FOREST BOUNDRY
SAN BERNARDINO NATIONAL FOREST
CP CAMP PAIVIKA
SCR SCHNEIDER CREEK
BF BARTON FLATS
BL BLUFF LAKE
UCC UNIVERISTY CONFERENCE CENTER
BP BREEZY POINT
COO CAMP O'ONGO
DL DEERLICK
HB HEART BAR
SF SKY FOREST
DW DOGWOOD
CAO CAMP OSCEOLA
HV HOLCOMB VALLEY
GVC GREEN VALLEY CREEK

Figure 1. Map of the San Bernardino National Forest with vegetation plots, e.g., BP, GVC, BF, and monitoring sites for precipitation (rectangle) at Lake Arrowhead and ozone (triangle) at Lake Gregory.

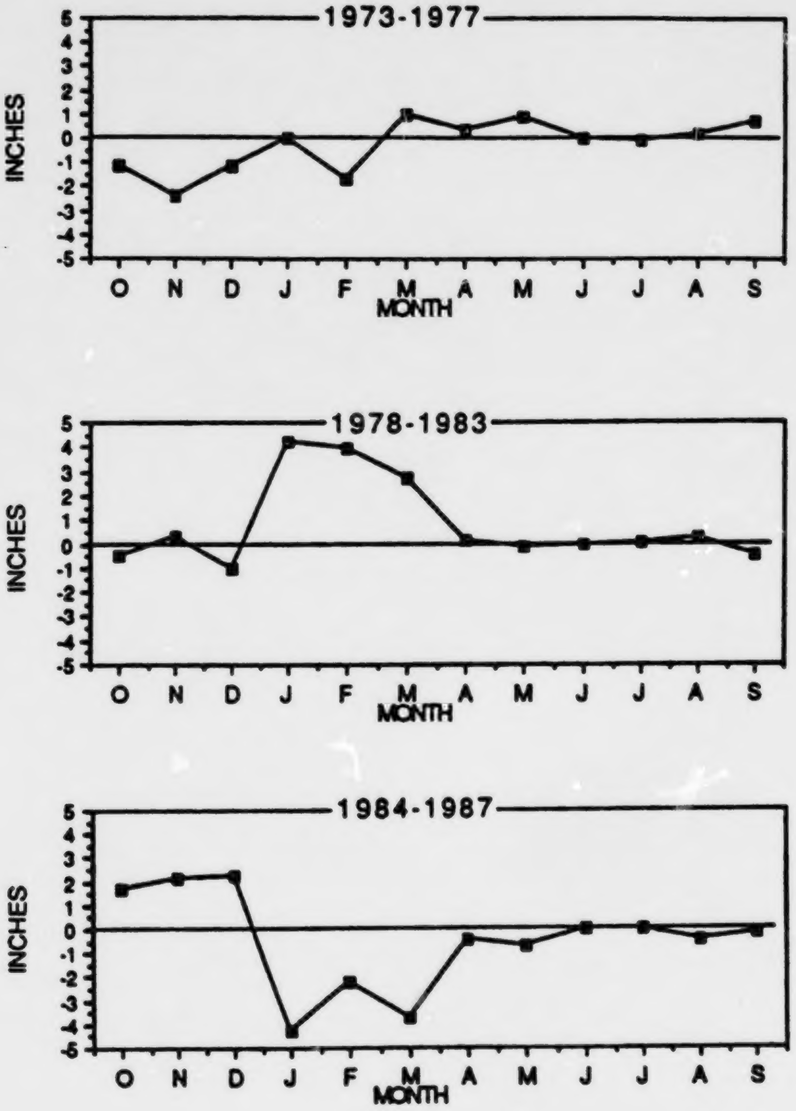

Figure 2. Departures of monthly precipitation amounts at Lake Arrowhead from the 1973-1987 monthly average during three periods: 1973-1977, 1978-1983, 1984-1987.

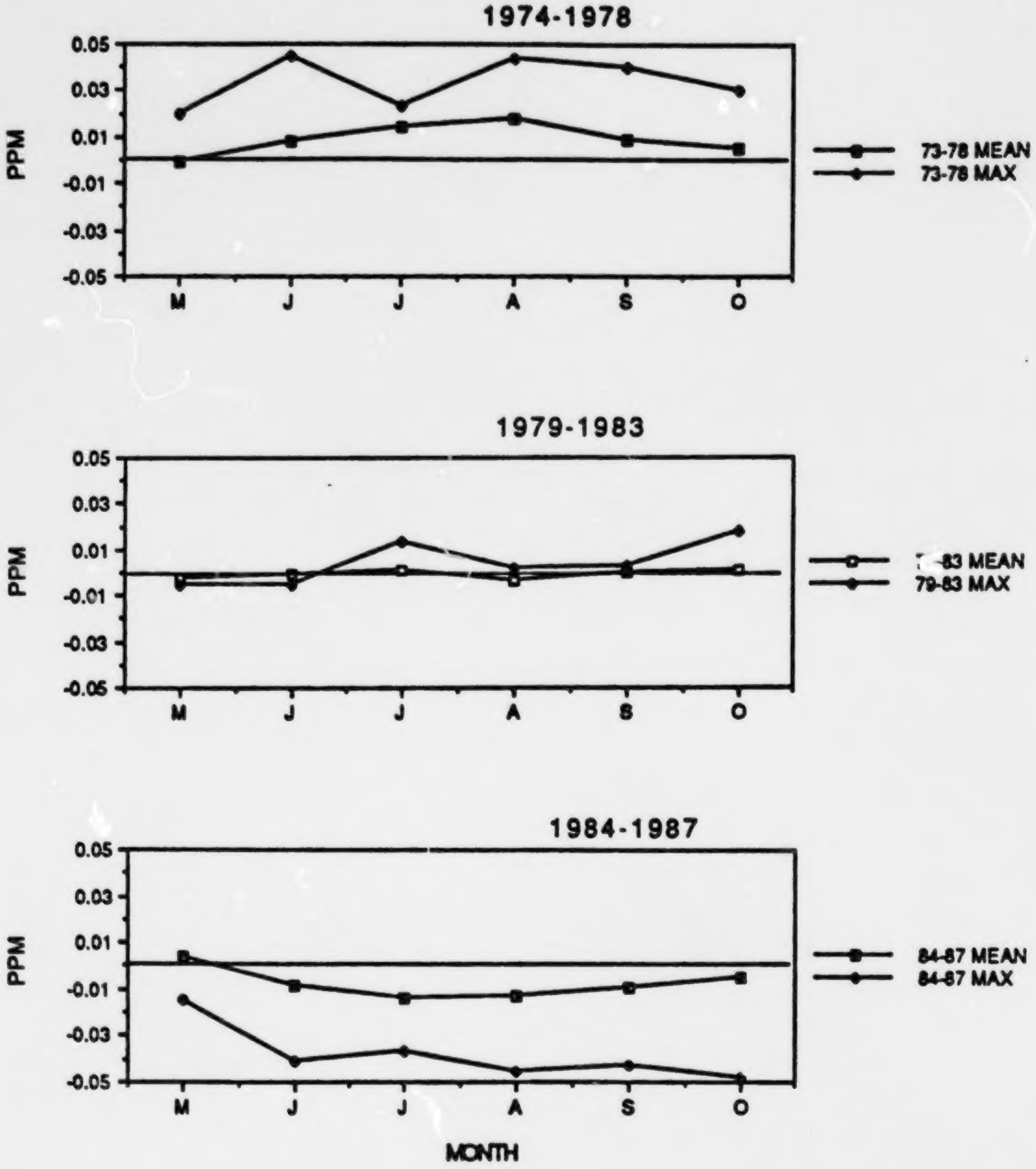

Figure 3. Departures of monthly 24-h ozone averages and averages of the monthly maximum concentration at Lake Gregory for May through October from the 1974 to 1987 averages during three periods: 1974–1978, 1979–1983, and 1984–1987.

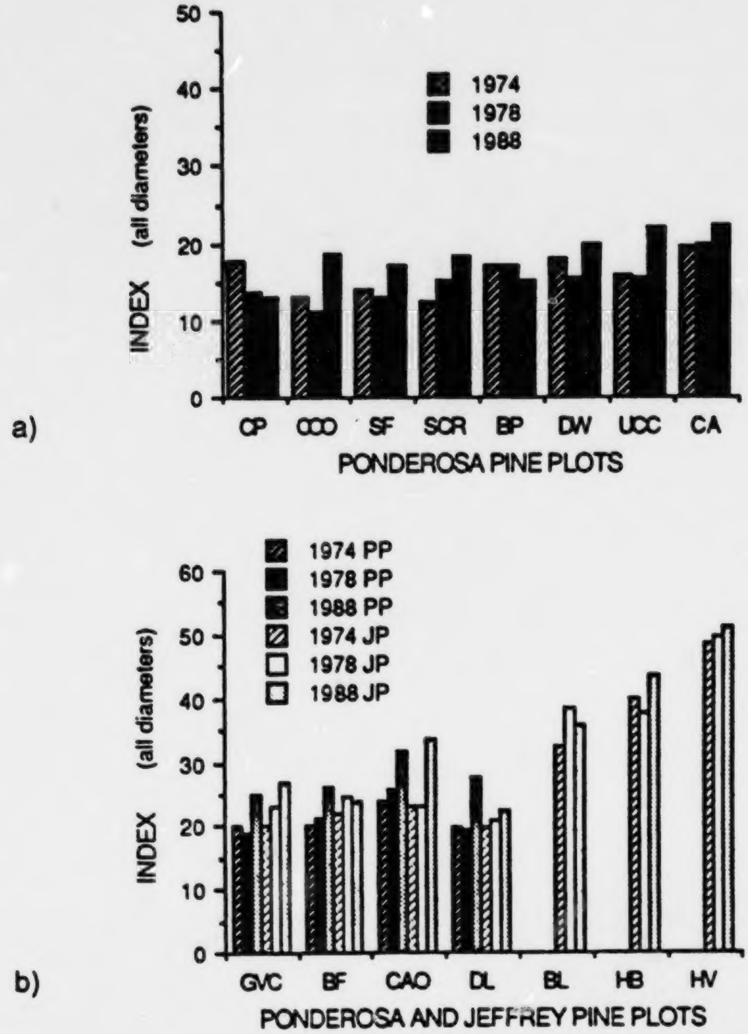

Figure 4. Average ozone injury indexes in 1974, 1978, and 1988, at each of 15 forest plots, including (a) ponderosa pine plots, and (b) plots with both species or Jeffrey pine alone.

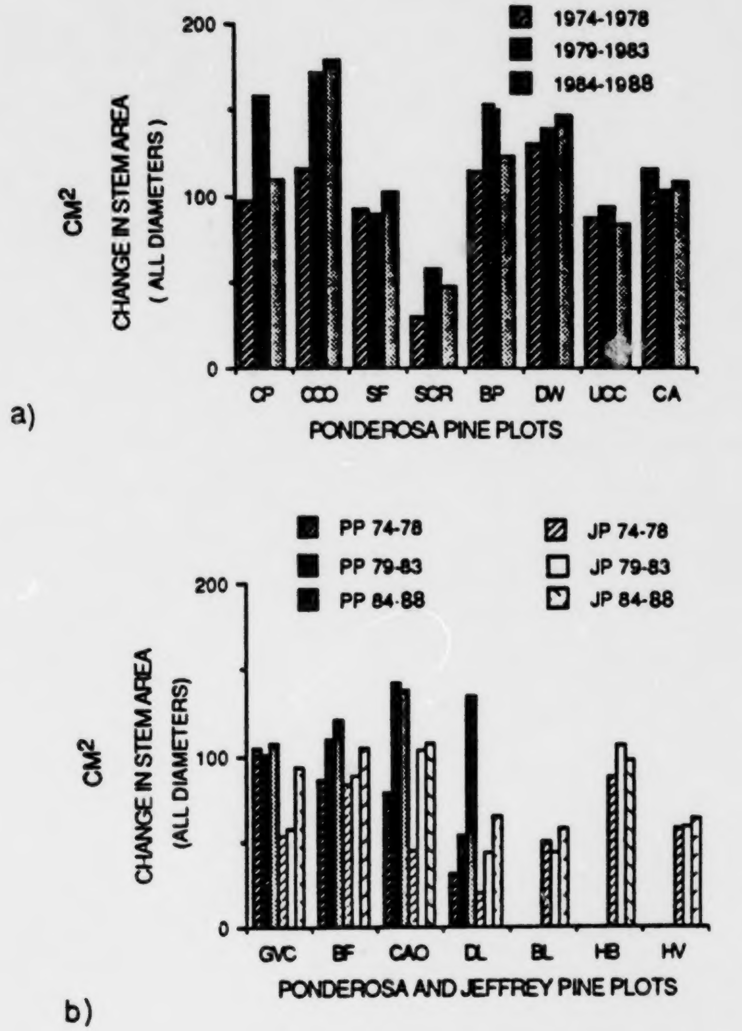

Figure 5. Average change in stem area during 1974-1978, 1979-1983, and 1984-1988 at 15 forest plots, including (a) ponderosa pine plots, and (b) plots with both species or Jeffrey pine alone.

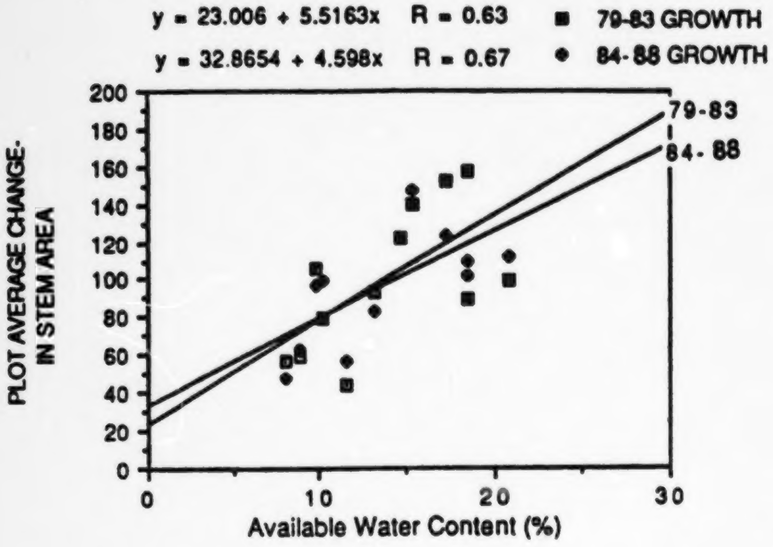

Figure 6. Relationship of average change in stem area during 1979–1983 and 1984–1988 with percent available soil moisture in the 0–90 cm zone at 13 plots.

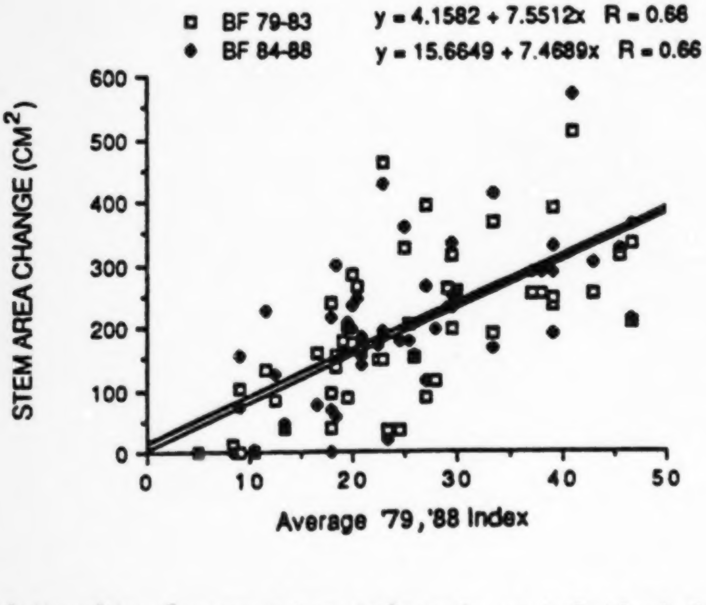

Figure 7. Relationship of ozone injury indexes in an individual plot (BF) to stem area changes during 1979-1983 (moist) and 1984-1988 (dry).

Current and Potential Threats to Biodiversity in Forests of the Lower Pacific Coast States

Sandra Henderson, Richard K. Olson, and Reed F. Noss

Environmental Research Laboratory– Corvallis
200 S.W. 35th St.
Corvallis, OR 97333

INTRODUCTION

Biodiversity refers to the diversity of life at multiple levels of biological organization. Three primary levels have been emphasized in recent literature[1]: (1) the diversity of species inhabiting a defined area; (2) the diversity of genetic material within species; and (3) the diversity of ecosystems or habitats in an area. The spatial arrangement of ecosystems across a landscape is recognized as an important higher-level aspect of biodiversity.[2] Equally as important as these pattern aspects of biodiversity are the geological, climatological, hydrological, evolutionary, and ecological processes that create and maintain biodiversity. A comprehensive approach to conservation of biodiversity must therefore address multiple patterns and processes in nature.[3,4]

Biodiversity has become an important environmental issue in the scientific community and, increasingly, among the general public. Many values associated with the environment (including such "public services" as maintenance of air and water quality, watershed protection, and soil building) depend on natural patterns and processes of biodiversity. A diversity of genetic material within wild species allows for future adaptive change and provides for genetic enrichment of domestic crops and livestock. Impoverishment of biodiversity at any organizational level may reduce ecological resistance or resilience. In addition, a growing number of Americans believe that species, ecosystems, and other elements of biodiversity are valuable in and of themselves.

Patterns and processes of biodiversity currently are deteriorating in most regions of the world, a problem that most biologists consider to be of crisis proportions. Many threats, such as the enhanced greenhouse effect, are global in scope. Estimates of the annual global rate of species extinction range from 1,000 to 10,000 times that before human intervention.[5] Many species have been severely reduced in numbers and geographic range. Loss of genetically distinct populations may be as serious as extinctions of entire species.[6] At a higher level of organization, whole communities such as the Florida scrub are being eliminated.[7]

Biodiversity in forests of the lower Pacific Coast States (Washington, Oregon, and California) faces current or potential threats from three primary anthropogenic stressors: land use practices, air pollution, and climate change. The following sections will describe forests and forest biodiversity in these three states, present examples of current and potential effects of the major stresses on these forests, and recommend actions to prevent further deterioration of biodiversity in these ecosystems. We limit our discussion in this paper to the above-ground terrestrial portion of forest ecosystems.

Preceding page blank

FORESTS OF THE LOWER PACIFIC COAST STATES

Forests cover 93 million acres (46%) of the land in the lower Pacific Coastal States.[8] Coverage ranges from 40% of the area of California to 55% of the land in Washington. Approximately half the forested land is federally owned, with most of the remainder privately held.

The U.S. Forest Service recognizes 12 broad forest types within this region, with major ones including Douglas-fir, hemlock-sitka spruce, ponderosa pine, spruce-fir and lodgepole pine.[8] Other classification schemes include many more forest types and more accurately reflect the diversity of forests in these three states.[9,10]

The forests of the Pacific Coast States are rich in biological diversity, as evidenced by the many tree species and associations they contain. However, the biodiversity of a forest is not limited to trees; it also includes herbaceous plants, bryophytes and hepatophytes, algae, fungi, protists, bacteria, and many groups of vertebrates and invertebrates. In most cases, the total species list of forest communities is poorly known. Some species, particularly of invertebrates and bacteria, have not yet been described by science. The assemblage of species into floras and faunas, distinct to regions, represents a higher order of biodiversity that is easily disrupted as human activities displace sensitive species and favor weedy, opportunistic species.

In addition to this "compositional" or taxonomic diversity, forests also can be characterized in terms of structural diversity. One extremely important component of structural diversity in old-growth Douglas-fir forests is coarse woody debris, which in Oregon and Washington, can approach 24,300 cubic feet and 178 tons per acre.[11] Juniper-grassland complexes of eastern Oregon and mixed conifer forests of the Sierra Nevada are dominated by ponderosa and Jeffrey pine and are much different in structure from the mesic Douglas-fir forests. Forest structure, in turn, determines what animal species will live there. Spotted owls, for example, appear to require the tall canopy and buffered microclimate of old-growth Douglas-fir forests, whereas pygmy nuthatches require an open physiognomy as in fire-maintained ponderosa pine stands. Collectively, the pattern of these forest types and species distributions across the region represents ecosystem and landscape diversity.

CURRENT AND POTENTIAL THREATS TO BIODIVERSITY

Biodiversity of forests in the lower Pacific Coast States is now adversely affected by land use practices and air pollution. Land use has by far the greatest effect, with air pollution a distant second. Forests are continually changing in composition as species respond individualistically to natural climate change.[12] Accelerated rates of climate change caused by enhanced greenhouse effects, could increase extinction rates dramatically, especially in fragmented landscapes.[13] These three threats are certain to interact to produce synergistic effects that will be difficult to predict or mitigate.

Forest Conversion

The most extreme alteration of forest biodiversity involves the conversion of forested ecosystems to nonforest land. In California between 1950 and 1980, forest lands totalling 837,000 acres were converted to agricultural or urban use.[14] About 40% of the converted forest area went to urban uses. Losses for specific cover types included 617,000 acres of hardwood woodlands, 80,000 acres of pine, 61,000 acres of redwood, 41,000 acres of mixed conifer, and

37,000 acres of other forest types. The figures for loss to urbanization do not include small parcels, subdivisions, and roads in predominantly rural areas. This more diffuse development increases the total forest acreage lost and eliminates or alters many of the structural and functional attributes of undisturbed forests through fragmentation of larger forest units.

The threat to forest biodiversity from land conversion and fragmentation varies among forest types and regions. Losses of valley foothill hardwoods in California between 1950 and 1980 equalled 7% of the total acreage of this forest type, compared to statewide losses of 2% of ponderosa/Jeffrey pine. However, in the Southern California and Central Sierra regions, 10% of the ponderosa/Jeffrey pine forests were converted during this period.[14] Because of their location in areas facing high conversion pressures mesa oak and walnut woodlands are among 32 California plant communities considered most endangered by The Nature Conservancy.[15]

Both urbanization and agricultural conversion are related to human population growth. Expanding populations utilize forest lands for residential and industrial purposes as well as for infrastructure such as roads, reservoirs, and transmission lines. All of these uses fragment habitats and increase artificial edges. Agricultural conversions of forest land often represent an attempt to replace agricultural land lost to urbanization (1.2 million acres in California between 1950 and 1980).

Forest losses have been driven by an increase in California's population from 10,586,223 in 1950 to 23,667,902 in 1980.[16] Both population growth and forest conversion are continuing in this state. A 1987 population of 28 million is projected to reach 37,347,000 million by 2010,[17] while forest conversion during this period is predicted to be 340,000 acres.[14]

Although the magnitude of California's growth produces the greatest impact on forests, Washington and Oregon also have rapidly expanding populations (74% and 75%, 1950-1980, respectively)[18,17] and attendant forest conversion. Total decreases of timberland rated "highly productive" in the lower Pacific Coast States from 1950 to 1980 totaled 1.2 million acres.[9] Of this 1.2 million acres, the greatest causes of loss were road building and grazing clearings in Oregon and urban expansion in the Puget Sound area of Washington.[9]

Forest management

When the most accessible or productive sites in a forest landscape are cut for timber or development, the remaining forest is fragmented into a patchwork of stands of varying sizes and degrees of isolation.[19] Limitations on clearcut size on public lands actually have increased the level of fragmentation.[20] Forest fragmentation has two components, both of which contribute to deterioration of biodiversity: (1) a reduction in the total amount of forest habitat in the landscape and (2) an apportionment of the remaining forest area into small, isolated fragments. Many biologists consider forest fragmentation to be the single greatest threat to biodiversity .[21]

Habitat reduction and insularity cause extinctions and shifts in species composition and abundance patterns through a variety of mechanisms.[22] One major class of problems is edge effects, which increase in importance in small forest patches with high edge:interior ratios. Forests below a certain size (about 10 ha in old-growth Douglas-fir) are entirely edge habitat and cannot be considered ecologically viable.[19,20] Whereas wildlife managers traditionally have managed lands to benefit edge-adapted game species, the weight of biological opinion on edge has shifted dramatically in recent years. Deleterious edge effects include shifts in abiotic variables and habitat structure from two to three tree-heights into forests from an edge, increasing "weediness" of animal and plant species composition, increased rates of nest predation and cowbird parasitism on birds, and loss of sensitive forest interior species.[23,22]

Forest management practices often fragment habitats and simplify habitat structure, and thereby alter biological diversity. The following discussion is most applicable to closed-canopied conifer forests, such as Douglas-fir forests on the western slope of the Cascades.

Two basic operations are common to all managed forests: tree harvest and tree planting. Two general classes of forest management differ in harvest methodology and pattern of regrowth: uneven-aged management (selective cutting) and even-aged management (clearcutting).[24] In the former, the harvest mimics the treefall gap disturbance process of relatively close-canopied old-growth forests, resulting in fine-grained patchiness and high structural and alpha (within-habitat) species diversity. In the latter, all the trees over a large area are cut. Unlike natural catastrophic disturbances, such as fire and windthrow, clearcutting removes all live wood and leaves little coarse woody debris. It also produces a pattern of smaller, more uniform patches and is repeated at intervals far shorter than natural catastrophes, thereby truncating succession long before old-growth characteristics develop.[25]

After clearcutting, site preparation, including slash burning, removes most of the residual coarse woody debris. Artificial regeneration (replanting) on clearcuts is usually with single tree species, and the resulting monoculture has a vastly reduced structural and compositional diversity compared to natural forests.[26] For example, although the Willamette National Forest in Oregon replants 15 species of trees, Douglas-fir and noble fir account for 91% of the replantings.[27] These monocultures have much higher densities of certain insect pests, and far fewer predators of these pests, and therefore are highly vulnerable to pest outbreaks.[28] Genetic diversity is also depressed in many replanted stands on National Forests, despite policies to collect seeds from multiple stands in appropriate ecological zones.[29,27] In addition, the intensive management associated with even-aged forestry requires increasing outlay of capital, time, energy, and polluting chemicals such as fertilizers, herbicides, and pesticides.

The solution to the problems associated with even-aged management is not simply to switch to selective cutting. If total yield is held constant, selective cutting will result in higher road densities and more disturbance with repeated human entry.[30] Roads, in particular, are a source of multiple impacts on natural ecosystems; sensitive species may be eliminated when road densities exceed a certain threshold.[31] An optimal silvicultural strategy might be to harvest and regenerate trees in a way that mimics natural disturbance and recovery processes, at both fine and coarse spatial scales. This strategy could include (1) occasional, selective removal of individual trees, and (2) periodic, long-rotation removals of trees over large areas while retaining many live trees and most coarse woody debris on site. Hence, structural diversity is maintained in the system. The Forest Service is experimenting with such modified clearcuts in the H.J. Andrews Experimental Forest, Willamette National Forest, Oregon.[32]

Old-growth Forests

Old-growth forests differ significantly from younger forests in species composition, structure, and function; much of the difference is related to the role of dead wood in these systems.[33,34] Coarse woody debris is a critical carry-over or legacy from old-growth forests into regenerating forests. When snags are removed from short-rotation stands following clearcutting of old-growth, 10% of the wildlife species (excluding birds) may be eliminated; 29% of the wildlife species may be eliminated when both snags and downed trees are removed from intensively managed forests.[35] Although snags and downed trees might not be considered productive components of a forest, there are actually many more living cells (i.e., fungi and bacteria) in a downed log than in a "live" bole. Many species depend on snags and logs for habitat. For example, in the Wallawa-Whitman National Forest in Oregon and Washington's Blue Mountains, some 39 species of birds and 23 mammals use cavities in snags, and 179 amphibians, reptiles, birds, and mammals use downed logs. Without these logs or snags, some species would disappear, resulting in a net loss of biodiversity.[24] All together, over 200 species of vertebrates use old-growth forests in the Pacific Coastal States, and at least 50 reach their highest densities in these communities.[33]

Old-growth forests have been so drastically reduced in this region that most ecologists favor a moratorium on their harvest. Nearly all the old-growth on private lands has been logged, so the timber industry has come to rely on National Forests and other public lands in order to maintain yields. Franklin and Spies[36] estimated that 60%–70% of the forest land in the Douglas-fir region was covered by old-growth in 1800, representing an area of about 6 million hectares. Today, no more than 10%[37] to 17%[25] of that forest remains, with an area of less than 1 million hectares. Earlier estimates of old-growth acreages, upon which National Forest plans for this region were based, appear to have been gross overestimates.[38] More than two-thirds of the remaining old-growth on public lands is not protected, and at least 40,000 acres are logged each year in Oregon and Washington alone. This reduction in old-growth forests represents a loss of one of the most significant reservoirs of biodiversity in the country.

Air pollution

Effects of regional air pollution on biodiversity in western forests are currently far less severe than those associated with intensive land use. However, effects have been demonstrated, and could increase in extent and magnitude through future increases in pollution (fueled by population growth), cumulative effects of pollution, and interactions between air pollution, land use, and climate changes.

The mixed conifer forests of the San Bernardino and San Gabriel Mountains of southern California have been exposed to increased levels of ozone since the early 1950s.[39] Effects include increased mortality of ponderosa pine and other sensitive species.[40] In addition, increased mortality of pollution-intolerant genotypes within species may lead to a reduction in genetic diversity. Changes in community structure as ozone-sensitive species are replaced by more tolerant species such as oaks and various shrubs, can lead to an increased frequency and severity of fires; these fires alter community structure further. This resulting, less diverse community may provide fewer recreational and economic "services".

Over a broader region, ozone damage to ponderosa and Jeffrey pine has been reported along the west slope of the Sierra Nevada as far north as Lake Tahoe.[41-43] Peterson and Arbaugh[44] and Peterson et al.[45] have shown reduced growth of individuals of Jeffrey pine and ponderosa pine. Effects of air pollution are now less severe in the Sierra Nevada than in the San Bernardino Mountains, but ozone levels are expected to remain at current levels for the near future[44] and cumulative effects of pollution are likely.

Global climate

Atmospheric concentrations of CO_2 have increased from pre-industrial levels of 270–290 ppm to a present concentration of 350 ppm.[46] Generated by combustion of fossil fuels and deforestation, CO_2 concentrations are currently increasing at a rate of 15 ppm per decade.[47] Combined with increases in other greenhouse gases such as methane, nitrous oxides and CFCs, higher CO_2 levels are predicted to cause increases in mean global temperature of from 1.5° C to 4.5° C by the year 2030.[47]

Predictions of increases in mean temperature for the lower Pacific Coast States vary considerably, depending on which atmospheric model is used,[47,48] but generally fall within the mean global range. Precipitation is expected to show little change. Under this scenario, plants will face greater water stress as effective moisture levels are reduced. The frequency of extreme temperatures and droughts will likely increase, as will the frequency of disturbances such as high winds and fires. These stresses are predicted to have dramatic effects on plant regeneration and forest composition, even though established forests may show considerable inertia.[49] Insect and pathogen outbreaks may also become more common. The more diverse old-growth forests are expected to exhibit greater resistance and resilience to all these effects than the already impoverished, intensively managed forests. Hence, maintaining a diversity of structure, tree species, and genotypes in managed forests would be a prudent strategy.[49]

Predicted effects of global climate change on western forests include reductions in species diversity in low elevation forests as well as elevational and latitudinal shifts in species ranges.[50] Species are most likely to be stressed at the edges of their ranges. Plant and animal species with low vagility, or that are prevented from migrating by a lack of habitat corridors, may become regionally extinct. Endangered species with limited distributions will be especially vulnerable to shifts in habitat conditions.[51,47] The major threat of climate change associated with enhanced greenhouse effects is not change itself—which has occurred repeatedly in the past—but rather the combination of two factors: (1) an extremely rapid rate of change, predicted to be some 10 to 40 times faster than similar changes during the Pleistocene and Holocene; and (2) habitat fragmentation, which has eliminated many natural avenues for species dispersal.[14,52]

Other stresses

Stresses other than those discussed so far may affect biodiversity in forests of the lower Pacific Coast States. Increased ultra-violet radiation, resulting from depleted stratospheric ozone, could have deleterious impacts on forest species. Point or non-point source pollution of surface waters in forests could threaten aquatic species. Introduced exotic species ("biotic pollutants") may outcompete native plants or animals, especially under stressed conditions. In all cases, these stressors would likely interact with land use practices, air pollution, and/or climate change, which makes predicting their effects on biodiversity even more difficult.

DETERMINATION OF HIGHEST RISK AREAS

High-risk areas for biodiversity would be: (1) areas with high species richness, numerous endemics, threatened and endangered species, genetically distinct populations, or rare or unique community types; (2) regional landscapes least resistant or resilient to stress; (3) regional landscapes of high ecological, economic, or sociocultural significance; (4) areas under intense population or economic pressure, and areas subject to high levels of pollutants or other stressors. Any area that fits more than one of these categories obviously would be high priority for monitoring and mitigative action.

For example, old-growth forests in northern California, Oregon, and Washington are at very high risk of losing biodiversity through intense logging. Rare species such as the spotted owl are dependent on old-growth forests for habitat. The Siskiyou Mountains in southern Oregon and northern California are a hot-spot of biodiversity, with unique old-growth forests and numerous endemic species.

Forests in southern and central California are at high risk on three levels. Biological diversity is high, pressures for conversion of forested lands are high due to the rapid human population growth and air emissions associated with increased urbanization have potential for adverse effects on remaining forests.

RECOMMENDATIONS

The magnitude of the threat to biodiversity in the lower Pacific Coast States warrants a strategy of concurrent research and protection/mitigation. An improved understanding of the components and processes of biodiversity is essential for the long-term preservation of diversity. However, enough is known to guide immediate action to reduce current risks. Recommendations for research and policy include:

(1) Conduct a regional inventory/survey of biodiversity.

At present, the status and distribution of the biological resources of the lower Pacific Coast States are very poorly known. A regional inventory and mapping of biodiversity is necessary to determine areas at greatest risk. Parallel to a complete biological survey, we need rapid surveys to identify centers of species richness and endemicity as well as locations of elements of biodiversity with particular sensitivity, ecological significance, or other indicator value in establishing linkages between biodiversity and forest ecosystem functions.

(2) Define relationships between population growth, land-use patterns, and trends in biodiversity.

Population growth at scales from local to global will influence biodiversity in the lower Pacific Coast States. While increases in regional population will affect biodiversity through land development and other direct uses, a growing national and world population will increase economic pressures on these forests. If world population doubles as projected in 40 years,[53] then emissions driving global climate change will likely increase. An understanding of these relationships can be used to identify areas where biodiversity is at highest risk and to develop policies for preventing and mitigating losses.

(3) Develop and implement forest management practices that maintain biodiversity while allowing continued utilization.

Although the interacting effects of multiple stressors on biodiversity will be difficult to disentangle, it is possible to develop a management strategy that is robust for many different stress scenarios. Some elements of a forest health strategy for multiple stressors would be to (a) minimize outputs of toxic and greenhouse gases, (b) stop deforestation and forest fragmentation, (c) reforest large areas and interconnect forest blocks by habitat corridors, (d) provide extra protection to hot-spots of biodiversity and high-risk areas, but with flexible reserve boundaries to allow adaptation to change, and (e) maintain options by providing a diversity of species, genotypes, and structure in managed forests.

The appropriate local management practices will vary between different forest types, depending largely on the natural disturbance and regeneration regime for each type. A strategy proposed for old-growth forests by Harris[19] utilizes a spatial and temporal cutting rotation designed to preserve the essential characteristics of the old-growth ecosystem, while allowing a sustainable harvest. Experiments to maintain structural, compositional, and functional diversity in cut-over areas by mimicking natural disturbance-recovery processes and landscape mosaic patterns[23,30] must be expanded. Rather than being thought of as just another of the "multiple uses" to provide for on public lands, biodiversity must become the organizing paradigm for forest management. All other forest uses and services ultimately depend on biodiversity.

(4) Increase public education.

Only if the value of biodiversity, the threats facing it, and the actions required to protect it are generally known, can sufficient support for those actions be generated. Because protecting diversity requires effort at both the individual and government levels, both the general public and policy makers need to be educated on this topic. Scientists in particular need to consider the needs of these two groups when disseminating results of their research.

(5) Accelerate targeted land purchases.

Also needed to limit further losses of biodiversity are continued purchases of preserves and migration corridors. Acquisitions can be targeted from the results of a regional biodiversity survey (Recommendation #1). Acquisition programs by private groups such as The Nature Conservancy, as well as state and federal agencies, should be expanded.

(6) Improve coordination between regulatory and land management agencies.

Regulatory agencies such as the U.S. EPA, California Air Resources Board, and Washington Department of Ecology must coordinate activities with land management agencies, including the U.S. Forest Service, Fish and Wildlife Service, National Park Service, Bureau of Land Management, and state Departments of Forestry. Biodiversity is a regional, and ultimately global, multimedia issue that cannot be effectively addressed piecemeal.

CONCLUSIONS

Biodiversity in forests of the lower Pacific Coast States faces immediate threats from nonsustainable land use practices as well as potential threats from climate change and other alterations of the global ecosystem. Deterioration of biodiversity in these forests can be minimized through a combination of near-term mitigation and management activities as well as long-term changes in environmental policy. Implementing a successful program will require the full participation of private individuals and groups, industry, state agencies, and federal agencies.

ACKNOWLEDGMENTS

We wish to thank Steve Cline, Rob DeVelice, Ross Kiester, Paul Schroeder, Jack Winjum, and two anonymous reviewers for their insightful reviews and comments.

The research described in this presentation has been funded by the United States Environmental Protection Agency and was conducted at EPA's Environmental Research Laboratory in Corvallis, OR, through contract #68-C8-0006 to NSI Technology Services Corporation. It has been subjected to the Agency's peer and administrative review and was approved for publication.

REFERENCES

1. Office of Technology Assessment, *Technologies to Maintain Biological Diversity*, U.S. Government Printing Office, Washington, D.C., 1987.

2. R.T.T. Forman and M. Godron, *Landscape Ecology*, John Wiley and Sons, New York, 1986.

3. R.F. Noss and L.D. Harris, "Nodes, networks, and MUMs: preserving diversity at all scales," *Environ. Manage.* 10:299 (1986).

4. R.F. Noss, "From endangered species to biodiversity," *A 15-Year Retrospective on the Endangered Species Act*, Island Press, New York, in press.

5. E.O. Wilson, "The current state of biological diversity," *Biodiversity*, National Academy Press, Washington, D.C., 1988, p. 3.

6. P.R. Ehrlich, "The loss of diversity: causes and consequences," *Biodiversity*, National Academy Press, Washington, D.C., 1988, p. 21.

7. G. Bass, "Secrets of the Florida scrub," *The Nature Conserv. Mag.*, 38(4):11 (1988).

8. USDA Forest Service, *An Assessment of the Forest and Range Land Situation in the United States*. Forest Resource Report No. 22, 1981.

9. M.G. Barbour and J. Major, *Terrestrial vegetation of California*, J. Wiley and Sons, New York, 1977.

10. J.F. Franklin and C.T. Dyrness, *Natural vegetation of Oregon and Washington*. USDA Forest Service General Technical Report. Portland, OR, 1973.

11. T.A. Spies and S.P. Cline, "Coarse woody debris in forests and plantations of coastal Oregon," *From the forest to the sea: a story of fallen trees*, Pacific Northwest Research Station, U.S. Department of Agriculture, Forest Service, Portland, OR., 1988, p. 5.

12. M.B. Davis, "Quaternary history and the stability of forest communities," *Forest Succession: concepts and applications*, Springer-Verlag, NY, 1981., p. 132.

13. R.L. Peters and J.D.S. Darling, "The greenhouse effect and nature reserves," *BioScience*, 35:707 (1985).

14. State of California, *California's forests and rangelands: growing conflict over changing uses*, California Department of Forestry and Fire Protection, 1988.

15. M.G. Barbour, "Californian upland forests and woodlands," *Terrestrial vegetation of North America*, Cambridge Univ. Press, New York, 1988, p. 132.

16. U.S. Bureau of the Census, *U.S. Department of Commerce, Projection of population of states by age, sex, and race, 1988 -2010*. Current Population Reports Series P-25, No. 1017, 1987.

17. U.S. Bureau of the Census, *U.S. Department of Commerce News*, CB87-205, December 30, 1987.

18. U.S. Bureau of the Census, "Characteristics of the population," *U.S. Department of Commerce 1980 Census of Population*, vol. 1., 1982.

19. L.D. Harris, *The fragmented forest: island biogeography theory and the preservation of biotic diversity*, University of Chicago Press, Chicago IL, 1984.

20. J.F. Franklin and R.T.T. Forman, "Creating landscape patterns by forest cutting: ecological consequences and principles," *Landscape Ecology*, 1:5 (1987).

21. B.A. Wilcox and D.D. Murphy, "Conservation strategy: the effects of fragmentation on extinction," *Am.Nat.* 125:879 (1985).

22. D.S.Wilcove, C.H. McLellan, and A.P. Dobson, "Habitat fragmentation in the temperate zone," *Conservation biology: the science of scarcity and diversity*, Sinauerr, Sunderland, MA., 1986, p. 237.

23. R.F. Noss, "A regional landscape approach to maintain diversity," *BioScience*, 3:700 (1983).

24. E.A. Norse, K.L. Rosenbaum, D.S. Wilcove, B.A. Wilcox, W.H. Romme, D.W. Johnston, and M.L. Stout, *Conserving biological diversity in our national forests*, The Wilderness Society, Washington, D.C., 1986.

25. T.A. Spies and J.F. Franklin, "Old-growth and forest dynamics in the Douglas-fir region of western Oregon and Washington," *Nat. Areas J.*, 8:190 (1988).

26. C. Maser, *The redesigned forest*, R & E Miles, San Pedro, CA, 1988.

27. D.S. Wilcove, "National forests: policies for the future," *Protecting biological diversity*, Vol. 2, The Wilderness Society, Washington, D.C., 1988.

28. T. Schowalter and J. Means, "Pests link site productivity to the landscape," *Maintaining the long-term productivity of Pacific Northwest Forest Ecosystems*, Timber Press, Portland, OR, 1988.

29. California Gene Resources Program, *Douglas-fir genetic resources: an assessment and plan for California*, National Council on Gene Resources, Berkeley, CA, 1982.

30. J.F. Franklin, "Natural diversity in temperate forests: lessons for our future landscapes," a lecture given at Oregon State University, Feb. 16, 1989.

31. R.F. Noss, "Protecting natural areas in fragmented landscapes," *Nat. Areas J.* 7(1):2 (1987).

32. S. Eubanks, USDA Forest Service, Willamette National Forest, private communication, 1988.

33. J.F.Franklin, K. Cromack, Jr., W. Denison, A. McKee, C. Maser, J. Sedell, F. Swanson, and G. Juday, *Ecological characteristics of old-growth Douglas-fir forests*, USDA Forest Service General Technical Report PNW-118, Portland, OR, 1981.

34. C. Maser, S.P. Cline, K. Cromack, Jr., J.M. Trappe, and E. Hansen, "What we know about large trees that fall to the forest floor," *From the forest to the sea: a story of fallen trees.* General Technical Report PNW-GTR-229. Portland, OR, 1988.

35. L.D. Harris and C. Maser, "Animal community characteristics," *The fragmented forest*, University of Chicago Press, Chicago, IL, 1984, p. 44.

36. J.F. Franklin and T.A. Spies, "Characteristics of old-growth Douglas-fir forests," *New forests for a changing world*. SAF, Bethesda, MD, 1984, p. 320.

37. The Wilderness Society, "Litigation update," *Wilderness*, 52 (183):6 (1988).

38. P.H. Morrison, *Old-growth in the Pacific Northwest: a status report.*,The Wilderness Society, Washington, D.C., 1988.

39. P. Miller, "Ozone effects in the San Bernardino National Forest," *Air Pollution and the Productivity of the Forest*, Proceedings of the Symposium, Washington, D.C., 1984, p. 161.

40. P. Miller, "Oxidant-induced community change in a mixed conifer forest," *Advances in Chemistry*, Series no. 122, 1973, p. 101.

41. J. Pronos and D.R. Vogler, *Assessment of ozone injury to pines in the southern Sierra Nevada*, USDA For. Serv. Pac. SW Region Forest Pest Manage. Rep 81-20., 1981.

42. J.R. Allison, *An evaluation of ozone injury to pines on the Eldorado National Forest*, USDA For. Serv. Pac. SW Region Forest Pest Manage. Rep. 84-16, 1984.

43. J.R. Allison, *An evaluation of ozone injury to pines on the Tahoe National Forest*, USDA For. Serv. Pac. SW Region Forest Pest Manage. Rep. 84-30, 1984.

44. D.L. Peterson and M.J. Arbaugh, "Growth trends in oxidant-stressed forests of the Sierra Nevada." Proceedings of APCA 81st Annual Meeting, Dallas, TX, 1988.

45. D.L. Peterson, M.J. Arbaugh, V.A. Wakefield, and P.R. Miller, "Evidence of growth reduction in ozone-stressed Jeffrey pine in Sequoia and Kings Canyon National Parks", *JAPCA* 37:96 (1987).

46. D. Rind, "A character sketch of greenhouse," *EPA Journal*, 15 (1):4 (1989).

47. U.S. EPA, "The Potential Effects of Global Climate Change on the United States: Draft Report to Congress," Vol. 1: Regional Studies. Office of Policy, Planning and Evaluation, Washington, D.C., 1988.

48. J.N. Woodman and C.S. Furiness, *Potential Effects of Climate Change on U.S. Forests: Case Studies of California and the Southeast*. U.S. Environmental Protection Agency, Office of Policy, Planning, and Evaluation, Washington, D.C., 1988.

49. J.F. Franklin, V.H. Dale, D. Perry, F.J. Swanson, M. Harmon, T.A. Spies, A. McKee, and D. Larson, "Effects of global climatic change on forests in northwestern North America," paper presented at World Wildlife Fund Conference on Consequences of the Greenhouse Effect for Biological Diversity, Washington, D.C., 1988.

50. J.W. Leverenz and D.J. Lev, "Effects of carbon dioxide-induced climate changes on the natural ranges of six major commercial tree species in the western United States," *The Greenhouse Effect, Climate Change, and U.S. Forests*, The Conservation Foundation, Washington, D.C.,1987, p. 123.

51. S. Henderson, "How it might be: species," *EPA Journal*, 15(1):21 (1989).

52. T.E. Lovejoy, "Conference overview," paper presented at World Wildlife Fund Conference on Consequences of the Greenhouse Effect for Biological Diversity, Washington, D.C., 1988.

53. W. Fornos, *Gaining people, losing ground: a blueprint for stabilizing world population*, Science Press, Ephrata, PA, 1987.

Comparisons of Aircraft and Satellite Sensors for Monitoring Air Pollution Effects on Forests

Christopher D. Elvidge[1]
James E. Vogelmann[2]
Carl A. Fox[1]

[1] *Desert Research Institute*
and Agricultural Experiment Station
University of Nevada System
P.O. Box 60220
Reno, NV 89506-0220

[2] *Institute for the Study of Earth, Oceans, and Space*
University of New Hampshire
Durham, NH 03824

INTRODUCTION

Air pollution, including acid rain and oxidant air pollution, has been a persistent phenomenon over the past five decades. Hydrocarbons released from industrial activity and vehicle emissions are photo-oxidized to produce oxidant air pollutants known to have adverse effects on many plant species. Figure 1 shows a photograph of forest damage in Vermont thought to be partially related to air pollution. Principal oxidant air pollutants include ozone, sulfates, nitrous oxide, nitrogen dioxide, and peroxyacetyl nitrate. These pollutants are generated primarily in urban areas and can reach damaging concentrations in the western United States where polluted air becomes trapped in valleys or against topographic barriers. Impacts on crops and forest ecosystems from topographically trapped oxidant pollutants are well documented. These impacts include slower growth rates, reduced leaf area index (LAI) values, increased susceptibility to disease or insect infestations, chlorosis, necrosis, growth form modifications, and gradual changes in species composition. In extreme cases, plant mortality can occur.

Remote sensing provides a tool for measuring the areal extent and level of vegetation damage from air pollutants. The unique spectral features of green vegetation in visible and near-infrared (NIR) wavelength regions can be readily measured and monitored using data acquired from airborne and satellite sensors. There are distinct spectral changes that occur as a direct consequence of air pollutiondamage in vegetation. Several additional factors make remote sensing attractive for the analysis of air pollution damage to vegetation. The data are readily available and large areas can be covered with a single data set. The digital data can be manipulated on a computer and coupled with field measurements to form biophysically based indices, such as images of LAI values.

Because of the high geometric fidelity of multispectral satellite images, the data can be readily registered to other spatially oriented data sets or attributes in Geographic Information Systems. Multiple coverages available from satellite sensors permit vegetation conditions to be monitored through time. Finally, today's airborne and satellite sensors obtain data with higher spectral resolution and longer NIR wavelengths than was possible with conventional air photography.

Reflectance Characteristics of Vegetation

The reflectance spectra of green leaves are presented in Figure 2. Green leaves have intense plant pigment absorptions in the visible (0.4 to 0.7 µm), high reflectivity referred to as the NIR plateau from 0.8–1.3 µm, and leaf water absorptions from 1.3–2.5 µm. Species related differences in the spectra can be noted in the shape of the pigment absorption region in the visible (0.4–0.7 µm), the depth of the water absorptions on the NIR plateau at 0.98 and 1.19 µm, and the relative height of the NIR plateau lobes centered at 0.9, 1.08, and 1.27 µm. The distinctive reflectance features of lignin and cellulose (Figure 3) are not present in the spectra of most green leaves due to intense leaf water absorption. The lignin and cellulose features are prominent in the spectra of dry leaves, litter, bark and wood.[1,2]

Distinct spectral changes occur in leaves as they senesce. Figure 4 shows reflectance spectra of chlorotic leaves from three species. The spectral differences are primarily in the 0.4–0.8 µm region. Intense pigment absorption is retained in the blue, while green and red reflectance increases. The chlorophyll A absorption near 0.68 µm persists and the red edge of the chlorophyll absorption (0.7–0.8 µm) shifts to shorter wavelengths. In addition, the leading edge of the NIR plateau (near 0.8 µm) begins to collapse into the red edge feature. As with green leaf spectra, the NIR absorption features of lignin and cellulose are not present in the yellow leaf spectra. The lignin/cellulose absorption features are only evident in dry plant materials.

Detection of Vegetation Stress and Damage

There are no universal symptoms of air pollution damage to vegetation. For instance, loss of LAI can be caused by air pollution, but can also be the result of insect infestations, drought, or other factors. Similarly, there are no universal spectral features that can be used to identify and quantify the level of vegetation damage from air pollution. For this reason some knowledge of local conditions and local phenomena are vital to the accurate interpretation and classification of the spectral indicators of air pollution damage in vegetation. If air pollution is documented at a particular set of sites, remote sensing may be useful in mapping the areal extent of damage and provide a rapid technique for monitoring the subsequent developments of air pollution damage in vegetation. In areas where no ground truth is available, remote sensing can still be used to identify sites where vegetation is damaged or stressed. Field checking is then required to determine the cause of the vegetation decline.

Air pollution is known to induce stress-related changes in forest canopies. These changes frequently include growth rates and leaf area index (LAI) values. Stressed trees can become more susceptible to attack from insects or disease. Foliar chlorophyll and water contents can be reduced. Longer term effects include tree mortality, alteration in growth forms, and changes in species composition. Below is a description of the spectral changes that occur as a result of specific symptoms associated with air pollution damage to vegetation. The value of the spectral signatures listed below can be enhanced substantially by registering data acquired on different dates in order to observe changes in plant communities induced by long-term exposure to air pollutants.

1. Changes or differences in (LAI) values are best discerned by contrasting the reflectance in the red and NIR.[3] These LAI related symptoms can be induced by reduced growth rates, necrosis, tree mortality, or changes in species composition.

2. Leaf water content of plant canopies can be monitored by combining bands from the NIR plateau (0.8–1.3 µm) with bands in the water absorption areas between 1.3 and 2.5 µm.[4] Radar imagery provides another means for monitoring leaf water content.

3. Changes in species composition can be best discerned using multiple bands and multiple dates of imagery. It is frequently possible to detect changes in species composition using three band color composites employing visible and NIR bands. In addition, a variety of statistical classification procedures can be used to map plant communities and changes in species composition between successive dates of imagery.

4. Necrosis and tree mortality will depress LAI values and increase the intensity of the lignin/cellulose absorptions in plant canopies. The lignin-cellulose spectral features are not widely recognized by the remote sensing community. However, recent laboratory[1,2] and airborne spectral measurements of NIR ligni-cellulose absorptions[5] suggest that the spectral features of dry plant materials could be used to indicate vegetation stress and forest damage induced by air pollution.

5. The chlorophyll content of plant canopies can be monitored with the wavelength position of the chlorophyll red edge. This feature is located between the intense chlorophyll pigment absorption at 0.68 µm and the high reflectance of the NIR plateau beyond 0.8 µm. The red edge is the sharpest feature of the green leaf spectrum. That is to say, it is the portion of the spectrum with the greatest change in reflectance per change in wavelength. It is now known that the position of the chlorophyll red edge shifts to longer or shorter wavelengths in response to changing phenologic or physiologic conditions in leaves.[6] Chlorosis induces the chlorophyll red edge to shift toward the blue end of the spectrum. The red edge has been a major focus of spectral studies of air pollution and acid rain damage to vegetation.[7-10] The relationship between the red edge position and chlorophyll content was first noted by Gates et al.:[11] "The position of this edge may be a good measure of the amount of chlorophyll within a leaf." Measurement of the red edge position requires higher spectral resolution than that offered by most airborne and satellite sensors. Collins[6] was the first investigator to measure red edge shifts using remotely sensed data. High spectral resolution (6 nm or less) is required in the 0.7 to 0.8 µm region in order to measure the wavelength position of the red edge. To date, only a handful of airborne instruments have been developed that are capable of accomplishing this task. No satellite sensor has been deployed with this capability.

AVAILABLE SENSORS

Both airborne and satellite sensors are available for monitoring air pollution effects on forest ecosystems. In this section, the characteristics of the major sensors will be described and compared.

Landsat MSS

The original earth observing satellite developed by NASA is the Landsat MSS (Multispectral Scanner). The first Landsat MSS was launched in 1972, and regular coverage has been maintained until the present. The Landsat MSS data has four bands between 0.5 and 1.1 µm. Two bands are in the visible and two are in the NIR. The spatial resolution of the data is 79 meters. By today's standards the spatial resolution and spectral resolution of Landsat MSS are coarse. The bandpasses are too broad to measure the chlorophyll red edge wavelength position, and no bands are present in the leaf water and lignin/cellulose absorption areas between 1.3 and 2.5 µm.

The great value of Landsat MSS data lies in the long period (17 years) over which data is available for use in multitemporal studies. Vogelmann[12] found a significant decrease in NIR reflectance between 1973 and 1984 Landsat MSS data on the Green Mountains of Vermont. Long-term forest records indicate that the area had sustained a substantial decline in forest vigor during the 1973-1984 period. Thedecrease in NIR reflectivity is consistent with a decrease in green biomass andan increase in dead branch materials associated with tree mortality.

Thematic Mapper

The Thematic Mapper (TM) was designed by NASA as the follow on to the Landsat MSS instruments. TM data covers a much wider spectral range (0.4 to 12.5 µm) than Landsat MSS data. The TM has three visible bands, three NIR bands, and one thermal infrared band. The TM bands are too broad to uniquely identify changes in the chlorophyll red edge wavelength position or in the intensity of lignin/cellulose absorption features. However, bands centered at 0.83, 1.65, and 2.22 µm have been used to monitor canopy moisture content. The spatial resolution of the visible and NIR data is 30, and the thermal infrared data has 120-resolution. In addition, TM data have 8-bit quantitization as opposed to the 6-bit quantitization of Landsat MSS. The TM data record extends back to 1982. Overall, TM data have proven to be considerably more useful spatially and spectrally than Landsat MSS data.

TM data have been successfully used to map the distribution of coniferous forest damage in airborne Thematic Mapper (ATM) data and satellite Thematic Mapper (TM) data of Vermont using NIR vegetation indices formed with bands on the NIR plateau (0.8-1.3 µm) and a leaf water absorption band at 1.65 µm.[13,14] Factors which affect this NIR vegetation index include LAI, leaf water content, and the proportion of green versus brown leaf materials in a plant canopy.

TM and ATM data were less useful in mapping air pollution damaged vegetation in the Santa Monica Mountains and the southern Sierra Nevada of California.[15] Coastal sage and chaparral communities were examined in the Santa Monica Mountains and yellow pine forests were examined in the southern Sierra Nevada. The air pollution damage in these areas were not as severe as the Vermont sites. In addition, the plant canopies in the California sites are less continuous than the Vermont sites, leading to a greater contribution of rocks, soils, and litter to the spectral response. The results of the California study[15] indicate that single dates of TM styled imagery will not be fully adequate to characterize air pollution damage in much of the western United States. Greater success may be afforded by analyses designed to detect change between successive dates of imagery. In addition, it may be useful to obtain imagery having higher spatial and spectral resolution than that offered by the broad band TM instruments.

SPOT

In 1986 the French government launched an earth observing satellite known as SPOT (Systeme Probatoire d'Observation de la Terre). SPOT data have a single visible-NIR (0.51-0.73 µm) band with 10-spatial resolution and three bands between 0.50 and 0.89 μm with 20-resolution. SPOT provides a substantial advantage over Landsat MSS and TM data in terms of spatial resolution. However, the SPOT bands are too broad to measure shifts in the position of the chlorophyll red edge, and there are no bands in the leaf water and lignin/cellulose absorption regions from 1.3 to 2.5 μm.

Airborne Visible/NIR Multispectral Scanners

A variety of airborne multispectral scanners with channels in the visible and NIR are available in the United States through government agencies or commercial services. These instruments can generally provide data with finer spatial resolution than the available satellite sensors. The most common airborne multispectral scanners have the seven TM bands, but additional bands are frequently available.

Airborne Imaging Spectrometers

Imaging spectrometers are a class of sensors that acquire imagery with fine spectral resolution (10 nm or less) in large numbers of bands. The fine spectral resolution is required to measure the wavelength position of the chlorophyll red edge, lignin/cellulose absorptions, and the depth of minor water absorptions on the NIR plateau at 0.97 and 1.19 μm. All imaging spectrometers now operating are airborne instruments. No satellite based imaging spectrometer data are currently available.

An imaging spectrometer known as AVIRIS (Airborne Visible/Infrared Imaging Spectrometer) has been built by NASA at the Jet Propulsion Laboratory. This instrument was initially flown in 1987. AVIRIS acquires data in 224 spectral bands between 0.41 and 2.45 μm with 20-m spatial resolution.[16] Preliminary results indicate that AVIRIS data will be useful in measuring the intensity of lignin/cellulose absorptions, leaf water absorptions, and species related differences in the shape of the visible portion of the spectrum.[5] It remains to be determined whether the 10-nm spectral resolution of AVIRIS is sufficient to adequately characterize the wavelength position of the chlorophyll red edge. The existing AVIRIS coverage is limited to a small number of NASA study areas.

The Programmable Multispectral Imager (PMI) of Moniteq Ltd. is a commercially available airborne imaging spectrometer with the capability of acquiring up to 288 spectral bands between 0.43 and 0.80 μm. These data have been used to measure red edge shifts in forest decline areas of Vermont that are suspected to be related to acid deposition.[7]

Airborne Spectroradiometers

Spectroradiometers are instruments that measure the intensity of solar radiation as a function of wavelength. These instruments are similar to imaging spectrometers, except that they acquire transects of data rather than images. Airborne spectroradiometers have been used extensively to identify stressed vegetation. The first report of this capability comes from Collins,[6] who found that the wavelength position of the chlorophyll red edge could be used to assess the phenological/physiological condition of crops. Airborne spectroradiometers have been used to detect chlorophyll red edge shifts in acid rain damaged forest canopies.[9,10]

Multispectral Thermal

Broad band thermal measurements can be used to measure temperature differences between plant canopies and provide a useful adjunct to multispectral visible/NIR data. However, instruments with single broad thermal bands, such as the TM, are unable to measure the fine spectral features that may be present in the thermal infrared. Recent laboratory studies[17,18] of the reflectance characteristics of plant materials in the thermal infrared (2.5–20 μm) have revealed a wide range of spectral features, some of which may prove to be of use in monitoring air pollution damage to vegetation. NASA operates a Thermal Infrared Multispectral Scanner (TIMS) with six bands in the 8–14 μm range. The TIMS bands are broad compared to the fine spectral features that can be measured in vegetation; no spectral features for vegetation have yet been identified in TIMS data. Sensors with higher thermal infrared spectral resolution will undoubtably be required to fully test the utility of this spectral region for the characterization of vegetation.

RADAR

There is a class of instruments that measure the backscatter returned from an active microwave beam (radar) to generate images of the earth's surface. These radar sensors can be aboard aircraft or spacecraft. Radar backscatter is sensitive to canopy moisture, canopy geometry, and the structural elements of the canopy (stems and trunks). Radar data have been used successfully to map species composition boundaries in forests.[19] Combining radar imagery with visible/NIR data has proven to provide a synergism in the analysis of vegetation characteristics.[20] Acquisition of radar imagery is problematic in many cases because of the limited availability of airborne and spaceborne radar imaging systems.

Airborne Video Systems

The previously discussed airborne and satellite data sets have several drawbacks that limit their applications in the monitoring of forest ecosystems. (1) Data are not analyzed in a real-time or even near real-time basis. Instead, data is not available until weeks or months after it has been acquired. (2) Because of the limitations of satellite orbits, data can only be acquired on certain dates. (3) The spatial resolution of the currently available satellite imagery is coarse, on the order of 10–80 meters. Finer spatial resolution is required for many land surface applications. These drawbacks have been successfully overcome with the development of visible/NIR airborne video systems. There have been several airborne multicamera video systems developed in the past several years.[21,22] These systems have been used to analyze vegetation conditions in forests, rangelands, and crops.[23-25] We expect multispectral airborne video systems to be used extensively in the future to detect and monitor air pollution damage in forests.

CONCLUSION

Remote sensing systems provide a means of mapping, quantifying, and monitoring types and conditions of vegetation. Vegetation stress and damage predictably alter both visible and NIR reflectance of forest canopies, and these reflectance changes can be used to assess forest condition. Current orbital systems capable of providing information regarding air pollution effects on forest ecosystems include the Landsat Multispectral Scanner (MSS), Thematic Mapper (TM), and the French satellite SPOT. Long-term changes in forest condition can be best ascertained using MSS data, which are available from 1972 to the present. However, because of their better spatial resolution, both SPOT and TM provide more precise information regarding current status of forest ecosystems. In addition, TM provides better spectral resolution than either SPOT or MSS, and thus is able to provide information regarding certain aspects of forest condition (e.g., water status) that is not obtainable using these other sensors. Note that each sensor has a number of advantages and disadvantages that must be considered when carrying out any remote sensing investigation. It is often beneficial to include data from several of the sensors in order to compensate for each other's weaknesses.

In addition to the orbital sensors described above, there are now many aircraft sensors that can be used to assess forest condition. Many of these are broad-band sensors that provide spectral data similar to those provided by the orbital sensors. The advantages of these airborne sensors are: (1) they provide better spatial resolution than the orbital sensors; (2) data acquisition is not constrained by orbital characteristics, and thus data may be acquired whenever necessary; and (3) bandpasses can be tailored for the application at hand with interchangeable filters. Airborne video systems provide an additional advantage with real-time color infrared display and near real-time data analysis capabilities.

Many aircraft sensors developed recently have the capability to acquire spectral information in narrow bands (high spectral resolution sensors). These advanced sensors provide reflectance data in spectral regions that are important for assessing forest health along the chlorophyll red edge and in areas of major lignin and cellulose absorptions. The technology for building, operating, and analyzing data for this new class of sensors is still evolving. However, it is expected that the information provided by high spectral resolution sensors will be extremely useful in analyzing the effects of air pollution on vegetation.

The need to assess the consequences of human activities on forest ecosystems is becoming increasingly apparent. It is important to monitor the state of health and condition of the vegetation from a number of biomes, determine which plant communities are affected, and to determine the location and the magnitudes of these effects at local and regional scales. Although much work is necessary to maximize biological information content in remotely sensed data, the processes involved are constantly evolving and improving. Remote sensing provides a means for obtaining useful perspectives on the status of forest ecosystems and has the potential for playing an important role in determining the severity of the effects of pollutant exposure on forests.

REFERENCES

1. C.D. Elvidge, "Reflectance characteristics of dry plant materials," Proceedings of the International Symposium on Remote Sensing of Environment, Environmental Research Institute of Michigan, 1987, p. 721.

2. C.D. Elvidge, "Visible and near infrared reflectance characteristics of dry plant materials," *International J. Remote Sensing*, submitted 1989.

3. D.L. Peterson, M.A. Spanner, S.W. Running, and K.B. Teuber, "Relationships of Thematic Mapper simulator data to leaf area index of temperate coniferous forests," *Remote Sensing of Environ.* 22:323 (1987).

4. R.E. Hunt, B.N. Rock, and P.S. Nobel, "Measurement of leaf relative water content by infrared reflectance," *Remote Sensing of Environ.* 22:429 (1987).

5. C.D. Elvidge, "Vegetation reflectance features in AVIRIS data," Proceedings of the International Symposium on Remote Sensing of Environment, 6th Thematic Conference, Remote Sensing for Exploration Geology, Environmental Research Institute of Michigan, 1988, p. 169.

6. W.E. Collins, "Remote sensing of crop type and maturity using high resolution features in the near infrared," *Photogrammetric Engineering and Remote Sensing* 44:43 (1978).

7. B.N. Rock, J.E. Vogelmann, D.L. Williams, A.F. Vogelmann, and T. Hoshizaki, "Remote detection of forest damage," *Bioscience* 36:439 (1986).

8. B.N. Rock, T. Hoshizaki, and J.R. Miller, "Comparison of *in situ* and airborne spectral measurements of the blue shift associated with forest decline," *Remote Sensing of Environment* 24:109 (1988).

9. D.L. Williams, "Remote sensing: tool for acid rain research," *Forest Industries* 19:31 (1986).

10. D.L. Williams, C.L. Walthall, and S.N. Goward, "Collection of in situ forest canopy spectra using a helicopter: a discussion of methodology and preliminary results," Proceedings of the Tenth International Symposium on Machine Processing of Remotely Sensed Data, Purdue University, 1984, p. 94.

11. D.M. Gates, H.J. Keegan, J.C. Schleter, and V.R. Weidner, "The spectral properties of plants," *Applied Optics* 4:11 (1965).

12. J.E. Vogelmann, "Detection of forest change in the Green Mountains of Vermont using Multispectral Scanner data," *International J. Remote Sensing* 9:1187 (1988).

13. J.E. Vogelmann and B.N. Rock, "Assessing forest decline in the coniferous forests of Vermont using NS-001 Thematic Mapper Simulator data," *International J. Remote Sensing* 7:1303 (1986).

14. J.E. Vogelmann and B.N. Rock, "Assessing forest damage in high elevation coniferous forests in Vermont and New Hampshire using Thematic Mapper data," *Remote Sensing of Environ.* 24:227 (1988).

15. W.E. Westman and C.V. Price, "Detecting air pollution stress in Southern California vegetation using Landsat Thematic Mapper band data," *Photogrammetric Engineering and Remote Sensing* 54:1305 (1988).

16. W.M. Porter and H.T. Enmark, "A system overview of the Airborne Visible/Infrared Imaging Spectrometer (AVIRIS)," *Airborne Visible/Infrared Imaging Spectrometer (AVIRIS): A Description of the Sensor, Ground Data Processing Facility, Laboratory Calibration, and First Results*, JPL Publication 87-38, 1987, p. 3.

17. C.D. Elvidge, "Thermal infrared reflectance of dry plant materials: 2.5 to 20.0 μm," *Remote Sensing of Environ.* 26:265 (1988).

18. J.W. Salisbury, "Preliminary measurements of leaf reflectance in the 8–14 μm region," *International J. Remote Sensing* 7:1879 (1986).

19. J. Cimino, A. Brandani, D. Casey, J. Rabassa, and S.D. Wall, "Multiple incidence angel SIR-B experiment over Argentina: Mapping of forest units," *IEEE Transactions in Geoscience and Remote Sensing* 52:343 (1986).

20. J.F. Paris and H.H. Kwong, "Characterization of vegetation with combined Thematic Mapper (TM) and Shuttle Imaging Radar (SIR-B) image data," *Photogrammetric Engineering and Remote Sensing* 54:1187 (1988).

21. D. King, J. Vlcek, and X. Yuan, "A 4-camera video sensor: Its performance and applications with special regards to forestry," Proceedings of the 11th Biennial Workshop on Color Aerial Photography and Videography in the Plant Sciences, American Society for Photogrammetry and Remote Sensing, 1987, p. 286.

22. P.R. Nixon, D.E. Escobar, and R.L. Bowen, "A multispectral false color video imaging system for remote sensing applications," Proceedings of the 11th Biennial Workshop on Color Aerial Photography and Videography in the Plant Sciences, American Society for Photogrammetry and Remote Sensing, 1987, p. 295.

23. D.E. Escobar, R.L. Bowen, H.W. Gausman, and G. Cooper, "Use of a near-infrared video recording system for detection of freeze-damaged citrus leaves," NASA AgRISTARS EW-U2-04351 JSC-18563, 1982.

24. J.H. Everitt, D.E. Escobar, M.A. Alaniz, and M.R. Davis, "Using airborne middle-infrared (1.45-2.0 um) video imagery for distinguishing plant species and soil conditions," *Remote Sensing of Environ.* 22:423 (1987).

25. P.R. Nixon, D.E. Escobar, and R.M. Menges, "A multiband video system for quick assessment of vegetal condition and discrimination of plant species," *Remote Sensing of Environ.* 17:203 (1985).

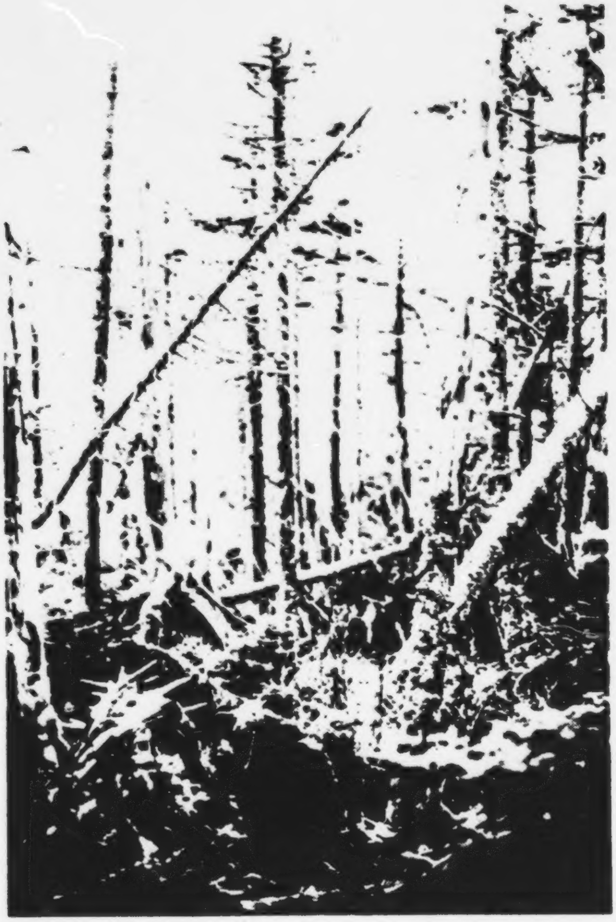

Figure 1. Forest decline damage at Camels Hump, VT. Damage is thought to be partially related to exposure to pollutants. Photo courtesy of the University of Vermont Botany Department.

produced from
available copy.

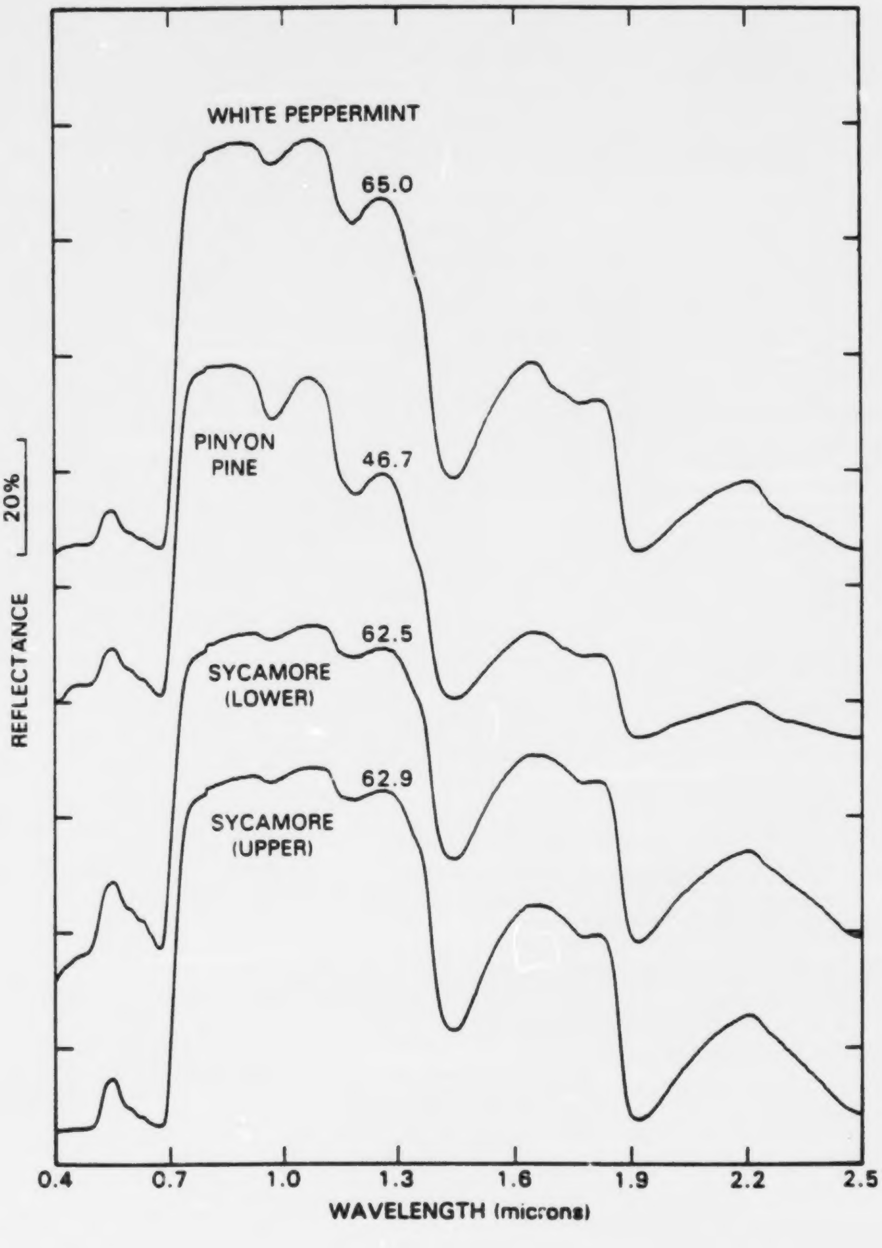

Figure 2. Laboratory reflectance spectra of green leaf materials. The spectra have been displaced vertically to avoid overlap. The reflectance at 1.3 um is provided for each curve. From Elvidge.[1]

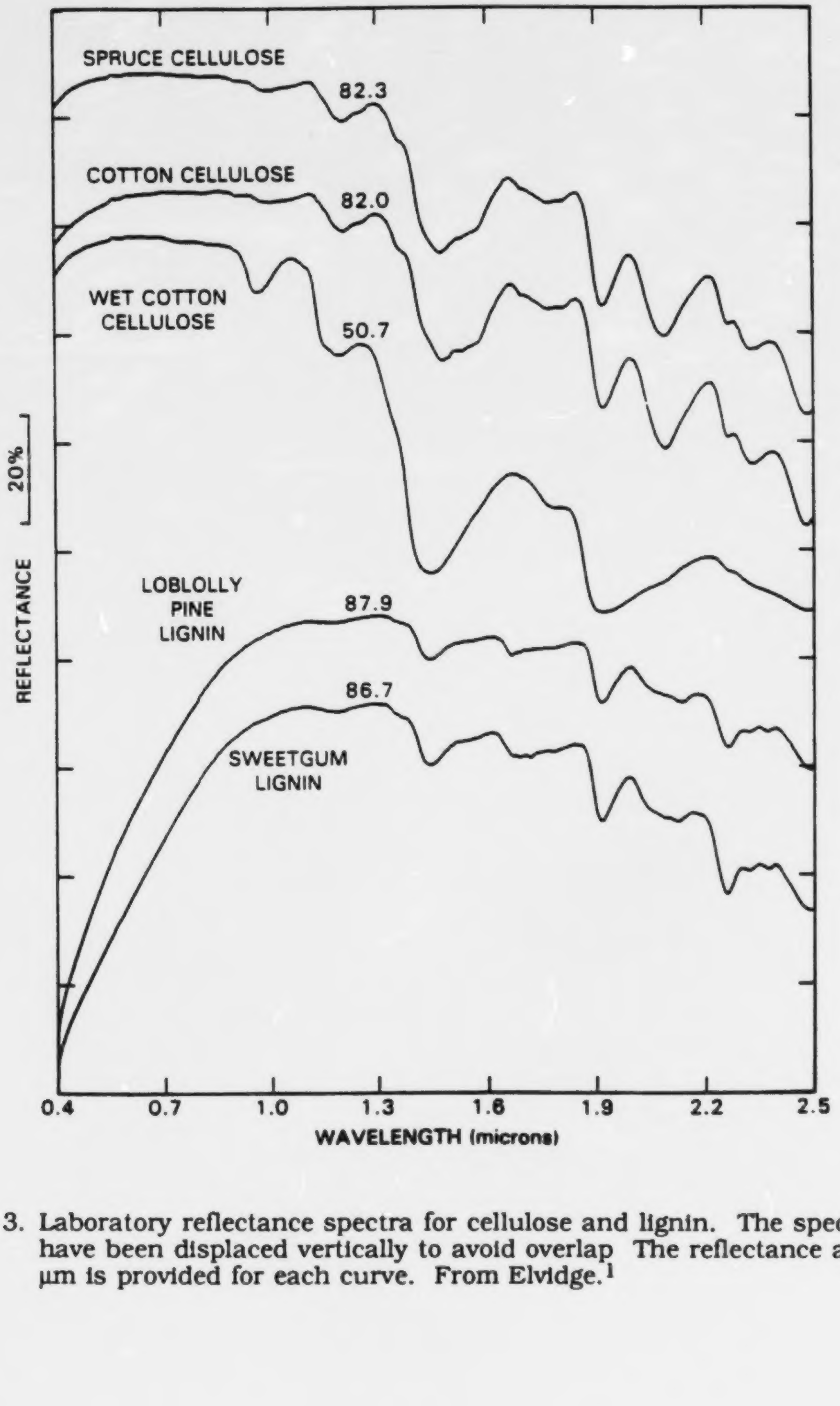

Figure 3. Laboratory reflectance spectra for cellulose and lignin. The spectra have been displaced vertically to avoid overlap The reflectance at 1.3 μm is provided for each curve. From Elvidge.[1]

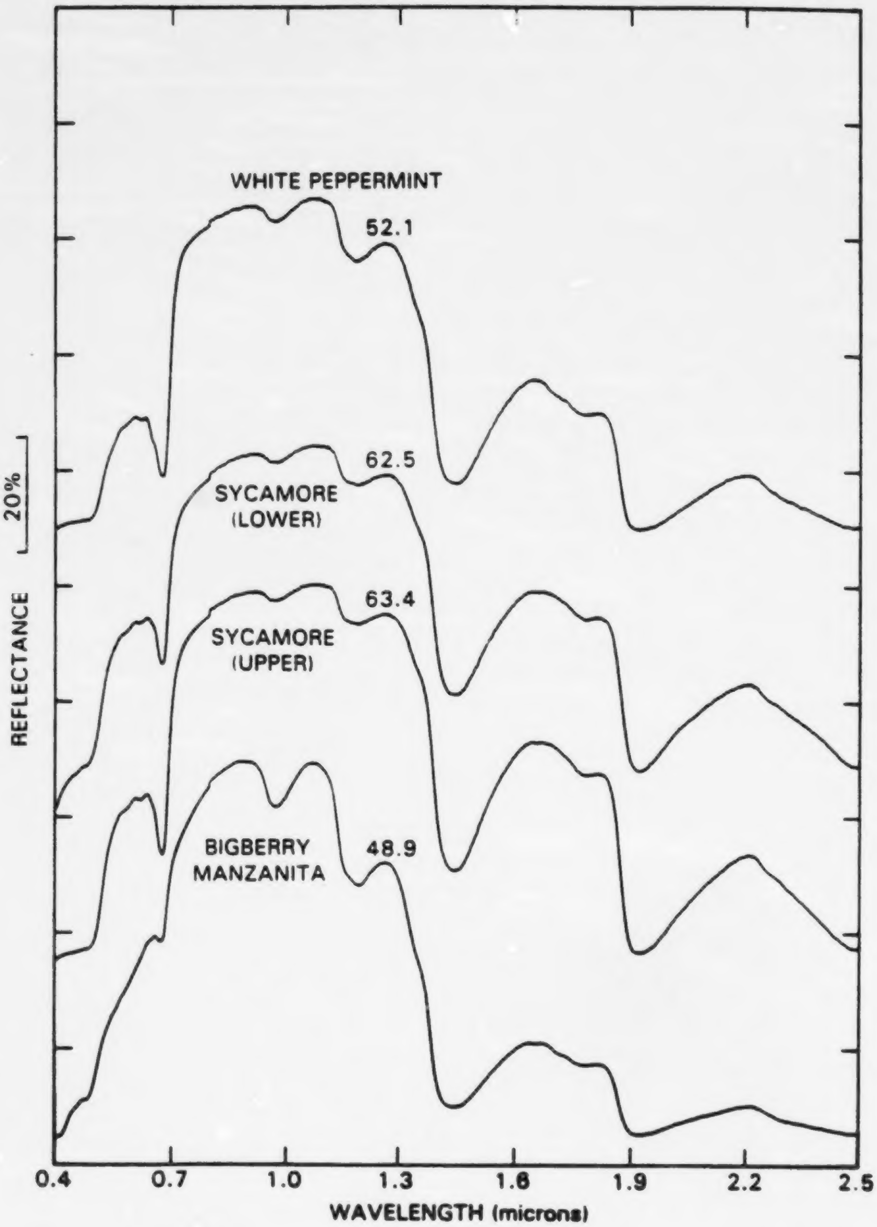

Figure 4. Laboratory reflectance spectra of chlorotic leaves. The spectra have been displaced vertically to avoid overlap The reflectance at 1.3 μm is provided for each curve. From Elvidge.[1]

Early Detection of Air Pollution Injury to Coniferous Forests Using Remote Sensing

Susan L. Ustin[1]
Brian Curtiss[2]
Scott N. Martens[1]
Vern C. Vanderbilt[3]

[1] *Department of Botany*
University of California
Davis, CA 95616

[2] *Center for the Study of Earth from Space*
University of Colorado
Boulder, CO 80309-0449

[3] *NASA Ames Research Center*
MS-242-4
Moffett Field, CA 94035

INTRODUCTION

Many recent studies have documented high levels of atmospheric pollutants in both urban and rural areas as evidence for actual or potential forest decline on regional scales.[1,2] Chronic exposure to atmospheric pollutants such as oxidants may produce significant changes to forested ecosystems, ranging from needle chlorosis, premature foliar loss, and altered canopy architectures under moderately severe exposures to tree mortality, reduced species diversity, and altered species distributions under severe chronic exposures. Early detection and efficient monitoring of forested ecosystems for symptoms of decline are of global significance.

Considerable difficulties arise in detecting and interpreting the spatial extent of air pollution injury in natural ecosystems, due to heterogeneity at all scales of most forested landscapes, and the importance of terrain and meteorological factors on the distribution and concentration of pollutants. The southern Sierra Nevada range provides a good example of the problems faced when trying to interpret regional-scale pollutant exposures and vegetation responses. In this region, weather patterns, known sensitivity of forest species, and evidence of foliar symptoms indicate the potential for oxidant-induced forest decline over much of the montane region.

The USDA Forest Service has monitored visual symptoms of oxidant injury on needles at numerous sites in the yellow pine forests (*Pinus ponderosa, P. jeffreyi*) since 1979.[3-6] Similar results are reported by the National Park Service.[7,8] At this stage of decline, considerable variation in foliage conditions exists among trees within and among stands. Symptoms are most severe in the southern Sierra Nevada and generally decrease toward the north. Symptoms of oxidant injury have increased in frequency and severity over the period of monitoring (J. Pronos, unpublished data). Current symptoms, slight to moderate in severity, include characteristic needle mottle chlorosis and crown thinning but little evidence for oxidant-induced mortality. Despite this database, regional extrapolations of ozone exposure in the forest zone are difficult because of the relatively few air quality monitoring stations in the montane region, the difficulty of modeling air flow patterns in complex terrain,

Preceding page blank

and difficulties in establishing and monitoring oxidant injury in sites with limited access.

Although aircraft and satellite sensors have the potential for monitoring ecosystem functioning, methods for detecting early stages of forest injury before tree mortality occurs have been of limited success.[9-11] Westman and Price[10] have concluded that current levels of forest damage are not detectable in this region using Landsat Thematic Mapper satellites. Field and aircraft instruments are now capable of high spectral and spatial resolution, improving the potential for early detection of forest injury. NASA's planned Earth Observation (EOS) Platform for the 1990s will carry a new generation of satellite sensors, which will include the high resolution imaging spectrometer (HIRIS). This sensor and the current airborne instrument, the advanced visible and infrared imaging spectrometer (AVIRIS), are capable of providing detailed spectral and spatial information useful for determining the physiological condition of forested ecosystems and for mapping spatial patterns associated with environmental stresses. Both sensors acquire data at sampling intervals of 10 nm in the 400- to 2500-nm spectral region. HIRIS acquires 192 spectral bands and AVIRIS acquires 224 bands in this region with spatial resolutions of 20 m by 20 m.

METHODS

Site Selection

Advanced visible infrared imaging spectrometer (AVIRIS) data were obtained from NASA along an 11 km wide flightline oriented to include the latitudinal gradient in oxidant injury symptoms in the yellow pine forest (Figure 1). We located stands within the flightline in which (1) ponderosa and/or Jeffrey pine was a dominant species within the forest and (2) that represented the range of foliar oxidant injury present, based on information from USDA Forest Service surveys and the topographic location of the site in relation to prevailing winds from the San Joaquin Valley. Foliage was sampled from 20 trees at six sites in Sequoia National Forest and Sequoia-Kings Canyon National Parks and at eight sites in Sierra and Stanislaus National Forests in September 1987. Site locations are listed in Table I. Based on analysis of the visible ozone injury data, we selected two sites (Site 1 = highest damage, Site 6 = lowest damage) to revisit in September 1988. Injury ranking, spectra, and chlorophyll were remeasured.

At each site a stratified randomly placed transect was determined within the forest, and the nearest dominant or codominant ponderosa pine at 20 m intervals was selected for sampling. Three branches were obtained from the south side of open-grown (non-shaded) foliage from 20 trees/site using 7-m pole pruners. The "healthiest" appearing branch was retained for subsequent measurements. Tree height varied with site and usually lower or mid-canopy foliage was obtained for measurements. Muir and Armentano[12] found upper and lower crowns did not differ in severity of chlorotic mottle or needle retention; thus, use of foliage from the lower crown should not have biased the results. Branch samples were tagged, placed in black plastic bags and stored in ice chests for transport to the spectrometer. In most cases, spectral measurements were made on the day of collection or the following day.[13] Spectral measurements for Sites 5 and 6 were made two days after collection. Supporting field measurements included species composition and basal area measurements (Relaskop) of the stand and canopy cover estimates from fisheye photographs. Photographs were analyzed for percentage canopy cover (1-sky) using elevation angle weighting.[14]

Foliar Damage Assessment

Pine needles are clustered into whorls corresponding to the year of development on branches. Within 24 h of collection, six characters were measured on each needle whorl on the branch samples using a modified method developed by the National Park Service.[15] Injury was visually estimated as a percentage of needle area damaged and assigned into three categories: ozone (based on chlorotic mottle), biotic (evidence for herbivory and/or pathogens), and abiotic (principally winter fleck and tip burn). Experienced National Park Service and USDA Forest Service scientists provided training in damage assessments, which included cross-comparisons of injury evaluations to verify our ability to discriminate various forms of damage. Percent needle retention was estimated from the scars left by abscissed fascicles. Whorl length (stem length occupied by remaining fascicles in each whorl) and needle length of three needles from each whorl were measured.

Chlorophyll Analysis

Chlorophyll A, chlorophyll B, and total chlorophyll were determined for each whorl of all branches at two sites (Sites 12 and 14) during the original measurement set (1987) and two sites (Sites 1 and 6) revisited during the following year. Chlorophyll extractions were made less than 48 h after the branches were cut and stored refrigerated in Ziploc® bags placed inside large black plastic bags. Samples were obtained from the midsection of the needles by cutting <1-mm slices across the bundle so that segments from all needles were included in the analysis. Needle pieces were weighed on a Mettler PE360 balance, placed in 50-ml centrifuge tubes with 10 ml cold reagent-grade acetone with 1% NH_3OH, and immediately ground using a Biospec Products, Inc., tissue homogenizer for approximately 10 sec until tissue particulates were clear of color. Tubes were then placed in an icebath and covered with tinfoil to prevent light-induced oxidation of the pigments until centrifuged at 10,000 Rev/min for 10 min in a Sorval RC-5B refrigerated centrifuge. One-milliliter supernatant samples in quartz tubes were analyzed in a Varian Techtron Model 635 spectrophotometer. Absorbance was measured at 663 and 645 nm against blank standards and chlorophyll A, B standards (Aldrich 25-825-3; 25-826-1). Chlorophyll A and B were determined using the equations of Anderson and Boardman.[16] A second set of needle material was weighed for fresh weight and dried in a 90° C oven. These samples were reweighed to obtain fresh weight/dry weight conversion factors.

Spectral Measurements

Reflectance spectra of pine needles were measured with the NASA Jet Propulsion Laboratories' PIDAS spectroradiometer (portable intelligent display and analysis spectrometer).[17] This instrument acquires reflectance measurements in 1-nm spectral bands in the visible and near-infrared (400–1100 nm) and in 5-nm spectral bands in the near- and shortwave-infrared (900–2450 nm). To estimate the bidirectional reflectance factor, each whorl of needles was fastened into a tight bundle using rubberbands at each end, and placed within the PIDAS field of view, 0.3 m from the 6° foreoptic, with the center line of the shoot perpendicular to the PIDAS optical axis. This produces a standardized viewing geometry, which is readily reproducible by other researchers, and reduces any confusion due to differences in specular reflectance. The needle bundle usually, but not always, filled the 1-cm diameter dark center field-of-view. Illumination was provided by a 1000-W quartzline lamp (GE FHM (Q1000T3/4) in a Smith-Victor Co. (Model 750) studio lamp with a PH stabilizer voltage regulator (Model AVR-1000W) to control fluctuations in light intensity. The lamp was located 0.45 m from the bundle at an angle of 45° to the center line of the shoot. Radiance values were converted to percent reflectance using measurements of a pressed Halon standard (polytetrafluoroethylene powder) of known reflectance.

Considerable effort was made to reduce specular reflectance from the whorls due to needle geometry and to eliminate backscattered light from other sources of reflectance. The needles in the whorls were held tightly bundled and suspended in front of the PIDAS by supporting the two bundle ends on a frame outside the field of view. Visual inspection showed no evidence of specular reflection from the needles for the directions of illumination (45° zenith and 0° azimuth) and reflection (0° zenith and 0° azimuth). A light-absorbing baffling behind the frame reduced the diameter of and trapped the portion of the incident light beam not intercepted by the needle bundle. A second light trap 0.8-m deep provided a black background directly behind the needle bundle within the field of view of PIDAS. Measurements showed that the radiance of the black background was less than 0.001 of the value of the radiance of a needle bundle. Each needle bundle was measured and rotated three times to obtain an average representing the spectral reflectance of each needle bundle.

Quality Control and Assessment

Standard quality control and validation procedures were used to determine precision and accuracy standards. Five to ten percent of the data were remeasured. All data presented in this paper are within acceptable EPA quality standards of accuracy and precision for the type of data presented.[18,19]

RESULTS AND DISCUSSION

Vegetation Reflectance Patterns

The reflectance curve illustrated in Figure 2 represents a typical pattern observed for healthy green vegetation. Reflectance (as a percentage of the reflectance of a perfect lambertian surface), is low in the visible (400-700 nm) and sharply increases in the near-infrared (800-1100 nm), and is relatively low again in the shortwave infrared (1550-1900 and 2100-2400 nm). This pattern contrasts with that of most soils and other natural materials. Many soils show a gradual increase in reflectance across the spectrum, although some minerals and clays have unique absorbance patterns in the 890-910 nm and 2100-2400 nm range.

Reflectance characteristics of forest canopies are dominated by photosynthetic pigment absorption in the visible (500-700 nm) spectral region, by leaf structure and canopy architecture in the near-infrared (800-1100 nm), and by water content in the shortwave infrared (1550-2400 nm). Recent research has suggested that changes in the chemical composition of tree canopies may be detected from aircraft and spaceborne platforms, which, if confirmed, could be used to infer information about changes in forest condition (Figure 2). Leaf and canopy chlorophyll,[20-23] nitrogen and lignin,[24-26] and cellulose[27,28] have been detected and quantified using high spectral resolution sensors.

As foliage becomes chlorotic and senescent under various sources of environmental stress, reflectance changes predictably by increasing in the visible region and decreasing in the near-infrared.[9] The spectral position of the 'red-edge' (the inflection point around 700 nm), appears to shift toward shorter or longer wavelengths around 700-720 nm as chlorophyll concentration decreases or increases, respectively. Ustin et al.[22] and Ustin and Curtiss[23] have shown that both increased reflectance in the visible region and shifts in the red-edge occur in ponderosa pine foliage exposed to a simulated seasonal oxidant fumigation in the summer range of exposures reported from southern Sierran monitoring stations.[29] The changes in reflectance were consistent with other evidence of increasing stress and symptoms of chlorosis. These results indicate that it is possible to nondestructively detect and quantify ozone injury using spectral assays under field conditions and that such injury may be detectable using spaceborne platforms, provided there is sufficient spectral and spatial resolution of the sensors.[23]

Field Measurements

Environmental Injury Rankings and Foliage Age. Mean foliar injury rankings show considerable variation among sites (Figure 3). A similar range of variation is found for within-site comparisons between trees (Tables II and III). All sites show a consistent trend with age: the oldest whorl exhibits the most severe needle mottle with less severe symptoms in younger growth ($r = 0.55$, $p < 0.0001$).

Few whorls show chlorotic mottle affecting greater than 20% of the needle surface. Only 3.3% of all whorls sampled were estimated to have oxidant symptoms exceeding 30% of the retained needle area. Nonetheless, all sites had chlorotic mottle symptoms on some whorls, and in all sites but one, foliar oxidant injury was found on some current (first year) or previous (second) years' needle whorls. Because of the generally slight symptoms on the first two years' growth and the small number of whorls per branch, the mean percent leaf area affected is quite small. Further, needle injury rankings did not extend over the full range but instead 95% of whorls were limited to less than 10% of the needle surface affected. Needles having high injury rankings (20-60%) were always in the oldest whorls on the affected branches, suggesting that abscission occurs substantially before the entire needle is affected. Thus, both mean needle age and chlorosis of the stand are affected by oxidant exposure.

Figure 3 suggests that biotic and abiotic needle damage do not closely follow the trend observed for oxidant damage, yet significant correlations were found ($p < 0.0001$) between ozone damage and biotic damage ($r = 0.24$) and between ozone damage and abiotic damage ($r = 0.30$). These relationships are dependent on the high oxidant rankings in the first four sites and need further study to determine if the statistical associations are biologically significant.

Because foliage injuries are cumulative, the age of oldest foliage retained is a good indicator of the general vigor of the stand. Oldest needle age is an indicator of the presence of some form of environmental stress; the type of stress can be inferred by assessment of the retained foliage. Age of oldest foliage on ponderosa pine varies markedly (Table II). Healthy ponderosa pines retain needles for 6 to 10 years.[7] Only 3 of 15 stands had needles as old as 6 years, and only 1 stand had many whorls of this age. Further, the age of the youngest whorl having chlorotic mottle was relatively young at most sites (Table III). We found a weak correlation ($r = -0.25$, $p < 0.0003$) between injury rankings and needle retention. However, we did observe that whorls having oxidant rankings exceeding 20% were always the oldest whorls on the branch.

These results demonstrate the problems in detecting early stages of forest decline using spectral techniques. The principal changes currently observed in the southern Sierra Nevada associated with oxidant foliar injury are slight canopy chlorosis, differences in mean needle age, and excessive crown thinning. Based on the sites we sampled, our data support the conclusion that such effects, though slight to moderate in severity, are widespread throughout much of the western slopes of the southern Sierra Nevada.[3-8] We have found that multivariate statistical methods for image analysis are too sensitive to extraneous site conditions, illumination, atmospheric effects, and instrument drift to be used successfully for detecting such subtle changes of forest condition. Alternatively, we have adopted a strategy of developing deterministic models based on spectral changes of foliage exposed to atmospheric pollutants. This approach has potential because AVIRIS and HIRIS instruments have sufficient spectral sampling to define unique spectral signatures.

Canopy Closure. Yellow pine forests are typically open growth stands. The percentage of canopy closure was calculated for 14 of the stands (Table IV). These values illustrate the range of canopy closure conditions present in different stands. Variation is principally influenced by the age of second growth forest and management practices and is largely unrelated to oxidant exposure. Although canopy thinning exists in sites having high ozone rankings, these effects were less prominent than other sources of environmental variation.

Spectral Measurements

Rationale. We measured reflectance on artifically arranged needle bundles rather than on the natural architecutral arrangements of the needles for three reasons. First, this approach permitted the best determination of the spectral light-absorbing and scattering properties of the needles. By bundling the needles together the chance of measuring a small change in chlorosis is enhanced because the close spacing increases the probability that any light scattered by one needle will be absorbed by another in the bundle. Second, bundling the needles reduced confounding reflectance changes due to differences in biomass between samples. Third, the natural architectural arrangement of the shoots could not be reproduced for the spectral measurements after removing the branches from the trees, therefore an arbitrary decision was required to standardize the measurement procedure. We designed the measurement process to address these sources of variation so that measurements would be readily reproducible.

We have concentrated on examining reflectance changes in the visible and near-infrared spectral regions because of correspondence to the observed visual symptoms of needle mottle and because these symptoms can be related to the physiological condition, through improved understanding of the action of oxidants on photosynthetic membranes and cumulative effects on growth. Mean spectral reflectance varied principally with needle age. The spectra in Figure 4 show the mean reflectance for whorls one and four, obtained from measurements from Site 12, a site ranked as having slight to moderate oxidant foliar symptoms (Figure 3). Increased reflectance is observed between 570 and 700 nm and decreased reflectance between 700 and 800 nm in the fourth-year foliage. This pattern illustrates a typical age-dependent pattern we have observed at all 15 sites. The first whorl (current year) has somewhat higher reflectance in this region than the second-year foliage. The second-year foliage has the lowest reflectance in the red region of the spectrum (600–670 nm). Foliage older than the second whorl has reflectance similar to the second year (i.e., no change) or has increasingly higher reflectance in this region. The oldest one or two years' foliage shows increased reflectance in the red region. These changes in band depth at the chlorophyll absorptance region are indicative of changes in needle chlorophyll concentration. Previous studies have reported good correlations between ozone exposure and reflectance in this region.[22,30,31] Nonetheless, while linear regressions between reflectance and chlorophyll concentration support a strong correlation,[22] significant scatter around the regression line is apparent, making predictive use difficult. We have hypothesized that this is due to changes in (a) molecular organization and structure of the chloroplast thylakoids, (b) to changes in photosynthetic pigment concentration, and (c) pigment composition.[22]

Reflectance Spectra. When all whorls within a site are averaged, we can examine spectral differences between sites related to oxidation exposures. Figures 5 and 6 show mean reflectance spectra for Sites 1 and 6, the sites having the greatest difference in ozone rankings. Figure 5 shows the response over the full spectral range, while Figure 6 shows details of the response in the visible and near-infrared spectral region. The greatest differences between sites are in the 400–1400 nm region. The spectral changes observed on foliage exposed to atmospheric pollutants are consistent with similar effects measured on foliage grown under controlled ozone fumigations.[22,23] Both normal developmentally determined senescence and oxidant injury apparently produce similar spectral changes but occur at differing foliar ages (Figures 4-6).

Red-edge Inflection. Changes in the inflection point in the wavelength region between 670 and 720 nm has been related to foliage chlorophyll content.[22,31-34] Rock et al.[34] have used the blue-shift to define spruce decline from Camels Hump, VT. The wavelength position of the red-edge inflection (REI) is determined by the point where the first derivative is maximum and the second derivative is zero. Because the exact wavelength at which the first derivative curve is at maximum is difficult to estimate, we approximated REI as the midpoint on the symmetric curve from the point where reflectance was half of the maximum value. A significant correlation between this wavelength and chlorophyll A, B, or total chlorophyll content was obtained.[22] A linear correlation was obtained between total chlorophyll (ug/g dry weight) and inflection wavelength over a 20-nm range.

$$\text{Chlorophyll} = -1.17 \times 10^5 + 169 \cdot (\text{REI wavelength, nm}) \qquad [1]$$
$$r = 0.72,\ n = 107,\ p < 0.001$$

Scatter around the regression decreases substantially when data for all whorls of the same age are averaged. In this case, the regression for the eight age class whorls is:

$$\text{Chlorophyll} = -6.24 \times 10^4 + 92.0 \cdot (\text{REI wavelength, nm}) \qquad [2]$$
$$r = 0.93;\ p < 0.001$$

Increased reflectance in the red region indicates a loss of band depth while the red-edge shift indicates band narrowing of the chlorophyll feature. At the molecular level such changes implicate alterations in the distribution of complexed forms of chlorophyll species[35,36] and/or alterations in thylakoid membrane structure and configuration.[37] Because of this sensitivity to photosynthetic pigments, it may be possible to link spectral changes directly with physiological models of pollutant injury or with growth models.

The blue-shift seen in the REI is sufficient to be detectable by scanners having the bandwidth resolution of AVIRIS and HIRIS. Under diverse environmental conditions found in the Sierra Nevada, it is uncertain whether a 1-2 band shift would be sufficient for detection without further processing of the image datasets.

An alternative way to examine the data is to look at individual age variance of the REI plotted by tree (Figures 7a–d). For example, we have chosen four sites that span the range of ozone rankings we measured (Figure 3; Sites 1, 6, 12, 14). The effect of individual tree variance within sites is best seen in terms of number of whorls present and the shape of the curves. Some trees maintain high red-edge values for several years while others decline after one or two years, as indicated by the shapes of the curves. A family of curves is found where the wavelength of the REI increases in the second whorl, followed by additional years at nearly the same wavelength until the final year of growth, which often shows a marked decrease in wavelength. The age at which these events occur varies with individuals and with sites and provides new insight into the site condition. Individuals having greater foliage vigor have shallow curves extending over several years while foliage at the other extreme has REI plots with steeply arched curves of only 1–3 years' duration. Wide variation in tree response to atmospheric pollutants within sites is similar to results of other studies.[3,7]

REI was replotted by age classes. The REI data were classified by the age of the oldest whorl on the branch. That is, all branches having eight years' growth were grouped together and the REI of each whorl averaged; branches having seven years' growth were grouped together, and so on until all branches from the site were classified. Figures 8a–d show the family of curves obtained when the mean foliage REI is classed by the age of the oldest whorls. Trees maintaining foliage of the same age class were found to respond similarly even when considerable differences in foliage age were found among trees at the same site. These results suggest that REI within sites could be used to detect differences in mean age and foliage condition, and differing REI means between sites could be used to detect early stages of oxidant injury. Similar magnitudes of red-edge shift were measured on seedling canopies from open-top chamber experiments.[23] When resampled at the 10-nm resolution of AVIRIS data, differences were still sufficient for detection.

A pattern closely similar to the family of REI curves is observed when mean needle chlorophyll content is plotted by whorl age after first grouping by the age of the oldest whorl (Figures 9a,b). Curves for chlorophyll A and B are very similar in shape with those presented for total chlorophyll. These results again demonstrate that the REI is a good approximation of needle chlorophyll. The chlorophyll A/B ratio declines slightly with age accounting for differences in curve shape between chlorophyll A and B.

Modeling Spectral Changes in AVIRIS or HIRIS Image Data. Because of the confounding problems associated with detecting subtle spectral changes due to environmental stresses in the presence of environmental heterogeneity and differing illumination conditions, we have approached the problem of detecting early stages of pollutant injury by assuming the signal received by a satellite or airborne sensor is a composite spectrum partially contributed to by all components on the surface (foliage, litter, wood, soils, rock types, and shadow/shade). Linear mixture methods using factor analysis for deconvolving the satellite or airborne datasets can be applied provided that the assumption of single scattering for photons within the canopy is valid. The open-growth ponderosa pine stands and the relatively sparse foliage may not violate this assumption excessively. More complex nonlinear techniques exist but require a better understanding of radiation transfer within the canopy than the current state of knowledge permits. The advantage of the linear mixing approach is that it relies on the multidimensionality in the spectral domain for detecting trends in spectra having the same general signature shape. Traditional approaches that have relied on band ratios or other limited-band combinations are inadequate to differentiate minor spectral differences in the presence of significant environmental "noise."[13,22,23] For vegetation, the spectral trends defined by the mixing lines can be interpreted based on well-characterized biophysical processes, e.g., chlorosis and senescence. The presence of spectral changes in other biochemical constituents in the canopy (e.g. cellulose or lignin features) can be included to define the mixing lines in the spectral dimension. Thus, with this approach it may be possible to model relatively subtle changes in spectral properties due to changes in the biochemical constituents of the canopy.

The success of mixture models depends on differences among the reflectance spectra of the surface components and on the various types of illumination, which vary with season, time of day, and topography.[13,38,39] The effects of illumination are largely removed by the analysis,[39,40] therefore eliminating a major obstacle to comparisons between scenes. We have modeled the detectability of spectral changes currently associated with oxidant pollutants under two types of potentially confounding environmental conditions: variations in total canopy cover and with illumination sources. Simple differences in the relative proportions of canopy and soils in the imaged pixel will not produce red-edge shifts even where changes in the chlorophyll absorption band depth are observed.[23] Similarly, backscattered reflectance off surrounding surfaces (e.g., other vegetation or soils/rock types) will not produce the spectral shifts observed under current levels of forest injury.[13]

We have not yet addressed the question of spatial resolution for the detection of these spectral effects. Because other species within the mixed conifer forest are less sensitive to ozone than ponderosa and Jeffrey pines, there is little likelihood that other species within the community will show spectral changes on the order of those for the yellow pines. For maximizing spectral differences, one may anticipate that the spatial resolution should be about 20-25% the size of a typical tree crown in order to have the greatest probability of obtaining spectra of illuminated foliage by the spaceborne scanner. AVIRIS and HIRIS will have a spatial resolution of 20 m and 30 m, respectively, a scale greater than most tree crowns. One solution to this dilemma is to coregister the images with panchromatic image data of smaller pixel size.[41] The French Space Agency's satellite sensor, Systeme Probatiore d'Observation de la Terre (SPOT) has 8 m resolution, and NASA has a 5 m resolution instrument planned for the EOS Platform which could be used to improve spatial resolution. Image scale issues are currently under investigation and a variety of promising techniques, such as semivariogram analyses, have been proposed.[42] Several promising techniques have been developed for estimating stand geometry and structural properties.[43-45] A stratified processing of the image data by sequentially using techniques to define the vegetation structure before applying stress detection algorithms may lead to improved detection of early stages of forest decline.

CONCLUSIONS

At this stage of oxidant injury in the yellow pine forests in the southern Sierra Nevada, considerable variation in foliage condition exists among individual trees within and between stands. The principal forest canopy changes associated with oxidant foliar injury are a slight canopy chlorosis, differences in mean needle retention, and excessive crown thinning. Our data support the conclusion that such effects, though slight to moderate in severity, are widespread throughout much of the western slopes of the southern Sierra Nevada.

Forest decline symptoms produce changes in canopy spectral properties that may be detectable with high spectral and spatial resolution. Field techniques using portable spectrometers for measuring spectral changes on foliage are now available and could be used to improve quantitative estimates of foliage condition. Standardized procedures could be developed using currently available technology for temporal and spatial comparisons and could replace current visual assessment methods subject to observer bias.

Satellite and aircraft imagery, with its synoptic sampling, provides a means of determining both spatial patterns and temporal changes provided techniques can be developed for detecting early stages of forest decline symptoms. Detecting current levels of oxidant injury in the southern Sierra Nevada from spaceborne scanners will require both high spatial and spectra resolution. Full use of the potential offered by the new high spectral scanners requires development of new methods for analyzing both spectral and spatial variability. Mixing models were discussed for defining spectral trends associated with foliage condition in multidimensional spectral data, and several techniques for spatial analyses.

ACKNOWLEDGMENTS

This research has been supported by the Environmental Protection Agency under grant #R-814274-01-0, the National Council of the Paper Industry for Air and Stream Improvement under grant # 2070, and through the California Space Institute grants #CS-18-87 and CS-37-88. Although partially funded by the EPA, this research does not necessarily reflect the views of the agency and no official endorsement should be inferred. We wish to thank William Caldwell, Peter Collins, James Doyle, Jennifer Fitzgerald, Yaffa Grossman, Brian Pederson, Douglas Ryden, Curtis Smith and Erik Ustin for assistance with the field measurements and to Curtis Smith for data entry and computer assistance.

REFERENCES

1. S.B. McLaughlin, "Effects of air pollution on forests: A critical review," *JAPCA* 35:512 (1985).

2. A. Wellburn, *Air Pollution and Acid Rain—The Biological Impact*, J. Wiley and Sons, New York, 1988.

3. J. Pronos and D.R. Vogler, "Assessment of ozone injury to pines in the southern Sierra Nevada, 1979/1980," *USDA Pacific Southwest Region, Forest Pest Management Report* No. 81-20, 1981.

4. J. Allison, "Evaluation of ozone injury on the Stanislaus National Forest," *USDA Pacific Southwest Region, Forest Pest Management Report* No.82-07, 1982.

5. J. Allison, "Evaluation of ozone injury to pines on the Eldorado National Forest," *USDA Pacific Southwest Region, Forest Pest Management Report* No. 84-16, 1984.

6. J. Allison, "Evaluation of ozone injury to pines on the Tahoe National Forest," *USDA Pacific Southwest Region, Forest Pest Management Report* No. 84-30, 1984.

7. D.M. Duriscoe, "Evaluation of ozone injury to Ponderosa and Jeffrey pines in Yosemite National Park, California. 1985 Survey Results," *USDI National Park Service.* Final Report, Air Quality Division, 1987.

8. D.M. Duriscoe, "Cruise survey of western yellow pine (*Pinus ponderosa* and *Pinus Jeffreyi*) for oxidant air pollution injury in Yosemite National Park, California, Draft Final Report," 1989.

9. R.D. Jackson, "Remote sensing of biotic and abiotic plant stress," *Ann. Rev. Phytopathol.* 24:265 (1986).

10. W.E. Westman and C.V. Price, "Detecting air pollution stress in southern California vegetation using Landsat Thematic Mapper band data," *Photogramm. Engin. and Remote Sens.* 54:1305 (1988).

11. B. Curtiss and S.L. Ustin, "The remote detection of early stages of air pollution injury in coniferous forests using imaging spectrometry," *Int. J. Remote Sens.* (in press).

12. P.A. Muir and T.V. Armentano, "Evaluating oxidant injury to foliage of *Pinus ponderosa*: A comparison of methods," *Can. J. For. Res.* 18:498 (1988).

13. B. Curtiss and S.L. Ustin, "The characterization of sources of illumination in a ponderosa pine (*Pinus ponderosa*) forest community using the portable instantaneous display and analysis Spectrometer," *SPIE Tech. Symp. on Optics, Electro-Optics, and Sensors.* Orlando, FL ,April 4-8, 1988. (in press).

14. P.M. Rich, "Video image analysis of hemispherical canopy photography," *First Workshop on Videography* Am. Soc. Photogramm. and Remote Sens., 1988 (in press).

15. K.W. Stolte and J.P. Bennett, "Standardized procedures for establishing permanent pine plots and evaluating pollution injury on pines," unpublished file report, USDI National Park Service, Air Quality Division, P.O. Box 25287 Denver, CO 80255, August, 1985.

16. J.M. Anderson and N.K. Boardman, "Studies on the greening of dark grown beans," *Aust. J. Biol. Science* 17:93 (1964).

17. A.F.H. Goetz, "The portable instantaneous display and analysis spectrometer (PIDAS)," *Proc. 3rd. Airborne Imaging Spectrometer Data Analysis Workshop*, June 2-4, 1987 Jet Propulsion Laboratory, JPL Publ. 87-30:8 (1987).

18. W.P. Robarge and I. Fernandez, "Quality assurance methods manual for laboratory analytical techniques," *U.S. EPA and USDA Forest Service Forest Response Program.* Environmental Research Laboratory, Corvallis, OR, 1986.

19. S.M. Zedaker and N.S. Nicholas, "Quality assurance methods manual for site classification and field measurements," *U.S. EPA and USDA Forest Service Forest Response Program.* Environmental Research Laboratory, Corvallis, OR, 1986.

20. H.W. Gausman, D.E. Escobar, and R.R. Rodriguez, "Discriminating among plant nutrient deficiencies with reflectance measurements," Proc. 4th. Biennial Workshop on Aerial Color Photography, *Am. Soc. Photogramm.* 39:13 (1973).

21. M.L. Tsay, D.H. Gjerstad, and G.R. Glover, "Tree leaf reflectance:a promising technique to rapidly determine nitrogen and chlorophyll content," *Can. J. For. Res.* 12:788 (1982).

22. S.L. Ustin, B. Curtiss, S. Martens, and V.C. Vanderbilt, "Use of high spectral resolution sensors to detect air pollution injury in conifer forests," in *Remote Sensing Applications for Acid Deposition*, L.K. Fenstermaker, Ed., U.S. EPA, Las Vegas, NV 89193-3478, 1988, p. 72.

23. S.L. Ustin and B. Curtiss, "Spectral characteristics of ozone treated conifers," *Environ. and Exp. Bot.* (in press).

24. D.L. Peterson, J.D. Aber, P.A. Matson, D.H. Card, N. Swanberg, C. Wessman, and M. Spanner, "Remote sensing of forest canopy and leaf biochemical contents," *Remote Sens. Environ.* 24:85 (1987).

25. C.A. Wessman, J.D. Aber, and D.L. Peterson, "Estimating key forest ecosystem parameters through remote sensing," *Proc. IGARSS '87* 2:1189 (1987).

26. C.A. Wessman, J.D. Aber, D.L. Peterson, and J.M. Melillo, "Remote sensing of canopy chemistry and nitrogen cycling in temperate forest ecosystems," *Nature* 335:154 (1988).

27. M.A. Spanner, D.L. Peterson, W. Acevedo, and P. Matson, "High resolution spectrometry of leaf and canopy chemistry for biogeochemical cycling," *Proc. Airborne Imaging Spectrometer Data Analysis Workshop.* April 8-10, 1985, Jet Propulsion Laboratory, JPL Publ. 85-41:92, 1985.

28. C.D. Elvidge, "Visible and infrared reflectance characteristics of dry plant materials," *Int. J. Remote Sens.* 26:265 (1988).

29. D. Vogler, "Ozone monitoring in the southern Sierra Nevada, 1976-1981," *USDA Pacific Southwest Region, Forest Pest Management Report* No. 82-17, 1982.

30. V.C. Runeckles and P.M. Rosen, "Effects of ambient ozone pretreatment on transpiration and susceptibility to ozone injury," *Can. J. Bot.* 55:193 (1977).

31. W.E. Westman and C.V. Price, "Spectral changes in conifers subjected to air pollution and water stress: Experimental Studies," *IEEE Trans. Geosci. and Remote Sens.* GE-26:20 (1988).

32. S.H. Chang and W. Collins, "Confirmation of the airborne biogeophysical mineral exploration technique using laboratory methods," *Econ. Geol.* 78:723 (1982).

33. W. Collins, "Remote sensing of crop type and maturity," *Photogramm. Eng. Remote Sens.* 44:43 (1979).

34. B.N. Rock, T. Hoshizaki and J.R. Miller, "Comparison of *in situ* and airborne spectral measurements of the blue shift associated with forest decline," *Remote Sens. Environ.* 24:109 (1988).

35. J.S. Brown, "Forms of chlorophyll in vivo," *Ann. Rev. Plant Physiol.* 23:73 (1972).

36. W. Junge, "Physical aspects of light harvesting, electron transport and electrochemical potential generation in photosynthesis of green plants," in *Encyclopedia of Plant Physiology*, A. Trebst and M. Avron, Eds., Photosynthesis I. NS. Photosynthetic Electron Transport and Photophosphorylation, 1977, p. 69.

37. W.W. Thomson, W.M. Dugger, and R.L. Palmer, "Effects of ozone on the fine structure of the palisade parenchyma cells of bean leaves," *Can. J. Bot.* 44:1677 (1966).

38. J.B. Adams, M.O. Smith, and P.E. Johnson, "Spectral mixture modeling: a new analysis of rock and soil types at the Viking Lander I site," *J. Geophys. Res.* 91:8098 (1986).

39. S.L. Ustin, J.B. Adams, C.D. Elvidge, M. Rejmanek, B.N. Rock, M.O. Smith, R.W. Thomas, and R.A. Woodward, "Thematic Mapper studies of semiarid shrub communities," *BioSci.* 36:446 (1986).

40. M.O. Smith, S.L. Ustin, J.B. Adams, and A.R. Gillespie, "A regional measure of sparse vegetation cover from multispectral images," (submitted 1989).

41. L.M. Wood, R.A. Schowengerdt, and D.J. Meyer, "Restoration for sampled imaging systems," Applications of Digital Processing IX, *Proc. SPIE Int. Symp. on Optical and Optoelectronic Applied Sciences and Engineering*, , 697:333, San Diego, CA, 1986.

42. P. Curran, "The semivariogram in remote sensing: An introduction," *Remote Sens. Environ.* 24:493 (1988).

43. X. Li and A.H. Strahler, "Geometric-optical modeling of a conifer forest canopy," *Trans. Geosci. and Remote Sens.* GE-23:705 (1985).

44. X. Li and A.H. Strahler, "Geometric-optical bidirectional reflectance modeling of a conifer forest canopy," *Trans. Geosci. and Remote Sens.* GE-24:906 (1986).

45. X. Li and A.H. Strahler, "Modeling the gap probability of a discontinuous vegetation canopy," *Trans. Geosci. and Remote Sens.* 26:161 (1988).

Table I. Location of study sites for spectral measurements.

Site Number and Descriptive name	township	range	section	latitude	longitude
1. Deer Ridge Sequoia NP	T16S	R29E		36°32'44"	118°46'40"
2. Eshom Creek	T14S	R28E	S20	36°41'45"	118°57'00"
3. Big Stump Ridge	T28E	T14S	S18	36°42'30"	118°52'30"
4. Verplank Ridge	TS	R28E	S19	36°47'00"	118°58'21"
5. Bacon Meadow	T14S	R28E	S3	36°43'55"	118°55'25"
6. Montecito-Sequoia	T14S	R29E	S19-20	36°41'56"	118°51'20"
7. Big Meadow	T14S	R29E	S18	36°42'29"	118°52'05"
8. Bass Lake	T6S-T7S	R22E	S32-S5	37°21'42"	119°34'30"
9. Lewis River	T5S	R21E	S,	37°25'12"	119°37'36"
10. Jerseydale Station	T4S	R19E	S35	37°33'06"	119°49'36"
11. Worman Road	T6S	R21E	S7	37°25'30"	119°42'36"
12. Harris Road	T5S	R21E	S18	37°29'54"	119°43'30"
13. Peterson Mill Road	T10S	R25E	S24	37°02'48"	119°18'18"
14. Soaproot Saddle	T10S	R25E	S29	37°06'00"	119°18'18"
15. Shaver Lake	T10S	R25E	S5	37°06'36"	119°16'30"

Table II. Frequency distribution of age of oldest whorl on ponderosa pine branches from 15 sites. Values are number of branches having oldest whorl in the age class. Whorl ages are numbered from current year = 1. Total number of needle whorls = 1189.

	Whorl Age, (Year of Initiation)								
	1987	1986	1985	1984	1983	1982	1981	1980	1979
Site #	1	2	3	4	5	6	7	8	9
1	1	7	5	5	2	0	0	0	0
2	0	2	6	7	4	0	1	0	0
3	0	0	9	5	5	1	0	0	0
4	0	0	3	6	5	6	0	0	0
5	0	0	15	5	0	0	0	0	0
6	0	0	0	0	5	7	6	2	0
7	0	1	2	2	10	3	2	0	0
8	0	2	11	7	0	0	0	0	0
9	0	2	6	11	1	0	0	0	0
10	0	6	14	0	0	0	0	0	0
11	0	8	9	3	0	0	0	0	0
12	0	0	8	11	0	0	0	0	0
13	0	2	8	10	0	0	0	0	0
14	0	1	9	9	1	0	0	0	0
15	0	3	4	7	5	0	0	0	0
Number of sites having oldest needle age in each age class	0	0	1	5	4	2	2	1	0

Table III. Presence of chlorotic mottle on ponderosa pine needle whorls.

Site	% branches with mottle	youngest age affected	
		whorl #	mean age
1	100	1	1.3
2	100	1	1.3
3	95	1	1.5
4	85	1	3.
5	70	2	2.6
6	25	5	6.0
7	60	2	3.9
8	75	1	2.4
9	40	2	2.6
10	50	2	2.6
11	40	2	2.6
12	70	1	2.6
13	65	2	2.6
14	60	2	2.4
15	85	2	2.6

Table IV. Mean (n = 20) percentage of canopy closure from 14 sites in ponderosa pine forests as estimated from fisheye photographs.

Site #	Percent canopy cover 1-sky cover (SD)
1	0.25 (0.05)
2	0.33 (0.05)
3	0.25 (0.06)
4	0.41 (0.15)
5	0.54 (0.07)
6	0.57 (0.11)
7	0.49 (0.08)
8	0.45 (0.08)
9	0.22 (0.05)
10	0.31 (0.04)
11	0.31 (0.11)
12	0.25 (0.06)
13	0.30 (0.06)
14	0.39 (0.11)

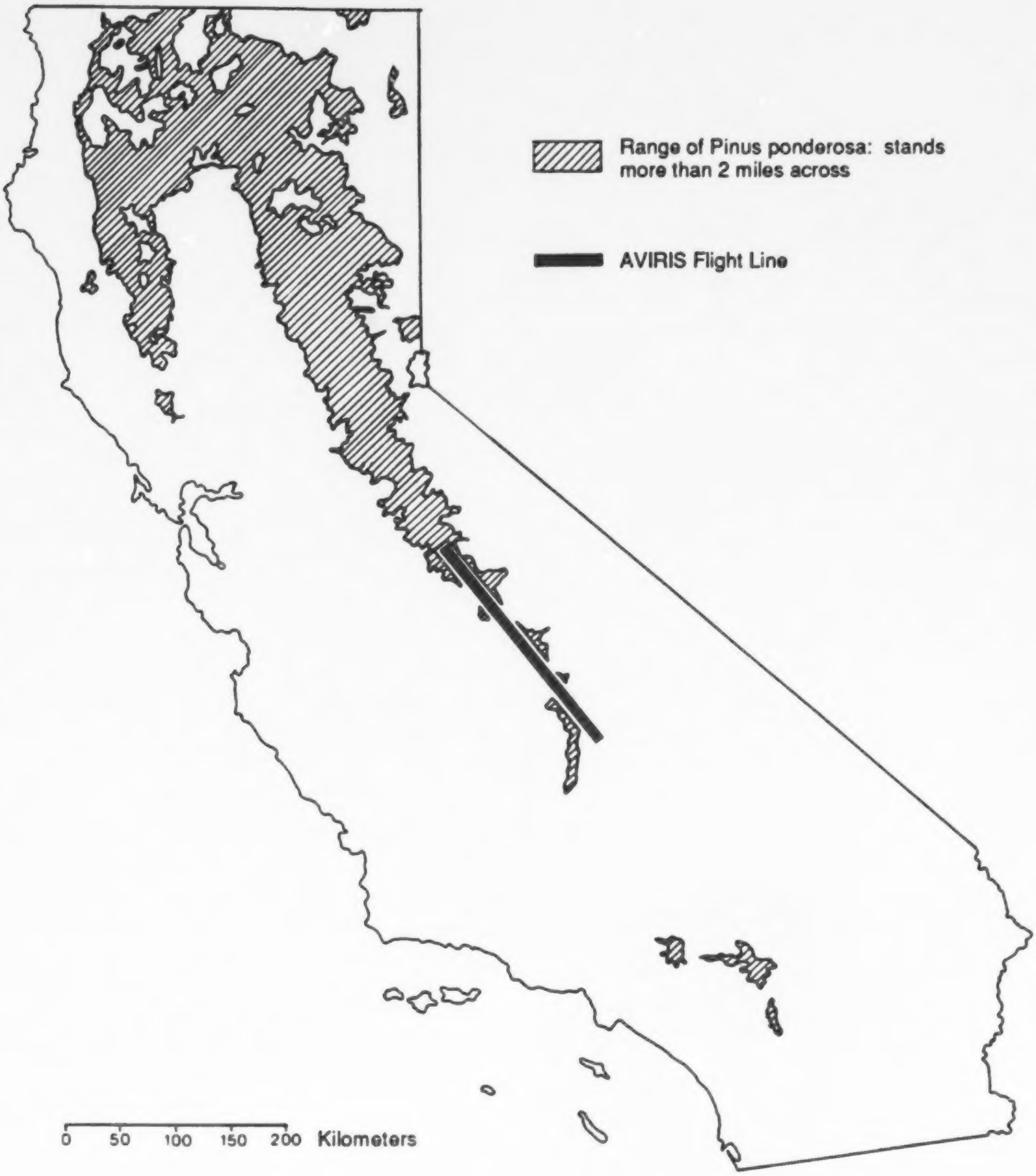
▨ Range of Pinus ponderosa: stands more than 2 miles across
AVIRIS Flight Line
0 50 100 150 200 Kilometers

Figure 1. Map of Study Area.

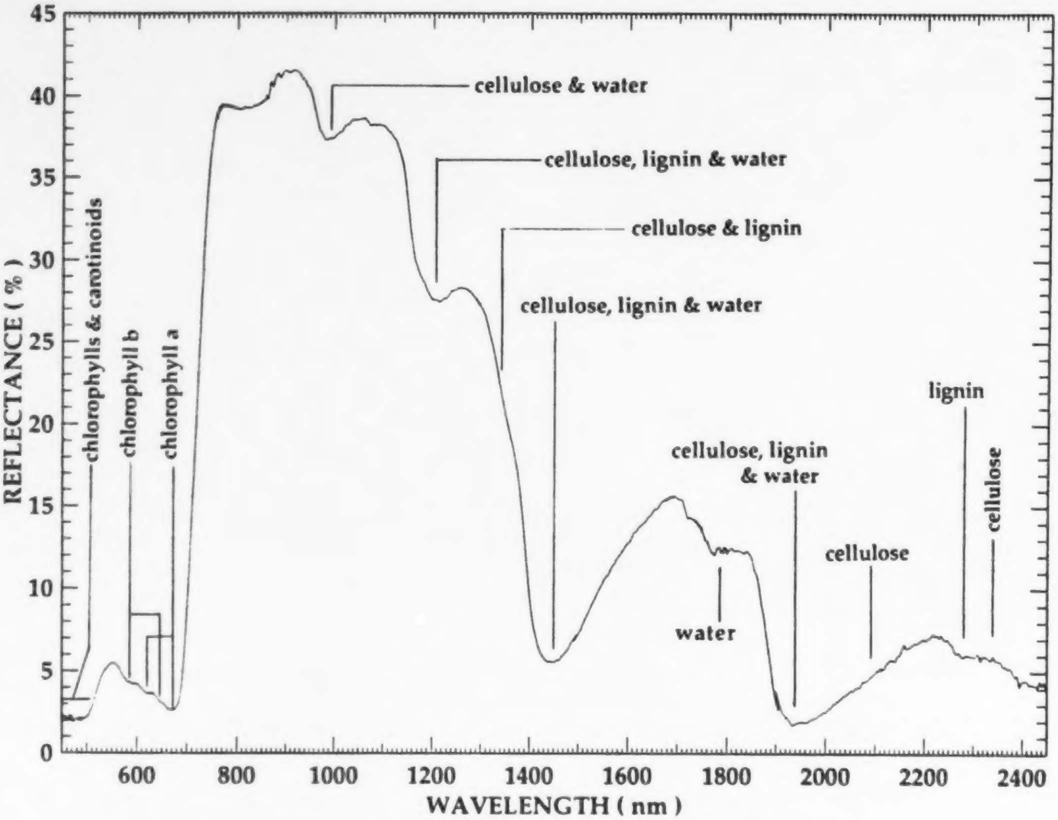

Figure 2. Typical reflectance spectrum of green vegetation in the visible (400-700 nm), near-infrared (700-1400 nm), and shortwave-infrared (1400-2400 nm). This example is of ponderosa pine foliage from 2-year-old seedlings grown under controlled conditions in open-topped chambers. Wavelength locations of major absorption features are indicated.

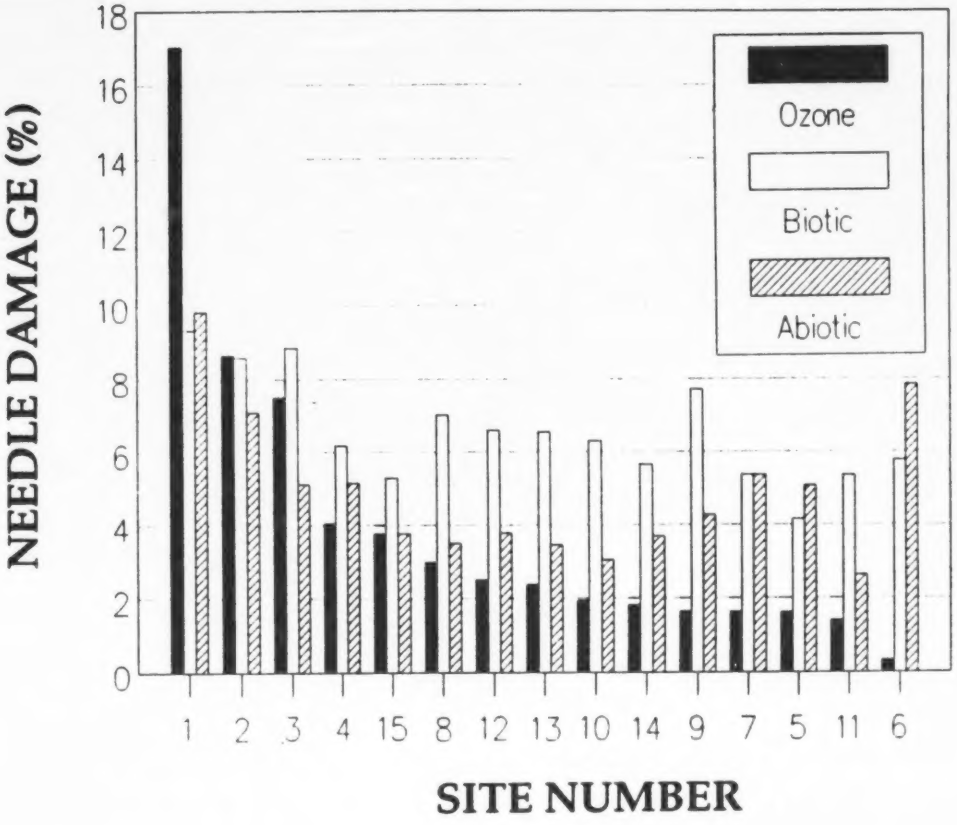

Figure 3. Mean foliar injury rankings for oxidant (solid bars), biotic (open bars), and abiotic (hatched bars), foliar damage symptoms from 15 sites in the southern Sierra Nevada. Measurements represent the mean of all whorls present on 20 branches per site. Sites are ranked by percentage needle area exhibiting symptoms of ozone damage.

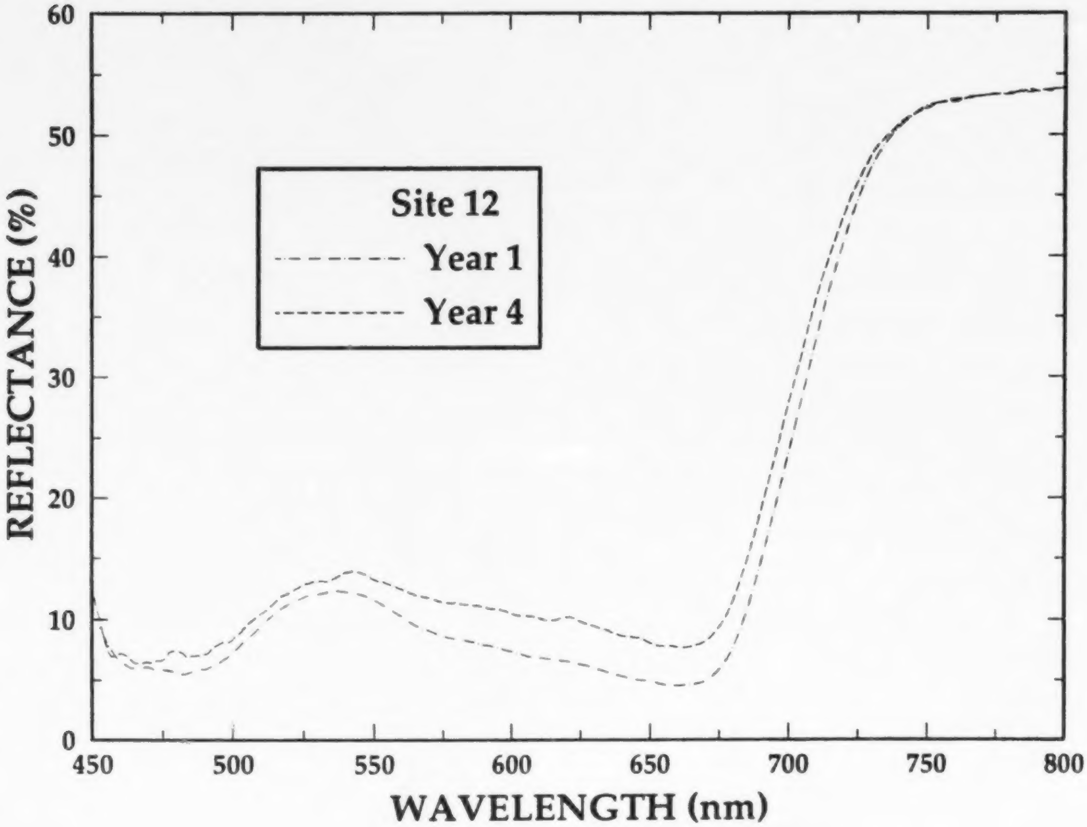

Figure 4. Differences in mean reflectance spectra from first- and fourth-year needle whorls measured at Site 12. Differences are due to developmental/age-dependent factors and cumulative oxidant injury. Sites with less oxidant injury do not exhibit age dependent differences of this magnitude.

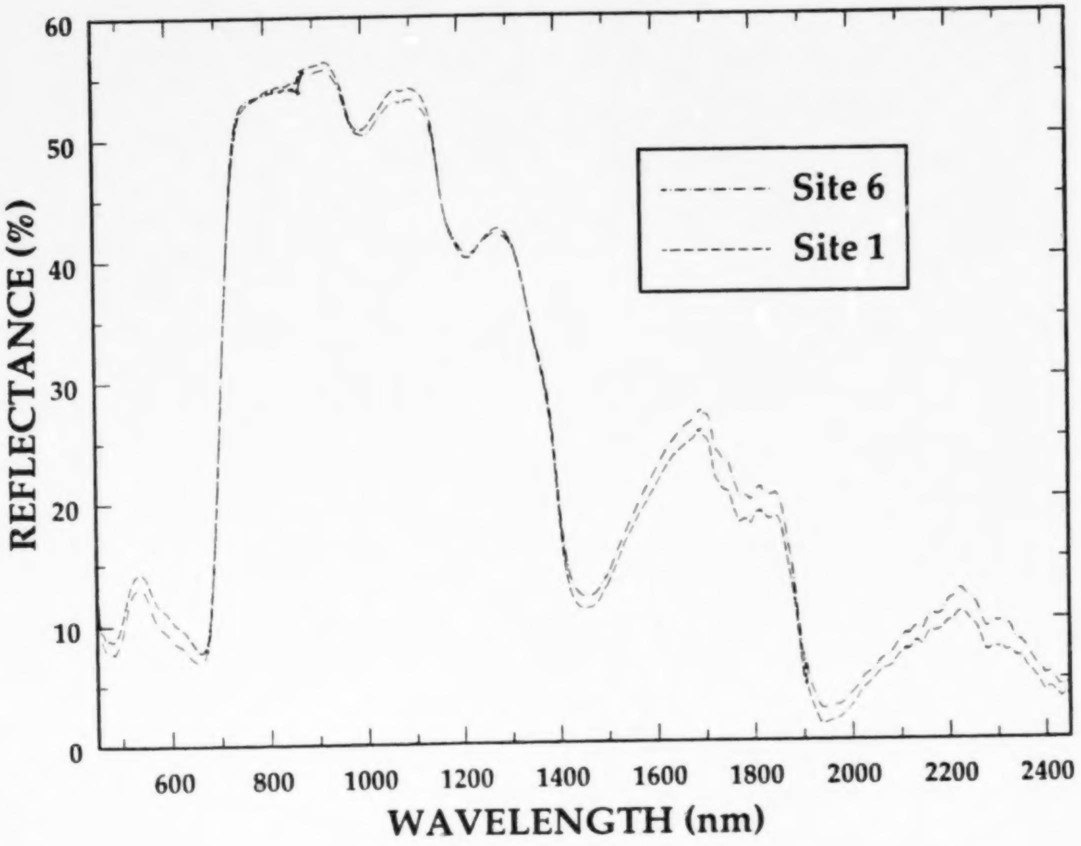

Figure 5. Mean reflectance spectra for all whorls from sites having the greatest difference in visual ozone injury ranking. Site 1 (-.-) has the highest injury ranking, and Site 6 (- - -) the lowest rank. Differences are primarily in the visible and near-infrared with little change in the shortwave infrared region. Note differences between sites in the lignin/nitrogen feature around 1350 nm.

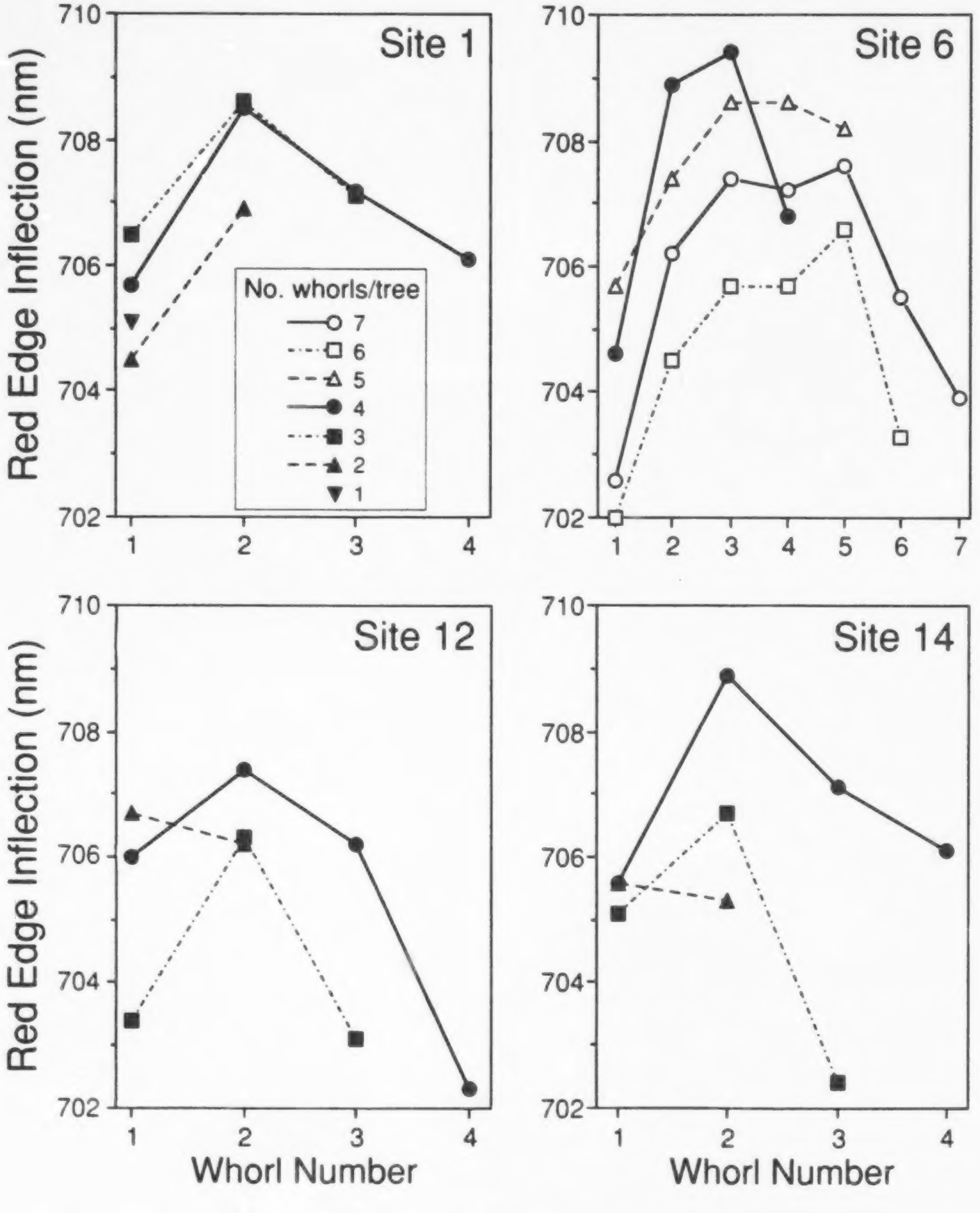

Figure 6. Mean reflectance spectra for the 450–800 nm region shown in Figure 4. Differences between sites in the chlorophyll absorptance band are easier to examine when the scale is enlarged.

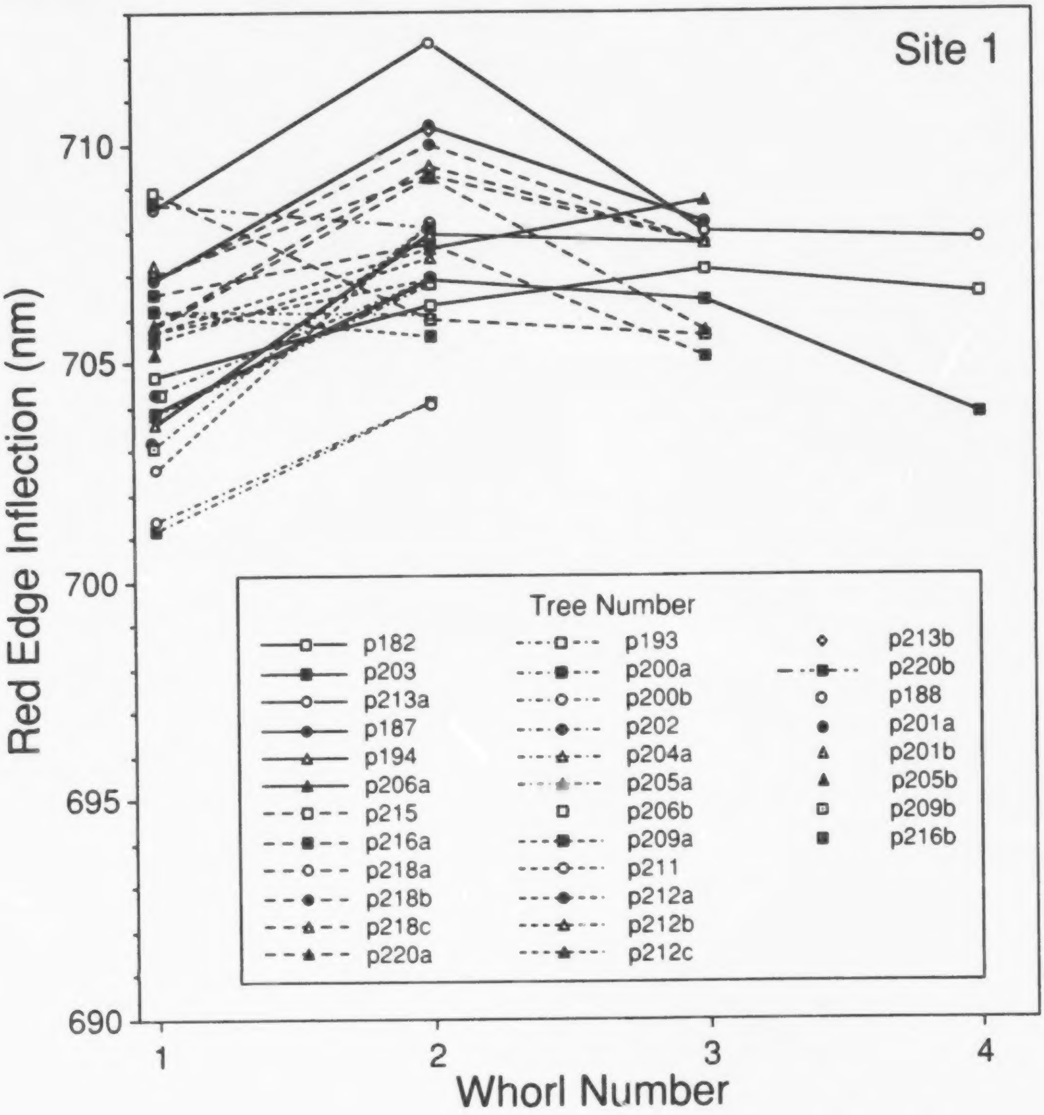

Figure 7a. Red-edge inflection point of tree foliage measured at four sites differing in ozone rankings. Each curve represents the REI point for foliage of different age on the branch; curves vary with years of needle retention. Branches were collected from different trees at the site: Site 1 (a), Site 6 (b), Site 12 (c), Site 14 (d). Note differences in axis scales.

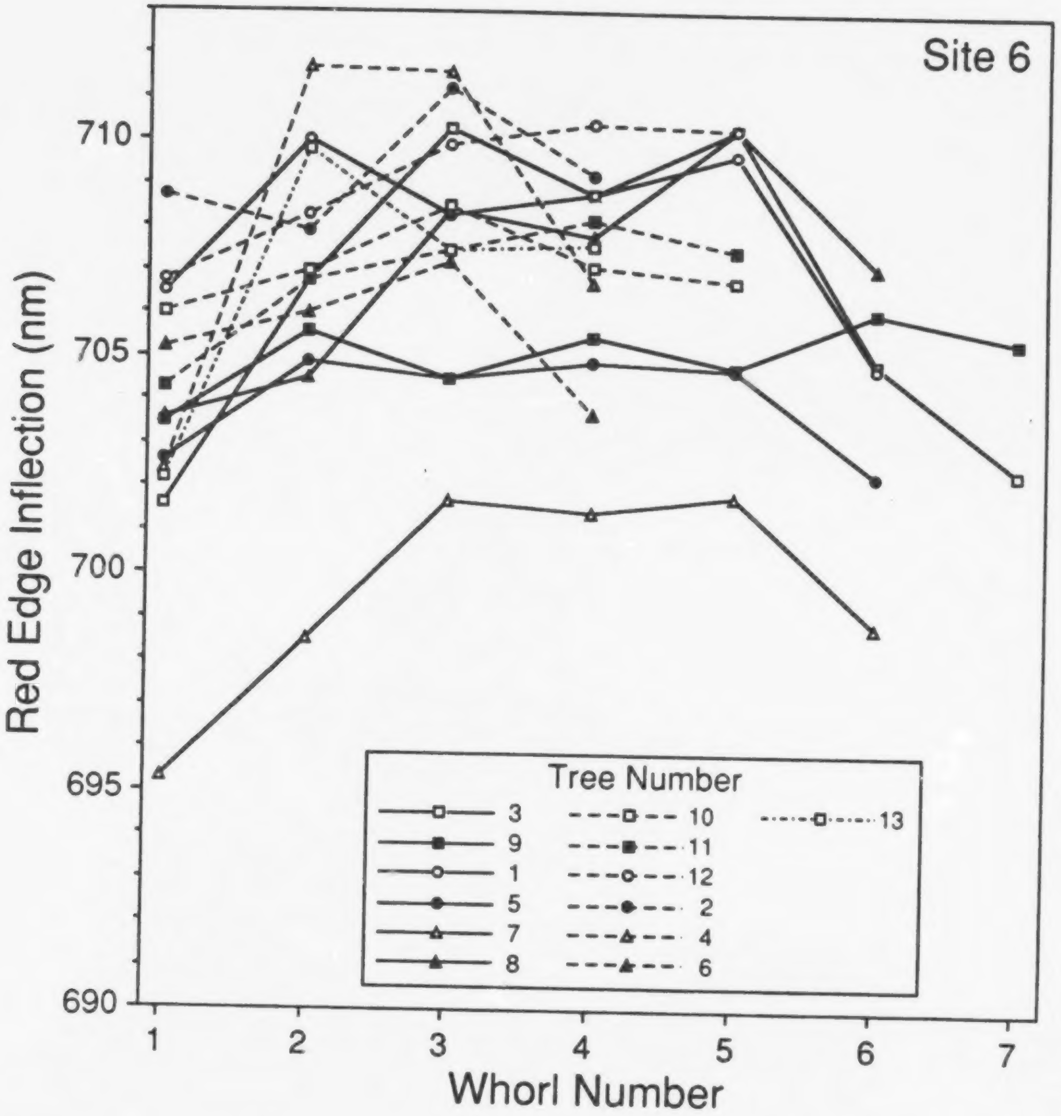

Figure 7b. Red-edge inflection point of tree foliage measured at four sites differing in ozone rankings. Each curve represents the REI point for foliage of different age on the branch; curves vary with years of needle retention. Branches were collected from different trees at the site: Site 1 (a), Site 6 (b), Site 12 (c), Site 14 (d). Note differences in axis scales.

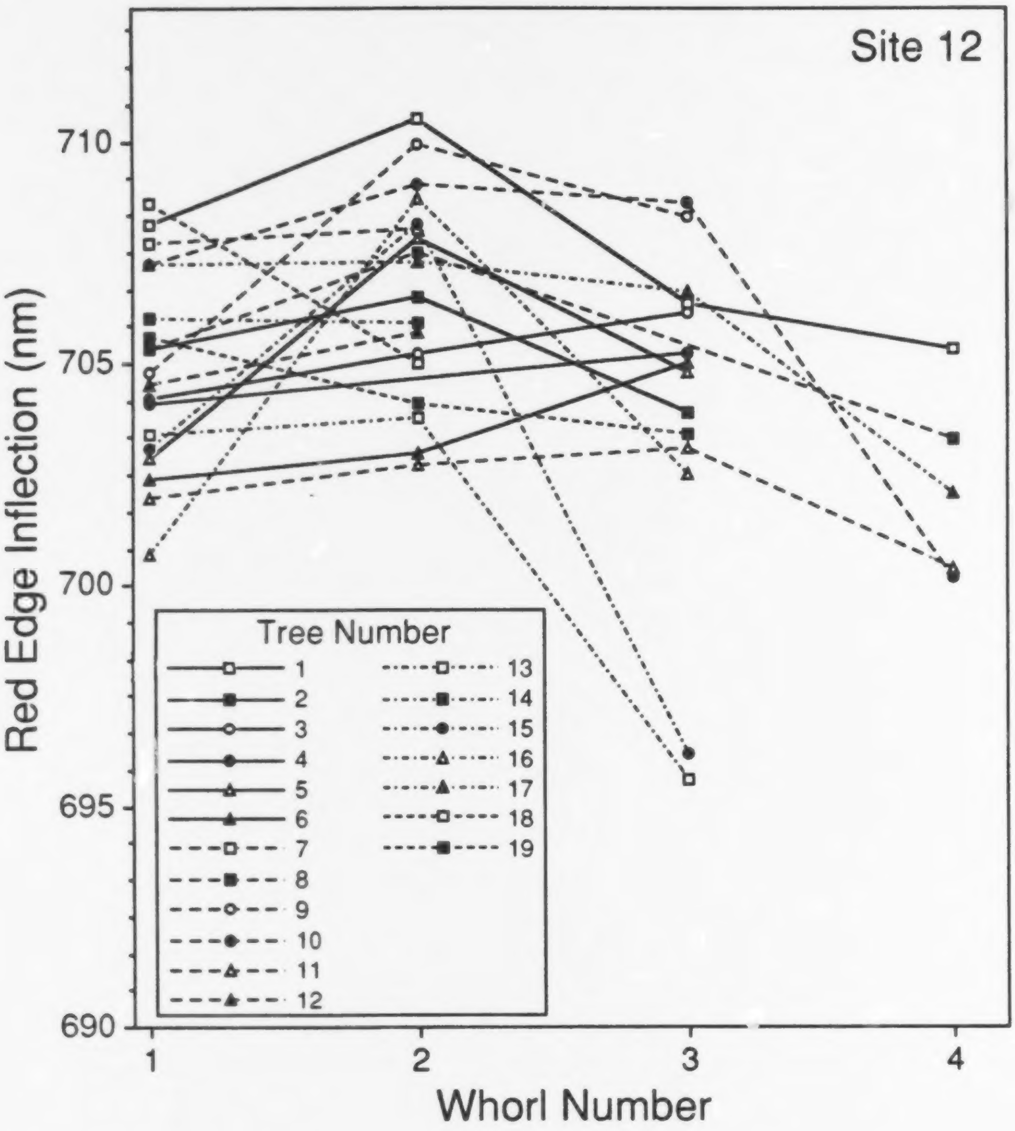

Figure 7c. Red-edge inflection point of tree foliage measured at four sites differing in ozone rankings. Each curve represents the REI point for foliage of different age on the branch; curves vary with years of needle retention. Branches were collected from different trees at the site: Site 1 (a), Site 6 (b), Site 12 (c), Site 14 (d). Note differences in axis scales.

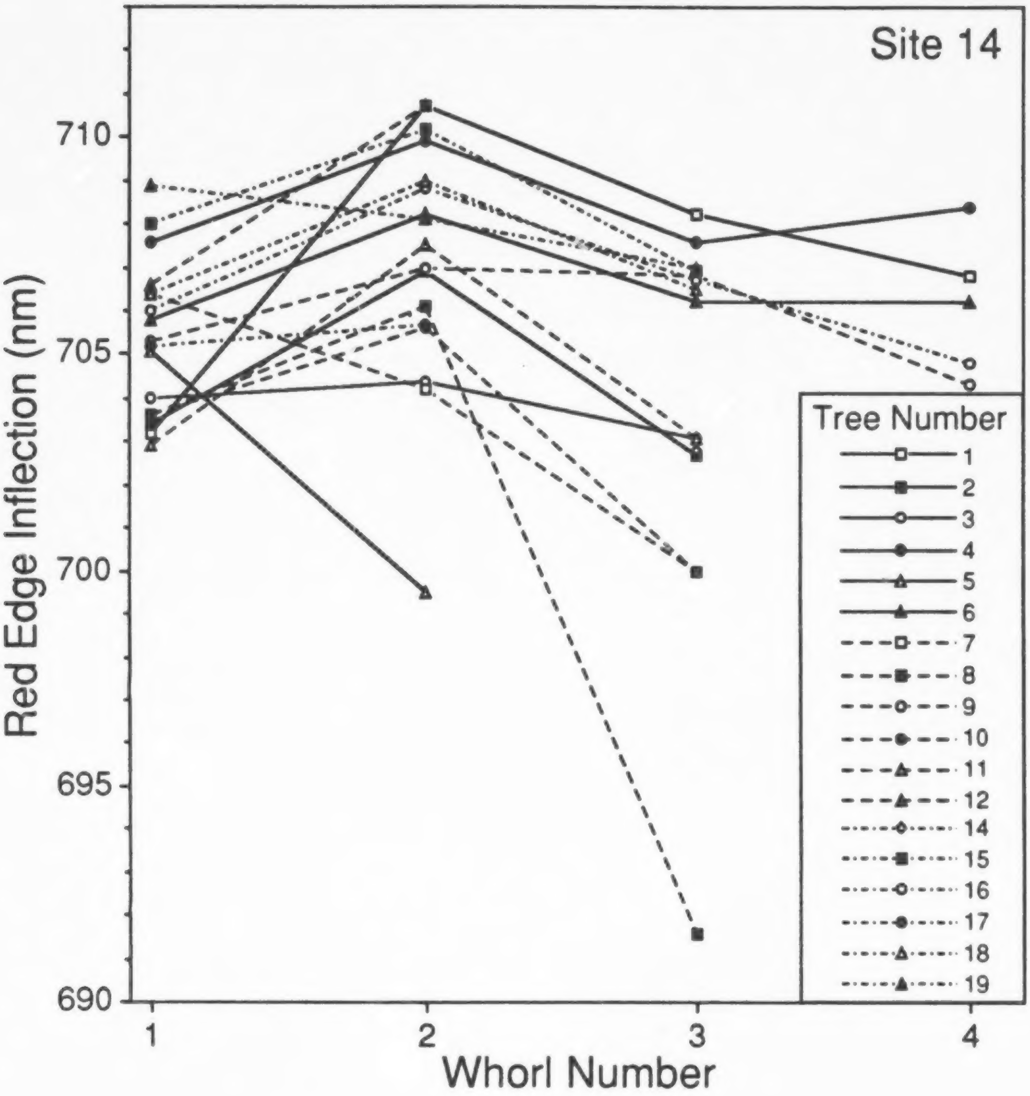

Figure 7d. Red-edge inflection point of tree foliage measured at four sites differing in ozone rankings. Each curve represents the REI point for foliage of different age on the branch; curves vary with years of needle retention. Branches were collected from different trees at the site: Site 1 (a), Site 6 (b), Site 12 (c), Site 14 (d). Note differences in axis scales.

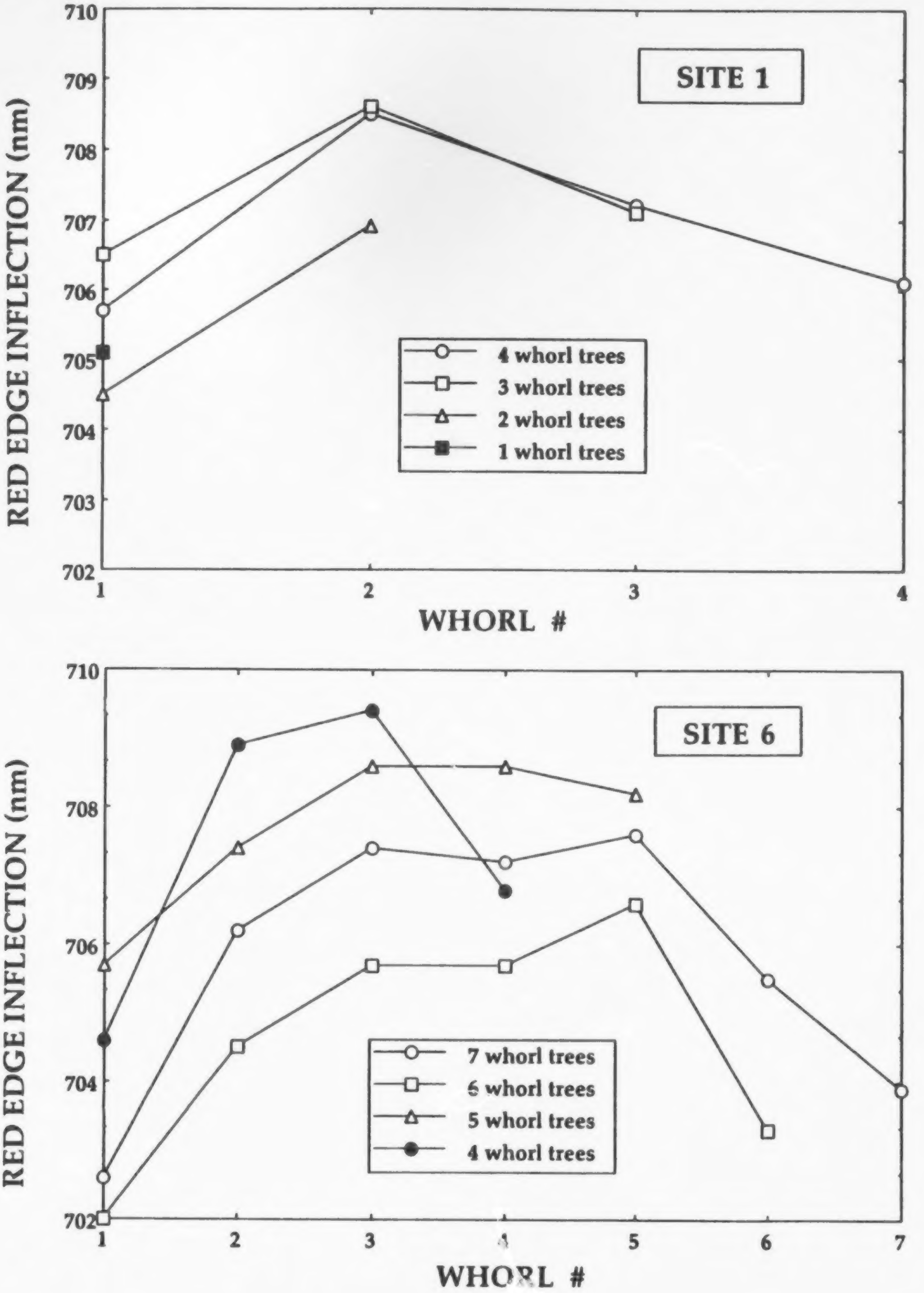

Figures 8a,b. Mean red-edge reflectance curves grouped by number of years of needle retention on branch. Branches having the needle classes of the same age have similar red-edge curves; Site 1 (a), Site 6 (b), Site 12 (c), Site 14 (d).

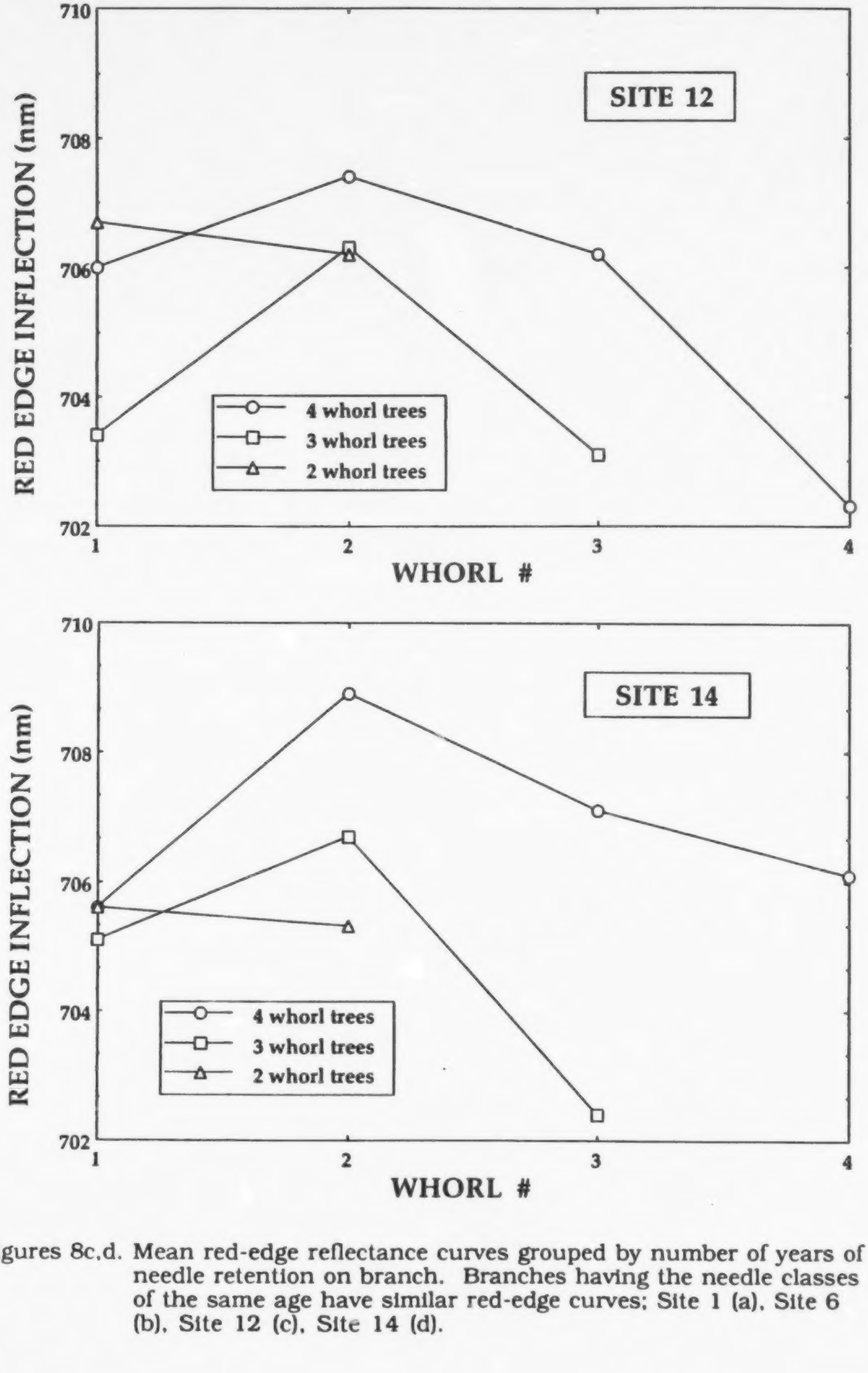

Figures 8c,d. Mean red-edge reflectance curves grouped by number of years of needle retention on branch. Branches having the needle classes of the same age have similar red-edge curves; Site 1 (a), Site 6 (b), Site 12 (c), Site 14 (d).

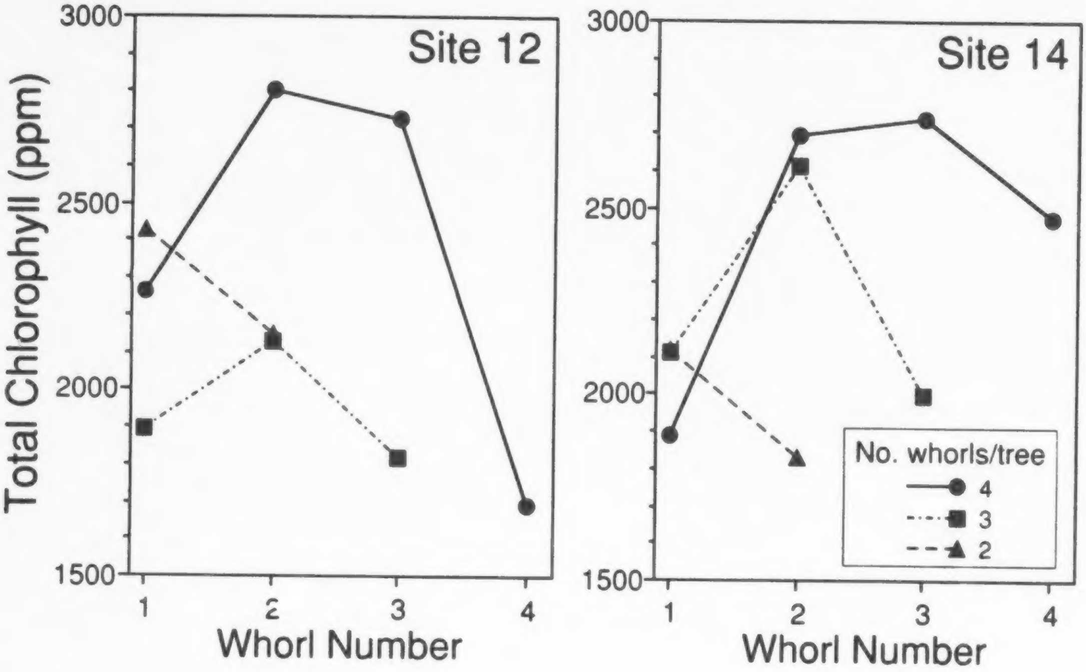

Figures 9a,b. Mean total chlorophyll (A+B) content (μg chlorophyll/g dry weight) of needle whorls from Sites 12 and 14. Curves represent branches having needle classes of the same age.

Use of Quality Control Procedures for Assessing Variation in Measurements of Forest Canopy Condition

Steven P. Cline, William G. Burkman, and Chris D. Geron

NSI Technology Services Corporation
U.S. EPA Environmental Research Laboratory
200 SW 35th Street
Corvallis, OR 97333

INTRODUCTION

Experimental results from the Forest Response Program (FRP),[1] a part of the National Acidic Precipitation Assessment Program (NAPAP), may be used to formulate environmental policy. Environmental policy decisions can be made with more confidence when the uncertainty associated with experimental data is known and is relatively low. Measurement variation is one component of the total uncertainty of experimental results. One goal of the Quality Assurance (QA) Project of the FRP is to document measurement variation associated with experimental data sets.

There are several reasons to document and control measurement variation. First, actual measurement variation has not been quantified for many of the biological variables used to assess the effects of air pollution on forests. This situation is especially common for field measurements. Second, some variation due to the measurement process is inevitable, and it may be relatively large for a difficult, inappropriate, or poorly defined or executed methodology. For example, observer variation composed 19-32% of the total variation associated with visual assessment of ozone-induced foliar injury of different crop species.[2] Third, many components of measurement variation are controllable through quality control (QC) procedures such as calibration, analysis of reference materials, and use of defined operating procedures and control charts.[3] These procedures appear particularly appropriate for field measurements because they provide a means of reducing one potentially confounding source of variation in a setting where variation is normally uncontrolled and large. In addition, comparability studies can be designed and implemented to facilitate the selection of the most appropriate measurement method in relation to the study goals. For example, for visual assessment of ozone-induced foliar injury to ponderosa pine (*Pinus ponderosa* Dougl. ex Laws.), a "hands-on" method was recommended over "remote" methods (e.g., binoculars) when accurate estimation of tree injury was required.[4] Finally, the reduction of measurement variation is usually cost effective because the amount of useable data increases; however, the cost of reducing measurement variation should always be evaluated. In most cases it is useful to ask "How much will it cost to increase the quality of data, and is this cost justified?"

The two primary purposes of this paper are to present estimates of measurement variation for some forest canopy and crown characteristics, and to discuss the use of QA procedures and QC data for reducing measurement variation. Examples from two FRP projects are used.

EXPERIMENTAL METHODS

Project 1

Background. A main objective of the project was to determine if oxidant-induced injury in ponderosa pine forests was detectable from remote sensing data. Aircraft-based spectral data were collected on a 145 km x 10 km flight line oriented north-south over the western slope of the southern Sierra Nevada of California and along an ozone concentration gradient.[5] Ground-based data were collected in 15 stands within the flight line to provide a ground-truth and a basis for relating remote spectral data to stand and canopy characteristics. Only stands dominated by ponderosa pine were selected. Other stand selection criteria included a range of exposures to ozone, easy access, and easy location on aircraft images.

A transect of 400 m was set out through the center of each of the 15 stands, usually in two 200-m parallel lines 50 m apart. Sampling points were established every 20 m along the transect, and each of the 20 points/stand were marked with a stake. This sampling design provided a spatial average for the site over an area of several pixels (one aircraft pixel = 20 m by 20 m).

Measurements. A black and white hemispherical (fisheye) photograph was taken at each of the twenty sampling points/stand using a camera equipped with a fisheye lens and mounted on a tripod. Before taking the photograph at each point, the camera was centered 25 cm above each point, aimed vertically, positioned so that north was at the top of each frame, and leveled. Exposures and f-stops were set manually and were not changed within a site. Photographs were taken when sun angles were low and were completed at a site in about 1 hr. After completing all photographs at a site, field replicates were collected by returning to the first sample point and rephotographing it using the same camera and settings. This was done at eight of the fifteen field sites. Within a site the photographer was always the same, but among sites they differed.

Exposed film was returned to the laboratory and analyzed in several steps. First black and white negatives were digitized using a video camera. As the camera scanned the negative, a brightness value was assigned to each pixel of a 500 x 500 grid. The brightness value assigned depended in part upon the f-stop setting on the scanning video camera. Generally the brightness levels of the negatives appeared either white, black, or gray. The white and black areas easily separated into either sky or canopy, but the gray area could be either. Consequently, the next processing step was to define a threshold brightness in order to assign each pixel in the gray area to either sky or canopy. Hemispherical photographs analyzed in two dimensions are distorted, having the pixels in the center of the photograph over-represented compared to the edge pixels. Distortion can be corrected by applying a standard algorithm to give the pixels equal weight. A summation of the pixels below and above the threshold brightness times their appropriate weighting factor produced the estimates of sky and canopy cover.

QC procedures. Variation due to single and combined steps of the measurement process were examined. First variation associated with the measurement of field replicates was examined (Type 1). Differences in field replicates estimated variation from all steps in the measurement process, including that from inaccuracies in relocating the original point for the replicate measurement, differences in leveling of the camera, changes in the lighting conditions since the original measurement, and changes in the laboratory analysis steps. In this analysis field replicate photographs were digitized with the video camera set at the same f-stop. Variation from the digitization step was examined next. This was the variation found when the same photographs were remeasured with the digitizing video camera set on the same f-stop (Type 2) and different f-stops (Type 3).

Finally the variation due to defining a threshold brightness and correcting for distortion was examined. Since both of these steps were performed late in the analytical process, they were examined within the context of earlier steps, including the collection of field replicates (Type 1), and remeasurement of the same photographs with the same f-stop (Type 2) and different f-stops (Type 3). Defining a threshold brightness to separate canopy and sky cover was a subjective decision and was suspected to be the largest source of variation in processing the photographs. In order to estimate the maximum magnitude of this variation, a single interpreter set the threshold brightness at the darkest sky brightness acceptable and at the lightest sky brightness acceptable for each photograph, remeasured them, and compared the difference. This produced a high and low estimate of sky cover, respectively, for each remeasured photograph. In addition the variation from weighting pixels of photographs was assessed by comparing high and low estimates of sky cover measured with and without applying the weighting algorithm. Deciding to use the weighting algorithm was also a subjective decision and its use was expected to have a large influence on cover estimates if the canopy was clumped rather than randomly distributed.

Project 2

Background. The major objective of this project was to determine the rate of change in sugar maple (*Acer saccharum* Marsh.) canopy conditions over a wide geographic area of the United States and Canada. The geographic area included the states of Maine, Massachusetts, Michigan, New Hampshire, New York, Vermont, and Wisconsin and the provinces included New Brunswick, Nova Scotia, Ontario, and Quebec. During the summer of 1988, 166 clusters of five plots, 20 m by 20 m each, were established through these states and provinces. One-half of the clusters were located in sugarbush stands tapped for maple sugar production and the other half in forest stands.

Measurements. The crown characteristics of 15,642 sugar maples were rated during a 6-week period beginning on July 15 and ending on August 31. Each sugar maple was rated for four crown characteristics: branch dieback, foliage transparency, foliage discoloration, and dwarfed foliage. To ensure that all sides of the crown were observed and to reduce individual bias, a crew of two rated each tree. Both observers agreed on the final rating for each of the four crown characteristics. Each crew used binoculars when necessary. Branch dieback, foliage transparency, foliage discoloration, and dwarfed foliage were rated in a 12-class system (Table I). The crown characteristics were defined as follows:

1. branch dieback—an estimate of the proportion of the tree crown area that contained branch dieback. Branch dieback was defined as the dieback that begins at the terminal end of a branch and progresses toward the main stem (as opposed to dieback that begins at the main stem and progresses outward to the branch tip).
2. foliage transparency—an area estimate of the proportion of skylight visible through the foliated portion of the tree crown.

3. foliage discoloration—an area estimate of the foliated portion of a tree crown that contains leaves some other color than green or a shade of green.

4. dwarfed foliage—an area estimate of the foliated portion of the crown that contains leaves that are obviously smaller (≤ half the size) than leaves on other nearby sugar maples.

QC procedures. During the same 6-week period, 843 sugar maples (5.4% of the total) were remeasured by various cooperator crews. Trees were remeasured on plots randomly selected within a cluster. The cluster that was selected generally was the closest geographic plot between various states and provinces. The length of time between measurements was determined by each cooperator. The remeasurements were classified into three different types: Type 1—the trees on a plot were remeasured by the same crew; Type 2—the trees were remeasured by a different crew from the same state or province; and Type 3—the trees were remeasured by a different crew from a different state or province. The project set an acceptable variation of ±1 class deviation for 90% of the observations within a plot.

Data Analysis

Several field measurements were made at each sampling site of project 1, but only the percent sky cover data were analyzed for this paper. Percent sky cover equalled 100% plant cover. The influence of each type of measurement procedure on percent sky cover estimates was analyzed separately. Graphical analysis consisted of plotting the difference between original and replicate measurements in relation to the ideal target (0% difference) and the stated project goal for precision (±10%). Measurement precision was estimated by the root mean square of the differences in replicate measurements.[3] were tested using Paired t-tests were used to test the null hypothesis of mean population differences equal 0.[6]

Several other field measurements were made on each sample plot of project 2, but only the discrete class ratings of sugar maple crown characteristics were analyzed for this paper. Data from forest and sugar bush stands were analyzed together, with deviations in class ratings based on the original rating. Analysis of the remeasurement data included comparisons of frequencies and graphical comparisons similar to those used in project 1. These types of analyses were employed because of an unbalanced study design, which was characterized by a mix of different remeasurement types with different stands, different elapsed times between remeasurements, and unequal sample sizes among remeasurement types and rating classes. In addition, and as in project 1, a similar null hypothesis was tested using paired t-tests, but the results of these statistical tests were interpreted cautiously and for consistency with the other analyses since underlying assumptions may have been violated due to the unbalanced design.

RESULTS

Project 1

Similar precision estimates (± 2.6–4.0%) were calculated for field replicates (Type 1) and for lab replicates digitized using either the same (Type 2) or different f-stops (Type 3) (Table II). Individual remeasurements usually differed <±10% from original measurements for each type of measurement procedure analyzed, but for Types 2 and 3 the remeasurements were consistently lower than the original measurements (Figure 1). This trend was consistent with the mean differences between remeasurements, which were significantly different than 0 for Types 2 and 3 (2.5 ± 3.9% and 3.1 ± 4.1%, respectively, P = 0.001), but not for Type 1.

A source of measurement variation of greater significance than precision was selecting a threshold brightness value, which controlled the high and low sky cover estimates. This analysis showed that for both unweighted and weighted estimates, the high and low means were significantly different for each of the three types of measurements analyzed (paired t-test, P = 0.01). Mean high sky cover estimates were 10–13% greater than low estimates (Table II). These results must be considered in their proper context, primarily that they represented a contrived "worst-case" example of the effects of using very different threshold values between remeasurements. In reality, all photographs in project 1 were analyzed by one interpreter, and it is unlikely that the same interpreter would introduce a large systematic difference between photographic remeasurements. The implications, however, remain important: the interpreter's decision about the threshold value is the crucial step in repeatability of the fisheye cover measurements. Consequently, when more than one interpreter is working on the same set of photographs, each must use consistent techniques to avoid introducing systematic differences. Systematic variation is also possible if personnel change year to year, as is likely in long-term monitoring projects. Such variation can be controlled by using one or more reference photographs to calibrate between observers, measurement sessions, and years. A plot of repeat measurements of these reference photographs on a control chart can be used to track performance and make necessary adjustments (instrument calibration, retraining) if drift becomes a problem.

Finally, weighting pixel values must be recognized as a potentially significant source of variation during processing of hemispherical photographs. This analysis showed that for both high and low sky cover estimates the unweighted and weighted means differed significantly for each of the three types of remeasurements analyzed (paired t-test, P = 0.01). Mean unweighted estimates were 4–5% greater than mean weighted estimates (Table II). This systematic difference can be reduced or eliminated if the same weighting procedure is used consistently to process all the photographs in a study, and if the data are reported as unweighted or weighted so that its comparability with data from different years or other studies can be evaluated.

Project 2

Same-crew remeasurements (Type 1) met the project goal for precision—±1 class deviation for 90% of the remeasurements within a plot—for foliage discoloration (96.6%), foliage transparency (95.2%), branch dieback (94.5%), but not for dwarfed foliage (88.3%) (Table III). Similarly, remeasurements by different crews from the same state/province (Type 2) met the precision goal for all variables, including dwarfed foliage. These results imply that if all measurements were made by the same crew or different crews from the same state/province, most rating changes of ±2 classes or greater would not be caused by measurement variation. In contrast, remeasurements made by crews from different states/provinces (Type 3) met the project precision goal of ±1 class for branch dieback (95.4%), but not for foliage discoloration (80.5%), foliage transparency (78.8%), and dwarfed foliage (73.5%). This result implies that if crews from different states/provinces make all the measurements, rating changes of ±2 classes (except branch dieback) could be caused by measurement variation. Furthermore, even rating changes of ±3 classes for dwarfed foliage and foliage discoloration could be caused by measurement variation, since the proportion of remeasurements within ±2 classes remained relatively low for these characteristics (82.1% and 81.5%, respectively).

Further graphical analysis of branch dieback and foliage transparency showed that the magnitude (i.e., the range) of remeasurement differences increased as the value of the original rating increased (Figures 2 and 3). A similar trend has been commonly found in analytical chemistry, where the absolute precision (i.e., the standard deviation) of replicate analyses increased with the concentration of the analyte.[7] This trend held for both variables and all remeasurement types, but the ranges were usually larger for foliage transparency than for branch dieback and for remeasurements made by different crews (Types 2 and 3) than for those made by the same crews (Type 1). For example, for Type 2 remeasurements of foliage transparency, the range of differences increased from 20 to 75% as original ratings increased from 0 to 30% (Figure 3b). In contrast, for Type 1 remeasurements of branch dieback the range of differences increased only from 0 to 20% as original ratings increased from 0 to 30% (Figure 2a). These results are consistent with the frequency tabulations in Table III.

In addition, the graphical analysis showed patterns of systematic difference between remeasurements, with remeasurements typically being greater than originals for low rating classes and but less than originals for higher rating classes. This pattern was most obvious for Type 3 remeasurements (Figures 2c and 3c), but was indicated to a lesser degree for the other remeasurement types and branch dieback. The cause of this systematic difference, which appeared to range from 5-10%, can not be determined exactly; however, one contributing factor could have been lack of "calibration" between the remeasurement crews. Another likely contributing factor was the unbalanced design, especially the different elapsed times among the remeasurement types. Elapsed times between measurements were ordered as follows: Type 3 (98% ≥ 7 days) > Type 2 (55% ≤ 6 days) > Type 1 (90% ≤ 1 day). The longer the time between measurements the greater the potential for larger changes in canopy condition and in observer perceptions or expertise. For example, a small positive correlation between remeasurement variation and elapsed time between measurements of foliage transparency was found for remeasurement Type 2 ($r = 0.17$, $P = 0.001$). This variation may be minimized by making remeasurements on the same day or requiring the same elapsed time between measurements, or by recording elapsed time between measurements so that the effects of different elapsed times can be examined and adjusted, if needed.

Finally, paired t-tests showed that the mean remeasurement differences were significant for Type 2 remeasurements of branch dieback and Type 1 remeasurements of foliage transparency. In addition, for foliage transparency the standard deviation of remeasurements increased from remeasurement Type 1 to 3; meanwhile, the opposite trend–decreasing standard deviation of remeasurements from Type 1 to 3–was shown for branch dieback. Furthermore, the paired t-tests did not detect the systematic difference shown by graphical analysis. Generally most of these results were inconsistent with the results of the other analyses. This may be due in part from the the unbalanced design, especially from uneven distributions of remeasurements among the rating classes and from possible changes in populations between remeasurements.

Overall the remeasurement data served several important uses. First, it quantified the lower limits for detecting change. In this study any real change of ±1 class or smaller for a tree cannot be reliably detected because of measurement variation. Second, the data provided some indication of the reliability of measurements of different tree crown characteristics. For example, in this remeasurement program branch dieback was most easily reproduced by all crews, and thus was more reliable for detecting trends than foliage discoloration and transparency and dwarfed foliage; however, the four crown characteristics had similar measurement precision when the same crews were used for all measurements. Finally, remeasurement data provided information for increasing the precision of data collected in the future. For example, the relative increase in quality of data (i.e., higher precision) by using the same crew for all measurements (Type 1) would have a cost—mainly the money needed to travel from site to site. This cost could be considerable in a project such as this, where a large geographical area is covered, and would probably not be justified because little quality was lost by using different crews from the same state/province (Type 2). In addition, if different crews from different states/provinces (Type 3) were used in future monitoring, branch dieback could be emphasized more because this variable can be measured with more precision than dwarfed foliage and foliage discoloration and transparency. Another option would be to attempt to reduce measurement errors of difficult variables by refining definitions and increasing training. Again, the cost of these activities must be evaluated. If the variables in question are biologically critical or sensitive, then the extra cost may be justified.

The collection and analysis of QC data is most beneficial when implemented early in survey projects such as this one. For example, a pilot study would ideally include not only a test of the experimental design, sampling procedures, and measurement systems, but also a test of the QA program. An integral part of the test QA program would be training sessions. Training sessions have several benefits: (1) introducing the personnel to the methodology; (2) early data collection to estimate measurement variation; (3) identifying ambiguities in the methodology and their contribution to measurement variation; and (4) the opportunity to revise methods so that variation is reduced before data collection starts. The results of a training session held prior to the start of this project were used to alter the procedure for rating individual trees; the revised procedure required a second observer for each crew. Both observers rated the tree separately, by viewing all sides, and then conferred and agreed upon one rating. This rating was more reliable than individual ratings because it more truly represented the whole crown and tended to average out observer bias.

Doing these types of exercises in a pilot or training setting solidifies the connection between experimentally important variables, the magnitude and sources of variation associated with the collection and measurement of those variables, and the types of QA activities and QC data needed to monitor, reduce, and document variation. Conducting these types of exercises prior to data collection increases the amount of potentially usable data, the quality of which is documented concurrently.

CONCLUSIONS

Several results can be drawn from this analysis of measurement variation during assessment of canopy cover and crown condition:

1. Estimation of canopy cover using hemispherical photography was quite precise. For example, measurement precision (as the root mean square of the differences in replicate measurements) of ponderosa pine canopy cover was ±2.6–4.0% and was similar for field and laboratory replicates

measured with the same and different f-stops. In contrast, systematic variation introduced by defining a threshold brightness and correcting for distortion was found to be potentially significant, but controllable by using a consistent methodology on all photographs and continuous monitoring with internal reference photographs.

2. Visual estimation of crown condition characteristics proved reasonably precise, and, as such, a viable method for detecting change in forest condition. For example, measurement precision (as frequency of remeasurements within ±1 class) of sugar maple crown condition ranged from 73.5–96.6% across all variables and remeasurement types. Measurement precision was lowest when the remeasurement crews were from different states/provinces (Type 3) and highest when remeasurements were done by the same crew (Type 1). The easiest variable to remeasure was branch dieback. Emphasis of this variable in future data collection sessions, use of the same crews for remeasurements (Type 1), and training field crews prior to data collection would improve data quality (i.e., higher precision), but the cost of these actions would have to be evaluated in relation to the relative gain in precision and the biological significance of the measurement variable. Under these circumstances, most ±2 class changes in an individual tree crown characteristic would not be due to measurement variation.

3. The QA activities and QC procedures discussed have general application, even though the data presented here were specific for these projects. In addition, the precision data for canopy cover and crown condition ratings can be used to estimate measurement variation until actual project data is available. Finally, the following general QA/QC guidelines are recommended regardless of forest type or measurement system: (1) implement training prior to data collection to increase the amount of potentially usable data, (2) use consistent methods and reference materials to control measurement variation during data collection, and (3) include detailed methods and QC data with study results to provide a basis for evaluating data quality and comparability with other studies.

These results have immediate usefulness to the two projects analyzed. In this sense the results are project specific and their generality remains in question. The QA Project of FRP is continuing to analyze and summarize QC data from other FRP projects for a variety of variables. At the end of this process more definitive estimates of measurement variation of canopy and crown condition and other variables can be stated.

ACKNOWLEDGMENTS

The funding for this research was provided by the US Environmental Protection Agency and the USDA Forest Service through the Quality Assurance Project of the Forest Response Program, under the National Acidic Precipitation Assessment Program. The data for project 1 were provided by S. Ustin and B. Curtiss from a study entitled "Remote Sensing of Forest Condition in the Western United States," funded through the FRP Western Conifers Research Cooperative. The data for project 2 were provided by the cooperating groups in the "North American Sugar Maple Decline Project" (USDA Forest Service, FPM; Canadian Forestry Service; Maine Forest Service; University of Massachusetts; Michigan State University; New Hampshire Department of Resources and Economic Development; SUNY College of Environmental Science and Forestry; Vermont Agency of Environmental Conservation; and

Wisconsin Department of Natural Resources). Project 2 was funded by the FRP Eastern Hardwood Research Cooperative (I. Millers, USDA Forest Service Northeastern Area, Durham, NH, and D. Lachance, Forestry Canada, Ste. Foy, Quebec; National Project Coordinators). The authors also thank T. Armentano, D. Coffey, H. Erickson, A. Hairston, P. Muir, C. Palmer, A. Sherman, and J. Watson for providing helpful review comments.

REFERENCES

1. P. Schroeder and A.R. Kiester, "The forest response program: national research on forest decline and air pollution," *J. For.* 87:27 (1989).

2. M.L. Gumpertz, D. Tingey, and W. Hogsett, "Precision and accuracy of visual foliar injury assessments," *J. Environ. Qual.* 11:549 (1982).

3. J. Taylor, *Quality assurance of chemical measurements*, Lewis Publishers, Inc., Chelsea, MI, 1987, 328pp.

4. P.S. Muir and T.V. Armentano, "Evaluating oxidant injury to foliage of *Pinus ponderosa:* a comparison of methods," *Can. J. For. Res.* 18:498 (1988).

5. D.L. Peterson, M.J. Arbaugh, V.A. Wakefield, and P.R. Miller, "Evidence of growth reduction in ozone-injured Jeffrey pine (*Pinus jeffreyi* Grev. and Balf.) in Sequoia and Kings Canyon National Parks," *JAPCA* 37:906 (1987).

6. W.J. Dixon and F. Massey, Jr., *Introduction to Statistical Analysis*, 3rd ed., McGraw-Hill Book Co., New York, 1969, 638pp.

7. M. Thompson, "Variation of precision with concentration in an analytical system," *Analyst* 113:1579 (1988).

Table I. Class percentage and range for estimates of sugar maple branch dieback, foliage transparency, foliage discoloration, and dwarfed foliage for project 2.

Class Percentage	Class Percentage Range
0	0
5	1–5
10	6–15
20	16–25
30	26–35
40	36–45
50	46–55
60	56–65
70	66–75
80	76–85
90	86–95
100	96–100

Table II. Measurement variation using hemispherical photography to estimate ponderosa pine canopy cover for project 1. Data are % sky cover = 100 - % canopy cover.

Remeasurement Type	Mean	Sm[a]	Sm[a] Relative	Sd[b]	Sd[b] Relative	N[c]
Field Replicates (Type 1)						
high sky cover unweighted	59.6[d,e]	11.3	19.0	2.6	4.4	16
low sky cover unweighted	46.6	14.1	30.4	3.1	6.7	16
high sky cover weighted	55.5	11.1	20.0	2.6	4.7	16
low sky cover weighted	42.4	13.5	31.9	3.3	7.8	16
Digitize same f-stop (Type 2)						
high sky cover unweighted	63.2	15.3	24.1	2.9	2.6	20
low sky cover unweighted	53.0	16.8	31.8	3.5	6.6	20
high sky cover weighted	58.9	15.2	25.7	3.1	5.3	20
low sky cover weighted	48.6	16.2	33.3	3.4	7.0	20
Digitize different f-stop (Type 3)						
high sky cover unweighted	65.7	11.0	16.7	3.2	4.9	36
low sky cover weighted	53.8	14.4	26.7	3.6	6.7	36
high sky cover weighted	60.9	11.0	18.1	3.7	6.1	36
low sky cover unweighted	48.7	13.9	28.5	4.0	8.2	36

[a] Sm = standard deviation of all measurements. Sm Relative=Sm/mean X 100.

[b] Sd = root mean square of differences in replicate measurements. Sd Relative=Sd/mean X 100.

[c] N=sum of original and replicate measurements.

[d] For each remeasurement type, means of high and low sky cover estimates were compared (paired t- test). Unweighted means and weighted means were compared separately. For each comparison in each data set, the means were significantly different (P = 0.01).

[e] For each remeasurement type, means of unweighted and weighted sky cover were compared (paired t-test). High and low means were compared separately. For each comparison in each remeasurement type, the means were significantly different (P = 0.01).

Table III. Percent of remeasurement values 0, ±1, and ±2 classes from original value for sugar maple branch dieback, foliage transparency, foliage discoloration and dwarfed foliage for project 2.

Remeasurement Type[a]	0	±1	±2	0	±1	±2	N[b]
	Branch Dieback			Foliage Transparency			
1	66.2	94.5	94.5	67.6	95.2	97.9	145
2	59.3	93.2	98.2	45.7	91.4	97.7	396
3	57.3	95.4	98.7	34.4	78.8	96.4	302
	Foliage Discoloration			Dwarfed Foliage			
1	71.7	96.6	100.0	67.6	88.3	93.1	145
2	62.9	96.0	98.7	81.8	96.5	98.0	396
3	48.7	80.5	81.5	56.0	73.5	82.1	302

[a] 1 = same crew, 2 = different crew, same state/province, 3 = different crew, different state/province.

[b] N = Number of trees remeasured.

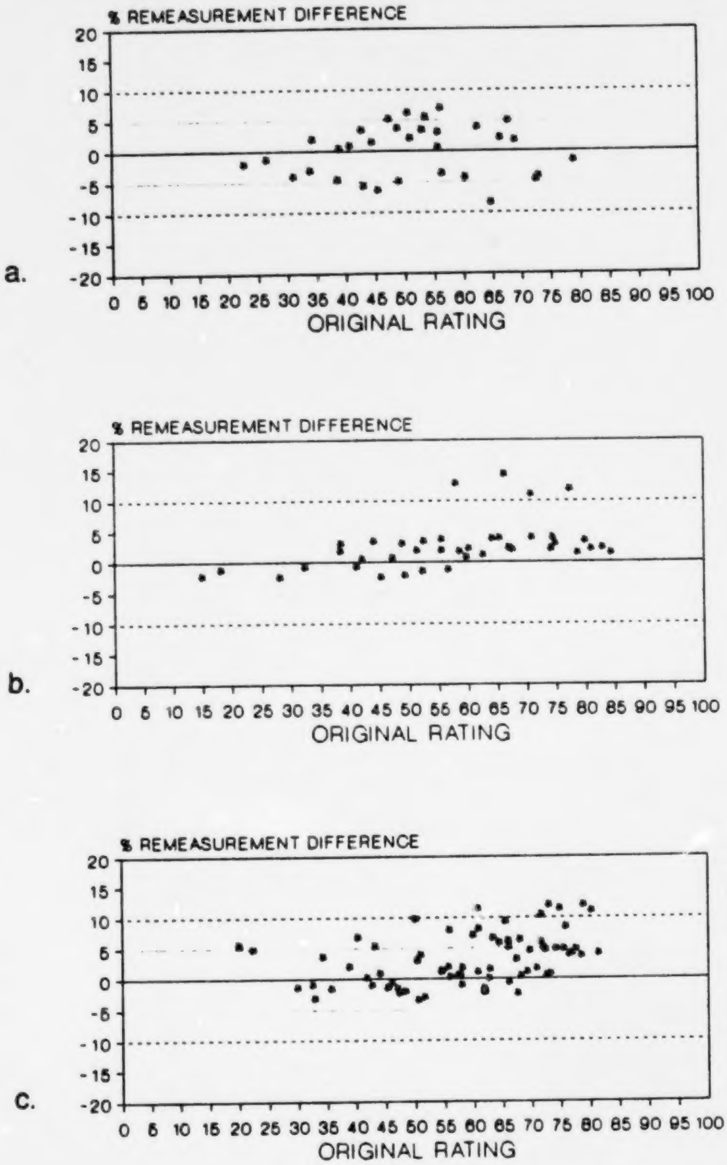

Figure 1. Percent (%) remeasurement difference for replicate measurements of ponderosa pine canopy cover by remeasurement type for project 1: (a) field replicates (Type 1), (b) digitize same f-stop (Type 2), and (c) digitize different f-stop (Type 3). % remeasurement difference = original % sky cover - replicate % sky cover.

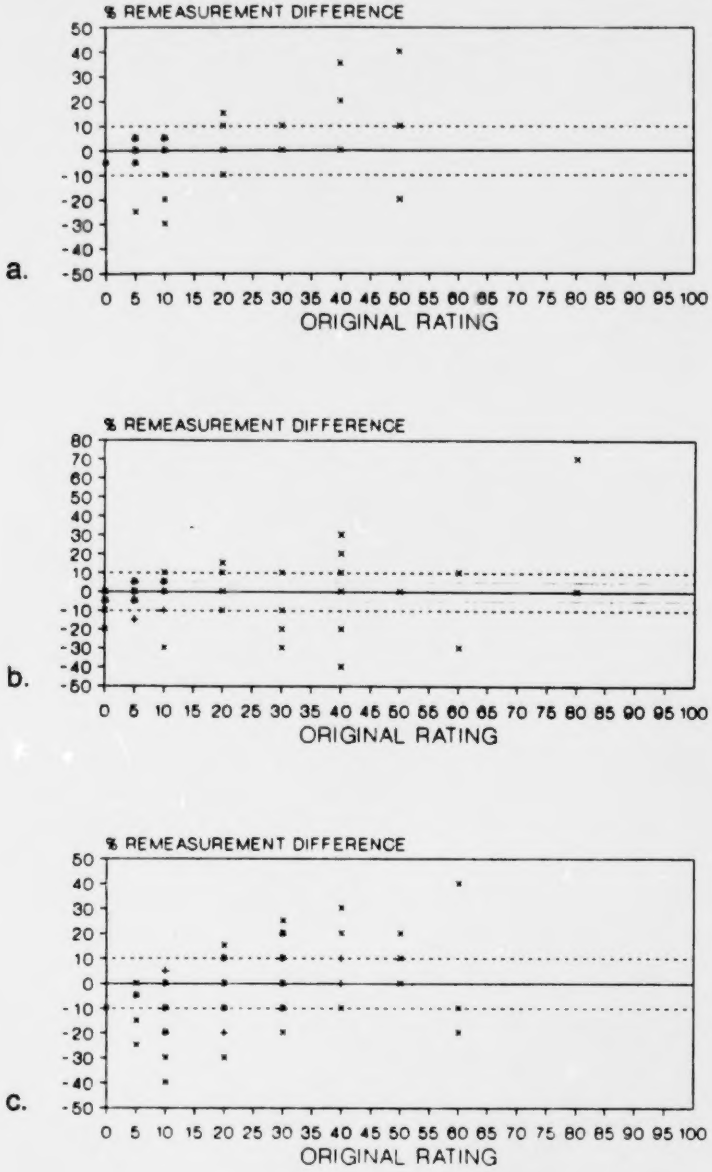

Figure 2. Percent (%) remeasurement difference for replicate measurements of sugar maple branch dieback by remeasurement type for project 2: (a) same crew (Type 1); (b) different crew, same state/province (Type 2); and (c) different crew, different state/province (Type 3). % remeasurement difference = original class rating - replicate class rating. Frequencies: x = <6, + = 6-10, and * = >10.

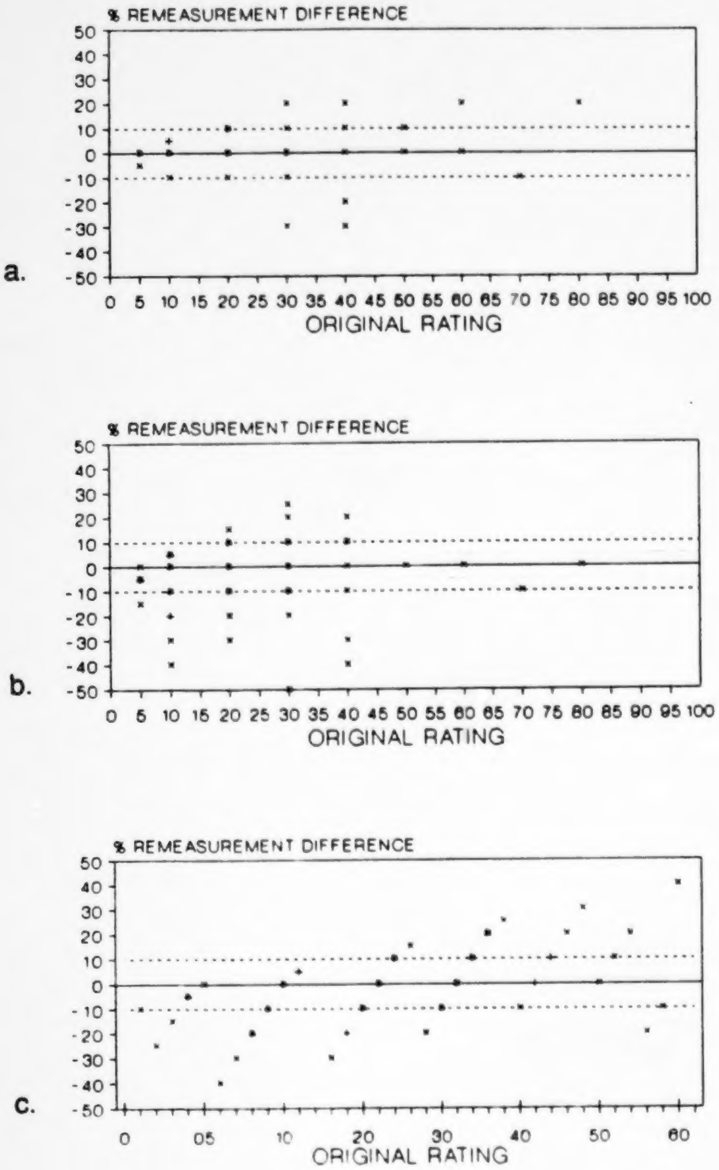

Figure 3. Percent (%) remeasurement difference for replicate measurements of sugar maple foliage transparency by remeasurement type for project 2: (a) same crew (Type 1); (b) different crew, same state/province (Type 2); and (c) different crew, different state/province (Type 3). % remeasurement difference = original class rating - replicate class rating. Frequencies: x = <6, + = 6-10, and * = >10.

Analysis of Growth Trends and Variation in Conifers from Arizona and New Mexico

Donald A. Graybill[1]
Martin R. Rose[2]

[1] *Laboratory of Tree-Ring Research*
University of Arizona
Tucson, Arizona 85721

[2] *Biological Sciences Division*
Desert Research Institute
University of Nevada System
P.O. Box 60220
Reno, Nevada 89506

INTRODUCTION

A major environmental policy issue in North America concerns whether there may or may not be a significant problem of forest damage due to acidic deposition or from other pollutants. Those pollutants may include SO_x, NO_x, O_3, H_2O_2, and various hydrocarbons and metals. Evaluation of that issue is being accomplished by various organizational units of the U.S. Forest Response Program[1] through in-house programs and by support of other researchers. Some efforts are focused on two testable hypotheses that are phrased as "Scientific Questions":

S.Q. 1.1 "Are changes in forest condition greater than can be attributed to typical trends and levels of natural variability?"

S.Q. 1.2 "What spatial patterns exist in forest condition and how do these patterns relate to spatial patterns of pollutant exposure?"

The research reported here is a summary of a regional case study[2] that uses dendrochronological techniques to explicitly address S.Q. 1.1. Since the approaches taken are regional in scope, the results of this work may also be useful in consideration of S.Q. 1.2. The specific sector of the southwest United States considered here (see Figure 1) was identified[3] as a region where such a study might have maximal value according to the following criteria: (1) coniferous forest type present; (2) high levels of atmospheric deposition occurring; (3) good baseline data on tree physiology, stand development, and ecosystem processes; and (4) existing forest inventory and dendrochronological databases.

In consideration of S.Q. 1.1, we use a series of analytical strategies to evaluate the nature of variability in the annual growth increments of 41 tree-ring chronologies that were developed for this project. Radial growth is commonly considered to be one single variable that is highly representative of forest growth in general,[4] although it is recognized that there are many other components of forest growth. Tree-ring series are particularly useful for this problem because they provide the *only* truly long-term annual records (200+ years) of forest condition that both precede and are concurrent with the urban and industrial pollution developments of the twentieth century. This permits the development of baseline characterizations of natural variability in

Preceding page blank

growth for times prior to suspected pollution effects and a search for deviations of recent growth from those norms. This kind of approach also has been used recently in other studies evaluating possible forest decline in the southwestern United States,[5] in the eastern United States,[6-8] and in Germany.[9]

One variable that we considered most suitable for those purposes is the standwide common variation in ring-width increment growth that is a record of natural macroclimatic variation. There are compelling reasons for this selection. First, a common, synchronous signal that can be identified and quantified for use in statistical hypothesis testing procedures is desirable. Second, understanding of empirical test results can profit from prior physiological studies[10,11] and models of tree-growth and climate[12] that have been developed using conifers in this region. Analytical techniques for working with those relationships are also reasonably well developed.[13] Finally, under conditions of pollution stress that lead to disruption of normal physiological activity through many potential routes,[14,15] the normal tree growth–climate relationship might expectedly change.

The Regional Setting

Extensive forests of commercial value, primarily ponderosa pine (*P. ponderosa*), arc across central Arizona and into western New Mexico, generally in and near the mountainous Mogollon Rim that separates the upland Colorado Plateaus from the desertic Basin and Range Province (Figure 1). Other economically important species include Douglas-fir (*Pseudotsuga menziesii*) and to a lesser extent, southwestern white pine (*P. strobiformis*), white fir (*Abies concolor*) and Engelmann spruce (*Picea engelmannii*). In the Basin and Range areas of south central and southeastern Arizona, the forests occur on several isolated mountain masses and generally include the same range of coniferous species just noted. Substantial portions of all mountainous regions are also forested with varying proportions of pinyon pine (primarily *P. edulis*), junipers (*Juniperus sp.*) and oaks (*Quercus sp.*).

It is apparent that the region of study has recently been experiencing relatively high levels of pollutant deposition. There also appears to be some spatial gradients in the amounts of deposition (Figure 1).[16,17] The sulfur appears to be primarily derived from nonferrous smelting activity in an area ranging from near the Arizona-Mexico border up to the base of the Mogollon Rim in central Arizona and then eastward along the Mogollon Rim to the copper mining areas of eastern Arizona and southwestern New Mexico. While some of the mining activity has an extensive history that extends back into the 19th century, the heaviest smelting activity appears to have taken place in the decades following World War II.[18,19] One study of visibility in the region found a declining trend from the middle 1950s to the early 1970s, hypothesizing that this was most likely due to corresponding increases in SO_2, NO_x, and hydrocarbon emissions.[20] Nitrates and hydrocarbons vary in source, but changes in them could be inferred from increases in population and attendant increases in total vehicle and other sources of emissions since mid-century in Phoenix and Tucson.

Sampling Approach

The overall collection strategy that we adopted was wide-ranging in coverage and exploratory in nature. Stands containing the species of primary economic importance (ponderosa pine and Douglas-fir) were most frequently sampled, but other conifers were also considered (Table I). Two cores per tree were extracted at breast height from 15 to 25 dominant to codominant trees in each collection. These generally ranged from 200 to more than 500 years in age. In two stands we also purposefully collected samples from an equal number of more youthful trees in the 100 year age range for eventual comparative purposes. The final chronologies that were developed are from stands in a variety of environmental settings that range from the forest interior to near the lower forest border. This kind of idealized transect should not, however, be interpreted as one ranging from 'extremely wet' to 'very dry'. There is prevailing aridity over the entire region. In the central area along the Mogollon Rim, the range of annual precipitation over the distribution of most ponderosa pine type forests is only 500-635 mm.[21]

Obtaining a broad initial overview of this nature appeared the most useful strategy in the absence of any prior knowledge that conifers in any single sector of the region were experiencing abnormal growth. However, the geographic distribution of stand collections was designed to be reasonably congruent with the larger area of known pollutant production. Given the relatively long-standing and known sources of pollution from copper smelting, approximately half of the collections were made in the southern isolated mountains and from the lower forested edges of the Mogollon Rim. Some stands in southern Arizona were also sampled due to their proximity to the rapidly growing cities of Tucson and Phoenix.

The Dendrochronological Background

At the most general level, dendrochronology can be defined as a science whose fundamental data are time series of annual growth layers from woody plants. These growth layers are universally assigned accurate calendar dates in all legitimate studies that attempt to generalize about the precise historical covariation of annual increment growth with human activity, environmental factors, or both. A procedure known as crossdating insures the integrity of date assignment by determining whether certain series may have either missing or multiple intra-annual growth bands for various years.[22] If tree-ring series are not reliably crossdated but are simply counted and then averaged to form a composite stand or regional chronology, the potential information they might hold regarding historical environmental variation can be completely lost.

Tree-ring series are considered to be a composite of signals that is known as an "aggregate model"[23,24]

$$R_t = f(B_t, C_t, D_t, E_t)$$

where R_t is a dated and measured series of ring widths and B_t is a biological growth trend that commonly decreases as a function of age. C_t is growth variation that is climatic in origin. D_t is a range of potential disturbance signals that may or may not be present. These can be unique to a single tree at one or more times, reflecting random events with respect to time such as lightning damage. These may also be common to many or most trees in a stand, representing events such as overstory harvest. E_t is growth variation that is unique to each series due to factors such as genetic or micro-site differences.

Chronology Development

Many of the dendrochronological procedures undertaken were designed to maximize a climatic signal and remove or control some of the others described above. Disturbance signals were initially minimized at time of collection by avoiding trees with obvious evidence of mechanical damage and by avoiding stands that had been affected by thinning.

Each ring width series was carefully crossdated and the widths were measured to the nearest 0.01 mm. The resultant time series were then individually standardized and converted to tree-ring indices. This removes the biological growth trend and results in a new time series that is more homeoscedastic than the ring widths. It also allows direct comparison of the variation in growth patterns of all trees, regardless of age or rate of growth.

The standardization process primarily involved the use of simple deterministic curves such as negative exponentials or straight lines to model age-related growth trends. This minimized the possibility of removing recent growth trends of interest that were not age related. In a limited number of cases we used cubic splines to remove disturbance signals in the pre-analysis periods, but they were not allowed to track the ring width data too closely. After carefully reviewing plots of the actual and expected values for each series, we are confident that no important trends were either removed or introduced by any of these procedures.

Once the indices for individual ring width series had been developed, they were averaged to form a mean value function index chronology for each collection. This process has the effect of reducing the unique error associated with each component series and maximizes the common climatic signal used for ongoing analyses.

The persistence (autocorrelation) structure is one additional characteristic of tree-ring index chronologies that requires consideration. This component must be identified and treated appropriately before moving to some stages of analysis. Temporal persistence in a tree ring chronology is present when successive values in the series are not independent, that is, when they can be partially predicted from past observations. The presence of significant persistence in time series that are being used in regression-based procedures results in the adverse consequence of the variance estimates becoming unreliable.

Because all of the chronologies had significant persistence, standard Box-Jenkins[25] ARMA protocol was used to identify a low order parsimonious model that might be used in removing it. This first required defining of the appropriate time span for model evaluation. Two factors were of concern: where to end and where to begin the model identification process with respect to the total series length. In terms of the end date, it was desirable to use a time period for model fitting that was thought to precede any period of probable abnormal growth. Both 1950 and 1960 were selected. They provide approximate turning points for post World War II expansion and increased pollution production as it may or may not be relevant in affecting tree growth during more recent decades in this region. In terms of a beginning date, the important issue is the presence of an adequate number of series in order to maintain model stability. The number of component series normally decreases in the earliest years of a chronology to a point where there is increasing variability due simply to sample size. We therefore determined the earliest year in which a subsample of series contained 90% of the common signal expressed in a chronology of all the trees.[26] Best-fit ARMA models were then developed using the length of series from that year to 1950 and again to 1960.

Autocorrelation was then removed from the index chronologies by prewhitening each entire series via the models that were established. In this data set, we think that this persistence is primarily biological in origin and that we did not remove any strong climate signals. None of the five state divisional precipitation annual sums in the study region (Arizona divisions 2,3,4,7 and New Mexico division 4) evidenced significant autocorrelation over the period of 1895–1986.

Preliminary Indications of Recent Growth Abnormalities

During these early stages of the research we discovered what may be a very straightforward indication of trend in recent growth that is not "typical" or apparently "natural" in terms of the ability of some trees to covary with annual precipitation. In the dating process we found that a moderate to substantial portion (up to about 50%) of the series from ponderosa pine in several stands could not be dated after times ranging from about 1920–50 to the final year of collection in 1986. In some cases, more than 40 rings are absent from samples during the period of 1920–86. The most extreme suppressions of growth were found in the post-1950 years. This was unexpected. Precipitation trends throughout the region show particularly high values near the beginning of the century with decline from the 1920s into drought conditions at mid-century. This is followed by substantial increases in moisture in the 1970s and 1980s.[27] Most tree-ring series with which we had experience in the two states were tracking this overall "u" shaped pattern[28,29] (see expected growth patterns in Figure 2). However, we had not been working with series from the Basin and Range area. Six of the seven chronologies exhibiting this period of growth suppression are from that southern sector of Arizona. Discussion of possible reasons for these kinds of apparent growth anomalies follows upon consideration of some of the quantitative aspects of climate and tree growth covariation.

Analytical Procedures

A tree ring–climate transfer function analysis was implemented to develop reliable predictive relationships of natural tree growth variation from climatic variation over the baseline periods thought to be free of major anthropogenic pollution inputs. Simple linear regression analyses were used and evaluated according to commonly used criteria.[30] The dependent variable was always a prewhitened tree-ring chronology while the independent variable was an annual precipitation sum of divisional data. Procedurally, statistical models were established in each period over two subintervals. That is, the intervals from 1897 to 1950 or 1960 were divided into halves. The first interval was initially used for calibration (model development) while the second interval was used for verification (model testing). Then the process was reversed, and the second interval was employed in calibrating the model while the first segment was used for verification. This split period calibration–verification approach during the baseline period was adopted in an attempt to test for time stability of the climate–tree growth system. Only after the split period results were evaluated was a final calibration established with the full baseline period data set. This exercise was necessary and prudent because the climatic data available during the baseline periods is only 55 to 65 years in length. All data were used to insure that the final calibration models were developed on the fullest possible range of data covariation.

Predictive relationships between divisional climatic data (August to July total precipitation) and each of the 41 prewhitened tree-ring chronologies were established during the two baseline periods. The final adjusted r^2 values for the full calibrations across the baseline periods were significant in all cases (alpha = 0.05). Those values were relatively constant per chronology for each period, but there were some differences by subarea. The range of values for the 20 chronologies in the south is slightly lower than for the 21 in the north

(0.09–0.45 vs 0.13–0.55, 1896–1950 period); the central tendencies are somewhat different (0.26 in the south, 0.38 in the north ($t = 3.69$, $p < 0.001$). The lower mean value in the south is primarily due to low calibration values for chronologies in the mountains near Tucson.

The equations derived from the analyses just described were used to estimate tree growth series in the 1951–86 and 1961–86 periods. The null hypothesis then considered was that the estimated growth should be reasonably similar to actual growth in the recent intervals. Failure to reject the hypothesis would support the contention that there has been no change in the climate/tree-growth relationship. Test implications are straightforward. The covariance between the predicted and actual growth should not be significantly different and should be similar to that of the model calibration period; the means of the predicted and actual growth should not be significantly different, and there should not be any anomalous trend in the actual growth that is not present in the predicted growth. Covariance was evaluated with Pearson's correlation coefficient and its square, the coefficient of determination, differences of means and central tendency were tested with the t test and the Wilcoxon matched pairs signed ranks test, and trends were tested with a sign test. An alpha level of 0.05 was set for all tests and these were two-tailed.

Alternatively, (1) the actual and predicted series may not exhibit significant covariance, or it may drop precipitously from that seen in the calibration period; (2) there may be a significant difference between the means of the actual and the predicted series; and (3) there may be a trend in the regression residuals. Inability to reject any of the alternative hypotheses indicates that the actual and predicted growth empirically differ in some manner. It does not necessarily mean that an anthropogenic impact on tree growth is the cause of the difference, merely that a difference exists and that some factor(s), including pollution, could be the causal agent(s). That pollution is actually the cause of any tree growth change would still remain to be demonstrated.

Results of the comparison of actual and estimated tree growth are summarized in Table II. During each of the recent test periods there were a limited number of cases where the covariation between actual and climatically predicted tree growth was not significant. However most of these were in the southern area. One other perspective concerns whether there were major changes in covariance from that found in the baseline periods to values observed in either of the recent test periods. In most cases this did not occur. Eight exceptions were simpy defined as those chronoligies that exhibit an r^2 value in either recent test period that was 50% or less of the calibration r^2 value in the respective baseline period. Five of these exceptions are from the southern area and all are from sites near Tucson. Four of those sites had a substantial number of series that could not be dated after 1950. (Those particular series, however, were not included in the chronologies that were used in these analyses.) Three-fourths of the series rejected in the sign test during both periods were in the south and consistently included three of the sites just noted, as well as one Douglas-fir and one pinyon collection from the mountains near Tuscon.

The results of the tests discussed so far indicate that a moderate number of sites have trees with recent growth anomalies. Results of the tests regarding central tendency provide continuing verification of that. Because the Wilcoxon and t-test results were very similar, only the latter are presented and discussed here. In an effort to evaluate some of those test results in a more stringent fashion, we rejected all cases where the adjusted r^2 value between actual growth and precipitation over the baseline calibration period was less than 0.25. A focus on the t-test results from this reduced sample indicates that for the region as a whole, 16 of 31 series (52%) have less growth than predicted by a model in the 1951–86 period while 11 of 29 (38%) demonstrate this in the 1961–86 period. These proportions are similar to those for the full data set (51%, 39%) and the values are substantially larger than might be expected. With an arbitrary alpha level of even 0.10, we would only expect three series per period to be rejected. There are, again, some hints at subregional differences in those test results. For example, in the 1961–86 time period 14 series in the north show no significant decrease in expected growth while five do. In the south those respective frequencies are four and six (Chi Sq. = 3.157, $p < 0.10$). Some of the north-south differences stem from the test results for Douglas-fir. For both test periods only one of four series (25%) in the north has significantly less growth than expected, but this is seen in five of six (83%) series in the south for the first test period and in four of five (80%) series after 1961.

Examples of some of the differences in actual and expected growth in project chronologies are shown in Figure 5. The upper series (a.) is ponderosa pine from an open grown stand in the north. It has reasonable covariance with precipitation before 1951 ($r^2 = 0.37$, $p < 0.001$) and an even higher value between the actual and expected growth for 1951 - 1986 ($r^2 = 0.50$, $p < 0.001$). However, the mean level of actual growth for that recent time period is significantly less than expected ($t = 4.892$, $p < 0.001$). The lower series (b.) is from a moderately dense Douglas-fir stand in the Santa Rita Mountains just south of Tucson. It has covariance of 0.42 ($p < 0.001$) with precipitation before 1951 and a similar value of 0.41 ($p < 0.001$) between actual and expected growth in succeeding years. There is a relatively high mean value for expected growth after about 1960 that corresponds to increased precipitation here, but the actual growth series does not demonstrate a correspondent increase ($t = 3.993$, $p < 0.001$).

Foliar Damage Estimates

Several stands that we sampled are in National Monuments. As part of a cooperative research effort with K. Stolte of the Air Quality Division, National Park Service, some of the trees were visibly evaluated for foliar damage that might be pollution related. This included ponderosa pine from the Gila Cliff Dwellings, NM (one stand), Chiricahua, AZ (one stand), Saguaro East, AZ (three stands), and Walnut Canyon, AZ (one stand). Single chronologies for Douglas-fir were also developed from the latter three locations. Additional chronologies from Saguaro Monument near Tucson include one of white fir, three of white pine, and one of pinyon pine. All trees used in developing these chronologies were also evaluated for foliar damage. In brief, only minimal damage was found. Eleven individual ponderosa pine trees in the Saguaro monument had limited evidence of ozone damage to needles. Only three of those appear to have growth decline in their post-1950 ring width record. However, it is possible that decreases in productivity (unexpected ring width decrease) may be observed prior to obvious foliar damage.

CONCLUSION

Two types of anomalous tree growth have been discovered in the mid to late twentieth century in this region that are perhaps different in degree rather than kind. In the most extreme cases, some trees in ponderosa pine stands, particularly some of those in southern Arizona, exhibit ring width growth patterns during recent decades that suggest mortality is imminent. Their external morphological characteristics, that is, foliage, do not immediately permit the same inference. In other less extreme cases, there are statistically significant differences in actual and climatically predicted tree-ring growth in terms of covariance, trend, and particularly mean value over the same period. These differences are most pronounced in southern Arizona and are most reliably documented throughout the region, in terms of sample numbers, for ponderosa pine and Douglas-fir.

Although empirical tests such as those undertaken here may be statistically significant, they only provide indications of the possibility that meaningful biological changes may be occurring. Bridging arguments that might begin to address the reasons for those changes in greater detail are needed. Therefore, a limited number of explanatory hypotheses for further consideration of these apparent growth anomalies are offered: (1) Lack of growth response to "ameliorating" moisture conditions of the late twentieth century is related to different intrinsic (genetic) tolerances of individuals to drought stress they experienced in mid century. (2) Anthropogenic activity resulted in chemical deposition that affected the tree growth–climate interaction. (3) Natural biological competition may be responsible for growth changes in some stands. (4) Any combination of the above may be possible. All require further testing.

Investigation of one of those alternatives is currently underway. Relatively wet conditions in the early twentieth century, combined with effective fire suppression by the U.S. Forest Service, may have encouraged establishment of a substantial number of trees. During the succeeding 30–60 years they may have provided serious competition with older individuals for water, soil nutrients, and ultimately, light. In the northern sector of the region researchers[31,32] have particularly noted the successful establishment of a large crop of ponderosa pine seedlings in 1919, a year of exceptionally high summer rainfall. A study has therefore been initiated to develop competition indices for trees of varying ages in many of the stands that we have evaluated throughout the region. This should allow us to determine if competition could be at least partially responsible for some of the seemingly anomalous growth patterns discerned here in the late twentieth century.

ACKNOWLEDGMENTS

This research was partially supported by funds provided by the Western Conifers Research Cooperative within the joint U.S. Environmental Protection Agency–USDA Forest Service Forest Response Program. The Forest Response Program is part of the National Acid Precipitation Assessment Program. This paper has not been subject to EPA or Forest Service review and should not be construed to represent the policies of either agency.

REFERENCES

1. R. Kiester, (Project Leader), *Research Plan*, Synthesis and Integration Project, Forest Response Program, U.S. EPA, Corvallis, OR, 1987.

2. D.A. Graybill and M.R. Rose, "Analysis of growth trends and variation in conifers from Central Arizona, I. Network chronology development and analysis," Final Report to the Western Conifers Research Cooperative, U.S. EPA, Corvallis, OR. Laboratory of Tree-Ring Research, University of Arizona, Tucson, 1988.

3. Western Conifers Research Cooperative. *1987 Research Plan*. U.S. EPA. Corvallis, OR, 1987.

4. C.C. Avery, and H.E. Burkhart, *Forest Measurements*, McGraw-Hill, NY, 1983.

5. M.R. Rose, "Recent forest growth trends in the western United States: 1700–1985," report submitted to Southern California Edison & West Associates. Laboratory of Tree-Ring Research, University of Arizona, Tucson, 1988.

6. E.R. Cook, "The use and limitations of dendrochronology in studying effects of air pollution on forests," *Proceedings of NATO Advanced Research Workshop: Effects of Acidic Deposition on Forests, Wetlands, and Agricultural Ecosystems*, Toronto, Canada , May 12-17, 1985.

7. A.H. Johnson, E.R. Cook, and T.G. Siccama, "Climate and red spruce growth and decline in the northern Appalachians," *Proceedings of the National Academy of Science, USA*, Volume 85, Applied Biology, Washington, D.C., 1988.

8. S.B. McLaughlin, D.J. Downing, T.J. Blasing, E.R. Cook, A.H. Johnson, and H.S. Adams, "An analysis of climate and competition as contributors to decline of red spruce in high elevation Appalachian forests of the eastern United States," *Oecologia* 72:487 (1987).

9. F.H. Schweingruber, R. Kontic, and A. Winkler-Seifert, "Application of annual ring analysis in investigations of conifer die-back in Switzerland." *Swiss Institute of Forestry Research, Report No. 253*, Aug. 1983, Birmensdorf, p. 6. In German, with English abstract.

10. J.M. Brown, The photosynthetic regime of some southern Arizona ponderosa pine, Ph.D. thesis, University of Arizona, Tucson, 1968.

11. C.A. Budelsky, "Variation in transpiration and its relationship with growth for *Pinus ponderosa* in southern Arizona," Ph.D. thesis, University of Arizona, Tucson, 1969.

12. H.C. Fritts, *Tree-Rings and Climate*, Academic Press, NY, 1976.

13. M.K. Hughes, P.M. Kelly, R.J. Pilcher, and V.C. LaMarche, Jr., *Climate from Tree-Rings*, Cambridge University Press, Cambridge, 1982.

14. T.T. Kozlowski and H.A. Constantinidou, "Responses of woody plants to environmental pollution," *Forest Abstracts* 47(1):5 (1986).

15. T.T. Kozlowski and H.A. Constantinidou, "Environmental pollution and tree growth," *Forestry Abstracts*, 47(2):105 (1986).

16. United States Environmental Protection Agency, *National Air Quality, Monitoring, and Emissions Trends Report, 1977*, EPA450/2-78-052, 1978.

17. P. Roth, C. Blanchard, J. Harte, H. Michaels, and M.T. El Ashry, *The American West's Acid Rain Test*, World Resources Institute and Energy and Resources Group, University of California, Berkeley, CA, 1985.

18. C.H. Dunning and E.H. Peplow, Jr., *Rock to Riches*, Southwest Publishing Co., Phoenix, AZ, 1959.

19. Arizona Department of Economic Security, *Arizona Occupational Profile*, Arizona Department of Economic Security, Phoenix, 1983.

20. J. Trijonis, "Visibility in the southwest—an exploration of the historical data base," *Atmospheric Environment*, 13:833 (1979).

21. R.L. Beschta, "Climatology of the ponderosa pine type in central Arizona," *Agriculture Experiment Station Technical Bulletin 228*. University of Arizona, Tucson, 1976.

22. M.A. Stokes and T.L. Smiley, *An Introduction to Tree-Ring Dating*, The University of Chicago Press, Chicago, IL, 1968.

23. D.A. Graybill, "Chronology development and analysis," In *Climate from Tree Rings*, M.K. Hughes, P.M. Kelly, J.R. Pilcher and V.C. LaMarche, Jr., Eds., Cambridge University Press, London, 1982, p. 21.

24. E.R. Cook, "On the decomposition of tree-ring series for environmental studies," *Tree-Ring Bulletin*, 47:37 (1987).

25. G.E.P. Box and G.M. Jenkins, *Time Series Analysis: Forecasting and Control*, Holden-Day, San Francisco, CA, 1976.

26. T.M.L. Wigley, K.R. Briffa, and P.D. Jones, "On the average value of correlated time series with applications in dendroclimatology and hydrometeorology," *Journal of Climate and Applied Meteorology*, 23:2:201 (1984).

27. N.O.A.A., State Divisional Climatic Data, 1895–1987, magnetic tape, National Climatic Data Center, Asheville, NC, 1988.

28. M.R. Rose, W.J. Robinson, and J.S. Dean, "Dendroclimatic reconstruction for the southeastern Colorado plateau," Manuscript, Final Report to Division of Chaco Research, National Park Service, Order No. PX7486-7-0121, 1982.

29. D.A. Graybill, "The reconstruction of prehistoric Salt River stream flow," Chapter 3 in *The 1982-1984 Excavations at Las Colinas, Environment and Subsistence*, C.A. Heathington, and D.A. Gregory, Eds., Archaeological Series 162, Volume 5, Part 1, Cultural Resource Management Division, Arizona State Museum, University of Arizona, Tucson, 1986.

30. N. Draper and H. Smith, *Applied Regression Analysis*, 2nd ed., Wiley, New York.

31. G.A. Pearson, "Management of ponderosa pine in the southwest," USDA Forest Service, *Agriculture Monograph* No. 6, 1950.

32. C.F. Cooper, "Changes in vegetation, structure, and growth of southwestern forests since white settlement," *Ecological Monographs* 30(2):19 (1960).

Table I. Numbers of tree-ring collections by species and subarea in the study region.

	PP[a]	DF	WP	PN	WF	Totals
North[b]	13	4		4		21
South	8	7	3	1	1	20
Totals	21	11	3	5	1	41[c]

a. PP (*Pinus ponderosa*)
   DF (*Pseudotsuga menzeisii*)
   WP (*Pinus strobiformis*)
   PN (*Pinus edulis*)
   WF (*Abies concolor*)

b. Northern collections are from the Mogollon Rim and Colorado Plateaus. Southern collections are from the Basin and Range sector of central and southern Arizona. See Figure 1 for location of these features.

c. This data set is derived from 1,747 core samples taken from 889 different trees. All core samples were dated and 1,150 were measured and standardized. More than 283,000 tree rings are represented in the 41 chronologies.

Table II. Test results of comparisons of actual and expected growth for 41 chronologies, 1951-1986 and 1961-1986.

Periods	Tests	No. of Chronologies[a]		
		Accept	Reject	
1951-1986	r^2	36	5 (4)[b]	
1961-1986	r^2	36	5 (4)	
		Accept	Reject$_i$	Reject$_d$
1951-1986	T	19	1	21 (13)
1961-1986	T	24	1 (1)	16 (11)
		Accept	Reject	
1951-1986	Sign	33	8 (6)	
1961-1986	Sign	29	12 (8)	

a. Accept = null hypothesis accepted.
   Reject = null hypothesis rejected.
   Reject$_i$ = reject, actual growth is greater than expected.
   Reject$_d$ = reject, actual growth is less than expected.

b. Numbers in parentheses are frequency of series in the southern sector with test rejections. Other numbers are totals for the 41 chronologies.

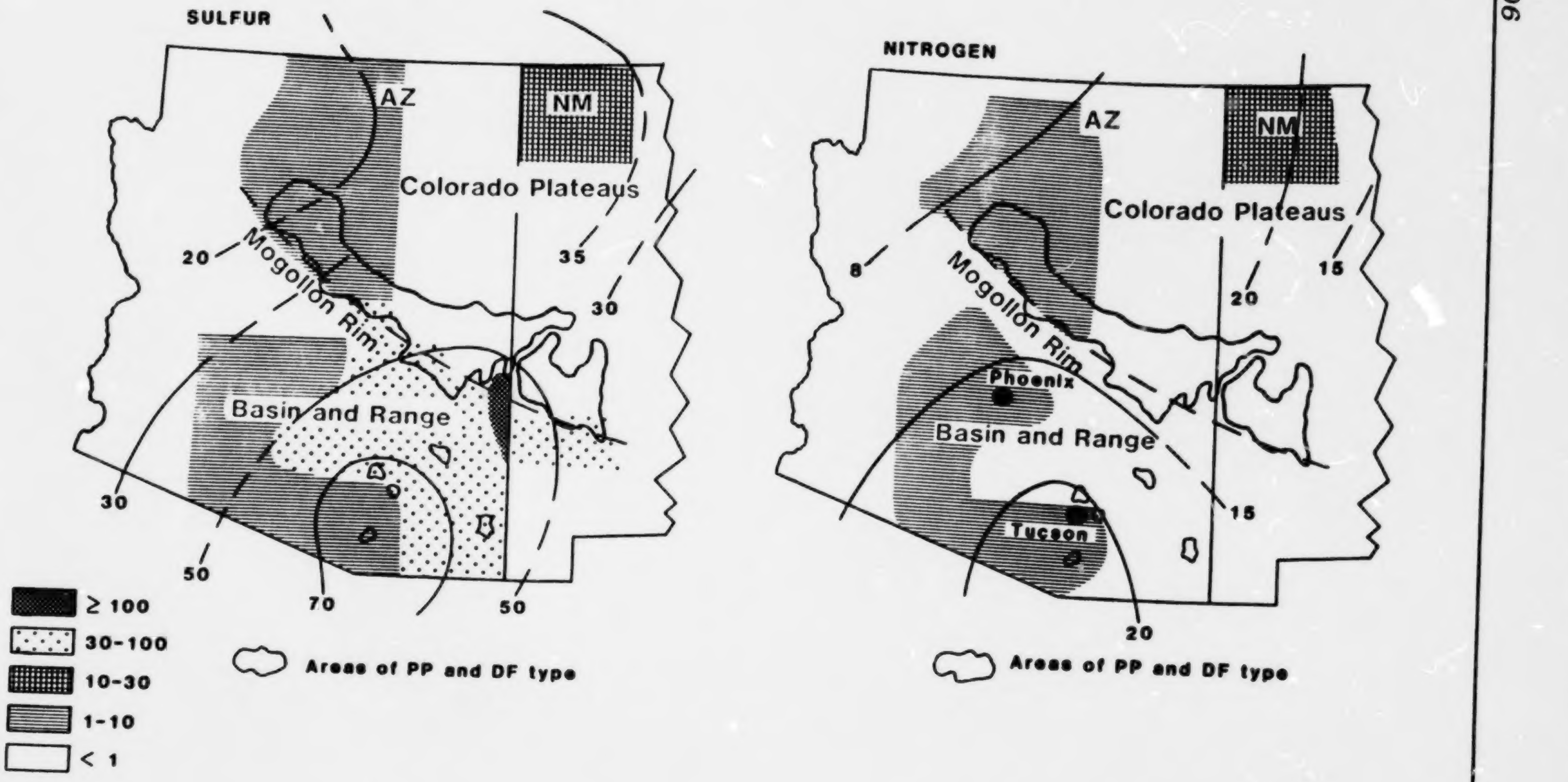
SULFUR
AZ
NM
Colorado Plateaus
Mogollon Rim
Basin and Range
20
35
30
30
50
70
50
≥ 100
30-100
10-30
1-10
< 1
Areas of PP and DF type
NITROGEN
AZ
NM
Colorado Plateaus
Mogollon Rim
Phoenix
Basin and Range
Tucson
8
20
15
15
20
Areas of PP and DF type

Figure 1. Southwestern physiographic features and chemical emissions and deposition, 1975.

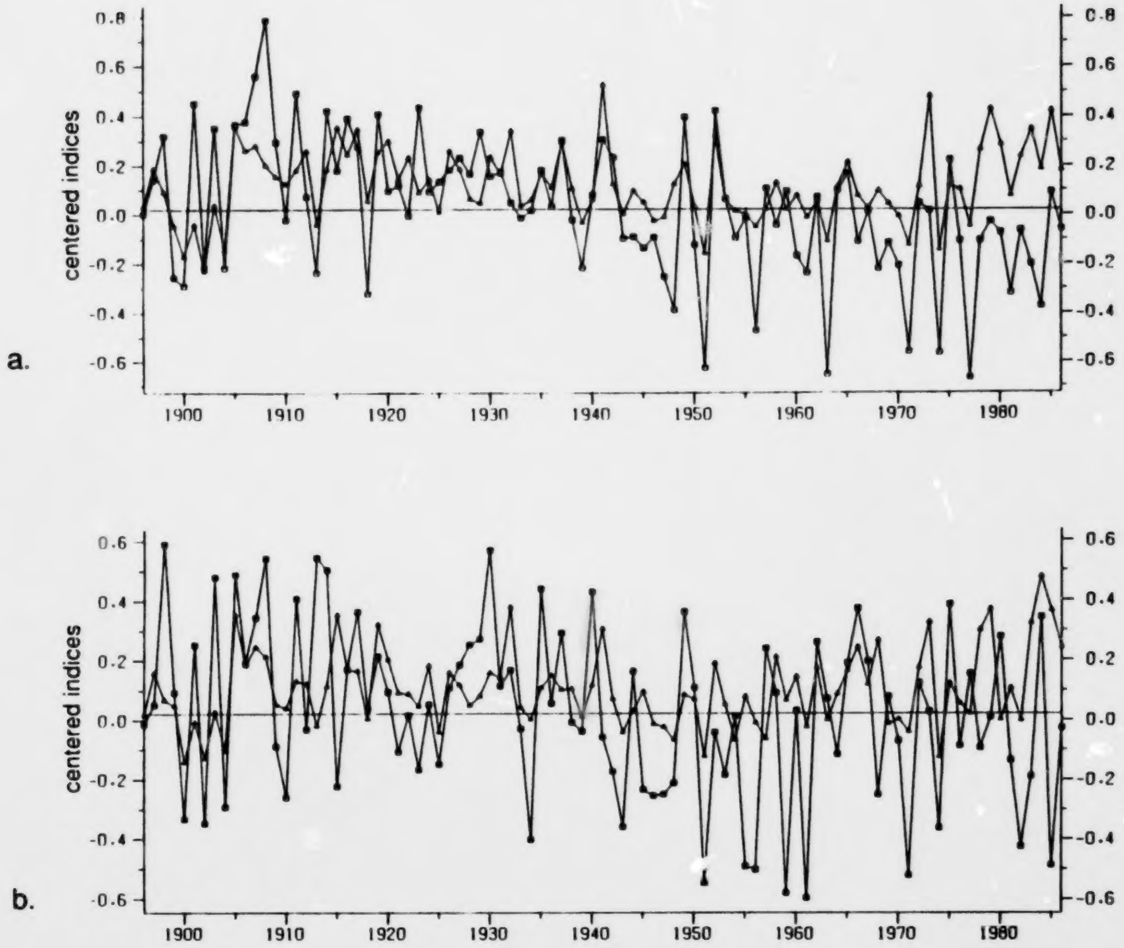

Figure 2. Actual and expected growth for ponderosa pine from Slate Mountain, central Arizona (a) and for Douglas-fir from the Santa Rita Mountains, southern Arizona (b). Triangles mark expected growth and squares mark actual growth.

Chapter Five

Growth and Physiological Mechanisms of Effect

Specific Leaf Weight and Other Characteristics of Ponderosa Pine as Related to Visible Ozone Injury	D.M. Ewell, L.C. Mazzu, and D.M. Duriscoe	411
Seasonal Physiological Responses of Ozone Stressed Jeffrey Pine in Sequoia National Park, California	M.T. Patterson and P.W. Rundel	419
Photosynthetic Response of Giant Sequoia Seedlings and Rooted Branchlets of Mature Foliage to Ozone Fumigation	N.E. Grulke, P.R. Miller, R.D. Wilborn, and S. Hahn	429
Potential Effect of Premature Needle Loss on the Foliar Biomass and Nutrient Retention of Lodgepole Pine	A.W. Schoettle	443
Effects of Photochemical Smog on the Growth and Physiology of Ponderosa Pine Seedlings Grown Under Nitrogen and Magnesium Deficiencies	A. Bytnerowicz and B.K. Takemoto	455
Sensitivity of Western Conifers to SO_2 and Seasonal Interaction of Acid Fog and Ozone	W.E. Hogsett, D.T. Tingey, C. Hendricks, and D. Rossi	469
Nutrient Effects on Responses of Willow and Alder to Ozone	C.S. Greitner and W.E. Winner	493

Preceding page blank

Specific Leaf Weight and Other Characteristics of Ponderosa Pine as Related to Visible Ozone Injury

D.M. Ewell[1]
L.C. Mazzu[2]
D.M. Duriscoe[3]

[1] *National Park Service*
Sequoia and Kings Canyon National Parks
Three Rivers, CA 93271

[2] *National Park Service*
Recreation Resources Assistance Division
1100 L Street NW, Room 2321
Washington, D.C. 20013

[3] *Eridanus Research Associates*
42403 Sierra Drive
Three Rivers, CA 93271

INTRODUCTION

Chlorotic mottle, or visible ozone injury, on pine foliage was associated with ambient ozone concentrations in southern California in 1962 by Miller et al.[1] Subsequently, in 1970, visible ozone injury was observed on ponderosa (*Pinus ponderosa* Laws.) and Jeffrey (*Pinus jeffreyi* Grev. and Balf.) pines under ambient ozone concentrations in the southern Sierra Nevada of California.[2] Reduced annual ring growth attributable to ozone exposure has been observed for Jeffrey pines but not ponderosa pines in Sequoia and Kings Canyon National Parks.[3,4] Results from a survey conducted in 1986 showed that 39% of the ponderosa and Jeffrey pines in Sequoia and Kings Canyon National Parks had visible ozone injury.[5]

Reductions in growth and photosynthesis correlate well with ozone exposure.[6,7] Specific leaf weight (leaf weight:leaf area ratio) correlates well with photosynthesis and can be used to estimate carbon uptake.[8,9] Reductions in specific leaf weight with increasing visible ozone injury were observed for ponderosa pine in the San Bernardino Mountains of California.[10] When photosynthetic measurements are not available or possible, specific leaf weight appears to be a good alternative for assessing ozone damage. In this paper, specific leaf weight is used to assess ozone damage on ponderosa pine trees that exhibit different levels of visible ozone injury.

EXPERIMENTAL METHODS

Needle tissue of ponderosa pine trees was sampled in late August, 1987, near Oriole Lake at 1525 m elevation in Sequoia National Park (see Figure 1). Mean annual precipitation is approximately 110 cm at this elevation with 95% falling between October and May. Approximately 30% falls as snow.[11] Mean daily temperatures for January and July are approximately 2° C and 20° C respectively.[11] The study site is on soils derived from dark granite diorite parent rock material.[12]

The Oriole Lake site was chosen for several reasons. The site is predominantly ponderosa pine that is fairly even-aged with many trees between 20 to 40 cm

Preceding page blank

dbh (pruneable crown). The trees at the site express a continuum of visible ozone injury. Slope, aspect, and soil type are uniform at the site. Since tree growth characteristics vary with season, leaf age, branch and canopy position, exposure, and tree stem diameter, we felt this site would minimize these variables.[9,13-17]

Visible ozone injury was estimated by observing the percent chlorotic mottle over the total surface area of each branchlet whorl. Trees were also grouped into 3 visible ozone injury classes (in order of increasing injury) as follows: (1) visible ozone injury on 3-year-old (1984) and older annual whorls, (2) visible ozone injury on the 2-year-old (1985) and older annual whorls, and (3) visible ozone injury on the 1-year-old (1986) and/or current year (1987) and older annual whorls. For the remainder of this paper, "injury" will be used when referring to visible ozone injury.

Trees were systematically selected by walking a swath through the forest until approximately ten trees were obtained in each injury class. There were 10, 9, and 11 trees in classes 1, 2, and 3, respectively.

Distal branchlets (ten per tree) were pruned from the south side at mid-crown position. Once pruned, branchlets were sprayed with water, sealed in plastic bags, and stored in ice chests. Within 24 hours of collection, the fascicles (including sheaths) from the 1-year-old (1986) whorls were weighed as a unit. Length of each needle was measured to the nearest 0.5 cm. Three fascicle diameters were taken per whorl. Diameters were measured at the proximal end of the fascicles (without sheath) using calipers.

Area was computed geometrically assuming the outside three-needle fascicle surface approximates a right cylinder and the inside fascicle wall surfaces approximate six right rectangles. Similar methods have been used by others.[18-20] Taper was assumed to be negligible since most of the taper occurs in the fascicle tip.

Using total needle length—L (cm) and average diameter—d (mm) for each whorl, the following equation was used for total whorl surface area:

$$\frac{\frac{2}{3}a + 2a}{100{,}000} = m^2 \qquad \text{where } a = \frac{d}{2} \times L \qquad [1]$$

The 1-year-old (1986) whorls were oven dried and weighed until weights did not significantly change on subsequent weighings to obtain dry weights. Specific leaf weight (SLW) was determined using the dry whorl weight divided by the fresh whorl area. "Saturated" moisture content (percent) was determined by dividing the difference between wet and dry weights by dry weight.

The Kruskal-Wallis one-way analysis of variance was used with the Mann-Whitney U statistic to determine significant differences at the tree level.[20] Statistical significance is reported at the p = 0.05 level.

RESULTS

SLW was significantly different between injury classes 1 and 3 (Figure 2a). There was a 12% decline in SLW between classes 1 and 3. There were no significant differences between the injury classes for "saturated" moisture content (SMC) but there was a slight increase from class 1 to classes 2 and 3 (Figure 2b).

Average branchlet injury ranged from 0.4% to 16.5% among the classes (Figure 3a). Average branchlet injury represents an estimate of the proportion of the tree's foliage that is affected by chlorotic mottle. There were 30% less whorls per branch between classes 1 and 2, and 22% less between classes 2 and 3 (Figure 3b).

The average needle count for 1-year-old (1986) whorls decreased by approximately 10% with increasing injury class (Figure 4a). There was a decrease in average needle dry weight for 1-year-old (1986) whorls between class 1 and classes 2 and 3. Average needle dry weight increased slightly from class 2 to 3 (Figure 4b). Average needle length and area for 1-year-old (1986) whorls did not show any consistent relationship with injury classes (Figures 5a and 5b).

DISCUSSION

SLW was found to decrease with increasing visible ozone injury, which indicates a negative effect of ozone exposure on photosynthetic capacity (Figure 2a). Coyne and Bingham presented similar results for ponderosa pine trees in the San Bernardino Mountains of southern California (1600 m).[10] They reported a range of SLW from 127 to 110 g/m^2 (injury class 1 to 3); this study's range was 113 to 101 g/m^2. They found significant differences between all three injury classes ("very slight," "slight to moderate," and "moderate to severe"). It is probable that injury classes 1 and 2 from this study would fall into their "very slight" class, and class 3 would fall into their "slight to moderate" class. Their classification system may better represent physiological processes related to visible ozone injury. The visible ozone injury found in the San Bernardino Mountains was much more severe than at the Oriole Lake study site.

Since "true" fresh weights were not measured, only a relative comparison can be made with "saturated" moisture content (SMC). SMC is a measure of the moisture holding capacity of the needles. SMC was not significantly different among the injury classes, which indicates a similar moisture holding capacity (Figure 2b). Without more information, the significance of this finding cannot be determined. The number of whorls per branchlet declined as injury class increased (Figure 3b). This has been reported before in many studies.[2,21] The number of needles on 1-year-old (1986) whorls also declined as injury class increased. A similar decline was observed for fumigated slash pine seedlings.[22] While Coyne and Bingham found needles to be shorter with increasing injury class, the data from this study were inconclusive (Figure 5a).[10] Likewise, needle area data did not show consistent results (Figure 5b). The large variability of the needle weight and morphology data indicate a larger sample size is needed before conclusions may be drawn.

The results from this study indicate that SLW does decrease with increasing visible ozone injury. Other studies have shown that SLW is highly correlated to photosynthesis which, in turn, is related to carbon uptake.[6-9] The decline in whorl retention and SLW with increasing visible ozone injury supports the conclusion that the trees at the Oriole Lake Study site have reduced photosynthetic capacity due to ozone exposure. While these results only apply to the area studied, others have reported similar results.[10,21,22] Results from this study indicate that the ponderosa pine trees at Oriole Lake are being affected by current ozone concentrations, and without effective pollution abatement programs the trees may continue to decline, or may decline at an acclerated pace if ozone concentrations increase in the future.

ACKNOWLEDGMENTS

We thank the Air Quality Division of the National Park Service (Denver, Colorado), without whose support this project would not have been possible. Appreciation also goes to the persons who assisted with the field and laboratory work including M.B. Stebleton and M.L. Heim (seasonal park technicians, Sequoia and Kings Canyon National Parks). Special thanks are extended to M.T. Patterson (University of California, Los Angeles) for his advice and support.

In addition, we thank H.W. Werner (Fish and Wildlife Biologist, Sequoia and Kings Canyon National Parks) for his guidance with the statistical analyses.

REFERENCES

1. P.R. Miller, J.R. Parmeter, Jr., O.C. Taylor, and E.A. Cardiff, "Ozone injury to the foliage of ponderosa pine," *Phytopathology* 53:1072 (1963).
2. P.R. Miller and A.A. Millecan, "Extent of oxidant air pollution damage to some pines and other conifers in California," *Plant Disease Reporter* 55:555 (1971).
3. D.L. Peterson and M.J. Arbaugh, "An evaluation of the effects of ozone injury on radial growth of ponderosa pine (*Pinus ponderosa*) in the southern Sierra Nevada," *JAPCA* 38:921 (1988).
4. D.L. Peterson, M.J. Arbaugh, V.A. Wakefield, and P.R. Miller, "Evidence of growth reduction in ozone-injured Jeffrey pine (*Pinus ponderosa* Grev. and Balf.) in Sequoia and Kings Canyon National Parks," *JAPCA* 37:906 (1987).
5. D.M. Duriscoe, *Cruise Survey of Western Yellow Pine* (*Pinus ponderosa* and *Pinus jeffreyi*) *for Oxidant Air Pollution Injury in Sequoia and Kings Canyon National Parks, California*, Final Report prepared by Eridanus Research Associates under contract for the National Park Service, Air Quality Division, Denver, Colorado, 1988.
6. J.S. Jacobson, "Ozone and Growth and Productivity of Agricultural Crops," in *Effects of Gaseous Air Pollution in Agriculture and Horticulture*, M.H. Unsworth and D.P. Ormrod, Eds, Butterworth Scientific, London, 1982.
7. P.R. Reich, "Quantifying plant response to ozone: a unifying theory," *Tree Physiology* 3:63 (1987).
8. *Plant Photosynthetic Production. A Manual of Methods*, Sestak, J. Catsky, and P.G. Jarvis (Eds.), Dr. Junk N.V. Publishers, The Hauge, 1971.
9. R. Oren, E.D. Schulze, R. Matyssek, and R. Zimmermann, "Estimating photosynthetic rate and annual carbon gain in conifers from specific leaf weight and leaf biomass," *Oecologia* 70:187 (1986).
10. P.I. Coyne and G.E. Bingham, "Variation in photosynthesis and stomatal conductance in an ozone-stressed ponderosa pine stand:Light response," *For. Sci.* 28(2):257 (1982).

11. N.L. Stephenson. *Climatic Control of Vegetation Distribution: The Role of the Water Balance with Examples from North America and Sequoia National Park, California.* Doctoral Dissertation. Cornell University. Ithaca. New York. 1988.

12. J.G. Moore and T.W. Sisson. *Preliminary Geologic Map of Sequoia and Kings Canyon National Parks, California.* U.S. Geological Survey. Open File Report 87-651. 1987.

13. S.B. McLaughlin and H.A.I. Madgwick. "The effects of position in crown on the morphology of needles of Loblolly pine (*Pinus taeda* L.)." *The Amer. Nat.* 80(2):547 (1968).

14. E.D. Schulze. M.I. Fuchs and M. Fuchs. "Spacial distribution of photosynthetic capacity and performance in a mountain spruce forest of northern Germany." *Oecologia* 29:43 (1977).

15. R.B. Smith. R.H. Waring. and D.A. Perry. "Interpreting foliar analyses from Douglas-fir as weight per unit leaf area." *Can. J. For. Res.* 11:593 (1981).

16. H. Hager and H. Sterba. "Specific leaf area and needle weight of Norway spruce (*Picea abies*) in stands of different densities." *Can. J. For. Res.* 15:389 (1985).

17. W.E. Westman. "Aboveground biomass. surface area. and production relations of red fir (*Abies magnifica*) and white fir (*A. concolor*)." *Can. J. For. Res.* 17:311 (1987).

18. T.T. Kozlowski. T.T. and. J.J. Schumaker. "Estimation of stomated foliar surface of pines." *Plant Physiology* 18:122 (1943).

19. W.R. Harms. "Estimating leaf-area growth in pine." *Ecology* 52(5):931 (1971).

20. Leland Wilkinson. *SYSTAT: The System for Statistics.* Evanston. Illinois. Systat. Inc.. 1986.

21. D.M. Duriscoe and K.W. Stolte. "Photochemical oxidant injury to western yellow pine (*Pinus ponderosa* Laws. and *Pinus jeffreyi* Balf.) in the National Parks of the Sierra Nevada of California." in *Proceedings of the 82nd Annual Meeting and Exhibition of the Air and Waste Management Association.* Anaheim. California. June 25-30. 1989.

22. W.E. Hogsett. M. Plotcher. V. Wildman. D.T. Tingey. and J.P. Bennett. "Growth response of two varieties of slash pine seedlings to chronic ozone exposures." *Can. J. Bot.* 63:2369.

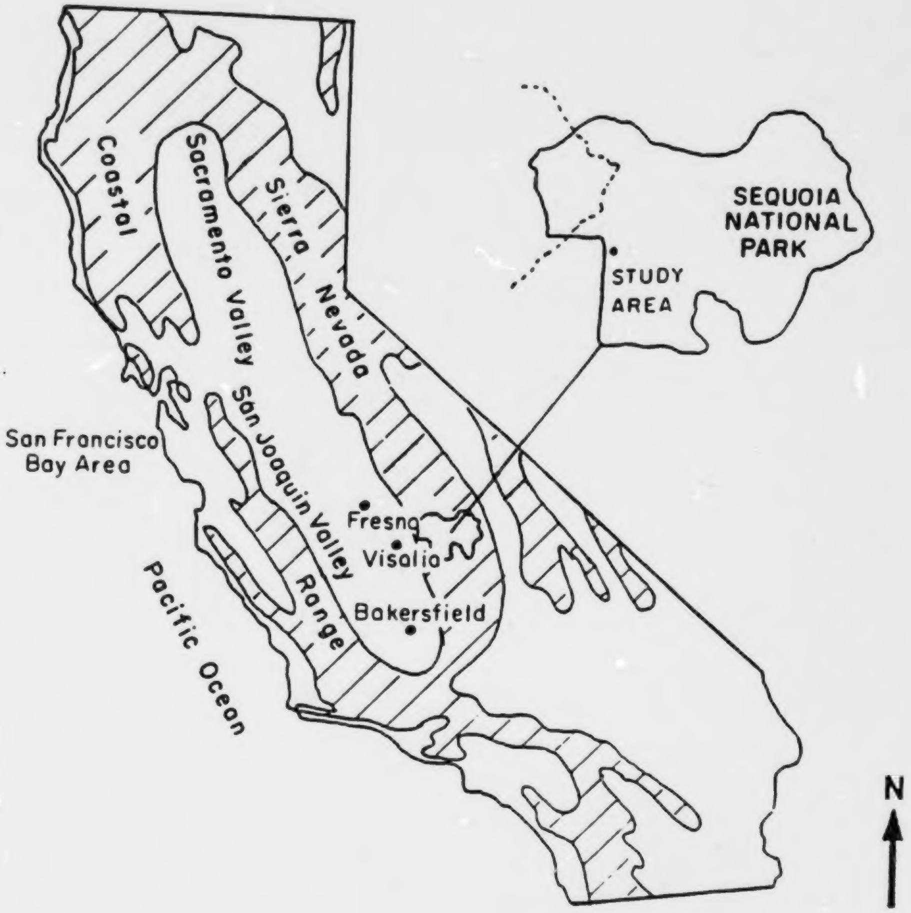

Coastal
Sacramento Valley
Sierra Nevada
San Joaquin Valley
Range
San Francisco Bay Area
Pacific Ocean
Fresno
Visalia
Bakersfield
SEQUOIA NATIONAL PARK
STUDY AREA
N

Figure 1. Map of Sequoia National Park with Oriole Lake Study site (hatched area indicates mountainous regions).

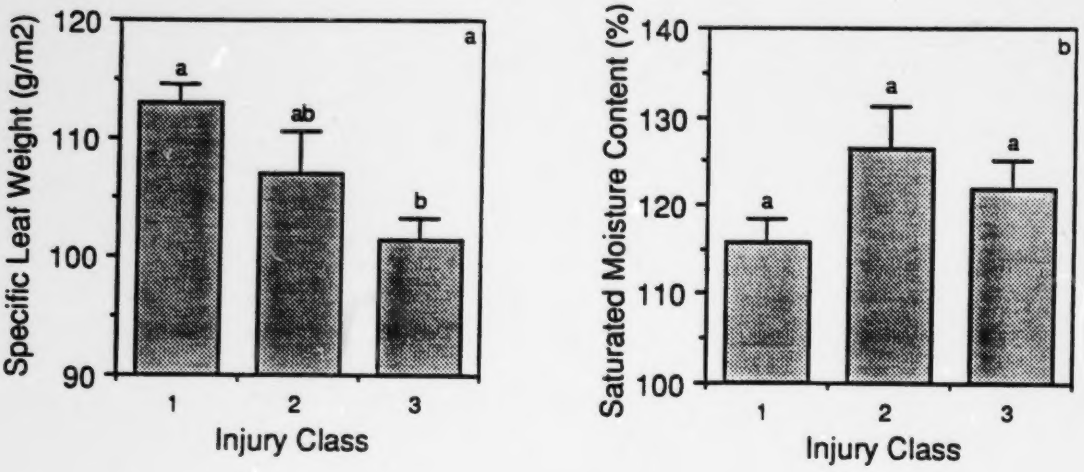

Figure 2. (a) Average specific leaf weight (g/m^2) and (b) Average "saturated" moisture content (%) for 1-year-old (1986) whorls by injury class. Similar letters denote no statistical differences between classes and bars represent standard error.

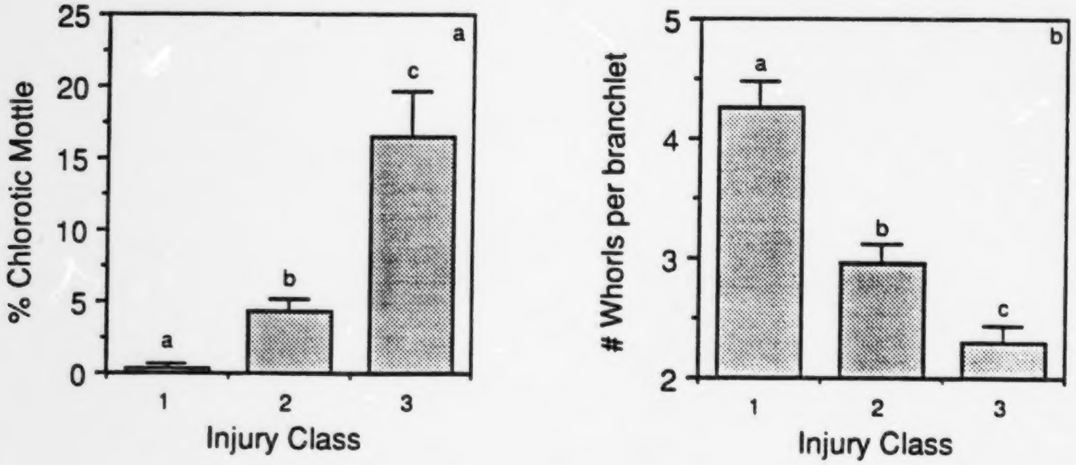

Figure 3. (a) Percent chlorotic mottle averaged over all whorls for each branchlet by injury class. (b) Average number of whorls per branchlet by injury class. Similar letters denote no statistical differences between classes, and bars represent standard error.

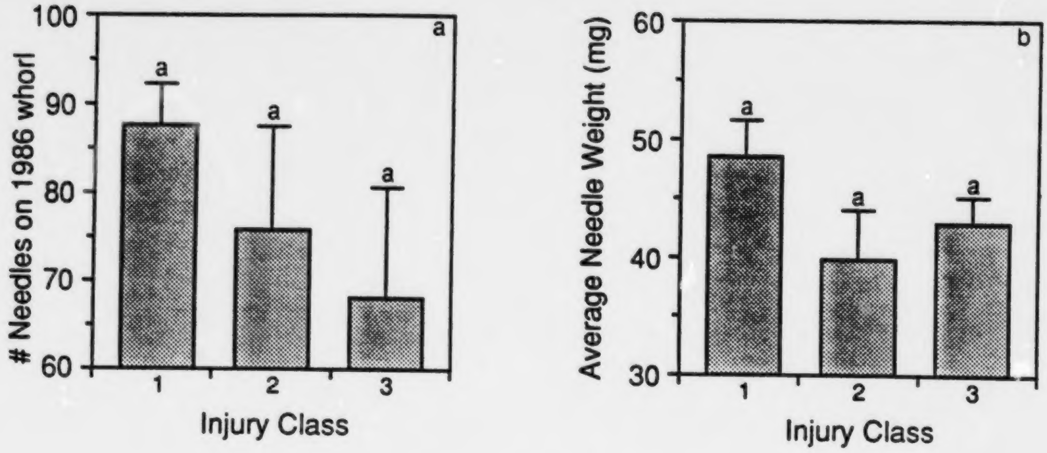

Figure 4. (a) Average number of needles and (b) Average needle weight (mg) on 1-year-old (1986) whorls by injury class. Similar letters denote no statistical differences between classes, and bars represent standard error.

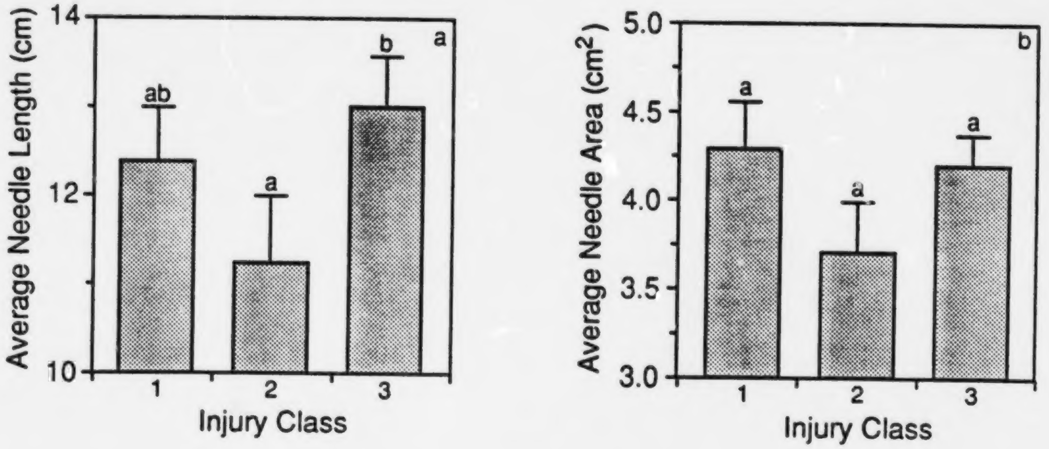

Figure 5. (a) Average needle length (cm) and (b) Average needle area (cm^2) on 1-year-old (1986) whorls by injury class. Similar letters denote no statistical differences between classes, and bars represent standard error.

Seasonal Physiological Responses of Ozone Stressed Jeffrey Pine in Sequoia National Park, California

Mark T. Patterson and Philip W. Rundel

Laboratory of Biomedical and Environmental Sciences
900 Veteran Avenue
University of California, Los Angeles
Los Angeles, California 90024

INTRODUCTION

Symptoms of ozone injury on Jeffrey pine (*Pinus jeffreyi*) are widespread throughout the southern Sierra Nevada mountains of California.[1-5] Chronic phytotoxic levels of ozone occur during summer months with daily ambient concentrations commonly peaking at over 0.1 ppm and 24 hour means ranging between 0.06 and 0.07 ppm/h (National Park Service data). Ozone-induced physiological damage resulting in reduced photosynthetic capacity and productivity has been measured in related pine species[6-9] and other conifer species.[10-12] However, most of the work describing ozone impacts on conifers has been based on short term greenhouse and plantation fumigations of seedlings. Very few field-oriented physiological studies have been conducted. Needle longevity of up to several years in many conifers complicates the assessment of ozone impacts because of the interactions of age and environment with multiple ozone exposures.

Seasonal variation in physiological responses to changing environmental parameters in an ozone-stressed population of Jeffrey pine was studied over an 18-month period. Diurnal courses and daily maximum rates of photosynthesis and stomatal conductances of ozone-resistant and -sensitive trees are compared. Stomatal response to vapor pressure deficits (VPD) between leaf and air, and photosynthetic responses to internal CO_2 concentrations (c_i) are used to discuss observed physiological differences between ozone-sensitive and -resistant groups of trees.

EXPERIMENTAL METHODS

Field studies were performed on natural populations of *Pinus jeffreyi* occuring in the mixed conifer montane forests of Sequoia National Park in the southern Sierra Nevada, California. These populations show a wide range of ozone injury symptoms. Two experimental categories of trees were defined—resistant and sensitive—based on the relative expression of visible ozone symptoms. Individuals resistant to ozone generally retained 4–5 years of needles and did not show any visible ozone injury symptoms. Sensitive individuals were defined as having retained only two years of needles (1986 and 1987 growth) with chlorotic mottle, a characteristic symptom associated with ozone injury. Visible ozone injury was expressed as a percentage of the total needle surface area covered by chlorotic mottle. Trees were selected for uniform size (5–8 m in height) and canopy position (open grown) to facilitate access to canopy and to minimize physiological differences caused by canopy position.

Photosynthesis and transpiration were simultaneously measured using a LICOR 6200 portable photosynthesis system. Leaf conductance values and intercellular CO_2 concentrations (c_i) were calculated from these parameters.[13]

Diurnal gas exchange measurements were made on representative trees in each sampling category. All diurnal measurements were taken with needles initiated in 1986. Maximum photosynthetic rates were measured during the morning hours when trees were most physiologically active. Ten to 20 trees of each sampling category were monitored bi-weekly during summer months when ozone levels were high and approximately bi-monthly during the rest of the year when ozone levels were low. Three replicates from each tree and needle age were taken during each sampling period. Predawn and midday water potentials were measured using a Schoalander-type pressure bomb.

Photosynthetic responses to c_i and stomatal responses to changing vapor pressure deficits (VPDs) between leaf and air were determined using a portable steady-state gas exchange system (Armstrong Enterprises). Desired CO_2 concentrations were mixed from cylinders of CO_2-free air and 1% CO_2 in nitrogen using mass flow controllers. VPD was controlled with a temperature-controlled copper block humidifier by cooling water-saturated air to a desired dew point temperature. Leaf temperatures and light levels were held constant (20° C and 800 $\mu mol/m^2/s$, respectively) for all measurements. Stomatal conductance and c_i values were calculated from equations derived by von Caemmerer and Farquhar.[13]

Ambient ozone levels were monitored by the National Park Service at a site adjacent to the study area. A Dasibi ultraviolet photometer was used to measure concentrations of ozone which were averaged over 24 hours and reported as hourly means.

RESULTS

Photosynthetic rates varied with season and between resistant and sensitive groups of trees (Figure 1). Stomatal conductance (g) also varied especially during periods of high VPD. Resistant trees maintained lower stomatal conductances, and consequently lower maximum photosynthetic rates during the 1987 growing season (July–September), than sensitive trees. However, this relationship reversed during the 1988 growing season. Maximum photosynthetic rates dropped in both groups of trees during the summer of 1988, but sensitive trees consistently maintained photosynthetic rates that were 20–30% lower than resistant individuals. By September, needles of sensitive trees had prematurely abscised. Resistant trees retained their needles, although both photosynthesis and stomatal conductance were at seasonal low values in September. A recovery of both stomatal conductance and photosynthesis after fall precipitation was evident in resistant trees.

Diurnal photosynthetic responses suggest different environmental factors being the most important in limiting daily photosynthetic gains during different seasons. Figure 2 shows representative photosynthetic and conductance rates over the course of a day in sensitive and resistant plants during summer and winter seasons. In summer, high VPDs reduce stomatal conductance which limits photosynthetic rates and consequently limits carbon gain. Winter photosynthetic rates are limited to a greater extent by light. Summer photosynthetic and conductance rates were lower for resistant trees than for those of sensitive trees, possibly reflecting a differential sensitivity of stomates to changes in VPDs.

Representative stomatal responses of sensitive and resistant trees to changes in VPD are presented in Figure 3. Over a range of VPD characteristic of field conditions, stomatal response to changing VPDs was relatively sluggish in trees showing ozone injury. Sensitive trees maintained greater stomatal conductances during periods of low relative humidity which may result in greater CO_2 and ozone uptake rates when compared to resistant trees.

Photosynthetic responses to internal CO_2 concentrations can be used to assess the general health of the photosynthetic apparatus.[13,14] Sensitive trees show a 25% slower initial increase in photosynthesis to increasing c_i indicating a lower carboxylation efficiency (Figure 4). CO_2 saturated photosynthetic rates were 20% lower for sensitive trees suggesting possible injury to electron transport or RuBP regeneration mechanisms of the photosynthetic apparatus. Both Stomatal responses to VPD and photosynthetic responses to c_i were determined from needles initiated in 1986 during the summer season of 1988.

Predawn and midday water potentials did not differ appreciably between the two experimental groups of trees. Predawn water potentials were lowest in the summer months, ranging between -1.5 and -1.3 MPa, and were highest in the fall and winter months, ranging between -1.1 and -0.7 MPa. Similar seasonal patterns of midday water potentials were measured with summer lows ranging between -2.1 and -1.8 MPa, and winter values ranging between -1.7 and -1.4 MPa. Water potential values cannot account for differences in sensitivities to ozone between resistant and sensitive groups of trees. However, loss of transpiring needle surface area in sensitive trees due to premature abscision may allow for greater stomatal conductances while maintaining a physiologically active range of tissue water potentials.

DISCUSSION

The physiological responses of an ozone-stressed population of Jeffrey pine showed differences both between seasons and between groups of ozone-sensitive and -resistant trees (Figures 1 and 2). Gross patterns of maximum photosynthetic rates and stomatal conductances were similar between the two experimental groups of trees; however, relative magnitudes differed. During the growing season in 1987, sensitive trees showed higher maximum photosynthetic rates and stomatal conductance values than resistant trees. This pattern changed during the next growing season (1988) when resistant trees exhibited higher photosynthetic rates but showed similar stomatal conductance values. These data suggest that the physiological expression of ozone injury may change with time and exposure and highlights the importance of long term studies. The initially higher assimilation rates of sensitive trees may reflect higher intrinsic stomatal conductances of sensitive individuals[8,14] or, conversely, may result from a photosynthetic compensation to injury.[15,16] Additional data are required to develop a more conclusive understanding of these results.

The results from the diurnal courses of stomatal conductance and photosynthesis indicate different limiting environmental factors during summer and winter seasons (Figure 2). Jeffrey pines are metabolically active throughout the year with substantial carbon assimilation occuring in winter months. The premature abscision of potentially photosynthetic needles in sensitive trees can lead to lowered stored reserves and lowered growth potential for the following growing season. In addition, the relatively higher stomatal conductance values in winter months for both sensitive and resistant trees indicate a greater susceptibility to injury during episodes of elevated ozone concentrations during the winter.

Differences in carboxylation efficiencies between resistant and sensitive trees are evident during the summer of 1988 (Figure 4). Sensitive trees exhibited a slower increase in photosynthesis as c_i was increased, and also showed lower maximum rates of photosynthesis to saturating levels of CO_2. These data suggest physiological damage to the photochemistry or biochemistry of the photosynthetic process in sensitive individuals[13] and support results obtained from other studies on ozone-stressed pines.[8,14]

Stomatal behavior may also be impaired in trees showing visible ozone injury. Guard cells of sensitive trees appear to be less responsive than guard cells of resistant trees to changes in VPD (Figure 3). As a consequence, sensitive trees had lower stomatal conductance values at high VPDs when compared to resistant trees. These results may explain, in part, the initially higher photosynthetic rates of sensitive trees during periods of low relative humidity. Moreover, episodes of high ozone levels are most frequently associated with hot, dry weather, and the impacts of ozone on physiological processes could differ between individual trees based on their stomatal control. Greater ozone uptake would occur in trees that maintained greater stomatal conductances. Stomatal function could be impaired by ozone-induced increases of membrane-bound permeability of guard cell plasmalemmas[15,16] or inhibition of membrane-bound K^+ pumps.[18] The difference between sensitive and resistant trees in stomatal behavior may reflect ozone-related damage to guard cells in sensitive individuals. Quantifying physiological responses of natural populations of Jeffrey pine to chronic exposures of ozone will require long term integration of ecological and physical environmental factors.

ACKNOWLEDGMENTS

This research is supported by the Air Quality Division of the National Park Service through a research contract from Holcomb Research Institute, Butler University. We thank the staff of Sequoia and Kings Canyon National Parks for their support and cooperation in the field. This work greatly benefited from support and discussions with Ken Stolte, David Parsons, Dan Duriscoe, and Diane Ewell.

REFERENCES

1. J. Pronos, D. Volger and R. Smith, "An evaluation of ozone injury in the southern Sierra Nevada," USDA Forest Service, Report No. 78-1, 1978.

2. W. Williams, "Air pollution disease in the Californian forests. A baseline for smog disease on ponderosa and Jeffrey pines in Sequoia and Los Padres National Forests," *Env. Sci. Tech.* 14:179 (1980).

3. T.E. Warner, D.W. Wallner, and D.R. Volger, "Ozone injury to ponderosa and Jeffrey pines in Sequoia National Park," *Proceedings First Biennial Conference of Research in California's National Parks*, University of California, Davis, 1982, p. 107.

4. D.W. Wallner and M. Fong, "Analysis of ozone injury to ponderosa and Jeffrey pines in Sequoia and Kings Canyon National parks, Final Survey results 1980-1982," Resource Management, Sequoia National Park, California, 1982.

5. D.M. Duriscoe, "Evaluation of ozone injury to selected tree species in Sequoia and Kings Canyon National Parks," Final Report No. 122, Holcomb Research Institute, Butler University, Indianapolis, Indiana, 1987.

6. J. Parmeter, R. Bega, and T. Neff, "A chlorotic decline of ponderosa pine in southern California," *Plant Dis. Rep.* 46:269 (1962).

7. P. Miller and M. White, "Ecosystems," in *Ozone and other photochemical oxidants*, Nat. Acad. Sci., Washington, D.C., 1977.

8. P. Coyne and G. Bingham, "Comparative ozone dose response of gas exchange in ponderosa pine stands exposed to long term fumigations," *JAPCA* 31:38 (1981).

9. P.J. Temple, "Injury and growth of Jeffrey pine and giant sequoia in response to ozone and acidic mist," *Env. Exp. Bot.* 28(1):37 (1988).

10. E. Tseng, T.R. Seller, and B.I. Chevone, "Effects of ozone and water stress on greenhouse grown Fraser fir seedling growth and physiology," *Env. Exp. Bot.* 28(1):37 (1988).

11. R. Zimmerman, R. Oren, E.D. Schulze, and K.S. Werk, "Performance of two *Picea abies* stands at different stages of decline," *Oecologia* 76:513 (1988).

12. G.E. Taylor, Jr., R.J. Norby, S.B. McLaughlin, A.H. Johnson, and R.S. Turner, "Carbon dioxide assimilation and growth of red spruce (*Picea rubens* Sarg.) seedlings in response to ozone, precipitation chemistry, and soil type," *Oecologia* 70:163 (1986).

13. S. von Caemmerer and G.D. Farquhar, "Some relationships between the biochemistry of photosynthesis and the gas exchange of leaves," *Planta* 153:376 (1981).

14. P. Coyne and G. Bingham, "Variation in photosynthesis and stomatal conductance in an ozone stressed ponderosa pine stand: light response," *Forest Sci.* 28:257 (1982).

15. S. von Caemmerer and G.D. Farquhar, "Effects of partial defoliation, changes in irradiance during growth at enhanced p(CO_2) on the photosynthetic capacity of leaves of *Phaseolus vulgaris* L.," *Planta* 160:320 (1984).

16. R.L. Heath, "Oxidant air pollutants and plant injury," in *Models in Plant Physiology and Biochemistry*, CRC Press, Boca Raton, Florida, 1987, p. 63.

17. L. Evans and I Ting, "Ozone-induced membrane permeability changes," *Amer, J. Bot.* 60:155 (1973).

18. P.J. Dominy and R.L. Heath, "Inhibition of the K^+-stimulated ATPase of the plasmalemma of pinto beans by ozone," *Plant Physiol.* 77:43 (1985).

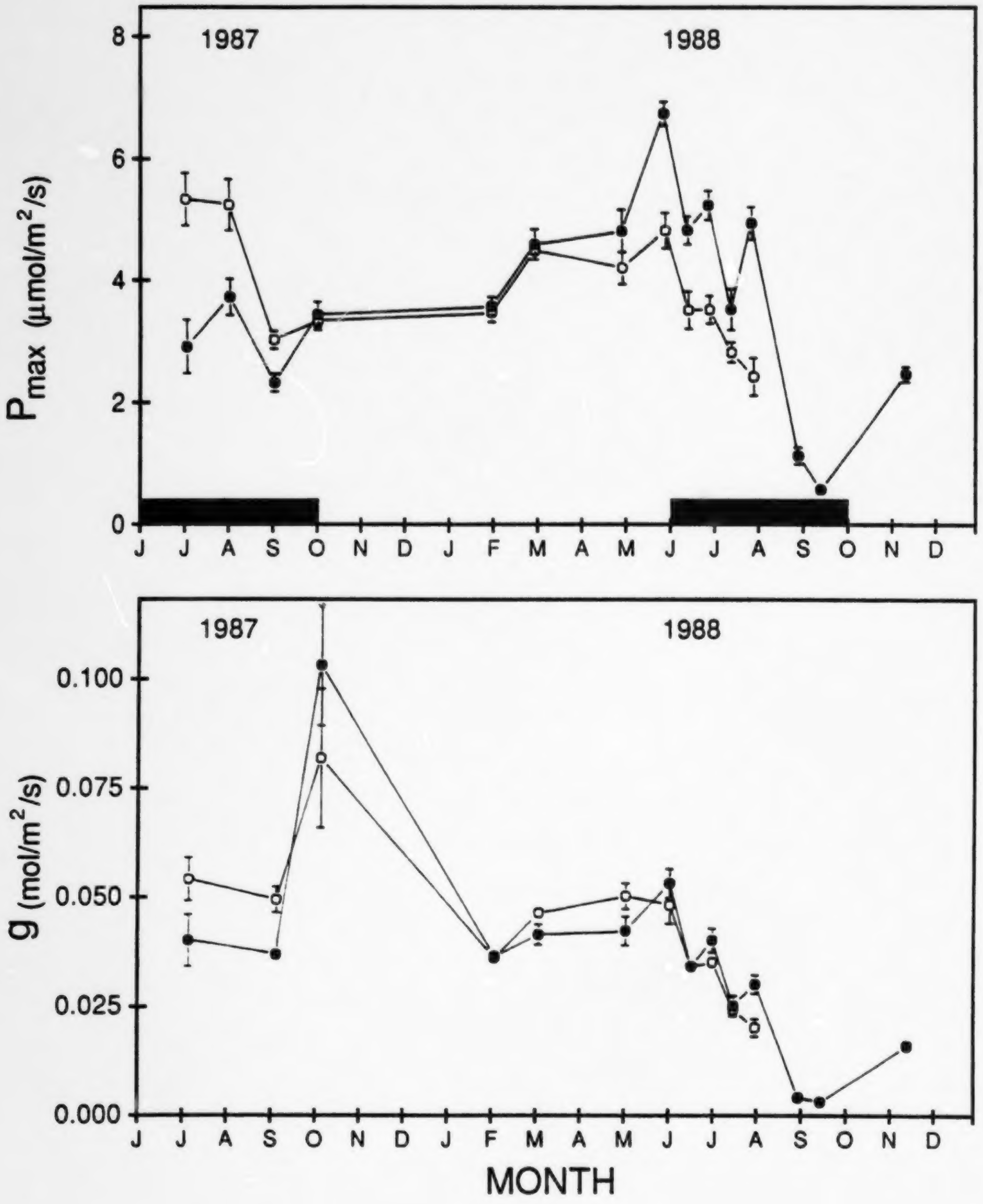

Figure 1. Seasonal course of maximum photosynthetic rates (Pmax) and stomatal conductance (g) in sensitive (open circles) and resistant (closed circles) groups of trees. Data points represent means ± SE; n=9-35. Bars at bottom of figure indicate periods of elevated ozone.

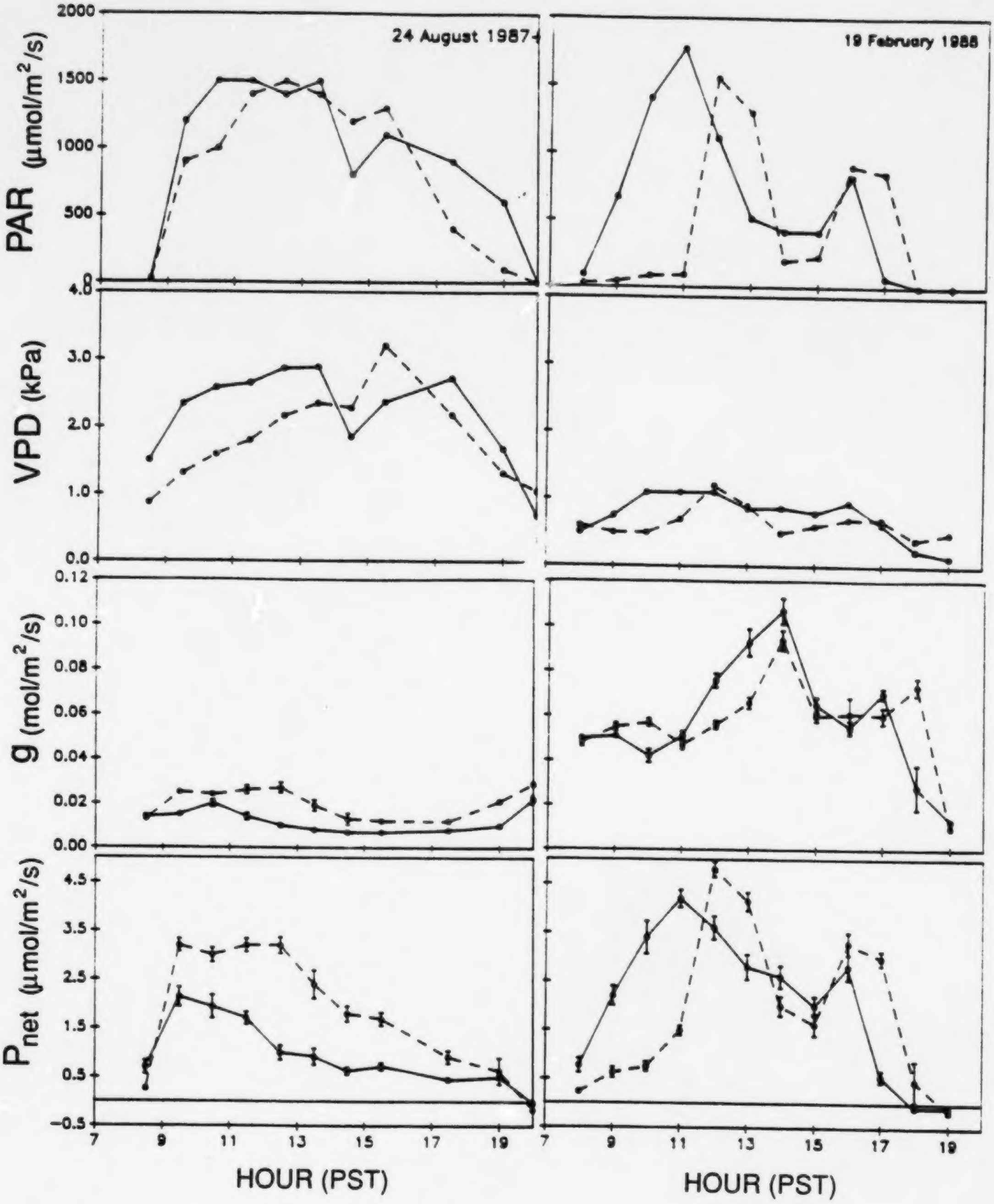

Figure 2. Summer and winter diurnal patterns of photosynthetically active radiation (PAR), vapor pressure deficits (VPD), stomatal conductance, and photosynthesis. Data represent means (± SE) of ten measurements from representative sensitive (dashed lines) and resistant (solid lines) trees.

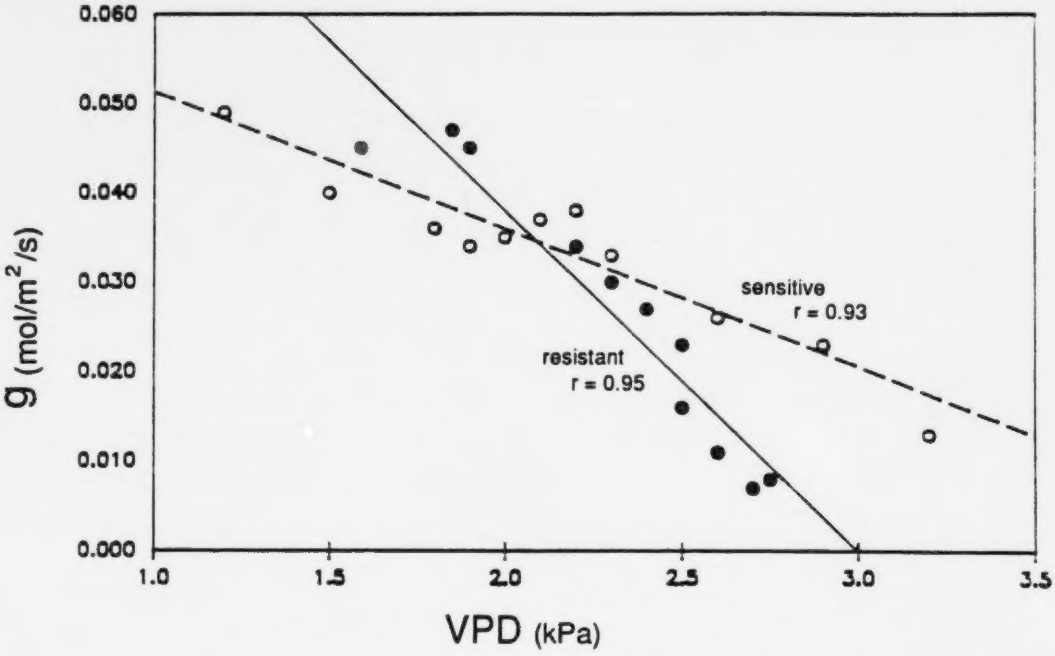

Figure 3. Stomatal responses (g) to changes in vapor pressure deficits (VPD). Sensitive individuals have a more sluggish response to changes in VPD than resistant trees, suggesting possible impairment of guard cell function. The r values presented are from least square regressions.

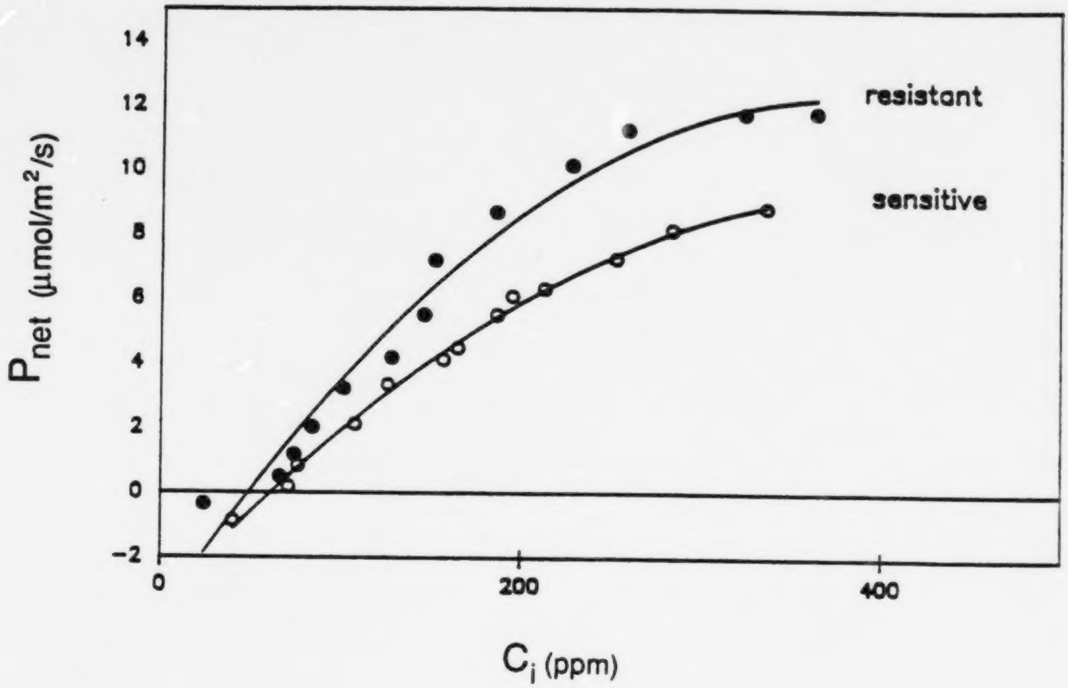

Figure 4. Photosynthetic assimilation (Pnet) responses to internal carbon dioxide levels (c_i). Sensitive individuals had ca. 20% chlorotic mottle over their needle surface area. Both responses were performed on needles initiated in 1986.

Photosynthetic Response of Giant Sequoia Seedlings and Rooted Branchlets of Mature Foliage to Ozone Fumigation

N.E. Grulke[1]
Paul R. Miller[1]
R.D. Wilborn[1]
and Sabine Hahn[2]

[1] *Forest Service, U.S. Department of Agriculture,*
Pacific Southwest Forest and Range Experiment Station
4995 Canyon Crest Drive
Riverside, CA 92507

[2] *Lehrstuhl Botanik II*
Institute Universitat Wurzburg
Wurzburg, West Germany

INTRODUCTION

Fossil fuel consumption results in the production of NO_x, SO_2, CO, and CO_2. The photolysis of NO_x and hydrocarbons yields ozone. Emissions produced in the San Francisco Bay area and in the San Joaquin Valley regularly reach the central Sierra Nevada Mountains.[1,2] Ozone levels commonly exceed 10 pphm within Giant Forest sequoia grove at Sequoia National Park, California (Figure 1). Current ambient ozone levels result in foliar injury to both ponderosa (*Pinus ponderosa* [Dougl.] Laws.) and Jeffrey pines (*P. jeffreyi* Grev. and Balf.),[3] and in decreased radial growth of large-diameter Jeffrey pines growing on poor sites.[4] Both ambient and elevated atmospheric ozone were shown to reduce shoot, root, and total plant biomass, and to induce visible injury on giant sequoia seedlings (chlorotic mottling, necrosis).[5]

Giant sequoia occupies a relatively narrow latitudinal (35°51'N to 39°03'N) and elevational zone (1,525 to 2,290 m) on the western slopes of the Sierra Nevada[6] in many disjunct groves. Low winter temperatures at higher elevations and latitudes, and increased drought stress and inadequate insulating winter snow cover at lower elevations and latitudes have been cited as the primary microenvironmental restrictions on the success of seedling establishment. Sequoia groves are found in moist drainages or meadow margins, with adequate light levels from seedling through sapling stages,[7,8], and typically depend on fire to clear duff layers for active seed germination.[9,10]

This study identifies the physiological effects of O_3 on seedlings and rooted branchlets of mature foliage of giant sequoia (*Sequoiadendron giganteum* Bucholz.). The physiological effects of O_3 are documented, but results frequently conflict. O_3 fumigation has been shown to have no effect on photosynthesis in some conifer species,[11,12] but has reduced conifer photosynthesis in most other studies of conifers.[13-18] Physiological responses of giant sequoia seedlings and rooted branchlets of mature foliage were tested after June through September treatments of clean air (charcoal-filtered air) and O_3 was applied at 50% above ambient levels (to dust-filtered, ambient air). For first-year seedlings, differences in light compensation point, net assimilation, and dark respiration were tested. The current year's tissue of

Preceding page blank

rooted branchlets was tested for differences in net assimilation and leaf conductance between control and elevated O_3 treatments. Net assimilation of rooted branchlets was also compared with that of seedlings.

METHODS

Research Site

The study site was located at 1,920 m elevation, in Giant Forest Grove, Sequoia National Park, 150 m west of the employee housing area at Highlands. Fumigation chambers operated from June 4 through September 15, 1988, with gaps in fumigation indicated in Figure 1 due to a lightning strike, system calibrations, and adjustment of the control program. Physiological characteristics of seedlings from two treatments were analyzed: (1) charcoal-filtered air (controls); and (2) ambient air with additional O_3 added to approximate a 50% increase in O_3 concentration (elevated O_3 treatment).

Three sequoia monarchs (>50 m tall) were present within 30 m of the study site, with a mixed understory of large sequoia saplings (25–30 m tall), white fir (*Abies concolor* [Gord. & Glend.] Lindl.), sugar pine (*Pinus lambertiana* Dougl.), and Jeffrey pine (*Pinus jeffreyi* Grev. & Balf.). Sequoia seeds were collected in 1987 at this site and germinated in March, 1988, in leach tubes (3.9 cm dia.) containing grove soil in greenhouses at the Riverside Fire Laboratory. Branchlet cuttings from mature trees (approximately 20 cm in length) were collected by park personnel in 1987, dipped in a root promoter, allowed to root under intermittent mist, and then potted in 10.2 cm square pots in a peat/perlite mixture. Seedlings and rooted branchlets were transferred to the field site in early June and received only water (no nutrients) at biweekly intervals through the growing season.

Fumigation

Fumigation chambers were 2.13 m in diameter and were 2.2 m high with an open top.[19] Chambers were constructed of 3 aluminum hoops with 4 supporting vertical aluminum tubes. The aluminum frame was covered with clear vinyl plastic (Kreen—mention of trade names or products is for information only and does not imply endorsement by the U.S. Department of Agriculture), with a single layer on the top half and a double layer plenum in the lower half of the wall through which treatment air was supplied through evenly spaced holes (2.5 cm dia.) on the interior wall. Blower boxes (1/3 hp squirrel cage) provided a chamber exchange rate of 2/min. Fiberglass dust filters were in place for all chambers, and activated charcoal filters were used also for control treatments.

Instrumentation was housed in a trailer on site. Dry air was provided by a heatless air dryer (Puregas, Model HF200) to an O_3 generator (Griffin Technics, Model GTC-0.5B). O_3 was supplied through 0.25-cm Teflon tubing to a stainless steel manifold, through precision rotometers (Matheson, Model E517A), then out to the elevated O_3 treatment chambers. A vacuum pump continuously sampled air from a central position in each chamber. Sample air from each chamber was directed to a scanning valve (Scanivalve, with custom made electronics), which allowed sequential sampling at 2.5 min intervals. Ambient air was sampled continuously upwind from chambers to prevent contamination. O_3 concentrations were determined with an O_3 photometer (Dasibi, Model 1000 AH), which was calibrated at 2-week intervals. Instantaneous O_3 concentration of the ambient air sample was used to control the voltage supplied to the generator to produce O_3 on demand. Fine adjustments in O_3 distribution to the chambers was achieved by manually adjusting the rotometers.

Treatments were applied 24 h daily. Data sampling intervals (O_3 concentrations, air temperature at seedling level, soil temperature at 5 cm, and total global radiation (LICOR 200SZ) were controlled by a GW-Basic control program on an AT&T computer (PC 6300)[20] in conjunction with a data acquistion system (Keithley System 570). Data were automatically stored on a disk and printed after each sampling interval (1 h).

Gas Exchange of Seedlings

Two seedlings from each of four chambers of each treatment (8 for control and 8 for elevated O_3) were sampled for gas exchange measurements. CO_2 exchange and leaf water vapor were measured with a LICOR 6200 photosynthetic system (Lincoln, NE) with an installed air bypass system. Measurements were made outside fumigation chambers. All plants were well-watered the evening before and the morning of gas exchange measurements. Each measurement included net assimilation (Net Ps), photosynthetic photon flux density (PPFD), air and leaf temperature, and vapor pressure deficits (VPD). Means and standard errors were obtained from 2 to 4 runs (3-4 observations of gas exchange averaged together per run) on each plant over 1-5 min. Leaf area for each seedling was determined by a photograph taken from directly overhead with a millimeter rule included for scale. Leaf surface area that intercepted light directly (overlapping needle surface area excluded) was determined by cutting out the image and weighing the replica. The photographic paper density was determined from three 1x10-mm strips from the ruler image included in each photograph.

A small cuvette (75.60 cm^3) was designed and constructed for measuring the gas exchange of the seedlings (Figure 2). The seedling cuvette was cylindrical, 6.8 cm tall, 3.8 cm dia., with a standard LICOR cuvette fan set at a 15° angle pointed down toward the container-grown seedling, generally 2-3 cm away from the foliage. The cuvette was contructed of Acrylite lined with Teflon film and a Mylar top. The inside of the cylinder was lathed to fit over the small seedling pots ("D" cell), and the contact between cuvette and pine cell was sealed with Terostat. The soil surface was sealed with a cylindrical disk of white foam, covered with self-sticking Teflon film. A radial slit was cut in the foam disk for the stem of the seedling. An empty cuvette analogous to the standard setup (without seedling, but with moistened soil under foam disk) was tested for leaks by monitoring gas exchange. The gas exchange of the empty cuvette was unmeasurable after gas exchange rates were adjusted for (small) CO_2 leak rates.

To develop seedling light response curves, four frames consisting of a light source (GE-ESD projection quartzline multi-mirror bulb, socket #2CX-30, Kennedy Webster, Chicago, IL), heat/light separation mirror (reflection 420-630 nm, Optical Coding Lab, Inc., Santa Rosa, CA), and neutral density filters (0.32 cm Plexiglas, 44% [model 2094] and 23% transmission [model 5054], S&W Plastic Stores, Riverside, CA) were constructed to control light intensity. Muffin fans (472 cc s) were used to remove heat from the cuvette and from behind the heat/light separation mirror on each frame. Temperature of the cuvette was generally 0.2° C greater than ambient air temperature, but did not exceed 0.6° C greater than ambient during measurements. Light response was determined during September 1-4, 1988, for a total of 16 individuals (2 seedlings per chamber, 4 replicate chambers per treatment, 2 treatments). It was possible to measure 4 light levels (averaging 22±1, 108±2, 743±16, 1854±9 μmol/m^2/s) for 4 individuals each morning before ambient VPD and air temperature became limiting (usually after 1030 h). Plants were allowed to equilibrate for 0.5 hr at each light level before gas exchange was measured, and were exposed to decreasing light levels. CO_2 concentrations and heat buildup from light sources were minimized by blowing ambient air into the field laboratory with a large blower box.

No differences between laboratory and external air temperature were found, and CO_2 concentration did not exceed 15 ppm CO_2 above ambient (average 360 vs. 345 ppm). Regression lines were fit to each plant light response after natural logarithm transformation of PPFD ($r \geq 0.956$), and each equation was used to calculate and test for differences in light compensation point with a 1-way ANOVA. Net assimilation at light saturation (1854±9 μmol/m^2/s) was tested with a 1-way ANOVA.

On September 5, 1988, net CO_2 assimilation was measured for 4 plants from each treatment (two replicate chambers per treatment) at 9 sampling periods during the course of 25 h. Gas exchange measurements were plotted for each plant measured, along with concurrent PPFD, air and leaf temperatures (combined for the two treatments), and VPD. Leaf temperatures did not differ significantly for seedlings exposed to the two treatments. Differences in dark respiration between the two treatments were tested between 1800 and 2000 h with a 1-way ANOVA. VPD averaged 2.5 kPa, and leaf temperature averaged 28° C during these measurements.

Gas Exchange of Rooted Branchlets

Five rooted branchlets from the two treatments (control, elevated O_3) were selected for gas exchange measurements. Selection of branchlets was based on production of new tissue since rooting. Too few branchlets rooted in each chamber to test two per chamber per treatment; therefore, data were combined from different chambers within a treatment for analysis. Gas exchange was measured on current year's growth of rooted branchlets from 5 plants in each treatment by using the standard 0.25 l cuvette designed by LICOR. Calculated boundary layer conductance was 2.40 mol $H_2O/m^2/s$ for a rectangle of moistened filter paper with typical leaf surface area. Measurements were made in the afternoon: VPD averaged 2.812±0.1 kPa, PPFD was 669±53 μmol/m^2/s, and air temperature averaged 27.8±0.5°C. Differences in net assimilation were tested between treatments with a 1-way ANOVA within foliage type and with Mann-Whitney U test between foliage types (seedlings and branchlets).

For 20 branchlets of multiple year's growth, a regression was developed between branchlet length and surface area. Leaf area of rooted mature branchlets was calculated by assuming that surface area of the branchlet could be approximated by geometric forms (cylinder for the appressed needle bases on the stem, and cones for the free needle tips). The equation for the regression was

$$y = 0.083x - 0.378 \quad (r = 0.978) \qquad [1]$$

where y is geometric surface area in cm^2 and x is branchlet length in mm.

RESULTS

Light Response of Seedlings

The light response of individual seedlings in control (charcoal-filtered) and elevated O_3 chambers (50% above ambient levels) showed considerable variability within a treatment (Figure 3). Light compensation point in elevated O_3 plants occurred at light levels twice that of controls (95.2±15.5 vs. 59.7±10.3 μmol/m^2/s), and differences were statistically significant at the p = 0.73 level (1-way ANOVA, F = 3.815). Net CO_2 assimilation at light saturation (≈1800 μmol/m^2/s, Fig. 3) differed significantly between control and elevated O_3 treatments (5.424±0.595 vs. 3.027±0.379 μmol CO_2/m^2/s; F = 11.528, p = 0.005). Dark respiration also differed significantly between control and elevated O_3 treatments (-2.546±0.362 vs. -5.286±0.655 μmol CO_2/m^2/s; F = 13.99, p = 0.006).

The difference in light response between the two treatments was tested with a repeated measures, 1-way ANOVA. The effects of elevated O_3 differed significantly (F = 7.416; p = 0.018), and the interaction between treatment and repeated measures was not significant (F = 2.221; p = 0.102). The regression equation for the control was

$$y = 1.526(\ln x) - 6.049 \qquad (r = 0.923) \qquad [2]$$

and for the elevated O_3 treatment was

$$y = 1.219(\ln x) - 6.025 \qquad (r = 0.852) \qquad [3]$$

where y is net assimilation in μmol/m^2/s and x is PPFD in μmol/m^2/s.

Diurnal Course of Seedling Net CO_2 Assimilation

The diurnal course of net CO_2 assimilation is presented for September 5, 1988 (Fig. 4). For most of the day, PPFD was low, generally 60-130 μmol/m^2/s, and VPD and leaf temperatures were extremely high at midday. Four sunflecks of >400 μmol/m^2/s occurred, all lasting 4–15 min (Fig. 4b), and CO_2 exchange was measured a total of 9 times during sunflecks. Net assimilation was graphed for each plant to avoid masking plant response to the infrequent sunflecks and to emphasize the variability in individual plant response to treatments. Plant response to the elevated O_3 treatment was highly variable. Two plants generally had greater net assimilation rates than controls, and two plants had lesser net assimilation rates. One of the plants later died (most negative response). By chance, the two plants exposed to elevated O_3 had greater net CO_2 assimilation and were measured during the three brief sunflecks at 1330 h, and one control plant was measured as light levels were rapidly increasing. An explanation for greater carbon uptake of elevated O_3 plants may be that stomatal control was maintained in control treatments during the high VPDs that occurred midday. However, leaf temperatures between control and O_3 treatments did not differ significantly (F = 0.258, p = 0.638) and do not support lower leaf conductance (and therefore lower assimilation rates) in controls.

Two light regimes were encountered during the diurnal measurements: relatively low light levels, and brief sunflecks. Because CO_2 exchange could not be measured simultaneously on both control and elevated O_3 plants during sunflecks, predicted net CO_2 assimilation based on light response regressions

(Figure 3; equations (2) and (3)) were used to estimate differences in carbon balance for the two treatments (Figure 5). This graph illustrates the probable differences in net carbon balance between the control and elevated O_3 plants. The predicted carbon balance was based on seedling response to light, when VPD, leaf temperature, and soil moisture were not limiting.

Comparison of Net Assimilation of Rooted Branchlets and Seedlings

Net CO_2 assimilation was compared for seedling and rooted branchlets in both treatments (Figure 6). No statistical differences were found between foliage types (seedlings vs. rooted branchlets, Mann-Whitney U test). Within a foliage type, only seedlings showed a significant reduction in net assimilation between control and elevated O_3 treatment (1-way ANOVA).

Similar to results obtained for seedling net CO_2 assimilation at light saturation (Figure 3), net CO_2 assimilation of seedlings was reduced by 44% in control vs. elevated O_3 treatments (4.16 vs. 2.35 μmol $CO_2/m^2/s$), and differences were statistically significant (1-way ANOVA, $F = 6.206$, $p = 0.028$). Comparing ontologically younger (seedlings) with older tissue (rooted branchlets) in control treatments, net CO_2 assimilation for seedlings was 20% greater than rooted branchlets. Although net assimilation of seedlings was measured at a slightly higher light level (743 ± 16 vs. 669 ± 53 μmol/m^2/s), the light level accounts for only 4% of the differences in net assimilation (using regressions developed in Figure 3). Net assimilation of branchlets exposed to elevated O_3 was reduced by 26% relative to controls, but differences were not significant (2.47 vs. 3.34 μmol $CO_2/m^2/s$). Rooted branchlets had greater variability in response to chamber treatments. However, the variability may reflect individual differences in the ability to root rather than differences in plant response to O_3.

Leaf conductance of rooted branchlets was low, and did not differ significantly between control (0.065 μmol $H_2O/m^2/s$) and elevated CO_2 treatments (0.036 μmol $H_2O/m^2/s$; $F = 2.736$, $p = 0.137$). Leaf conductance values cannot be compared between seedlings and rooted branchlets because of the difference in the way leaf area was determined for the two foliage types.

DISCUSSION

These results strongly suggest that elevated atmospheric O_3 concentrations adversely affect carbon balance in giant sequoia seedlings. Significant differences in light compensation point, net assimilation at light saturation, and dark respiration were found between controls and elevated O_3 treatments (Figure 3). Non-simultaneous gas exchange measurements masked differences in diurnal carbon balance between the two treatments (Figure 4). However, predicted CO_2 exchange of control and elevated O_3 plants for a typical light environment of generally low PPFD (60-130 μmol/m^2/s) with brief sunflecks ($4 > 400$ μmol/m^2/s lasting < 15 min each) demonstrate a probable difference in carbon balance between control and elevated O_3 seedlings (Figure 5).

The importance of sunflecks for seedling survival has been demonstrated previously for giant sequoia seedlings,[9,10] other conifer seedlings,[21] and for survival and reproduction of other understory plants.[22,23] Plant response time to increase in PPFD at the initiation of sunflecks could not be measured accurately with available equipment. Because of the infrequent and ephemeral nature of sunflecks and their importance in maintaining positive carbon balance for understory plants.[21] It is important to address the effects of O_3 on response time to sunflecks in future research on giant sequoia seedlings.

Higher light compensation points and reduced net assimilation at light saturation (Figure 3) imply that with increased atmospheric O_3, giant sequoia seedlings will require higher light levels and longer durations of light to maintain a positive carbon balance. Previous research on the interaction of light level and O_3 injury has shown that low light levels and elevated O_3 adversely affect root/shoot ratio, root weight, and height growth of sequoia seedlings relative to high light levels and elevated O_3. Visible symptoms of O_3 injury were also greater, and shoot weight decreased in low vs. high light levels and elevated O_3.[24] High light levels compensating for reduced net assimilation in elevated O_3 treatments is the most likely explanation for the interaction between light and O_3 level.

Rooted branchlets in elevated O_3 treatments had lower net assimilation rates than those of controls (Figure 6). Differences in net assimilation were not statistically significant, but may be biologically important. This observation requires further investigation because no visible signs of O_3 injury have been observed on mature foliage of giant sequoia. Small changes in carbon balance of branches may cumulatively and significantly affect whole tree carbon balance and individual longevity.

In both the seedling and rooted branchlets, individual plant response to elevated O_3 was highly variable. Half of the O_3-fumigated plants had similar carbon balance to control plants, and half had greatly depressed net assimilation and increased dark respiration (Figure 3). Population variability in response to O_3 fumigation (reduction in net assimilation) has also been described for white pine,[25] and some individuals may be more resistant to O_3 injury than others. This variability in plant response may explain some of the discrepancies in reported photosynthetic response to O_3. Future research with genetic variability, tissue age, carefully controlled fumigation and calculation of stomatal O_3 concentrations, preliminary comparison of plants before fumigation, and component analysis of photosynthesis may also clarify apparent discrepancies in plant response to O_3.

ACKNOWLEDGMENTS

We thank J. Wilborn for assistance throughout the field season. T.J. Arkebauer provided essential information for operation of the LICOR 6200, programming alterations for leak calculation, and specifications for the control of light intensities. J. Welles and D. McDermitt at LICOR provided valuable assistance over the phone while we were in the field. This project would not have been possible without the support of the staff at Sequoia National Park, specifically D. Parsons and D. Ewell, and K. Stolte at the Air Quality Division, National Park Service.

REFERENCES

1. C.D. Unger, "The transport of photochemical smog in the Central Valley and the Sierra Nevada Mountains of California," in: *Proc. of the Conf. on Sierra Nevada Meteorology*. Am. Met. Soc. Boston, MA, 1978, p. 38.

2. D.L. Blumenthal, T.B. Smith, D.E. Lehrman, R.A. Rasmussen, G.Z. Whitten, and R.A. Baxter, "Southern San Joaquin Valley Ozone Study," Final Report for Western Oil and Gas Association, Los Angeles, CA. Contract No. 84-8.0.05(2)-07-01 by Sonoma Tech., Inc., and Systems Applications, Inc., STI Report 94100-510-FR, (1985).

3. J. Pronos, D.R. Vogler, and R.S. Smith, Jr., "An evaluation of ozone injury to pines in the southern Sierra Nevada," Report No. 78-1. FIDM, USDA Forest Service, Regional Office, San Francisco, CA, 1978.

4. D.L. Peterson, M.J. Arbaugh, V.A. Wakefield, and P.R. Miller, "Evidence of growth reduction in ozone-injured Jeffrey pine (*Pinus jeffreyi* Grev. & Balf.) in Sequoia and Kings Canyon National Parks," *JAPCA* 37(8):906 (1987).

5. P.R. Miller, "Root and shoot growth during early development of *Sequoiadendron giganteum* seedlings stressed by ozone," Abstract 4-29-2. XIV International Botanical Congress, Berlin.

6. J.D. Blick, "The giant sequoia: a study in autecology," Contract report for the Western Region, National Park Service, 1963.

7. P.W. Rundel, "Habitat restriction in giant sequoia: the environmental control of grove boundaries," *Am. Mid. Nat.* 87:81 (1972).

8. N. Stark, "The environmental tolerance of the seedling stage of *Sequoiadendron giganteum*," *Am. Mid. Nat.* 80:85 (1968).

9 J.L. Donaghey, "The properties of heated soils and their relationships to giant sequoia germination and seedling growth," M.S. Thesis, San Jose State University, San Jose, CA, 1969.

10. R.J. Hartesveldt and H.T. Harvey, "The fire ecology of sequoia regeneration," *Tall Timbers Fire Ecology Conf. Proc.* 7:65 (1967).

11. L. Skarby, E. Troeng, and C. Bostrom, "Ozone uptake and effects on transpiration, net photosynthesis and dark respiration of Scots pine," *For. Sci.* 33(3):801 (1987).

12. J.D. Barnes and A.W. Davison, "The influence of O_3 on the winter hardiness of Norway Spruce," *New Phyt.* 108(2):159 (1988).

13. R.L. Barnes, "Effects of chronic exposure to O_3 on photosynthesis and respiration of pines," *Environ. Poll.* 3:133 (1972).

14. P.B. Reich and R.G. Amundson, "Ambient levels of ozone reduce net photosynthesis in tree and crop species," *Sci.* 230:566 (1985).

15. E.C. Tseng, J.R. Seiler, and B.I. Chevone, "Effects of O_3 and water stress on greenhouse-grown Fraser fir seedling growth and physiology," *Env. Exp. Bot.* 28(1):37 (1988).

16. P.I. Coyne and G.E. Bingham, "Comparative ozone dose of gas exchange in a ponderosa pine stand exposed to long-term fumigations," *JAPCA* 31:38 (1981).

17. D.B. Botkin, W.H. Smith, and R.W. Carlson, "Ozone suppression of white pine net photosynthesis," *JAPCA* 21:778 (1971).

18. P.R. Miller, J.R. Parmeter, Jr., B.H. Flick, and C.W. Martinez, "Ozone dosage response of ponderosa pine seedlings," *JAPCA* 19:435 (1969).

19. A.S. Heagle, R.B. Philbeck, H.H. Roger, and M.B. Letchworth, "Dispensing and monitoring ozone in open-top chambers for plant effects studies," *Phytopath.* 69:15 (1979).

20. W.E. Hogsett, D.T. Tingey, and S.R. Homan, "A programmable control system for determination of the effects of pollutant exposure regimes on plant growth," *Atmos. Environ.* 19:1135 (1985).

21. S.L. Ustin, R.A. Woodward, M.G. Barbour, and J.L. Hatfield, "Relationship between sunfleck dynamics and red fir seedling distribution," *Ecology* 65(5):1420 (1985).

22. R.W. Pearcy and H. Calkin, "Carbon dioxide exchange of C_3 and C_4 tree species in the understory of a Hawaiian forest," *Oecologia* 58:19 (1983).

23. R.L. Chazdon and R.W. Pearcy, "Photosynthetic responses to light variation in rainforest species: I. Induction under constant and fluctuating light conditions," *Oecologia* 69:517 (1986).

24. P.R. Miller, R.D. Wilborn, S.L. Schilling, and A.P. Gomez, "Ozone injury to important tree species of Sequoia and Kings Canyon National Parks," Final Report, submitted to Air Quality Division, National Park Service, U.S.D.I., Denver, CO, 1988.

25. D.B. Botkin, W.H. Smith, R.W. Carlson, and T.L. Smith, "Effects of ozone on white pine saplings: variation in inhibition and recovery of net photosynthesis," *Environ. Poll.* 3:273 (1972).

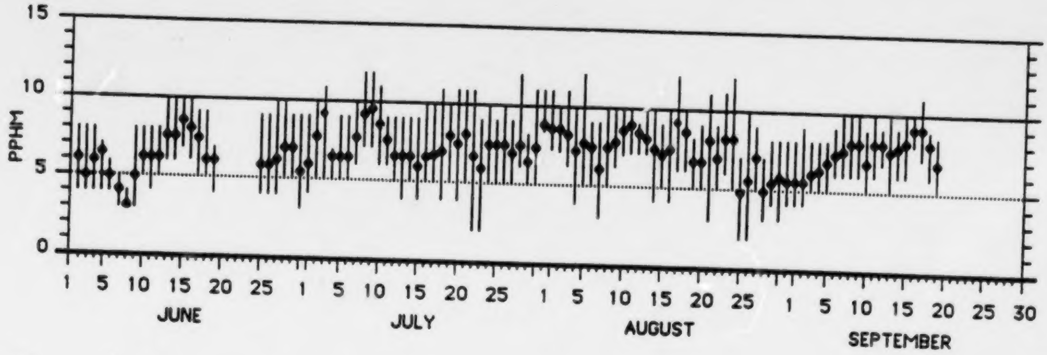

Figure 1. Seasonal course of maxima and minima ambient ozone concentration at study site during the growing season in 1988. Lowest ozone concentrations were often in the morning from 0700 to 0900, and highest ozone concentrations occurred between 1500 and 1700 h.

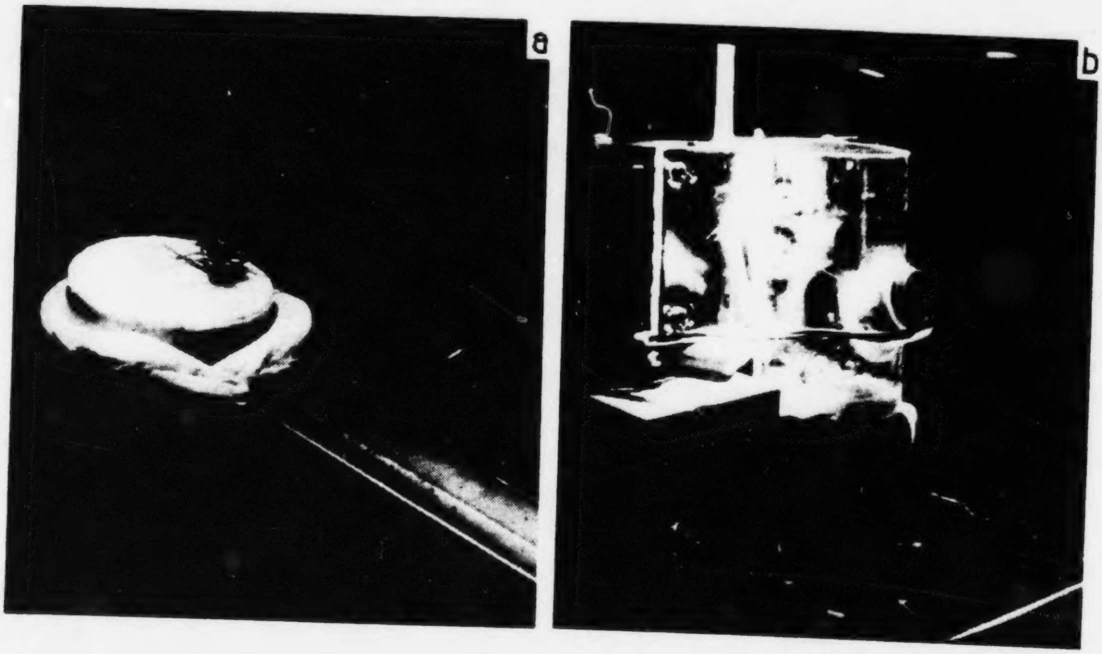

Figure 2. (a) Seedling with Teflon-covered foam disk to seal off soil and root respiration. (b) Seedling in cuvette under artificial light source during determination of light response. Plexiglass plate on cuvette was attached to standard sensor housing of the LICOR 6200 photosynthetic system.

produced from
available copy.

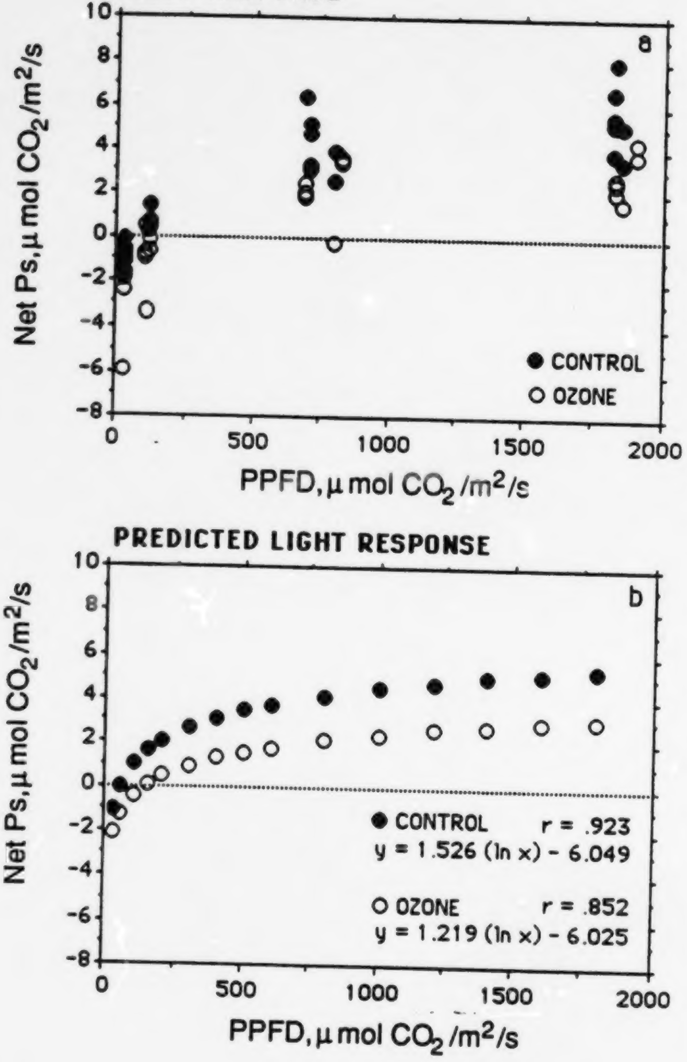

LIGHT RESPONSE

PREDICTED LIGHT RESPONSE

Figure 3. Light response of sequoia seedlings from control and elevated O_3 chambers. Each point in (a) represents the average net assimilation for two to four observations per seedling. Standard errors are not presented for clarity of points, but in most cases are within the boundaries of the circle. Points in (b) represent calculated net Ps from regressions fit to treatment groups in (a).

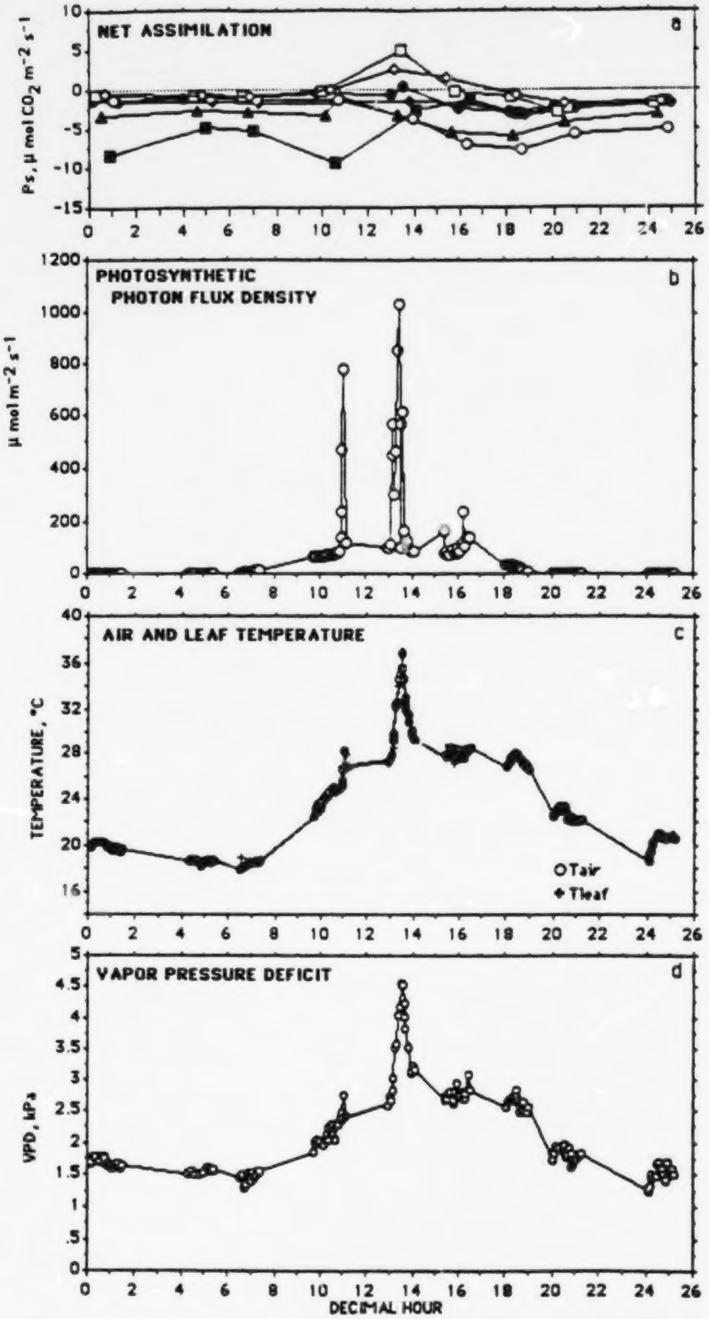

Figure 4. Diurnal course of (a) CO_2 balance (closed symbols represent control; open symbols represent elevated O_3 plants); (b) PPFD; (c) air and leaf temperature; and (d) VPD for control and elevated O_3-treated sequoia seedlings. Net assimilation is presented for all 8 plants to illustrate variability in treatment response.

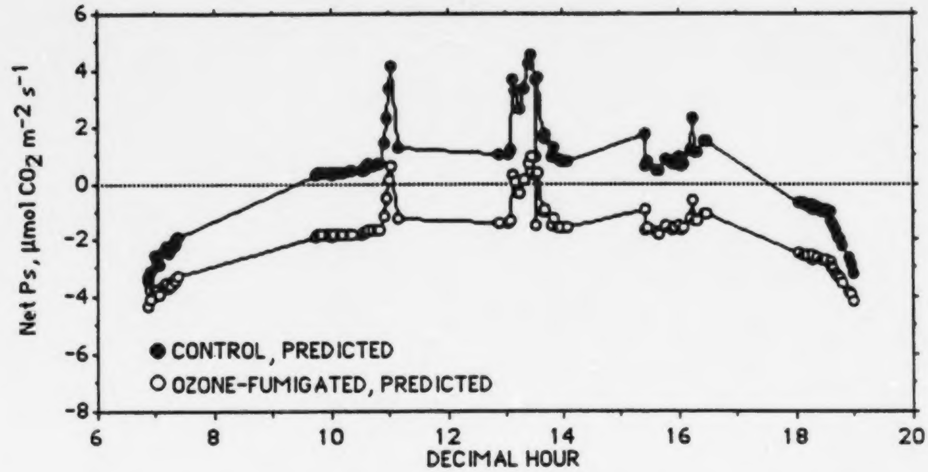

Figure 5. Predicted net CO$_2$ assimilation of seedlings for daylight hours as predicted from the diurnal course of PPFD (Figure 4) and regression lines for light response developed for the two seasonal treatments (Figure 3).

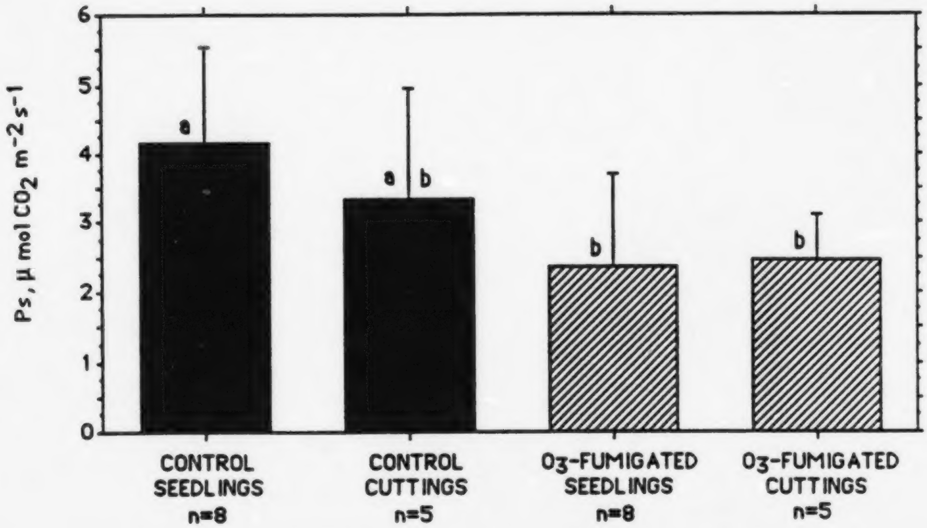

Figure 6. Net CO$_2$ assimilation of seedlings and rooted branchlets of mature foliage from control and seasonally fumigated O$_3$ chambers. Bar represents mean and standard deviation for each group. Differences between treatments and foliage type were tested with a 1-way ANOVA. Different letters denote statistically significant ($p = 0.001$) differences.

Potential Effect of Premature Needle Loss on the Foliar Biomass and Nutrient Retention of Lodgepole Pine

Anna W. Schoettle

USDA Forest Service
Rocky Mountain Forest and Range Experiment Station
240 W. Prospect St.
Ft. Collins, CO 80526

INTRODUCTION

One of the first symptoms of ozone damage to conifers is reduced leaf longevity.[1] The reduction in needle cohort retention is first observed in the lower portion of the crown and progresses upward through the crown.[1] As leaves age, their photosynthetic productivity is reduced by both physiological changes within the leaves and the quality of the environment that surrounds them.[2] Therefore, the leaves that abscise prematurely from trees in ozone-impacted areas are those with the presumed lowest productivity within the crown. The contribution of these old leaves to the carbon assimilation and nutrient reserves of the canopy is unclear.

Reports of reduced radial growth in mature conifers due to ozone are accompanied by reduced leaf retention.[3] Younger trees, however, can show reductions in leaf retention without observable impacts to radial growth.[3] While it seems clear that reductions in leaf longevity precede growth reductions, it is uncertain if the loss of the old leaves is partially or totally responsible for the decreased radial growth.

Lodgepole pine (*Pinus contorta* ssp. *latifolia* Engelm.) was used as a model species to address two questions: (1) What resources would be lost from the canopy by premature leaf abscission? and (2) Is it possible that the loss of these resources could contribute to subsequent reductions in radial growth? I first report on the natural distribution of foliar nutrients and biomass in the canopy of lodgepole pine in its present unimpacted condition in Colorado. Secondly, I discuss which resources would be lost following several different intensities of simulated ozone injury on leaf longevity. Finally I discuss how these impacts could cause growth reductions in lodgepole pine and compare the results to observations made in areas that are already impacted by chronic ozone exposure.

METHODS

Terminology

Throughout this paper I will refer to a "branch" as an axis that originates from the bole of the tree. The terminal of a branch is foliated. A "lateral" is a foliated axis that originates from the main axis of a branch or from another lateral. Therefore, the foliage of a branch is supported on the terminal of the main axis and on the attached laterals. The term "foliar whorl retention" is used throughout this paper to mean the maximum age of existing foliage on a given lateral. A lateral with a whorl retention of 10 means there were needles present in 11 cohorts, that is, current year needles and needles that were produced annually for the previous 10 years. This term is being used as a synonym of "maximum leaf longevity" and "needle retention." A "foliar age class" is the foliage that was still attached to the segment of a lateral that was produced in a given year. Bud scale scars on the axis of the laterals were used to locate and identify each annual growth segment and the age of the attached foliage.

Site

The site, just east of Fraser, CO in the central Rocky Mountains at an elevation of 3200 m, supported an even-aged lodgepole pine stand with a mean tree age of 75 years and a stand density of 2133 stems/ha. The height of the trees in the stand varied by less than one meter, with a mean height of 12.8 m. This site was selected because it is currently receiving low pollutant deposition. The central Rocky Mountains offer the opportunity to assess the distribution of biomass and nutrients within the canopy of healthy trees uncomplicated by the subjective selection of healthy vs. declining trees in an impacted site.

Sampling

Four representative trees in the stand were felled in August of 1987. The foliated portion of each canopy was divided into three segments of equal length. The average length of the canopy for the four trees was 8.3 m (± 1.3 m). Two branches were removed at the bole from the middle of each canopy third, for a total of six branches removed per tree. Each branch was dissected into its component laterals, and the foliage from each lateral was divided and sorted by needle age. The foliage was oven dried at 80° C and weighed. The proportion of the total foliage on the branch (sum of foliage weights for all of the laterals) for each needle age class was calculated and averaged for the two branches for each canopy section and for each tree. Total foliar biomass was estimated from the cross-sectional sapwood area at 1.4 m above the ground by using the equations of Pearson et al.[4] The distribution of foliar biomass by canopy third for each tree was estimated using the ratios of Gary.[5] The biomass of each age class in each canopy position was computed.

Nutrient Analysis

The pooled foliage samples for each age class from all of the laterals from each branch were ground in a Wiley mill (40 mesh) and digested by standard methods.[6,7] Calcium, magnesium, and potassium were detected by inductively coupled plasma spectroscopy, and nitrogen and phosphorous were determined using a flow injection analyzer (Lachet, Mequon, WI). Nutrient concentrations are expressed on a leaf dry weight basis.

Simulation Scenarios

Four scenarios were developed to reflect the progression of ozone injury to pines, as observed in California[1,3] (Table I). Ozone exposure first reduces needle retention in yellow pines on laterals in the lower portion of the crown. As exposure to ozone is increased, the reduction in whorl retention progresses upward through the crown. In the most extreme ozone exposure conditions, laterals throughout the canopy show severe reductions in needle retention. Four scenarios were generated that simulate this progression of effects (Table I). The Natural scenario is the distribution of biomass and nutrients within the trees in the current condition. Scenario 1 simulated the initial stages of impact, where whorl retention was reduced by 30% only in the lower third of the canopy. The level of impact was increased in Scenario 2 to include reductions in whorl retention in all canopy positions. Scenario 3 simulated an extreme condition of ozone impact with 60% reduction in whorl retention throughout the canopy.

These scenarios are, of course, a simplification of the natural progression of ozone injury. Discussion of these scenarios includes several assumptions and conditions: (1) entire needle cohorts are abscised; (2) no acceleration of needle loss within surviving cohorts is included when whorl retention is reduced; (3) no effective biomass loss due to needle mottling is considered; and (4) nutrient content of remaining cohorts remains unaffected by the impact scenarios. Each of these conditions will lead to an underestimation of the impact of each scenario on the resources of the canopy. It has been shown that ozone accelerates the age-induced decline in photosynthetic productivity of leaves and may, in fact, be the cause for premature leaf senescence.[8] The incorporation of this impact into these scenarios will have to be delayed until more information is available regarding the natural progression of aging in lodgepole pine needles. By ignoring this and other symptoms such as mottling and accelerated needle thinning,[9] the scenarios are conservative with respect to the actual impacts of ozone. These scenarios are intended to address only the effects of the loss of age cohorts on biomass and nutrient resources.

RESULTS

Foliar whorl retention in lodgepole pine can range from 5 to 22 years in the central Rocky Mountains. The average whorl retention across this region for this subspecies (*latifolia*) is 13 years.[10] Biomass distribution by canopy position and age class is shown in Figure 1. Whorl retention was consistently greater in the lower third of the canopy than the middle or upper portions. This trend was not statistically significant when one considers only the four trees that were sampled in this stand, yet in a larger study that included this site as well as ten others, the effect of canopy position on whorl retention was significant.[10] For this reason, each scenario of potential ozone impact was applied to each canopy third rather than to the average distribution of age classes throughout the canopy.

The biomass distributions within each canopy position by leaf age were different. The upper third of the crown had 43% of the foliar biomass in the current to 2-year-old needle age classes, where as the same age classes accounted for only 27% of the foliage in the base of the canopy (Table II). The bottom of the canopy had a greater proportion of needles in the age classes greater than 10 years old than those in the other canopy positions.

The proportion of total foliar biomass in each age class declined steadily after the needle age of 2 years (Figure 2). Needle expansion is complete in this species by the end of the second growing season. One third of the foliar biomass was found to be in current to 2-year-old needles (Table II). more than 50% of the needle biomass was in age classes 3 through 9, and the foliage greater than 10 years old accounted for an average of 16% of the total leaf biomass.

Foliar nutrient concentrations varied with leaf age (Figure 3). Potassium, phosphorous, nitrogen, and magnesium concentrations all declined with needle age while calcium increased.

There were no differences among the concentrations of nutrients by canopy position. There were, however, trends in foliar nutrient concentrations between canopy positions that are consistent with position effects reported by others.[11] In applying the scenarios to this data set, I conducted all of the simulations to each canopy position and computed total nutrient resources by multiplying the biomass and nutrient concentrations for that position. The data for each canopy position were combined to generate the estimate for the resources of the total canopy. The results from each tree were then averaged.

The foliar age class distribution within the canopy of lodgepole pine, as simulated by each scenario of ozone impact, is shown in Figure 4. The reduction of whorl retention in the lower portion of the canopy by 30% (Scenario 1) removed only a small percentage of the total foliar biomass (Table III). The total nutrient content of the foliage decreased by percentages comparable to those observed for the biomass. The reduction of leaf longevity by 60%, 40%, and 20% in the lower, middle, and upper crown thirds, respectively, had a much greater effect on canopy resources (Scenario 2). Biomass was reduced by 24% from the natural condition, whereas N, P, K, and Mg were reduced by only 21%. Foliar calcium content was reduced by 34% from the control condition. The severe reduction in maximum needle longevity of 60% throughout the canopy (Scenario 3) reduced the foliar biomass and N, P, K and Mg contents by approximately 40%. Calcium retention was reduced by more than 50%.

CONCLUSIONS

Foliar biomass was not distributed evenly by age class throughout the canopy of lodgepole pine. The top of the canopy had a greater proportion of foliar biomass in the young age classes than any other canopy portion, due to the greater number of young growing points. Many of the laterals in this canopy third were totally foliated since the life span of the foliage was greater than the age of the lateral. The age class distribution of foliage in the lower canopy third more closely reflected the foliage distribution on a single lateral. The decline in biomass with leaf age in the lower canopy was due to needle thinning with time, and was influenced to a lesser extent by the establishment of new laterals. A similar pattern was observed in the middle portion of the canopy.

The foliar nutrient concentrations were not affected by canopy position, contrary to the findings of Wells and Metz.[11] The effects noted for other *Pinus* species were evident as trends in this study, but were not statistically significant. The concentrations of N, P, K and Mg (dry weight basis) declined with leaf age. This decline has been attributed to translocation of the nutrients to new tissues and to increases in leaf specific weight with age.[11] Generally 50% of the N, and greater than 50% of the P,K, and Mg within conifer foliage is assumed to be mobilized from leaf tissue prior to abscission.[12] Calcium, however accumulated with leaf age and is not mobile for translocation prior to senescence.[12]

The cohort loss described for other pine species in California[1] was simulated by comparing the percent reductions in maximum needle longevity observed there against the lodgepole pine trees analyzed in the absence of ozone stress. Not until whorl retention was reduced by an average of 40% throughout the canopy (Scenario 2) was even 24% of the total foliage biomass lost. The scenarios applied are conservative because accelerated needle thinning with ozone exposure, which would increase the estimate of foliage lost was not included. Radial growth declines were observed in Jeffrey pine at this level of reduced leaf longevity[3] but were not observed for ponderosa pine, even when whorl retention was reduced 60% by ozone exposure.[13] This level of impact on lodgepole pine would be the equivalent at least a 40% reduction in foliar biomass (Scenario 3). Due to the similarity of branching patterns between lodgepole pine and other pines, this estimate of foliage loss is probably a fair estimate of biomass losses for ponderosa pine, within the assumptions of the scenarios.

While it is clear that ozone affects leaf longevity before growth is reduced, the significance of this symptom with respect to reductions in radial growth is uncertain. Chabot and Hicks[14] demonstrated that alterations in leaf longevity could greatly affect carbon gain per leaf structure, which would then impact the plant's carbon balance. Few experiments have tested the effect of leaf longevity on growth. Most defoliation studies have focused on simulating insect- or pathogen-caused defoliation in the young needle age classes. Experimental pruning treatments would be expected to have a lesser effect on net carbon gain of the tree than defoliation due to the pruning of both net photosynthesizing and respiring (branch) tissues. These data will not give information on the effect of the removal of old foliage. One artificial defoliation study[15] does address the importance of leaf longevity by demonstrating a radial growth decrease in sapling pines caused by repeated removal of old leaves. The percentage of the leaf biomass removed was only 20%, suggesting that radial growth may decline from an impact similar to that imposed by Scenario 2 in lodgepole pine. McLaughlin et al.[16] presented physiological data that show old needles of white pine contribute significant amounts of carbohydrates to new growth.[16]

The evergreen growth form has been suggested to function as a nutrient conservation mechanism.[17] A considerable amount of the canopy nutrient storage capacity would be lost by premature leaf senescence for lodgepole pine. Calcium uptake would decrease with reduced needle retention. The annual demand for N, P, K, and Mg would not be expected to change with the scenarios applied (assuming that the production of new foliage remained constant), yet the cycling rate of nutrients through the canopy would be altered. The nutrient use efficiency (carbon gain per unit nutrient) would also be reduced as a consequence of reduced foliar longevity. A reduction in needle retention could affect the nutrient cycling within the stand. The time scale of these changes is probably much longer than the life span of the trees themselves and probably would not contribute to growth reductions in the early stages of ozone exposure.

This simulation demonstrates that: (1) premature needle drop of the oldest cohorts must be extensive before foliar biomass is reduced appreciably; (2) most of the critical foliar nutrients are translocated from old needles as they age so that a reduction in whorl retention reduces canopy nutrient retention less than biomass; (3) reduced whorl retention would reduce the carbon gain per leaf structure and per nutrient assimilated, which would reduce the efficiency of the foliage and may lead to reductions in growth; and (4) reduced nutrient retention in the canopy caused by an increase in the rate of leaf turnover may make the nutrient cycling in the stand more leaky.

We would expect that reductions in leaf longevity caused by chronic ozone exposure would reduce the positive carbon balance of trees. The expression of this impact on radial growth would depend on the carbon allocation pattern of the individual. We need to better understand the dynamics of carbon assimilation through the life span of long-lived leaves as well as how the patterns of carbon allocation may change with tree age. This understanding would help us to predict and understand how needle retention relates to tree vigor and how ozone exposure affects tree growth.

REFERENCES

1. P.R. Miller and A.A. Millecan, "Extent of oxidant air pollution damage to some pines and other conifers in California," *Plant Dis. Rep.* 55:555 (1971).

2. C. Field, "Leaf age effects on the carbon gain of individual leaves in relation to microsite," in *Components of productivity of Mediterranean-climate regions—Basic and applied aspects*. N. S. Margaris, and H.A. Mooney (Eds.), Dr. W. Junk, 1981, p. 41.

3. D.L. Peterson, M.J. Arbaugh, V.A. Wakefield, and P.R. Miller, "Evidence for growth reduction in ozone-injured Jeffrey Pine (*Pinus jeffreyi* Grev. and Balf.) in Sequoia and Kings Canyon National Parks," *JAPCA* 37:906 (1987).

4. J.A. Pearson, T.J. Fahey, and D.H. Knight, "Biomass and leaf area in contrasting lodgepole pine forests," *Can. J. For. Res.* 14:259 (1984).

5. H.L. Gary, "Crown structure and distribution of biomass in a lodgepole pine stand," USDA Forest Service Research Paper RM-165, 1976, 20pp.

6. J.L. Havlin and P.N. Soltanpour, "A nitric acid plant tissue digest method for use with inductively coupled plasma spectrometry," *Comm. in Soil Science and Plant Analysis* 11:969 (1980).

7. J.A. Parkinson and S.E. Allen, "A wet oxidant procedure suitable for the determination of nitrogen and mineral nutrients in biological material," *Comm. in Soil Science and Plant Analysis* 1:6 (1975).

8. P.R. Miller and J.R. Parmeter, "Effects of ozone injury to Ponderosa pine," *Phytopathol.* 8:57 (1967).

9. P.R. Miller and R.E. Van Doren, "Ponderosa and Jeffrey pine foliage retention indicates ozone dose response," USDA Forest Service Gen. Tech. Rep. PSW-58,

10. A.W. Schoettle, "Natural variability of needle retention on *Pinus contorta* spp. *latifolia*," in *Proceedings Acid Deposition and Forest Decline—An International Symposium*," Rochester, NY, October, 1988, p. 41.

11. C.G. Wells and L.J. Metz, "Variation in nutrient content of loblolly pine needles with season, age, soil, and position on the crown," *Soil Sci. Soc. Am. Proc.* 27:90 (1963).

12. H.G. Miller, "Carbon x nutrient interactions—the limitation to productivity," *Tree Physiol.* 2:373 (1986).

13. D.L. Peterson and M.J. Arbaugh, "An evaluation of the effects of ozone injury on radial growth of Ponderosa Pine (*Pinus ponderosa*) in the Southern Sierra Nevada," *JAPCA* 38:921 (1988).

14. B.F. Chabot and D.J. Hicks, "The ecology of leaf life spans," *Ann. Rev. Ecol. Syst.* 13:229 (1982).

15. D.A. Rock and A.G.D. Whyte, "Partial defoliation and growth of 5-year-old radiata pine," *N.Z.J. For. Sci.* 6:40 (1976).

16. S.B. McLaughlin, R.K. McConathy, D. Duvick, and L.K. Mann, "Effect of chronic air pollution on photosynthesis, carbon allocation, and growth of white pine trees," *Forest Sci.* 60:28 (1982).

17. C.D. Monk, "An ecological significance of evergreenness," *Ecology* 47:504 (1966).

Table I. Summary of simulation scenarios.

Canopy Position	Natural	% Reduction in Whorl Retention Scenario 1	Scenario 2	Scenario 3
Top	0	0	20	60
Middle	0	0	40	60
Bottom	0	30	60	60

Table II. Percentage of foliar mass in each needle age class.

Foliar Age Class	Total	Canopy Position Top	Middle	Bottom
C - 2	33	43	32	27
3 - 9	51	46	47	44
> 10	16	11	21	29

Table III. Effect of each scenario on the distribution of foliar biomass and nutrient content.

			% reduction			
Scenario	Biomass	N	P	K	Ca	Mg
Natural	0	0	0	0	0	0
1	4	4	4	3	7	4
2	24	21	21	18	34	23
3	40	37	36	32	53	40

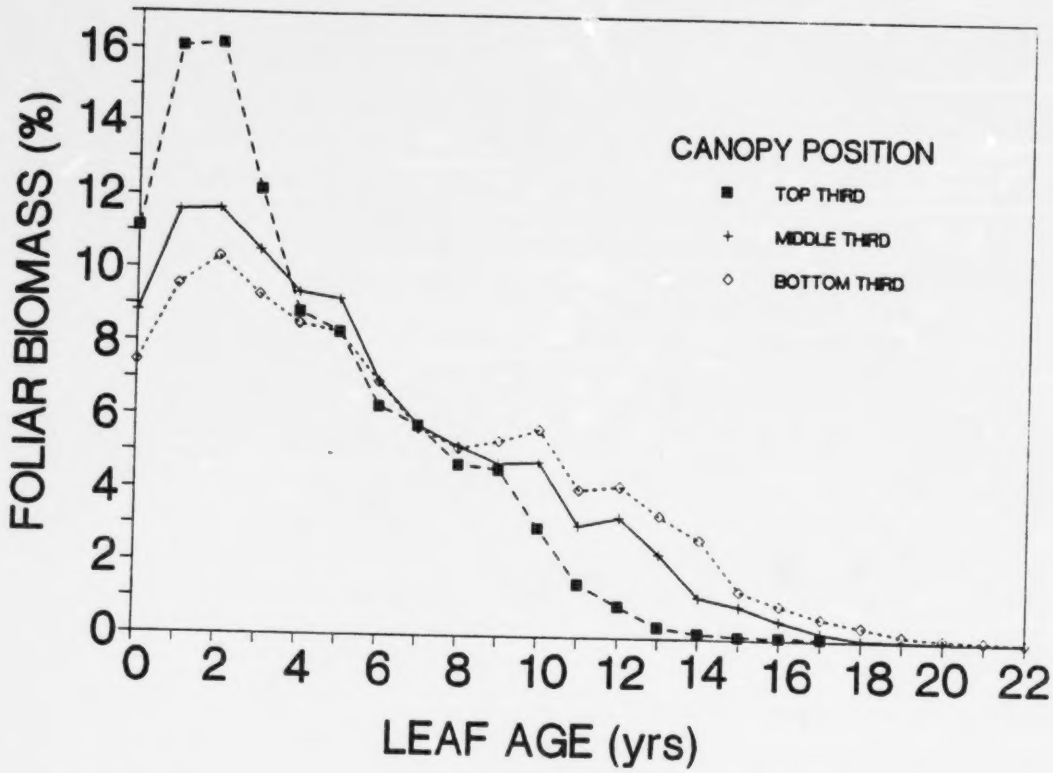

Figure 1. The age distribution of foliar biomass within each canopy third for *Pinus contorta* ssp. *latifolia*. Average for four trees; the average standard error was 0.75%.

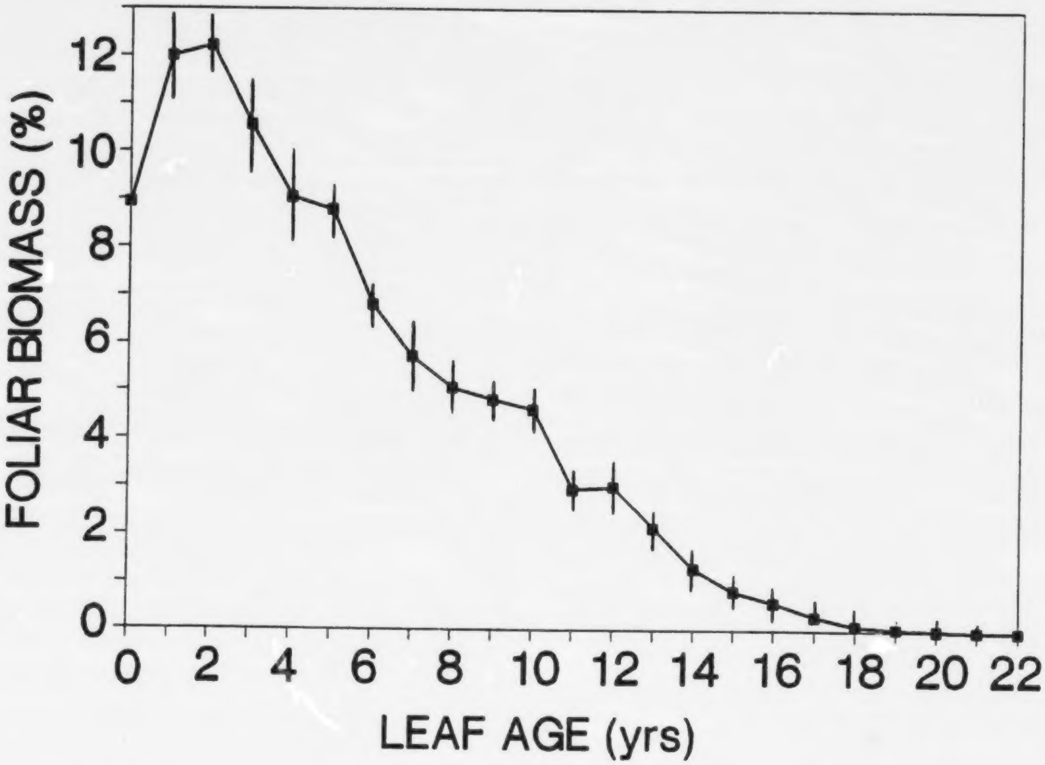

Figure 2. The age distribution of foliar biomass as a percent of total canopy foliage. Average for four trees (±standard error).

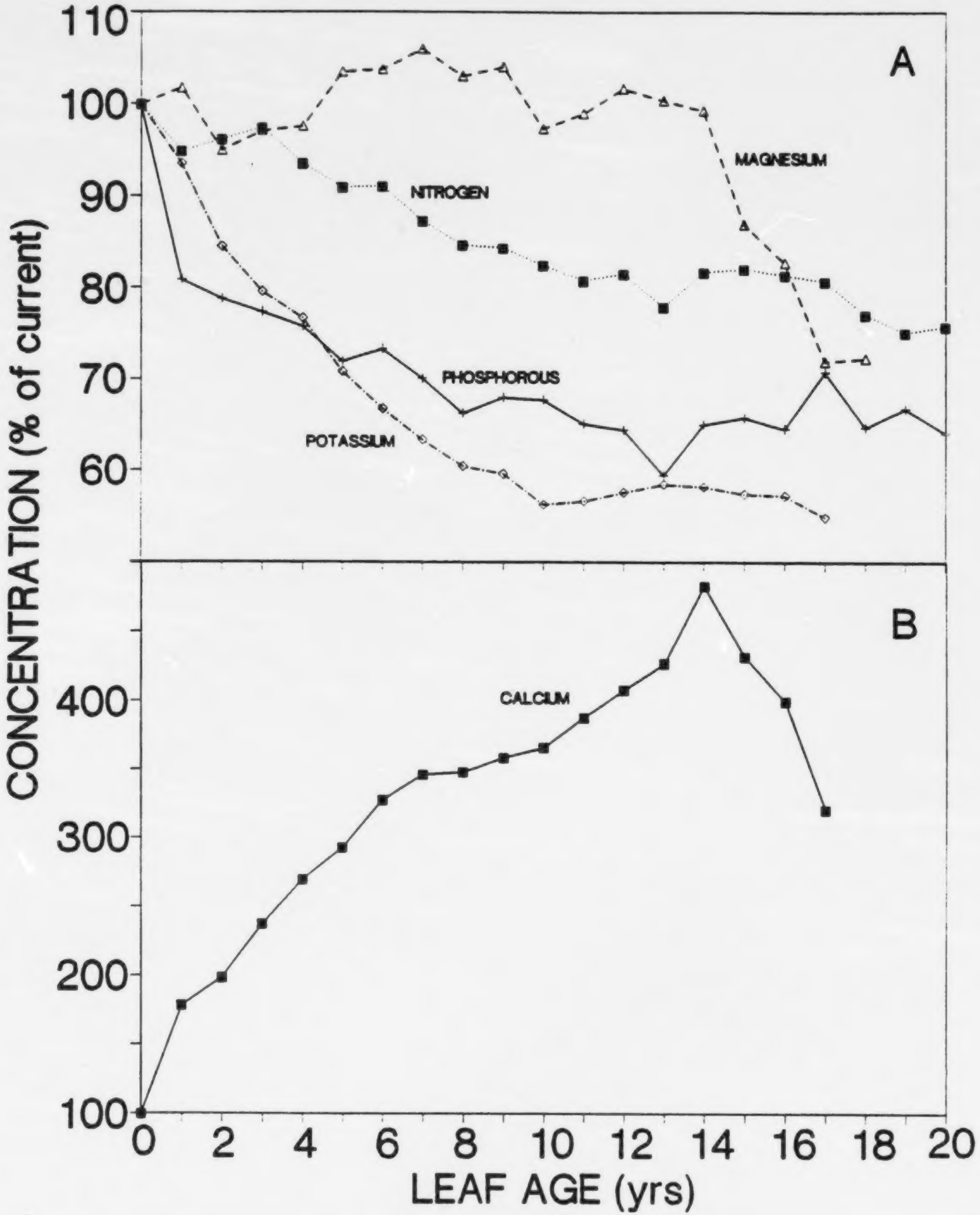

Figure 3. Percent change in nutrient concentration with leaf age as compared to the concentration in current year leaves. N,P,K and Mg are shown in the graph A, and calcium is shown in graph B. These data are averaged for canopy position and for the four trees. The concentration in the current leaves was 0.962%,0.122%, 0.654%,0.147%, 0.149% for N, P, K, Mg and Ca, respectively. All concentrations are on a leaf dry weight basis.

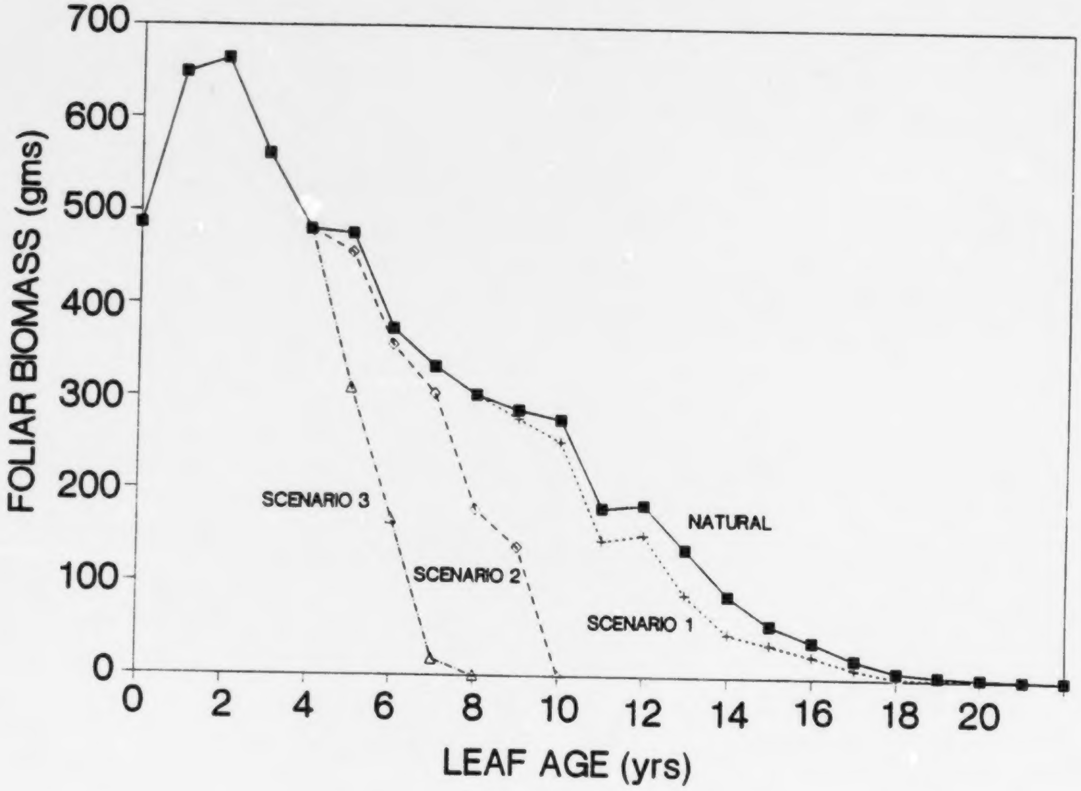

Figure 4. The age distribution of foliar biomass for each scenario condition (see text for details). Averaged over four trees.

Effects of Photochemical Smog on the Growth and Physiology of Ponderosa Pine Seedlings Grown Under Nitrogen and Magnesium Deficiencies

Andrzej Bytnerowicz and Brent K. Takemoto

Statewide Air Pollution Research Center
University of California
Riverside, CA 92521

INTRODUCTION

Coniferous trees that exhibit deficiencies of Mg, Ca, or Zn are believed to be more sensitive to O_3 injury than trees with a sufficient supply of nutrients.[1] Ponderosa pine (*Pinus ponderosa*) in the San Bernardino National Forest exposed to high concentrations of photochemical smog showed nutritional imbalances such as decreased concentrations of N, P, K, Ca, and Mg.[2] No systematic studies have yet been performed on how nutritional imbalances in soil affect the susceptibility of coniferous trees to photochemical smog in the mountains surrounding the South Coast Air Basin (e.g., the Los Angeles Basin).

Information on the effects of soil deficiencies of N and Mg on growth, physiology, injury development, and chemical composition of ponderosa pine exposed to ambient concentrations of photochemical smog is essential for understanding forest damage in Southern California. In the Los Angeles Basin valleys, very high concentrations of gaseous and particulate air pollutants have been recorded.[3,4,5] The monthly 24-h average concentrations of O_3 in the summer at Tanbark Flat of the San Dimas Experimental Forest, San Gabriel Mountains, were about two-fold higher than in various Basin locations. Concentrations of NO_2, particulate NO_3^-, and particulate NH_4^+ were also high at this location.[6] Deposition fluxes of airborne NO_3^- and NH_4^+ to the foliage of *Ceanothus crassifolius*, an important shrub of the chaparral ecosystem, in the San Dimas Experimental Forest was much higher than of any other ion.[7,8]

It has been shown that elevated levels of O_3 may cause a reduction of growth and increased damage to coniferous forests in the San Bernardino and San Gabriel Mountains.[9] However, very little information is available on the physiological basis for the effects of ambient levels of O_3 on ponderosa pine seedlings. Also, little is known about the effects of ambient concentrations of gaseous and particulate nitrogen pollutants (important components of photochemical smog) on forest trees. To address these problems, a two-year field study at Tanbark Flat was initiated in 1988. During the entire photochemical smog season of 1988, ponderosa pine seedlings were exposed to various combinations of ambient and subambient levels of gaseous and particulate components of photochemical smog combined with deficiencies of N and Mg in the artificial soil medium. During this first year of the study, we investigated injury development, growth changes, physiological process rates, and deposition fluxes of atmospheric ions to the foliage. The study will be continued during the 1989 season. Some results from the 1988 season investigations are presented in this paper.

EXPERIMENTAL METHODS

Study Site

The study was performed at Tanbark Flat (elevation 800 m) in the San Dimas Experimental Forest in the San Gabriel Mountains of southern California. The site is in the South Coast Air Basin, approximately 35 km northeast of downtown Los Angeles, and represents air pollution characteristics typical for the mountain ranges surrounding Los Angeles Basin, including the areas where ponderosa pine grows.[6,10,11]

Plant Propagation

Two-year old ponderosa pine seedlings from seed zone #522 located in Shasta County, CA, (elevation of 750 m) were used in the study. The seedlings were planted into 18 x 40 cm pulp pots filled with 50% perlite and 50% vermiculite potting mixture on February 8 and 9, 1988. After planting the trees were kept in a lathhouse in Riverside until April 5, 1988. Average 24-h concentration of ozone in Riverside during that time was 2.5 pphm; 1-h averages did not exceed 19 pphm. During that time the trees were watered as needed with a modified Hoagland's solution (1:100) until they were fully established. On April 5, 1988, the trees were moved to open-top chambers at Tanbark Flat. Shade cloth (to achieve a 55% reduction of light intensity) was installed over the plants in the chambers. Shade cloth was also installed over the top and on the sides of the plants in the outside chamberless plots. The walls of the chambers were also whitewashed to uniformly reduce the light intensity in the entire chamber. Light intensity was reduced to the same level in all the plots to provide a better environment for growing the pine seedlings– this species naturally grows at higher elevations in Southern California where air and soil temperature are lower than at Tanbark Flat.

Exposure to Photochemical Smog

Trees were exposed to ambient and subambient concentrations of gaseous and particulate components of photochemical smog in six open-top chambers.[12,13] Additionally, two outside chamberless plots were used for studying the effects of chamber enclosures. The following types of filtration were used to create the four different air quality treatments:

- Ambient I [NF(50%)]: Airguard type DP 2-60 Media extended surface air filters of 45-55% filtration efficiency for 2 μm diameter particles (Airguard Industries, Inc., Louisville, KY).
- Ambient II [NF(99%)]: Farr Riga-Flow 200 air filters of 99.7% filtration efficiency of 2 μm diameter particles (Farr Co., Los Angeles, CA).
- Clean Air [CF(99%)]: Farr Riga-Flow 200 air filters and Barnebey-Chaney Model FJ 062 high velocity filter housing with 12 panels containing activated charcoal.
- Ambient Air [AA(0%)]: No chamber enclosure.

The levels of gaseous and particulate pollutants in the chambers and in the ambient air plots are summarized in Table I.

Fertilization of Plants

Plants were also exposed to four different fertilization regimes: complete supply of nutrients (comp), 50% N deficiency (N def), 50% Mg deficiency

(Mg def), and 50% N and 50% Mg deficiency (N and Mg def). The solutions were prepared by dissolving the chemicals in deionized water and adjusting the acidity of the solutions with concentrated acetic acid to pH 3.5 ± 0.2. At this pH all the chemicals used for making the nutrient solutions were dissolved. Stock fertilizer solutions diluted 100-fold with a fertilizer proportioner (pH of the solutions about 4.5) were provided to the pots. Trees were watered once a week, except during 2 extremely hot weeks (September 6–20, 1988) when they were watered twice a week. Approximately 800 mL of fertilizer solution was applied to each pot per watering.

Monitoring Gaseous Air Pollutants

Air samples from each of the experimental plots were analyzed hourly. Concentrations of O_3 were measured with a Dasibi Model 1003 AH analyzer, NO and NO_2 with a Monitor Labs 8440 Analyzer, and SO_2 with a Meloy Model SA 285 Analyzer. A Cyborg ISAAC 41A data acquisition system and Apple II+ computer were used to collect and store air monitoring data. All analyzers were calibrated every 4 weeks.

Determination of Concentrations of Atmospheric Ions

Ambient concentrations of NO_3^-, SO_4^{2-}, NH_4^+ , Cl^- and F^- were determined every sixth day during the study. The concentrations of atmospheric ions inside open-top chambers and in the outside plots were determined during an intensive 72-h experiment in the middle of the smog season. Atmospheric ions were collected with sample trains consisting of an aluminum cyclone,[14] Sierra Instruments constant flow air sampler model No. 113, and Nylasorb 47 mm filters with a 1μm pore-size held in Nucleopore polycarbonate filter holders. The cyclones were of the design developed by John and Reischl,[15] with the addition of a Teflon coating on the internal surfaces to minimize the absorption of gaseous HNO_3. Airflow through the systems was maintained at 22 L/min, providing a 50% cutoff of 2.5 μm diameter particles. Fine particles (<2.5 μm) as well as HNO_3 vapor and NH_3 were absorbed on nylon filters. Coarse particles (>2.5 μm) were deposited inside the cyclone. For chemical analysis, the filters were extracted in 0.0024 M Na_2CO_3 + 0.0030 M $NaHCO_3$ solution.[16] Concentrations of anions (i.e., NO_3^-, SO_4^{2-}, Cl^-, F^-) were determined with a Dionex 4000i ion chromatograph, and NH_4^+ was determined with a Technicon TRAACS 800 analyzer (U.S. Forest Service, Forest Fire Laboratory, Riverside, CA).

Determination of Ionic Deposition Fluxes to Foliage

Determinations of deposition fluxes of ions to plant foliage were made over the entire duration of the study on two replicate seedlings per plot as described earlier.[8] About 200 mL of deionized-distilled water was dispersed on 5–10 cm long branches with a polyethylene sprayer for about 1 min. Plant rinses were collected in polyethylene bottles and stored at -18° C prior to analysis. Concentrations of anions were determined with a Dionex 4000i ion chromatograph; concentrations of NH_4^+ were determined with a Technicon TRAACS 800 analyzer. All chemical analyses were performed at the U.S Forest Service, Forest Fire Laboratory (Riverside, CA).

Assessment of Injury Development

Development of foliar injury symptoms was assessed before the air pollution exposures were started and were reassessed once each month during the experiment. Injury was rated by the same observer during the entire experiment and was calculated as percentage of total needle area injured for each individual plant.

Growth Measurements

Seedling diameter at the cotelydon mark (d) and height (h) were measured monthly. To estimate stem volume, values of d^2h were calculated.

Physiological Measurements

Stomatal conductance of water vapor, net photosynthesis, transpiration, and dark respiration were measured twice each month, between 1000 and 1500 PST with a LICOR 6000 portable photosynthesis system (Lambda Instruments, Lincoln, NE). Chlorophyll fluorescence was measured with a Plant Stress Meter (Polartech, Umea, Sweden). Values of F_0 (nonvariable fluorescence), F_m (maximal fluorescence), and F_v (variable fluorescence) were measured. Values of F_v/F_m (a measure of the photochemical efficiency of photosystem II) were calculated by the meter's microprocessor.[17]

Experimental Design and Statistical Analysis

The experiment was designed as a randomized block with replicate plots; air quality was the main plot factor and fertilization was a sub-plot factor. Two replicate chambers and chamberless plots were used for air quality treatment. Eight individual seedlings per each fertilization regime per plot were used. All trees were used for measurements of injury and growth. Three randomly selected seedlings from each fertilization regime plot were used to measure gas exchange and chlorophyll fluorescence. Measurements of dry deposition were performed on two trees per plot. Statistical analysis of injury, growth, and physiological data was done using analysis of variance according to the procedure described by Steel and Torrie.[18]

RESULTS

Concentrations of Air Pollutants

Concentrations of O_3 were highest in July and lowest in April. Over the entire season, 1-h average concentrations of O_3 were the highest in the early afternoon (1400-1500 PST). The 24-h concentrations of O_3 in outside plots were always higher than 3 pphm. There was no difference between the levels of O_3 in the outside plots and in the NF (50%) or NF (99%) open-top chambers. The 24-h average concentrations of O_3 inside the CF (99%) chambers were always below 2 pphm. The 24-h average concentrations and 1-h maximal concentration O_3 in the outside plots and in the CF (99%) chambers for the entire experiment (April to October 1988) are presented in Table II.

The highest concentrations of NO_2 occurred in August and the lowest in April. The highest 1-h average concentrations generally occurred in the late afternoon (1600–1700 PST). The concentrations of NO_2 in the NF (50%) and NF (99%) chambers did not differ appreciably from the outside plots. In the CF (99%) chambers, the 24-h average NO_2 concentrations were below 2 pphm. The 24-h average concentrations and 1-h maximal concentrations of NO_2 in the outside plots for the entire experiment are presented in Table II.

Concentrations of NO and SO_2 were low during the entire experiment. Maximum ambient concentrations of NO did not exceed 1.6 pphm, and the concentrations of SO_2 were below 1.2 pphm during the entire experiment.

Ambient concentrations of NO_3^- and NH_4^+ in the fine fractions of aerosols were the highest among the ions studied. Concentrations of NO_3^- ranged from 59.6 to 385.7 nM/m^3 during the study, and the highest concentrations were found in August, October and November. Concentrations of NH_4^+ were between 32.4 and 427.0 nM/m^3, with the greatest values in October and November. Concentrations of SO_4^{2-} ranged between 6.6 and 132.3 nM /m^3. The highest concentrations of this ion also occurred in October. Ambient concentrations of ions in the fine fraction of particles were similar to the levels determined in the same site during the 1985 season.[6] Concentrations of the selected ions inside open-top chambers and in the outside plots are presented in Table III. In the NF (50%) chambers, the concentrations of NO_3^-, NH_4^+, and SO_4^{2-} were reduced to 51.8-60.2%, 37.4-83.0%, and 56.2-131.4% of the levels in the outside plots, respectively. The lowest concentrations of all the studied ions were determined in the CF (99%) chambers. The levels of NO_3^-, NH_4^+, and SO_4^{2-} in the NF (99%) chambers were only slightly higher than in the CF (99%) chambers.

Deposition of Ions to Foliage

Over the entire season, deposition fluxes of the studied ions in the outside plots were significantly higher than inside the open-top chambers. There was a trend toward lower deposition fluxes in the CF (99%) chambers than in other chambers, and this trend was significant for the NH_4^+ ion. No differences in deposition fluxes of ions between the NF (50%) and NF (99%) chambers were seen during the entire season (Table IV).

Injury Assessment

Over time, increased injury to 1987 needles of seedlings in the different air quality and fertilization treatments was seen. In October, the trees grown in the CF(99%) treatment had the highest number of individuals with low total injury; however, no statistically significant effects of air quality were found. The 1988 needles showed very little injury during the entire study, and no effects of either air quality or fertilization were seen.

Growth Changes

No significant effects of air quality on tree growth were seen during the entire photochemical smog season. The September data are shown as examples of the measured values (Table V). There was a tendency of better tree growth in the outside plot compared to tree growth in the open-top chambers. Relative to the effects of fertilization, the trend was toward slower growth in the N deficient trees. These trees had smaller diameter and d^2h values than trees from other treatments.

Physiological Changes

Few significant differences or trends indicative of physiological alterations among the treatments were seen during most of the study. A general description of the physiological data is given in this chapter, and the results of physiological measurements collected in September are shown as examples of the measured values (Table VI).

Plants grown in CF (99%) air exhibited a trend toward higher rates of stomatal conductance than plants grown in NF (99%) air during 4 out of 5 months of measurements. However, these differences were significant only in July. Plants exposed to ambient levels of gaseous pollutants in combination with low amounts of dry deposition generally exhibited higher stomatal conductance rates than plants receiving high amounts of dry deposition, but no significant differences were observed. A 50% reduction in N fertilization caused significant decreases in stomatal conductance during May, June, and July. A 50% reduction Mg fertilization appeared to have the opposite effect: a trend toward higher stomatal conductance rates in Mg deficient plans was seen during all 5 months of measurements, but significantly higher readings were noted only in July.

Gaseous or particulate components of photochemical smog did not cause any significant changes in net photosynthesis of the 1987 or 1988 needles. With respect to fertilization, plants receiving 50% reduced N fertilization exhibited significantly lower rates of photosynthesis than plants receiving a full supply of N from May through July. Seedlings supplied with 50% Mg exhibited significantly higher rates of photosynthesis only in May.

No significant effects of gaseous or particulate pollutants on dark respiration were seen during the entire study. However, the N deficient plants had significantly lower rates of dark respiration in June, July, and August. No effects of reduced supply of Mg on dark respiration were seen during the entire study.

Air quality and fertilization effects on transpiration were similar to those observed for stomatal conductance. Although there were no significant air quality effects, reduced N and Mg fertilization caused significant alterations in some instances. The reduced supply of N caused lowered transpiration rates in May, June, and July. In June, transpiration rates in the plants with the reduced supply of Mg were significantly higher than in plants receiving full supply of this nutrient.

With respect to chlorophyll fluorescence, the ratio of F_v/F_m was not significantly affected by either component of air quality. However, for most of the measurements, a trend toward a lower F_v/F_m ratio was seen for the NF (50%) plants, indicating a possible negative effect of photochemical smog. During the entire experiment, the N deficient plants showed decreased F_v/F_m ratios compared to N sufficient plants, but the only statistically significant difference occurred in August. No significant effects of reduced Mg on chlorophyll fluorescence were determined during the entire study.

The results in this paper should be treated as preliminary, reflecting responses of trees to photochemical smog and nutritional deficiencies during a single season. The exposures to photochemical air pollutants will continue during the 1989 photochemical smog season. The measurements performed during the 1988 experiment will be repeated during the 1989 season, creating an opportunity for the further assessment of the differences or trends observed during the first year of exposures. Other parameters such as bud development, changes in biomass of plant organs, concentrations of plant pigments, and chemical content of plant tissues will also be studied in the 1989 season. Continuation of the study during the second year will allow for determining if the changes or trends observed during the first year of exposures are permanent or temporal.

CONCLUSIONS

Various components of photochemical smog at high ambient levels had no pronounced effects on the growth of ponderosa pine seedlings. However, seedlings exposed to decreased levels of gaseous oxidants in charcoal-filtered air showed a tendency toward low needle injury and greater stomatal conductance rates than the seedlings grown in nonfiltered air containing ambient levels of oxidants.

Trees exposed to low, subambient levels of particulate air pollutants showed a tendency toward higher rates of stomatal conductance than trees exposed to high levels of particulate air pollution.

Deficiency of N in the growing medium affected seedlings much more than any other factor, causing decreases in stomatal conductance, photosynthesis, dark respiration, transpiration and chlorophyll fluorescence.

Deficiency of Mg in the growing medium did not effect changes in any of the measured parameters, with the exception of increased transpiration.

ACKNOWLEDGMENTS

The authors wish to than the California Department of Forestry for providing the plant material for this research and the U.S. Forest Service for allowing access to the site. We would also like to thank Mr. Phil Dawson, Mr. Lynn Morrison, Mr. Raul Guillermo Torres-Jardon, Mr. Adam Johnson, Ms. Joanne Wolf, Ms. Minn Poe, and Mr. Ian Gocka of the Statewide Air Pollution Research Center of the University of California, Riverside for their excellent technical assistance. The research was conducted under Contract No. SCE 1557906 from the Southern California Edison Company. The mention of specific products does not constitute a guarantee or warranty by the University of California, or the Southern California Edison Company, nor does it imply endorsement of that product to the exclusion of other products.

REFERENCES

1. H.W. Zoettl and R.F. Huettl, "Nutrient supply and forest decline in Southwest Germany," *Water, Air & Soil Pollut.* 31:449 (1986).

2. R. Glauser, P.L. Gesper, and R.J. Arkey, "Nutrient dynamics—a comparison of a healthy with a severely OAP affected *Pinus ponderosa* Laws. in the San Bernardino National Forest of California. Part II. Nitrogen, phosphorus, potassium, calcium, and magnesium gains and losses," Unpublished manuscript, UC Berkeley.

3. B.R. Appel, E.M. Hoffer, Y. Tokiwa, and E.L. Kothny, "Measurements of sulfuric acid and particulate strong acidity in the Los Angeles Basin," *Atmos. Environ.* 16:589 (1982).

4. D. Grosjean, "Distribution of atmospheric nitrogenous pollutants at a Los Angeles smog receptor site,"*Environ. Sci. Technol.* 17:13 (1983).

5. S. Kumar and D.P. Chock, "An update on oxidant trends in the South Coast Air Basin of California," *Atmos. Environ.* 18:2131 (1984).

6. A. Bytnerowicz, P.R. Miller, D.M. Olszyk, P.J. Dawson, and C.A. Fox, "Gaseous and particulate air pollution in the San Gabriel Mountains of southern California," *Atmos. Environ.* 21:1749 (1987).

7. P.J. Riggan, R.N. Lockwood, and E.N. Lopez, "Deposition and processing of airborne nitrogen pollutants in Mediterranean-type ecosystem of southern California," *Environ. Sci. Technol.* 19:781 (1985).

8. A. Bytnerowicz, P.R. Miller, and D.M. Olszyk, "Dry deposition of nitrate, ammonium, and sulfate to a *Ceanothus crassifolius* canopy and surrogate surfaces," *Atmos. Environ.* 21:1749 (1987).

9. P.R. Miller, O.C. Taylor, and R.G. Wilhour, "Oxidant air pollution effects on a western coniferous forest ecosystem," *Environ. Res. Brief*, EPA-600/D-82-276 (1982).

10. P.R. Miller, M.H. McCutchan, and B.C. Ryan, "Influence of climate and topography on oxidant air pollution concentrations that damage conifer forests in southern California," *Effects of Air Pollutants on Forest Trees, VII International Symposium of Forest Fume Damage Experts.* Forstliche Bundesversuchanstalt, Wien. Vol. I:585-608 (1972).

11. P.R. Miller, O.C. Taylor, and M.P. Poe, "Spatial variation of summer ozone concentrations in the San Bernardino Mountains," Presented at the 79th Annual Meeting of the Air Pollution Control Association, Minneapolis MN, June 22-27, 1986.

12. A.S. Heagle, D.E. Body, and W.W. Heck, "An open-top field chamber to assess the impact of air pollution on plants," *J. Environ. Qual.* 2:365 (1973).

13. W.W. Heck, W.W. Cure, J.O. Rawlings, L.J. Zaragosa, A.S. Heagle, H.E. Heggestad, R.J. Kohut, L.W. Kress, and P.J. Temple, "Assessing impacts of ozone on agricultural crops: I. Overview, " *JAPCA* 34:729 (1984).

14. W. John, S.M. Wall, and J.L. Ondo, "Measurement of dry acid deposition in California," Presented at the 77th Annual Meeting of the Air Pollution Control Association, San Francisco, CA, 1984, 16pp.

15. W. John and G. Reischl, "A cyclone for size-selective sampling of ambient air," *JAPCA* 30:872 (1980).

16. Dionex Application Note 2 (1978).

17. G. Oquist and R. Wass, "A portable microprocessor operated instrument for measuring chlorophyll fluorescence kinetics in stress physiology," *Physiol. Plant.* 73:211 (1988).

18. R.G.D. Steel and J.H. Torrie. *Principles and Procedures of Statistics*, McGraw-Hill Book Co., NY, 1980, 633pp.

Table I. Gaseous and particulate components of photochemical smog in the chambers and in outside plots.

Concentration of Photochemical Smog Components	Open-Top Chambers			
	Ambient I [NF (50%)]	Ambient II [NF (99%)]	Clean Air [CF (99%)]	Ambient Air [AA (0%)]
Gaseous, ambient	+	+		+
Gaseous, low subambient			+	
Particle, ambient				+
Particle, high subambient	+			
Particle, low subambient		+	+	

Table II. Concentrations of O_3 and NO_2 at Tanbark Flat during the 1988 growing season

		24-h average		1h maximum	
	Month	Ambient[a]	CF (99%)	Ambient	CF(99%)
O_3(pphm)					
	April	4.32	1.10	16.6	2.7
	May	5.87	0.92	25.1	3.3
	June	6.17	0.94	20.4	3.1
	July	7.73	1.25	23.1	5.0
	August	7.31	1.15	22.4	4.1
	September	6.18	1.00	18.8	3.0
	October	5.09	0.84	16.9	2.3
NO_2(pphm)					
	April	0.69	0.54	3.2	2.0
	May	1.91	0.61	7.7	2.6
	June	2.34	0.71	6.9	2.4
	July	2.56	0.86	5.8	2.4
	August	3.22	1.25	8.7	3.5
	September	2.23	0.93	7.8	3.4
	October	1.34	0.55	6.0	1.8

[a] Ambient concentrations of pollutants measured in the outside chamberless plots. Concentrations in the NF (50%) and NF (99%) chambers were the same as in the outside plots.

Table III. Concentrations of ions in open-top chambers and in outside plots during an intensive study (nM/m^3).

Treatment Description			Ion		
	NO_3^- [a]	SO_4^{2-} [b]	NH_4^+ [c]	Cl^- [d]	F^- [e]
			September 21/22, 1988		
AA (0%)	89.4	19.4	60.8	13.8	3.4
NF (50%)	48.3	10.9	22.8	5.1	2.6
NF (99%)	18.5	13.6	3.7	9.7	1.7
CF (99%)	8.4	3.2	0.9	0.0	0.0
			September 22/23, 1988		
AA (0%)	101.9	16.9	61.3	48.9	20.3
NF (50%)	61.4	22.2	41.3	42.4	22.0
NF (99%)	21.4	1.4	0.0	0.0	0.0
CF (99%)	2.5	2.8	0.0	0.0	0.0
			September 23/24, 1988		
AA (0%)	188.6	46.0	125.5	7.1	6.2
NF (50%)	97.7	41.0	104.2		
NF (99%)	37.5	13.6	27.9	9.0	4.4
CF (99%)	22.9	12.4	19.5	2.8	

[a] 1 nM/m^3 = 0.063 µg/m^3
[b] 1 nM/m^3 = 0.096 µg/m^3
[c] 1 nM/m^3 = 0.018 µg/m^3
[d] 1 nM/m^3 = 0.036 µg/m^3
[e] 1 nM/m^3 = 0.019 µg/m^3

Table IV. Deposition fluxes of ions (µM/m^2/h) to 1988 ponderosa pine foliage, August 12-26, 1988. [a]

			Ion		
Treatment	NO_3^-	SO_4^{2-}	NH_4^+	Cl^-	F^-
AA (0%)	1.376a	0.128a	0.418a	0.081a	0.084a
NF (50%)	0.251b	0.020b	0.215b	0.023b	0.000b
NF (99%)	0.249b	0.011b	0.213b	0.022b	0.000b
CF (99%)	0.080b	0.009b	0.050c	0.020b	0.000b
LSD[b]	0.533	0.059	0.160	0.037	0.025

[a] Mean values representing averages of two observations, where each observation is the mean of two measurements. Dissimilar letter designations for each column (ion), indicate significant differences at $p < 0.05$ (Duncan's New Multiple Range Test).

[b] LSD = least significant difference at $p < 0.05$.

Table V. Effects of air quality and fertilizer chemistry on ponderosa pine growth (September 1988).[a]

	Measured Parameter		
Treatment	Diameter (d) (mm)	Height (h) (cm)	d^2h (cm^3)
Air Quality (AQ)			
CF (99%)	9.54	30.63	29.31
NF (99%)	9.49	31.57	30.01
NF (50%)	9.52	30.40	28.83
AA (0%)	9.97	32.35	34.33
LSD	2.45	4.83	20.92
Fertilizer Chemistry (FC)			
Comp	9.78	30.97	31.35
N def	8.91	30.57	25.99
Mg def	10.05	31.24	32.95
N + Mg def	9.78	32.17	32.23
LSD	0.96	3.77	9.03
ANOVA Results (values of p)			
Block	0.987	0.538	0.816
AQ	0.949	0.578	0.917
FC	0.351	0.597	0.444
AQ x FC	0.445	0.461	0.427
CV (%)	9.2	11.1	27.1

[a] Mean values for measured growth parameters. Each value represents the average of two observations, where each observation is the mean response of eight plants.
LSD = Least significant difference at $p < 0.05$.

Table VIa. Effects of air quality and fertilizer chemistry on physiology of 1987 ponderosa pine needles (September 1988).

	Measured Parameter				
Treatment	Stomatal Conductance[a] (mM/m^2/s)	Net Photosynthesis[a] (μM/m^2/s)	Dark respiration[a] (μM/m^2/s)	Transpiration[a] (μM/m^2/s)	Chlorophyll Fluoresence[b] (F_v/F_m)
Air Quality					
CF (99%)	37.0	1.12	0.95	1143	0.776
NF (99%)	35.3	1.29	0.97	1179	0.769
NF (50%)	31.5	1.01	1.00	1144	0.768
LSD[c]	23.8	1.25	0.28	457	0.024
N Concentrations (N)					
100%	34.1	1.08	1.01	1156	0.779 y
50%	35.1	1.20	0.94	1154	0.762 z
LSD[c]	6.5	0.27	0.18	154	0.013
Mg Concentrations (Mg)					
100%	32.1	1.08	0.96	1098	0.767
50%	37.1	1.20	0.98	1213	0.774
LSD[c]	6.5	0.27	0.18	154	0.013

Table VIb. Effects of air quality and fertilizer chemistry on physiology of 1987 ponderosa pine needles (September 1988).

	Measured Parameter				
Treatment	Stomatal Conductance[a] (mM/m^2/s)	Net Photosynthesis[a] (µM/m^2/s)	Dark respiration[a] (µM/m^2/s)	Transpiration[a] (µM/m^2/s)	Chlorophyll Fluoresence[b] (F_V/F_m)
N x Mg Interactions (N x Mg)					
Comp	34.6	1.15	1.01	1172	0.782 y
N def	29.7	1.01	0.92	1024	0.752 z
Mg def	33.6	1.01	1.01	1141	0.776 y
N + Mg def	40.5	1.40	0.95	1284	0.772 y
LSD[c]	9.2	0.38	0.25	218	0.018
ANOVA Results (values of P)					
Block	0.75	0.92	0.22	0.78	
AQ	0.66	0.67	0.83	0.93	0.616
N	0.74	0.33	0.38	0.97	0.012*
Mg	0.12	0.31	0.85	0.13	0.294
N x Mg	0.07	0.051	0.79	0.06	0.042*
AQ x N	0.63	0.45	0.93	0.45	0.407
AQ x Mg	0.07	0.09	0.09	0.019	0.198
AQ x N x Mg	0.98	0.13	0.10	0.77	0.709
CV (%)	19.4	29.1	21.7	11.1	3.6

[a] Mean values representing the average of four observations, where each observation is the mean response of three plants.

[b] Mean values representing the average of three observations, where each observation is the mean response of two plants.

[c] LSD = Least significant difference at $p < 0.05$.

* Significant at $p < 0.05$. For each treatment effect separately, means followed by dissimilar letter designations indicate statistically significant differences at $p < 0.05$ (Duncan's New Multiple Range Test).

CV (%) = coefficient of variations.

Sensitivity of Western Conifers to SO_2 and Seasonal Interaction of Acid Fog and Ozone

W.E. Hogsett[1]
David T. Tingey[1]
Craig Hendricks[2]
Deborah Rossi[2]

[1] *U.S. EPA*
Environmental Research Lab, Corvallis
Corvallis, Oregon

[2] *NSI, Inc.*
Corvallis, Oregon

INTRODUCTION

The increased concern for forest health and the role of anthropogenic depositions, including acidic/wet deposition and gaseous air pollutants, has led to the need to understand which forest species face the highest risk to atmospheric deposition. In order to address this issue for the western United States, many important western conifer species have been assessed with regard to seedling growth response to each of three different deposition scenarios likely to occur in the western United States. The exposure scenarios include (1) acid fog (fall-winter)/ozone (summer) in a seasonal interaction of each pollutant over the year, (2) acid fog only in fall-winter exposure, or (3) SO_2 gaseous pollutant over the fall and winter months. Seasonal interaction of the pollutants, rather than concurrent pollutant combinations represent a realistic exposure scenario for much of the climatic conditions of the coastal western United States, and the Cascade and Sierra foothills. The fumigation regimes reflect the seasonality of deposition duration, frequency of events, and chemistry for fog; and the seasonality of the frequency and distribution parameters of O_3 and SO_2 characteristic of selected regions of the West. The fumigation periods are those months when these depositions occur primarily.

Five species were selected for study based on economic and ecological importance in the West. These included Douglas-fir, ponderosa pine, lodgepole pine, western hemlock, and western redcedar. Douglas-fir and ponderosa pine were screened at both our laboratory and the Forest Service Fire Lab at Riverside, CA. A study similar to the one reported here has also been conducted at Riverside under the direction of Dr. Paul Miller. Seedling sensitivity was assessed as a growth response over two growing seasons, including the spring following the previous year's pollutant exposure. The various responses to the exposure scenarios for the first year's study are reported here. The study was repeated a second year, and these results are briefly presented.

METHODS

Pollutant Exposure Regimes

Pollutant exposures are conducted on a year-round schedule in modified open-top chambers[1] under natural environmental conditions employing simulated ambient exposure regimes for each pollutant. The exposure regimes were

Preceding page blank

developed from regional ambient air quality data. The methods of constructing the individual pollutant exposure regimes follow.

Acid Fog. The acidic fog exposure regimes were constructed from worst-case ambient fog data for the purposes of a screening study. Constructing the simulated ambient exposure regimes for acidic fog involves both selection of a fog chemistry (pH and ion concentration) and modeling the temporal dynamics of selected regional or site-specific fog events. Henninger Flats, CA, was selected as the site for the fog chemistry because this site had some of the most severe pH values for published fog analyses in the West.[2] The ion concentration of the pH 3.1 experimental treatment (Table I) are near the median ion concentrations for Henninger Flats, and the pH is near the median pH of 2.9 for the site.[2] Additional experimental treatments (pH 2.1 and pH 5.6) were created by increasing or decreasing the ion concentrations, but keeping the nitrate-to-sulfate ratio approximately 2:1 (Table I). The pH 2.1 treatment represents the extreme value from the Henninger Flat site and the ionic concentrations for the pH 3.1 and 2.1 fog fall within the range of those observed at Henninger Flat.[2] The pH 5.6 fog is representative of the ion concentrations for typical radiation-type fogs.[3]

Although fog chemistry was available from some western sites, no corresponding event frequency and duration data were available from these same monitoring sites for a sufficient time period to permit modeling the temporal dynamics of fog. Since the fog chemistry selected for the regimes represented what is perhaps a worst-case scenario, the coastal region of the West (west of the Cascades and Sierras) was chosen to obtain event frequency and duration. The coastal regions have the highest frequency of occurrence on an annual basis of fog deposition within the West (greater than 60 days), and the preponderance of occurrences are in the winter months.[4]

Two sites that represent the Coastal West region with sufficient available data were Portland and Eugene, OR. Hourly data of fog occurrence from 1948 to 1964 at these two airport sites were obtained from Dr. Kelly Redmond, Climatic Research Institute, Oregon State University. The data included visibility in miles recorded hourly and specific descriptions of meteorological events each hour including fog. One kilometer was chosen as the visibility limit because it represents the international definition of fog[5]; however, other limits were employed for maximum visibilities in the analysis for comparison of different fogs in the stochastic model. The limits included 1/8, 1/4, 1/2 and 1 mile, as well as 1 kilometer. The summary statistics derived for the Oregon data were similar to those for coastal regions through California and Washington. [6]

The fog exposure regimes were constructed with a stochastic simulation model using distribution functions that best described the three components of fog we chose to model for the regimes. The three components were: (1) the hours of the day the visibility coincided with the definition of fog (start hour); (2) the duration of the fog; and (3) the length of time since the last fog event (gap length). The summary statistics for the two sites were similar. The analysis of the relationship between frequency of events and month of the year indicated a more frequent occurrence during winter months. Consequently, only the winter months were used in the analysis.

The hour the fog event started was best described with a normal distribution, with most of the observations occurring in the early morning hours. The duration and gap length for each site were best described with exponential functions, showing distinctly skewed distributions. The relationship between the three components indicated no correlation between gap and duration, a slightly negative correlation between gap and start hour (-0.1), and a slightly positive correlation (+0.1) between start hour and duration. Box-Jenkins type time series modeling of duration and gaps indicated these variables were best modeled as independent exponential events (independent of each other). For this profile development, the start hour was also treated as a random, independent variable described with a normal distribution. A random variable model was used to generate simulated regimes for fog. In the model, both gaps and duration were assumed to be independent, identically distributed exponential random variables. The gaps were assumed to have a mean of 3.1 days, to resemble the gaps at Portland and Eugene. The mean duration was assumed to be 4.2 h for the same reason. The start hour was modeled as a normal distribution with a mean of 4 a.m. and a standard deviation of 4 h. Twenty-four simulations were generated and one was selected for generating a 60-day regime. The simulant selected had features that approximate the average for all the simulants (Figure 1). Treatment levels have the same temporal regime, but different pH values and their related ionic composition. The 60-day regimes were repeated as needed for the entire exposure period.

Ozone. Finding sufficient hourly ozone monitoring data from rural and remote areas in the West was difficult. Consequently, the ozone exposure regimes were constructed from air quality data of the upper Midwest, including rural and remote sites in Minnesota, Wisconsin, and Michigan. The exposure regimes were constructed averaging the following air quality characteristics over the 7-month period of April-October from ten monitoring sites across the region: (1) frequency of occurrence of hourly concentrations in 0.01 ppm increments; (2) percentile distributions; (3) duration of concentrations; and (4) length of time between episodes or peak events.[7,8] These average values were then used to construct a 30-day hourly concentration regime that reflects the ambient air quality characteristics of the region (Figure 2). The 30-day profile is repeated continuously over the designated exposure period or growing season. A range of treatments was created by increasing the hourly concentrations greater than or equal to 0.07 ppm by 60% and 80% (Figure 2). The resulting regimes are within 1-2 standard deviations of the mean frequency of occurrence of concentrations from the regional mean values. A statistical summary of the three ozone treatments is given in Table II. The 7-h mean is taken for the typical period of 9 a.m.–4 p.m. and the maximum 7-h concentration period.

Although constructed from upper Midwest air quality data, the exposure regimes are quite similar to hourly ozone concentrations and their temporal distributions observed from recent monitoring in the Cascades southeast of Seattle[9] and the Sequoia National Park in California.

Sulfur Dioxide. The SO_2 exposure regimes were constructed from air quality data selected from the SAROAD database from sites in the West that represented worst-case scenarios for the point-source pollutant. The initial site selection included Miami (Gila County), AZ, Greenlee County, AZ, Bannock County, ID, Shoshoni County, ID, Anaconda-Deer Lodge, MT, and Lewis and Clark County, MT. All of these sites were associated with smelters and were analyzed for the years 1979–83. The two Arizona sites had the most severe exposures and were selected to construct the profiles because of the intensity of the concentrations during 1981–83 and the completeness of the data. Analysis and subsequent construction of the exposure regimes for gaseous SO_2 was handled differently than that for O_3. A stochastic modeling approach was used to more accurately describe the extreme fluctuations in concentrations that occur with a point-source pollutant (i.e., brief periods at high, extreme concentrations, as well as extended periods when the concentration is below or near the detection limit of the analyzer). The analysis involved modeling the components of the site air quality with time-series models and then constructing an experimental exposure regime from the stochastic simulation model. The components of air quality that were modeled were: (1) episode duration; (2) the time between episodes or gap length; (3) episode start time; (4) maximum concentration; (5) time of maximum concentration; (6) relationship of maximum concentration and episode duration;, and (7) relationship of maximum concentration and hourly SO_2 concentration during that episode. The mathematical distributions of each of these components and their relationship to one another over time were determined.

The season with the highest concentrations was winter (December–February) at both sites. Since these higher values consistently occurred over all years, only winter months were used to construct the exposure profiles. An additional consideration in using only the winter months was the observation that at least some perennials exhibited increased sensitivity to SO_2 during the winter.[10] The concentration of hourly SO_2 was analyzed in terms of episodes using a threshold value of 30 ppb and length of gap (i.e., time between episodes). Threshold values of 10, 60, 100, 150, and 250 ppb were also used, and the results were similar to those with 30 ppb. The distribution of maximum SO_2 concentration was also determined for the episodes. Finally, the correlations between these three components (episode length, gap length, and episode maximum) were determined.

In addition to the episode variables mentioned above, the time variables of the air quality were also analyzed. This analysis included start hour for the episode and the hour at which the maximum occurs. The time variables at the two Arizona sites were different, which probably reflected meteorological differences at the two locations. The start hour of an episode was more frequently around noon at Greenlee, while the start hour at Miami was not consistent. The time of day the maximum concentration occurred was midday at Greenlee and in the early morning hours at Miami.

The mathematical functions describing each of the above components of point-source air quality were used in a Box-Jenkins type time series model to generate a number of simulated exposure profiles. Twenty simulants were generated by the model and one was selected that had component characteristics that were about average for all the simulants. This simulant was rerun in the model with a 24 x 60 matrix generating the hourly SO_2 concentrations for a 60-day exposure profile. The base profile is shown in Figure 3. Additional treatments were created by reducing the concentration of all peaks in the base profile by 33% and 67%, and the event frequency of the base profile by 33% and 67% (Figure 4). Table III gives a number of summary statistics for the SO_2 profiles.

Exposure Treatments

The first pollution scenario was summer ozone exposure followed by acid fog exposure during winter months. The ozone exposure period in the first year's study was 134 days beginning June 13, 1986, and the treatment levels included: (1) 30-day sum of 31 ppm and 7-h mean of 0.067 ppm (Figure 2), (2) 30-day sum of 34 ppm and 7-h mean of 0.071 ppm (Figure 2), and (3) charcoal-filtered air. Winter acid fog exposures followed the summer ozone exposure. Three treatment levels were employed and each had the same temporal regime (Figure 1), but with different pH values (5.6, 3.1, 2.1) and their related ionic composition (Table I). The fog exposure period was 60 days. The second deposition scenario of only acid fog employed the same fog exposure regimes as above, but with only two species, ponderosa pine and Douglas-fir, and no previous exposure to ozone. The third pollutant scenario was SO_2 exposures during the winter months. Four treatment levels were employed (Figure 3): (1) 66 ppb 60-day mean; (2) 42 ppb 60-day mean; (3) 21 ppb 60-day mean; and (4) charcoal-filtered control.

Plant Culture

Seedlings (1/0) of each species were obtained from commercial growers and from known seed sources and regions. Douglas-fir was from Oregon seed zone 452 (2000 ft, western Cascades). Western hemlock and western redcedar were from Oregon seed zone 052 (Northern Coast Range). Ponderosa pine was from California seed zone 522 (2000 ft, western Sierra). Lodgepole pine was from Washington seed zone 821 (3500 ft, Colville National Forest). Seedlings were transplanted with minimum disturbance of the root ball to Dee-cells (2.5" x 10") in Pro-Mix:Perlite (1:1 v/v) and supplied with a balanced nutrient at least one day per week, but not more than two days per week. Normal wet/dry cycles in soil moisture were maintained for optimal growing conditions.

Seedlings were selected from the whole population to increase the uniformity of the experimental population prior to beginning the study. The initial selection was based on seedling vigor and intact apical bud. From this resultant population, seedlings were selected primarily based on stem diameter (approximately 1-2 mm range) and secondarily on height.

Design

The experimental design for each exposure scenario utilized a hierarchical structure with seedlings randomized to the chambers, and stratified by pretreatment diameter. In the ozone/acid fog exposure study (Table IV), the ozone treatment levels were replicated three times, with 20 seedlings of each species in each chamber (60 seedlings per treatment). Following the ozone season, all seedlings from each chamber were then randomly assigned to acid fog chambers. Each acid fog treatment was replicated twice, giving a total of six chambers with 20 seedlings of each species in each of two replicate chambers (for a total of 40 seedlings per treatment). The other two pollutant scenarios, acid fog only, or SO_2 only exposure, utilized the same design but with 20 seedlings of each species in each of two replicate chambers for a total of 40 seedlings per treatment (Tables V and VI). After the appropriate exposure period, the seedlings were maintained in the nursery area to assess bud elongation and biomass the following spring and summer. The time of completion of bud elongation and spring growth varied among the five species. The experimental design was repeated in a second study (1987-88), but the number of seedlings of each species assessed with each chamber replica was increased from 20 to 24 with three chambers per treatment.

Two basic types of growth assessment were conducted during and following the different exposure periods: (1) weekly or biweekly assessment of change in stem diameter and height on the same plants over the exposure periods, "repeat measurements" (20 seedlings per species per chamber), and (2) final destructive harvests for assessment of changes in biomass and spring bud growth, conducted the spring and summer following the exposure periods.

The variables included: needle, stem, and root dry weight; number and length of branches; needle number by developmental stage; bud number; and bud elongation. The final harvest utilized 10 plants per species per chamber for the ozone/acid fog exposure and 20 plants per species per chamber for the acid fog only and SO_2 only exposures.

A pretreatment harvest of 40 seedlings of each species preceded each of the three exposure studies to evaluate the relationship of pretreatment biomass (stem, needle, and root dry weight), and stem diameter and height. Pretreatment measurements of diameter and height of the experimental seedlings provided covariates for statistical analysis of the repeated measures data.

Analysis of variance or covariance was used to assess treatment effects. Table VII is an example of the parameters for analysis of variance for final harvest biomass variables. Transformations of the data were used due to nonconstant variances and nonadditivity. A natural log transformation was used for height, diameter, bud elongation, and dry weight variables. Proportion variables used an arcsin square root transformation, and count variables used a square-root transformation. With repeated measurements of stem height, diameter, and bud elongation on the same plants, multivariate repeated measures techniques were used. Covariates included pretreatment stem height and diameter. More specific treatment comparisons were made using polynomial contrasts and Bonferroni multiple comparison techniques.

RESULTS

The study began in June 1986 with ozone exposures followed by acid fog exposures that began in March 1987. Sulfur dioxide exposures began in January 1986 and were completed April 13, 1987. Final assessment of growth alterations from the various exposure scenarios was not completed until September 1987 in order to fully assess the second year's growth resulting from the previous season's exposures.

The study was repeated a second year with an equivalent population of seedlings for each of the five species. Ozone exposure studies were conducted from June to October 1987, and were followed by acid fog exposures from December 1987 and until April 1988. SO_2 exposures began in December 1987 and continued until April 1988. Bud elongation and final assessment of growth variables began in April 1988 and were not completed until September 1988.

Seedling Growth Response

Table VIII presents a compilation of all significant ($P < 0.1$) treatment effects on growth observed in each of the five species after one year (1986–87) of seasonal exposure to the three scenarios. Briefly, all species exhibited growth over time in all measured variables (e.g., increase in height and diameter over the year) and bud growth the following spring. Certain growth variables were significantly altered with one or all exposure scenarios (Table VIII). This alteration was, in most instances, a reduction compared to control treatments, but there were several instances of growth increases in some variables, especially winter SO_2 exposure and acidic fog (Table VIII).

Repeated measures of height and diameter. Only western hemlock exhibited significant reductions in growth rate of height ($P < 0.05$) and diameter ($P < 0.025$) during exposure to ozone and acid fog. The growth rate slowed sooner in seedlings exposed to the higher ozone regime compared to charcoal-filtered air controls or the lower ozone concentration regime (Figure 4). At the final harvest, the hemlock seedlings exposed to ozone/acid fog were reduced 10% in height compared to controls. Redcedar was also significantly affected by the ozone/acid fog exposure scenarios. However, an increase in the rate of height growth ($P < 0.10$) was seen with exposure (Figure 4), and at final harvest the height of exposed seedlings had increased 8-12% over controls. The only other species exhibiting alterations in height or diameter with ozone/acid fog exposure was ponderosa pine, but this was not seen until the following spring in the second season of growth. A 10% reduction in height and diameter ($P < 0.005$) compared to controls was exhibited. No acid fog ozone interaction was observed.

Bud elongation in the spring/summer following the ozone x acid fog exposure period (June 1986–April 1987) was a "repeated measure" on the same plants, beginning with bud break during the spring and continuing until it was judged that bud elongation was complete and/or next season's bud was set. Bud elongation rate was reduced in western hemlock ($P = 0.06$) and ponderosa pine ($P = 0.06$) with both levels of ozone (Figure 5). Acidic fog at pH 2.1 also significantly reduced bud growth in hemlock ($P = 0.09$), but not any other species (Figure 6). On the other hand, western redcedar exhibited increased bud elongation rate with the highest ozone level ($P < 0.005$) and with acidic fog of pH 2.1 ($P < 0.05$) compared to controls (Figure 6). Only Douglas-fir bud elongation was unaffected by ozone/acid fog exposures. Winter SO_2 exposure caused significant increases in bud elongation in all species except lodgepole pine, which exhibited an increase in stem dry weight (Table VIII, Figure 7). The fastest growth rate and the resultant increased bud length did not necessarily result from exposure to the highest SO_2 concentration in all species. In the case of western redcedar, the fastest growth rate was observed in the seedlings exposed to the lowest SO_2 concentration (B x 0.67).

Final biomass harvest. Measures of biomass after spring growth following the previous year's exposures showed significant growth changes in all species, but the extent of the changes was notably different between the five species. Ponderosa pine ($P = 0.05$), hemlock ($P = 0.05$), and Douglas-fir ($P = 0.10$–0.15) all exhibited significant reductions in needle (total and certain age classes), stem, and root dry weight when exposed to ozone and acid fog. Table IX illustrates percent changes in these variables compared to charcoal-filtered air controls as a result of the two ozone treatment levels. In addition to these ozone main treatment effects with the ozone/acid fog exposure scenario, acid fog main treatment effects were observed in Douglas-fir as reduction in biomass of current year needles ($P = 0.05$). Significant reductions in bud elongation ($P = 0.09$) and root/needle dry weight ratio ($P = 0.10$) were noted in hemlock (Table X). Western redcedar, unlike the other species, exhibited significant increases in growth variables as ozone treatment effects (Table IX), acid fog effects (Table X), and ozone/acid fog interactions. Only root dry weight was reduced significantly below controls with exposure (Tables IX, X). Lodgepole pine biomass was apparently not significantly affected with exposure to ozone and acid fog.

The study was repeated with the identical treatment levels of all three exposure scenarios beginning June 1987 and continuing through October 1988 for final assessments of growth. The growth alterations observed were similar in this exposure season, with ponderosa pine exhibiting the largest number of growth measures altered with ozone/acid fog exposure, including reductions in stem, needle, and root biomass, as well as diameter. Unlike the previous year, a slight increase in spring bud growth with the lower ozone treatment was seen. Western redcedar again showed the least susceptibility to the exposure regimes. Unlike the previous year, lodgepole exhibited significant alterations in growth measures as a result of the ozone exposure, including reductions in root and needle biomass. Acid fog only and the SO_2 exposures, as with the 1986-87 exposures, caused significant increases in bud elongation the following spring and, unlike the previous year, increases in needle biomass.

DISCUSSION

Alterations in any of the growth variables, either during or following the exposure periods, are the criteria for assessing relative sensitivity among the 5 species. Based simply on the number of growth measures reduced by one season's exposure, ponderosa pine and hemlock are somewhat more responsive to the ozone/acid fog deposition scenario than the other three species, with lodgepole pine being the least responsive. Some species exhibited increases in one of the several measures of growth with exposure. Western redcedar exhibited significant increases rather than decreases in a number of the growth variables as a result of ozone/acid fog exposures, including the following spring's bud elongation. Hemlock and redcedar appeared to be more responsive to acid fog at both pH 3.1 and 2.1 than the other species. In addition, only these two species exhibited any visible needle injury to the fog exposures. The scenario of acid fog alone was assessed in just two of the species, both of which exhibited increases in height as a result. Douglas-fir also showed increases in stem diameter and stem dry weight, but reduction in root dry weight with pH 2.1. Exposure to SO_2 during the winter months, like the acid fog only exposures, appeared to cause increases in several growth variables. The most prevalent was an increase in spring bud elongation. It is important to note that most growth effects with treatment, in particular changes in biomass, did not occur during the time period of the exposure, but rather at the end of the following spring/summer bud elongation period. If growth had been monitored only during the period of exposure, the resultant alterations in growth from the ozone/acid fog treatment would not have been detected. It is interesting to note that, at least from one years' exposure results, reduction in spring bud elongation occurs with ozone/acid fog exposure, and increases in rate and length occur with winter SO_2 exposures in all the species screened but one, lodgepole pine. This measure of spring bud elongation rate and final length attained is perhaps reflective of the impact of the particular deposition scenario on carbohydrate reserves accumulated in the bud during the ozone/acid fog exposure period and the role these reserves play in growth of the bud the following spring. It is important to remember that the observations reported here are from the first season's exposures, and only general reference to the second exposure season's responses are reported.

The two exposure studies, however, generally agree on biomass reductions for various seedling tissue components following spring growth. Based on these measures of growth and response to these particular deposition scenarios, ponderosa pine appears to be the most sensitive conifer to ozone/acid fog exposures. Western redcedar and lodgepole pine appear to be the least susceptible. Douglas-fir and western hemlock had intermediate response. Acidic fog exposures alone and SO_2 exposures were both notable in causing many growth measures to be increased above controls. None of the biomass measures for any of the species exhibited any reductions greater than 10% with these exposure scenarios. However, there were increases in biomass of needles, stem, and spring bud elongation from 7-30% above controls in all species. The cause of this increase in biomass and bud elongation is under study. The increases in needle and stem biomass as well as the reduced or unchanged root biomass with acidic fog or SO_2 exposure resulted in reduced root/shoot ratios in hemlock, ponderosa pine, and Douglas-fir. This imbalance in allocation may have a detrimental effect on growth and seedling establishment with continued multi-year exposures. With only one year of exposure, however, speculation seems premature and offers an area of future study.

ACKNOWLEDGMENTS

We gratefully acknowledge the State of California Department of Forestry and Fire Protection for supplying ponderosa pine seedlings.

REFERENCES

1. W.E. Hogsett, D.T. Tingey, and S.R. Holman, "A programmable exposure control system for determination of the effects of pollutant exposure regimes on plant growth." *Atmos. Environ.* 19:1135 (1985).

2. J.M. Waldman, J.W. Munger, D.J. Jacob, and M.R. Hoffman, "Chemical characterization of stratus cloudwater and its role as a vector for pollutant deposition in a Los Angeles pine forest," *Tellus* 37B:91 (1985).

3. Sandro Fuzzi, R.A. Castillo, J.A. Juisto, and G.G. Lala, "Chemical composition of radiation fog water at Albany, New York, and its relationship to fog microphysics," *J. Geophysical Res.* 89:7159 (1984).

4. Robert G. Stone, "Fog in the United States and adjacent regions," *The Geographical Rev.* 26:111 (1936).

5. National Weather Service, Federal Meteorological Handbook, 1980.

6. U.S. Department of Commerce, "Incidences of low ceilings and low visibilities in U.S. Pacific coastal regions," Weather Division Headquarters, Army Air Forces.

7. A.S. Lefohn, W.E. Hogsett, and D.T. Tingey, "A method for developing ozone exposures that mimic ambient conditions in agricultural areas," *Atmos. Environ.* 20:361 (1986).

8. A.S. Lefohn, W.E. Hogsett, and D.T. Tingey, "The development of sulfur dioxide and ozone exposure profiles that mimic ambient conditions in the rural southeastern United States," *Atmos. Environ.* 21:659 (1986).

9. R.L. Edmonds and F.A. Basabe, "Ozone concentrations above a Douglas-fir forest canpoy in western Washington, U.S.A.," *Atmos, Environ.* 23:625 (1989).

10. M.E. Whitmore and T.A. Mansfield, "Effect of long-term exposures to SO_2 and NO_2 on *Poa pratensis* and other grasses," *Environ. Pollut.* 31:217 (1983).

Table I. Ionic composition of acid fog treatments

Component	pH 2.1 (ueq/l)	pH 3.1 (ueq/l)	pH 5.6 (ueq/l)
H^+	9610	1240	124
Na^+	1080	570	130
K^+	160	40	4
NH_4^+	2360	590	59
Ca^{2+}	150	150	15
Mg^{2+}	840	210	21
Cl^-	5040	210	21
NO_3^-	5960	1490	149
SO_4^{2-}	3200	800	80
OH^-	0	300	153
Total Cations	14200	2800	353
Total Anions	14200	2500	250

Table II. Seasonal statistical summary of ozone exposure profiles

	7-hr mean (ppm)		12-hr mean (ppm)	30-day integrated sum (ppm-h)		
Profile	9am–4pm	11am–6pm	9am–9pm	>0	>0.07	>0.10
Base	0.053	0.055	0.050	27	5	1
Base*1.6	0.063	0.067	0.060	31	11	9
Base*1.8	0.067	0.071	0.064	34	14	12

Table III. Summary statistics for SO_2 exposure profiles

	Base SO_2	Base*0.67	Base*0.33
60-day mean (ppb)	65.78	42.18	20.93
60-day sum (ppb-h)	94716	60741	30135
Number Hrs > 30 ppb	369	318	270
Number Days 24 h avg > 0.14 ppm	8	3	0
Number Days max 3-h	12	4	0

Table IV. Ozone/Acid fog exposure scenario for the '86–87 exposure season with elements of design and measurements taken

Time Period	Duration (Days)	Pollutant	Design	Treatment	Measurements
3/01/86–6/10/86				nursery site	Seedling selection
6/10/86–10/17/86	134	Ozone	3 chambers/treatment 20 seedlings/species /chamber	C 67 71 7-h means (ppb)	Pretreatment harvest (40 seedlings) Repeated measures (4x)
10/17/86–3/01/87				seedlings held in open-tops seedlings from each chamber	
3/01/87–5/01/87	60	Acid Fog	2 chambers/treatment 10 seedlings/species /chamber	pH 5.6 pH 3.1 pH 2.1	Initial measurements Repeated measures visible injury (2x)
4/12/87–					Bud elongation measurements
5/01/87–9/15/87				nursery site	Repeated measures Bud elongation only
7/14 (Douglas-fir) 9/03 (ponderosa pine) 9/12–9/15 (western hemlock, western redcedar, lodgepole pine)				final harvest	Destructive harvests of all seedlings for biomass, stem height, diameter, terminal bud elongation Visible injury

Table V. Acid Fog Exposure Schedule for the '86–87 exposure season with elements of design and the measurements taken.

Time Period	Duration (Days)	Pollutant	Design	Treatment	Measurements
3/01/86–3/01/87	----------------	----------------	----------------	nursery site	Seedling selection
3/01/87–5/01/87	61	Acid Fog	2 chambers/treatment 20 seedlings/species /chamber	pH 5.6 pH 3.1 pH 2.1	Pretreatment Biomass Harvest (40 seedlings) Pretreatment measures (ht, dia.) Visible injury (day 50 & 85) Final Measures (ht, dia.)
5/10/87–9/22/87	----------------	----------------	----------------	nursery site	
5/20/87					Visible injury Repeated Measures terminal bud elongation
8/17 (ponderosa pine)					final harvest
9/22 (Douglas-fir)					Destructive Harvest of all seedlings for biomass, final height, stem diameter and bud length Visible injury

Table VI. SO_2 Exposure Schedule for the '86–87 exposure season with elements of design and the measurements taken.

Time Period	Duration (Days)	Pollutant	Design	Treatment	Measurements
3/01/86–1/01/87	------------	------------	------------	nursery site	
					Seedling selection
1/13/87–4/13/87	90	SO_2	2 chambers/treatment	C, Base, B*0.67, B*0.33	Pretreatment Biomass Harvest (40 seedlings)
			20 seedlings/species /chamber		Visible injury (day 50 & 85) Final Measures (ht, dia.)
4/13/87–9/15/87	------------	------------	------------	nursery site	
5/13/87					Visible injury
					Repeated Measures terminal bud elongation
8/10 (Douglas-fir) 9/09 (ponderosa pine) 9/17 (western hemlock, lodgepole pine) 9/29 (western redcedar)				final harvest	Destructive harvest of all seedlings for biomass, final height, stem diameter, and bud length

Table VII. Analysis of variance F-values for effects of ozone(O_3)/acid fog(AF) on ponderosa pine needle dry weight.

Source of variation	df	F-value
Model	53	2.22
O_3 Trt[a]	2	13.40[b]
O_3 CH(O_3 Trt)	6	1.74
AF Trt[c]	2	0.28
AF CH(AF Trt)	3	1.34
O_3 Trt*AF Trt[d]	4	2.05
O_3CH*AFCH(O_3 Trt*AF Trt)	36	1.17
Error[e]	123	0.076

[a] Test of hypothesis using the Ozone chamber(Ozone treatment) mean square as the error term.

[b] F-values significant at 0.01

[c] Test of hypothesis using the AcidFog chamber(AcidFog treatment) mean square as the error term.

[d] Test of hypothesis using the ozone chamber*acidfog chamber(ozone treatment*acidfog treatment) mean square as the error term.

[e] Mean square error from the analysis of variance.

Table VIII. Summary of exposure treatment effects with three different scenarios over one year. ('86–87) The listing of a variable indicates a significant reduction with at least one of the treatment levels from control treatment ($P < 0.1$) unless noted as *, which indicates a significant increase above control ($P < 0.1$).

Species	Ozone + Acid Fog				Acid Fog only	SO_2
	Ozone Treatment Effect		Acid Fog Effect	Ozone x Acid fog		
	Repeated Measures	Final Biomass[a]	Final Biomass	Final Biomass	Final Harvest	Final Harvest
ponderosa pine	bud[b]	ht., dia., NDW, 2NW, 2NC, SDW, RDW	–	–	ht*, R/N	bud*, 2NC
Douglas-fir	–	NDW, 1NW, 3NW	3NW	–	ht.*, dia.*, SDW*, RDW	bud*, dia., 2NW, 2NC
western hemlock	ht., dia., bud	ht., NDW SDW, RDW	bud R/N	–	NA	bud*, RDW R/N
western redcedar	bud*, ht.*	ht.*	bud* NDW*, SDW* RDW, R/N	R/N	NA	bud*, ht*
lodgepole pine	bud	–	–	–	NA	SDW*

[a] measurements taken after bud elongation in the spring/summer following the exposure periods (ozone: May–Oct.; acid fog: Feb.–Apr.; SO_2: Feb.–Apr.)

[b] bud = spring bud elongation rate or the final length of apical bud after spring elongation
ht. = stem height
dia. = stem diameter
NDW = needle dry weight
SDW = stem dry weight
RDW = root dry weight
R/N = root/needle dry weight ratio
xNW = needle dry weight by age class (x=1, 2, or 3)
xNC = needle number by age class (x=1, 2, or 3)
NA = species not included in treatment

Table IX. Changes in biomass after spring growth following previous year's exposures to ozone/acid fog. Alterations due to ozone averaged over all fog treatments and reported as percent difference from charcoal-filtered control. Significantly different from charcoal-filtered control in Bonferroni T test at 0.05 level is marked (*).

Species	Needle Dry Weight		Stem Dry Weight		Root Dry Weight		Root/Needle Ratio	
	High O_3	Low O_3	High O_3	Low O_3	High O_3	Low O_3	High O_3	Low O_3
ponderosa pine	-33.6*	-27.3*	-36.3*	-20.8*	-43.6*	-33.0*	-9.3	-5.2
Douglas-fir	-19.2	-18.1	-14.8	-14.4	-20.5	-17.6	-2.4	+1.6
western hemlock	-11.0*	-4.5	-20.5*	1.0	-29.8*	-2.6	-4.9	+1.9
western redcedar	-3.0	+10.1	+8.0	+12.0	-14.6	-1.0	-14.7	-11.1
lodgepole pine	+9.0	-11.0	+14.0	+3.0	-6.1	-9.8	-15.5	+1.2

Table X. Changes in biomass after spring growth following previous year's exposures to ozone/acid fog. Alterations due to acidic fog averaged over treatments and reported as percent difference from pH 5.6 fog for an acid fog treatment effect. Significant at the level of 0.05 is marked (*) from multiple comparison Bonferroni test.

Species	Needle Dry Weight		Stem Dry Weight		Root Dry Weight		Root/Needle Ratio	
	pH 3.1	pH 2.1	pH 3.1	pH 2.1	pH 3.1	pH 2.1	pH 3.1	pH 2.1
ponderosa pine	+4.6	+2.4	+3.8	-1.0	+1.0	-5.0	-4.5	-8.0
Douglas-fir	+10.0	+1.6	+9.8	+2.3	+6.3	-12.5	-4.1	-14.2
western hemlock	0.0	+2.0	+2.8	+4.7	-17.0	-22.0	-17.0	-24.0*
western redcedar	+6.0	+10.1	+6.0	+11.6	-6.2	-20.2*	-14.8	-30.2
lodgepole pine	+4.0	+16.0	+4.0	+1.0	+3.8	-3.1	0.0	-19.5

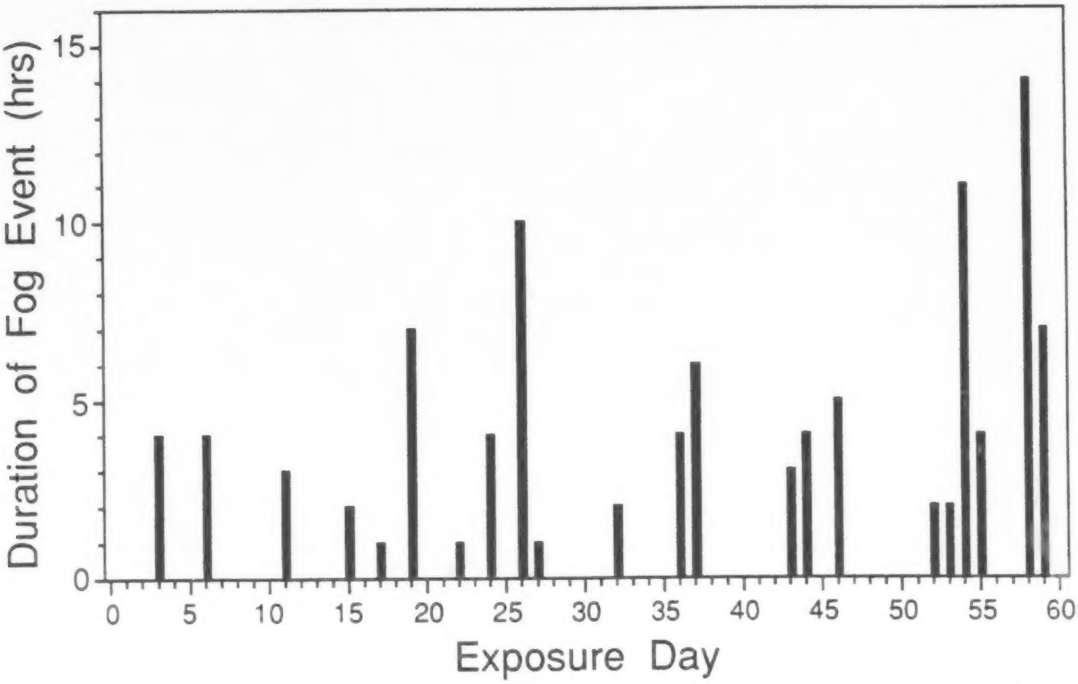

Figure 1. Simulated exposure regime for acid fog giving duration and frequency of events over a 60-day period.

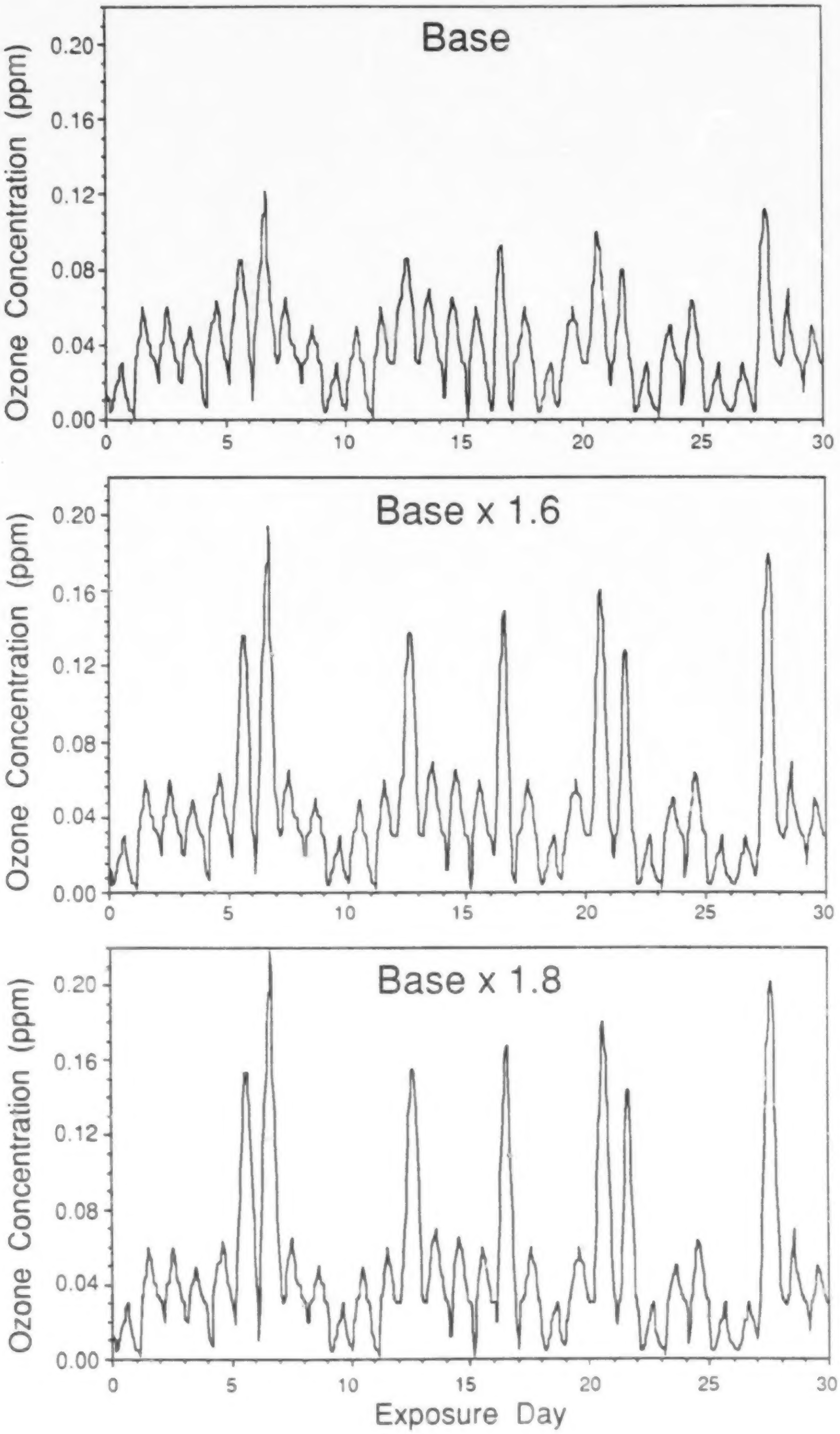

Figure 2. Simulated exposure regimes for ozone. Note that the 'BASE' regime was employed only in the '87–88 exposure season. The 30-day regimes were repeated over the 134-day ('86–87 season) and 126-day ('87–88 season) exposure period.

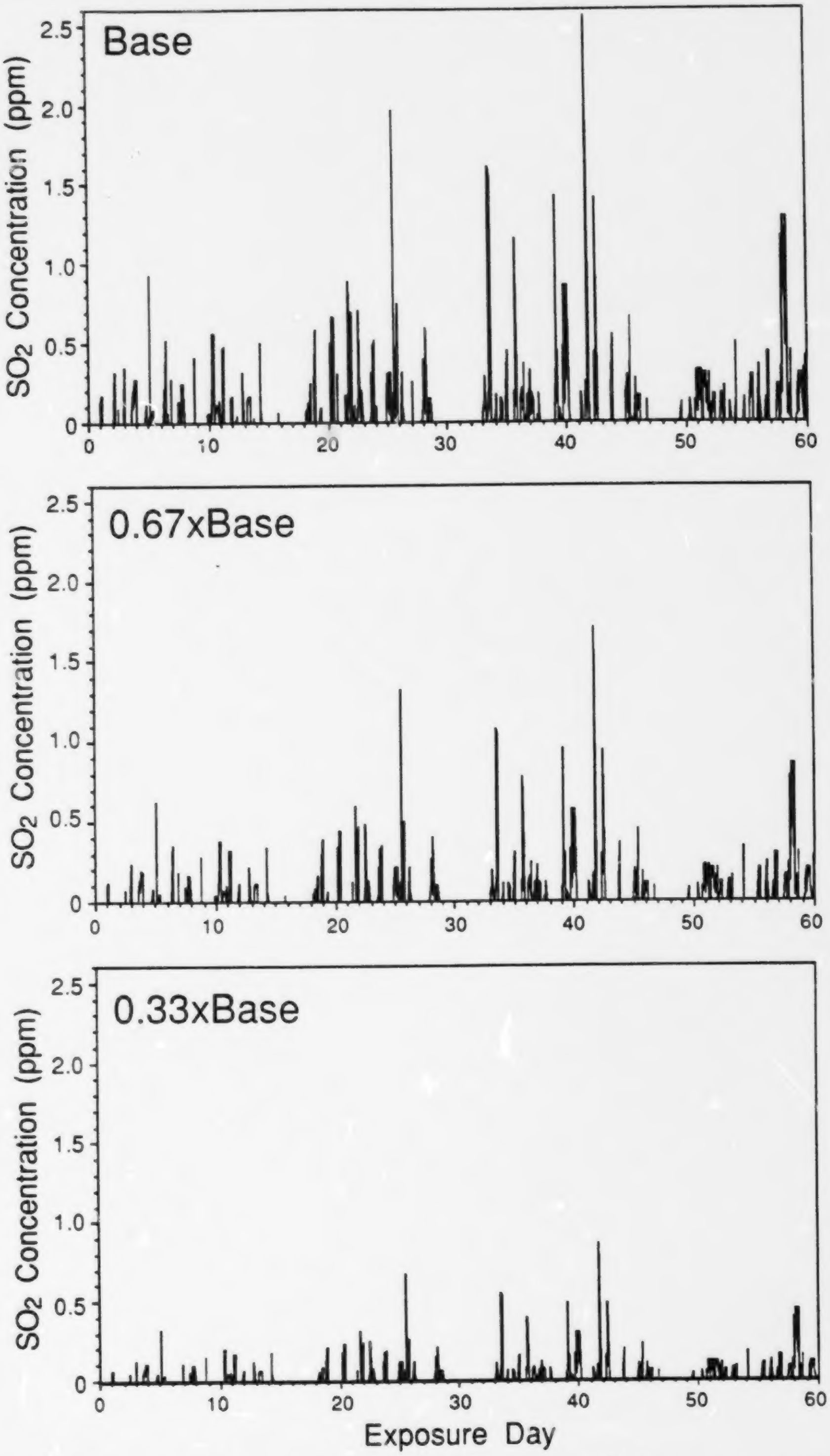

Figure 3. Simulated exposure regimes for SO$_2$. The 60-day exposure regimes were repeated over the 90-day exposure periods during the fall and winter months of '86–87 and '87–88.

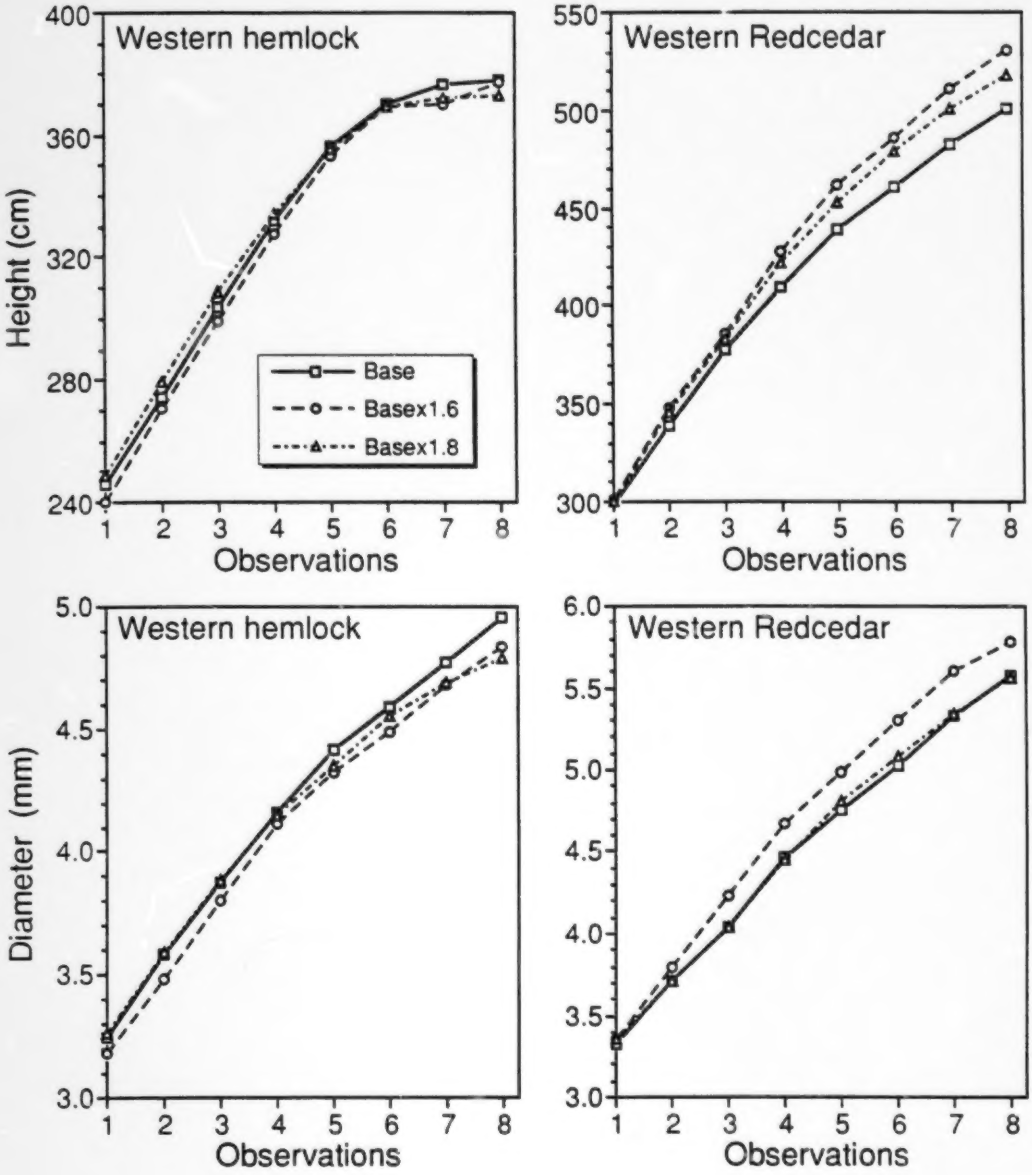

Figure 4. Changes in height and diameter of western hemlock and western redcedar over the 134-day ozone exposure period of the ozone/acid fog exposure scenario ('86–87 season). The average standard errors for western hemlock diameter: Control = 1.006; Base*1.6 = 1.006; Base*1.8 = 1.006; height: Control = 1.006; Base*1.6 = 1.006; Base*1.8 = 1.006. For western redcedar diameter: Control = 1.012; Base*1.6 = 1.012; Base*1.8 = 1.012; height: Control = 1.011; Base*1.6 = 1.012; Base*1.8 = 1.011.

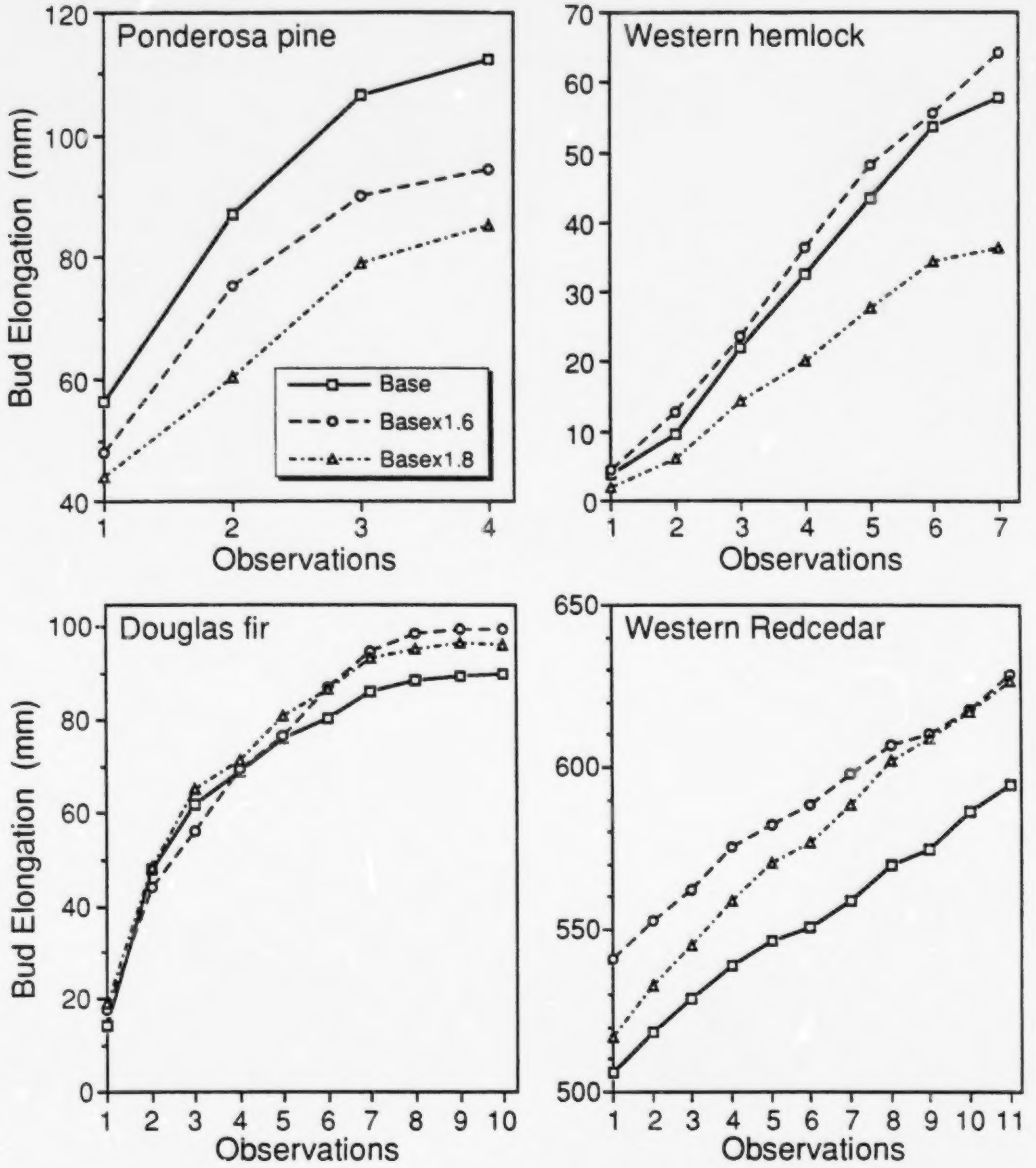

Figure 5. Spring bud elongation following ozone and acid fog exposure. The plots reflect the average ozone effect over all fog treatments. Average standard errors for ponderosa pine were: Control = 1.617; Base*1.6 = 1.475; Base*1.8 = 1.507. For Douglas-fir: Control = 1.872; Base*1.6 = 2.268; Base*1.8 = 1.877. For western hemlock: Control = 2.614; Base*1.6 = 1.916; Base*1.8 = 3.3422. For western redcedar: Control = 1.133; Base*1.6 = 1.096; Base*1.8 = 1.114. Control is charcoal-filtered air.

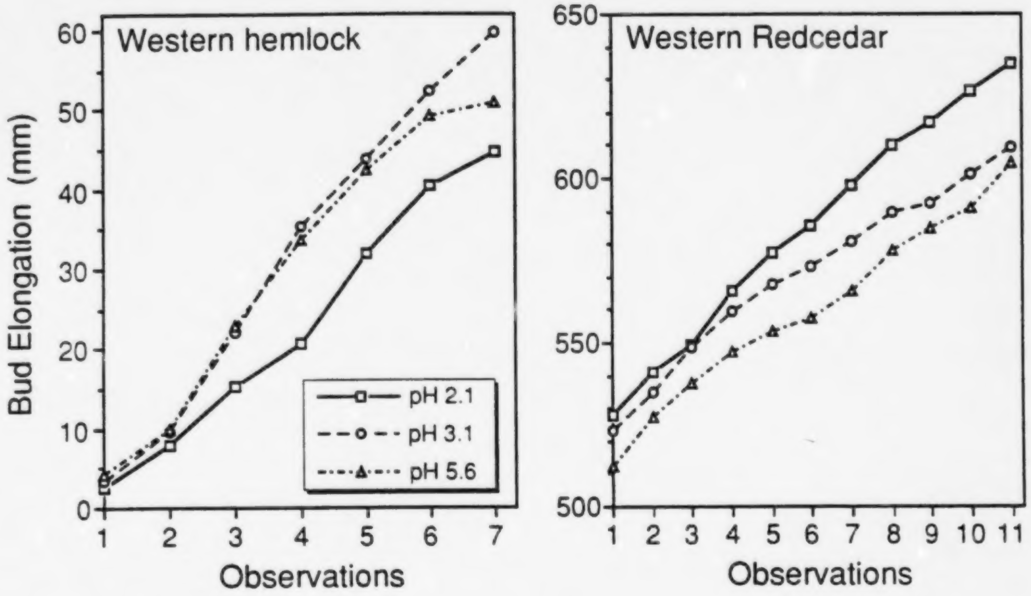

Figure 6. Spring bud elongation following ozone and acid fog exposure scenario. The plots reflect the average fog effect over all ozone treatments. Average standard errors for western hemlock were: pH 5.6 = 2.630; pH 3.1 = 2.672; pH 2.1 = 2.676. For western redcedar: pH 5.6 = 1.116; pH 3.1 = 1.119; pH 2.1 = 1.116.

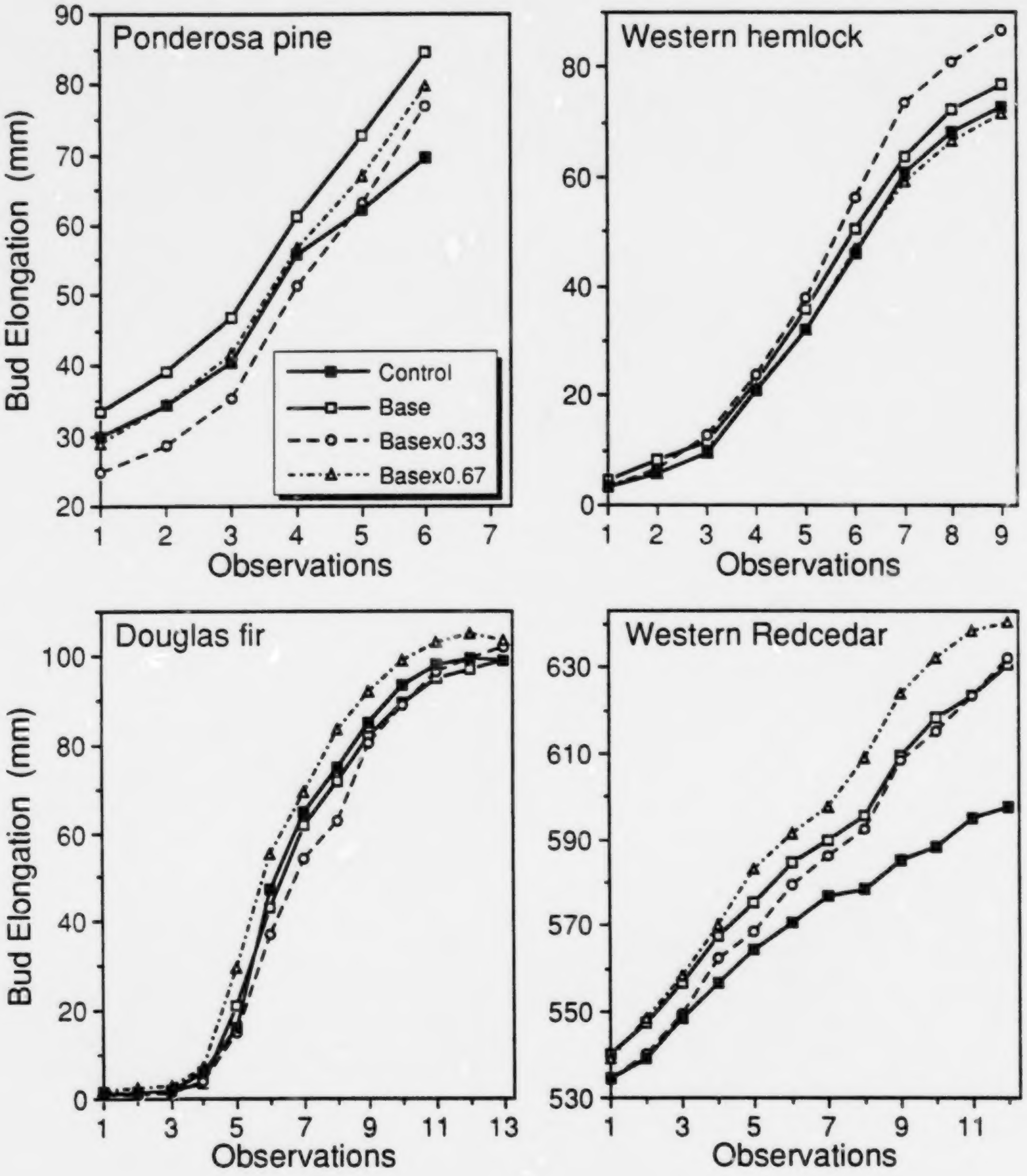

Figure 7. Spring bud elongation as affected by 90-day SO_2 exposure. Average standard errors for ponderosa pine were: Control = 1.053; Base = 1.053; Base*0.67 = 1.053; Base*0.33 = 1.053. For Douglas-fir: Control = 1.208; Base = 1.209; Base*0.67 = 1.205; Base*0.33 = 1.214. For western hemlock: control = 1.112; Base = 1.115; Base*0.67 = 1.3113; Base*0.33 = 1.112. Control is charcoal-filtered air.

Nutrient Effects on Responses of Willow and Alder to Ozone

Carol S. Greitner and William E. Winner

General Science Department
Oregon State University
Corvallis, OR 97331-6505

INTRODUCTION

Nutrient status is known to influence plant response to air pollution. Unfortunately, mechanisms of this interaction are not well understood, with no general trends apparent from the reports in the literature. It is important to understand any nutrient-air pollutant interaction, both for considering fertilizer applications for crops in highly polluted areas and for evaluating pollutant effects on plants in forests and other natural settings. In regions where acid deposition occurs, nutrient availability may change, thereby altering the response of crops and native vegetation to gaseous pollutants such as O_3 and SO_2.

To make matters more complex, most crops and native plants grow with rhizosphere symbionts including mycorrhizae and nitrogen fixing bacteria. These organisms play important roles in increasing availability of nutrients such as N, P, and K to plants. Air pollutants may influence the symbiosis, thereby altering the capacity for plants to acquire nutrients and to respond to air pollution.

One goal of this paper is to synthesize the current understanding in this area by examining reports in the literature in which plants were raised under various nutrient regimes and exposed to O_3. We have not considered studies with SO_2 and acid deposition due to the complication that these air pollutants include elements that are nutrients in themselves.

Another goal is to probe nutrient-air pollutant interactions with a simple plant system without rhizosphere symbionts. We conducted a laboratory study with willow (*Salix nigra* Marsh.) to attempt to determine (1) if nutrient status affected this species' sensitivity to O_3 and (2) if visible injury was associated with growth reduction. Willow was chosen because stem cuttings readily produce adventitious roots, making it possible to quickly obtain many genetically-alike individuals.

A final goal of this paper is to relate O_3-nutrient interactions to the capacity for rhizosphere symbionts to influence plant response to O_3. This involved exposing alder (*Alnus serrulata* Aiton. Willdenow) with and without root nodules formed by the nitrogen-fixing actinomycete *Frankia* to filtered air or O_3. Thus high and low nitrogen treatments were provided by the presence and absence respectively of the rhizosphere symbiont. Gas exchange parameters were measured. In addition, stable carbon isotope ratios were analyzed for both nodulated and unnodulated plants.

Current Understanding

Nutrients are seldom at optimal levels for plants. In general, during vegetative growth phases, plants compensate for nutrient oversupply and undersupply in order to (1) maximize growth under prevailing conditions and (2) maximize acquisition of limiting resources.[1] Nutrient levels are typically below optimal: plants compensate by increasing root:shoot ratios.[2] Interestingly, air pollutants are known to cause decreases in root:shoot ratios.[3-5] Thus plants exposed to both insufficient nutrient supply and air pollution are coping with stresses that would independently force resource partitioning in opposite directions. The "ideal" of optimal nutrient level and clean air results in a carbon allocation pattern balanced between roots and shoots (Figure 1a). Nutrient deficiency in clean air leads to a shift in allocation to enhance root growth at the expense of shoot growth (Figure 1b). When nutrients are at optimal levels but O_3 is present, the allocation pattern is shifted in the opposite direction and shoot allocation is dominant (Figure 1c). The overall plant size may also be reduced. The effect of combining nutrient deficiency and O_3 exposure is largely unknown (Figure 1d). Of principal concern then is the relative strength of these interacting stresses as they drive plant morphology in opposite directions.

Nitrogen is generally thought to be widely limiting for plant production in both agricultural and forested systems. However, excess N has the potential to damage some forests because balances in growth between roots and shoots may be disrupted by direct fertilization of the canopy.[6] N is positively correlated with metabolic capacity: plants raised at high N have higher photosynthetic capacities and stomatal conductances than plants raised at low N.[7,8] These metabolic parameters are directly related to air pollution sensitivity (i.e., high conductance results in high pollutant absorption rates).[9-11]

N status is also known to alter plant sensitivity to air pollution, but results vary from study to study. Tobacco plants grown at optimal N level showed more foliar injury than plants grown at either deficiency or luxury levels in one report,[12] but in another case injury was enhanced by both deficiency and excess of N.[13] N had no interaction with O_3 in growth of fescue and ladino clover.[14] High N concentrations made *Lemna minor* more susceptible to loss of chlorophyll induced by O_3.[15]

K is involved in stomatal control[2] and therefore may influence the amount of O_3 absorbed by leaves. Plants raised under K deficiency might be unable to open stomata as widely as plants whose K supply was not limiting. K-deficient plants might therefore absorb less O_3 and express less injury. Studies with silver maple[16] and tomato[17] gave results compatible with this scenario. In contrast, soybean and pinto bean grown at low K showed more foliar injury than at high K.[18]

Increased levels of P were associated with increased visible injury in tomato.[19] High levels of S protected against both visible injury and loss of chlorophyll induced by O_3 in beans.[20] Hybrid poplars grown at half the recommended rate of NPK fertilizer had more visible injury than unfertilized plants and those raised using the recommended fertilization rate.[21] Relative proportions of individual nutrients appear to be important in injury expression.[15]

Studies on nutrient impact on plant susceptibility to O_3 have been conducted with different species, nutrient levels, and O_3 doses. Few studies have involved more than one or two species or nutrient elements; thus drawing general conclusions about nutrient-pollutant interactions is difficult. Experiments involving several species and relating visible injury to changes in growth and physiology are needed.

EXPERIMENTAL METHODS

Willow Study

Branches were collected from a single *Salix nigra* shrub in the Jefferson National Forest, Montgomery County, VA in October, 1985. Cuttings were placed in trays of Promix (Premier Brands, Inc., New Rochelle, New York) under mist in a filtered-air greenhouse with a 16-h light photoperiod. After 4 weeks, cuttings with roots and leaves were removed from the mist and transplanted to individual 0.7 liter pots containing Promix. About a month later, roots of the cuttings were washed free of potting mix and transplanted to 0.7 liter pots containing an inorganic mixture of 1 volume clay to 3 volumes vermiculite. Plants were fertilized with 1 (low nutrient plants), 2 (medium nutrient), or 3 (high nutrient) grams slow-release Osmocote 14-14-14 (NPK) fertilizer (Sierra Chemical Company, Milpitas, CA) per pot.

For each of the three fertilizer levels, 12 plants were randomly selected to be exposed to O_3-free charcoal-filtered air (controls), 12 to be exposed to 0.06 ppm O_3 (low O_3) and 12 to be exposed to 0.12 ppm O_3 (high O_3). O_3 was generated from pure O_2 by electrical discharge. Fumigations began about 4 weeks after fertilization and were conducted in continuously stirred tank reactors (CSTRs) equipped with 1000 W metal halide lamps. Plants were fumigated an average of 4 h per day for 18 days in a 27-day period. Six chambers were used for the study (two control, two low O_3 and two high O_3), and six plants grown at each nutrient level were placed in each chamber. Plants were returned to the greenhouse after exposures. The day after each fumigation, foliage was inspected for visible injury, with percent leaf area necrotic estimated to the nearest 5% for each plant. When only a trace of injury (necrosis of less than 5% of the total leaf area) occurred, the plant was given a rating of 1%.

During the 11th exposure, one chamber of control plants was lost due to equipment malfunction. Therefore, the number of control plants per nutrient treatment in the final harvest was six, half that of the low and high O_3 exposures. Foliar injury had not been observed on any of the plants in the low or high O_3 chambers after 11 exposures; therefore the mean concentrations were doubled to an average of 0.12 ppm in the low and 0.24 ppm in the high O_3 chambers in order to determine the sensitivity of *S. nigra* to O_3. There were seven exposures to the increased concentrations, and the final harvest took place 2-3 days after the last fumigation. Roots were washed to remove potting mix, and the plants were separated into roots, stems, and leaves. Leaf areas were measured with a Hayashi Denko AAM-5 area meter. Samples were dried in a forced-air oven for 48 h and weighed to 0.01 mg. Means and standard errors of the means were calculated.

Alder-*Frankia* Study

Alnus serrulata seeds were collected from a single clump of stems in the Jefferson National Forest in November 1985. Seeds were surface sterilized in bleach (5.25% sodium hypochlorite) for 5–10 minutes, rinsed in deionized H_2O, and soaked in deionized H_2O for 3 days. Seeds were drained, placed in a plastic bag, and stratified for 41 days in a cold room (about 4° C) followed by 3 days in a freezer (about -10° C). Seeds were sown in pots containing a 1:3 v:v mixture of clay and vermiculite in the filtered air greenhouse with a 16-h light photoperiod. Seedlings emerged after several weeks and were watered daily. About 3 months after sowing, seedlings were transplanted to individual 0.7 liter pots containing 0.5 g Osmocote 14-14-14 fertilizer.

Five and a half months after planting, 17 seedlings were selected to be inoculated with *Frankia*. Root nodules collected in the field were washed in deionized H_2O, blotted dry, weighed, surface sterilized in bleach for 15 minutes, and rinsed in deionized H_2O. The nodules were ground with a mortar and pestle, with sufficient deionized H_2O to make a 0.07 g/ml suspension. Two milliliters of the suspension were injected into the potting mix in several locations near the roots in each pot. Seventeen other seedlings received deionized H_2O. By approximately 2.5 months after inoculation, new leaves of the successfully nodulated plants were observed to be larger and greener than those of unnodulated plants.

Fumigations began in the CSTRs 8.5 months after seeds were sown. Exposures to either 0.12 ppm O_3 or O_3-free air were administered for 27 out of 29 days for periods ranging from 4 to 11 h per day. Fumigated plants were exposed to O_3 for a total of approximately 164 hours. Plants were returned to the lighted greenhouse bench following each fumigation to maintain the 16-h daylight regime. Eight chambers were used for the study (four O_3 and four O_3-free control), and one pot each of nodulated and unnodulated alder was selected for treatment in each chamber.

A LI-COR LI-6200 photosynthesis system was used for gas exchange measurements inside the fumigation chambers, which had doors equipped with gloves for cuvette manipulation. Measurements were made 24 and 29 days into the fumigation period, with the two days' data combined and analyzed together. A young, fully expanded leaf of each control and O_3-treated seedling was measured when plants were in the chambers in filtered air between fumigations (a total of four readings per treatment taken on each of the two measurement days). Leaves of O_3-treated plants were measured again at least one hour after exposure to O_3 began. Photosynthesis, stomatal conductance, and internal CO_2 concentration were calculated by the system software. Ambient CO_2 concentrations in the cuvette were less than 387 ppm immediately before measurements were taken. Means for the eight readings for each treatment were calculated, and significant differences were based on the standard error of the mean. Linear regressions were calculated for plots of photosynthesis versus conductance for each treatment.

Total foliage was collected from each plant, dried at 60° C for 48 hours and ground to pass through a #40 mesh. Samples were analyzed for stable carbon isotope ratios by Dr. James Ehleringer, University of Utah.[22]

RESULTS

Simple Nutrient Supply System: Willow Study

Foliar Injury. No injury was visible after 11 exposures (45.5 hours) at the original mean O_3 concentrations of 0.06 and 0.12 ppm. After one 4-h exposure to the doubled concentrations, injury appeared on many plants exposed to the high O_3 treatment. O_3-induced foliar injury first appeared as dark purple areas on the laminas of middle-aged leaves in particular, and older and younger leaves to a lesser extent. Injured areas became necrotic, and when injury covered a large area, leaf abscission was common. Area of abscised leaves was not included in the evaluation; therefore the percent leaf area injured scores of highly injured plants sometimes decreased with increasing number of fumigations as an artifact of the scoring procedure. Thus the total leaf area lost as a result of exposure to high O_3 is under-represented by the visible injury scores for the most severely injured plants in the later fumigations.

In the high O_3 treatment, percent leaf area injured of high and medium nutrient plants was greater than that of low nutrient plants (Figure 2). Number of plants showing injury after each fumigation increased with fertilizer level until all plants exposed to high O_3 expressed some foliar injury (Figure 3). Thus nutrients also influenced the percentage of plants showing injury (Figure 3).

Similar patterns of foliar injury development were observed for the low O_3 treatment. Percent leaf area injured was low (means of 1-2%, with no plant showing more than 5% leaf area necrotic) at all nutrient levels. Injury appeared earliest on the high nutrient plants, and the number of plants expressing visible injury increased with increasing fertilizer level at low O_3 (Figure 4).

Surprisingly, foliage was not injured when plants were initially exposed to O_3 at 0.12 ppm for 11 fumigations, yet injury appeared on the plants previously exposed to 0.06 ppm after two fumigations at 0.12 ppm. Injury was observed on at least half of the low O_3 plants of each nutrient treatment after seven fumigations at 0.12 ppm. Since there were leaves of all ages on the plants throughout the experiment, it is unlikely that this effect was simply a matter of leaf age or the exposure timing in the plant life cycle. Rather, the previous exposure to 0.06 ppm seems to have predisposed the low O_3 plants to injury by 0 12 ppm. Possibly, initial exposure to 0.12 ppm O_3 induced rapid partial stomatal closure in plants that had never been exposed to O_3, but exposure to 0.06 ppm O_3 did not. The stomata might have acclimated to O_3 at a low concentration and then failed to close when subsequently exposed to 0.12 ppm.

Analysis of Willow Growth. Willow cuttings responded to increasing nutrient levels with increases in leaf area and in dry weights of leaves, stems, and roots (Table I). Leaf weight and area increased with nutrient level within all air pollution treatments. Root and stem weights always were greater at medium than at low nutrient level. High nutrient plants sometimes, but not in all cases, had greater stem and root weights than did medium nutrient plants.

Root-to-leaf ratios were calculated to detect changes in resource allocation patterns (Table II). Root-to-leaf ratios were expected to decrease with increasing fertilizer application rate. This tended to be true for low and high O_3 plants, but the trend was not as clear for control plants, perhaps due to the smaller number of controls. High nutrient control plants did however have a lower root-to-leaf ratio than either the low or medium nutrient controls.

Mean leaf area decreased with increasing O_3 within all nutrient treatments (Table I). In all cases, there was a trend for mean leaf weight to decrease with increasing O_3 (Table). Stem weight was unaffected by O_3. The only large effect of O_3 on root weight was a 34% reduction for medium nutrient high O_3 plants.

High O_3 caused a mean decrease in leaf area of 28% and a similar decline in leaf weight (25%, Table I) for low nutrient willow cuttings. Mean percent foliar injury was not large enough (maximum recorded was 10%) to account entirely for the loss in leaf area or weight. Root-to-leaf ratio increased, showing that resource allocation had shifted to favor growth of roots at the expense of leaves (Table II). The declines in leaf area and weight relative to controls were apparently a result of both losses from necrosis and changes in allocation patterns. At low O_3, low nutrient plants had only a trace of injury, yet leaf area and weight declined (by 19% and 15% respectively, Table I). Again, root-to-leaf ratio tended to increase compared with controls (Table II). Resource allocation shifts favoring root growth seemed to be solely responsible for the decline in leaf growth for low nutrient, low O_3 willows. These results for low nutrient plants indicate that nutrient deficiency was stronger than O_3 in influencing allocation.

For medium nutrient plants exposed to high O_3, leaf weight declined 25%, which was similar in value to the percent area necrotic (more than 16%) and percent decline in leaf area (19%) (Table I). Root weight decreased 34% relative to controls. Root-to-leaf ratios decreased with increasing O_3 level for medium nutrient plants, as expected (Table II). Carbon allocation shifted to favor leaf growth at the expense of root growth and may have helped compensate for the loss of foliage due to necrosis. Apparently, medium nutrient plants were not nutrient deficient and responded to the atmospheric stress by shifting allocation to the foliage.

High nutrient willow cuttings exposed to high O_3 had a mean decrease in leaf area of at least 19% and in leaf weight of 12% (Table I) relative to the corresponding controls. Unexpectedly, root-to-leaf ratios tended to increase with increasing O_3 in high nutrient plants (Table II). This increase was a consequence of O_3-caused reduction in leaf weight, along with a tendency for root weight to increase with O_3. The explanation for this trend is not clear. The high nutrient level did not appear to have induced toxicity symptoms.

Complex Nutrient Supply System: Alder-*Frankia* Study

O_3-caused injury symptoms were not observed on any leaves. Unnodulated plants always had lower photosynthesis (Figure 5) and stomatal conductance (Figure 6) as well as higher CO_2 internal values (Figure 7) than did nodulated alders, presumably as a consequence of N deficiency. Mean photosynthetic rate of nodulated plants was not decreased by O_3 (Figure 5). Plants without *Frankia* had about a 40% decrease in mean photosynthesis in response to O_3 (Figure 5), which although not statistically significant, could be of biological importance. In addition, conductance of nodulated and unnodulated plants tended to increase with O_3 treatment, both during fumigation and in filtered air (Figure 6). Normally, factors that increase conductance make CO_2 more available to mesophyll cells and photosynthesis also increases.

Wong, Cowan, and Farquhar[7] observed that photosynthetic capacity and conductance were closely and positively correlated in *Zea mays*. Lange, Beyschlag, and Tenhunen[23] cited several studies showing a linear relationship between CO_2 assimilation and conductance. To test whether such a linear relationship existed for alder, photosynthesis was plotted against conductance for leaves of control plants and plants that had received O_3.

Photosynthesis and conductance were positively correlated for control seedlings (Table III). No significant positive correlation was found for leaves of nodulated or unnodulated O_3-fumigated plants measured during exposures (Table III) because leaves that had high conductance had lower photosynthesis values than expected.

Gas exchange rates of leaves of O_3-treated nodulated and unnodulated seedlings were also measured in filtered air to determine whether O_3 effects lasted beyond the fumigation period. Photosynthesis and conductance were correlated (Table III) for leaves of nodulated plants. Thus the relationship between photosynthesis and conductance for O_3-treated leaves of nodulated plants recovered in clean air. However, photosynthesis and conductance were only weakly correlated for O_3-treated leaves of unnodulated plants measured in filtered air (Table III). N deficiency apparently reduced the capacity for these leaves to return completely to the expected relationship between photosynthesis and conductance.

Sensitivity to O_3 was associated with high conductance for leaves of both nodulated and unnodulated plants, presumably because leaves with high conductance absorb more air pollutant. In addition, leaves with high values of conductance or photosynthesis are more metabolically active, and high rates of metabolism may confer sensitivity to air pollutants.[9] If the observation that the leaves with highest metabolic rates are also most sensitive physiologically to O_3 is generally true, then it would appear that those leaves contributing most toward productivity are most vulnerable to O_3.

Stable carbon isotope ratios, expressed as delta ^{13}C values, were measured for leaves of control nodulated and unnodulated alders (Figure 8). Leaves of plants lacking *Frankia* had significantly more negative delta ^{13}C values than plants with the symbiont. These values, which are an integrated expression of the physiological status of the plants throughout their growth, agreed with the instantaneous gas exchange measurements. The CO_2 internal value (Figure 7) was higher for unnodulated plants, indicating that ribulose bisphosphate carboxylase was able to discriminate against ^{13}C to a greater extent in unnodulated than in nodulated plants. This resulted in the more negative delta ^{13}C values for the N-deficient plants. N deficiency evidently reduced photosynthesis more than conductance, since CO_2 internal values were higher for unnodulated alders. Determining delta ^{13}C values for control and O_3-treated plants raised at various nutrient levels would provide more information on the effect of nutrition on O_3 response.

DISCUSSION

Most reports in the literature on O_3-nutrient interactions have focused on visible injury. The results are mixed: often plants raised at optimal nutrient levels showed enhanced O_3-induced foliar injury, but there are many exceptions. Few studies have examined nutrient influence on O_3-caused effects on growth or physiology; these areas require more attention. One important feature of air pollution and nutrient stress interactions that has long been overlooked involves biomass partitioning between roots and shoots. Since air pollution stress results in partitioning favoring shoots and nutrient deficiency results in partitioning favoring roots, the combination of these two stresses together places the fate of photosynthate in question. No concepts have emerged that enable the prediction of carbon partitioning for plants faced with these two stresses.

For willow, increased nutrient status resulted in increased visible injury. However, nutrient-deficient plants were more sensitive to O_3-induced reductions in leaf area than were plants raised at higher nutrient levels. Thus foliar injury, which is recognized as a poor predictor of growth responses to gaseous pollutants, is quite misleading in this study. More specifically, high foliar injury occurred for plants that were more resistant to O_3 on the basis of growth analysis.

Nutrient level and O_3 influenced carbon allocation patterns. The willow study showed that nutrient deficiency can be so severe as to prevent the biomass partitioning expected in response to O_3. The effect of poor nutrition was stronger for low nutrient willows than the effect of O_3 in determining carbon allocation because leaf area and weight decreased relative to controls, but root weight did not. At higher levels of nutrient availability, nutrients and O_3 both seemed to influence partitioning. In medium nutrient plants, carbon allocation shifted to favor leaf growth at the expense of root growth, in agreement with the general finding that air pollutants affect root growth more than shoot growth. Whether O_3 stress can ever be severe enough to override nutrient deficiency and dominate partitioning has not been determined.

The alder-*Frankia* system is more complex than the willow system in several ways. For example, photosynthate in the willow system is partitioned only between roots and shoots. In the alder system, photosynthate can go to roots, shoots, and symbiont. Carbon allocated to the symbiont can be viewed as either lost from the plant or as a third allocation pool that is well integrated with the tree. The rules for stress effects on carbon allocation are understood for roots and shoots, but the rules governing allocation to *Frankia* are unknown.

In addition, *Frankia* can play a direct role in uncoupling alder from the constraints of soil N. Thus, interpreting the relative nutrient status of alder in stress experiments is difficult. More specifically, we could manipulate N content in potting media for willow and be certain of low, medium, and high N treatments. For alder, low soil N enhances the *Frankia* symbiosis, and activity of the symbiont can contribute substantial amounts of N to a low fertilizer treatment. Thus obtaining alder at high and low N levels is not simple. Our study exploits the fact that photosynthetic capacity is an excellent assay for foliar N because the two are correlated.

The results with alder can be viewed in context of those for willow. Some leaves from unnodulated alders had such poor nutritional status that O_3 had no effect on gas exchange; the same was true for nodulated alder. Only leaves with high conductance showed an O_3 response for plants in both nutrient treatments. Thus as with willow, the severity of one stress (low nutrients) can be so profound that the effects of a second, lesser stress (O_3) are overwhelmed. These experiments were conducted with species native to the eastern United States; however, species of *Alnus* and *Salix* occur throughout the Pacific Northwest. The effects of nutrient and symbiont status on plant response to O_3 reported here are expected to be similar for western members of these two genera. Changes in photosynthesis and carbon allocation patterns observed in these studies may be general plant responses that are applicable to a wide range of woody species.

However, the possibility exists that for some species or conditions, altering the fertilizer level will have no effect on plant response to O_3. That is, O_3 may cause the same percent reduction in growth for plants of low and high nutrient status. This might be expected in species in which nutrient deficient individuals have the same photosynthetic rate and same percent foliar nitrogen, but smaller overall biomass, as for high nutrient plants. Additional work with other species will reveal whether the results reported here for willow and alder are widely applicable or restricted to these experimental conditions.

ACKNOWLEDGMENTS

This research was supported by U.S. Department of Energy Grant DE-FG05-85ER60312 to W.E.W. We thank James Ehleringer for the isotope analysis and helpful comments.

REFERENCES

1. A. J. Bloom, F. S. Chapin III, and H. A. Mooney, "Resource limitation in plants—an economic analogy," *Annu. Rev. Ecol. Sys.* 16:363 (1985).

2. H. Marschner, *Mineral Nutrition of Higher Plants*, Academic Press, San Diego, 1986, 674pp.

3. R. A. Reinert, D. S. Shriner, and J. O. Rawlings, "Responses of radish to all combinations of three concentrations of nitrogen dioxide, sulfur dioxide, and ozone," *J. Environ. Qual.* 11:52 (1982).

4. D.T. Tingey, W.W. Heck, and R.A. Reinert, "Effect of low concentrations of ozone and sulfur dioxide on foliage, growth and yield of radish," *J. Amer. Soc. Hortic. Sci.* 96:369 (1971).

5. L. Walmsley, M.R. Ashmore, and J.N.B. Bell, "Adaptation of radish *Raphanus sativus* L. in response to continuous exposure to ozone," *Environ. Pollut., Ser. A* 23:165 (1980).

6. S.B. McLaughlin, "Effects of air pollution on forests—a critical review," *JAPCA* 35(5):512 (1985).

7. S.C. Wong, I.R. Cowan, and G.D. Farquhar, "Stomatal conductance correlates with photosynthetic capacity," *Nature* 282:424 (1979).

8. C. Field and H.A. Mooney, "The photosynthesis-nitrogen relationship in wild plants," In *On the Economy of Plant Form and Function*, T.J. Givinish, Ed., Cambridge University Press, Cambridge, 1986, p. 25.

9. W.E. Winner and H.A. Mooney, "Ecology of SO_2 resistance: II. Photosynthetic changes of shrubs in relation to SO_2 absorption and stomatal behavior," *Oecologia* 44:296 (1980).

10. W.E. Winner and H.A. Mooney, " Ecology of SO_2 resistance: III. Metabolic changes of C_3 and C_4 *Atriplex* species due to SO_2 fumigations," *Oecologia* 46:49 (1980).

11. P.B. Reich and R.G. Amundson, "Ambient levels of ozone reduce net photosynthesis in tree and crop species," *Science* 230:566 (1985).

12. I.A. Leone, E. Brennan, and R.H. Daines, "Effect of nitrogen nutrition on the response of tobacco to ozone in the atmosphere," *JAPCA* 16 (4):191 (1966).

13. F.D.H. MacDowall, "Predisposition of tobacco to ozone damage," *Can. J. Plant Sci.* 45(1):1 (1963).

14. R.A. Montes, U. Blum, and A.S. Heagle, "The effects of ozone and nitrogen fertilizer on tall fescue, ladino clover, and a fescue-clover mixture. I. Growth, regrowth, and forage production," *Can. J. Bot.* 60:2745 (1982).

15. L.E. Craker, "Effects of mineral nutrients on ozone susceptibility of *Lemna minor*," *Can. J. Bot.* 49:1411 (1971).

16. T.L. Noland and T.T. Kozlowski, "Influence of potassium nutrition on susceptibility of silver maple to ozone," *Can. J. For. Res.* 9:501 (1979).

17. I.A. Leone, "Response of potassium-deficient tomato plants to atmospheric ozone," *Phytopathology* 66:734 (1976).

18. J.A. Dunning, W.W. Heck and D.T. Tingey, "Foliar sensitivity of pinto bean and soybean to ozone as affected by temperature, potassium nutrition and ozone dose," *Water Air Soil Pollut.* 3:305 (1974).

19. I.A. Leone and E. Brennan, "Ozone toxicity in tomato as modified by phosphorus nutrition," *Phytopathology* 60:1521 (1970).

20. N.O. Adedipe, G. Hofstra, and D.P. Ormrod, "Effects of sulfur nutrition on phytotoxicity and growth responses of bean plants to ozone," *Can. J. Bot.* 50:1789 (1972).

21. R. Harkov and E. Brennan, "The influence of soil fertility and water stress on the ozone response of hybrid poplar trees," *Phytopathology* 70(10):991 (1980).

22. C.S. Greitner and W.E. Winner, "Increases in delta ^{13}C values of radish and soybean plants caused by ozone," *New Phytol.* 108:489 (1988).

23. O.L. Lange, W. Beyschlag, and J.D. Tenhunen, "Control of leaf carbon assimilation—input of chemical energy into ecosystems," in *Potentials and Limitations of Ecosystem Analysis* (E. D. Schulze and H. Zwolfer, Eds.), *Ecological Studies* vol. 61, Springer-Verlag, New York, 1987, p. 148.

Table I. Dry weights (gm) and leaf areas (cm^2) of *Salix nigra* cuttings grown at three nutrient levels and exposed to filtered air or low (0.06 ppm increased to 0.12 ppm) or high (0.12 ppm increased to 0.24 ppm) O_3. Values are means (n=6 for controls, n=12 for O_3-treated cuttings) ± standard errors.

Treatment	Dry Weights (gm)			Leaf Areas (cm^2)
	Leaves	Stems	Roots	
Control, Low Nutrient	2.23 ± 0.22	1.78 ± 0.27	2.85 ± 0.67	620 ± 53
Control, Med. Nutrient	3.23 ± 0.26	2.94 ± 0.27	4.98 ± 0.71	915 ± 54
Control, High Nutrient	3.76 ± 0.24	3.35 ± 0.23	3.68 ± 0.55	1088 ± 67
Low O_3, Low Nutrient	1.89 ± 0.14	1.77 ± 0.17	3.12 ± 0.39	504 ± 37
Low O_3, Med. Nutrient	3.14 ± 0.22	2.91 ± 0.29	4.50 ± 0.66	895 ± 53
Low O_3, High Nutrient	3.65 ± 0.25	3.25 ± 0.29	4.16 ± 0.63	1037 ± 60
High O_3, Low Nutrient	1.70 ± 0.15	1.73 ± 0.17	2.88 ± 0.41	444 ± 36
High O_3, Med. Nutrient	2.78 ± 0.15	2.64 ± 0.13	3.27 ± 0.33	737 ± 39
High O_3, High Nutrient	3.30 ± 0.24	3.22 ± 0.29	4.23 ± 0.55	878 ± 50

Table II. Root:leaf ratios of *Salix nigra* cuttings grown at three nutrient levels and exposed to filtered air or low (0.06 ppm increased to 0.12 ppm) or high (0.12 ppm increased to 0.24 ppm) O_3. Values are means n=6 for controls, n=12 for O_3-treated cuttings) ± standard errors.

O_3 Treatment	Low Nutrient	Medium Nutrient	High Nutrient
Control	1.30 ± 0.25	1.54 ± 0.21	0.95 ± 0.11
Low O_3	1.59 ± 0.16	1.39 ± 0.14	1.07 ± 0.13
High O_3	1.69 ± 0.18	1.19 ± 0.12	1.25 ± 0.11

Table III. Regression statistics for plots of photosynthesis versus conductance for leaves of nodulated *Alnus serrulata* seedlings.

Treatment	r^2	alpha	Slope	Y-Intercept
Controls				
Nodulated	0.617	0.025	18.18	3.53
Unnodulated	0.692	0.01	31.01	-2.02
O_3-treated in filtered air				
Nodulated	0.654	0.025	40.35	-3.15
Unnodulated	0.323	0.25	13.26	-1.55
O_3-treated in O_3				
Nodulated	0.167	0.50	-12.35	10.89
Unnodulated	0.400	0.10	-6.55	1.88

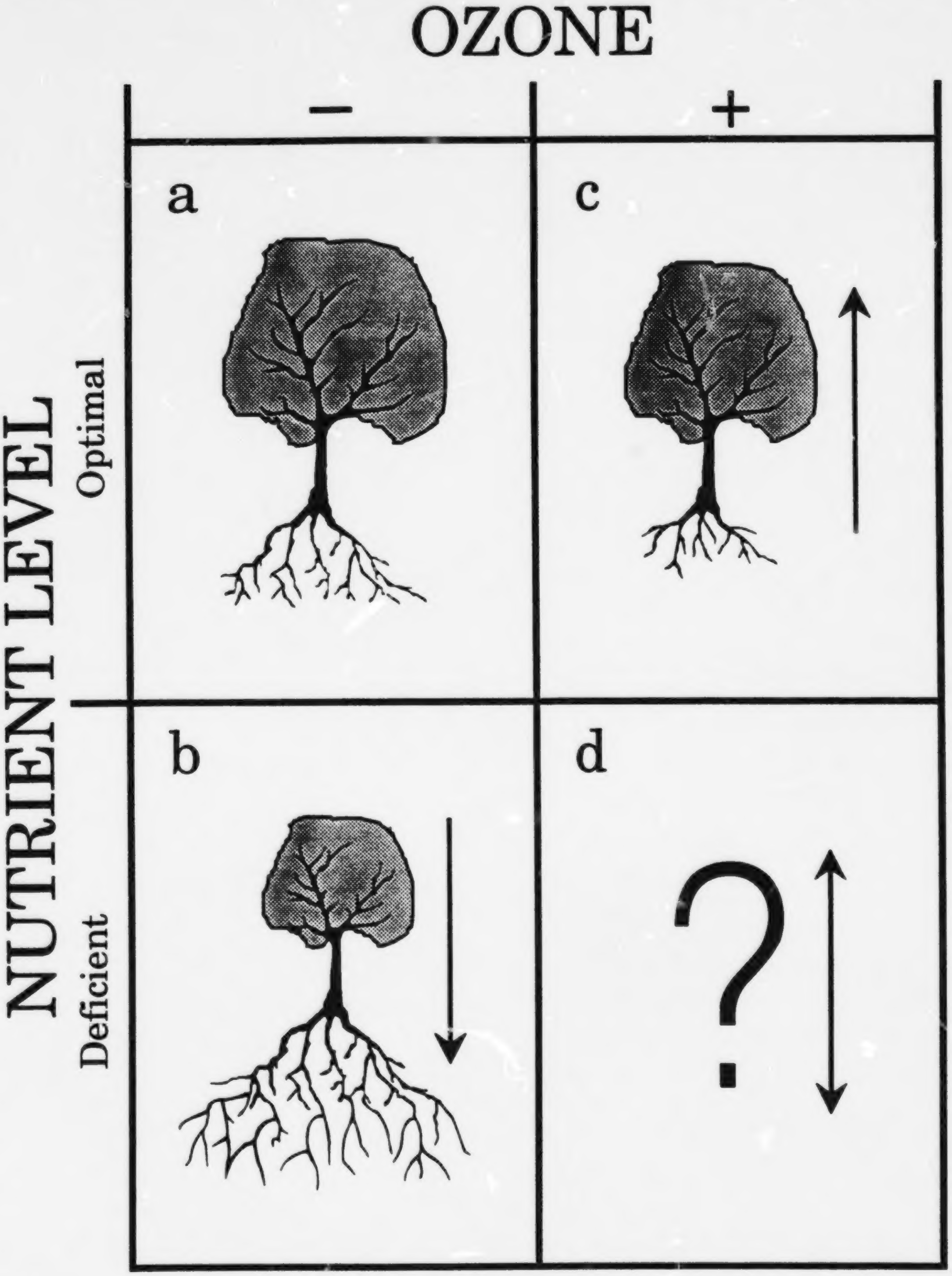
OZONE
−
+
NUTRIENT LEVEL
Optimal
Deficient
a
c
b
d
?

Figure 1. Hypothesized changes in plant growth form with nutrient deficiency and/or ozone exposure. Arrows indicate direction of allocation shifts in response to stress. See text for details.

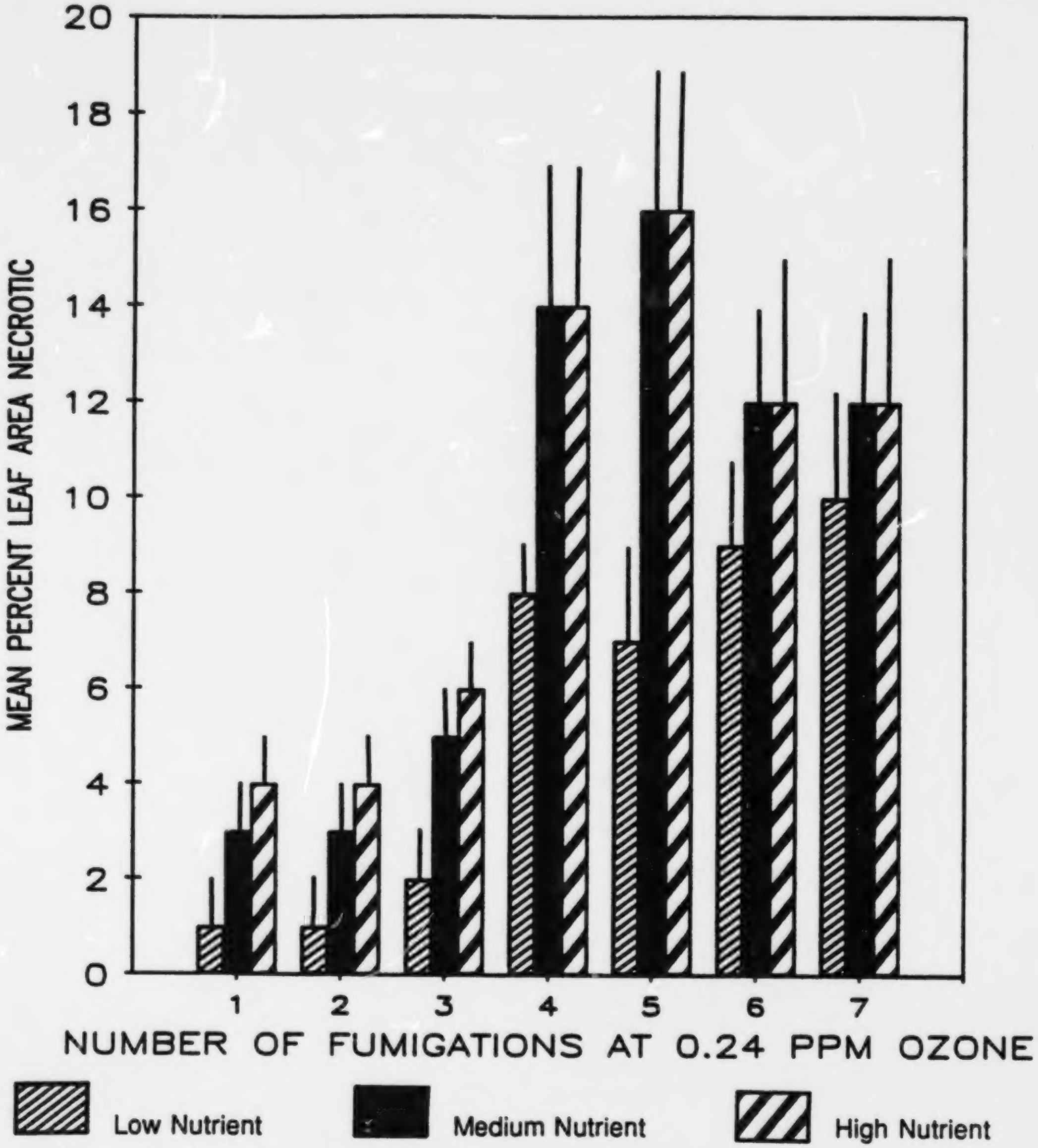

Figure 2. Influence of nutrient status on percent leaf area necrotic in *Salix nigra* cuttings after 11 four h exposures to ozone at 0.12 ppm and a series of four h exposures at 0.24 ppm. Each bar represents the mean of 12 plants (± SE).

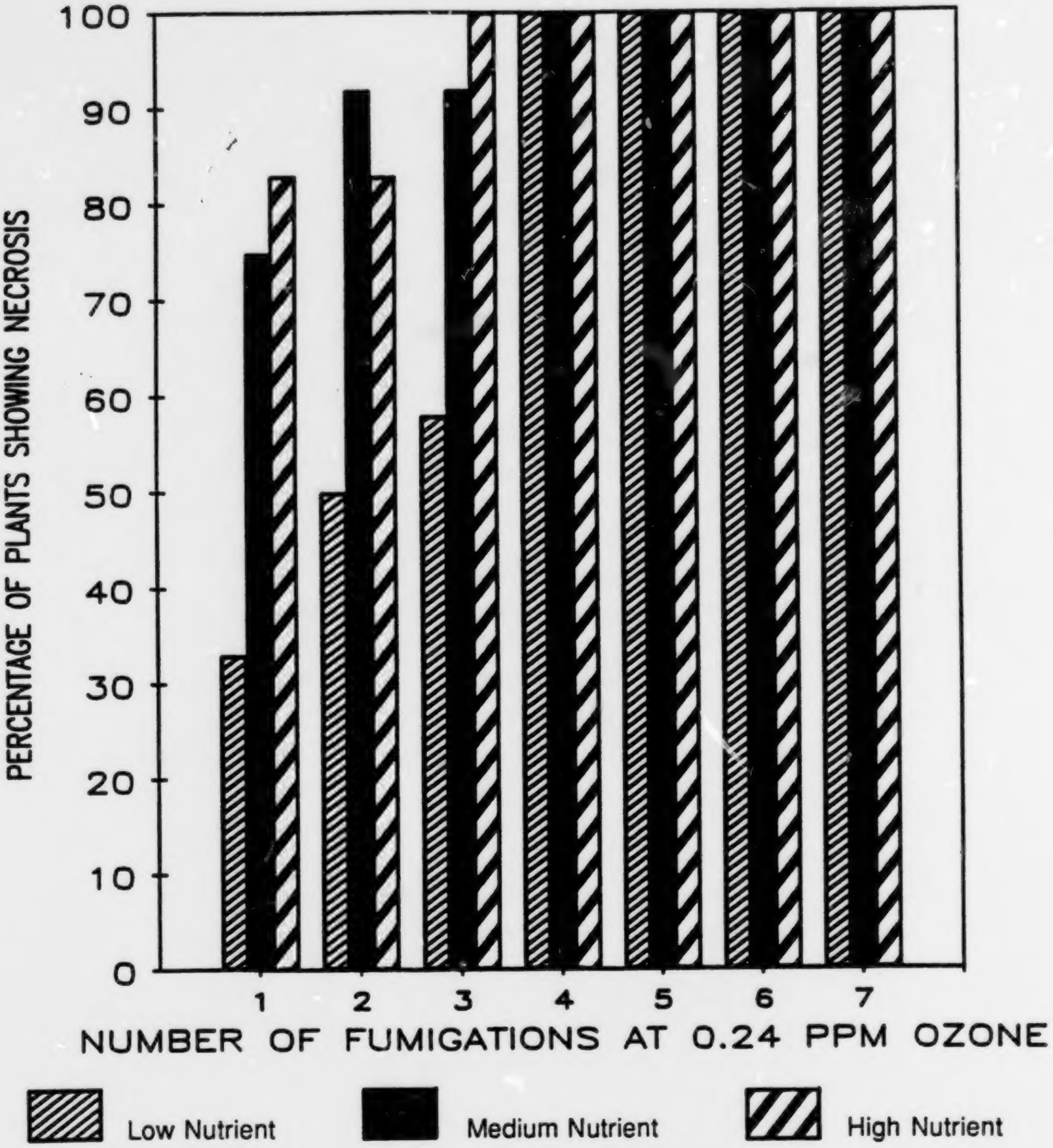

Figure 3. Influence of nutrient status on the percentage of *Salix nigra* cuttings (N=12) showing necrosis after 11 four h exposures to ozone at 0.12 ppm and a series of four h exposures at 0.24 ppm.

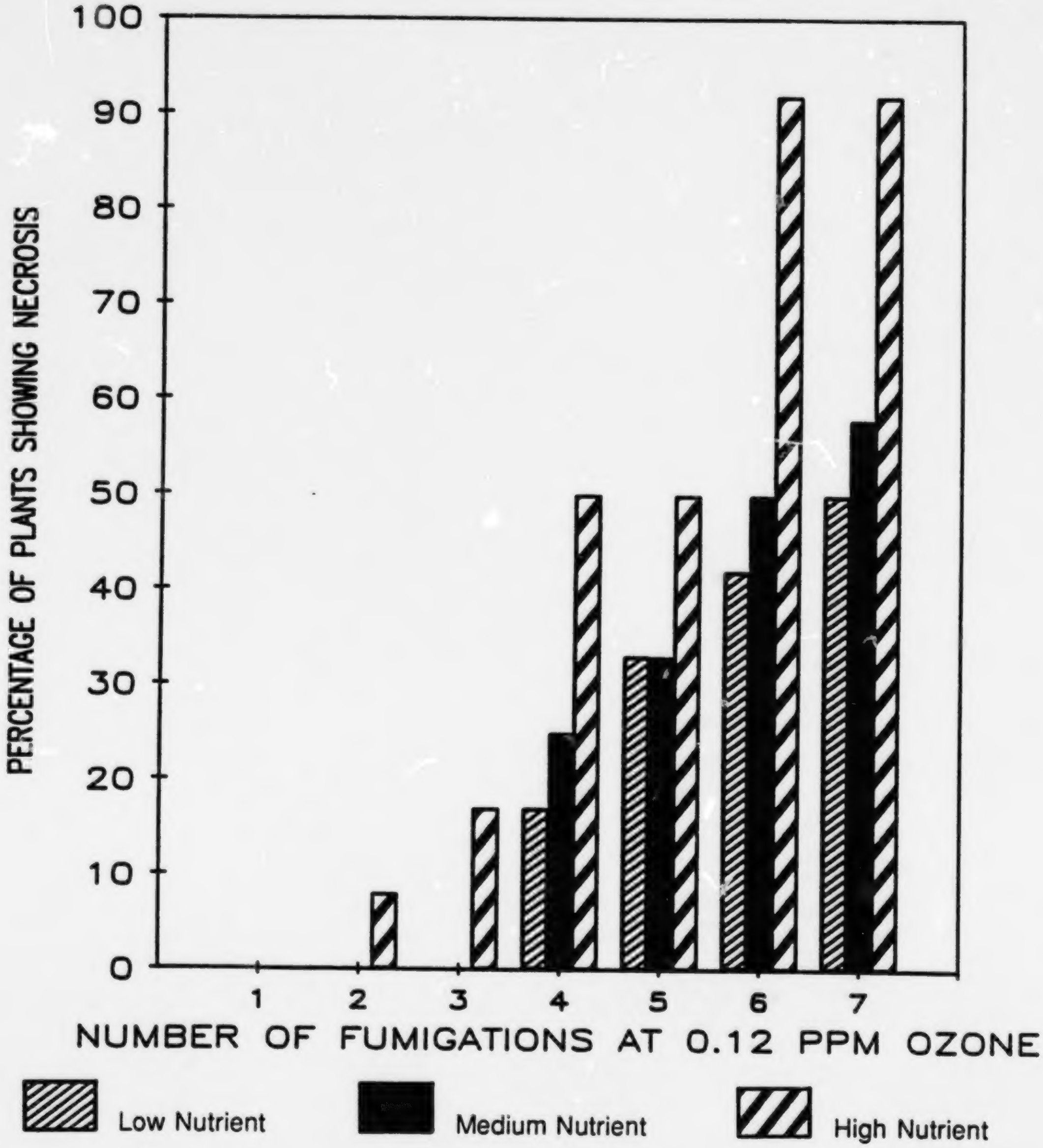

Figure 4. Influence of nutrient status on the percentage of *Salix nigra* cuttings (N=12) showing necrosis after 11 four h exposures to ozone at 0.06 ppm and a series of four h exposures at 0.12 ppm.

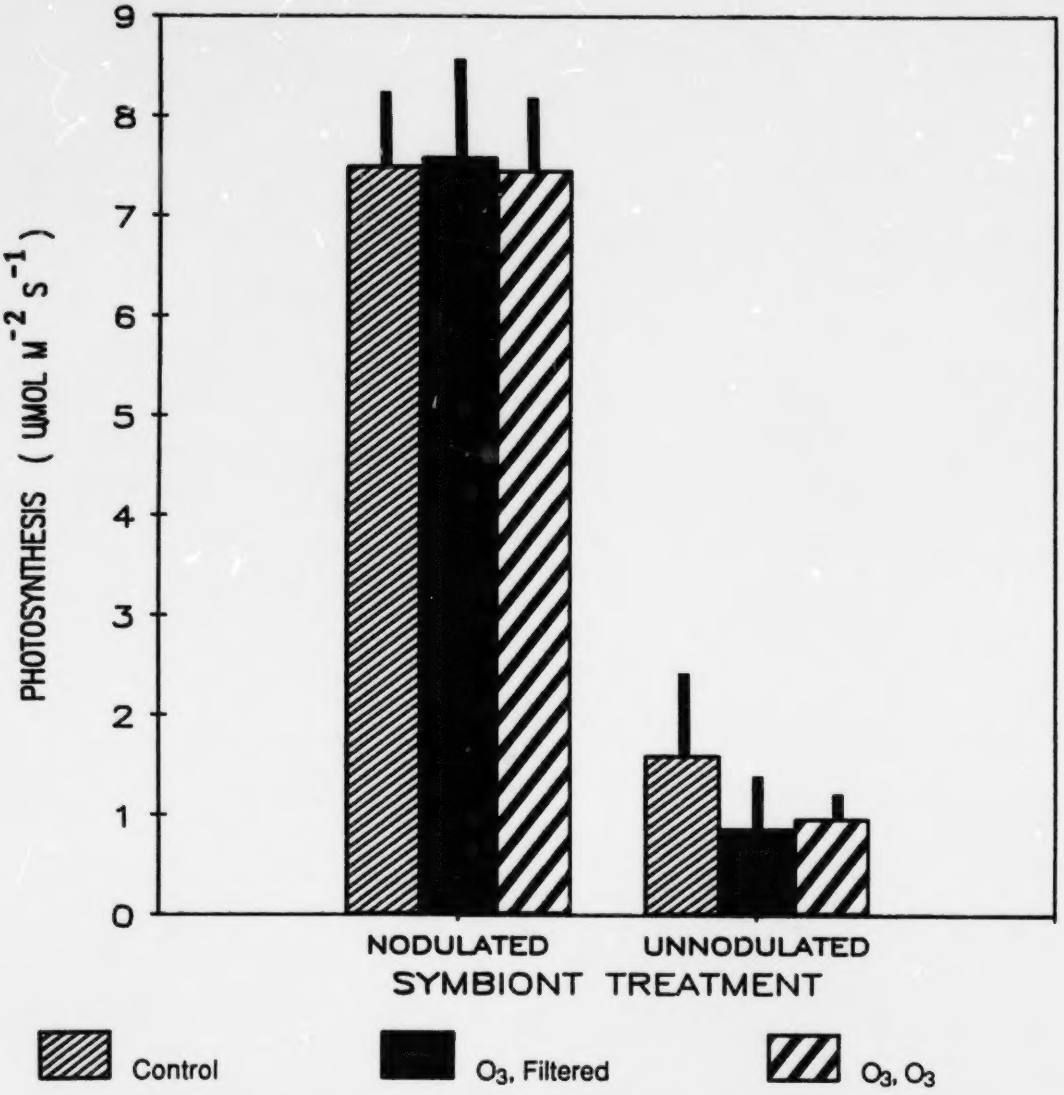

Figure 5. Photosynthesis of nodulated and unnodulated *Alnus serrulata* seedlings exposed to filtered air (control) or 0.12 ppm ozone. Ozone-treated plants were measured in filtered air and in ozone. N=16 for controls; N=8 for ozone-treated. Bars are means ± SE.

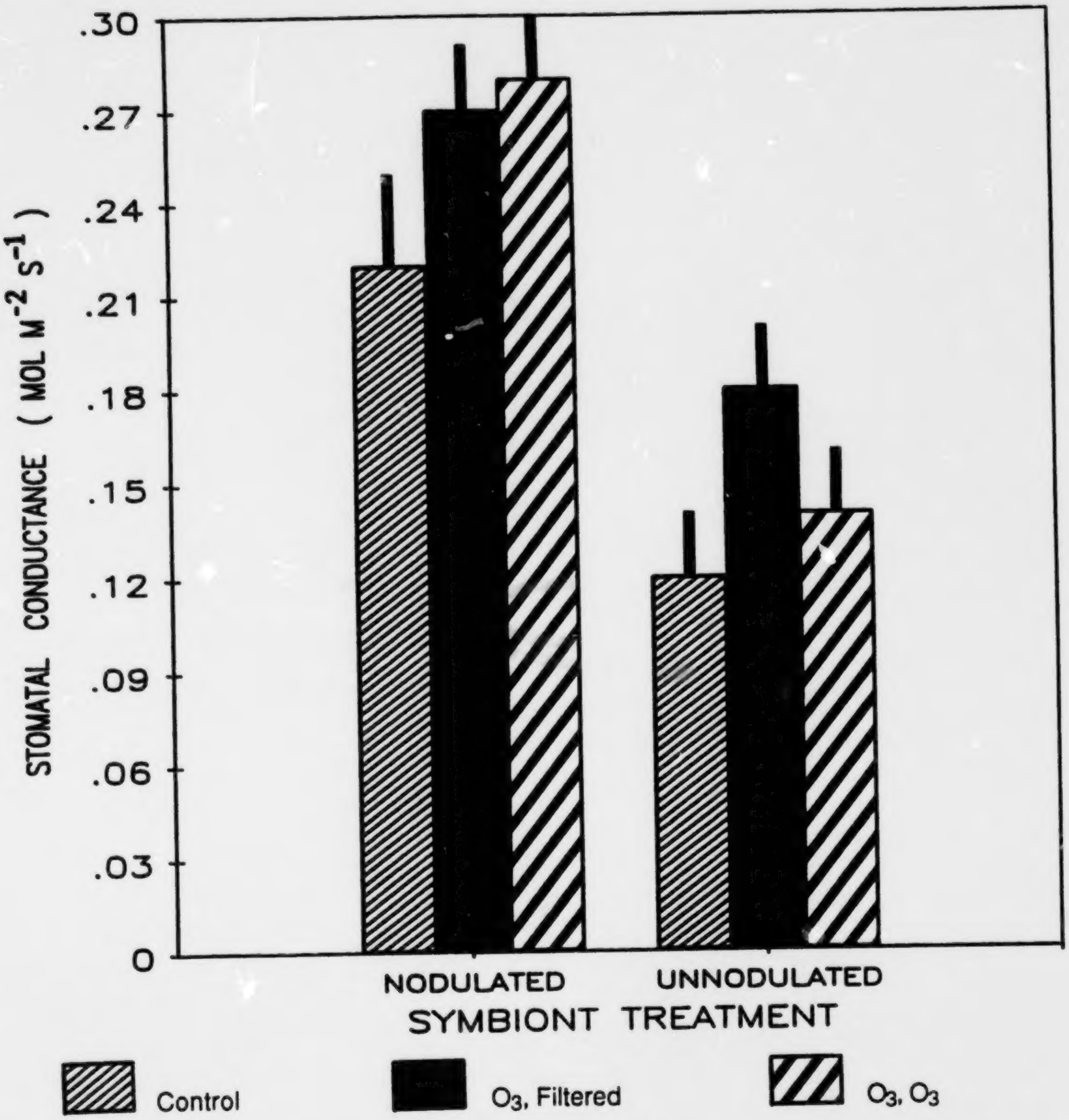

Figure 6. Stomatal conductance of nodulated and unnodulated *Alnus serrulata* seedlings exposed to filtered air (control) or 0.12 ppm ozone. Ozone-treated plants were measured in filtered air and in ozone. N=16 for controls; N=8 for ozone-treated. Bars are means ± SE.

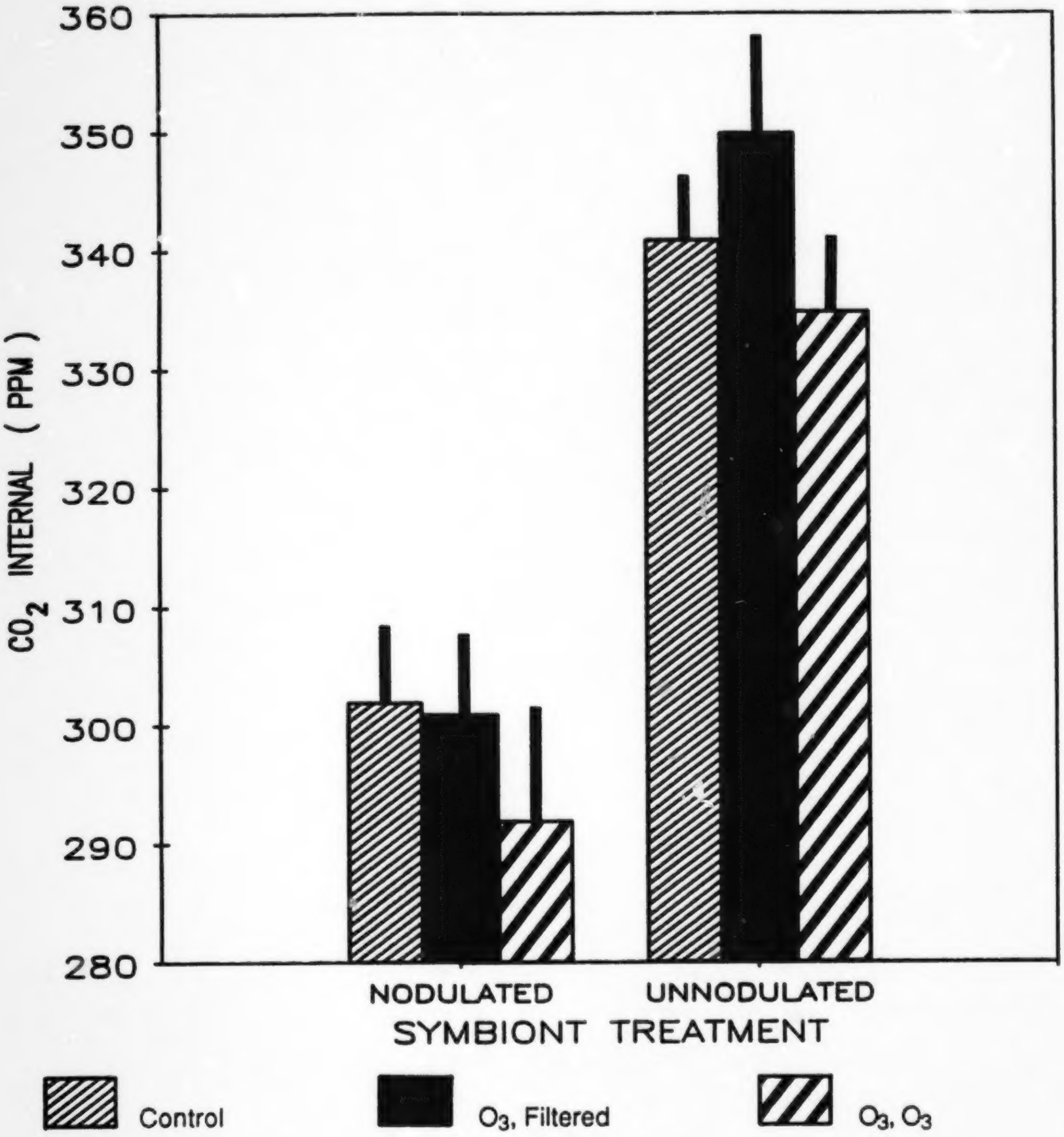

Figure 7. Internal CO_2 concentration of nodulated and unnodulated *Alnus serrulata* seedlings exposed to filtered air (control) or 0.12 ppm ozone. Ozone-treated plants were measured in filtered air and in ozone. N=16 for controls; N=8 for ozone-treated. Bars are means ± SE.

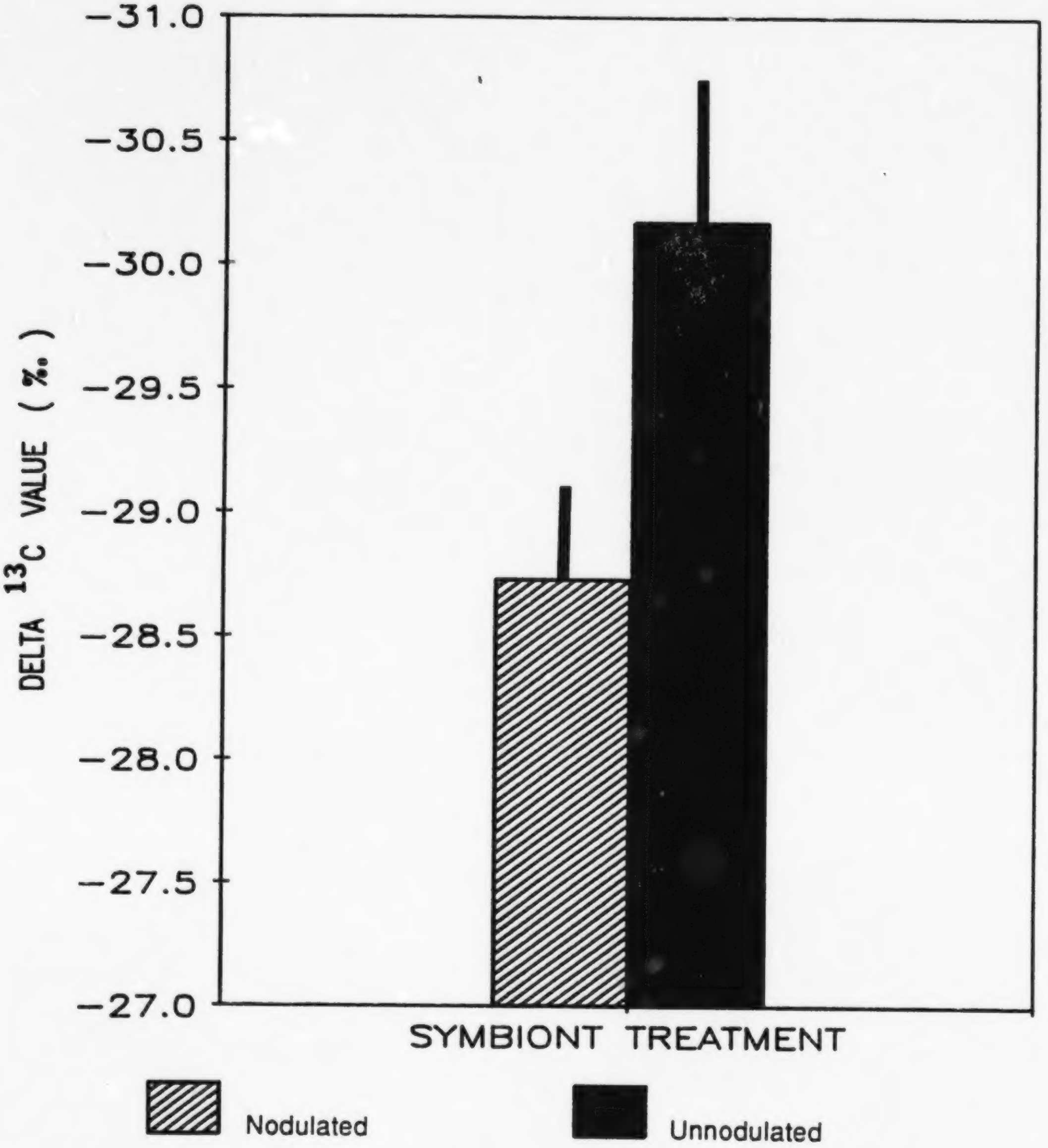

Figure 8. Delta ^{13}C values of foliage of nodulated and unnodulated *Alnus serrulata* seedlings. N=4; bars are means ± SE.

Chapter Six

Response of Soils to Atmospheric Deposition

The Effect of Nitrogen Accumulation and Nitrification on Soil Chemical Properties in Alder Forests	H. Van Miegroet, D.W. Cole, D. Binkley, and P. Sollins	515
Forest Soil Sulfur Pools and SO_4^{2-} Adsorption and Desorption Capacity Following Elevated Inputs of SO_4^{2-}	R.B. Harrison, D.W. Johnson, and D.E. Todd	529
Soil-Solution Equilibria in Lysimeter Leachates Under Red Alder	J.O. Reuss	547
Sensitivity of Forest Soils in the Western U.S. to Acidic Deposition	D. Binkley	561

The Effect of Nitrogen Accumulation and Nitrification on Soil Chemical Properties in Alder Forests

Helga Van Miegroet[1]
Dale W. Cole[2]
Dan Binkley[3]
Phil Sollins[4]

[1] *Environmental Sciences Division*
Oak Ridge National Laboratory
Oak Ridge, TN 37831-6038

[2] *College of Forest Resources*
AR-10
University of Washington
Seattle, WA 98195

[3] *Forest and Wood Sciences*
Colorado State University
Fort Collins, CO 80523

[4] *School of Forestry and Environmental Studies*
Yale University
New Haven, CT 06521

INTRODUCTION

Nitrogen availability commonly limits growth in many forests throughout the world.[1] Alders (*Alnus* spp.) are N-fixers, which are often found as early successional species on recently deglaciated or exposed soils, on alluvial flats, and on riverbanks. Because of this ability to utilize atmospheric N_2 and increase soil N content, the use of alder is sometimes advocated for forest site improvement or as an alternative to N fertilization in N-limited forest stands.[2-4] Reported N-fixation rates for red alder (*A. rubra* Bong.), a lowland species in the northwestern United States, range from 50 to 320 kg/ha/yr[5-9]; values for Sitka alder [*A. sinuata* (Regel) Rydb.], which is found in Alaska, throughout Canada, and at higher elevations in Oregon and Washington are somewhat lower.[4,9,10]

Nitrification is a microbial process that strongly depends on N availability and is restricted in many N-stressed forest soils by the strong competition for NH_4^+ between plants and microbes.[11-13] Nitrogen enrichment by N-fixation may stimulate this process, as indicated by the elevated NO_3^- levels reported for soil, solution, and streamwater samples from alder forests.[7,14-18] During nitrification, NH_4^+ is oxidized into the anionic NO_3^- form while H^+ ions are released into solution. This process thus has the ability to acidify both soil and soil solution because of (1) the internal H^+ production during this process and (2) the lack of NO_3^- adsorption by the clay surfaces,[19-22] which facilitates downward leaching of base cations with mobile NO_3^- as counter-ion following cation displacement from the exchange complex by the H^+ ions. In more acid soils with low base saturation, the increase in ionic strength of the solution may lead to Al mobilization.[23]

By studying the effects of such natural NO_3^- production, we can increase our understanding of the potential effects of atmospheric acid deposition on forest soil and solution chemistry. Indeed, in many ways nitrification represents a worst-case scenario of possible soil acidification in that (1) the strong acid is formed within the soil system rather than passing through the canopy and forest floor; (2) internal NO_3^- production usually indicates a lack of N-stress[11-13] and thus minimal influence of uptake on NO_3^- retention, whereas NO_3^- added from the atmosphere can be immobilized by the trees and microbes when the system is N-limited; and (3) NO_3^- is not typically adsorbed and therefore highly mobile in soils,[19-22] whereas atmospheric acid deposition often also includes SO_4^{2-} which can be retained through adsorption in sesquioxide-rich horizons.[19-20]

This paper examines the effect of alder occupancy on soil chemical properties, based on information reported in the literature and on data from selected studies in Washington and Oregon. We will assess the role of nitrification as an acidifying process and will evaluate its influence on soil sensitivity to further acidification. Finally, the implication of these findings with respect to soil response to acid deposition is discussed.

METHODS

Site Description

The three main sites used for this analysis are the University of Washington's Thompson Research Center, the U.S. Forest Service Wind River Experimental Forest in Washington, and the U.S. Forest Service Cascade Head Experimental Forest on the Oregon coast.

The Thompson site (TS) is located 56 km southeast of Seattle, WA, in the foothills of the Cascade Mountains. Mean annual temperature is 9.8° C, mean annual precipitation is 130 cm, most of which falls as rain between October and March. Soil and solution properties are compared between a Douglas-fir (*Pseudotsuga menziesii* [Mirb.] Franco) stand planted in the 1930s following clearcutting of the old-growth forest in the early 1900s and subsequent wildfires around 1920, and a pure stand of red alder established naturally adjacent to it a few years later where conifer was not planted. Both forest types are underlain by a gravelly sandy loam soil of glacial origin (Dystric Entic Durochrept–Alderwood Series). More detailed descriptions of soil properties and forest composition are published elsewhere.[17,24]

The Wind River site (WR) is located in southwestern Washington at about 625 m elevation. Mean annual temperature is 9° C, and annual precipitation averages about 220 cm, with about 75% falling between November and March. A snowpack of 1–2 m is common. The topography is rolling with slopes ranging from 0 to 60%. The area was on the eastern edge of a large wildfire in 1902, and the site also burned in 1922 and 1927. It was planted with Douglas-fir seedlings from an off-site source in 1929. In 1933, a 22-m wide strip was interplanted with red alder seedlings to provide a firebreak across the plantation. The soil has a silty clay loam texture (Andic Haplumbrept–no series classification) and developed from a combination of andesitic and rhyolitic parent material, with some pumice and basaltic gravel.

The Cascade Head study site (CH) is located near the Oregon coast at an elevation of 180 m. Mean annual precipitation is about 240 cm with little snowfall. The average temperature for July is 20° C, and for January 10° C. Freezing temperatures are uncommon. The stand where the measurements were taken is about 8 ha in size, covering moderate slopes of about 15%. The land had been cleared for agriculture but was abandoned in about 1925; it regenerated naturally with various conifer species (Douglas-fir, Sitka spruce [*Picea sitchensis* (Bong.) Carr] and western hemlock [*Tsuga heterophylla* (Raf.) Sarg.]) and red alder. In 1935, the 8-year-old forest contained about 4500 conifers per hectare and 3000 red alders per hectare. A 0.2-ha plot was established in 1935 and thinned to 2800 stem per hectare by removing all alders and many smaller conifers (pure conifer plot). Another 0.2-ha plot remained undisturbed and served as reference for comparison (mixed conifer-alder). Some soil chemistry data from these plots were described earlier.[5]

Chemical Analysis and Calculation Methods

The total N content of the systems was calculated from Kjeldahl N analysis of overstory, understory, forest floor samples taken in each plot, and total biomass estimates for these components. Soil samples were taken by depth and analyzed for total N and total C, exchangeable bases, and pH (in water and 0.01$\underline{M}$ $CaCl_2$). Cation exchange capacity at TS was determined following extraction with 1$\underline{N}$ NH_4Cl and exchangeable Al was calculated from the difference between CEC and the sum of exchangeable bases. At the two other sites exchangeable Al was determined directly on 1$\underline{N}$ KCl extracts, and CEC was calculated from the sum of exchangeable cations. The TS soil solutions were collected with ceramic lysimeter plates (15-cm diameter) at 10-kPa tension placed in triplicate below the forest floor and at 10-cm and 40-cm soil depth. Ten tensionless lysimeters (i.e., 25 cm x 25 cm galvanized square steel pans) were placed at 70-cm soil depth at CH and WR. Earlier publications contain more detailed descriptions of stand characteristics, aboveground sampling, total biomass calculations,[25] and soil and solution sampling and analysis procedures for the Thompson site[17-18] and for the Wind River and Cascade Head sites.[26-27]

Nitrogen mineralization and nitrification potential were determined at TS through in situ incubation by using the buried bag technique.[28] Several soil cores were taken seasonally to a depth of 15 cm in each plot over a 15-month period, placed in plastic bags, and buried beneath the forest floor for 1 month. Preincubation and postincubation samples were analyzed for KCl-extractable NH_4-N and NO_3^-N; net mineralization was calculated from the difference between final and initial inorganic N concentration.[13] In the CH and WR sites, annual N mineralization was calculated from a sequence of monthly on-site incubations of soil cores (0–15 cm depth) in PVC tubes with resin bags over an 18-month period.[26]

Acid and base neutralization were determined on five replicate soil samples originating from 0–7 cm and 7–15 cm depth in the TS Douglas-fir and red alder stands. Increasing amounts of acid (HCl) or base ($Ca(OH)_2$) were added to a 20-g air-dried sieved (<2 mm) soil at a solution-to-soil ratio of 2.5:1, corresponding to an addition of 0, 5, 10, 20, 40, 80, and 160 (for acid only) $mmol_c$ of H^+ or OH^- per kilogram of dry soil.[25] The soil pH was determined within 24 h and again after 3 weeks. The acid-buffering intensity was determined graphically from the titration curves as the amount of H^+ needed to cause a one unit pH decrease below the pH in water, (i.e. the slope of the titration curve at pH_{water}.) Buffer capacity was determined as the amount of H^+ needed to lower the pH to an endpoint of pH = 4. Similar titrations were done for soils from the other sites.[27]

RESULTS

Soil N Enrichment and Nitrification

Several past studies using alder chronosequences on a particular soil or comparisons between nonalder stands and alder stands of different ages (Table I) have documented a progressive increase in the N content of soils and forest floors with increasing alder stand age, ranging from 26 to 300 kg/ha/yr. The stands that contained alder in our studies also showed net accretion in total ecosystem N content over the corresponding pure conifer stands of 78 kg N/ha/yr (TS) over a 50-year period,[7,25] and 74 kg N/ha/yr(CH) and 51 kg N/ha/yr (WR) for 55 years.[26]

This N enrichment under alder resulted in a greater soil N mineralization and nitrification potential as suggested by the elevated NH_4^+ and NO_3^- levels in alder soils[29] or determined during laboratory incubation[30] or field mineralization studies (Table II). The annual nitrification rates calculated for the pure conifer stands ranged from <1 to approximately 15 kg/ha/yr, while in pure alder and mixed alder-conifer forests 100–115 kg NO_3^- N/ha was produced annually in the soil. The negative net ammonification at the Thompson site suggests that nitrification of NH_4^+ exceeded NH_4^+ input from mineralization, causing a net decline in soil levels within the buried bag. Because NO_3^- is not typically retained in the soil through adsorption[19-22] and because biological N immobilization was unlikely in these N-enriched systems, NO_3^- leached out of the rooting zone with the percolating solution. Adjusting for the N input from the atmosphere, on the order of 5 kg/ha/yr,[17,26] net annual NO_3^- leaching losses were 3 kg N/ha (WR), 36 kg N/ha (CH), and 30 kg/ha (TS) (Table II).

Nitrification as a Source of Acidification

Since little NO_3^--N entered directly from the atmosphere (e.g., Table III), all NO_3^- must have been produced internally. The oxidation of N_2 to NO_3^- causes a net release of one H^+ ion per molecule NO_3^- formed; assuming that all NO_3^- leaching losses were ultimately derived from atmospheric N_2, net H^+ release rates with the production of this NO_3^- were 200 mol_c/ha/yr (WR), 2500 mol_c/ha/yr (CH), and 3500 mol_c/ha/yr (TS). The latter two internal H^+ production rates are equivalent to the acid input with precipitation of pH 3.8–3.6 (assuming 150 cm of annual rainfall). At the Thompson site, an additional 300 mol_c/ha/yr of H^+ entered the soil via precipitation, and 300 mol_c/ha/yr was generated internally from carbonic acid dissociation associated with root and microbial respiration.[18]

Acidity and acidification cannot be described by a single index, and the terms "capacity" and "intensity" have been used in this regard.[31] Capacity usually refers to the total storage of protons or Al, or exchangeable bases associated with the solid phase. Intensity refers to the concentration in solution at a particular time, or to solution pH for H^+. Changes associated with acidification are usually more pronounced in terms of intensity than capacity.[31] Various earlier papers on the influence of alder on soil properties have mostly reported a significant decline in soil pH and/or base saturation (Table I), but few contain information on soil solution chemistry or the mechanisms involved in the observed changes. As illustrated in Figure 1 (TS) the soil solution responded to higher acid input in the alder soil by a significant pH decline in the upper part of the soil profile (forest floor and A-horizon), where most of the nitrification also took place.[16-18] The H^+ flux below the litter layer and A-horizon was lower than would be expected based on the increase in NO_3^- loading. It further decreased with soil depth; less than 2% of the total annual H^+ input to the solutions percolated beyond the B-horizon, irrespective of the origin and magnitude of the H^+ sources (Table III). This indicated strong solution pH buffering against acidification particularly in the forest floor and A-horizon.

The concurrent increase in total cation leaching (Table III) and the significant drop in base saturation under alder (Table IV) would initially suggest that cation displacement from the exchange sites is the mechanism involved, and some comparative studies have indeed shown a decrease in exchangeable base content under alder versus pure conifer or mixed alder-conifer stands.[5,29] These findings are by no means consistent, however, and in some instances, no change or a net increase in the concentration of some exchangeable cations has been reported[4,18,32-34] (Table IV). Furthermore, the net cation leaching output from the alder soils represented a large fraction of the exchangeable pool between 0- and 45-cm soil depth for some cations[17] and could not be sustained very long by the exchange complex without some replenishment (i.e., through increased weathering).

The composition of the cation exchange complex provided further evidence for accelerated weathering rates under alder. Indeed, the reported decline in base saturation often appeared to result from a combination of the two factors: (1) a significant increase in cation exchange capacity, associated with greater soil organic matter contents under alder[5,33] and (2) increased occupancy of these exchange sites by Al (or exchange acidity), presumably derived from accelerated weathering of Al-silicate minerals. This weathering process and the hydrolysis reactions of the Al released could also account for part of the solution pH buffering. A slight increase in amorphous (oxalate-extractable) Al in the upper horizons of the alder versus the Douglas-fir soil supports the possible breakdown of Al minerals that may further contribute to the increase in cation exchange capacity.[35] The Al soil-solution equilibrium reactions in question are discussed more extensively by Reuss.[41] This compositional change of the cation exchange complex is in turn reflected in lower pH values of alder soils (Table IV).

Increasing the ionic strength of the percolating solution in such acid soils, as is occurring as a result of nitrification, will mobilize Al in solution through the so-called "salt effect," that is, the preferential displacement of polyvalent over divalent and monovalent cations from the exchange complex.[23,41] Higher Al concentrations were measured in the alder A-horizon leachates than in the corresponding solutions under Douglas-fir,[25,41] but the effect was attenuated deeper in the soil profile.[41] There was also a decline in solution alkalinity (from 49 $\mu mol_c/L$ in the Douglas-fir A-horizon to 1.4 $\mu mol_c/L$ under alder) because of this increase in inorganic (strong acid) anion load. This was consistent with the model developed for increased solution SO_4^{2-} concentrations due to atmospheric deposition on soil water alkalinity.[36] Despite this initial sharp decline, the alkalinity of the solution leaching out of the alder rooting zone remained positive (36 $\mu mol_c/L$ in the red alder B-horizon vs. 52 $\mu mol_c/L$ under Douglas-fir), thus minimizing the potential negative effects of strong acid anion inputs on the chemistry of lake and stream water.[36] Similar results were also obtained from the deep lysimeter at Cascade Head (a significant decrease from 291 $\mu mol_c/L$ under the conifer to 86 $\mu mol_c/L$ under the mixed alder-conifer stand). Lower nitrification and NO_3^- leaching rates at Wind River did not have a large impact on soil solution chemistry.

Buffering and Resistance to Further Acidification

The soil titration experiments indicated that acid and base neutralization reactions proceeded rapidly and that prolonging the equilibration time from 24 h to 3 weeks did not significantly affect the titration results. Consequently, only the 24-h results will be discussed. The lower pH values, in response to base additions, indicated greater titratable acidity of alder soils compared to the corresponding conifer soils (Figure 2). The increased acidity of red alder soils (Table IV) did not greatly diminish their ability to neutralize additional H^+ inputs, as indicated by the similarity of the H^+ addition-pH response curves between the corresponding alder and Douglas-fir soils. The acid neutralization capacity, (i.e., the amount of acid needed to reduce the soil pH to pH = 4) did not significantly differ between soil depths at a given site or between corresponding Douglas-fir and red alder soils from a given depth. At the Wind River and the Cascade Head sites where the acid neutralizing capacity was calculated to an endpoint of pH = 3, a decline was measured in the upper soils of the alder sites (259 vs. 220 $mmol_c$/kg at WR and 429 vs. 227 $mmol_c$ /kg at CH). Differences disappeared at greater depth, and integrated over the entire soil volume to a depth of 70 cm, there was no net loss of acid neutralizing capacity in the more acid mixed conifer-alder sites.[27] The buffer intensity or slope of the titration curve, which expresses the resistance against a further pH decline, was significantly larger in the alder than in the corresponding Douglas-fir soils and was greatest in the upper soil horizon. Thus, although alder soils were acidified through prolonged strong acid input, they resisted further acidification more strongly than the less-acid conifer soils.

CONCLUSIONS

Comparisons between soils subject to large, chronic strong acid inputs via natural processes and the same or similar soils subject to less total acid input are useful to assess changes in soil chemistry that may be induced by atmospheric acid deposition. The soil and solution changes associated with prolonged high nitrification rates in N-rich soils constitute a worst-case scenario in that the strong acid is generated within the soil profile (i.e., the buffering action of forest canopies is not taken into account), and the acid anion (NO_3^-) is not typically retained in the soil through adsorption. In addition, internal acid production often exceeded reported atmospheric acid input rates even in highly polluted areas.

The acidification of the system can be seen most rapidly in the solution composition, that is, through a drop in solution pH, mobilization of Al from the exchange complex in the upper horizons, and a reduction in solution alkalinity. However, observed decline in solution pH was far less than expected from the strong anion release, indicative of strong solution buffering, presumably through exchange reactions and/or accelerated weathering. By the time solutions leached out of the rooting zone, differences in chemistry between the two systems had strongly diminished. This illustrates the importance of soil depth in assessing potential impacts of strong acid inputs on the chemistry of water draining out of forested areas into streams and lakes. We found that the soils subjected to prolonged action of nitrification had higher titratable and exchangeable acidity, which was further reflected in the significantly lower soil pH. Despite past acidification, these soils had apparently not lost their ability to neutralize additional H^+ inputs, and actually seemed to resist further acidification more strongly than the less acidic conifer soils. Although there is some danger in extrapolating these results, our studies may serve as an illustration of the potential changes in soil and solution chemistry caused by chronic strong acid input and of the strong buffering that may take place.

ACKNOWLEDGMENTS

This research has been funded by the Electric Power Research Institute under contract RP-2621 with Martin Marietta Energy Systems, Inc., under contract DE-AC05-84OR21400 with the U.S. Department of Energy, and by the National Science Foundation under contract BSR-841678 with Oregon State University. Publication No. 3296, Environmental Sciences Division, Oak Ridge National Laboratory.

REFERENCES

1. G. Abrahamsen, "Acid precipitation, plant nutrients, and forest growth," in *Ecological impacts of acid precipitation*, D. Drablos and A. Tollan, Eds., The Norwegian interdisciplinary research programme: Acid precipitation—Effects on forest and fish, Oslo-As, Norway, 1980, p. 58.
2. W.A. Atkinson and W.I. Hamilton, "The value of red alder as a source of nitrogen in Douglas-fir/alder mixed stands," in *Utilization and management of alder*, D. G. Briggs, D.S. DeBell and W.A. Atkinson, Eds., USDA For. Serv. Gen. Tech. Rep. PNW-70, U.S. Government Printing Office, Washington, DC, 1978, p. 337.
3. J.C. Gordon and C.T. Wheeler, *Biological nitrogen fixation in forest ecosystems: foundations and applications*, Martinus Nijhoff/Dr. Junk, Publishers, The Hague, The Netherlands, 1983.
4. D. Binkley, J.D. Lousier, and K. Cromack Jr., "Ecosystem effects of sitka alder in a Douglas-fir plantation," *For. Sci.* 31:26 (1984).
5. J.F. Franklin, C.T. Dyrness, D.G. Moore, and R.F. Tarrant, "Chemical soil properties under coastal Oregon stands of alder and conifers," in *Biology of alder*, J.M. Trappe, J.F. Franklin, R.F. Tarrant, and G.M. Hansen, Eds., USDA PNW Forest Range Exp. Stn., Portland, Oregon, 1968, p. 157.
6. J. Zavitkovski and M. Newton, "Effect of organic matter and combined nitrogen on nodulation and nitrogen fixation in red alder," in *Biology of alder*, J.M. Trappe, J.F. Franklin, R.F. Tarrant, and G.M. Hansen, Eds., USDA PNW Forest Range Exp. Stn., Portland, Oregon, 1968, p. 209.
7. D.W. Cole, S.P. Gessel, and J. Turner, "Comparative mineral cycling in red alder and Douglas-fir," in: *Utilization and management of alder*, D.G. Briggs, D.S. DeBell and W.A. Atkinson, Eds., USDA For. Serv. Gen. Tech. Rep. PNW-70, U.S. Government Printing Office, Washington, DC, 1978, p. 327.
8. D.S. DeBell and M.A. Radwan, "Growth and nitrogen relations of coppiced black cottonwood and red alder in pure and mixed plantings," *Bot. Gaz. (Chicago)* 140:5102 (1979).
9. D. Binkley, "Nodule biomass and acetylene reduction rates of red alder and Sitka alder on Vancouver Island, B.C.," *Can. J. For. Res.* 11:281 (1981).
10. R.F. Tarrant, "Nitrogen fixation in North American forestry: research and application," in *Biological nitrogen fixation in forest ecosystems: foundations and applications*, J.C. Gordon and C.T. Wheeler, Eds., Martinus Nijhoff/Dr. Junk Publishers, The Hague, The Netherlands, 1983, p. 261.
11. P.M. Vitousek, J.R. Gosz, C.C. Grier, J.M. Melillo, W.A. Reiners, and R.L. Todd, "Nitrate losses from disturbed ecosystems," *Science* 204:469 (1979).

12. S.J. Riha, G.S. Campbell, and J. Wolfe, "A model of competition for ammonium among heterotrophs, nitrifiers, and roots," *Soil Sci. Soc. Am. J.* 50:1463 (1986).

13. D. Binkley and S.C. Hart, "The components of nitrogen availability assessment in forest soils," *Adv. Soil Sci.* 10:57 (1989).

14. R.F. Tarrant, "Stand development and soil fertility in a Douglas-fir/red alder plantation," *For. Sci.* 7:238 (1961).

15. R.N. Coats, R.L. Leonard, and C.R. Goldman, "Nitrogen uptake and release in a forested watershed, Lake Tahoe Basin, California," *Ecology* 57:995 (1976).

16. D. Binkley, J.P. Kimmins, and M.C. Feller, "Water chemistry profiles in an early- and mid-successional forest of coastal British Columbia," *Can. J. For. Res.* 12:240 (1982).

17. H. Van Miegroet and D.W. Cole, "The impact of nitrification on soil acidification and cation leaching in a red alder forest," J. Environ. Qual. 13:585 (1984).

18. H. Van Miegroet and D.W. Cole, "Acidification sources in red alder and Douglas-fir soils—Importance of nitrification," *Soil Sci. Soc. Am. J.* 49:1274 (1985).

19. D.W. Johnson and D.W. Cole, "Anion mobility: relevance to nutrient transport from forest ecosystems," *Environm. Internat.* 3:79 (1980).

20. D.W. Johnson, D.W. Cole, H.Van Miegroet, and F.W. Horng, "Factors affecting anion movement and retention of four forest soils," *Soil Sci. Soc. Am. J.* 50:776 (1986).

21. T. Kinjo and P.F. Pratt, "Nitrate adsorption: II. In competition with chloride, sulfate, and phosphate," *Soil Sci. Soc. Am. Proc.* 35:725 (1971).

22. L. Wiklander, "The influence of anions on adsorption and leaching of cations in soils," *Grundfoerbaettring* 26:125 (1976).

23. J.O. Reuss, "Implications of the calcium-aluminum exchange system for the effect of acid precipitation on soil," *J. Environ. Qual.* 12:591 (1983).

24. D.W. Cole and D.W. Gessel, *Cedar River Watershed—a program for studying pathways, rates and processes of elemental cycling in a forest ecosystem*, University of Washington, Institute of Forest Products, For. Resources Monograph #4, University of Washington, Seattle, 1968.

25. H. Van Miegroet, *Role of N status and N transformations in* H⁺ *budget, cation loss and S retention mechanisms in adjacent Douglas-fir and red alder forests*, Ph.D. Dissertation, University of Washington, Seattle, 1986.

26. D. Binkley, P. Sollins, R. Bell, D. Sachs, and D. Myrold, "Nitrogen biogeochemistry of adjacent conifer and alder/conifer ecosystems," (in review).

27. D. Binkley and P. Sollins, "Acidification of soils in mixtures of conifers and red alder," (in review).

28. C. Eno, "Nitrate production in the field by incubating the soil in polyethylene bags," *Soil Sci. Soc. Am. Proc.* 24:277 (1960).

29. W.B. Bollen and K.C. Lu, "Nitrogen transformations in soils beneath red alder and Douglas-fir," in *Biology of alder*, J. M. Trappe, J.F. Franklin, R.F. Tarrant, and G.M. Hansen, Eds., USDA PNW Forest Range Exp. Stn., Portland, Oregon, 1968, p. 141.

30. H. Van Miegroet, D.W. Johnson, and D.W. Cole, "Soil nitrification as affected by N fertility and changes in forest floor C/N ratio in four forest soils," (in review).

31. J.O. Reuss and D.W. Johnson, *Acid deposition and acidification of soils and waters*, Ecol. Studies 59, Springer-Verlag, New York, 1986.

32. F.C. Ugolini, "Soil development and alder invasion in a recently deglaciated area of Glacier Bay, Alaska," in *Biology of alder*, J.M. Trappe, J.F. Franklin, R.F. Tarrant and G.M. Hansen, Eds., USDA PNW Forest Range Exp. Stn., Portland, Oregon, 1968, p. 115.

33. K. Van Cleve and L.A. Viereck, "Distribution of selected chemical elements in even-aged alder (*Alnus*) ecosystems near Fairbanks, Alaska," *Arct. Alp. Res.* 4:239 (1972).

34. D. Binkley, "Ecosystem production in Douglas-fir plantations: interactions of red alder and site fertility," *For. Ecol. Manage.* 5:215 (1983).

35. D.W. Johnson, Oak Ridge National Laboratory, Personal Communication.

36. J.O. Reuss and D.W. Johnson, "Effect of soil processes on the acidification of water by acid deposition," *J. Environ. Qual.* 14:26 (1985).

37. R.L. Crocker and J. Major, "Soil development in relationship to vegetation and surface age at Glacier Bay," *J. Ecol.* 43:427 (1955).

38. K. Van Cleve, L.A. Viereck and R.L. Schlentner, "Accumulation of nitrogen in alder (*Alnus*) ecosystems near Fairbanks, Alaska," *Arct. Alp. Res.* 3:101 (1971).

39. B.T. Bormann and D.S. DeBell, "Nitrogen content and other soil properties related to age of red alder stands," *Soil Sci. Soc. Am. J.* 45:428 (1981).

40. D.S. DeBell, M.A. Radwan, and J.M. Kraft, *Influence of red alder on chemical properties of a clay loam soil in western Washington*, USDA For. Serv. PNW For. Range Exp. Stn. Res. Paper PNW-313, Portland, Oregon, 1983.

41. J.O. Reuss, "Soil-solution equilibria in lysimeter leachates under red alder," Proceedings of the 82nd Annual AWMA Meetings, Anaheim, CA, 1989.

Table I. Summary of studies on the effect of alder species on soil and solution properties.

Location–alder species Type of study	Properties measured	Reference
Alaska (Glacier Bay), *A. sinuata* Deglaciation chronosequence	Soil N, soil pH soil organic C	37
Washington (Wind River), *A. rubra* Conifer vs. alder-conifer stand (27 years)	Soil N, soil pH, CEC, exch. bases	14
Alaska (Glacier Bay), *A. sinuata* Deglaciation chronosequence	Soil genesis, % calcite soil N, soil pH, CEC, exch. bases, H^+, forest floor organic C	32
Oregon (Cascade Head, Widow Creek), *A. rubra* Conifer vs. alder-conifer stand (30 & 40 yr)	Soil N, NH_4, NO_3, C/N, soil pH, CEC, exch. bases, %BS, P, soil organic C	5,29
Alaska, *A. sinuata* Floodplain chronosequence soil organic C	Soil N, soil pH, CEC, exch. bases, Mn, P,	33,38
Washington (Olympia), *A. rubra* Alder chronosequence (9-45 yr) vs. Douglas-fir	Soil N, soil pH, soil organic C, exch. bases, S, SO_4-S, extract. Fe, Mn, Cu, Zn	39,40
British Columbia, *A. rubra* Mixed alder/conifer (17 yr) vs. conifer old-growth (70-90 yr)	Soil pH, CEC, exch. bases, NH_4, solution pH, NO_3, soil and forest floor organic C	16
Washington (Skykomish), *A. rubra*	Soil N, pH,	34
British Columbia (Mt. Benson), *A. rubra* alder/conifer vs. Douglas-fir (23 yr)	soil organic C, exch. bases	
British Columbia (Mt. Benson), *A. sinuata* Mixed alder/conifer vs. conifer (23 yr)	Soil N, pH, P, soil organic C, exch. bases	4
Washington (Thompson Site), *A. rubra*	Soil N, soil pH,	17,18
Alder vs. Douglas-fir stand (50 yr)	CEC, exch. bases, % BS, solution pH, NO_3	

Table II. Annual N mineralization (0-15 cm depth) and leaching rates for the conifer and alder sites at the Thompson site (25), the Wind River Experimental Forest, and Cascade Head (26).

Location Ecosystem	Mineralization[a] NH_4^+	NO_3^-	Total	Net Leaching[a,b] NH_4^+	NO_3^-	Inorg. N
Thompson Site						
Douglas-fir	12	5	17	<1	<1	<1
Red alder	-14	114	101	<1	49	49
Wind River						
Conifer	<1	0	<1	<1	<1	1
Alder/conifer	27	99	126	4	3	7
Cascade Head						
Conifer	15	14	29	4	8	12
Alder/conifer	7	116	123	2	36	38

[a] kg/ha/yr

[b] Leaching to 40-cm depth at the Thompson site and to 70-cm depth in the Wind River and Cascade Head sites.

Table III. Three-year average annual water flux, and H^+, NO_3^-, and HCO_3^- input and output budget for the Douglas-fir and red alder ecosystem at the Thompson site (25).

Ecosystem Flux	H_2O cm	Cations[a]	H^+ [a]	NO_3^- [a]	HCO_3^- [a]
Douglas-Fir					
Precipitation	158	790	303	154	139
Throughfall	105	1220	122	14	76
Forest floor	51	1440	82	14	136
A-horizon	102	1380	12	8	504
B-horizon	111	1550	28	11	578
Red Alder					
Precipitation	158	790	303	154	139
Throughfall	105	1160	57	23	413
Forest floor	60	3490	265	2370	43
A-horizon	102	4030	263	4400	14
B-horizon	124	4800	52	3680	447

[a] mol_c/ha/yr

Table IV. Difference in soil acidity expressed by pH in water, pH in $CaCl_2$, exchangeable base concentration, exchangeable Al, and percent base saturation between conifer and alder forests at the three study sites (mean with standard deviation in parentheses, followed by significance of difference between alder and Douglas-fir soils at a given depth: • p = 0.1; •• p = 0.05).

Location Stand Depth (cm)	pH_{water}	pH_{CaCl_2}	CEC^{a,b}	Exch. Bases^{b}	Exch. Al^{a,b}	BS %
Thompson Site						
Douglas-fir						
0-15	5.3(0.2)••	4.5(0.2)••	99••	13	89(15)••	12.5(5)••
15-30	5.3(0.2)••	4.8(0.2)••	89••	11	81(16)••	11.5(6)••
30-45	5.3(0.1)••	4.7(0.1)••	79••	7	72(15)••	9(5)
Red alder						
0-15	4.5(0.3)••	4.0(0.2)••	149••	11	136(25)••	7(3)••
15-30	4.8(0.2)••	4.4(0.1)••	128••	9	119(25)••	7(3)••
30-45	4.9(0.2)••	4.4(0.2)••	118••	11	107(29)••	8.5(5)
Wind River						
Conifer						
0-15	5.4(0.1)•	4.3(0.1)	48•	16	32(7)	32•
15-40	5.3(0.1)•	4.3(0.1)	36•	8	28(7)•	22•
40-65	5.2(0.1)•	4.1(0.1)	109	26	83(30)	24•
Alder/conifer						
0-15	5.1(0.3)•	4.3(0.2)	77•	34	42(5)	45•
15-40	5.1(0.2)•	4.2(0.1)	62•	16	46(3)•	26•
40-65	5.0(0.2)•	4.1(0.1)	96	15	81(10)	16•
Cascade Head						
Conifer						
0-15	5.4(0.4)•	4.4(0.4)•	126•	37	89(6)•	29•
15-30	5.4(0.2)•	4.4(0.2)•	72	21	51(16)	29•
30-60	5.2(0.2)•	4.3(0.2)	64•	11	53(12)	17•
Alder/conifer						
0-15	4.3(0.4)•	3.7(0.3)•	152•	14	138(4)•	9•
15-30	4.8(0.4)•	4.1(0.1)•	92	16	76(17)	18•
30-60	4.8(0.3)•	4.2(0.1)	54•	5	49(9)	9•

[a] Thompson site: CEC determined by 1N NH_4Cl extraction, exch. Al calculated by difference between CEC and sum of exchangeable bases; Cascade Head and Wind River: exch. Al determined on 1N KCl extract, CEC calculated from sum of exch. Al and exchangeable bases.

[b] $mmol_c/kg$

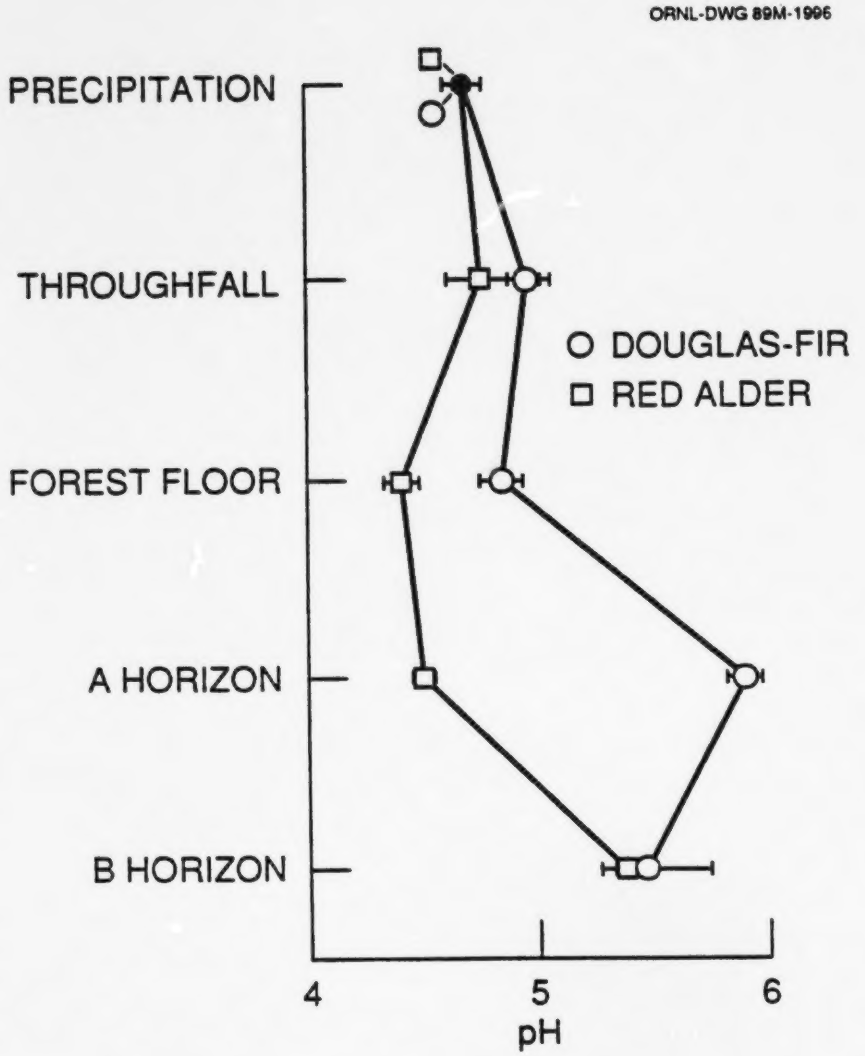

Figure 1. Average pH of precipitation, throughfall, forest floor, A-horizon and B-horizon solutions in the Douglas-fir and red alder stands at the Thompson Research Center [1981-1984 mean and standard deviation].[25]

ORNL-DWG 89M-1997

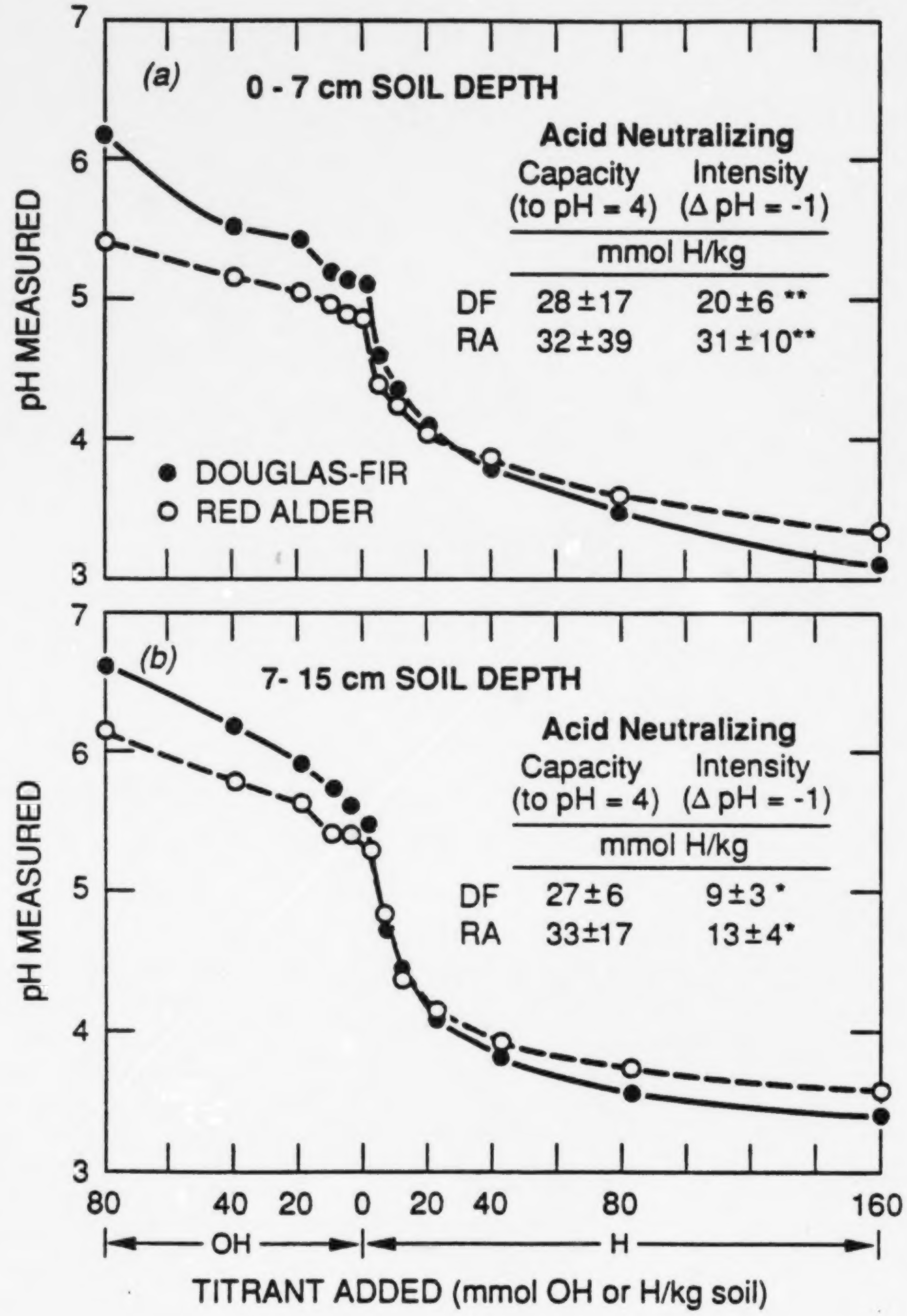

Figure 2. Mean soil pH vs. amount of H^+ or OH^- added to Douglas-fir and red alder soils at the Thompson Research Center and calculated acid neutralizing capacity and intensity [mean and standard deviation (n = 5), followed by significance of difference (* p = 0.1; ** p = 0.05)] for (A) 0-7 cm soil depth and (B) 7-15 cm soil depth.[25]

Forest Soil Sulfur Pools and SO_4^{2-} Adsorption and Desorption Capacity Following Elevated Inputs of SO_4^{2-}

Robert B. Harrison[1]
Dale W. Johnson[2]
Donald E. Todd[3]

[1] *College of Forest Resources*
AR-10
University of Washington
Seattle, WA 98195

[2] *Desert Research Institute*
University of Nevada
P.O. Box 60220
Reno, NV 89506

[3] *Environmental Sciences Division*
Oak Ridge National Laboratory
P.O. Box X
Oak Ridge, TN 37831

INTRODUCTION

Much concern has been expressed over the influences of elevated inputs of certain anions (notably SO_4^{2-} and NO_3^-) and their associated acidity on cation leaching from forest ecosystems.[1,2] Various factors typically influence ecosystem response to acid inputs, including vegetation and soil factors, topographic factors, and natural and human-caused factors such as land use and fire.[3] The mobility and retention in soils of S from inputs of acid SO_4^{2-}, in particular, have received considerable attention because SO_4^{2-} retention can result in reductions in cation leaching when an accompanying cation is coadsorbed with the SO_4^{2-} anion.[2,4,5]

Whether or not SO_4^{2-} will be mobile in a forest soil, incorporate into the soil organic matter, or be inorganically retained in the soil depends on a soil's inherent SO_4^{2-} retention properties, and the present S status of the soil. The chemical characteristics, as well as the total pool of S in the forest soil, are important in determining the nature of S cycling in the system. For example, Figure 1 illustrates some potential cycles for SO_4^{2-} input into a forest soil, the transformations that may occur, the forms retained in the soil, and the mechanisms for loss from the soil.

Forest ecosystems exhibit vastly different total S contents, and highly variable chemical characteristics of the S in those ecosystems.[6-9] As shown in Figure 1, soil S may be retained by a variety of different mechanisms, including both organic and inorganic forms. Both are typically important in most forest soils. Forest ecosystems that contain soils exhibiting substantial amounts of retention of SO_4^{2-}, regardless of whether that retention is by organic incorporation or by mineral adsorption and precipitation, are considered to be at least partially resistant to accelerated cation leaching.[10-14]

Considerable effort has been and is presently being made to evaluate the potential retention of SO_4^{2-} in soils to better estimate ecosystem susceptibility to accelerated cation leaching caused by increased atmospheric inputs.[15,16] It is clear from numerous research results that S retention in a forest ecosystem increases as the input levels of SO_4^{2-} into that forest increase, and that this can lead to net cation conservation in the short term. However, it it less clear whether at least part of S retention is permanent when input levels of SO_4^{2-} are decreased. Several previous studies indicate that a portion of inorganic SO_4^{2-} is irreversibly retained in the long term.[17-19] Gradual solubility of this residual SO_4^{2-} results in increased levels of solution SO_4^{2-} well past the time of the original applications.[20-22] This paper gives results from a study of soil sulfur pools in 20 forest ecosystems in the United States, Canada, and Norway, as well as observed SO_4^{2-} retention and release in soils collected from those forest ecosystems.

EXPERIMENTAL METHODS

Site Descriptions

We describe the results of a study of soil S pools, soil properties, and SO_4^{2-} adsorption and desorption in soils from a variety of forest ecosystems under investigation as part of the integrated forest study on effects of atmospheric deposition (IFS). This is an integrated nutrient cycling study being conducted in 20 forest ecosystems in the United States, Canada, and Norway. The sites studied represent a variety of physiographic locations and local climates, present and past atmospheric deposition levels, vegetation types, and soil chemical and physical properties. Figure 2 shows the approximate location of the study sites in the United States, Canada, and Norway, and Table I summarizes site properties.

Site vegetation includes pure and/or mixed stands of hardwoods and conifers, depending on location. Stand elevation ranges from 60 to 1800 m above sea level, including mountain slope and valley locations. Three soils orders, including Ultisols, Inceptisols, and Spodosols, are represented.

Soil sampling and analysis

Soil samples were collected by cooperators at the 20 sites of the IFS by horizon, air-dried, sieved to 2 mm, and stored in air-tight glass jars at room temperature prior to analysis. In some cases soil horizons were composited, and in other cases only one soil pit was sampled for each soil sample. Samples were analyzed for a variety of properties, including pH, total C by LECO combustion, pyrophosphate, oxalate and dithionite-citrate, extractable Fe and Al. The Fe and Al fractions extracted by these methods have been loosely termed as (1) organically bound (Al_o and Fe_o), (2) amorphous (Al_a and Fe_a) or (3) crystalline (Al_c and Fe_c), where the sodium pyrophosphate extraction is considered to remove organically bound, the oxalate extraction to remove organically bound plus amorphous, and the dithionite-citrate-bicarbonate extraction to remove organically bound, amorphous and crystalline Fe and Al.[23]

This methodology has been investigated for soil Fe,[24] and the classifications are thought to be accurate for Fe in many soil samples. However, the methodology has not been thoroughly investigated for soil Al. Since the extractions were done on individual and not sequential samples, the relative values of each Fe or Al fraction would be determined by difference, thus:

$$Fe_o = Fe_p, \qquad [1]$$

$$Fe_a = Fe_o - Fe_p, \text{ and} \qquad [2]$$

$$Fe_c = Fe_d - Fe_o \qquad [3]$$

Total S and soil sulfur fractions

Soil S was analyzed by a variety of methods including total soil S by alkaline oxidation and HI reduction,[25] HI reducible by HI reduction, insoluble phosphate desorbable SO_4^{2-} by exhaustive phosphate solution displacement and ion-chromatographic determination of SO_4^{2-},[23] and water soluble SO_4^{2-} by miscible displacement of SO_4^{2-} with deionized water. Soil S was then divided into the four fractions as follows:

$$\text{carbon bonded sulfur (C-S)} = \text{total S} - \text{HI reducible} \qquad [4]$$

$$\text{ester } SO_4^{2-} = \text{HI } SO_4^{2-} - \text{phosphate desorbable } SO_4^{2-} \qquad [5]$$

$$\text{adsorbed } SO_4^{2-} = \text{phosphate desorbable } SO_4^{2-} - \text{water soluble } SO_4^{2-} \qquad [6]$$

$$\text{water } SO_4^{2-} = \text{water soluble } SO_4^{2-} \qquad [7]$$

There are other operational methods available to fractionate soil S, such as Raney-Ni,[26] but the large number of samples to be evaluated made it impossible to utilize every method. The operational procedures chosen for determining S chemistry are not exact, but they do offer a useful way of classifying the myriad chemical forms of S in a systematic and reproduceable way.

SO_4^{2-} adsorption capacity and desorption reversibility

SO_4^{2-} adsorption/desorption and desorption reversibility was measured by use of a constant-rate vacuum extractor.[23] Two different leaching sequences (desorption-extraction and adsorption-desorption-extraction) completed on two separate soil samples (1a-1b and 2a-2b-2c; Figure 3) with an influent rate of 1.4 cm/h (25 g soil loosely packed in a cylinder 2.5 cm in diameter) were followed for each soil sample (with three replications for several of the soil samples, one soil sample only for others) studied in order to give the following information:

The typical adsorption-desorption-extraction pathway of soil SO_4^{2-} vs .solution concentration for a soil exhibiting irreversible SO_4^{2-} adsorption is shown in Figure 3. Solution samples were collected and analyzed for pH, electrical conductivity, and SO_4^{2-} (by ion chromatography) in 50-ml increments in order to track the progress of SO_4^{2-} saturation of the soils. When the solution concentration of the effluent was equal to that of the influent (0.25 $\underline{\text{mM}}$ SO_4^{2-}), the soil was considered to be SO_4^{2-} saturated at the input concentration.

RESULTS

Soil sulfur pools and fractions

Total soil S in subsurface soil horizons ranged from 0.5 mmol/kg in the Florida slash pine C horizon to 26 mmol/kg in the Maine red spruce "B" horizon, a range of nearly two orders of magnitude. The distribution of total S in subsoil horizons is shown in Figure 4, and in general, total S decreases from northern sites to southern sites. The exceptions are the Duke loblolly pine site, which had a history of application of S-containing superphosphate fertilizer, and the Smokies sites which have much higher S inputs than most other southern sites. The total S concentrations of the 11 soil samples analyzed from Washington state sites ranged from 2.9 to 20.8 mmol/kg. In general, the total S concentrations of the western soils were higher than the average for all other soils and were lowest in the A2 horizons of those soils.

In general, surface soil horizons had much higher contents of total S than subsurface soil horizons. Surface soil horizons typically had greater than 80% of total S in the organic fraction (carbon bonded S and ester SO_4^{2-}) compared to the inorganic fraction (phosphate or water soluble SO_4^{2-}), whereas subsoil horizons varied widely in S fraction distribution (from greater than 80% to less than 10% organic). Figure 5 illustrates the inorganic vs. organic S fractions for all of the soils of the study, sorted by soil order and site. Most soils showed a relative decrease in organic S with increasing soil depth. For instance, the organic S fraction decreased from 90% in the Cedar River Douglas-fir A1 horizon to less than 10% in the B22 horizon. However, this was not true of the Findley Lake and Red Alder soils in the other two western sites.

Since the total S of most sites decreased with soil depth, and the organic fraction was high in all soil horizons, organic mechanisms of S retention were predominant in the rooting zones of most sites. However, in some sites, notably the Ultisols in the southeastern United States, the subsoil horizons contain a high proportion of adsorbed SO_4^{2-} and inorganic mechanisms of S retention predominate. The strong, direct relationship between S and organic matter can be seen in Figure 6, where total S is plotted vs organic C. The phosphate and water soluble SO_4^{2-} pools are inversely related to organic matter concentration of the soil (Figure 7). If the phosphate and water soluble pools of SO_4^{2-} are subtracted from total S, a much stronger relationship between organic S and total C emerges (Figure 8). Thus, the ability of forest ecosystems to retain S by organic incorporation appears to be directly related to the total C pools of the soil and, in some respects, can be estimated by this relationship.

SO_4^{2-} adsorption

Observed SO_4^{2-} adsorption-desorption-extraction curves generally followed the form of Figure 3, indicating most soils showed irreversible SO_4^{2-} adsorption. Subsoil horizons showed SO_4^{2-} adsorption ranging from 0.2 to 5.0 mmol SO_4^{2-}/kg soil (Figure 9) from 0.25 mM SO_4^{2-} solution. There were typically large differences in observed SO_4^{2-} adsorption between soil horizons. For instance, the Beech Gap B and BC horizons showed large differences in SO_4^{2-} adsorption (0.3 vs. 0.8 mmol/kg SO_4^{2-} adsorbed, respectively). There were also some differences in SO_4^{2-} adsorption and native SO_4^{2-} levels in similar soil horizons between sites in the same area, though not as great as the differences between soil horizons.

Several soil properties appeared to be correlated with observed SO_4^{2-} adsorption. The concentration of oxalate (amorphous) or dithionite/citrate (crystalline) extractable Al was most closely correlated with SO_4^{2-} adsorption. This observation has been seen in several previous studies.[23,27,28,18] For instance, Figure 10 shows the relationship between SO_4^{2-} adsorption and oxalate extractable Al. Very noticeable in this figure is the lack of high levels of oxalate Al in the weathered Ultisols despite a range of SO_4^{2-} adsorption. If the values for Ultisols are removed, the observed SO_4^{2-} adsorption vs Al relationship is relatively strong ($r^2 = 0.68$). No soil property measured correlated well with observed SO_4^{2-} adsorption for samples from Ultisols, though it appeared that extractable Fe might be considerably more important than Al for these soils, as has been seen in other studies.[21,17,10,29,28]

Since initial soil-forming processes are also thought to create SO_4^{2-} adsorption sites in soil parent material in the first place,[30] estimating SO_4^{2-} adsorption by looking at soil properties is likely to be a somewhat complicated undertaking, since processes that (1) create SO_4^{2-} adsorption sites, (2) remove SO_4^{2-} adsorption sites, and (3) compete with SO_4^{2-} for sites must all be taken into account. In general (the Duke "B2t" sample is an exception), soils showing the highest levels of water soluble SO_4^{2-} were those that showed minimum SO_4^{2-} adsorption. This observation is logical, since soluble SO_4^{2-} pools would revert to insoluble SO_4^{2-} pools with time, and in general, highly soluble SO_4^{2-} in soils is thought to be related to S deposition history. Total S, ester-SO_4^{2-}, and phosphate desorpable SO_4^{2-}, however, showed no such trend. All soil samples showing substantial SO_4^{2-} adsorption (from 0.25 m$\underline{M}$ $CaSO_4$) also showed increased SO_4^{2-} desorption over untreated samples upon water extraction (with the exception of the Smokies "B" horizons), indicating that SO_4^{2-} adsorption was at least partially reversible.

SO_4^{2-} desorption reversibility

The reversibility of SO_4^{2-} adsorption is very important since irreversibly adsorbed SO_4^{2-} represents a pool permanently removed from inorganic leaching. In the present study there are two measures of SO_4^{2-} adsorption reversibility. One is the change in phosphate-extractable SO_4^{2-}, since it would be expected that irreversibly or slowly reversible adsorbed SO_4^{2-} would increase in an insoluble inorganic pool. The second measure of irreversibly adsorbed SO_4^{2-} is the difference between native soluble SO_4^{2-}, SO_4^{2-} adsorbed from $CaSO_4$ inputs, and SO_4^{2-} desorbed after $CaSO_4$ treatment (see Figure 3), as follows:

$$\text{Irreversibly adsorbed} = 2c - 1b \qquad [8]$$

$$\text{Irreversibly adsorbed} = 1a + 2a - 2b \qquad [9]$$

Ten out of fifteen subsoils showed irreversible adsorption based on increases in phosphate-extractable SO_4^{2-} (as in equ. [8]); 9 of 15 soils showed irreversible adsorption based on equ. [9].

Despite air drying and the potential perturbations associated with this practice on SO_4^{2-} incorporation and mineralization processes, most soil samples showed conservation of added SO_4^{2-}. In other words, SO_4^{2-} adsorbed from solution was recovered quantitatively by water or phosphate extraction, or:

$$1a + 2a - 2b \approx 2c - 1b \qquad [10]$$

These observations suggest that inorganic processes are dominant in these air-dried soils and that inorganic adsorption is likely to be the most important factor in controlling SO_4^{2-} concentrations in waters equilibrating with these soils. For example, the B2ir horizon in the Findley Lake Pacific Silver fir site had 0.1 mmol/kg of native water-soluble SO_4^{2-} and only 0.6 mmol/kg of phosphate extractable SO_4^{2-}. The soil retained 5.0 mmol SO_4^{2-}/kg upon treatment with 0.25 m*M* SO_4^{2-} solution, far more than the native adsorbed pools combined. A water leaching resulted in removing 3.1 mmol/kg of this retained SO_4^{2-}, and an additional phosphate extraction removed 2.7 mmol SO_4^{2}/kg. The result is conservation of added SO_4^{2-}. Applying eq. [10], we see that the net difference is 0.1 mmol SO_4^{2-}/kg, an insignificant amount.

The path that soil sampled from the "Bs" horizon of the Findley Lake Pacific Silver fir site and the Duke Loblolly pine B2t followed (the equivalent of Figure 3) is shown in Figure 11. Note that the entire path 2a-2b-2c results in approximately the same final result (fluxes summed) as the path 1a-1b (about -0.9 mmol/kg). Based on this balancing of fluxes, we could safely conclude that organic processes are not extremely important for determining SO_4^{2-} movement in this soil horizon. However, the possibility that S incorporation and mineralization rates are important but at a balance cannot be precluded. Since net production or loss not seen in this balancing was observed in several of the other sites, we would have to conclude that incorporation (possibly two sites, but differences not significant) or mineralization (significant in two sites) might be important in several other sites. In future studies of inorganic SO_4^{2-} adsorption, this kind of checkbook balancing should be done to the extent possible to be certain that SO_4^{2-} is not retained in or released from unmeasured pools.

In the sequence of adsorption-desorption-extraction in the Findley Lake "Bs" horizon, 2.3 mmol SO_4^{2-}/kg soil or 38 % of added SO_4^{2-} was retained irreversibly by the phosphate-extractable SO_4^{2-} pool. This represents a considerable pool of SO_4^{2-} relatively permanently removed from inorganic cycling. The effects of time on the permanence of this retention are questionable. Researchers have noted that time has a positive influence on SO_4^{2-} adsorption,[31] but another researcher[28] saw no correlation between SO_4^{2-} desorption and time. Permanent SO_4^{2-} adsorption appears to be an important property of many soils.

Implications for acidification of western soils

The number of sites located in the western United States evaluated as part of the Integrated Forest Study are extremely limited (3 of 20). However, soil samples collected from these three western sites exhibited high levels of SO_4^{2-} adsorption and adsorption irreversibility. Thus, based on this data it appears that a consideration of SO_4^{2-} adsorption would be necessary to understand the potential impacts of increases of acidic inputs into western forests. The three sites studied do represent important soil and forest types, with both glacial and tephric impact on soil development. It is particularly important to note that glacially affected sites have generally been assumed to show very low levels of SO_4^{2-} adsorption[32]; whereas two of the western sites (the Douglas-fir and Red Alder sites) have developed on glacial outwash and exhibit high levels of SO_4^{2-} adsorption. Thus it appears that a combination of tephra deposits and parent material effects on soil development may be much more important than recent glaciation for determining the susceptibility of these soils to accelerated cation leaching from elevated levels of acidic deposition.

CONCLUSIONS

Organic concentrations of S are generally highest in the surface forest soil horizons. Organic S typically constitutes 80% or more of total S in these horizons and is strongly correlated with soil organic C content. However, inorganic SO_4^{2-} can sometimes account for most of the total S in forest ecosystems, particularly forested Ultisols in the southeastern United States. This is because inorganic SO_4^{2-} generally increases with soil depth, and the higher relative bulk of the subsoil versus surface horizons leads to a the dominant pools of S being located in the subsoils in some forest ecosystems.

SO_4^{2-} adsorption is an important property of most subsoils examined in the 20 sites of the Integrated Forest Study, including the three western sites, which had among the highest levels. Many subsoils are capable of retaining high amounts of SO_4^{2-} from solution. However, many northeastern United States sites and southest sites at high altitude are low in SO_4^{2-} adsorption potential. Upon reducing solution concentrations, most soils showed irreversible SO_4^{2-} adsorption to varying degrees. The role of the reversibility of SO_4^{2-} adsorption is critical in assessing the response of forest ecosystems to reduced levels of S inputs.

ACKNOWLEDGMENTS

This research was sponsored in part by the Office of Health and Environmental Research, U.S. Department of Energy, under Contract No. DE-AC05-84OR21400 with Martin Marietta Energy Systems, Inc. and by the Electric Power Research Institute as part of the Integrated Forest Study on the Effects of Atmospheric Deposition.

REFERENCES

1. N. Van Breemen, "Dissolved aluminum in acid sulfate soils and in acid mine waters," SSSAP 37:694 (1973).

2. D.W. Johnson and D.W. Cole, "Sulfate mobility in an outwash soil in western Washington," *Water, Air and Soil Pollut.* 7:489 (1977).

3. C.A. Aas, "Investigation of sulfate adsorption characteristics in selected piedmont soils using a radioactive tracer and ion chromatography," M.S. Thesis, Clemson University, 1985.

4. C.S. Cronan, W.A. Reiners, R.C. Reynolds, Jr., and G.E. Long, "Forest floor leaching: contributions from mineral, organic and carbonic acids in New Hampshire subalpine forests," *Science* 200:309 (1978).

5. G. Abrahamsen and A.O. Stuanes, "Effects of simulated rain on the effluent from lysimeters with acid, shallow soil, rich in organic matter," Proc., Int. conf. ecol. impact acid precip., Norway, SNSF project, 1980.

6. M.E. Watwood and J.W. Fitzgerald, "Sulfur transformation in forest litter and soil: results of laboratory and field incubations," *Soil Sci. Soc. Am. J.* 52:1478 (1988).

7. M.B. David and M.J. Mitchell, "Transformations of organic and inorganic sulfur: importance to sulfate flux in an Adirondack forest soil," *JAPCA* 35:39 (1987)

8. J.W. Fitzgerald, T.C. Strickland, and W.T. Swank, "Metabolic fate of inorganic sulphate in soil samples from undisturbed and managed forest ecosystems," *Soil Biol. Biochem.* 14:529 (1982).

9. T.C. Strickland, J.W. Fitzgerald, J.T. Ash, and W.T. Swank, "Organic S transformations and S pool sizes in soil and litter from a southern appalachian hardwood forest," *Soil Sci.* 143:453 (1987).

10. D.W. Johnson, D.W. Cole, and S.P. Gessel, "Acid precipitation and soil sulfate adsorption properties in a tropical and in a temperate forest soil," *Biotropica* 11:38 (1979).

11. J.J. Lee and D.E. Weber, "Effects of sulfuric acid rain on major cation and sulfate concentrations of water percolating through two model hardwood forests," *J. Environ. Qual.* 11:57 (1982).

12. C.S. Cronan, "Consequences of sulfuric acid inputs to a forest soil," in *Atmospheric Sulfur Deposition*, D.S. Shriner, C.R. Richmond and S.E. Lindberg, Eds., Environmental Impact and Health Effects, Ann Arbor Science Publishers, Inc., Michigan, 1980.

13. R.D. Fuller, C.T. Driscoll, G.B. Lawrence, and S.C. Nodvin, "Processes regulating sulfate flux after whole-tree harvesting," *Nature* 325:707 (1987).

14. A.R. Huete and J.G. McColl, "Soil cation leaching by acid rain with varying nitrate-to-sulfate ratios," *J. of Environ. Qual.* 13:366 (1984).

15. R.B. Harrison and D.W. Johnson, "Atmospheric deposition and cation leaching," in B.G. Blackmon and R.S. Beasley, *Mid-South Symposium on Acid Deposition*, Univ. of Arkansas, Monticello, 1986, p. 42.

16. N.E. von Freiesleben, "Sulfate mobility in an acid Danish forest soil," *J. Environ. Qual.* 17:278 (1988).

17. L.A.G. Aylmore, M. Karim, and J.P. Quirk, "Adsorption and desorption of sulfate ions by soil constituents," *Soil Sci.* 103:10 (1967).

18. N.J. Barrow, "Effects of adsorption of sulfate by soils on the amount of sulfate present and its availability to plants," *Soil Sci.* 108:193 (1969).

19. R.F. Wright, E. Lotse, and A. Semb, "Reversibility of acidification shown by whole catchment experiments," *Nature* 334:670 (1988).

20. E. Bornhemisza and R. Llanos, "Sulfate movement, adsorption, and desorption in three Costa Rican soils," *Soil Sci. Soc. Am. Proc.* 31:356 (1967).

21. T.T. Chao, M.E. Harward, and S.C. Fang, "Movement of S35 tagged sulfate through soil columns," *Soil Sci. Soc. Am. Proc.* 26:27 (1962).

22. S.S.S. Rajan, "Adsorption and desorption of sulfate and charge relationships in allophanic clays," *Soil Sci. Soc. Am. J.* 43:65 (1979).

23. D.W. Johnson and D.E. Todd, "Relationships among iron, aluminum, carbon, and sulfate in a variety of forest soils," *Soil Sci. Soc. Am. J.* 47:792 (1983).

24. J.A. McKeague, J.E. Brydon, and N.M. Miles, "Differentiation of forms of extractable iron and aluminum in soils. *Soil Sci. Soc. Am. Proc.* 35:33 (1971).

25. M.A. Tabatabai and J.M. Bremner, "Use of the Leco automatic 70-second carbon analyzer for total carbon analysis in soils," *Soil Sci. Soc. Am. Proc.* 34:608 (1970).

26. W.A. DeLong and L.E. Lowe, "Note on carbon-bonded sulphur in soil," *Can. J. Soil Sci.* 42:223 (1961).

27. H. Nommik, K. Larsson, and U. Lohm, "Effects of Experimental Acidification and Liming on the Transformation of Carbon, Nitrogen and Sulphur in Forest Soils," Report No.: SNV-PM-1869, 1984.

28. B.R. Singh, "Sulfate sorption by acid forest soils: 2. Sulfate adsorption isotherms with and without organic matter and oxides of aluminum and iron," *Soil Sci.* 138:294 (1984).

29. R.L. Parfitt and R.S.C. Smart, "The mechanism of sulfate adsorption on iron oxides," *Soil Sci. Soc. Am. J.* 42:48 (1978).

30. S.M. Hasan, R.L. Fox, and C.C. Boyd, "Solubility and availability of sorbed sulfate in Hawaiian soils," *Soil Sci. Soc. Amer. Proc.* 34:897 (1970).

31. N.J. Barrow and T.C. Shaw, "The slow reactions between soil and anions: 7: effect of time and temperature on contact between an adsorbing soil and sulfate," *Soil Sci.* 124:347 (1977).

32. B.P. Rochelle, M.R. Church, and M.B. David, "Sulfur retention at intensively studied sites in the U.S. and Canada," *Water Air Soil Pollut.* 33:73 (1987)

Table I. Characteristics of sites of the Integrated Forest Study.

Study area	Primary Vegetation	Soil series Soil order	State	Physiographic Location	Elev. (m)
Cedar River	Red Alder	Alderwood series Durochrept	WA	valley	100
Cedar River	Douglas-fir	Alderwood series Durochrept	WA	valley	100
Findley Lake	Pacific Silver fir	Chikamin series Andept	WA	mountain basin	1100
Oak Ridge National Lab	Loblolly pine	Cecil series Typic Hapludult	TN	valley	300
Smokies	Red spruce, Fraser fir	Burton series Inceptisol	NC	mountain slopes	1800
Smokies	American beech	Burton series Inceptisol	NC	mountain slopes	1800
Oak Ridge National Lab	Yellow Poplar	Fullerton series Typic Palcudult	TN	valley	300
Oak Ridge National Lab	Chestnut Oak	Tarklin series Typic Fragiudult	TN	valley	300
Camp Branch	White Oak	Lily series Udult	TN	plateau	550
Coweeta Hyd. Lab	Oak-hickory	Fannin series Hapludult	NC	mountain slopes	700-800
Coweeta Hyd. Lab	White pine	Fannin series Hapludult	NC	mountain slopes	800 1100
Duke Forest	Loblolly pine	Appling series Typic Hapludult	NC	piedmont	215
Whiteface Mtn.	Red spruce Balsam fir	Becket series Orthod	NY	mountain slopes	1000 1500
Huntington forest	Mixed hardwoods	Becket series Orthod	NY	slopes	530
Turkey Lakes	maple-birch	Turkey series Orthod	Ontario, Canada	valley	350
Norway	Norway spruce	Typic Udipsamment	Norway	valley	202
B.F. Grant Forest	Loblolly pine	Cecil series Ultisol	GA	piedmont	160
Florida	Slash pine	Pomona series Spodosol	FL	coastal plain	50
Maine	Red spruce	Shirley series typic Haplorthod	ME	rolling hills	60

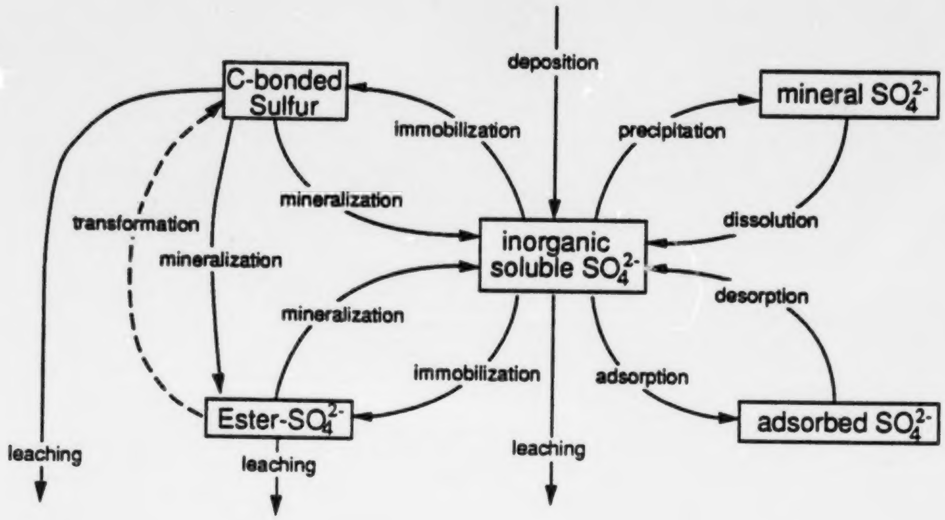
deposition
C-bonded Sulfur
mineral SO_4^{2-}
immobilization
precipitation
mineralization
transformation
dissolution
inorganic soluble SO_4^{2-}
mineralization
desorption
mineralization
immobilization
adsorption
Ester-SO_4^{2-}
adsorbed SO_4^{2-}
leaching
leaching
leaching

Figure 1. Pathways of SO_4^{2-} flow into, within, and through the soil component of a terrestrial system.

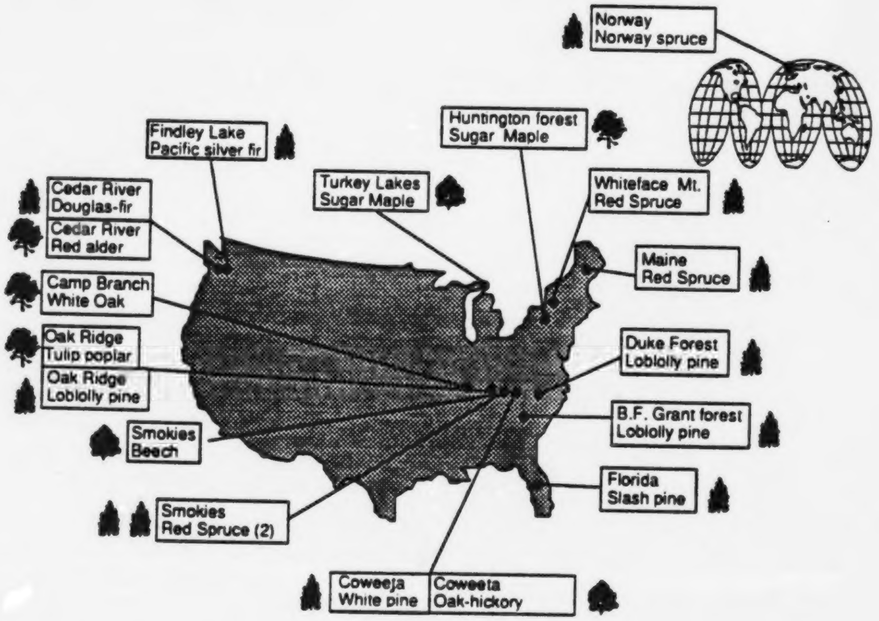
Norway
Norway spruce
Findley Lake
Pacific silver fir
Huntington forest
Sugar Maple
Cedar River
Douglas-fir
Turkey Lakes
Sugar Maple
Whiteface Mt.
Red Spruce
Cedar River
Red alder
Maine
Red Spruce
Camp Branch
White Oak
Oak Ridge
Tulip poplar
Duke Forest
Loblolly pine
Oak Ridge
Loblolly pine
B.F. Grant forest
Loblolly pine
Smokies
Beech
Florida
Slash pine
Smokies
Red Spruce (2)
Coweeja
White pine
Coweeta
Oak-hickory

Figure 2. Sites of the Integrated Forest Study.

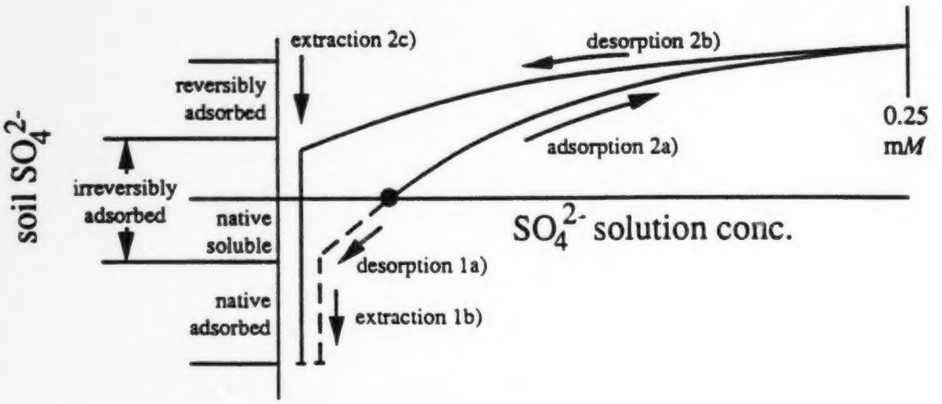
soil SO_4^{2-}
reversibly adsorbed
irreversibly adsorbed
native soluble
native adsorbed
extraction 2c)
desorption 2b)
adsorption 2a)
0.25 mM
SO_4^{2-} solution conc.
desorption 1a)
extraction 1b)

procedure followed and sulfate fraction measured

1a) Deionized water leaching until the effluent SO_4^{2-} concentration < 0.025 mM. Gives a measure of native water soluble SO_4^{2-}.

1b) Following procedure "1b" samples are extracted with 1000 ppm P as NaH_2PO_4 until the SO_4^{2-} concentration drops below the detectable limit for this matrix. Gives a measure of the native insoluble adsorbed SO_4^{2-}.

2a) Adsorption leaching with 0.25 mM $CaSO_4$ solution until the concentration of the percolate reaches 0.25 mM. Gives SO_4^{2-} adsorption from a 0.25 mM solution.

2b) Following procedure "2a" samples are leached with deionized water as in "1a". The value "1a + 2a - 2b" gives a measure of reversible SO_4^{2-} adsorption.

2c) Samples from 2b are extracted with phosphate as in "1b". The results of "2c - 1b" give a measure of irreversibly adsorbed SO_4^{2-} from SO_4^{2-} adsorption sequence in 2a.

Figure 3. Schematic of SO_4^{2-} adsorption-desorption-reversibility sequence.

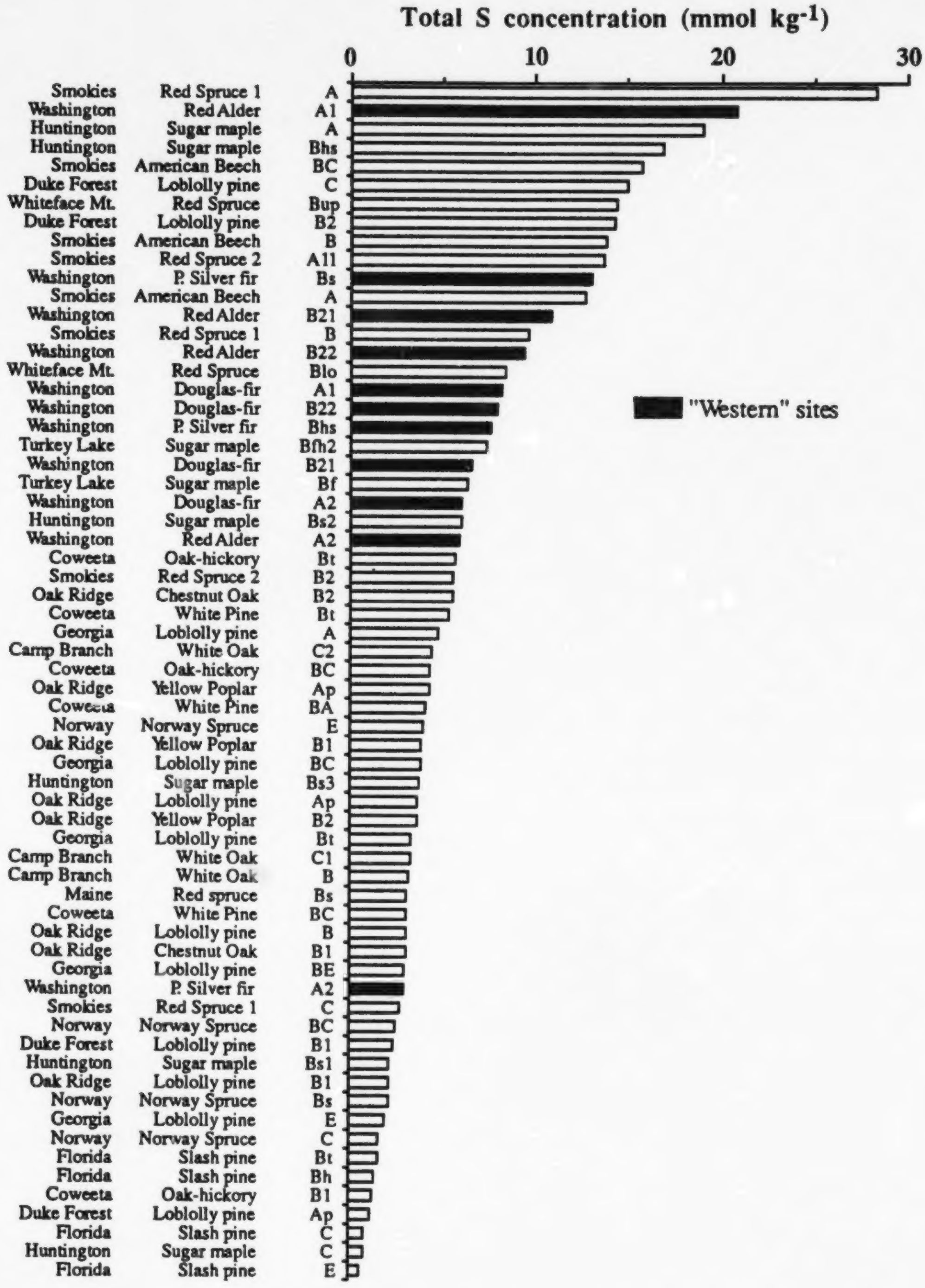

Figure 4. Soil total S concentration sorted from highest to lowest concentration.

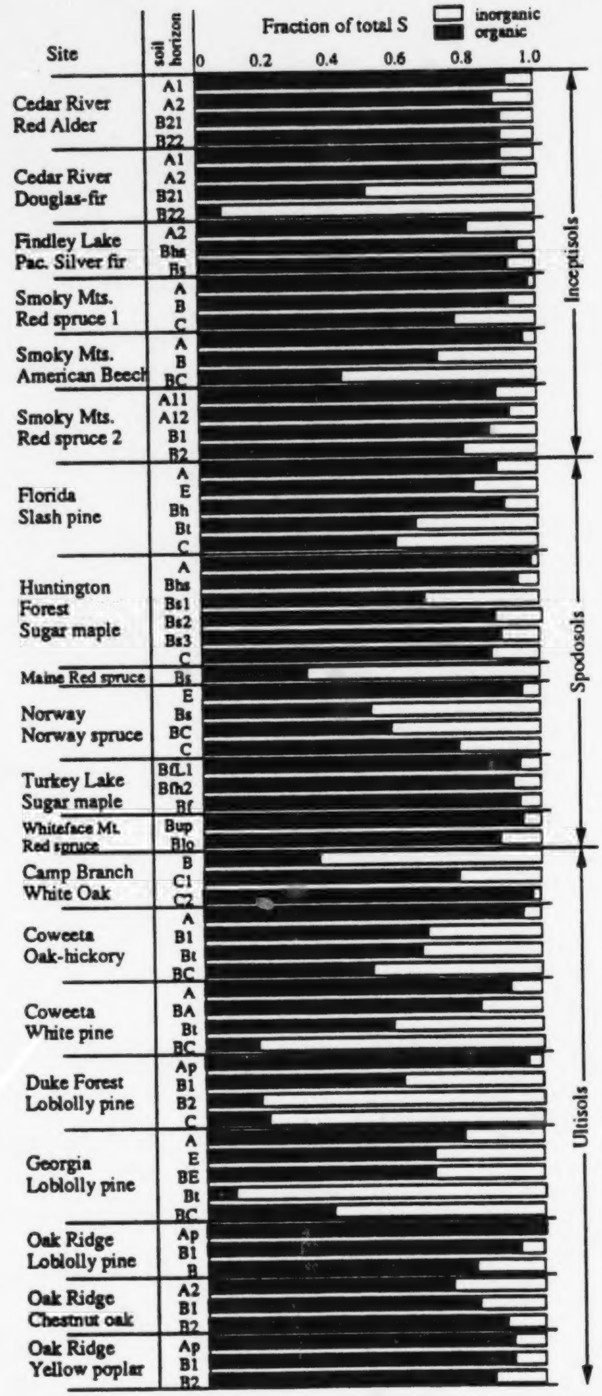

Figure 5. Soil organic versus inorganic fractions by soil order and site.

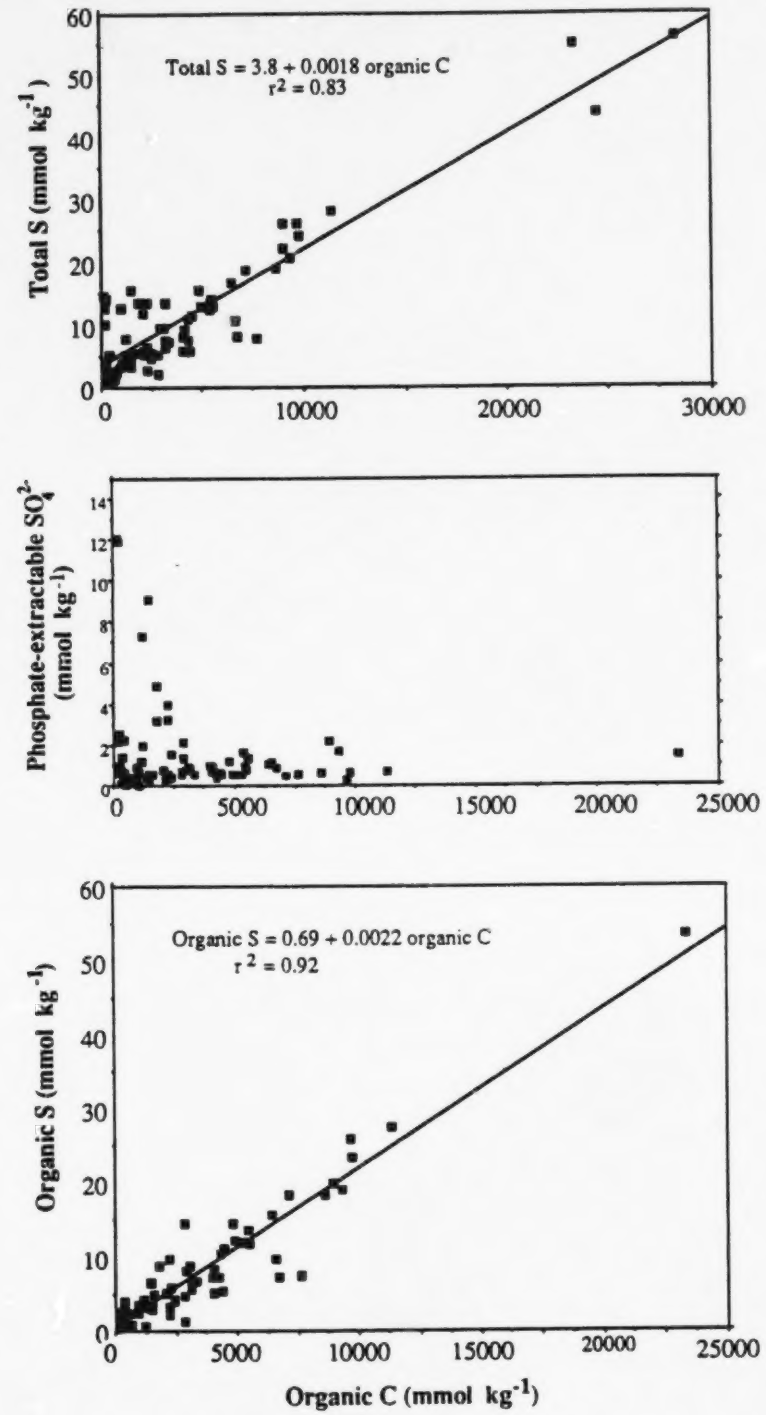

Figures 6-8. Total, inorganic and organic S versus total C.

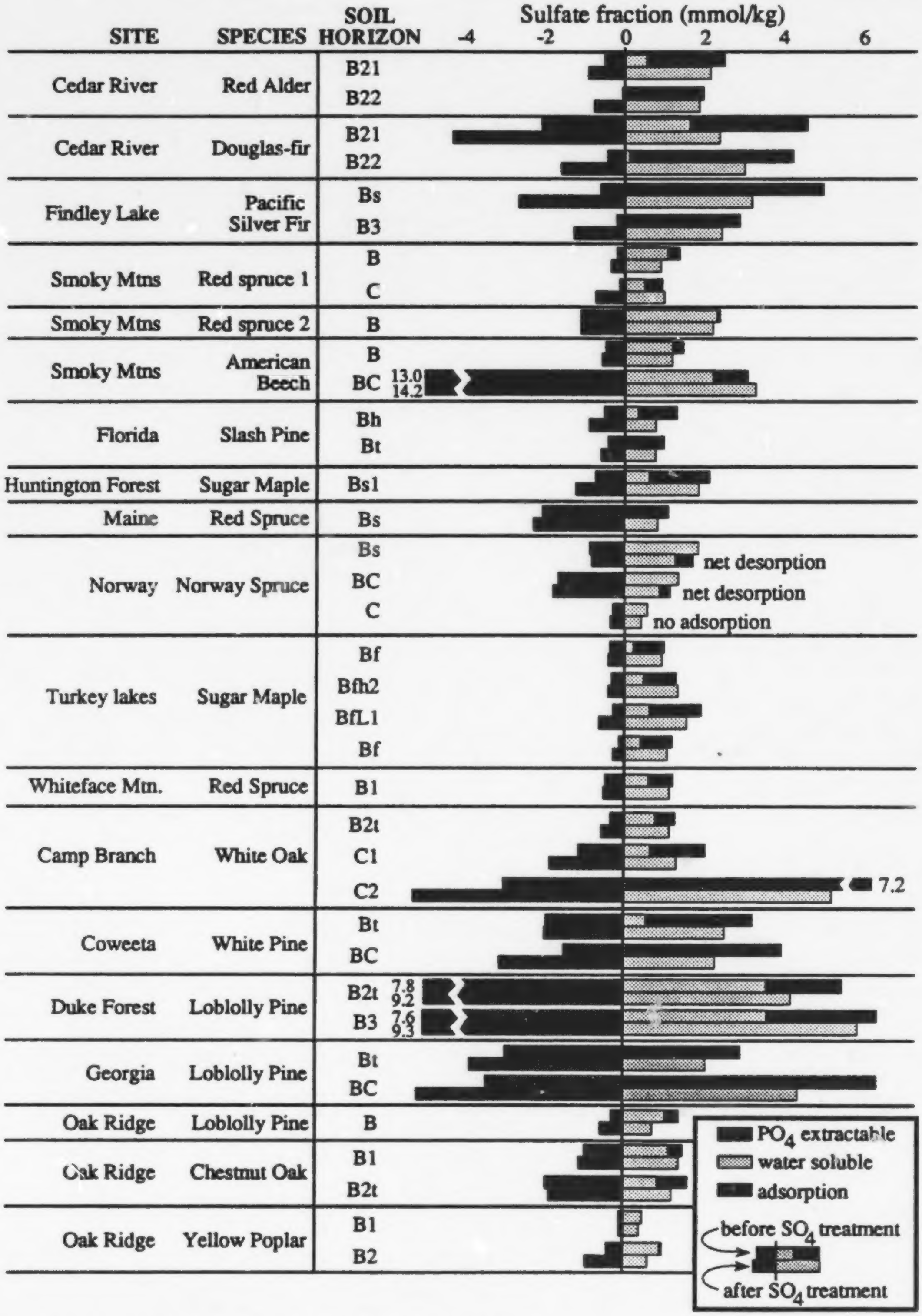

Figure 9. SO_4^{2-} adsorption, desorption, and extraction totals for soils studies in the Integrated Forest Study.

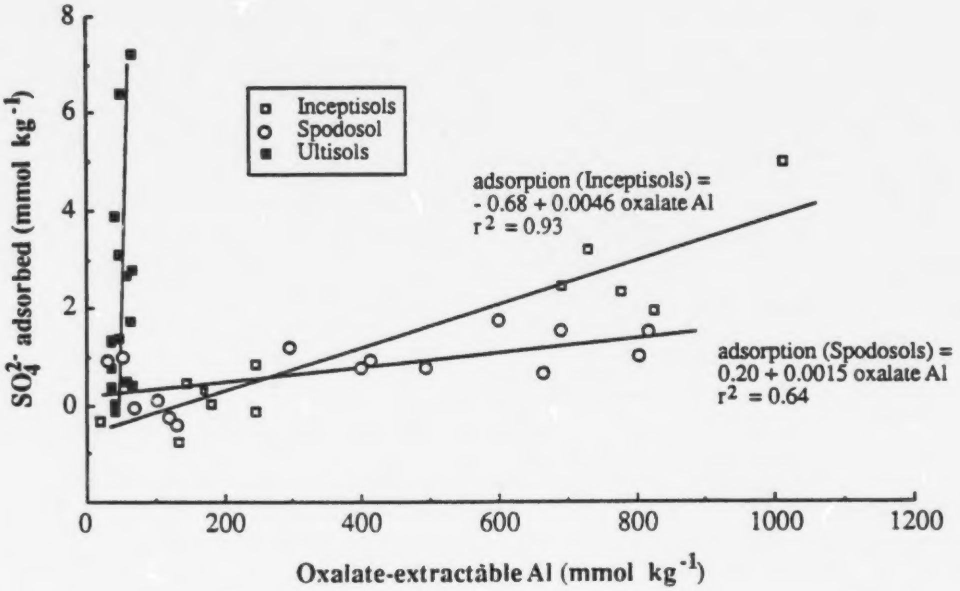

Figure 10. $SO_4{}^{2-}$ adsorbed versus oxalate extractable Al.

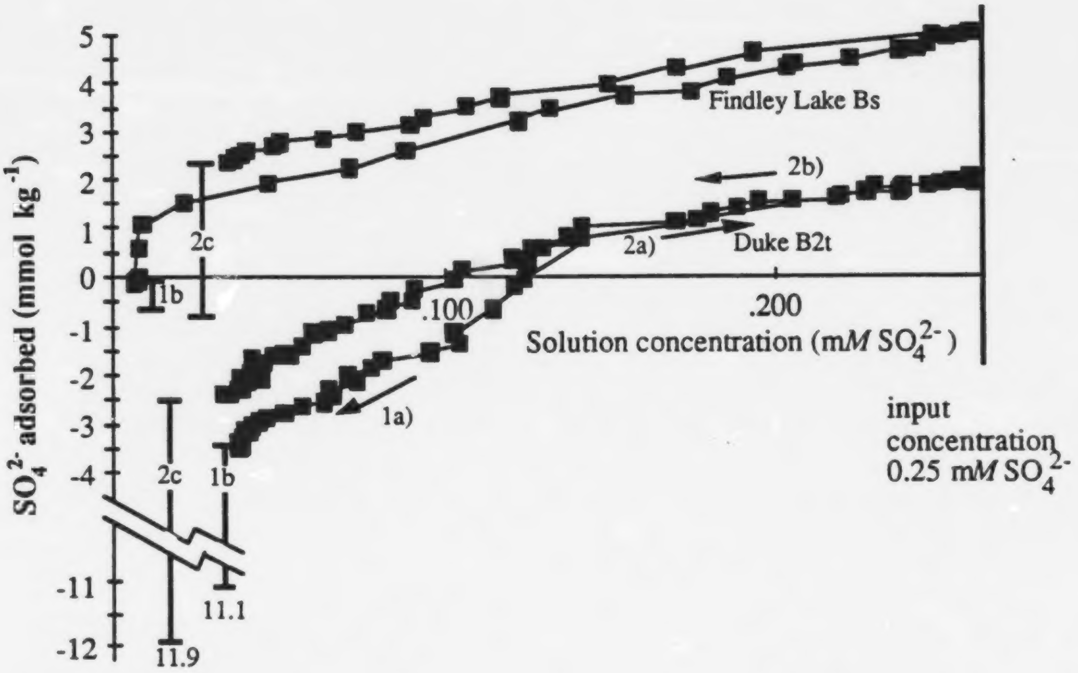

Figure 11. SO_4^{2-} adsorption, desorption, and extraction sequences for Findley Lake Bs and Duke Forest B2t horizon.

Soil-Solution Equilibria in Lysimeter Leachates Under Red Alder

John O. Reuss

Department of Agronomy
Colorado State University
Fort Collins CO, USA 80523

INTRODUCTION

Changes postulated to occur in acid soils as a result of acid deposition include increased cation export and mobilization of monomeric forms of aluminum. These changes can, in turn, cause significant changes in the composition of surface waters. A number of models have been proposed to predict the probable effects of acid deposition on surface waters.[1-8] Reliable tests of the relationships used in these models are difficult to achieve experimentally. Nitrogen fixation in red alder (*Alnus rubra* Bong.) forests is accompanied by high rates of nitrogen cycling. Rapid mineralization allows substantial oxidation of ammonia to form nitric acid (HNO_3). This process provides both a substantial input of free H^+ and an increase in the ionic concentration of the soil solution on a seasonal basis.[9] This paper discusses the changes in cation concentrations in response to this input to test some key assumptions in these models, particularly the model of Reuss and Johnson.[7,8]

MATERIALS AND METHODS

Soil leachates were collected under a stand of red alder located at the University of Washington Thompson Research Center in the Cedar River Watershed about 55 km southeast of Seattle, WA over a 27-month period starting in January, 1983. The soil belongs to the Alderwood series, which is a Dystric Entic Durochrept.[10]

Leachates were collected at 28-day intervals from 15 cm diameter tension lysimeters at 10 kPa[11] installed in triplicate at the lower limit of the A horizon (10 cm) and near the lower limit of the B horizon (40 cm). Leachates were analyzed for Na^+, K^+, Ca^{2+}, Mg^{2+}, NH_4^+, NO_3^-, SO_4^{2-}, HCO_3^-, $H_2SO_4^-$, HPO_4^{2-}, pH, and electrical conductivity. Soil samples were taken in duplicate from opposite walls of adjacent pits. Exchangeable cations and CEC (Table I) were measured at soil pH using a neutral salt extractant (NH_4Cl). Additional information concerning sampling and analytical procedures may be found in Johnson et al.[12] and Van Miegroet and Cole.[9]

Aluminum was not measured but the total charge associated with Al species can be inferred from the deficits in cation charge relative to the sum of the anions. The activity of Al^{3+} was calculated using the relationship,

$$(Al^{3+}) = \frac{Al_T}{3/\gamma_3 + 2K_1^\circ/\gamma_2(H^+) + K_2^\circ/\gamma_1(H^+)^2} \qquad [1]$$

where the parentheses denote activity, γ_i represents the activity coefficient for ions with valence i and $[Al_T]$ represents the total charge in moles (+)/L associated with the monomeric Al species. $K_1°$ and $K_2°$ are the equilibrium constants for the hydrolysis of Al^{3+} to form $Al(OH)^{2+}$ and $Al(OH)_2^+$, and are taken as $10^{-5.02}$ and $10^{-9.30}$, respectively.[13] The (H^+) is known from solution pH, the activity coefficents are calculated using the Davies form of the Debye Huckel equation,[13] and the ionic strength is calculated from electrical conductivity.[14]

RELATIONSHIPS TESTED

Key processes that are quantitatively described in most acid deposition effects models include the dissolution or precipitation of aluminum minerals, cation exchange, and the equilibrium between H^+ and HCO_3^- ions in solution and gaseous CO_2. The aluminum dissolution-precipitation reaction is commonly described in terms of the reaction of H^+ with aluminum tri-hydroxide minerals.

$$3H^+ + Al(OH)_3 = Al^{3+} + 3H_2O. \qquad [2]$$

The equilibrium expression for eq. [2] may be written,

$$(Al^{3+}) = K°(H^+)^3, \qquad [3]$$

where the parentheses denote molar activity. Equation 3 may also be used to describe Al^{3+}-H^+ exchange, so its validity in acid soils may not necessarily require the presence of any particular solid phase.[15] Some authors, however, have suggested that the relationship observed in acid forest soils may be better described by using an exponent less than 3.0 in eq. 3.[16,6]

Ion exchange has been described both in terms of H-Ca exchange[1-3] and in terms of Al-Ca exchange.[4,5,7,8] The most common exchange relationships employed are those of Gaines and Thomas (1953)[17] and Gapon (1933).[18] For Al-Ca exchange these may be written as follows:

Gaines-Thomas

$$K_{gt(Al\text{-}Ca)} = \frac{(Ca^{2+})^3(AlX)^2}{(Al^{3+})^2(CaX)^3}. \qquad [4]$$

Gapon

$$K_{gp(Al\text{-}Ca)} = \frac{(Ca^{2+})^{1/2}(AlX)}{(Al^{3+})^{1/3}(CaX)}. \qquad [5]$$

where $K_{gt(Al\text{-}Ca)}$ and $K_{gp(Al\text{-}Ca)}$ are the respective selectivity coefficients, (Ca^{2+}) and (Al^{3+}) are the solution activities, and CaX and AlX denote the fraction of the exchange sites occupied by Ca^{2+} and Al^{3+}, respectively.

When solved for the activity of Al^{3+}, eq. 4 becomes,

$$(Al^{3+}) = \frac{(Ca^{2+})^{3/2}(AlX)}{K_{gt(Al\text{-}Ca)}{}^{1/2}(CaX)^{3/2}}. \qquad [6]$$

Similarly from the Gapon we obtain,

$$(Al^{3+}) = \frac{(Ca^{2+})^{3/2}(AlX)^3}{K_{gp(Al\text{-}Ca)}{}^3(CaX)^3}. \qquad [7]$$

Similar relationships can be obtained for Al–Mg exchange, or for combined Al–(Ca+Mg) exchange. In soil, the exchangeable ions are normally far in excess of those in solution, thus CaX and AlX may be regarded as constant for relatively short term effects. Therefore, both eqs. 6 and 7 predict that as total solution strength varies, exchange processes would take place in a manner such that Al^{3+} activity would be directly proportional to the 3/2 power of the Ca^{2+} activity. Because the Al^{3+} increases relatively more rapidly than Ca^{2+}, a simple increase in total solution strength will bring about a disproportionate increase in the Al^{3+} in solution.

If the system is modelled in terms of H^+–Ca^{2+} exchange, the Gaines-Thomas relationship can be written as,

$$\frac{(Ca^{2+})}{(H^+)^2} = \frac{K_{gt(H\text{-}Ca)}(CaX)}{(HX)^2}. \qquad [8]$$

Again assuming that the total of exchangeable ions is very much greater than those in solution, the right hand side of eq. 8 may be taken as a constant and be written,

$$pH + (1/2)\log\,(Ca^{2+}) = K_L\,. \qquad [9]$$

where $K_L = (1/2)\log(K_{gt(H\text{-}Ca)}(CaX)/(HX)^2)$. A similar relationship is obtained using the Gapon equation, except that in this case $K_L = \log(K_{gp(H\text{-}Ca)}(CaX)/(HX))$. K_L is also the well known "lime potential" of Schofield and Taylor (1955),[19] which tends to remain constant even though pH may vary with solution strength. The relationship between the lime potential, Al–Ca exchange, and the pH dependence of the Al^{3+} relationship may be understood by combining eqs. 3 and 4 to obtain,[20,4]

$$pH + (1/2)\log(Ca^{2+}) = (1/6)\log\,(K^{\circ 2}K_{gt(Al\text{-}Ca)}(CaX)^3/(AlX)^2). \qquad [10]$$

Thus, the lime potential may be expressed in terms of aluminum solubility, the Gaines-Thomas Al–Ca selectivity coefficient, and the exchange fractions of Al and Ca. A similar expression may be derived for the Gapon relationship.

For exchange between ions of equal valence, it is commonly assumed that the ratio of the activity of the ions in solution will be directly proportional to the ratio on the exchange, i.e., for Mg^{2+}–Ca^{2+} exchange,

$$K_{gt(Mg\text{-}Ca)} = \frac{(Ca^{2+})(MgX)}{(Mg^{2+})(CaX)}. \qquad [11]$$

The acid neutralizing capacity (ANC) is commonly defined by,

$$[ANC] = [HCO_3^-] + 2[CO_3^{2-}] + [OH^-] - [H^+]. \qquad [12]$$

In water ANC is conservative, i.e., it is not affected by changes in $[HCO_3^-]$ or $[H^+]$ brought about by changes in CO_2 partial pressure,

$$CO_2 + H_2O = H^+ + HCO_3^-\,. \qquad [13]$$

The equilibrium expression for eq. 13 is given by

$$(H^+)(HCO_3^-) = K_C(CO_2)g. \qquad [14]$$

where $(CO_2)_g$ is the partial pressure in MPa and K_C at 25° C is $10^{-6.81}$. However, in soils where exchange processes are important, the ANC of the soil solution may be highly dependent on the CO_2 partial pressure.[7,8] This dependency arises because if CO_2 is increased, exchange processes will replace part of the H^+ brought into solution with Ca^{2+}. Because of this exchange buffering, in order to maintain the equilibrium required by eq. 14, the solution HCO_3^- will be increased much more than the H^+ concentration. The net effect is to replace exchangeable Ca^{2+} with H^+ while increasing both Ca^{2+} and HCO_3^- in solution, thereby increasing the solution ANC [eq. 12].

When acid soils are impacted by strong acids, the H^+ may also be consumed by processes that bring Al species into solution [eq. 2]. The acidity is thus stored as "acid cation" Al species, and when these solutions are transferred to the surface water, they are buffered against an increase in pH by the reverse reaction. When dealing with these solutions, the definition of ANC as given by eq. 12 is inadequate because the acidity stored as Al species is not taken into account. For acid soil solutions, where $[OH^-]$ and $[CO_3^{2-}]$ may be neglected, ANC is more appropriately defined by,

$$[ANC] = [HCO_3^-] - [H^+] - n[Al]^{n+}\ , \qquad [15]$$

where n^+ is the average charge on the Al species. This definition of ANC accounts for the acidity stored as Al species and is used in this paper. It should also be noted that ANC defined in this way is numerically equal to the sum of the "base cations" minus the conservative or "mineral" anions. This becomes apparent from eq. 16, which is a rearrangement of the charge balance equation for the ions present in significant amounts in these solutions.

$$[HCO_3^-] - [H^+] - n[Al]^{n+} = 2[Ca^{2+}] + 2[Mg^{2+}] + [K^+] + [Na^+] - 2[SO_4^{2-}] - [NO_3^-] - [Cl^-]\ . \qquad [16]$$

The model of Reuss and Johnson[7,8] consists essentially of eqs. 3, 4, 13, and 16, plus the equilibrium equations for the formation of $Al(OH)^{2+}$ and $Al(OH)_2^+$. Inputs include the respective equilibrium constants, the CO_2 partial pressure, and the concentration of the conservative anions. The equations are solved simultaneously for the concentrations of the remaining ions.

RESULTS AND DISCUSSION

The results reported are from the leachates collected at 10 cm. While some similar trends are found in the 40 cm leachates, the generally higher base saturation levels and lower NO_3^- concentrations at this depth tended to attenuate the effects of interest. Time course plots for the NO_3^- levels in the leachates from the three replicate lysimeters at the 10 cm depths are shown in Figure 1. Nitrate concentrations as high as 2500 µmol/L were observed in the fall, but generally fell to about 100 µmol/L by early spring.

The formation of more than 2500 µmol NO_3^-/L (Figure 1) by the oxidation of $-R-NH_2$ compounds would result in the formation of an equal amount of H^+ or a pH of 2.6. If the starting point were NH_4^+, twice that amount of H^+ would be formed, resulting in a solution pH of 2.3. In fact, the lowest pH observed was 4.26, or 55 µmol H^+ per liter. This attenuation clearly indicates that the cation concentration in the leachates is controlled largely by dissolution and exchange processes such as those discussed in the previous section. A plot of ANC versus

NO_3^- is shown in Figure 2. The slope of -0.36 indicates that on the average, about 36% of the charge on the NO_3^- ion was balanced by the acid cations (H^+ and Al species), while 64% was balanced by base cations (i.e., Ca^{2+}, Mg^{2+}, Na^+, and K^+). Unfortunately, the solutions were not analyzed for aluminum. However, on examination of the cation-anion balances, substantial cation deficits were observed in solutions with low pH. When these deficits are plotted against pH (Figure 3), the pattern observed is typical of that for a pH-Al plot as predicted by eq. 3 above. The effect of pH is unmistakeable, and the data tend to follow a curve that would indicate a solubility slightly below that of amorphous $Al(OH)_3$. The most plausible explanation for pH dependent cation deficits that follow this pattern seems to be that they are due to inorganic Al species. While a direct analytical determination would be preferable, none were made. Furthermore, a direct determination may well have been seriously confounded by the presence of organic complexes.[21] The possibility that aluminum in solution might be due in part to release from the ceramic lysimeter plates was considered. However, tests on similar plates indicate that aluminum release at or above pH 4.0 is insignificant.[22] While organic anions may be an important constituent of forest soils, these would tend to cause apparent anion deficits rather than the observed cation deficits. Some negative values (Figure 3) were observed, and these may be due to either organic anions or analytical noise. As these tend to be small in relation to the large cation deficits observed at low pH, the contribution of organic anions would not have a major effect on the observed pattern. Therefore, it was concluded that in these solutions the cation deficits provide a satisfactory assay for the charge associated with uncomplexed inorganic aluminum species.

This also leads to the conclusion that eq. 3 as used in a number of current models provides a satisfactory description of the pH-Al^{3+} relationship for these leachates. The value selected for log K° is 9.1. This is based on a visual fit, as the common curve fitting techniques were found to induce biases and/or distortions. For example, using a logarithmic transformation introduces a bias due to rejection of points with negative cation deficits and distortions caused by small differences at low Al^{3+} levels having a large effect on the transformed values. Non-linear techniques based on minimizing the sum of squares for deviations underestimate K° because points only slightly to the left of the steep portion of the line will have very large deviations.

As shown by eqs. 6 and 7, applying either the Gapon or Gaines-Thomas relationship would predict that Al^{3+} activity should be proportional to the 3/2 power of the Ca^{2+} activity. Plots of Al^{3+} against the divalent cations (not shown) are clearly non-linear. However, when plotted against the 3/2 power of Ca^{2+}, there is no indication of non-linearity (Figure 4); the inherent assumption of zero intercept is supported by the low value of $\underline{t}$ (Table 2). Similar results are obtained using either Mg^{2+} or (Ca^{2+}+ Mg^{2+}) to the 3/2 power as the independent variable. The reason for the outlier in Figure 4 is not known. It was not included in the regression, as it was judged that the remaining points are more likely to reflect the true slope. To avoid possible biases due loss of aluminum from solution resulting from pH rise associated with CO_2 degassing of solutions containing HCO_3^-,[7] this test was confined to solutions with ANC less than -50 μmol/L.

Using the slopes of the (Al^{3+}) versus $(Ca^{2+})^{3/2}$, $(Mg^{2+})^{3/2}$, and $(Ca^{2+}+Mg^{2+})^{3/2}$ relationships and the respective exchange fractions from Table I, the selectivity coefficients were calculated for both the Gaines-Thomas and the Gapon relationship (Table II). The log K_{gt} values ranged from 0.27 to 1.55, while log K_{gp} values ranged from 0.49 to 1.11. In both cases the highest values were for Al–Mg exchange, reflecting the fact that Mg^{2+} is more easily displaced from the exchange sites than is Ca^{2+}. This is also clearly reflected in the linear relationship between (Mg^{2+}) and (Ca^{2+}) in solution ($r^2 = 0.906$). The ratio of $(Mg^{2+})/(Ca^{2+})$ in solution is 2.49 times the ratio on the exchange sites.

These results confirm the (3/2) power relationship between (Al^{3+}) and the activity of the divalent ions, as would be predicted by either of the exchange equations. However, these data do not allow us to evaluate the effect on solution composition of changes in exchangeable cations that may occur over time. Therefore, no inferences can be drawn concerning which of the two exchange equations is more appropriate for modelling purposes.

These data may also be used to test the constancy of the lime potential [eq. 9]. Again, excluding solutions with ANC above -50 µmol/L and one observation with pH 5.67 and ANC -168 µmol/L, the remaining 38 observations have a mean lime potential of 2.71 with a standard deviation of 0.123. An expected lime potential may be calculated from eq. 10 using the exchange fractions from Table I, the previously determined value of 9.1 for log K°, and 0.55 for the log of the Gaines-Thomas Al–(Ca+Mg) selectivity coefficent (Table II). This expected value of 2.65 compares well with the mean of 2.71 found in the solutions. A completely independent estimate of the lime potential obtained from measuring pH, Ca^{2+}, and Mg^{2+} in three soil samples after equilibration with 0.01 $\underline{M}$ $CaCl_2$ gave a value of 2.65 with a standard deviation of 0.15. These results support the assumption of a constant value of the lime potential as used in several models.

These models also predict that acidic soil solutions may have positive ANC as a result of the interaction of exchange processes with above ambient CO_2 levels present in soil gases. When released to the surface environment where exchange processes are no longer important and CO_2 is near ambient, the pH of such waters may increase to 6.0 or above.[7,8] The theoretical relationship between ANC and pH for ambient CO_2 ($10^{-4.5}$ MPa) as calculated by simultaneous solution of eqs. 12 and 14 (neglecting OH^- and CO_3^{2-}) is shown in Figure 5. At negative ANC, observed pH is well above the values calculated in this manner. However, when aluminum buffering processes are taken into account, the agreement between predicted and observed pH is reasonable. These predicted values are approximately those that would be obtained by a simultaneous solution of eqs. 2, 14, and 15 for (H^+), (HCO_3^-), and (Al^{3+}) using a value of 9.1 for log K°. Actual calculations, however, also take into account the $Al(OH)^{2+}$ and $Al(OH)_2^+$ species.

Note that the leachates from a soil with pH 4.56 (1:1 soil:water) varied from pH 4.26 to 6.37. While changes in soil solution pH would be expected as solution strength varied from less than 50 $\mu mol_c/L$ to more than 2000 $\mu mol_c/L$, these changes would be unlikely to exceed a few tenths of a pH unit. The models based on the equations discussed here predict that at low solution strengths, positive ANC may develop in acidic soil solutions. Further, when degassed to ambient CO_2 levels, the pH of the leachates may rise to 6.0 or more.[7] This effect is evident in Figure 5. It should also be understood that the changes in soil solution pH, leachate pH, and ANC are most likely due to the solution strength (i.e., the "salt effect"). The effect is similar to the reduction observed when soil pH measured in a salt solution is compared to pH measured in water. It arises as a result of the interaction of the exchange and dissolution processes with the charge balance constraint. It is readily demonstrated by a model incorporating these interactions.[8] Unless there are significant changes in exchangeable base status, a similar effect would occur whether changes in solution strength resulted from inputs of HNO_3 or a neutral salt such as $Ca(NO_3)_2$. In the longer term, however, inputs of a neutral salt would raise the base saturation, while base saturation would be lowered by long term inputs of acid resulting in a net export of base cations. The pH rise that occurs when low ionic strength leachates from acid soils emerge into the lower CO_2 environment of the atmosphere has major ecological significance, because drainage waters from acid soils are often neutral or even alkaline.

CONCLUSIONS

In this acid soil, the seasonal changes in NO_3^- concentrations under red alders were accompanied by the depression of ANC to large negative values. This depression averaged about 36% of the NO_3^- increase, while the remaining 64% was balanced by base cations, confirming the importance of cation exchange processes in determining solution composition.

The negative ANC that develops in response to high NO_3^- levels is largely in the form of Al^{3+} rather than H^+. The aluminum buffering that occurs in the system is consistent with a log K° [eq. 2] value of about 9.1. The results confirm that the Al^{3+} activity remains proportional to the 3/2 power of the Ca^{2+} or $(Ca^{2+} + Mg^{2+})$ activity over a wide range of total solution concentrations. The results also confirmed that the $(Mg^{2+})/(Ca^{2+})$ ratio in solution remains constant. These results support the assumption of constant values for these parameters, which is inherent in several current models used to describe the effects of acid depositon applied to acid soils. Furthermore, these results support the related assumption that the lime potential, defined as $pH - (1/2)\log(Ca^{2+})$, remains constant even though pH varies in response to changes in solution concentration.

These models predict that in acid soils the solution ANC may change from positive to negative as solution concentration increases and that this change is reversible if the composition of the exchange phase remains reasonably constant. The results clearly indicate these effects and the substantial changes in leachate pH that accompany the changes from positive to negative solution ANC.

ACKNOWLEDGMENTS

Contribution by Colorado Agricultural Experiment Station, Project No. 6232. The research described in this article has been funded in part by the EPA/NCSU Acid Precipitation Program (a Cooperative Agreement) between the U.S. Environmental Protection Agency and North Carolina State University. It has not been subjected to EPA's peer review policy and, therefore, does not necessarily reflect the views of the Agency. No official endorsement should be inferred.

The author wishes to express his appreciation to D. W. Cole and H. Van Miegroet of the College of Forest Resources, University of Washington–Seattle, for providing the data used in the analyses reported here.

REFERENCES

1. J.O. Reuss, "Simulation of soil nutrient losses resulting from rainfall acidity, *Ecol. Modell.* 11:15 (1980).

2. N.H. Christopherson, H.M. Seip, and R.F. Wright, "A model for streamwater chemistry at Birkenes Norway," *Water Resour. Res.* 18:977 (1982).

3. C.W. Chen, S. Gherini, R.J.M. Hudson, and J.D. Dean, *The integrated lake watershed acidification study. Vol. 2. Model principles and procedures*, Rep. No. EA-3221, Electric Power Research Institute, Palo Alto, CA, 1983.

4. J.O. Reuss, "Implications of the Ca-Al exchange system for the effect of acid precipitation on soils," *J. Environ. Qual.* 12:591 (1983).

5. B.J. Cosby, R.F. Wright, G.M. Hornberger, and J.N. Galloway, "Modelling effects of acid deposition: Assessment of a lumped parameter model of soil and streamwater chemistry," *Water Resour. Res.* 21:51 (1985).

6. P.R. Bloom and D.F. Grigal, "Modelling soil response to acidic deposition in nonsulfate adsorbing soils," *J. Environ. Qual.* 12:489 (1985).

7. J.O. Reuss and D.W. Johnson, "Effects of soil processes on the acidification of water by acid deposition," *J. Environ. Qual.* 14:26 (1985).

8. J.O. Reuss and D.W. Johnson, *Acid deposition and the acidification of soils and waters*, Ecological Studies Series #59, Springer-Verlag, New York, 1986, 115pp.

9. H. Van Miegroet and D.W. Cole, "The impact of nitrification on soil acidification and cation leaching in a red alder ecosystem," *J. Environ. Qual.* 13:586 (1984).

10. D.W. Cole and S.P. Gessel, *Cedar River research—a program for studying pathways, rates and processes of elemental cycling in a forest ecosystem*, Institute of Forest Research, University of Washington, College of Forest Resources contribution 4. University of Washington, Seattle, WA, 1968.

11. D.W. Cole, "A system for measuring conductivity, acidity, and rate of flow in a forest soil," *Water Resour. Res.* 4:1127 (1968).

12. D.W. Johnson, D.W. Cole, F.W. Horng, H. Van Miegroet, and D.W. Todd, *Chemical characteristics of two forested Ultisols and two forested Inceptisols relevant to anion production and mobility*, Oak Ridge National Laboratory, Environ. Sci. Division Pub. 1670, Oak Ridge National Laboratory, Oak Ridge, TN, 1981.

13. W.L. Lindsay, *Chemical Equilibria in Soils*, Wiley Interscience, NY, 1979.

14. R.A. Griffin and J.J. Jurinak, "Estimation of activity coefficients from the electrical conductivity of natural aquatic systems and soils extracts," *Soil Sci.* 116:26 (1973).

15. W.L. Lindsay, Peech, and J.S. Clark, "Determination of aluminum ion activity in soil extracts," *Soil Sci. Soc. Am. Proc.* 23:266 (1959).

16. U.K. Misra, R.W. Blanchar, and W.J. Upchurch, "Aluminum concentration of soil extracts as a function of pH and ionic strength," *Soil Sci. Soc. Amer. Proc.* 38:897 (1974).

17. G.L. Gaines and H.C. Thomas, "Adsorption studies on clay minerals: A formulation of the thermodynamics of exchange adsorption," *J. Chem. Phys.* 21:714 (1953).

18. E.N. Gapon, "On the theory of exchange adsorption in soils," (In Russian, original not seen) *J. Gen. Chem. USSR.* 3:144 (1933).

19. R.K. Schofield and D.W. Taylor, "Measurements of the activities of bases in soils," *J. Soil Sci.* 6:137 (1955).

20. R.C. Turner and J.J. Clark, "Lime potential and degree of base saturation of soils," *Soil Sci.* 99:194 (1964).

21. F.E. Adams, and P.J. Hathcock, "Aluminum toxicity and calcium deficiency in acid subsoil horizons of two coastal plains soil series," *Soil Sci. Soc. Amer. J.* 48:1305 (1984).

22. D.W. Johnson, private communication, 1987.

Table I. Soil pH, exchangeable cations, and cation exchange capacity for the A horizon.

Exchangeable cations (NH_4Cl)	$cmol_c/kg$	Fraction of CEC
Ca^{2+}	1.03	.102
Mg^{2+}	0.16	.016
K^+	0.30	.030
Al (by difference)	8.56	.852
CEC (NH_4^+ by NaCl extract)	10.05	

pH (1:1 soil:water) = 4.56

Table II. Regression parameters for the regressions involving Al^{3+}, Ca^{2+}, and Mg^{2+} ion activities ($\mu mol_c/L$) in leachates from the 10 cm depth. Selectivity coefficients are calculated from the slope without intercept. The exchange fractions are shown in Table 1.

	Independent Variable (X)			
	$(Ca^{2+})^{3/2}$	$(Mg^{2+})^{3/2}$	$(Ca+Mg)^{3/2}$	(Ca^{2+})
Dependent Variable (Y)	(Al^{3+})	(Al^{3+})	(Al^{3+})	(Mg^{2+})
r^2	0.699	0.597	0.691	0.906
Intercept	0.69	7.55	1.91	-1.40
t for intercept	0.14	1.45	0.39	-0.63
Slope	0.0193	0.0621	0.0113	0.339
Slope w/o intercept	0.0195	0.0706	0.0117	0.391
log selectivity coefficients				
Gaines-Thomas	0.27	1.55	0.52	-
Gapon	0.49	1.11	0.51	-
Mg-Ca	-	-	-	0.396

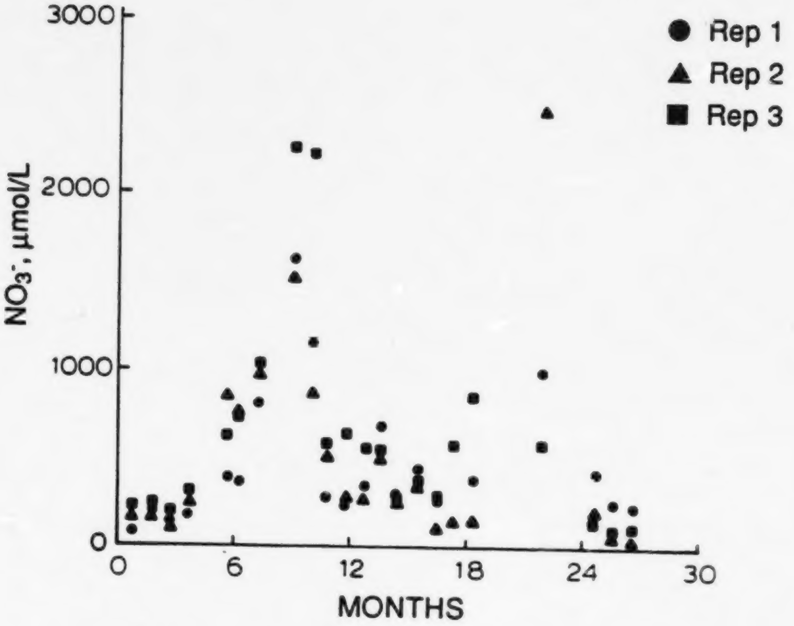

Figure 1. Variations in NO_3^- concentrations (µmol/L) in samples from three lysimeters placed near the base of the A horizon (10 cm) under red alders. Starting time is Jan. 1, 1982.

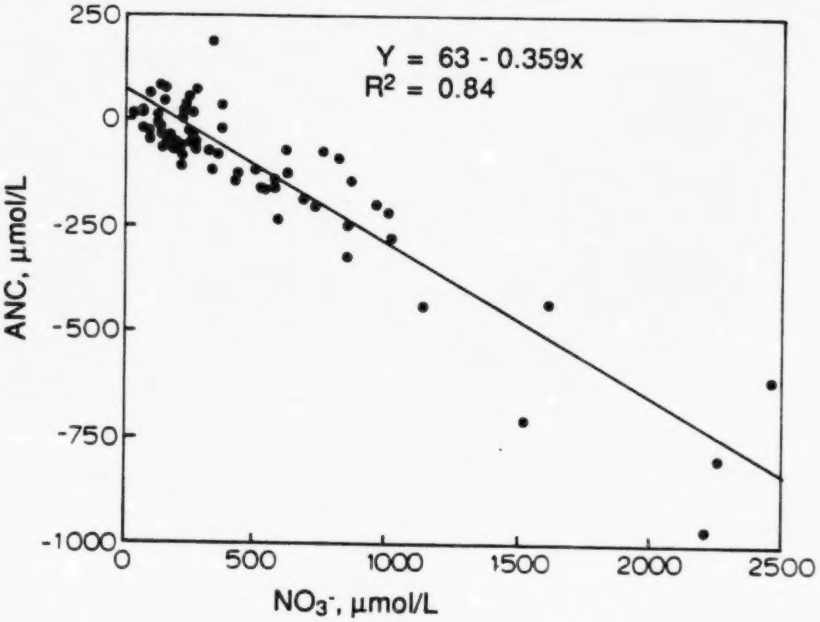

Figure 2. Acid neutralizing capacity (ANC) of leachates from the A horizon as a function of NO_3^- concentration.

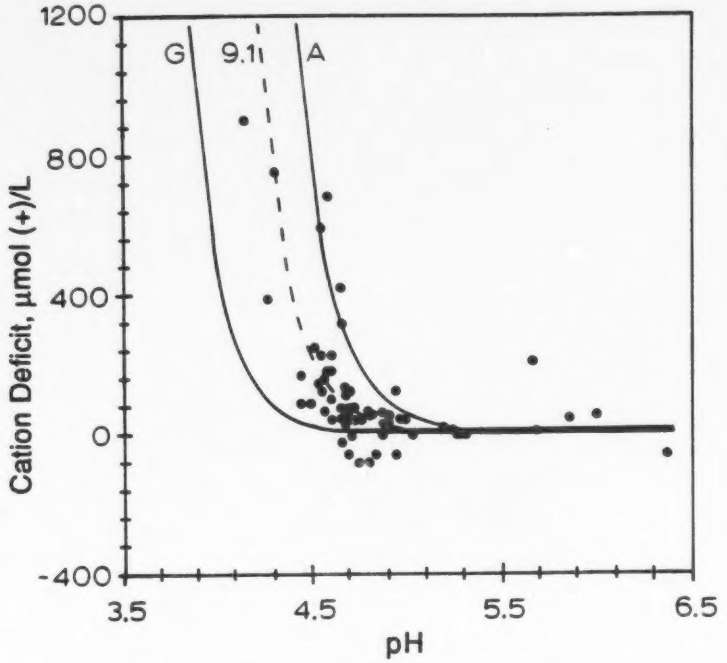

Figure 3. Observed cation deficits as a function of pH. Lines designated A and G represent the total charge associated with Al species for amorphous $Al(OH)_3$ (log K° = 9.66) and gibbsite (log K° = 8.04), respectively. The dashed line shows the total charge for log K° = 9.1.

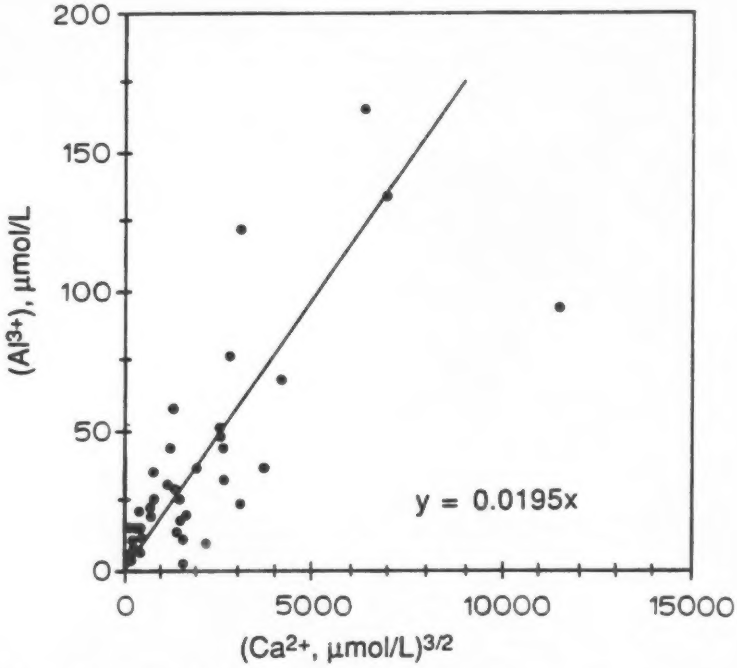

Figure 4. Al^{3+} activity in leachates from the A horizons as a function of the activity of Ca^{2+} to the 3/2 power.

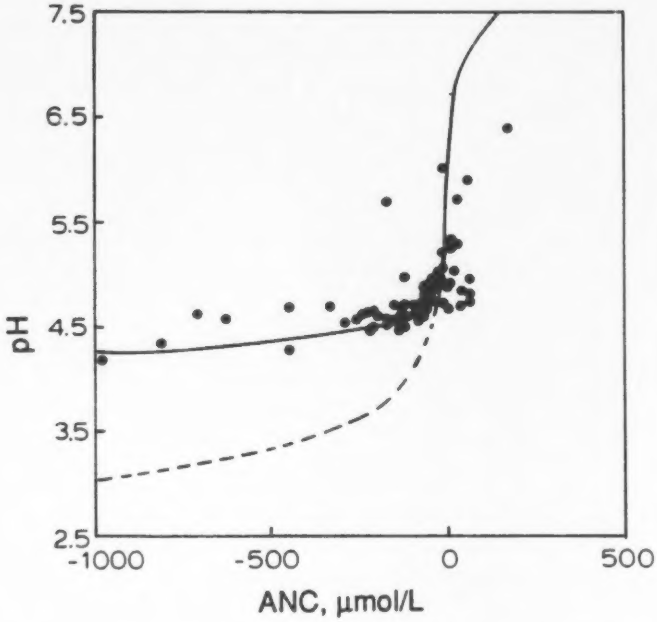

Figure 5. pH of leachates from the A horizon as a function of ANC. The theoretical relationships are shown for $10^{-4.5}$ MPa CO_2, without considering aluminum buffering (dotted line), and with aluminum buffering (solid line) assuming a log K° value of 9.1.

Sensitivity of Forest Soils in the Western U.S. to Acidic Deposition

Dan Binkley

Dept. of Forest and Wood Sciences
Colorado State University
Ft. Collins, CO 80523

INTRODUCTION

A central issue surrounding the effects of acidic deposition on ecosystems is the potential acidification of soils. Potential problems with acidified soils include impaired plant nutrition, toxicity of high concentrations of aluminum in soil solution, and acidification of aquatic ecosystems receiving water that drains from acidified soils. Some experts are skeptical about the potential of acidic deposition to acidify forest soils because forest soils are often acidic under unpolluted conditions.[1] However, many studies that have directly assessed long-term changes in forest soil chemistry have found rates of acidification that ranged up to 1 pH unit within 50 years.[2-12] Most of these studies have attributed the soil acidification to the effects of species or stand development over time, without a direct assessment of the role of acidic deposition. The implication is that natural forest processes, such as production of carbonic acid from root respiration and the accumulation of nutrient cations in biomass, can acidify some forest soils on a time scale of decades. If rates of acidic deposition are of a similar or greater magnitude, then deposition should be expected to accelerate acidification of sensitive soils.

No long-term data sets exist for the chemistry of forest soils in the western United States, making it difficult to assess the sensitivity of soils in the region to acidic deposition. In the southeastern United States, long-term data on soil acidification are also sparse, but indirect approaches such as analysis of computerized data bases and dynamic computer simulations have provided preliminary assessments.[13] Published estimates of the proportion of sensitive soils in that region range from less than 10% to greater than 50%. Computerized data sets in the western United States are not currently amenable to such a regional evaluation of western forest soils.[14] As an alternative, this paper summarizes the current state of an on-going effort to synthesize and interpret available evidence on the senstitivity of western forest soils being carried out as part of the Western Conifers Research Cooperative. After a brief overview of soil acidification, studies from California that have examined soil sensitivity to acidification are discussed. Similar studies are lacking for the rest of the region, but biogeochemical studies in Oregon and Washington provide helpful information. The final portion of the paper examines the processes that might serve to neutralize acidic deposition and discusses the implications for forest productivity.

SOIL ACIDIFICATION

Soil acidity is most commonly characterized by measurements of pH, but this is only one aspect of soil acidity. The concentration of H^+ maintained in solution depends on the equilibrium between the solution and the exchange complex of the soil. For many forest soils, the quantity of H^+ in soil solution at a single time is less than 1 $kmol_c$/ha, whereas the exchange complex may contain

Preceding page blank

much more than 1000 $kmol_c/ha$.[15] Changes in soil pH derive from changes in the exchange complex that influence the equilibrium with the solution. Four types of changes in the exchange complex are possible.[5,13] An increase in the size of the exchange complex, such as an accumulation of humic acids in soil organic matter, would tend to lower soil pH. A decrease in the proportion of the exchange complex occupied by alkali+alkaline earth cations (so-called base saturation) would lower soil pH. This represents increased protonation of the exchange complex, and increased protonation of a given acid results in a lower equilibrium pH of the solution. The third type of change in the exchange complex is a change in the selectivity of the exchange complex for H^+ (or Al^{3+}), which is equivalent to changing the pK_a of acids in a solution. A fourth way to change the equilibrium between the H^+ in solution and the exchange complex is to change the ionic strength of the soil solution. If a salt solution is added to a soil, the cation equilibrates with the exchangeable pool of cations, and the resultant suite of cations in solution may contain more H^+ than were present at lower ionic strengths.

Of these four factors that determine soil solution pH, acidic deposition is generally viewed to have a potential impact on the degree of dissociation of the exchange complex (alkali+alkaline earth saturation [AES], or base saturation), and on the ionic strength of the solution passing through the soil. The acidification of soils depends both on the quantity of H^+ deposited from the atmosphere (and other sources of H^+), and the processes that may neutralize the H^+. In forest soils, the major neutralizing mechanisms are mineral weathering, sulfate adsorption, and plant assimilation of nitrate and sulfate. The potential adverse effects of soil acidification could include increased concentrations of aluminum in solution, increased leaching losses of nutrient cations from the soil (with risk of impaired plant nutrition), and decreased solution alkalinity (with implications for reduced buffering of aquatic ecosystems).

CALIFORNIA

A wide range of studies of soil sensitivity to acidification has been conducted in California, funded primarily by the California Air Resources Board, the electric utilities, and by the National Park Service. Several of these have included alpine systems as well as forests.

In one of the first studies, McColl[16] performed leaching experiments on 17 forest soils primarily from granitic parent materials in Shasta, Fresno, and Siskiyou counties. Surface soils from each pedon were leached with solutions ranging in pH from 5.5 to 2.0 in a mechanical vacuum extractor for 2 h. The leachates were collected and analyzed for a variety of properties. He found that ability of the soils to buffer added H^+ related well to the concentration of alkali+alkaline earth cations on the exchange complex. Soils with less than about 70 $mmol_c/kg$ of alkali+alkaline earth cations appeared to be very sensitive to acidification. In general, the sensitivity of soils tended to increase with elevation.

Weintraub[17] assessed the sensitivity of two alpine watersheds (Eastern Brook Lake and Emerald Lake) in the Sierra Nevada to acidification. Her approach involved mineralogic assays, estimates of weathering rates based on changes in mineralogic composition, and laboratory acidification experiments. She concluded that these watersheds would be very sensitive to acidification, due to the shallow depth of soils (where present) and low weathering rates. Assuming 10,000 years of weathering in the present landscapes, the estimates of weathering rates represented an annual consumption of only about 0.1 kmol H^+/ha, which is probably similar to the current rates of H^+ deposition in the Sierra. The response of soil columns to acid additions in the laboratory demonstrated that the rate of weathering might increase if H^+ loading increased, but this increase was judged to be small relative to observations from similar experiments on other soils.

Wyels[18] developed titration curves for 24 Sierran soils and used these in conjunction with a soil sensitivity scheme to assign the soils to three sensitivity classes. Six categories of properties were current pH, saturation of the exchange complex with alkali+alkaline earth cations, cation exchange capacity, organic carbon, soil depth, and parent material. Some properties, such as pH, were weighted more heavily in her rating system than others, such as soil depth. This scheme led to classifying 6 soils as very sensitive to acidic deposition, 15 soils as sensitive, and 3 soils as unsensitive. Of the soils she rated as very senstitve, 3 of them had less than 70 $mmol_c$/kg of alkali+alkaline earth cations.

Huntington and Akeson[19] developed a soil resource inventory for the central part of Sequoia National Park. Although no estimates of sensitivity to acidification were made, chemical analyses of some representative pedons provided data on pH and exchangeable cations. The variation among soils within the same family was surprisingly high. For example, the top 25 cm of one coarse-loamy, mixed, mesic Xeric Haplohumult had over 150 $mmol_c$/kg of alkali+alkaline earth cations and a pH of 6.7, whereas another of the same family with a pH of 6.1 had less than 70 $mmol_c$/kg of these cations. No trend in the concentration of alkali+alkaline earth cations was apparent across soil orders (Entisols, Inceptisols, Alfisols, and Mollisols); only soils with a cryic temperature regime (high elevation) had consistently low concentrations of these exchangeable cations.

Intensive characterization of aspects of biogeochemical cycles at the Emerald Lake Watershed in the Sierra Nevada[20] showed that the intermittent, shallow soils of this alpine watershed are very low in exchangeable alkali+alkaline earth cations (<15 $mmol_c$/kg). Laboratory assays of potential weathering rates produced estimates that were an order of magnitude higher than for some soils in the northeastern United States, but this estimate is difficult to evaluate without information on the mineralogic composition of the soils at Emerald Lake.

The most thorough study in the region was performed by Liu,[21] using 12 pedons from 4 watersheds (including Eastern Brook Lake and Emerald Lake). His analyses included the basic soil chemistry parameters, titration curves, analyses of the cations removed during the H^+ titrations, and point of zero net charge (PZNC, the pH at which anion exchange capacity equals cation exchange capacity). He concluded that the difference between the current soil pH and the PZNC could be used to indicate the primary process that currently regulates pH. Specifically, if (pH - PZNC) was greater than 2.2 but less than 3.1, cation exchange reactions appeared to provide most of the buffering of added H^+. If the difference was between 1.3 and 2.4, both aluminum dissolution and cation exchange were the major buffering processes. Weathering of aluminosilicate minerals was indicated if the difference was below 0.9. Liu also developed a simple acidification model and estimated that pedons from the East Brook Lake watershed were very well buffered with respect to 100 years of acidic deposition at a relatively low rate of 0.18 kmol H^+/ha annually. The buffering in the most sensitive soils arose from dissolution of aluminum minerals. This process results in decreased solution alkalinity and increased export of aluminum to aquatic systems. All soils studied by Liu had less than 20 $mmol_c$/kg of exchangeable alkali+alkaline earth cations.

Estimates of ecosystem H^+ budgets are not available for any of the intensively studied sites in California, so it is difficult to evaluate the likely impacts of current (or future) rates of acidic deposition relative to natural ecosystem processes. However, two watersheds in the Sierra Nevada have been examined with the ILWAS model,[22] and some implications for likely changes in soil acidity are evident.

The ILWAS model was calibrated for the Blue Lake Watershed in a joint project funded by Pacific Gas and Electric Company.[23] The small watershed is underlain by metasedimentary and granodioritic bedrock, and soil covers only about 20% of the watershed. The vegetation is dominated by ponderosa and Jeffrey pines (*Pinus ponderosa* and *P. jeffreyi*). The lake is typical of moderate-to-high elevation lakes in the Sierra Nevada, with moderately poorly buffered water (30–70 μmol_c/L ANC) of near-neutral pH. After calibrating the ILWAS model with intensively collected field data, 5 acidification scenarios were simulated for 21 years: base case (current deposition), doubled rate of sulfuric acid or nitric acid deposition, and halved rate of deposition for each acid. The current rate of sulfate deposition led to no change in pH in 21 years, whereas doubling the rate decreased lake water pH by 0.05 units. Most of the deposited H^+ was buffered in the soil by the exchange complex, and much of the sulfate that reached the lake was consumed in redox reactions. The increased rate of nitric acid deposition actually led to an increase in lake alkalinity and pH, due to assimilation or reduction of the nitrate. Decreasing the deposition rate of sulfate or nitrate had no effect on lake pH. Although these simulations did not assess soil acidification directly, a lack of change in the poorly buffered lake suggests that no significant acidification of the soil would have occured.

The application of the ILWAS model to Eastern Brook Lake in the central Sierra Nevada did not include intensive calibration with field data, so the simulation projections are tentative.[24] Eastern Brook Lake has greater alkalinity (about 70–250 μmol_c/L ANC) than Blue Lake, and 10 year simulations with a five-fold increase in sulfate deposition lowered lake pH by only 0.04 units.

Collectively, these California studies indicate that some Sierran soils may be sensitive to acidification if rates of deposition increased to levels found in parts of the eastern United States and Europe.

OREGON AND WASHINGTON

In comparison with California, the sensitivity of soil to acidification has received very little little attention in other western states. The best information related to soil acidification in forests in the western United States comes from ecosystems where N-fixing alders greatly accelerate ecosystem N cycling and nitrate leaching.[12] These studies indicate that when acidification occurs under the influence of alder, it results in part from the input of H^+ from nitrification (coupled with nitrate leaching) of perhaps 1–3 kmol H^+/ha annually and from the accumulation of strongly acidic organic matter. Where acidification has not occurred with alders, there seems to have been minimal nitrification and nitrate leaching. In combination, these studies indicate that some soils in the Pacific Northwest would be acidified (with decreases in soil pH, exchangeable alkali+alkaline earth cations, and solution alkalinity, coupled with increases in aluminum concentrations in soil solutions) if the rates of acidic deposition resulted in net inputs of H^+ on the order of 1 to 3 kmol H^+/ha annually. The current rate of acidic deposition in the Pacific Northwest U.S. is only about 0.05 to 0.20 kmol H^+/ha annually,[25] so the present effects of acidic deposition on soil chemistry should be much less pronounced than the effects of alder.

Detailed H^+ budget information is available for three conifer forests in Oregon and Washington, and two of these are paired with adjacent alder/conifer ecosystems. In Sweden, Sollins[26] developed the first H^+ budget for a forest ecosystem, and later Sollins et al.[27] developed the first H^+ budget for a forest in the western United States. In a 450-year-old Douglas-fir forest in the Cascade Mountains of Oregon, precipitation contributed only about 0.1 kmol H^+/ha annually. The accumulation of nutrient cations in biomass generated about 0.6 kmol H^+/ha, and the production and dissociation of carbonic acid in the soil generated a remarkable 5.4 kmol H^+/ha annually. Assuming no net ecosystem acidification, they calculated that the rate of H^+ consumption in weathering in this Typic Dystrochrept was about 7.1 $kmol_c$/ha annually. This rate is very high, but given that the output of alkali+alkaline earth cations in streamwater exceeded 4 $kmol_c$/ha, it appears feasible.

Near the coast of Oregon, Binkley and Sollins[4] examined components of H^+ budgets for adjacent 55-year-old mixed conifer and alder/conifer ecosystems on a Typic Dystrandept. Precipitation contributed less than 0.1 kmol H^+/ha annually, compared with a rate of cation accumulation in biomass of about 0.7 $kmol_c$/ha annually in both stands. The formation and dissociation of carbonic acid contributed about 0.9 $kmol_c$/ha of H^+ in both ecosystems, whereas the high rate of nitrate leaching contributed an additional 2.0 $kmol_c$/ha of H^+ to the alder/conifer ecosystem.

Binkley and Sollins[4] also examined components of H^+ budgets for a pair of 55-year-old Douglas-fir and alder/Douglas-fir ecosystems on a poorer soil (Andic Haplumbrept). Precipitation again contributed less than 0.1 kmol/ha of H^+, and cation accumulation in biomass (aboveground biomass plus forest floor) contributed 0.3 and 0.6 $kmol_c$/ha annually in the Douglas-fir and the mixed ecosystems, respectively. Nitrate leaching was negligible in both ecosystems, but the formation and dissociation of carbonic acid was greater in the mixed ecosystem (1.0 $kmol_c$/ha annually) than in the Douglas-fir ecosystem (0.4 $kmol_c$/ha).

D. Cole and associates at the University of Washington are developing information on H^+ budgets for three forests as part of the Integrated Forest Study of the Electric Power Research Institute and Oak Ridge National Laboratory. Information on these ecosystems should be published within the next two years.

These H^+ budgets for Pacific Northwest forests indicate that within-ecosystem biogeochemical processes contribute far greater inputs of H^+ than is received from atmospheric deposition. The acidification that occurred under the influence of alder appears to have resulted in large part from the 1 to 3 $kmol_c$/ha annual input of H^+ from nitrification coupled with nitrate leaching. These studies, along with others discussed by Van Miegroet et al.[12] indicate that the biogeochemical effects of alders can lead to substantial changes in soil chemistry. If rates of acidic deposition in this region rose to the level found in parts of the eastern United States and Europe, similar changes in soil chemistry might occur in the absence of alder.

OTHER STATES

Very little work has examined the sensitivity of soils to acidification in other western states. A variety of projects examining soil development in primary succession sequences have documented rapid delines in pH in both glacial retreat seres[28-30] and riverside terraces.[31] Colonization by plants leads to rapid acidification (0.5–2.0 units within 100 years) of the soils. At the other environmental extreme, plantations of *Eucalyptus* and nitrogen-fixing *Albizia* trees (alone and in combination) lowered the pH of a Typic Hydrandept soil in Hawaii from 5.9 to 5.2–5.5 in just 48 months.[32]

The USDA Forest Service is conducting an intensive study on acidification of a high-elevation watershed in southeastern Wyoming. The Glacier lakes Experimental Watershed ranges from 3300 m to 3660 m in a glaciated basin with fractured quartzite bedrock. Forests occupy a small portion of the watershed, and are dominated by Engelmann spruce (*Picea engelmannii*) and subalpine fir (*Abies lasiocarpa*). The forested soils are Cryoboralfs, with $\text{pH} < 5$ and base saturation of <30%.[33] Direct assessments of soil sensitivity to acidification have not been done, but the current rate of acidic deposition in the region is probably too low to have a large effect.

The National Park Service has a major project in the Loch Vale Watershed in Rocky Mountain National Park. The watershed ranges from 3100 m to 4000 m in elevation, with bedrock composed of biotite gneiss and granite.[34,35] Soils cover only about 6% of the watershed, and the forested (spruce and fir) soils are predominantly Cryoboralfs with very low pH (<4) and low base saturation (<35%). Mast[34] estimated the rate of denudation of cations from the watershed to be about 0.6 kmol_c/ha, which is probably a good estimate of the rate of consumption of H^+ in weathering. About 40% of the weathering release of cations comes from traces of calcite (in hydrothermally altered fraction of the bedrock).[34] Although the current rate of weathering is low, it exceeds the current rate of acidic deposition.

WEATHERING

Weathering of carbonate and silicate minerals consumes H^+ to replace bonds with silica formerly occupied by aluminum, calcium, magnesium, potassium, sodium, and other ions. The precise quantity of H^+ consumed depends upon the rate of weathering and the specific stoichiometry of each reaction, including any subsequent hydrolysis associated with aluminum ions. Most reports of weathering rates in forest soils around the world fall below 2 kmol_c/ha annually.[36,10] (Very few estimates are available for western forests of the consumption of H^+ in mineral weathering.) For the five studies available in this region, the range spans from 0.1 kmol H^+/ha annually for an alpine granitic parent material in the Sierra Nevada to well over 5 kmol H^+/ha for easily weathered volcanic breccia and carbonates (Table I). In the absence of adequate data, the only reasonable inference at a regional scale is that some forest soils probably have very little capacity to buffer H^+ inputs through weathering, whereas others have large buffer capacities. If rates of acidic deposition increased in the region, the weathering capacities of the soils would be a high-priority topic.

SULFATE ADSORPTION

The adsorption of sulfate by iron and aluminum oxides can displace OH^- which then consumes H^+ to form water. Later desorption may regenerate the acidity. For these reasons, the geochemical adsorption of sulfate (and the reversibility of the reaction) are important components of soil acidification. Sulfate immobilization by microbes also involves consumption of acidity. Unfortunately, both of these processes are very difficult to assess under ambient conditions, and interpretations relative to changes in rates of sulfate deposition are problematic. The quantity of information on sulfate adsorption in western conifer forests is as sparse as the information on weathering. Harrison et al.[37] presents data on sulfate adsorption for the three Washington sites involved in the Integrated Forest Study of the Electric Power Research Institute and Oak Ridge National Laboratory. All sites adsorbed added sulfate from solution, and part of the adsorbed sulfate entered pools that were not readily extractable, implying that the adsorption was at least partially irreversible. The Emerald Lakes study site in the Sierra Nevada also appeared to have some sulfate adsorption capability.[20] Too little information is available to allow regional inferences to be made.

FOREST NUTRITION

Acidic deposition interacts with forest nutrition in three major ways. First, N and S are essential plant nutrients, and where the supply rates of these nutrients limits forest growth, the deposition of nitric and sulfuric acids would probably stimulate growth. Indeed, assimilation of nitrate or sulfate involves neutalization of H^+.[2] Second, the increased ionic strength of soil solutions could lead to accelerated leaching losses of essential alkali and alkaline-earth cations. Finally, elevated solution concentrations of aluminum could be toxic to root or microbes, or could interfere with the uptake and use of calcium and magnesium.

The current availability of nitrogen probably limits the growth of most forests in the region,[38-40] and increases in the rate of nitric acid deposition would probably increase growth. Sulfur limitations are less common, but do appear important in regulating the growth response of Douglas-fir to nitrogen fertilization in some cases.[41] Little is known of the degree to which the availability of nutrient cations limits forest growth in the west. At least some lodgepole pine forests appear to be limited by K^+ availability,[40] and presumably these forests might be at risk from any reduction in K^+ supply resulting from acidic deposition. In the cases where the exchangeable pools of calcium, magnesium, and potassium have been reduced in the presence of alders, there is no indication (based on foliage analysis) that the supply rates of these nutrients have become limiting.

No cases of aluminum toxicity to trees have been demonstrated under normal conditions in forests in the region, but this might reflect an absence of sufficient information rather than an absence of a problem. Although a variety of excellent seedling studies have examined threshold levels of aluminum concentrations that affect seedling development for species from the eastern United States,[42-47] similar studies are lacking for the west. Some research from Europe has suggested that the critical level of Ca:Al (molar ratio) is about 1:1; I am not aware of any soil solution data for the Western U.S. that approaches this level.

SUMMARY AND RESEARCH NEEDS

The current rates of acidic deposition are low in the western United States compared with the east and with Europe.[25] The current rates of deposition probably pose little risk to conifer forests in the region. A variety of lines of evidence suggest that the chemistry of forest soils in the region may be sensitive to changes in biogeochemical cycles. If acidic deposition rates increased substantially, the chemistry of many forested soils in the region would probably change significantly. The implications of such changes aren't clear, however, because information is scanty on the degree to which tree growth is limited by the availability of cation nutrients or the concentrations of aluminum in soil solutions. We are continuing this assessment as part of the Western Conifers Research Cooperative by parameterizing computer simulation models with data sets representative of major forest types in the region and by simulating responses to changes in atmospheric deposition. Our tentative suggestions for future research include experimental manipulations of plots to validate model predictions and establishment of long-term plots (with and without manipulations) to monitor changes in soils that appear to be especially sensitive.

ACKNOWLEDGMENTS

I thank K. Tonnessen for providing a wealth of hard-to-find information and R. Goldstein and C. Chen and associates for providing information on the ILWAS projects. Three anonymous reviewers provided remarkably helpful comments on an earlier draft. This project was funded primarily through Kilkelly Environmental Associates as part of the Western Conifers Research Cooperative, within the joint U.S. EPA and USDA Forest Service Forest Response Program. Support for portions of this work was provided by NSF Grant #BSR-8416768 and by the the Integrated Forest Study of the Electric Power Research Institute and Oak Ridge National Laboratory. This paper has not been subjected to policy review and should not be construed to represent the policies of either the EPA or the Forest Service.

REFERENCES

1. M.A. Tabatabai, "Physicochemical fate of sulfate in soils," *J. Amer. Phys. Chem. Assoc.* 37:34 (1985).

2. M. Anderson, "The effects of forest plantations on some lowland soils. I. A second sampling of nutrient stocks," *Forestry* 60:69 (1987).

3. D. Binkley and D. Valentine, "Fifty-year effects on biogeochemistry in replicated plantations of green ash, white pine, and Norway spruce," in review.

4. D. Binkley and P. Sollins,"Biogeochemistry of adjacent conifer and alder/conifer ecosystems," in review.

5. D. Binkley, D. Valentine, C. Wells, and U. Valentine, "An empirical analysis of factors contributing to 20-year decline in soil pH in an old-field plantation of loblolly pine," *Biogeochemistry* 10:in press (1989).

6. D. Brand, P. Kehoe, and M. Connors, "Coniferous afforestation leads to soil acidification in central Ontario," *Can. J. of For. Res.* 16:1389 (1986).

7. U. Falkengren-Grerup, "Long-term changes in pH of forest soils in Southern Sweden," *Environ. Poll.* 43:79 (1987).

8. D.W. Johnson, G.S. Henderson, and D.E. Todd, "Changes in nutrient distribution in forests and soils of Walker Branch Watershed, Tennessee, over an eleven-year period," *Biogeochemistry*, in press (1987).

9. A.E. Johnston, K.W.T. Goulding, and P.R. Poulton, "Soil acidification during more than 100 years under permanent grassland and woodland at Rothamstead," *Soil Use Manage.* 2:3 (1986).

10. S.I. Nilsson, "Critical deposition limits for forest soils," in *Critical Loads for Nitrogen and Sulfur: Report from a Nordic Working Group*, J. Nilsson, Ed., Nordisk Ministerrad Miljo Rapport 1986:11, p. 37.

11. C.O. Tamm and L. Hallbacken, "Changes in soil pH over a 50-year period under different forest canopies in SW Sweden," *Water, Air, Soil Poll.* 31:337 (1986).

12. H. Van Miegroet, D. Cole, D. Binkley, and P. Sollins, "The effect of nitrogen accumulation and nitrification on soil chemical properties in alder forests," 82nd Annual AWMA meetings, Anaheim, CA, 1989.

13. D. Binkley, C. Driscoll, H. Allen, P. Schoeneberger, and D. McAvoy, "Acidic Deposition and Forest Soils: Context and Case Studies in the Southeastern United States," *Ecological Studies* #72, Springer-Verlag, New York, 1989, p. 150.

14. R. Turner, personal communication.

15. D. Binkley and D. Richter, "Nutrient cycles and H^+ budgets of forest ecosystems," *Adv. Ecol. Res.* 16:1 (1987).

16. J. McColl, "Effects of acid rain on plants and soils in California," Final Report submitted to California Air Resources Board, Contract #A8-136-31, 1981, p. 111.

17. J. Weintraub, "An assessment of the susceptibility of two alpine watersheds to surface water acidification: Sierra Nevada, California," MS thesis, Dept. Geology, Indiana University, 1986, p. 186.

18. W. Wyels, "The buffering capabilities of Sierra Nevadan soils exposed to simulated acid precipitation," MS thesis, University of California, Davis, CA, 1986, p. 188.

19. G. Huntington and M. Akeson, *Pedologic investigations in support of acid rain studies, Sequoia National Park, California; Soil resource inventory of Sequoia National Park, Central Part.*, National Park Service, 1987.

20. L. Lund, A. Brown, M. Lueking, S. Nodvin, A. Page, and G. Sposito, "Soil processes at Emerald Lake Watershed," Final Report, submitted to California Air Resources Board, Contract #A3-105-32, 1987, p. 114.

21. W. Liu, "The sensitivity of selected soils from the Sierra Nevada to acidic deposition," Ph.D. dissertation, University of California, Riverside, 1988, p. 102.

22. S. Gherini, C. Chen, L. Mok, R. Goldstein, R. Hudson, and G. Davis, "The ILWAS model: formulation and application," *Water, Air and Soil Pollution* 26:425 (1985).

23. D. Gilbert, T. Sagraves, M. Lang, R. Munson, and S. Gherini, *R&D Lake Acidification Assessment Project: Blue Lake Acidification Study*, Pacific Gas and Electric Company, Dept. of Research and Development, San Ramon, CA, 1989.

24. C. W. Chen and L.E. Gomez, "Application of the ILWAS Model to Eastern Brook Lake-Watershed in the Sierra Nevada Mountains," Prepared for Southern California Edison Co., and Electric Power Research Institute, by Systech Engineering, Lafayette, CA, 1988.

25. M. Böhm, "Regional characterization of air quality across the coniferous forests of the western United States," Proceedings of the 82nd Annual AWMA meetings, Anaheim, CA, 1989.

26. P. Sollins, *Preliminary annual element budgets for the 120-year pine stand at Jadraas.* Memo 761221, Swedish Coniferous Forest Project, Uppsala, 1976.

27. P. Sollins, C. Grier, F. McCorison, K. Cromack, Jr., R. Fogel, and R. Fredriksen, "The internal element cycles of an old-growth Douglas-fir ecosystem in western Oregon," *Ecol. Monogr.* 50:261 (1980).

28. R. Crocker and B. Dickson, "Soil development in recessional moraines of the Herbert and Mendenhall Glaciers, southeastern Alaska," *J. Ecol.* 45:169 (1957).

29. R. Crocker and J. Major, "Soil development in relation to vegetation and surface age at Glacier Bay, Alaska," *J. Ecol.* 43:427 (1955).

30. F. Ugolini, "Soil development and alder invasion in a recently deglaciated area of Glacier Bay, Alaska," In *Biology of Alder*, J. Trappe, J. Franklin, R. Tarrant, and G. Hansen, Eds., USDA Forest Service, Portland, OR, 1968, p. 115.

31. K. Van Cleve, personal communication.

32. D.S. DeBell, C.D. Whitesell, and T.H. Schubert, "Using N_2-fixing *Albizia* to increase growth of *Eucalyptus* plantations in Hawaii," *For. Sci.* 35:64 (1989).

33. D. Fox, R. Hopper, and P. Walthall, personal communication.

34. M.A. Mast, "A laboratory and field study of chemical weathering with special reference to acid deposition," PhD thesis, University of Wyoming, Laramie, 1989, 176pp.

35. P.M. Walthall, "Acidic deposition and the soil environment of Loch Vale Watershed in Rocky Mountain National Park," PhD thesis, Colorado State University, Ft. Collins, 1985, 148pp.

36. J.P. Kimmins, D. Binkley, L. Chatarpaul, and J. DeCatanzaro, "Biogeochemistry of temperate forest ecosystems: literature on inventories and dynamics of biomass and nutrients," Information Report PI-X-47 E/F, Canadian Forestry Service, Petawawa, Ontario, 1985, p. 227.

37. R. Harrison, D. Johnson, and D. Todd, "Forest soil sulfur pools and SO_4^{2-} adsorption and desorption capacity following elevated inputs of SO_4^{2-}," 82nd Annual AWMA meetings, Anaheim, CA, 1989.

38. R. Miller, P. Barker, C. Peterson, and S. Webster, "Using nitrogen fertilizers in management of Coast Douglas-fir. I. Regional trends of response," in *Douglas-fir: Stand Management for the Future*, C. Oliver, D. Hanley, and J. Johnson, Eds., Contribution #55, College of Forest Resources, University of Washington, Seattle, 1986, p. 290.

39. R.F. Powers, "Forest fertilization in California," in *I.U.F.R.O. Symposium on Forest Site and Continuous Productivity*, R. Ballard and S. Gessel, Eds., USDA Forest Service General Technical Report PNW-163, Portland, OR, 1983, p. 388.

40. G.F. Weetman, "Nutrition and fertilization of lodgepole pine," in *Proceedings--Future Forests of the Mountain West: a Stand Culture Symposium*, W. Schmidt, compiler, USDA General Technical Report INT-243, 1988, p. 231.

41. J. Blake, S. Webster, and S. Gessel, "Soil sulfate-sulfur and growth responses of nitrogen-fertilized Douglas-fir to sulfur," *Soil Sci. Soc. Amer. J.* 52:1141 (1988).

42. T.C. Hutchinson, L. Bozic, and G. Munoz-Vega, "Responses of five species of conifer seedlings to aluminum stress," *Water, Air, Soil Poll.* 31:283 (1986).

43. J.K. Kelly, J.D. Joslin, F.C. Thornton, M. Schaedle, and D. Raynal, "A comparison of the response of red spruce seedlings to Al in soil and in solution culture," *Agr. Abstr.* 1987:260 (1987).

44. F.C. Thornton, M. Schaedle, and D.J. Raynal, "Effects of aluminum on growth, development, and nutrient composition of honeylocust (*Gleditsia triacanthos* L.) seedlings," *Tree Phys.* 2:307 (1986).

45. F.C. Thornton, M. Schaedle, and D.J. Raynal, "Effect of aluminum on the growth of sugar maple in solution culture," *Can. J. For. Res.* 16:892 (1986).

46. F.C. Thornton, M. Schaedle, and D.J. Raynal, "Effects of aluminum on red spruce seedlings in solution culture," *Environ. Exper. Bot.* in press, 1987.

47. J.D. Joslin, "Predicting the response of red spruce seedlings to soil Al," *Agr. Abstr.* 1987:260 (1987).

48. D. Marchand, "Rates and modes of denudation, White Mountains, eastern California," *Amer. J. Sci.* 270:109 (1971).

49. J. L. Clayton, "An estimate of plagioclase weathering rate in the Idaho Batholith based upon geochemical transport rates," in *Rates of Chemical Weathering of Rocks and Minerals*, S. Colman and D. Dethier, Eds., Academic Press, New York, 1986, p. 453.

Table I. Weathering estimates (kmol H^+/ha consumed annually) for Western U.S. ecosystems.

Location	Vegetation	Parent Material	Rate	Reference
White Mountains, California	Mixed conifer	Dolomite	8.8	48
White Mountains, California	Mixed conifer	Adamellite	1.3	48
Cascades, Oregon,	Douglas-fir	Volcanic breccia	7.1	27
Sierra Nevada, California	Alpine	Granodiorite	0.1	17
Idaho Batholith	Mixed conifer	Plagioclase	0.7	49
Rocky Mountains, Colorado	Spruce, Fir	Gneiss, Granite	0.6	34

Index of Authors

Arbaugh, M.J. 293
Basabe, F.A. 33
Bicknell, S. 147
Binkley, D. 515, 561
Borys, R.D. 105
Böhm, M. 73, 221
Braus, J. 171
Burkman, W.G. 379
Bytnerowicz, A. 455
Cahill, T.A. 207
Caine, J. 171
Chang, W.L. 33
Cline, S.P. 379
Cole, D. W. 515
Curtiss, B. 351
Daly, C. 247
Duriscoe, D.M. 261, 411
Edmonds, R.L. 33
Elvidge, C.D. 337
Ewell, D.M. 411
Fox, C.A. 337
Garcia, J.A. 3
Geron, C.D. 379
Gomez, A.P. 309
Graw, R. 105
Graybill, D.A. 395
Greitner, C.S. 493
Grulke, N.E. 429
Hahn, S. 429
Harrison, R.B. 529
Hazlett, D.L. 177
Henderson, S. 325
Hendricks, C. 469
Hogsett, W.E. 469
Johnson, D.W. 529
Kopcewicz, B. 15
Krupa, S.V. 193
Larson, T.V. 33
Legge, A.H. 193
Martens, S.N. 351
Mazzu, L.C. 411
McBride, J.R. 309
Miller, D.F. 105
Miller, P.R. 309, 429
Muir, P.S. 73
Nagamoto, C. 15
Noss, R.F. 325
Olson, R.K. 325
Parungo, F. 15
Patterson, M.T. 419
Pedersen, B.S. 207, 279
Peterson, D.C. 247
Peterson, D.L. 293
Reuss, J.O. 547
Richards, L.W. 51
Robinson, L.J. 293
Rose, M.R. 395
Rossi, D. 469
Rundel, P.W. 419
Schilling, S.L. 309
Schoettle, A.W. 443
Sievering, H.J. 171
Snider, J.R. 3
Sollins, P. 515
Stolte, K.W. 261
Takemoto, B.K. 455
Tingey, D.T. 469
Todd, D.E. 529
Unger, C.D. 137
Ustin, S.L. 351
Van Miegroet, H. 515
Vanderbilt, V.C. 351
Vogelmann, J.E. 337
Vong, R.J. 117
Wilborn, R.D. 429
Winner, W.E. 493
Zeller, K.F. 177

Preceding page blank

Index of Subjects

Page numbers indicate the first page of each paper or papers in which the accompanying subject is discussed.

A
Abies concolor, 395
Acer saccharum, 379
acid neutralizing capacity, 547
acidification, 515, 529, 561
aerosol formation, 51
airborne sampling, 51
Alaska, 73
Alberta, 193
Alnus, 493, 515, 547, 561
aluminum, 515, 547
ammonia, 193
ammonium, 51
anion mobility, 529
Arizona, 221, 395

B
biological diversity, 325
boundary layer, 177
British Columbia, 117

C
California, 51, 73, 147, 207, 221, 247, 261, 279, 293, 309, 325, 351, 379, 411, 419, 429, 455, 561
Canada, 193
canopy exchange, 171
carbon allocation, 493
carbonyl compounds, 51
carboxylation efficiency, 419
Cascade Mountains, 33, 73, 529
cation exchange, 547
cation leaching, 529
chlorophyll, 337, 351, 411
climate change, 325
cloud, 3, 15, 33, 51, 73, 105, 147, 221
CO_2, 193
Colorado, 15, 73, 105, 171, 177, 221, 443

D
defoliation, 443
delta ^{13}C, 493
dendrochronology, 293, 395
deposition velocity, 177
dry deposition, 105, 171, 177, 193, 455

E
eddy correlation, 177
Elk Mountain Observatory, 3
Emerald Lake, 207, 561
emission, pollutants, 137, 221
extractable aluminum, 529

F
fog, 33, 73, 147
fog, effects, 469
foliage distribution, 443
foliage longevity, 443
foliage morphology, 411
foliar injury, 261, 279, 293, 309, 337, 351, 379, 395, 411, 419, 455, 469
foliar leaching, 171
foliar nutrients, 443
foliar washing, 171
fragmentation, forest, 325
Fortress Mountain, 193
Frankia, 493
Front Range, 15, 73, 171

G
growth, tree, pollutant effects on, 293, 309, 395, 443, 455, 469, 493

H
habitat destruction, 325
hemispherical (fisheye) photography, 379
human population growth, 325
hydrogen peroxide, 51

I
Idaho, 221
ILWAS model, 561
image processing, 351

L
Lake Tahoe, 279
leaf area index, 177, 337
lifted condensation level, 3
light compensation point, 429
lime potential, 547

M
measurement precision and bias, 379
meteorology, 137, 193, 207
methane sulfuric acid, 117

micrometerology, 177
Montana, 73, 221

N
N-fixation, 515
Nevada, 221, 279
New Mexico, 73, 221, 395
nitrate, 51, 73, 171, 193, 455, 515, 547
nitric acid, 51, 193
nitrification, 515
nitrogen oxides, 221
nitrous acid, 193
nucleation scavenging, 117
nutrient retention, 443

O
old-growth forests, 325
open-top chambers, 455, 469
Oregon, 73, 117, 221, 325, 515, 561
organic acids, 547
ozone, ambient concentrations, 51, 177, 193, 207, 247, 279, 309, 455
ozone, effects, 247, 261, 279, 293, 309, 351, 411, 419, 429, 455, 469, 493
ozone, exposure profiles, 469
ozone transport, 193, 207, 279

P
particulates, 105, 193, 455
permanent plots, 261, 279, 309
pH, 193
pH-CO_2 relationships, 547
photochemical smog, 455
photosynthesis, 411, 419, 429, 455, 493
Pinus contorta, 171, 443, 469
Pinus edulis, 395
Pinus jeffreyi, 261, 279, 309, 419, 561
Pinus ponderosa, 261, 279, 293, 309, 325, 351, 379, 395, 411, 455, 469, 561
Pinus strobiformis, 395
pollutant transport, 137, 221
precipitation, 15, 105, 117, 137, 147, 193, 221, 309
Pseudotsuga menziesii, 325, 395, 469, 515, 561

Q
quality assurance and control, 379

R
remote sensing, 337, 351
respiration, 429, 455
risk analysis, 247
Rocky Mountains, 3, 73, 105, 171, 193, 443
root:shoot ratio, 469, 493

S
Salix, 493
San Bernardino Mountains, 247, 309
sea salt, 33, 51, 73, 117, 147
Sequoia National Park, 137, 147, 207, 261, 351, 411, 419, 429
Sequoia sempervirens, 147
Sequoiadendron giganteum, 429
shortgrass steppe, 177
Sierra Nevada, 73, 137, 207, 247, 261, 279, 293, 351, 411
soils, 515, 529, 547, 561
soil moisture availability, 309
specific leaf weight, 411
spectral reflectance, 337, 351
stomatal behavior, 419, 429
sulfate, 51, 73, 171, 193, 455
sulfate adsorption, 529, 561
Sulfur IV, 51
sulfur dioxide, ambient concentrations, 193, 221
sulfur dioxide, effects, 469
sulfur mineralization, 529

T
throughfall, 171
Thuja plicata, 469
Tsuga heterophylla, 469
thunderstorms, 137
trace metals, 51

U
Utah, 221

V
vapor pressure deficit, 419

W
Washington, 33, 73, 117, 221, 325, 515, 529, 547, 561
water use efficiency, 419
weathering, mineral, 529, 561
Weibull distribution, 193
wet deposition, 15, 105, 117, 137, 147, 193, 221
Wyoming, 3, 73, 221